UNIVERSITY OF CAPE TOWN
IYUNIVESITHI YASEKAPA • UNIVERSITEIT VAN KAAPSTAD

Leakage Characterisation in Bulk Pipes using Pressure Tests

Prepared by:

Dietmar Eckart Niebuhr

For:

Prof. J. E. van Zyl

In part requirement of:

Master of Science in Engineering

Submission date: February 2019

Institution: University of Cape Town

Faculty: Engineering and Built Environment

Department: Civil Engineering

Plagiarism Declaration

1. I know that plagiarism is wrong. Plagiarism is to use another's work and to pretend that it is one's own.

2. I have used the Harvard Convention for citation and referencing. Each significant contribution to and quotation in this report that forms the work or works of other people has been acknowledged.

3. This report is my own work.

4. I have not allowed and will not allow anyone to copy my work with the intention of passing it as his or her own work.

5. This dissertation has been submitted to the Turnitin module and I confirm that my supervisor has been provided with the report and no concerns have been revealed.

Student no: NBRDIE001 Name: Dietmar Eckart Niebuhr

Date: 07 February 2019 Signature: Signed by candidate

Abstract

The supply of water is becoming increasingly strained as the demand for this essential and limited resource continues to increase. A significant amount of this resource is, however, lost through leakage. Not only does this result in a waste of a precious resource, but it also leads to a direct loss of revenue, especially considering that value has been added to the leaking water through collection, storing, purifying and pumping. A great deal of research has been done on reducing water leakages in distribution networks, however, leakage in bulk pipelines has received comparatively little attention thus far.

In this study, bulk pipelines in the field were tested with a pressure testing device developed by the University of Cape Town. With this device, a range of pressures were applied to various pipeline sections and the corresponding leakages were measured, resulting in characteristic pressure-leakage relationships. The Fixed and Variable Area Discharge (FAVAD) and the empirical N1 leakage models were then applied to interpret the pressure-leakage relationships.

Thirteen tests were attempted on pipeline sections ranging from 300 mm to 600 mm in diameter, and pressure tests were successfully performed on eight of the thirteen sections. Even though the effectiveness of the testing technique is dependent on the sealing capability of the isolation valves, it was found that most valves sealed effectively, with only two pipelines sections failing to isolate.

The high elevation differences along the length of the pipelines were found to have a dominating effect on the characteristics of the leak, which made it possible to roughly estimate the most likely leak locations by comparing the observed leak characteristics to those found in literature for similar conditions. The dependence of the leak characteristics on the location means that both have to be determined simultaneously. This can benefit the analysis, as some locations may be excluded based on their unrealistic leakage characteristics. However, it also means that there will be uncertainty with regards to the true location and leakage characteristics for sections of the pipe where the leakage characteristics are realistic.

Nonetheless, the measured leakage rate together with the estimated leak characteristics provided valuable information on the pipeline conditions, making it possible to rank the pipelines according to the severity of their conditions, for optimal allocation of maintenance resources.

Through practical tests, the study shows that pressure testing is an effective, simple and low cost technique to assess leakage in bulk pipelines. It causes minimal interference to the pipe operation, requires little downtime and the data can be processed in minimal time.

Acknowledgements

I would like to express my deepest appreciation for

- Professor Kobus Van Zyl, who enthusiastically guided me, encouraged me and always speedily replied to any queries I had;
- Mr. Trevor Westman from the City of Tshwane Municipality, who went out of his way to identify and make pipes available for this study;
- Mr 'Bossie' Boshoff from the City of Tshwane Municipality, who willingly and patiently assisted with accessing testing sites and providing operational support during all tests on the Tshwane infrastructure;
- The Thembisile-Hani Municipality and Ceenex (PTY) Ltd, an engineering consultancy firm, for identifying and making pipes available for testing in the KwaMhlanga area;
- My wife, for her constant encouragement, support and patience.

Contents Page

Appendices

List of Figures

List of Tables

List of Symbols

Q	Flow rate (m^3/s)
t	Time (s)
k_E	Price of electricity ($)
γ	Specific weight of water (N/m^3)
ρ	Density of water (kg/m^3)
g	Gravitational constant (m/s^2)
f	Friction Factor (Colebrook-White)
E	Modulus of elasticity
E_R	Relaxation modulus (MPa)
v	Poisson's ratio of the material
$\mathcal{V}$	Kinematic viscosity (m^2/s)
C_d	Orifice coefficient / Discharge coefficient
C_E	Emitter coefficient $\left(m^{5/2}/s\right)$
ζ	Orifice resistance coefficient
d	Pipe diameter (m)
s	Pipe wall thickness (m)
H_s	Static head (m)
H_d	Demand head (m)
H_f	Frictional head loss (m)
H_l	Leakage fraction (m)
ΔH	Differential pressure head (m)
H	Total leak discharge pressure head (m)
V	Velocity (m/s)
V_o	Velocity of outgoing flow (m/s)
V_i	Velocity of incoming flow (m/s)
Z_o	Height above reference level of outgoing flow (m)
Z_i	Height above reference level of incoming flow (m)
P_o	Pressure of outgoing flow (Pa)
P_i	Pressure of incoming flow (Pa)
ΔP	Differential pressure (Pa)
A	Actual, pressure dependant leak area (m^2)
A_o	Initial, pressure independent component of leak area (m^2)

A_{out}	Cross-sectional area of leak flow (outgoing flow) (m^2)
A_i	Cross-sectional area of pipe or flow source (incoming flow) (m^2)
A_e	Elastic and reversible change in leak area (m^2)
A_v	Visco-elastic component of leak area (m^2)
α	Emitter exponent (*usually 0.5*)
x	Fractional location (m)
N_c	Kinetic energy coefficient of vena contracta of leak flow (*J*)
A_c	Area of vena contracta of leak flow (m^2)
V_c	Velocity of vena contracta of leak flow (m^2/s)
N_i	Kinetic energy coefficient of pipe or flow source
ε_j	Coefficient of jet (leak flow) contraction
ε	Absolute Wall Roughness (m)
$\varepsilon_{circ/long}$	Strain (m)
E	Elastic Modulus (Pa)
K_L	Minor loss coefficient
m	Head-area slope of leak (m^{-1})
m_{vu}	Head-area slope for visco-elastic material (m^{-1})
m_e	Head-area slope for elastic material (m^{-1})
k_v	Expansion ratio for visco-elastic material
k_{vu}	Ultimate expansion ratio for visco-elastic material at 1000 seconds
L_c	Length of crack (m)
l	Length of pipe (m)
P_w	Wetted perimeter of flow (m)
σ_l	Longitudinal stress along pipe (N/m^2)
τ_σ	Relaxation time of strain during constant load (s)
M	Mass (kg)
C_{N1}	Leakage coefficient
$N1$	Leakage exponent
n_a	Component of N1 value relating to pipe material
n_q	Component of N1 value relating to leak dimensions
N_L	Leakage number
R_e	Reynold's number
DWS	Department of Water and Sanitation
PCAE	Pipe Condition Assessment Equipment

Chapter 1

1 Introduction

1.1 Background

The demand for water, an already strained resource in many countries and areas, is increasing, while cities are continuing to expand and populations are continuing to grow. Urbanisation, population growth, migration and industrialisation are all contributing to this ever increasing need for water (United Nations, 2015; World Bank, 2016). Water resources are, in contrast to the demand, diminishing. This is, due to the increase in demand, increased polluting of water sources, as well as the impact of climate change. It is, therefore, inevitable that a crisis will arise if current trends and behaviour persist.

An unacceptable amount of this precious resource is, however, lost unnecessarily, with one of the main contributors being pipeline leakage. By monitoring the condition and leakage of distribution and transfer pipes, effective intervention can be implemented to reduce these losses.

A lot of research focuses on reducing leakage from water distribution networks. The leakage from bulk transfer systems must, however, not be overseen, as large amounts of scarce and expensive water may be lost through these systems without water utilities realising it.

The University of Cape Town has developed testing equipment for assessing and characterising leakage in distribution networks. The technique uses pressure tests to obtain a relationship between the combined leakage flow rate of a pipe or a pipe network and the pressure in the pipe. The characteristics of the leakage can then be investigation by interpreting the pressure versus leakage relationship and applying the Fixed and Variable Area Discharge concept, as well as the empirical N1 equation.

Following the successful implementation of this technique on distribution networks, new equipment was developed by René Nsanzubuhoro, under the supervision of Professor Kobus van Zyl (2016), for the assessment of bulk distribution pipes.

This study investigates the application of the condition assessment technique with the newly developed equipment to effectively assess bulk distribution pipes, and in particular, bulk distribution pipes encountered in South Africa.

1.2 Aims and Objectives

The aim of this study is to investigate and verify the application of the newly developed pipe condition assessment equipment for testing bulk distribution pipes in the field, using proven models, which are based on the pressure-leakage relationship, to characterise leakage and assess pipe conditions.

The objectives of this study are as follows:

- Conducting a comprehensive literature review covering the significance of the water leakage problem in general, current assessment techniques, as well as the theory associated with the models used to interpret pressure-flow leakage characteristics.
- Identifying bulk pipelines in the field that can be tested with this equipment.
- Performing pressure tests using the newly developed pipe condition assessment equipment for bulk pipelines.
- Analysing the test data by using proven pressure-flow leakage models, in particular the FAVAD and N1 concepts.
- Demonstrating the ease and effectiveness of applying pressure tests for characterising leakage and for investigating pipe conditions.
- The development of an Excel spreadsheet tool that interprets the test data effectively, with minimal time and effort.
- Ranking the tested pipes according to the severity of their condition.

1.3 Scope

The scope of the study is confined to the pressure testing of bulk distribution and transfer pipelines in the field, using the equipment provided by the University of Cape Town, and the subsequent interpretation of the test data.

The interpretation of the test data is confined to the application of the Fixed Area and Variable Discharge (FAVAD) concept. The N1 leakage number concept is also incorporated into the study, due to its wide use and its common occurrence in literature.

Only bulk transfer or distribution pipes were tested. The scope is deliberately not confined any further on the sample of pipes to be tested, as it was deemed beneficial if the pipes vary in terms of diameters, pipe materials, applications and lengths.

Finally, all observations that could contribute to better understanding and improving future applications of the technique is reported and discussed.

1.4 Layout of Dissertation

The dissertation consists of five chapters:

- **Chapter 1: Introduction**
  In the first chapter, the need for this study is discussed and a brief background is given. This is followed by a definition of the aim of the study and a list of its objectives. The scope then indicates which work shall be included or excluded from the study.

- **Chapter 2: Literature review**
  The literature review then takes the reader through a broad overview of the dire water situation and how a reduction of leakage through improved water and leak management can assist in improving the situation. Existing pipe condition assessment techniques are then discussed, after which the review starts to focus on the technique of characterising pipeline leakage through pressure testing. Both the N1 and FAVAD leakage models are then presented in detail, including the results from studies applying these concepts in the field.

- **Chapter 3: Methodology**
  The methodology then presents the pressure testing equipment, as well as a description of the testing procedure. The method for identifying and selecting the pipe sample for testing is also explained, followed by a detailed description of an Excel spreadsheet tool that was developed to assist with analysing and interpreting the test data.

- **Chapter 4: Results and discussion**
  The results from the tests are then discussed, starting with a detailed presentation for the first test results. This is followed by a discussion of the remainder of the tests, with the detail of the reporting for each subsequent test reducing, as the observations become more repetitive. The results for all tests combined are then summarised at the end of this chapter.

- **Chapter 5: Conclusions and recommendations**
  In the final chapter, the summarised results are discussed, and recommendations for further experimentations and investigations are made.

Chapter 2

2 Literature Review

2.1 Introduction

Initially, the study explores the current state of water infrastructure and water leakage management in the world and in South Africa. The impact and consequences of leakage and water losses are then discussed and highlighted, followed by a section on the factors contributing to high water loss.

Existing means of intervention are explored, which include a review of the strengths and shortcomings a number of direct and indirect leakage detection and condition monitoring techniques.

The study then focuses on condition assessment techniques that are based on the use of pressure tests to characterise individual leaks and leaks in systems. The fundamental theory is explained, followed by an exploration into two well-known methods that are based on the pressure-flow relation, namely the fundamental FAVAD and the empirical N1 power equation techniques.

After reporting on the success of the FAVAD equation for assessing water distribution systems, the study concludes with an assessment of the research available for the application of this technique on bulk transfer pipelines.

2.2 Common Terminology and Definitions

2.2.1 IWA Water Balance

The IWA water balance, as shown in Figure 2-1, provides a break-down of the watering entering a system and indicates how much water is lost through real losses, such as leaks, how much water is lost through apparent losses and how much water is consumed.

<table>
<tr><td rowspan="8">System Input Volume</td><td rowspan="4">Authorised Consumption</td><td rowspan="2">Billed Authorised Consumption</td><td>Billed Metered Consumption</td><td rowspan="2">Revenue Water</td></tr>
<tr><td>Billed Unmetered Consumption</td></tr>
<tr><td rowspan="2">Unbilled Authorised Consumption</td><td>Unbilled Metered Consumption</td><td rowspan="6">Non-Revenue Water</td></tr>
<tr><td>Unbilled Unmetered Consumption</td></tr>
<tr><td rowspan="4">Water Losses</td><td rowspan="2">Apparent Losses</td><td>Unauthorised Consumption</td></tr>
<tr><td>Metering Inaccuracies</td></tr>
<tr><td rowspan="3">Real Losses</td><td>Leakage on Transmission and/or Distribution Mains</td></tr>
<tr><td>Leakage and Overflows at Utility's Storage Tanks</td></tr>
<tr><td>Leakage on Service Connections up to point of Customer Metering</td></tr>
</table>

Figure 2-1: Water Balance Example (A Lambert & Hirner, 2000)

Starting from the left-hand side of Figure 2-1, of the total *System Input Volume*, the *Authorised Consumption* is the only water that is intended to be supplied. The rest of the system input comprises of *Water Losses*, which the supplier should strive to minimise as much as possible.

Authorised Consumption is only distinguished from *Revenue Water*, by including *Unbilled Metered* and *Unbilled Unmetered Consumption.* In a South African context, an example of *Unbilled Metered* consumption would be the Free Basic Water allocated to every household. The use of fire hydrants in emergencies would be an example of *Unbilled Unmetered* consumption. *Non-Revenue Water (NRW)* refers to the entire portion of the *System Input Volume* that is not billed and that is lost through losses. It also includes authorised use of unbilled water.

Apparent Losses refer to the unauthorised consumption of water due to theft or illegal use, as well as the perceived losses resulting from meter inaccuracies. *Apparent Losses* are apparent, as the water is consumed, and not really lost. *Real Losses*, in turn refer to the physical losses from the system, which cannot be accounted for and which are not consumed (A Lambert & Hirner, 2000).

2.2.2 Background Losses and Bursts

Background losses are real losses that result from very small and undetectable leaks with typically low flow rates (A Lambert & Hirner, 2000). These leaks are difficult or impossible to detect while the pipe is buried (Clayton & van Zyl, 2007)

Bursts are large individual leaks that can often appear on the ground surface or can be detected with active leakage detection methods (Clayton & van Zyl, 2007)

2.2.3 Unavoidable and Current Annual Real Losses

Every pipe-line and distribution system will leak to a small, but acceptable, extent. To completely stop leakage in a pipe system is not possible, as the costs drastically increase as the leakage approaches zero. In 1956 Ledochowski (1956) already referred to such a minimum leakage when he suggested that leakage below one gallon per hour, per inch diameter, per mile under test pressure is acceptable.

The Unavoidable Annual Real Losses (UARL) predicts the acceptable real losses for a pipe that is in a good condition (S Hamilton, McKenzie, & Seago, 2006), and takes into account a number of factors that contribute to the acceptable loss rate. The UARL indicator takes into consideration the continuity of supply, length of mains, number of service connections, location of customer meters and average operating pressures. In its basic form, UARL can be presented as

$$UARL = (18 \times L_m + 0.80 \times N_C + 25 \times L_P) \times P \quad \textbf{2-1}$$

L_m (km) is the length of the main pipe (km), N_C is the number of off-takes or service connections, L_P (km) is the combined length of all pipe from the off-take on the main to the customer meter, and P is the average operating pressure. The resulting UARL value is in litres/day (S Hamilton et al., 2006).

Current Annual Real Losses (CARL) includes all the real losses, including UARL.

2.2.4 Infrastructure Leakage Index

The Infrastructure Leakage Index (ILI) is a non-dimensional water leakage indicator that relates the leakage to the minimum leakage level assumed possible in a network. The ILI indicator is defined as the ratio of the CARL over the UARL. It was developed to accurately indicate the performance of a system in comparison to other systems, taking into account all the factors which are considered when calculating the UARL (S Hamilton et al., 2006). These factors include the continuity of supply, length of mains, number and location of service connections, as well as the operating pressure.

As an example, An ILI of 1 indicates the minim possible leakage, equivalent to a UARL of 1, and should be strived for. An ILI of 10, as an example, indicates 10 times the minimum possible leakage (Mckenzie, Siqalaba, & Wegelin, 2012).

A report by Liemberger et al., (2017), commenting on the IWA Best Practices for 'Performance Indicators for Water Supply Systems', supports using ILIs as performance indicators, as they are based on the UARL, which has been proven to be robust in application through sensitivity studies and many years of studying. Hundreds of ILIs have been calculated in countries across the world.

In this same report, however, criticisms obtained by the ILI in the 2nd edition of IWA Best Practices, on a possible shortcoming relating to its dependency on pressure, are addressed. The UARL is dependent on pressure, as seen in Equation 2-1. If the pressure is reduced through, for example pressure management, the resulting ILI may, in some cases, increase. For this reason, the average operating pressure must best accompany the ILI number.

2.3 The Current State of Water

2.3.1 International State of Water

According to an UN assessment, two-thirds of the world's population will have insufficient water supply by the year 2020 (Rogers, 2014). By 2025 it is estimated that 1.8 billion people will be living in countries or regions with absolute water scarcity, with two-thirds of the population living under water stressed conditions (United Nations, 2012).

Müller (2016) quotes from the 2014 WHO/UNICEF report that 748 million people globally did not have access to improved drinking water by 2012, of which 325 million people were in sub-Saharan Africa. Under the business-as-usual scenario, the global water deficit is expected to stand at 40% by 2030 (United Nations, 2015). This is, if it is assumed that there is no significant change in people's behaviour and priorities, and no technological, economic and policy developments.

This increase in demand is largely due to population growth, income growth and the rising of living conditions. Industrialisation and increases in production, as well as urbanisation and migration has also resulted in an increased demand in certain areas (United Nations, 2015).

In many countries, water scarcity is further increased by climate change. Climate change has different effects on different regions of the world, leading to either increases or decreases in temperatures and precipitation, as well as to the occurrence of more extreme weather events, such as prolonged droughts and extreme flooding (United Nations, 2012). Generally, however, climate change tends to cause decreased precipitation in countries that already experience low precipitation (de Wit & Stankiewicz, 2006), thereby contributing to the worrying trends in water scarcity.

The outlook of the international state of water is therefore not positive, and necessary intervention must be put in place to counter the worrying trend of ever increasing water deficit, especially in countries that are already experiencing water scarcity, such as the sub-Saharan African countries.

2.3.2 State of South Africa's Water

South Africa is a water scarce country with an annual runoff of less than 13% of the world average (W. A. Wegelin, Mckenzie, Herbst, & Wensley, 2010). According to the definition of the total actual renewable water resources (TARWR) per person per year, South Africa is rated as the 29th driest country out of 193 countries (Muller et al., 2009).

In addition, a large proportion of South Africa's demands come from inland areas, where the economy and urban settlements have advanced in response to mining opportunities, but which are far from major water sources. With rainfalls in South Africa varying radically across the country, as well as from season to season, the limited water resources are unevenly spread across the country (Muller et al., 2009). It is therefore especially important that South Africa's water sources are allocated effectively and efficiently.

A report by the Institute for Security Studies provides evidence that South Africa is overexploiting its water resources at a national level, with water withdrawals exceeding the sustainable supply available (Hedden, ISS, & WRC, 2016). In this study, the sustainable supply refers to the supply available from currently utilised water resources, and excludes potential resources not yet utilised. It further uses reliable forecasting tools that make use of a number of indicators, to predict that the demand of water in South Africa will increase over the next 20 years.

Factors leading to this increase in demand include GDP growth per capita, increased access to piped water, an increase in urban population, an increase in industrial use, as well as an increase in agricultural use. The expected growth according to each water use sector is illustrated in the pie charts in Figure 2-2.

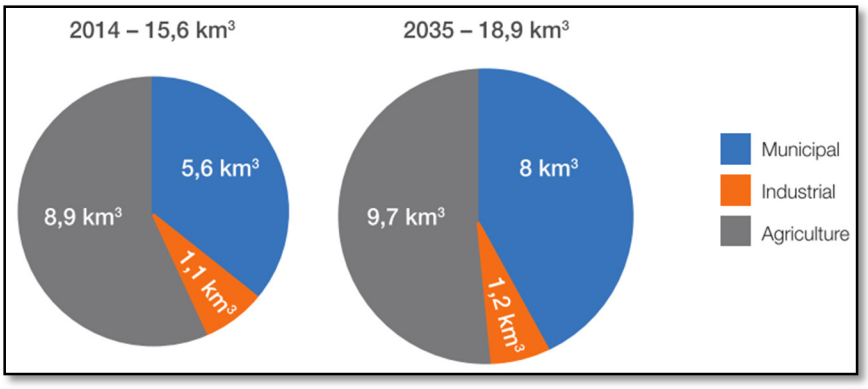

Figure 2-2: Increase in overall water withdrawals according to sector (Hedden et al., 2016)

According to this study, the planned infrastructure and strategies to increase the supply in South Africa will lead to a total annual supply of 17,8 km^3 by the year 2035, which is still lower than the 18,9 km^3 demand predicted for that year. This means that, according to this report, the overexploitation of this resource will increase in the next 20 years, even with the optimistic assumption that all planned reconciliation strategies will effectively be implemented before then.

This is further illustrated in Figure 2-3, which displays total withdrawals and total sustainable supply, as well as the reduction in withdrawals due to a planned intervention aimed at water conservation and water demand management (WCWDM). For clarity, even though the legend in Figure 2-3 refers to 'Total Supply', the graph refers to the total sustainable supply available. The total sustainable supply available was calculated by considering all the large-scale reconciliation strategies, amongst others, the National Water Resource Stragies of the Department of Water and Santiaion.

Figure 2-3: Forecast of water withdrawals and water supply (Hedden et al., 2016)

Climate change also has a negative effect on the rainfall in South Africa. This is illustrated in a study by de Wit and Stankiewicz (2006), in which they predict the expected changes in precipitation over the next century due to climate change. They clearly indicate how different areas are differently affected, with drier areas generally becoming drier, while precipitation is expected to increase in areas currently experiencing high rainfall.

As illustrated in Figure 2-4, South Africa falls in the region where drier conditions can be expected in the future, with a drop of more than 10 percent in perennial drainage density expected in parts of the country before the end of this century (de Wit & Stankiewicz, 2006). Similarly, the Intergovernmental

Panel on Climate Change (IPCC) forecasts that the western and south-western regions of South Africa will be at higher risk for droughts over the 21st century due to climate change (Hedden & Cilliers, 2014).

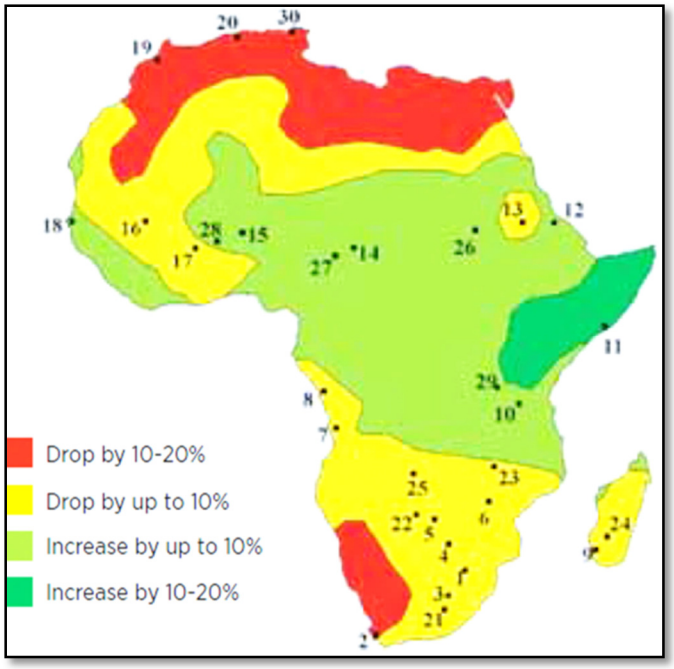

Figure 2-4: The predicted change in perennial drainage density in Africa due to climate change over the century starting in 1979-1998 and ending in 2070-2099 (de Wit & Stankiewicz, 2006)**.**

Müller et al (2009) predict, based on a number of studies, that even though a high proportion of available water is already used, enough water will be available in South Africa to meet the country's short and long-term needs. According to Müller et al, the main problems lie with the limited financial resources and institutional capabilities available to utilise the available water effectively. Already in 2009 Müller et al expressed that a water crisis may arise if the right investments, innovations and management decisions were not implemented at the right time.

The drought in South Africa of the years 2015 to 2016, which is perceived as the worst drought in 23 years, has highlighted how strained the country's water resources are, with a number of news articles now reporting on South Africa's 'water crisis'. During this drought eight out of the nine provinces have been declared disaster areas and a number of communities were faced with dry taps (Essop, 2016).

The preservation and effective use of water has therefore not received enough attention in South Africa, and the consequences are beginning to show.

2.3.3 Consequences of Water Scarcity

Water scarcity can have detrimental consequences. It not only deprives people of one of their basic needs, but can also result in serious social, environmental and economic consequences.

All agricultural foods, for instance, strongly depend on the availability of water, with more than 70% of the world's freshwater withdrawals consumed by the agricultural sector (United Nations, 2012). Water scarcity therefore has a direct impact on the sustainable supply of food, which amongst water itself, is one of the basic human needs.

Health risks also increase with water scarcity, with a number of water-borne diseases emerging form poor hygiene and sanitary conditions resulting from water scarce conditions (United Nations, 2012). In addition, when pipes routinely run dry, diseases can enter the water supply system due to the backflow of contaminated water into the depressurised water pipes through pipe defects.

Water scarcity also has economic consequences. In fact, the above social consequences ultimately contribute to the economic consequences. In addition, water is also an essential input to the industry, as well as the production of electricity. If water is scarce it will directly limit the expansion of industries critical to sustainable development, which would also include the food production and energy sectors (United Nations, 2015).

The World Bank has therefore recently sent out a stern warning to developing countries about the economic impact of water scarcity on their economies, and reports that water scarcity can lead to growth declines of up to 6% of GDP in the countries most affected by climate change (World Bank, 2016).

Ultimately water scarcity will affect the living conditions, jobs and livelihoods of a vast number of people (Muller et al., 2009), carrying with it a number of far reaching consequences.

2.4 The Current State of Leakage and Water Loss

2.4.1 An International Perspective

In the year 2006, the total cost of non-revenue water worldwide was already estimated at $\$14x10^9$ per year, with the contribution of developing countries amounting to one third of this amount (Kingdom, Liemberger, & Marin, 2006). In the same year, a study on more than 900 water utilities in 44 developing countries revealed an average NRW level of 35%, with even higher overall levels expected due to the poor performing utilities not being able to contribute to this study (Kingdom et al., 2006).

Kingdom et al argued that $\$2.9x10^9$ could be saved annually in developing countries by halving the NRW, and that enough water would then become available to serve an additional $90x10^6$ people. Considering that the NRW in developed countries is less than half of the NRW of developing countries, this goal should be achievable (Kingdom et al., 2006).

2.4.2 Water Losses in South Africa

In 2012, a study on the national municipal water losses in South Africa was carried out by McKenzie et al (2012). Unfortunately, only 132 of the possible 237 municipalities approached provided acceptable water loss data that could be used in this study. Assuming that the data obtained from the municipalities is accurate, and considering the likelihood that the municipalities providing the data were the better run municipalities, this study is expected to provide a rather optimistic, but useful indication of the condition of South Africa's municipal water infrastructure.

In this study, the non-revenue water, excluding the unbilled free basic water allowance, was estimated to be 36.8%. Most of the non-revenue water, or 25.4% of the total supplied water, constitutes losses through physical leakage. This approximates to around $1580x10^6$ m^3/annum, similar to the total supply of Rand Water, South Africa's largest water utility, amounting to approximately $R7.2x10^9$ in lost revenue (Mckenzie et al., 2012).

The apparent losses, however, vary considerably between the municipalities, with losses estimated at 80% in some municipalities and at only 5% in others, which again hints at possible inaccuracies in the municipal data.

The optimistic NRW of 36.8% is similar to the world average of 36.6%, which is high compared to developed countries, but low compared to developing countries. Similarly, the estimated average ILI value of 6.8 was found to be on par with the world average (Mckenzie et al., 2012).

In a more recent study (DWS & Sussens, 2015), the eight largest metropolitan municipalities, which serve 40% of the South African population, were assessed.

The study summarises the results in an IWA water balance as depicted in Figure 2-5. In this study, NRW is estimated at 34.3%, and the ILI is estimated at 5.4. This report, however, emphasis the fact that this water balance only represents the state of the municipalities that cooperated in this study, and possibly indicates an optimistic state of South Africa's water systems.

<table>
<tr><td rowspan="4">System Input Volume

2159
(100%)</td><td rowspan="2">Authorised Consumption

1537
(71.2%)</td><td>Billed Authorised Consumption
1418
(65.7%)</td><td>Revenue Water
1418
(65.7%)</td></tr>
<tr><td>Unbilled Authorised Consumption
120 (5.6%)</td><td rowspan="3">Non-Revenue Water
741
(34.3%)</td></tr>
<tr><td rowspan="2">Water Losses
622
(28.8%)</td><td>Commercial Losses
175 (8.1%)</td></tr>
<tr><td>Real or Physical Losses
447 (20.7%)</td></tr>
</table>

Figure 2-5: South Africa's National Water Balance in 2013/2014 (klx10^6/a) (DWS & Sussens, 2015)

In all of the studies (Mckenzie et al., 2012), (W. Wegelin, Barnard, & Mckenzie, 2016), (DWS & Sussens, 2015), the concern was highlighted, that a significant amount of municipalities, especially in rural areas, could not report on the volumes entering and leaving their networks. This indicates that these municipalities are potentially not aware of problems in their infrastructure and that they are probably not implementing Water Demand Management.

In 2015, of 237 municipalities, 15% have not submitted water loss information to authorities in the last 6 years, 45% have submitted poor, erratic loss information that is of little use, while only 40% maintain reasonable to good water balance information (W. Wegelin et al., 2016).

Reasons were found to be, amongst others, a limited understanding of water losses and the urgency of reducing them (W. Wegelin et al., 2016), as well as a lack of resources and metering, ignorance and apathy (Mckenzie et al., 2012). In a general study on developing countries, Kingdom et al

(2006) also observed poor reporting and allocated this to a common lack of national reporting systems that collect and consolidate information on the utility performance. Appropriate planning is therefore impossible.

Even though South Africa's water losses, based on the available data, appear to be on par with world norms, considering that this is a water scarce country, South Africa has a significant scope for savings through reducing water losses.

According to DWS studies (Mckenzie et al., 2012), a realistic target of 25% NRW is achievable over a period of 10 years (starting from 2012), if approximately $R2x10^9$ is invested annually. Similarly, by reducing the current ILI of 5.4 for the eight largest municipalities to a realistically achievable value of 3, an annual saving of $R1.6x10^9$ can be made (DWS & Sussens, 2015).

Whereas in the past, developing new infrastructure was the obvious answer to alleviating water shortages, this might not be the case today. A large portion of South Africa's water resources are already intensely utilised and new infrastructure is not always socially, environmentally or economically viable, because most of the cheaper schemes are already developed. More attention must now be given to the management of the demand which includes, amongst others, the management and reduction of water losses.

2.5 Reducing Water Losses

2.5.1 Poor Water Management

As water infrastructure ages, it deteriorates structurally and hydraulically. This leads to significant impacts on the water quality, water lost, system reliability and efficiency. Water infrastructure must therefore be effectively and continuously managed to limit the impacts and to ensure renewal of the system when it is most cost effective to do so.

Unfortunately, in many systems, large volumes of water are lost without any intervention taking place. Gonzalez-Gomez et al (2011), as cited in (van den Berg, 2015), conclude in their study of high NRW in developing countries, that the main reason for the high NRW can be attributed to a lack of incentives, not enough funds allocated to reduction of water losses, as well as a lack of knowledge about NRW.

A similar deduction was made in another study (Frauendorfer & Liemberger, 2010), in which it is recommend that utility owners must be made aware that they are "sitting on a goldmine" and that their staff must be incentivised by informing them of the consequences and effects of NRW.

Water related services, as well as the financing for water infrastructure, operations and maintenance, remain under-prioritised in most countries (United Nations, 2015). Especially in poorer countries, the main priority, and therefore the bulk of the already limited funding, is often allocated to short-term achievements, such as increasing access to basic services (Muller, 2016). This often results in a lack of commitment to maintaining and improving the existing infrastructure.

In South Africa, for instance, even though a significant portion of the national budget is made available for water infrastructure projects, the funding is implemented disproportionally with an emphasis on new water resource infrastructure, and insufficient focus on water conservation and demand management (WCWDM) (W. Wegelin et al., 2016), as well as a lack of attention to the maintenance, refurbishment and replacement of ageing existing infrastructure.

The poor condition of the ageing water infrastructure of the local Department of Water and Sanitation was highlighted by the most recent SAICE Infrastructure Report Card ((SAICE), 2011) grading, which awarded a D- for all water infrastructure, only one reward grading level above E, which would indicate infrastructure unfit for purpose. This report also cites that a focus on quantity, rather than quality infrastructure, together with a 'serious shortage' of skilled personnel and officials are main reasons for the poor condition. According to this report, even though major

advances were made in developing new infrastructure to increase provision since 1994, the weighted average age of the existing infrastructure was 39 years in 2011. This is worrying concern which highlights the fragile state of South Africa's infrastructure and the importance of quality water management.

2.5.2 Combating Poor Water Management in South Africa

In South Africa, a lot of focus has been placed on the implementation of Water Conservation and Water Demand Management (WCWDM) strategies that reduce leakage in municipal networks.

The Department of Water and Sanitation (DWS) has developed strategies since the year 2004 aimed at reconciling water demand with water availability in municipal water supplies. In 2013, the national water resource strategy emphasised WCWDM for metropolitan areas and large cities.

A recent report for DWS shows the progress of these reconciliation strategies in the municipalities which are situated in the large water supply systems of South Africa (W. Wegelin et al., 2016). This report showed that, by 2015, only two of the eight large water supply systems achieved savings close to the targeted savings; two achieved savings which were far short from the targeted savings; two showed negative savings (increased leakages); and two were not able to provide sufficient data to determine their savings. In total, the eight water supply systems showed a saving of 2.1% for the year 2015, 7.6% below the targeted saving.

In a similar internal study by DWS, which specifically focused on the effectiveness of the reconciliation strategies of the eight largest municipalities in South Africa, concern was raised due to the limited impact of the national WCWDM strategies (DWS & Sussens, 2015). As displayed in Figure 2-6, no clear trend in water loss reduction can be observed since the implementation of WCWDM strategies. In the contrary, an increase was witnessed in the 2013/2014 assessment year. The system input volume has also continually increased, breaching the maximum target value.

Figure 2-6: Metropolitan NRW and System Input Volume (SIV) trends. SIV target refers to 2013/2014. (DWS & Sussens, 2015)

The municipalities of one province, the Western Cape, outperformed the rest, with some municipalities operating close to their economic levels of leakage, with water losses below 15% (W. Wegelin et al., 2016) and an approximate ILI value of 2.3 (DWS & Sussens, 2015). In contrast, a number of other municipalities were not even able to provide water balance data, showing their ignorance to implementing the WCWDM strategies. It is also important to note that in some municipalities with economic significance, large budgets and formal infrastructure, savings were often barely visible if not non-existent.

Largely in response to the lack of commitment of all municipalities to implement reconciliation strategies, the "No Drop" certification was recently designed and is currently being implemented. This certification programme will assess, verify and validate the water use efficiencies of municipalities (Herbst & Raletjena, 2015). An assessment of every water supply system will be made on a yearly basis and a score will be given to each municipality. The program aims to acknowledge good practice, but also to direct necessary regulatory and support interventions to remedy non-compliance. The underlying aim is to encourage continuous improvement in water use efficiency and water management.

Little focus, however, is placed on the efficient management of bulk transfer lines outside of the municipalities. Often the monitoring and maintenance of bulk transfer lines is neglected first, because the detection, location and repair costs of unreported bursts are significantly higher than on distribution mains, leading to many utilities excluding these from their leak detection

programmes (Kevin Laven, 2012). Yet, WCWDM strategies for water boards and state-owned bulk pipelines are not as rigorously encouraged, in comparison to those of municipalities.

With often only a small proportion of leaks visible above the ground (Rogers, 2014), it is of concern that numerous transmission mains may have never been properly surveyed and may have accumulated a large backlog of unreported leaks, which the water utilities are not aware of. Laven (2012) therefore suggests that the surveying of bulk transmission mains must be included in reconciliation strategies.

2.5.3 Leakage and Condition Assessments for Effective Water Management

Water losses identified on the IWA water balance can consist of physical or real losses, and apparent losses, such as unauthorised consumption through illegal connections and metering inaccuracies. It is important that all these types of losses are known and that strategies are put in place to counter them. This study will, however, focus on strategies aimed at preventing physical losses resulting from pipeline leakage.

For effective water leakage management a strategy must be developed and put in place. Farley (2003) presented five central questions that must be answered when developing such a leakage strategy:

1. How much water is being lost?
2. Where is it being lost?
3. Why is it being lost?
4. What strategies can be introduced to reduce losses?
5. How can the strategies be maintained?

The first step, therefore, requires a detailed assessment of the water entering and leaving the system. This view is supported by Rogers (Rogers, 2014), who states that an immediate and precise way of quantifying leakage is needed, that is not subject to measurement errors. In a study of leakage management technologies in the UK, the EPA (Environmental Protection Authority, 2007) also suggests that, before any pipe testing strategy is developed, the approximate water losses must first be determined with available equipment, such as flow meters.

The results can be summarised in the form of an IWA water balance, which accurately allocates the entire system input volume to the various categories of users and water losses. Maintaining accurate IWA water balance data is also essential to determine baselines and setting targets (W. Wegelin et

al., 2016). With the water loss data known, the most critical pipelines can be identified and assessed in priority sequence (Bennis, Fares, Guemouria, & Dubois, 2011) (Prinsloo, Wrigglesworth, & Webb, 2011).

If a pipe, however, does not leak excessively, it might not be economically feasible to invest into a leakage reduction strategy. Accurate leakage and water balance data is therefore also required to determine the cost of treating and pumping the water that never reaches the customer. A capital investment, that increases exponentially as the maximum allowable leakage is lowered, will be needed to recover it. An optimum balance therefore exists between savings and investment, which is specific to each network (Rogers, 2014) or transfer pipe.

It is therefore advisable that the economic level of leakage for every pipe system is determined before a decision is made on the most ideal leakage strategy for that pipe system (Farley, 2003) (Environmental Protection Authority, 2007). The total elimination of all leaks will never be economically, nor physically feasible, and thus the economic level of leakage can be used as a guideline to determine whether a leakage reduction strategy is justifiable (Fantozzi & Lambert cited in (Bennis et al., 2011)).

If the NRW is found to be allocated to physical losses, comprehensive assessments or surveys of the pipe infrastructure can be carried out to verify the leakage accurately, as well as to assess the pipe condition. The type of deterioration mechanisms present, the existing and potential failure modes, as well as the expected frequencies of the failures are valuable data on which the risk of the asset can be determined (Liu, Kleiner, Rajani, Condit, & Wang, 2012).

Based on this data, an engineering evaluation can be conducted to identify and prioritise pipes and pipe sections in need of repair or replacement. Funds, tools and available technologies can then be pro-actively allocated to where they are most needed (Prinsloo et al., 2011).

Leakage control strategies that make use of such leakage and condition assessments, have major advantages over passive leakage control strategies that determine the need for rehabilitation and replacement of pipes based on historic criteria such as the number of recent failures, age, material and risk. With condition assessments and condition monitoring, the water utility has the necessary data to properly maintain their pipelines and to identify only specific sections in need of replacement, instead of replacing the entire pipeline (Prinsloo et al., 2011), saving considerable costs.

It should be clear, that the above steps to developing and implementing a sound water leakage strategy, strongly depend on information available on the condition of the pipe system. Therefore, in cases where the condition of the pipe infrastructure is not known, an efficient and preferably low cost pipe condition monitoring technique would be of great benefit for the successful implementation of effective water strategies.

2.5.4 Benefits of Combating Leaks

A reduction of leaks in systems will lead to a narrowing of the gap between supply and demand of water and can thereby lead to the postponement or avoidance of large investments in new water supply infrastructure (Dobbs et al., 2013),(Colombo & Karney, 2002). Leak reduction should therefore be regarded as being equivalent to the acquirement of new water sources, which are much more expensive to develop and have much more environmental and social consequences. This is especially true if the impact of transferring water from its source up to the location of a leak is considered.

Kingdom et al (2006) already suggested in the year 2006, that reducing physical leakage could save approximately $215 to $500 per cubic meter of water leaked per day in developing countries. Investing into NRW reduction should therefore result in excellent return on investment. In summary, as cited by Hope, (1996 in (Colombo & Karney, 2002)), an old quote reads as follows: “There is no water-supply in which some unnecessary waste does not exist, and there are few supplies, if any, in which the saving of a substantial proportion of that waste would not bring pecuniary advantage to the Water Authority”.

Colombo and Karney (Colombo & Karney, 2002) developed Equation 2-2 for calculating the additional cost of operating a leaking system that is pressurised by pumps:

$$P_E = k_E \gamma Q((1+a)\{H_d + H_f[1 + ax(a+2)]\} - (H_d + H_f))t \qquad \textbf{2-2}$$

Where $a = \frac{C_E(H_d+(1-x)H_f-H_{gw})^{\alpha}}{Q}$

And k_E equals the unit price of electricity; γ represents the specific weight of water, Q the demand flow, C_E the emitter coefficient in $(m^{5/2}/s)$, H_d the demand head, H_f the head loss due to friction, α the emitter exponent (usually 0.5), x the fractional location of the leak and t the analysis duration. H_{gw} is assumed to be 0 for unsaturated soil.

The following must be noted with this equation:

- This cost does not include the cost of the treatment of the water which is ultimately wasted, further contributing to the economic losses of a leaking system.
- The equation is only applicable to pumped systems. In South African distribution systems, however, water is usually first transferred into high level reservoirs, from where the water gravity feeds into the network. In such a case, if leakage exists in the network or on the gravity line, only the cost of pumping to the reservoir would be considered.

In a study on the non-revenue water of developing countries, the benefits of reducing leakage, or NRW in general, was presented by examples of deliverables that could be achieved at the cost saved by reducing the NRW by a half (Kingdom et al., 2006). Based on 2006 figures, for example, such a reduction could translate to an additional $8x10^9$ cubic meters of treated and pumped water to customers, or treated water access to an additional 90 million people.

Investments into water infrastructure result in a number of secondary economic benefits (United Nations, 2012). For instance, upstream investments can lead to more consistent flows, which result in smaller storage capacity requirements, thereby saving costs on the infrastructure required for urban waterworks. Industrial users, farmers and other users not only save costs if the water supply is more reliable, but also make use of new economic opportunities that present themselves with increased access to a reliable water supply (United Nations, 2012).

It can also be mentioned here that leakage reduction has further advantages in addition to the major advantage of reducing NRW. Leaks also, for instance, undermine roadways by eroding the underlying soil (Price & Reed, 1989) (Colombo & Karney, 2002) and can recharge aquifers at a sufficient rate to pose a risk to building foundations (Price & Reed, 1989).

2.6 Current Leakage Detection and Condition Monitoring Techniques

Various condition monitoring techniques exist for investigating the structural integrity of pipes, as well as leakage from pipes. In this section, a number of the common techniques are discussed.

This section distinguishes between direct and indirect condition assessment techniques. Direct assessment techniques assess pipe condition and leakage by identifying defects through visual inspections or by analysing signals emitted directly from defects. In this section, the direct techniques are divided into assessments performed externally, by assessing the pipe from the outside, and assessments performed internally. Some internal direct assessment techniques can be applied to pipelines in operation while others require the pipes to be dry and out of operation.

Indirect condition assessments involve the analytical interpretation of data obtained from conditions induced onto pipe systems.

2.6.1 Direct Pipe Assessment Techniques Applied Externally

2.6.1.1 Leak Noise Correlators:

With this acoustic method, leakage noise is measured at two locations along the pipeline, and is then transmitted to a device that determines the position of the leak by measuring the time shift between the maximum correlations of the two signals. The noise can be measured by either hydrophones, which are underwater microphones, low-frequency vibration sensors (Gao, Brennan, Joseph, Muggleton, & Hunaidi, 2005), or a combination of both (Stuart Hamilton & Charalambous, 2013; Liu et al., 2012). To record these signals, access to the pipe is required at various points along the pipeline. Vibration sensors or accelerometers are limited to metallic pipes and can be attached to pipe fittings without requiring direct access to the water, while hydrophones require suitable access points for direct exposure to the water (Stuart Hamilton & Charalambous, 2013).

The delay between the two measurements is caused by the one sensor being closer to the leak compared to the other sensor. With the propagation velocity of the sound in water known, as well as the distance between the two sensors, the location of the leak can be detected.

Multiple leaks can be detected between the two sensors, as each leak will have its unique signal peak. This peak varies considerably on metal pipes, while the peaks on plastic pipes vary much less and are therefore harder to distinguish (Hunaidi, Wang, & Bracken, 2004).

A difficulty that arises when implementing acoustic leak detection to large diameter pipelines, such as bulk transmission lines, is that the intensity of the sound waves weaken at faster rates as the diameters of the pipes increase (Kevin Laven, 2012), (Hao et al., 2012). Larger pipes also result in lower pipe rigidity and consequently lower predominant frequencies that are more susceptible to low-frequency interference (Hunaidi et al., 2004). This leads to the requirement of more access points at closer proximity to each other, posing a problem to bulk transmission lines, where access to the pipe is limited in comparison to distribution networks.

The performance of this type of acoustic leak detection, and acoustic leak detection in general, can also be greatly compromised by high environmental acoustic noise that can hide sounds emitted from leaks, especially for low water pressure pipes (a. Cataldo et al., 2014), (Hunaidi et al., 2004).

A further drawback of this method is that its effectiveness is dependent on a number of factors that influence the amount of noise created by leaks. Higher pressure pipe leaks, for instance, generate more noise than low pressure leaks (Hunaidi et al., 2004). Small pinhole leaks and leaks created by corrosion pits emit clear noise signals, while large splits, leaking valves and leaking joints emit lower noise levels not easily detected by acoustic methods (Hunaidi et al., 2004), (Rogers, 2014). Also, if the pipe is below the water table, the acoustic signals are muffled (Hunaidi et al., 2004).

Pipe material has a significant effect, with a large amount of signal attenuation experienced in plastic pipes, while signals travel furthest in metal pipes. Rigid pipe materials also lead to higher predominant frequencies that are less susceptible to low-frequency interference (Hunaidi et al., 2004). It is therefore clear that this method is not equally effective for all types of pipe systems. Large, low pressure pipe bursts in plastic pipes, for instance, are harder to detect than small, high pressure pinhole leaks in steel pipes (Rogers, 2014).

The method further requires a highly skilled and experienced operator that is able to identify and distinguish between leakage signals and acoustic noise (Hunaidi et al., 2004).

2.6.1.2 Ground Penetrating Radar (GPR):

The Ground Penetrating Radar (GPR) method is a direct assessment technique that surveys the ground in the general vicinity of the pipe by sending high frequency electromagnetic pulses from a device that is guided over the pipe on the ground surface. The waveforms obtained from the pulse reflections from various materials in the vicinity of the tested region are then plotted and analysed, and the materials with sufficiently differing electrical characteristics can then be distinguished from each other on these plots (Lai, Chang, Sham, & Pang, 2016).

This method can be used for the leak detection of all pipe material types, as it indicates leaks by detecting certain changes in the di-electric characteristics of the soil surrounding a leak, irrespective of the pipe material (Hunaidi & Giamou, 1998).

A number of studies, however, confirm that GPR is highly sensitive to changes in moisture and GPR showed limitations in highly conductive soil types, such as clay and silty soils (Costello, Chapman, Rogers, & Metje, 2007; Hunaidi & Giamou, 1998; Stampolidis, Soupios, Vallianatos, & Tsokas, 2003).

GPR is also susceptible to any conductive objects in the vicinity of the pipe (a. Cataldo et al., 2014), with noise dominating the waveform plots at depths deeper than 3m (Hunaidi & Giamou, 1998). Even to successfully survey at depths of between 2m and 3m, the conditions must be very favourable.

Further, for successful leakage detection, highly skilled staff is required to accurately interpret the waveform plots, which is also a time consuming and expensive process (Hao et al., 2012).

2.6.1.3 Electrical Resistivity Tomography (ERT):

With this method, the electrical resistivity of the soil is measured by injecting current into the ground with electrodes and measuring the potential difference between the electrodes (a. Cataldo et al., 2014). The resistivity is simply calculated by Ohm's law and is then mapped to illustrate the variation of resistivity in the soil surrounding the pipe. The potential leaks are then pinpointed by identifying areas of low resistivity, which indicate moist soils or water filled cavities.

A disadvantage of this method is that it requires electrodes to be inserted into the ground at regular and frequent intervals, which can be time consuming, especially if the condition of the ground is not favourable. Further, the results are easily distorted by other anomalies in the ground that influence the resistivity (a. Cataldo et al., 2014).

2.6.1.4 Ultrasonic Guided Waves Technology:

With this method, a sleeve fitted with a transducer and a ring of dry-coupled piezoelectric elements, which act as both emitters and receivers, is positioned around the outer circumference of the conductive pipe. Waves at frequencies below 100 kHz are emitted and the reflections of the waves are recorded and analysed (Leinov, Cawley, & Lowe, 2015). Signals are reflected from both the

front and back ends of defects, allowing the size of the defect to be estimated from the time lag between the two signals.

The depth of the defects can be roughly estimated from the amplitude of the reflected signal, because it has been found that the depth is roughly proportional to the amplitude of this signal. Numerous defects can be identified with this technique by separating the reflected signals (Tse & Wang, 2009). This method is ideal for identifying corrosion in steel pipes even before any failure occurs (Hao et al., 2012).

This method is, however, strongly compromised by the limited distance of pipe that can be analysed from the fixed probe position. The effective range is only 30m (Liu et al., 2012) for pipes above the surface, and even less for buried pipes, because more energy is lost to the surrounding medium.

Another drawback is that this method can only be applied to continuously conductive pipes, such as welded steel pipes. This method can also not indicate whether the defects are on the inside or outside of the pipe.

2.6.1.5 Time Domain Reflectometry (TDR):

With this direct method, an electromagnetic signal is generated and transmitted through a transmission line that is buried in close proximity to the pipe. The signal is partially reflected back as it encounters varying degrees of electric impedance. By analysing the return signal, the soil condition and moisture content of the soil surrounding the pipe can be plotted along the length of the transmission line (a. Cataldo et al., 2014).

The ideal application requires a transmission line with two wire threads to be installed alongside the pipe during the laying of the pipe (A. Cataldo, De Benedetto, Cannazza, Piuzzi, & Giaquinto, 2015). This allows for quick pipe condition surveys (a. Cataldo et al., 2014) and can easily be modified to allow for continuous, real-time monitoring for the entire life of the infrastructure (A. Cataldo et al., 2015).

This method has also been successfully applied to existing underground conductive pipes by placing a conductive wire on the ground surface directly above the pipe (A. Cataldo, Cannazza, Benedetto, & Giaquinto, 2012). The pipe and the wire on the ground surface act as the sensing element, requiring the pipe to be electrically continuous.

Pipe lengths of up to 300m can be surveyed with one single measurement, which amounts to approximately 6 km of pipe per day (a. Cataldo et al., 2014).

The biggest limitation to this technique is that a transmission line must either be installed during the initial laying of the pipe, or the pipe must be electrically continuous. The real-time monitoring capability is only available for new pipe installations, as it requires the transmission line to be installed underground along the pipe.

2.6.1.6 Thermal Imaging or Infrared Thermography

With the thermal imaging technique, a visual representation of infrared energy is obtained with a device recording detailed images of the pipe and surrounding soils. The device is usually flown at a height of 600m above the ground (Stuart Hamilton & Charalambous, 2013) and gathers thermal images that can indicate the presence of water in the soil surrounding the pipe, signifying a possible leakage site.

The wet soil is identified by the difference in temperature on the soil surface caused by the increased humidity resulting from the presence of the water in the soil (Shakmak & Al-Habaibeh, 2015).

The thermal imaging equipment can be carried at the desired height over the vicinity of the pipe by various means, such as drones, helium balloons or airplanes (Shakmak & Al-Habaibeh, 2015). Figure 2-7 illustrated the use of a quad-copter drone for carrying the sensing equipment.

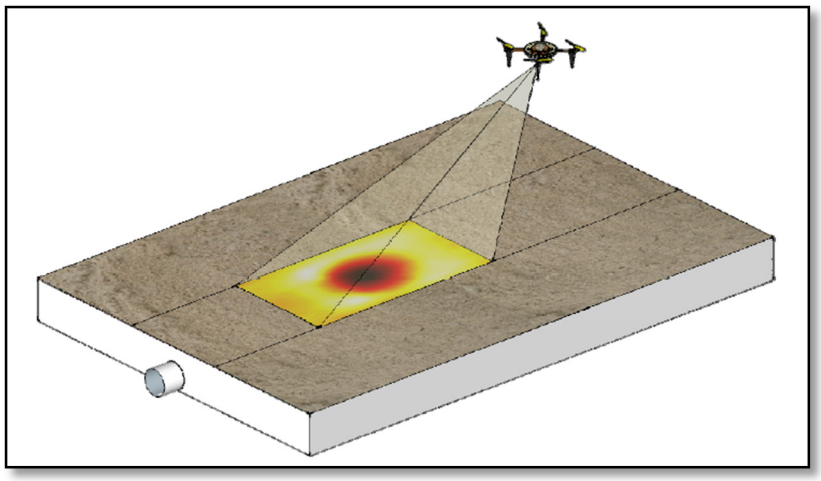

Figure 2-7: Illustration of a Quad-copter Drone surveying a pipeline with infrared thermography (Shakmak & Al-Habaibeh, 2015)

Limitations to this technique are that the technique requires soil conditions to be relatively dry, and therefore tests are limited to dry seasons in dry countries (Shakmak & Al-Habaibeh, 2015). Further limitations are that the method only provides a map of radiant energy and does not provide the cause of the extra energy. Skilled interpretation, which requires considerable man hours, is therefore required for analysing the data (Stuart Hamilton & Charalambous, 2013).

2.6.1.7 Other Externally Applied Direct Methods

Other direct methods include methods that are known to be less effective and less economically viable for large scale pipe surveying, such as the following devices: noise loggers, listening rods, ground microphones (Hunaidi et al., 2004),(Hao et al., 2012) and gas injection methods. These will not be elaborated on further in this study.

2.6.2 Direct Pipe Assessment Techniques Applied to Wet Pipelines

2.6.2.1 SmartBall:

One way of implementing acoustic leak detection to bulk distribution pipes, is by bringing the acoustic sensor closer to the source of the sound (Kevin Laven, 2012). This can be achieved by implementing devices that travel inside the pipeline during operation.

The SmartBall is an untethered and free-swimming ball, fitted with acoustic monitoring equipment. The acoustic listening equipment is fitted inside an aluminium sphere which is located in the centre of the foam ball. The device is launched through any 100mm diameter flanged pipe opening isolated by a valve, and is propelled by the flow of the water through the pipe. Receivers are positioned at regular intervals along the length of the pipeline to detect and calculate the location of the travelling ball.

Since it was commercially introduced in 2006, this method has rapidly gained popularity and has now become a common pipeline leak detection technique in many countries (Liu et al., 2012).

One major advantage of this system is that it is small and untethered allowing it to pass through valves and other obstacles commonly encountered in large pipelines, and bringing it into a close range to all potential leaks. The round shape of the device also ensures that noise generated from the shape is kept at minimal levels, largely eliminating external interferences (Oliveira, Ross, & Trovato,

2011). This allows for the detection of leaks smaller than 0.4 litres per minute, depending on the pipe material and leak type (Prinsloo et al., 2011).

This method also allows for the pipe to be surveyed in minimal time while remaining in full operation. A case study of this technique applied to an oil pipeline showed that a 21km long pipeline can be surveyed in less than 13 hours (Oliveira et al., 2011).

A disadvantage of this technique is that it does not provide additional information other than location and a rough estimate of the severity of the leak (Liu et al., 2012). The severity can only be roughly estimated, because the noise measured by the device is dependent on a number of factors, including pipe material, pipe pressure, leak size and leak type.

In addition, leaks in low pressure pipes can easily be overlooked due to the low level of noise emitted from such leaks, especially in the presence of ambient noise.

2.6.2.2 Sahara system

The Sahara system is a tethered, in-line leak detection technique that uses highly sensitive acoustic hydrophones to identify leak locations. It makes use of a carrying device that is fitted with a parachute, which uses the flow of the live pipeline to pull the system through the entire length of the pipe. Any tap point of 50mm or larger, such as the ones used for air valves, can be used as an insertion point for this device, and lengths of up to 2 km can be surveyed on one pass (Webb, Mergelas, & Laven, 2009).

Leak locations and rough estimates of the leak sizes are identified by the distinct noises of leaks detected by the apparatus. An operator with a locating tool tracks the device and marks the location where a leak signal is sensed (Webb et al., 2009).

The system has also been successfully used to inspect a pre-commissioned pipe with no water flow, by using a dragline to pull the device through the length of the pipe (Mergelas & Henrich, 2005). The device can also be adapted to perform CCTV inspections by replacing the sensing equipment with a video camera and lighting system (Webb et al., 2009).
One of the main advantages of the system is its compact size when the parachute is in collapsed position, enabling the device to travel through obstacles in the pipeline, as well allowing for the device to be easily introduced into the pipe through small pipe openings (Prinsloo et al., 2011). The

technique is also not limited to any pipe material and it is claimed that the device can detect leaks as small as 1L/hour, depending on the leak characteristics (Mergelas & Henrich, 2005).

Disadvantages are that access to the pipe of at least 50 mm in diameter is required for the insertion of the device, and only pipelines larger than 300 mm in diameter can be assessed with this device (Mergelas & Henrich, 2005).

Further, the device is limited to operating pressures of 16 bar (Webb et al., 2009), which is a significant disadvantage for long transmission lines, which often operate in excess of 30 bar.

Additionally, the device, in its standard form, requires flow in the pipeline, and a variety of operational and physical modifications are required for the device to effectively function in pipes that are not in operation (Mergelas & Henrich, 2005).

Finally, expensive and skilled operators are required to operate and setup the device, as well as to trace the device from the ground surface.

2.6.2.3 Ultrasonic In-line Inspection:

The ultrasonic in-line inspection method is used to detect either cracks or metal thinning through the emitting and receiving of high frequency waves from equipment installed on a carrying device that is pulled through the pipe. The waves are transmitted vertically through the pipe wall and reflections from the pipe features, such as from the inner and outer wall of the pipe, are recorded and analysed according to the time-of-flight principle. With this analysis, a high resolution data image of the pipe wall thickness can be obtained (Orazem, 2014).

Similarly, the signals can be emitted from slanted probes, causing the signals to propagate through the pipe at angles. These signals then reflect back from vertical cracks in the pipeline, which are difficult to detect with vertical reflections (Orazem, 2014).

One of the main drawbacks to this technique is its high cost, due to the length of time required for this labour intensive pipe inspection, as well as the cost of the equipment (Liu et al., 2012).

Also, similarly to other acoustic methods, the leak detection efficiency is strongly dependant on the amount of noise emitted from the leak. The pipe material, pipe pressure, leak size and leak type therefore have similar influences on the probability of leak detection, in comparison to the leak-noise correlators discussed in paragraph 2.6.1.1.

The pipe must further must be completely filled with water, because the method requires a coupling medium between the equipment and the pipe wall (Orazem, 2014).

2.6.2.4 Remote Field Eddy Current Technique (RFET):

With this method, a transmitter coil is energised by a low-frequency alternating current resulting in the formation of a magnetic field in the pipe wall. Flux lines from the magnetic field generate a voltage across the pipe wall, which in turn generates eddy currents. A receiving coil positioned at a certain distance from the transmitter coil then senses the alternating magnetic fields created by the eddy currents.

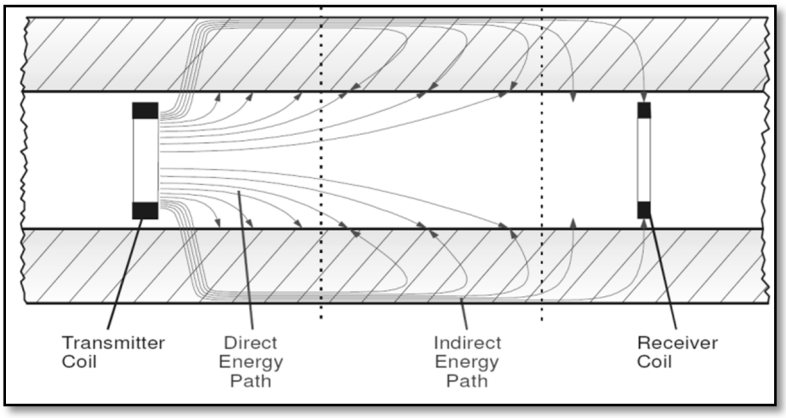

Figure 2-8: RFET Setup (Innospection, n.d.)

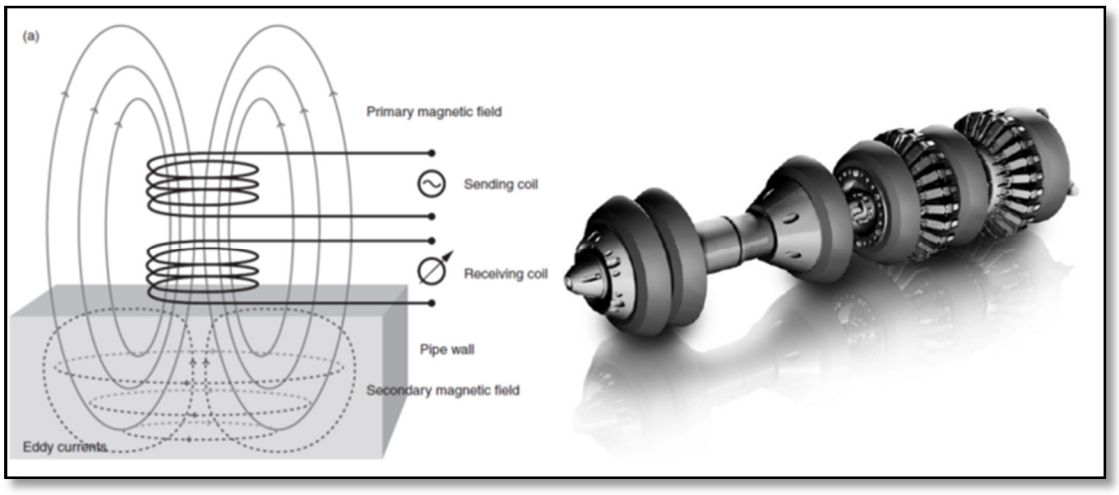

Figure 2-9: RFET flow diagram (Orazem & Tribollet, 2008) **and commercially available carrying device** (Orazem, 2014)

The phase as well as the voltage amplitude of the incoming signal is recorded by the receiver coil. The phase is used to identify the defect depth, while the signal amplitude can be analysed to estimate the defect volume.

Commercial tools are available for in-line inspections of pipes up to 700 mm (PICA, n.d.). The tools, known as HydroScopes or HydraSnakes, consist of a carrying device, a transmitting coil and a receiver coil. These devices can operate in wet or dry conditions and are either pulled through the pipe with a cable, or can be pumped through the system.

One advantage of this method is that no intimate contact with the pipe wall is required, allowing the system to function effectively, even if the pipe is lined or covered slightly with sludge or sand.

The Broadband Electromagnetic (BEM) technique is a similar method to the conventional RFET method discussed above, except that a broad range of frequencies between 50 Hz and 50 kHz (Liu & Kleiner, 2013) are transmitted instead of a single frequency. The advantage of this method is faster inspection speeds. Although commercially available, this method is not common.

The Remote Field Eddy Current / Transformer Coupling (RFEC/TC) technique functions on a similar principle, but was developed for pre-stressed concrete pipes (PCP) to identify the locations of broken wires in the concrete pipe walls. It is one of the most common methods of condition assessment for PCP (Prinsloo et al., 2011). A system, called the PipeDiver, is commercially available to perform this exact function. It is a flexible untethered and buoyant device that travels the length of the pipe using the flow of the water inside the live pipe.

The RFET method can, however, only be applied to ferritic pipes, while the RFEC/TC technique is only suitable for pre-stressed concrete pipes. Both techniques require the pipeline to be accessible for insertion and removal of the carrying device.

Another drawback of this technique is the low frequencies (10Hz to 1 kHz) at which this method is effective, resulting in a slow inspection speed (Innospection, n.d.), although newer technologies allow for surveying speeds of between 5m and 15m/min (PICA, n.d.).

This technique is also easily influenced by conductive debris or external electrical noise. The technique is therefore highly dependent on the skills and experience of the operator to distinguish potential pipe defects from this noise (Liu et al., 2012). Further, although the method detects internal and external flaws with equal effectiveness, it cannot distinguish between internal and external defects.

2.6.2.5 Magnetic Flux Leakage (MFL) Detection:

This direct, in-line inspection method is one of the oldest methods of ferrous pipe inspection (Orazem, 2014), and is accurate at determining any changes in pipe wall thickness, including the detection of corrosion pits.

Large magnets induce a saturated magnetic field, resulting in a magnetic flux distribution in the pipe wall. In perfect pipes, the magnetic flux field will be homogeneous, but damaged areas cause abrupt reductions in magnetic permeability, increasing the resistance to flux, and therefore causing the flux to change direction. Flux leakage therefore occurs at the pipe defects where the material is thinner and incapable of carrying all the magnetic flux. The flux leakage can then be detected to pinpoint the location of the defect (Liu et al., 2012).

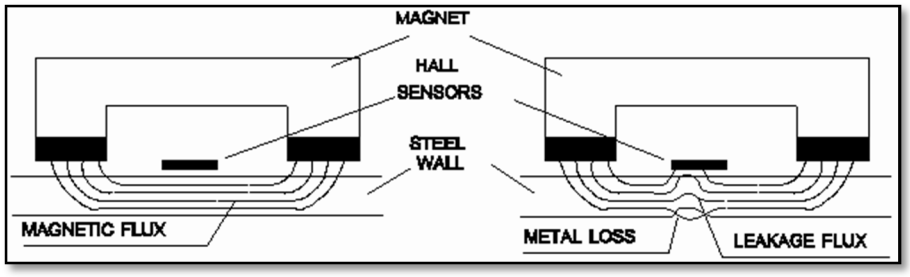

Figure 2-10: Illustration of the basic principle of Magnetic Flux Leakage

Most MFL techniques require direct contact with a cleaned, unlined pipe surfaces for efficient functioning, as well as to avoid damage to the pipe lining (Liu et al., 2012). New advancements, however, allow this method to function effectively without pipe wall contact by guiding a carrying device through the length of the pipe that is fitted with the magnets and sensors which it keeps at a constant distance from the pipe wall. This allows for accurate assessments of epoxy lined and even cement mortar lined pipelines. The applicability of this method for identifying pipe defects has been verified for large mortar lined steel pipes of up to 2 m in diameter (Hannaford & Melia, 2010).

Since recently, this method is also available in the form of a ‘smart pig’ that is pulled through the length of the pipeline (Orazem, 2014), eliminating the original requirements that the pipe must be taken out of operation, emptied and cleaned before implementation.

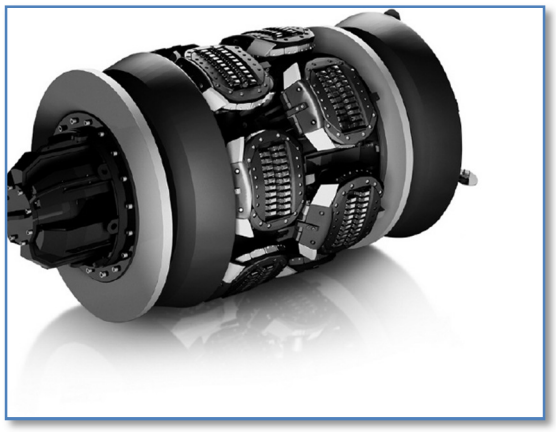

Figure 2-11: MFL Inspection equipment mounted to a carrying device, commonly referred to as a 'smart pig' (Orazem, 2014)

MFL, in general, is limited to ferrous pipes and it has also been found to be unreliable for detecting short and shallow defects (Hao et al., 2012). The close contact between the magnets and the pipe wall can also easily lead to lining damage (Liu et al., 2012). Further, if the direction of the induced magnetic field is aligned to the direction of the defect, the effectiveness of the device to identify thin defects, such as cracks, is limited (Orazem, 2014).

Limitations to the in-line method that utilises a 'smart-pig' are that the pipeline must be accessible to pigs and may not contain features that hinder the free movement of pigs, such as sharp bends and butterfly isolation valves.

The more common MFL techniques, that still require the pipeline to be emptied and cleaned, remain time consuming and require the pipe to be out of operation for the entire duration of the inspection. In a cited case study, for instance, the surveying of a 2m diameter, 12km long pipe required a ten week downtime period (Hannaford & Melia, 2010). Further, for this method to be effective, the pipeline must first be emptied and cleaned thoroughly prior to the inspection (Hao et al., 2012).

2.6.3 Direct Pipe Assessment Techniques Applied Inside Dry Pipes

2.6.3.1 Closed-circuit Television (CCTV) Inspection:

Closed-circuit television (CCTV) inspection is a direct, in-line condition assessment technique that utilises a carrier device fitted with a camera, which captures and transmits video and images to a ground station as it travels through the pipeline (Liu & Kleiner, 2013). The autonomous and tethered device is inserted into the emptied pipeline and is remotely operated from a surveillance unit.

Major disadvantages of this system are the slow pace at which a pipe is analysed and the fact that the pipe must be emptied and remain out of operation for the entire duration of the investigation. The device is commonly limited to a speed 15 cm/s (Liu & Kleiner, 2013) to allow for quality recordings, and stops frequently to assess suspect locations in the pipeline, resulting in extensive downtime. Although a lot of research and development has taken place to allow for automatic crack detection, interpretation of the footage is mostly performed manually by an experienced operator, which makes this method expensive and time consuming (Costello et al., 2007).

Newer side scanning evaluation technology (SSET) is, however, now available, which generates 360^{o} images of the pipe surface (Liu & Kleiner, 2013), considerably reducing the amount of time required for scanning the pipeline.

Unfortunately, this method can still only be used to assess the interior of the pipeline, and gives little indication on the depth and seriousness of detected cracks (Hao et al., 2012). Further, limitations exist on the sizes and types of leaks that can be detected through visual inspection, and the method is highly dependent on the skills of the operator (Hao et al., 2012).

2.6.3.2 Laser Scan:

This is a direct, in-line inspection method and involves a scanning device which is fitted on an autonomous and tethered carrying device. A laser projects a ring of light onto the inner surface of the emptied pipe and a camera captures the reflections of the emitted light which are then, through a time-of-flight approach, used to digitally reconstruct the profile of the pipe inner pipe wall (Liu & Kleiner, 2013).

The advantage of this method is that the reconstructed profile can be unfolded and manipulated to allow for effective review and analysis to detect and pinpoint potential pipe corrosion (Liu & Kleiner, 2013). This method is superior to normal CCTV inspection in terms of its capabilities for detecting potential leak sites.

This method is, however, limited by its long surveying time, as well as the fact that the pipeline must be taken out of operation and emptied for the duration of the assessment.

Similar to other visual inspection techniques, limitations still exist on the sizes and types of leaks that can be detected with this technique.

Further, the colour and roughness of the pipes play a significant role in the effectiveness of this method. Data processing is also required to compensate for errors induced during the scanning, making this a time consuming process (Liu & Kleiner, 2013).

2.6.4 Indirect Pipe Assessment Techniques

2.6.4.1 Conservation of Mass or Mass Flow Technique:

Conservation of mass techniques require the measurement of flow into and out of the pipeline, with mass flow technique appearing to be the easiest and most common of these techniques. The mass flow technique can accurately determine the existence of leaks, as well as the combined intensity of all the leaks. It, however, lacks the ability to locate the leaks (Ostapkowicz, 2016).

The mass flow technique is achieved by simply installing flow meters at the beginning and at the end of the pipeline under inspection. The difference in the flow entering and leaving the pipe indicates the amount of leakage from the system, with accuracy solely dependent on the flow meters used. Flow conditions other than steady state conditions also negatively influence the accuracy of this method, partially due to the delay in the pipe inlet and outlet flows in respect to the pressure changes (Turkowski & Bratek, 2007).

2.6.4.2 District Metering Area (DMA) Methodology:

The District Meter Area (DMA) methodology is an adaption of the mass flow technique, and is used specifically on distribution networks to narrow down the potential portion of the network where leakage occurs, and to improve the control over the existing leakage (Macdonald & Yates, 2005)

With this method, a large network is divided into a number of sections known as DMAs, with each section preferably supplied by a single supply. The inflow is then measured and monitored with a flow meter. The measured inflow can be compared to the expected usage, which can either be based on historic usage patterns, or can be assumed to be zero when the boundary valves of the DMA are

closed or the flow is recorded during certain night hours when usage is expected to be zero. This process is then carried out for each DMA, resulting in a clear overview of all the leakage in the network, and the allocation of leakage to each DMA (Macdonald & Yates, 2005; Rogers, 2014).

In a study on the feasibility of the implementation of DMA's in North America, some limitations are highlighted (Macdonald & Yates, 2005). One limitation concerns the dependence of this method on the accuracy of the flow meter, which must detect low leakage flows in pipelines intended for much higher maximum flows. In addition, not all existing networks allow for splitting the network into similar DMA's with single supplies. The method is also not ideal for DMA's in series, such as with the case of bulk transmission lines.

2.6.4.3 The Step Test Method:

The step test can be implemented as a continuation to the DMA method to further refine the potential location of the leak. It is used to identify specific isolatable sections of pipe that are responsible for the leakage of a greater network or length of pipe. The step test method is therefore also suitable for identifying leaking sections of transmission lines.

With this method, DMAs or long sections of pipes are closed off at the boundary valves. Flow into the system is then monitored as sections of pipe are progressively isolated from the larger DMA or pipe. Leaking sections are identified by measuring the drop in flow resulting from the isolation of the relevant section, which is roughly equal to the leakage from that section (Rogers, 2014). The identified sections can then be analysed further with other techniques more suitable for pinpointing the exact location of the leak (Boulos & Aboujaoude, 2011).

A night step test is a form of the step test applicable to distribution networks, where the test is performed during certain night hours when the demand is expected to be close to zero. This therefore eliminates the need for the boundary valves of the DMA to be closed (Rogers, 2014).

Limitations are that consumption during the test period must remain stable (Boulos & Aboujaoude, 2011). The effectiveness of the method to pinpoint leaking areas is also limited by the length or size of the sections that are isolatable.

2.6.4.4 Pinpointing a Leak through Conservation of Mass

Ledochowski (Ledochowski, 1956) effectively used a conservation of mass method to narrow down the location of a leak, if it is known that only a single leak exists. This method is based on the

principle, that if two sets of pipe pressure and leakage flow rate data are available, and the leakage is assumed to be categorised by the generic orifice equation, the pressure can be separated into an elevation component and an applied pressure component by solving the orifice equations 2-3 and 2-4 simultaneously:

$$Q_1 = C_d H_s^{0.5} \quad \textbf{2-3}$$

$$Q_2 = C_d (H_s + \Delta H)^{0.5} \quad \textbf{2-4}$$

In equations 2 and 3, Q refers to the leakage flow, H_s and ΔH refer to the static and the applied head respectively, and C refers to the orifice coefficient. The elevation of the leak is then determined from the calculated head value. By calculating the leak elevation, the potential leak site can be obtained from the pipeline profile.

Tests were carried out by isolating a section of the pipe and applying a test pump to a convenient connection point on the pipe. In the annotated diagram illustrated in Figure 2-12, the testing equipment is described.

A pump transfers water from a supply drum into the pipe. Shortly before the feeder pipe enters the pipe section under test, a bypass splits from the feeder pipe and returns the water supplied by the pump back into the supply drum. Two control valves, one on the feeder branch and the other on the bypass branch, can be adjusted to control the flow into the pipe section and to maintain the desired pressure. A pressure relief valve, which is fitted just after the pump and also feeds into the bypass, is set to a maximum allowable pipe pressure to protect the pipeline from becoming over-pressurised. A pressure gauge indicates the current system pressure.

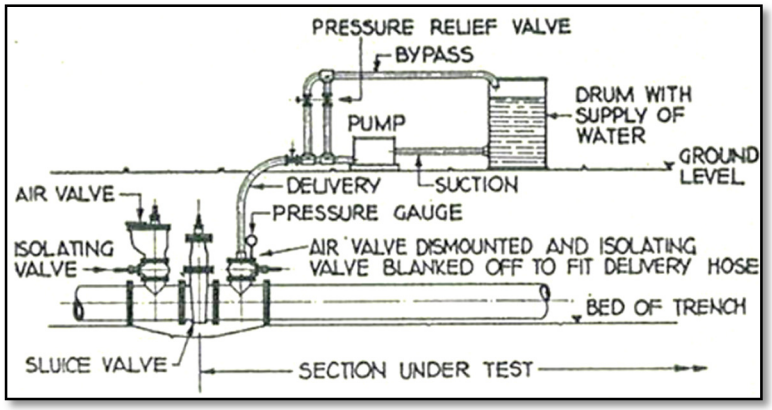

Figure 2-12: Apparatus used by Ledochowski to estimate burst elevation (Ledochowski, 1956)

A desired pressure is maintained in the pipeline by adjusting the control valve on the delivery line and bypass line, effectively splitting the excess supply from the desired supply, while the pump maintains a constant speed. The leakage or flow rate at the desired pressure level is obtained by measuring the drop in water level in the supply drum, provided that the leakage is less than the delivery capacity of the pump.

Ledochowski, however, encountered difficulties in maintaining a desired pressure and taking accurate readings, due to the vibrations caused by the running pump and partially closed gate valves. These difficulties could nowadays be overcome by installing a variable speed motor to drive the pump at the desired flow rate, instead of throttling the flow with control valves, or by using improved components that result in fewer vibrations.

Another method was proposed by Ledochowski for more accurately obtaining two sets of pressure and flow relations. With this method, the pump is switched on until the desired pressure in the pipe is achieved and then switched off, resulting in a backflow of water into the supply drum. The water that flows back into the supply drum is measured in conjunction to the resulting pressure drop, providing the first pressure-flow relation.

Thereafter, the pipe is pressured again. This time, the isolation valves must remain closed, so that no water can exit the pressured pipe, except through the leak. Time and pressure readings then form a time-pressure relation, from which a second pressure-flow relation can be calculated. With these two relations, the relationship between pressure and leakage rate can be plotted, from which the approximate leak elevation can be obtained by solving the two orifice equations simultaneously.

This system proved advantageous in identifying the elevation of large leaks and thereby assisting in locating those leaks on systems with considerable slopes. This method is, however, only suitable for estimating the leak location if only one leak exists on the pipe section under test.

2.6.4.5 The Inverse Transient Method

Transient flows can be described as the unsteady flows of fluids caused by changes in steady-state operating conditions. Any change in operating conditions is translated into pressure waves travelling at approximately sonic velocity from the point where the change is imposed. The transients can be in the form of a single identifiable alteration or an oscillating, periodic or pulsating disturbance (Van Vuuren, 2014).

Transient waves have excellent propagation properties due to their low frequency and higher energy, causing them to attenuate little over long distances (Karney, Khani, & Halfawy, 2009). These waves therefore travel over the entire length of the pipeline, while maintaining their characteristics.

All pipeline features alter the transient waves to some extent, resulting in the accumulation of a vast amount of data upon analysis of the wave. This data can then be used to reveal the approximate location and characteristics of pipeline features, such as leaks (Colombo, Lee, & Karney, 2009).

Leaks, for instance, generally cause a sudden pressure drop due to the absorption of energy by the leak, and can be identified by analysing the time of flight of the wave and the characteristic wave speed of the pipeline (Colombo et al., 2009).

The inverse transient method and frequency domain techniques obtain leak information from transients with the inverse method. That is, instead of using system characteristics to determine the system's state, the known system state is used to identify system characteristics, such as leaks (Colombo et al., 2009).

With the inverse transient method, hydraulic transients with known intensity are intentionally imposed into the pipeline at various locations and the dynamic transient data is then recorded at predetermined points along the pipeline. A set of expected data is then generated from a computational model which simulates the same transient events in the pipeline. The input parameters and model algorithms are varied until model results are obtained that agree best with the data recorded. The model data is then compared to the set of dynamic data (Karney et al., 2009).

With accurate model fitting, deviations between the two sets of data indicate pipe defects, such as leaks (Karney et al., 2009). The location of the possible leak can be directly determined by identifying the location where the deviation between the two data sets occurs.

This method, however, has a number of challenges. It can, for instance, become very complex and time consuming to mathematically model a long pipe section with all of its components, and the resulting models often depend on a number of assumptions for pipe parameters such as pipe wall friction (Karney et al., 2009). This method is therefore prone to model input and model structure errors by the operator (Colombo et al., 2009), such as the incorrect input of system characteristics and numerical mistakes.

A further challenge is system noise and distinguishing leak signals from signals caused by other system features (Colombo et al., 2009). Air cavities in the pipeline, for instance, cause discrepancies between the actual and modelled results (Turkowski & Bratek, 2007), often raising false alarms.

2.6.4.6 Frequency Domain Technique

The frequency domain analysis technique is an alternative to the Inverse Transient method, and is less dependent on the accuracy of the transient model. With this method steady, oscillatory flow is induced in the pipeline by operating a valve downstream of the pipe to a set pattern. The frequency response of the system is measured and analysed at the downstream valve for a range of frequencies. The response is then compared to a modelled frequency response for the pipe without leaks, which is numerically calculated from the known pipe characteristics (Mpesha, Gassman, & Chaudhry, 2001) (Colombo et al., 2009). An example of the typical response behaviour for a leaking pipe is shown in Figure 2-13.

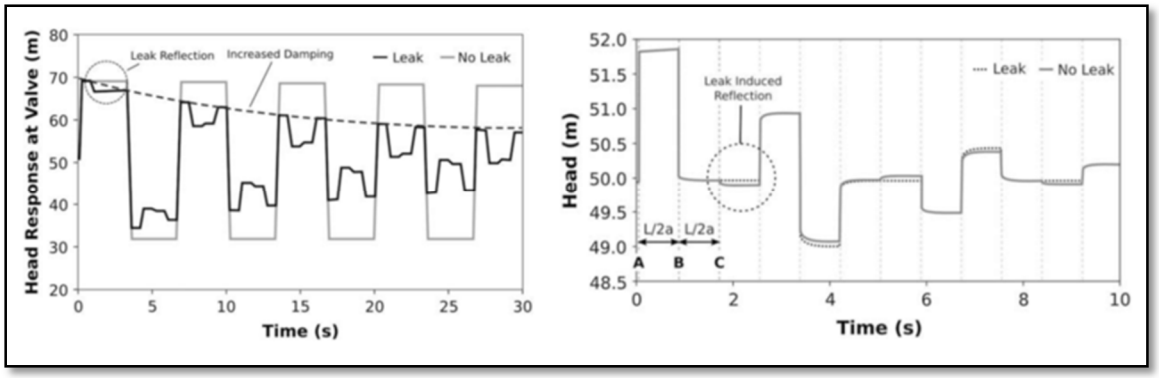

Figure 2-13: Two examples showing the comparison of transient pressure waves for the intact system and leaking system after the downstream valve is closed.

Obtaining the expected frequency response at the closing valve is much simpler and requires much less computational input in comparison to the Inverse Transient Method. The leaks and leak magnitudes are then identified from the amplitudes of the measured frequency response (Mpesha et al., 2001).

An advantage of the transient analysis approach is that the method only causes a disruption in the operation of the pipe for a short period. Further, all actions and measurements are taken at one location on the pipeline (Mpesha et al., 2001). A drawback of this method is, however, that transient states must be created through the opening and closing of valves, abnormal to the normal operation of the plant. This leads to an increased risk of failure of the pipeline and may require the operating

conditions to be constrained (Karney et al., 2009). Furthermore, this technique requires highly qualified operators, due to the complexity of the interpretation of the results (Ostapkowicz, 2016).

The state of development of this technology is accurately summarised by the following statement made by Colombo et al (2009) in the conclusion to a literature study on transient based leak detection methods: "While all have bestowed upon the technique some measures of approval, carefully contrived hypothetical examples and heavily controlled laboratory trials with the most rudimentary systems do not yet achieve the level of validation required for a strategy that must work in complex systems under a wide range of conditions."

A number of field tests have been carried out and are reported in literature. Although these tests prove that the above methods can be successful in identifying and pinpointing leakage, this method remains too complicated and error prone for successful commercial implementation. Significant work is still needed to develop this method into a practical leak detection method (Colombo et al., 2009)(Karney et al., 2009).

2.6.4.7 Negative Pressure Wave and Gradient Methods

These are condition monitoring techniques that can detect abrupt new leaks, such as pipe bursts, from the transient waves transmitted by these events. In steady state conditions, when a burst occurs in a pipe, it will generate negative pressure waves into both the upstream and downstream direction of the pipeline. With the negative pressure wave method, the waves can be detected with sensitive sensors at either end or, preferably, at multiple locations on the pipeline. The leak location can then be calculated using the measured time of flight of the upstream and downstream wave in conjunction with the pipe wave speed.

The gradient method requires multiple sensors on the pipeline which detect the degree of attenuation of the pressure waves created by the leak. The degree of wave attenuation over distance can be graphed as straight lines that intersect at the leak location (Ostapkowicz, 2016).

These methods can, however, only be used to detect and locate large bursts and cannot be used to detect existing or slowly increasing leaks (Ostapkowicz, 2016).

2.6.5 Summary of Existing Techniques and Shortcomings

The most optimal leak detection or condition assessment technique may vary from case to case, because the limitations and benefits of the various techniques may carry different weightings, which depend on the characteristics of a number of factors, such as the location of the pipe.

As discussed in paragraph 2.5.1, limitations that are result in poor water management in many developing countries, such as South Africa, include insufficient financial allocation, a critical shortage of skilled labour and a lack of incentives. In addition, many of these countries are further characterised by a large dependence on existing water supply networks, little abundance in supply, as well as water scarcity in general.

When taking these characteristics into account, the large number of leak detection and pipe condition monitoring techniques that exist, as presented in this section of the study, all come with one or more of the following important limitations:

- The testing equipment is highly specialised and expensive, resulting in high operating costs for the duration of the test.
- The assessment method is dependent on highly skilled labour which is scarce and expensive.
- The method is labour intensive and time consuming, making assessments of long lengths of pipe expensive.
- The method requires the pipeline to be taken out of operation and/or emptied, which results in water loss and supply interruptions.

It is therefore clear that further research and development on improved leak detection and condition assessment techniques is warranted, as all the techniques discussed have one or more important limitations.

2.7 Observations on Leak Formation

2.7.1 Pipe Failure Modes

Van Zyl and Clayton (2007) briefly discuss the phenomenon that different materials fail in certain characteristic ways. Asbestos cement pipes commonly fail through longitudinal cracks, while leaks in steel and cast-iron pipes commonly result from corrosion holes. Circumferential cracks are also more common in small diameter cast iron pipes due to bending.

Greyvenstein and Van Zyl (2007) performed tests on pipe failure samples from the field. Assuming that the samples reflect typical failures, they confirm the statements made by Clayton and van Zyl above. For instance, all three asbestos cement samples failed from longitudinal cracks, which ended in bell shaped cracks, as shown in the left picture of Figure 2-14.

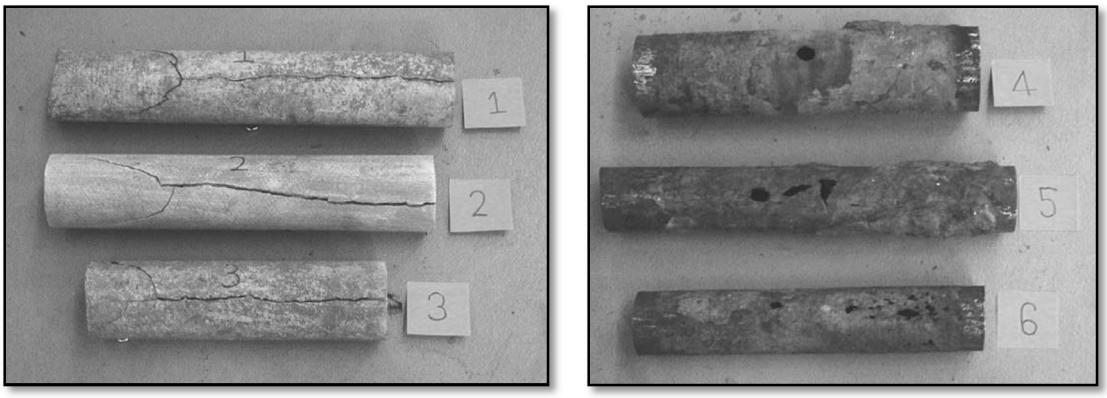

Figure 2-14: Asbestos Cement and Steel pipe failures from the field (Greyvenstein & Van Zyl, 2007)

In the same study, three steel pipe sections were taken from the field. All showed clear wall thinning resulting from corrosion, with two samples showing failures resulting from corrosion holes. The corrosion holes varied in shape and size, as shown in the right picture in Figure 2-14.

Although only briefly discussed in this paragraph, an understanding of this behaviour can contribute to an improved understanding of the type of leakage that can be expected in an existing pipe system.

2.7.2 Factors Affecting Leak Frequency

Understanding the factors that affect the leak frequency is important when developing and performing leakage assessments, as an accurate expectation of the frequency will assist in the interpretation of assessment technique results.

With a number of pipeline inspections being continuously conducted across the world, a large amount of data should already exist from which clear trends should be extractable. Laven & Lambert (K Laven & Lambert, 2012; Kevin Laven, 2012) identified this as an opportunity to source leak data of unreported leaks from two international acoustic leakage detection service providers. The data analysed consists of acoustic leak detection surveys performed with the Sahara system (see paragraph 2.6.2.2), comprising over 3000km international transmission lines spread across 25 countries.

Similarly, Rezaei et al. (Rezaei, Ryan, & Stoianov, 2015) also investigated the factors affecting leak frequency by analysing historic burst records from a UK water utility, amounting to almost 78 000 failure records over a ten year period between 2003 and 2013. The mean size diameters of the pipes investigated by Rezaei et al. are, however, smaller than the ones investigated by Laven and Lambert.

The results of these two studies are not directly comparable, because the study by Rezaei et al. is based on the occurrence of reported leaks over a specified period of time, while the study by Laven & Lambert is based on unreported leaks that could have accumulated over an indefinite period of time.

Laven and Lambert (2012) start off by investigating the impact of geographic location on the leak frequency. It is clear from Table 2-1, that Europe has the highest leak concentration. Laven and Lambert suggest that this phenomenon can be partially attributed to the old age of the pipes in Europe and partially to the pipes in Europe consisting largely out of cast iron, which is seen later in Table 2-2 to significantly contribute to burst frequency.

Table 2-1: Burst frequency for different geographic regions (K Laven & Lambert, 2012)

Region	Distance (km)	Leaks	Unreported Leaks/100 km
Worldwide	3221	2966	92
North America	711	496	70
Latin America	186	40	22
Europe	1583	2023	128
Africa	383	244	64
Asia & South Pacific	298	150	50
Middle East	60	13	22

In Table 2-2 the leak frequencies according to pipe material by Laven and Lambert and by Rezaei et al. are shown. In Laven and Lambert's study, welded steel pipes are seen to contribute the least to burst frequency and cast iron the most. Rezaei et al. also show that Cast Iron pipes contributed to the most leaks, but their study did not include welded steel or concrete pipes.

Table 2-2: Burst frequency for different pipe materials (K Laven & Lambert, 2012)

	Laven & Lambert: Unreported Burst Frequency over unknown time period.			**Rezaei et al: Reported Burst Frequency over 10 years.**
Material	**Distance(km)**	**Leaks**	**Leaks/100 km**	**Leaks/km**
Cast Iron	1127	1871	166	326
Ductile Iron	199	142	71	75
Steel	296	87	29	-
Concrete	961	417	43	-
Asbestos Cement	-	-	-	187
Polyvinyl Chloride	-	-	-	143
Polyethylene	-	-	-	99

In Laven and Lambert's study, the pipe diameter has an interesting effect on the burst frequency, with the frequency increasing with decreasing pipe diameter, except for pipes below 600 mm, for which the burst frequency was observed to be lower than pipes within the 600 to 900 mm range. The small sample size of pipes with smaller than 600 mm pipe diameters may, however, have contributed to this observation.

The study by Rezaei et al. showed a linear relationship for the pipe diameter effect, with leak frequency decreasing with diameter size. They suggest that the increase in wall thickness with pipe diameter results in the improved resistance of failure of larger pipes.

Table 2-3: Burst frequency for different pipe diameters (K Laven & Lambert, 2012)

	Laven & Lambert: Unreported Burst Frequency over unknown time period.			Rezaei et al: Reported Burst Frequency over 10 years.
Diameter (mm)	**Distance (km)**	**Leaks**	**Leaks/100 km**	**Leaks/100 km (approximate)**
<100				**205**
100-150				**192**
150-250				**142**
250-400				**58**
400-600				**40**
>600				**25**
<600	**47**	**31**	**66**	
600-900	**302**	**267**	**88**	
1050-1500	**399**	**141**	**35**	
>1500	**368**	**52**	**14**	

In Laven and Lambert's study, age showed a strong and consistent correlation to the unreported burst rate in the form of a linear relationship. This strong correlation suggests that leaks are forming and accumulating consistently at approximately 1.6 bursts per 100km per year. It is, however, noted that the available data mostly represents pipes older than 40 years, with the highest leakage detected on pipes of approximately 120 years of age. The possibility therefore exists that the slope is exaggerated by the primitive pipe types used in the late 19th century, and that the representation is not as accurate for determining the leak frequency of newer and more advanced piping systems. The study by Rezaei et al. confirmed a strong correlation between burst rate and age.

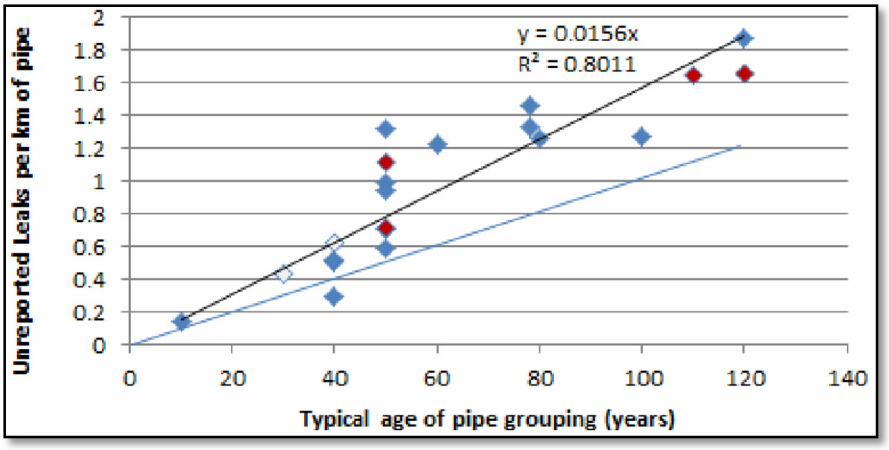

Figure 2-15: Unreported burst prevalence by age (Kevin Laven, 2012)

It must be noted that the above correlations were determined with the assumption that the pressure heads remain constant and regular. Rezaei et al. explore the impact of pressure fluctuation on pipeline failure rates. Their study involved the estimation of the pressure variations of various DMAs, and comparing the pressure variations with the historic data on reported burst frequencies for the respective DMAs. A positive correlation between rate of failure and the exposure of pipes to high pressure variations was observed, as shown below in Figure 2-16.

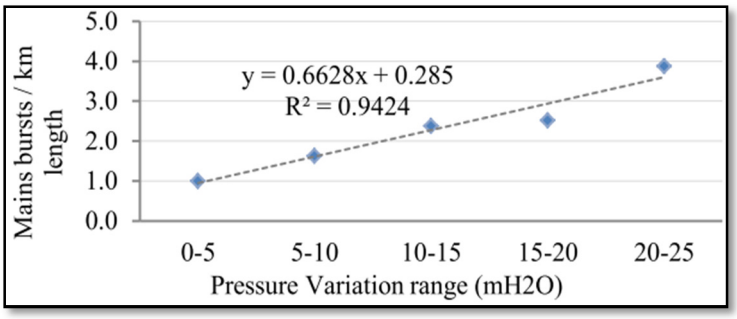

Figure 2-16: Burst frequency versus pressure variation range (Rezaei et al., 2015)

They argue that small pipeline defects, installation damage, or corrosion impacted areas, can propagate into cracks as a result of cyclic loading caused by pressure fluctuations.

The magnitudes of static pressure heads also have a strong influence on leak frequency, as pointed out in an overview of literature by Lambert (Allan Lambert, 2000). He briefly refers to three case studies that indicate a strong leak frequency versus pressure head relationship:

- In Australia, a 40% reduction in pressure of a distribution network led to a 55% decrease in leak frequency.
- Similarly, in Auckland, New Zealand, a pressure reduction of 71 to 54 meters led to leak frequencies last seen 8 years previously.
- Pressure management in Brazil led to a reduction in reported leak frequencies from 155 leaks to 95 per month.

Pressure, therefore, appears to show the strongest relation to leak frequency and will be investigated further in the following sections.

2.8 Pressure-Flow Relationships for Leakage Characterisation

2.8.1 Pressure Dependence of Leak Flow

There is a clear relation between leakage and pressure, which is often ignored or not known by many utilities. For instance, in an international overview of literature on pressure-leakage relationships, Lambert (2000) states that only utilities in Japan have quoted their leakage statistics with reference to pressure before the year 2000.

According to Lambert's broad literature overview, it becomes apparent that leakage in distribution systems is considerably more sensitive to pressure than had often been predicted. He mentions that in Japan, where it can be argued that leakage is best understood, the leakage rate is estimated, as a rule of thumb, to increase by 1.15% for every 1% increase in average pressure. This is a considerably stronger relationship than most utilities would have expected at the time.

The high impact of pressure is validated in a number of case studies. As an example, a study by Charalambous (2005) on 15 DMAs in Lemesos, Cyprus, where pressure reduction was implemented to reduce leakage, clearly confirms the strong relationship between pressure and leakage. In this study, gravity fed DMAs were identified with robust boundaries, minimal ground level variation and single entries. All DMAs consisted of a combination of uPVC, MDPE and asbestos pipes. By installing a pressure reducing valve at each DMA entry, the pressures were controlled in order to maintain the minimum pressure required for maintaining the standard of service to customers. In this case, it led to an overall pressure reduction of 32%.

With continuous flow monitoring, minimum night flows were measured. By comparing the losses of one month before, to the losses of one month after the pressure reduction, a reduction of approximately 38% in background and locatable losses was experienced. Also, by comparing the number of leaks reported in the 7 months preceding the pressure reduction to the 7 months following the reduction, a reduction of 40-45% in reported leaks was experienced.

This case is but one example of many similar case studies (Allan Lambert, 2000). With pressure being the main contributor to leakage rate, understanding the relationship between pressure and leakage is vital for the characterisation of leaks, validating further exploration of this field.

2.8.2 Torricelli's Equation and the Orifice Equation

The Torricelli's equation is a well-known equation used to characterise flow through an orifice caused by a pressure difference. The equation relates the velocity of the flow out of an orifice to the pressure head before the orifice:

$$V_o = \sqrt{2g(Z_i - Z_o)} \qquad \textbf{2-5}$$

The illustration in Figure 2-17 will be used as the basis for the derivation of Torricelli's equation, and illustrates gravity-fed flow through an outlet pipe at the bottom of a tank. The energy equation or the Bernoulli's equation can be applied to two points, one on either side of the orifice, depicted by the small outlet pipe of the tank.

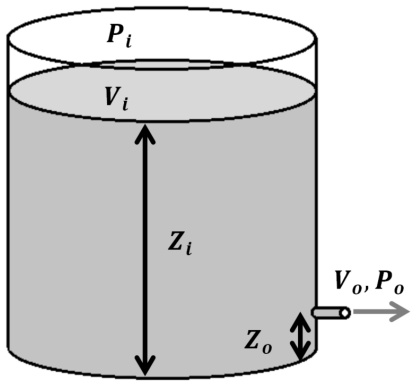

Figure 2-17: Tank with outlet for Illustration of Torricelli's Equation

Equation 2-6 and 2-7 show the energy equation, with P_i and P_o equal to the pressure at the surface and outlet of the tank, V_i and V_o equal to the velocities of the dropping tank level and the outlet flow, and ρ equal to the density of the fluid.

$$\boldsymbol{P_o + \rho g Z_o + \frac{1}{2}V_o^2 = P_i + \rho g Z_i + \frac{1}{2}V_i^2} \qquad \textbf{2-6}$$

Or

$$\boldsymbol{\frac{P_i - P_o}{\rho g} + \frac{V_i^2 - V_o^2}{2g} + Z_i - Z_o = 0} \qquad \textbf{2-7}$$

By realising that the surface area of the tank is much larger in comparison to the surface of the tank outlet, and by noting that, due to the conservation of mass, the flow rate of the dropping tank can be

equated to that of the outlet, the velocity of the dropping tank level, V_i, can be assumed to be zero. The pressures are all gauge pressures and cancel each other out due to the negligible difference in elevation. Finally, if the head loss is assumed to be negligible, the equation can be rearranged to equation 2-5, Torricelli's equation.

Similarly, Bennis et al (2011) show that the Torricelli's equation can be derived from the energy equation (equation 5) to characterise a leaking pipe. Through conservation of mass it can be shown that the velocity of flow across a pipe's longitudinal section will be negligible in comparison to the velocity of the flow across the leak section, justifying the kinetic energy component $V_i^2/2g$ to be set to zero.

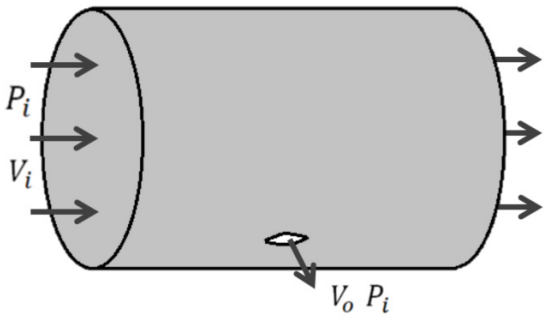

Figure 2-18: Pipe section with leak for illustration of Torricelli's Equation

Also, by assuming that the pipe wall is very thin, the term $Z_o - Z_i$ can be assumed to equal 0. The pressure on the outside of the pipe, P_o can also be assumed negligible if it is assumed that no resistance to the flow exists outside of the pipe if, for instance, the soil is well drained. The energy equation therefore simplifies to Equation 2-8, which simplifies to the Torricelli's equation, with H equal to the pressure head in the pipe:

$$\boldsymbol{V = \sqrt{\frac{2P_i}{\rho}} = \sqrt{2gH}} \qquad \textbf{2-8}$$

The above assumptions, however, oversimplify real world conditions, and are only useful to simplify the equation to the above form. To counter the effect of the simplifications imposed by the above assumptions, a coefficient is introduced. A flow rate equation thus results as follows, and is called the orifice equation (Deyi, Van Zyl, & Shepherd, 2014):

$$\boldsymbol{Q = AV = C_d A\sqrt{\frac{2P_i}{\rho}} = C_d A\sqrt{2gH}} \qquad \textbf{2-9}$$

C_d represents a coefficient, while A represents the area of the leak. From Equation 2-9 it can be noted here, that the orifice relation has the form of a power equation, as represented by Equation 2-10 below:

$$\boldsymbol{Q = ah^b}$$

2-10

Where $a = C_d A\sqrt{2g}$ and $b = 0.5$ (M. Ferrante, Brunone, Meniconi, Capponi, & Massari, 2014). It must, however, be stressed here, that in order for the equation to remain true to the underlying theory of the orifice equation, the exponent must equal 0.5, otherwise the equation becomes an empirical estimation if the leak flow.

Idelchik has proposed calculations for the coefficient of the orifice equation in his Handbook of Hydraulic Resistance (Idelchik, 1966), by incorporating a kinetic energy coefficient of the vena contracta, N_c, and an orifice resistance coefficient ζ:

$$C_d = \frac{1}{\sqrt{N_c+\zeta}} \quad with \quad N_c = \frac{1}{A_c}\int \left(\frac{V_o}{V_c}\right)^3 dA$$

2-11

A_c and V_c are the vena contracta area and velocity respectively. This relation is an attempt to define the orifice velocity in respect to the contraction of the jet that passes through the orifice. The contraction is dependent on the orifice shape, and therefore this relation effectively relates the orifice velocity to the orifice shape:

$$V = C_d \frac{\sqrt{2gH}}{\sqrt{1-N_i\left(\frac{A_{out}}{A_i}\varepsilon C_d\right)^2}} \quad with \quad N_i = \frac{1}{A_i}\int \left(\frac{V_o}{V_i}\right)^3 dA$$

2-12

In equation 2-12, A_{out} and A_i represent the areas of the orifice and the pipe/vessel respectively, and N_i represents the kinetic energy coefficient of the pipe/vessel. ε is the coefficient of jet contraction, that depends on the orifice characteristics, such as the inlet edge. It is calculated by dividing the area of the contracted section of the jet by the orifice area.

The relationship proposed by Idelchik is still limited and is only able to characterise thin, inflexible materials – characteristics which are not commonly associated with leaks in the field.

The Orifice and Toricelli's equations remain difficult to implement for characterising leakage in pipes in the field, as all factors are not taken into consideration by the equation.

Already in 1956, Ledochowski (1956) showed that the standard orifice equation with an exponent value of 0.5 seldom accurately reflects observed leak characteristics. In field tests on newly installed pipes, exponent values of 1.5 were, for instance, observed for leaks that occur through flexible and flanged joints, due to the rubber material allowing for expansion of the leak with increased pressure.

Ferrante et al. (2014) suggest in a brief review of literature on pressure versus leak flow relationships, that, for the concept of the orifice equation to be effectively used on real pressurised pipe systems, the equation must be extended to include

- the change in leak area with change in pressure and discharge in the pipe,
- the ground conditions around the pipe,
- and the effect of the stream flow in the pipe.

Van Zyl (2014), in a review of literature on the theoretical modelling of pressure and leakage in distribution systems, adds the following additional influential factors:

- The leak hydraulics, which distinguish between laminar, transitional and turbulent flow.
- The pipe material behaviour, which influences the change in area and shape of the leak in relation to the changes in pressure inside the pipe.

The above shortcomings of the orifice equation are confirmed by a number of experimental and field investigations (Clayton & van Zyl, 2007; Schwaller, van Zyl, & Kabaasha, 2015), (May 1994, in (Van Zyl, 2014)).

The N1 and FAVAD equations are common adaptions of the orifice equation, with the N1 equation empirically deviating from the 0.5 exponent value of the orifice equation, while maintaining the basic form of the power equation (Equation 2-10); while the FAVAD equation improves the orifice equation fundamentally by incorporating the effect of the variable area of the leak. These approaches are discussed in more detail in paragraphs 2.8.3 and 2.8.4.

2.8.3 The FAVAD Equation

2.8.3.1 The FAVAD Equation for Leaks with Elastic Material Behaviour

The Fixed and Variable Area Discharge (FAVAD) concept was introduced by May in 1994 to explain the variation of leakage rate with pressure as witnessed in field tests on various pipes in the United Kingdom. The concept is based on the orifice equation and incorporates the effects of the variation in area of the leak by assuming a linear relationship for the variation in area with pressure (May 1994, in (Van Zyl, 2014)).

This linear relationship was later confirmed by Cassa et al (2010) by means of a finite element study on the behaviour of holes and cracks in various common pipe materials under elastic loading conditions. It was shown that the variation in area with pressure can be represented by Equation 2-13 for all pipe materials, leak shapes and sizes, provided that the variation occurs in the elastic range:

$$A = A_0 + mH \tag{2-13}$$

In this equation A_0 refers to the initial area if no pressure is applied, m represents the head-area slope and H the discharge pressure head. This relationship was again confirmed for pipe materials with linear-elastic properties in another finite element study by Ssozi et al (2015) and an experimental study conducted by Ferrante (2011).

The experimental study by Ferrante was performed by cyclically pressurizing a steel pipe section containing a leak and by increasing the maximum pressure head with every cycle. All the leakage flow versus pressure head points were observed to follow a distinct curve, until a certain maximum pressure was reached, after which the points appear to follow another curve.

The points were converted to resemble leak area versus pressure head by calculating the area from the observed flow using Torricelli's law. A linear relationship resulted for the portion of the curve below a certain maximum pressure, confirming the relationship represented by Equation 2-13 for elastic material behaviour. For higher pressures, the relationship changes due to plastic behaviour.

Ferrante confirmed this behaviour with stress gauges close to the leak, which indicated linear cyclical behaviour up to characteristic maximum pressure, after which non-linear and non-cyclical leak behaviour was observed.

With the linear area-pressure relationship confirmed, the fixed area assumed in the orifice (Equation 2-9) can be replaced with the variable area relationship, resulting in the FAVAD equation for linear-elastic leak behaviour:

$$Q = C_d\sqrt{2g}(A_0 H^{0.5} + mH^{1.5}) \tag{2-14}$$

This version of the FAVAD equation differs slightly from the original equation proposed by May, in that it proposes that all leak areas vary linearly with pressure, while May suggested that some leaks are fixed and other are variable.

The FAVAD equation thus defines the leakage through the initial area plus the leakage through the additional area created by the expansion of the leak area under pressure. These two components are clearly represented in the FAVAD equation, with the first term identical to the orifice equation, and the second term accounting for the variation in flow under pressure according to the head-area slope.

Studies have been conducted to determine the head area slope value. Cassa & van Zyl (2014) quote relations that were derived for the head-area slopes of different leak types in another study by Cassa & van Zyl, using finite element modelling:

$$m_{long} = \frac{2.93157 \cdot d^{0.3379} \cdot L_c^{4.80} \cdot 10^{0.5997(\log L_c)^2} \cdot \rho \cdot g}{E \cdot s^{1.746}}$$

$$m_{spiral} = \frac{3.7714 \cdot d^{0.178569} \cdot L_c^{6.051} \sigma_l^{0.0928} \cdot 10^{1.05(\log L_c)^2} \cdot \rho \cdot g}{E \cdot s^{1.6795}}$$

$$m_{circular} = \frac{1.64802 \times 10^{-5} \cdot L_c^{4.87992662} \cdot \sigma_l^{1.09182555} \cdot 10^{0.8276316(\log L_c)^2} \cdot \rho \cdot g}{E \cdot s^{0.33824224} \cdot d^{0.186376316}}$$

2-15

In Equation 2-15, L_c equals the length of the crack in metres, σ_l represents the longitudinal stress in N/m^2, d the internal pipe diameter and s the pipe wall thickness in metres. The material effects are also incorporated by the inclusion of the modulus of elasticity E in these equations.

De Miranda et al (2014) also derived a 'physically-based analytical' formula to predict leakage in linear-elastic pipes with longitudinal cracks. This formula also takes into account pipe material and pipe geometry properties. De Miranda et al considered the longitudinal strip of material alongside the crack of the pipe to be similar to a classical beam with elastic restraints, and derived the following formula for the head-area slope of the FAVAD equation:

$$m = \frac{6\rho g L_c \left(\frac{d}{2}\right)^4 \pi (1-v^2)}{E s^3 a} \; where \; a = \left(\left(\frac{s_0}{s}\right)^2 \left(\frac{C_1 L}{d/2}\right)^{-C_2} + 1\right)$$

2-16

In Equation 2-16, v represents the Poisson's ratio of the material and a represents a correction coefficient, with s equal to the pipe thickness and s_0 referring to a reference thickness. C_1 and C_2 are coefficients that must be calibrated.

This equation was validated by De Miranda et al through comparison with published experimental results of leakage exponents. Good correlations with the predictions of Cassa and van Zyl (2013) (cited in (de Miranda et al., 2014)), as well as of a number of other experimental results were achieved for various leak types and pipe materials.

2.8.3.2 FAVAD Equation for Leaks with Visco-Elastic Material Behaviour

For elasto-plastic and viscoelastic pipe materials the pressure versus leakage area behaviour is not linear, as confirmed by Ferrante (2011) in the experimental study already discussed in paragraph 2.8.3.1.

In Ferrante's study, a pressure head was cyclically applied and relaxed upstream of a leak in a test piece over a period of time, with the maximum head increasing in for each new cycle. It was observed that the leak flow followed the same cyclical trend until a certain maximum head was reached, after which the minimum flow started to increase in each new cycle. This proves that the relationship between pressure and flow deviates from its linear nature as the pressure exceeds a certain value, indicating the onset of non-cyclical plastic deformation resulting in an ever increasing leak area.

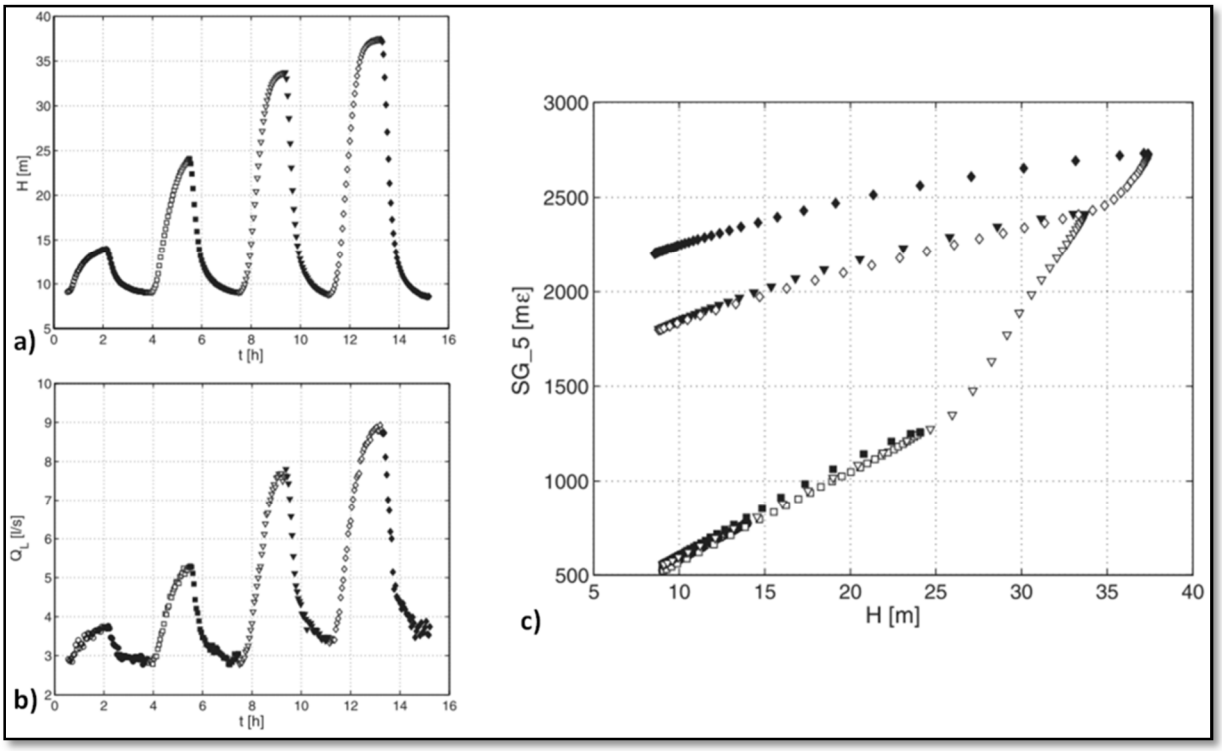

Figure 2-19: a) Cyclical application of head upstream of leak, b) cyclical flow response, c) cyclical stress strain behaviour (Marco Ferrante, 2011)**.**

By measuring the radial strains in the vicinity of the leak with strain gauges, it was clearly observed how the linear strain-pressure relationship holds up to a certain point, after which the strain accelerates. Ferrante therefore proposes that the leak head versus discharge relationship must be modelled with its behaviour over time taken into account.

In another experiment by Ferrante (2011) on longitudinal leaks in polyethylene pipes, the pressure on a test section was varied with a control valve and the hysteresis curves were recorded in both the head

versus discharge plane and the head versus strain plane. Clear hysteresis curves where observed with the paths for increasing and relieving pressure running parallel to each other.

Although the viscoelastic behaviour deviates from the linear leak area versus pressure head relationship, Ferrante (Marco Ferrante, 2011), (Marco Ferrante et al., 2011) observed a clear correlation between the leak area and pressure head and the stresses versus strains relationship, even when plastic deformations occur.

In a finite element analysis study by Ssozi et al (2015), the viscoelastic behaviour of high density polyethylene (HDPE) and polyvinylchloride (PVC) pipes was investigated. Round holes, longitudinal and circumferential cracks were investigated in both materials. The pipes were simulated to experience various pressure loadings over a period of 100 000 seconds and the change in leak area was determined at regular time intervals for each pressure loading.

According to Ssozi et al, viscoelastic behaviour results in the occurrence of creep, stress relaxation and hysteresis. Creep can be defined as time-dependant strain resulting from a constant stress applied to a material, and stress relaxation can be defined as the decrease in stress in the material when a constant strain is applied.

A clear proportional relationship between the total deformed leak area, which includes the time-dependant visco-elastic deformation, and the elastically deformed leak area was observed.

The relationship between leak area and pressure was found to be close to linear for any given time. Linear viscoelastic behaviour was therefore assumed, and it was observed that the total increase in leak area under viscoelastic conditions was always proportional to the elastic deformation. Equation 2-17 was proposed for the total variable leak area of leaks in visco-elastic pipe materials:

$$A(t) = A_0 + \Delta A_e + \Delta A_v(t)$$

2-17

The time-dependant visco-elastic leak area variation (A_v) is defined as follows:

$$A_v(t) = (1 - e^{-\frac{t}{\tau_\sigma}}) \frac{a\Delta P}{E_R}$$

2-18

By considering the variables of the FAVAD equation, Ssozi et al. propose that the total slope m_{vu} for linear viscoelastic materials can be estimated by m_{vu}:

$$m_{vu} = k_{vu} m_e = \frac{k_{vu} A_2 - k_{vu} A_1}{H_2 - H_1}$$

2-19

Where m_{vu} and m_e are the ultimate viscoelastic and time-dependant elastic area-head slopes, respectively, and k_{vu} is the ultimate ratio of total area deformation to elastic area deformation:

$$k_v = \frac{\Delta A(t)}{\Delta A_e} \text{ and } k_{vu} = \frac{\Delta A(100000s)}{\Delta A_e}$$

2-20

ΔA_e represents the elastic change in area, which can be predicted with a linear relationship, and ΔA_v represents the viscoelastic change in area, which is time dependant. $A(t)$ can be calculated by adding the initial, elastic and viscoelastic areas:

$$\boldsymbol{A(t) = A_0 + \Delta A_e + \Delta A_v}$$

2-21

Ssozi et al. further suggest that the creep witnessed in viscoelastic behaviour will stabilise only approximately 12 hours after the stress is applied. This means that leaks in real distribution systems, where pressures vary continuously, will be in a constant state of creep. Ssozi et al therefore suggest that, when leakage rates are measured, at least 12 hours are allowed for the system to stabilise first.

2.8.4 The N1 Equation

2.8.4.1 Concept and Basic Form

Unlike the orifice, Torricelli's and the FAVAD equation, which are all fundamental equations, the N1 equation is an empirical relation that has the same form than the orifice equation, but uses empirically adapted exponent values that deviate from the fundamental exponent value of 0.5, to more accurately simulate the observations made in the field:

$$\boldsymbol{Q = C_{N1} H^{N1}}$$

2-22

Note that the N1 Equation is the same as the power equation (Equation 2-10). Should C_{N1} be set to $C_d A\sqrt{2g}$, and with an $N1$ exponent value of 0.5, this equation would be equivalent to the orifice equation (Equation 2-9).

The N1 exponent and the leakage coefficient can be estimated by measuring the average pressure zone head and the leakage of a system before and after pressure management. The N1 exponent can then be calculated by dividing the N1 equation before pressure management by the N1 equation after pressure management, resulting in the elimination of the unknown leakage coefficient $\boldsymbol{C_{N1}}$.

$$\frac{Q_1}{Q_2} = \left(\frac{H_1}{H_2}\right)^{N1} or\ Q_1 = Q_2\left(\frac{P_1}{P_2}\right)$$

2-23

With the N1 exponent known, the leakage coefficient C_{N1} can easily be calculated.

Through experimental methods and field tests fairly accurate leakage characterisations have been obtained by fitting observed flow-pressure curves with curves obtained from the N1 equation with varying N1 exponent values.

The N1 exponent values are found to vary considerably in practice, with ranges between 0.36 and 2.79 obtained in field and experimental studies on leaks and water distribution systems in various countries.

In an experimental investigation by Greyvenstein & van Zyl (2007), for instance, N1 values of between 0.4 and 2.3 were observed for individual leaks. In this study, a number of failed pipes of various materials which exhibited a range of different leak types were tested in a controlled environment.

Walski et al (2009) summarises and tabulates the N1 values obtained from various field and experimental studies in a literature review.

Table 2-4 and Table 2-5 partially originate from this study, but have been extended considerably to include the results of even more studies encountered during this literature study.

Table 2-4 contains N1 exponent values from controlled tests on individual and clustered leaks, while Table 2-5 contains N1 exponents for systems with multiple leaks. The application of the N1 equation to multiple leaks is discussed in more detail under Paragraph 2.8.6.1.

Table 2-4: N1 exponents for controlled leaks reported in literature (extended from (Thomas Walski et al., 2009))

Author	N1 Values	Conditions
Ogura (1979) (in (Schwaller & Van Zyl, 2014))*	1.39-1.72	Slits
(Hiki, 1981)	0.5	Drilled holes
May (1994) (in (Thomas Walski et al., 2009))*	0.5 1.5 2.5	Fixed area Size = f(pressure) Longitudinal
Thornton & Lambert (Thornton & Lambert, 2005)	0.5 0.5-1.0 >1.0 0.5- 2.0 0.8-1.0	Circular holes, Re > 4000 Small circular leaks in general Corrosion clusters Longitudinal cracks: Length to Width ratio L/W = low L/W = high (for PVC pipes) AC pipes
Walski et al. (T. Walski, Bezts, Posluzny, Weir, & Whitman, 2006)	0.66-0.76	Drilled holes
Walski et al. (Thomas Walski et al., 2009)	0.47-0.74** Mean = 0.58 Median = 0.54	Slits and holes of various lengths and sizes for a number of pipe diameters in PVC pipe.
Greyvenstein and Van Zyl (Greyvenstein & Van Zyl, 2007)	0.52 1.38-1.85 0.79-1.04 0.41-0.53 0.67-2.3	Round Hole Longitudinal PVC Longitudinal AC Circumferential Corrosion steel
Noack and Ullanicki (2007) (in (Thomas Walski et al., 2009))*	0.5-1.2	f(soil permeability)
Ashcroft & Taylor (in (Allan Lambert, 2000))*	1.39-1.72 1.23-1.97 1.52	10 mm slit in plastic pipe 20 mm slit in plastic pipe Avg under varying pressure
*These works are not referenced in this study, and can be found in references indicated **These are exponent values resulting from a slightly adapted N1 equation that eliminates effect of system demand changes.		

Table 2-5: N1 exponents for systems observed in field studies and reported in literature (extended and adapted from (Thomas Walski et al., 2009)**)**

Author	N1 Values	Conditions
Lambert (Allan Lambert, 2000)	0.52-2.79 0.5 1.5	Literature UK metal pipes UK plastic pipes
Lambert (1997) (in (Schwaller et al., 2015))*	0.36-2.79	Literature
Thornton & Lambert (Thornton & Lambert, 2005)	0.5-1.6	Function of ILI, based on Literature
Farley and Throw (2003)(in (Cassa & Van Zyl, 2014))*	0.70-1.68 0.63-2.12 0.52-2.79	UK (1977) Japan (1979) Brazil (1999)
Ogura (1979) (cited in (Allan Lambert, 2000))*	1.15	Average in steel distribution systems in Japan.
Deyi, van Zyl & Shepherd (Deyi et al., 2014)	0.18-3.33	Mainly plastic distribution systems in South Africa.
Charalambous (Charalambous, 2005)	0.64-2.83 Avg = 1.47	Field study on 15 DMAs in Cyprus for mixed AC, PVC and MDPE pipes
*These works are not referenced in this study, and can be found in references indicated		

It is clear that the N1 values witnessed in experimental and field studies vary significantly, with a number of factors affecting the leakage rate versus pressure relationship.

The following disadvantages of the N1 equation, however, were noted by Schwaller & van Zyl (2015), and place the improved FAVAD equation as a more favourable alternative for future use:

- The N1 equation is empirical and not founded on fundamental fluid mechanics theory. The overall form of the equation is based on orifice theory, but the constants can only be determined experimentally.
- The values of the constant (C_{N1} and $N1$) are in fact not constant, but change with pressure.
- The units of C_{N1} include the variable N1, which complicates the equation and makes it difficult to interpret and distinguish between the factors affecting the N1 exponent and the constant C_{N1}.

In addition to the above factors, the C_{N1} constant and N1 exponent do not provide a lot of information on the characteristics of a leak. Ferrante (2011), also demonstrates, by experimenting with leaks in thick and thin steel and polyethylene pipes, that leaks cannot be accurately characterised by this equation, as the variation of the leak area with head is not accurately represented. Even though the N1 exponent does provide an indication of how sensitive the leak is in respect to pressure variation, it fails to accurately model a direct relationship between pressure and leakage area.

2.8.4.2 Alternative Forms and Adaptions of the N1 Equation

A number of attempts have been made to improve the n1 equation. Walski et al (2009) argue that it is important to know the component of flow that is pressure dependant and the component that varies with pressure. An equation with a similar form to the N1 equation was therefore developed that separated these two flows:

$$Q = K_p P^n + K_L P^n$$

2-24

As seen in the above equation, both terms have the same exponent n. Walski et al (2009) argue, based on their experimental studies, that with the equation in this form, the leak can be fairly accurately characterised by setting n to 0.5 and determining K_p and K_L, thus, effectively solving two orifice equations.

By using Equation 2-24, Walski et al. observed a much smaller variation in exponent values than often reported in literature. They observed exponent values ranging between 0.48 and 0.76 for longitudinal slits and between 0.47 and 0.54 for round holes in pipes with varying pipe diameters. Walski et al. argue that the higher N1 values commonly found in field studies are often due to measurements that do not take the pressure variation caused by system demand variation into account. It is therefore important to fully understand what component of system demand is pressure dependant.

Similarly, Bennis et al (2011) split the N1 exponent into three components, namely the component relating to a normal orifice equation, a component relating to the rigidity of the pipeline material, n_a ,and a component relating to the dimensions of the hole, n_q.

$$N1 = 0.5 + n_a + n_q$$

2-25

The variation of n_a and n_q were studied separately under various conditions. n_a was found to diminish as the diameter of the leak increased. It also diminished as the pressure reduction percentage increased, as shown by Figure 2-20, resulting in N1 values close to 0.5 for large holes measured over high pressure reduction ranges. An exponential equation for n_a was therefore proposed, which is a function of the pressure reduction range:

$$n_a = be^{-a\Delta P}$$

2-26

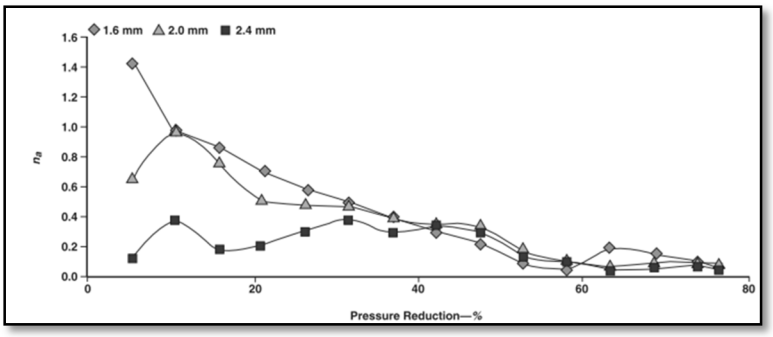

Figure 2-20: Relationship between n_a and the percentage pressure reduction for different sized leaks in PVC pipes (Bennis et al., 2011)**.**

All the above variations of the N1 equation aim at incorporating a pressure dependant component, such as the variable area component already incorporated into the FAVAD equation. Unlike the FAVAD equation, however, the adapted N1 equations remain empirical.

2.8.5 Factors affecting N1 and FAVAD parameters

The two preceding paragraphs 3.5.5.12.8.3 and 2.8.4 explain the N1 and FAVAD concepts, as well as the variation of their respective parameters observed in the field. With a basic understanding of the N1 and FAVAD concepts provided, the factors which contribute to this variation are briefly discussed in the following paragraphs.

2.8.5.1 Material Properties

Cassa and van Zyl (2010) numerically investigated the effect of pressure on cracks in water supply pipes for a range of different crack and material types using finite element methods.

By simulating the elastic behaviours of uPVC, steel, cast iron and asbestos-cement, Cassa and van Zyl, found that uPVC showed the greatest pressure-area slopes, followed by steel, cast iron and then asbestos cement. Cassa and van Zyl also confirm the linear relationship, as suggested by the FAVAD equation, between the leak area and pipe pressure for all pipe materials investigated, provided that the materials remain within their elastic range.

Similarly, in terms of N1 exponents, the same sequence was observed, with uPVC pipes showing the highest N1 values and asbestos-cement the lowest. It must, however, be noted that this study only simulates leaks numerically, and even though attempts were made to replicate real water supply systems, the results remain theoretical.

This material effect was, however, also observed in an experimental study by Bennis et al (2011). Bennis et al. obtained the N1 exponent values of drilled holes in pipe test pieces ranging in diameter from 20 mm to 35 mm. Through comparison of the N1 exponent values of PVC pipes to those of steel pipes under various pressure reduction ranges, they found that the leakage is always greatest in flexible pipes.

In a literature review, Thornton and Lambert (Thornton & Lambert, 2005) reaffirm this material effect by plotting N1 values in relation to the infrastructure leakage index (ILI) for various pipe material flexibilities, as shown in Figure 2-21, where variable 'p' is a measure of the rigidity of the material. A 'p' value of 100% refers to fully rigid pipes, while a value of 0% refers to fully flexible pipes. According to Thornton and Lambert, the relations of Figure 2-21 were developed by the 'Pressure Management Team', and are based on a broad range of international test data. It was used to predict a number of exponents obtained from field test and proved to replicate the test data with acceptable accuracy.

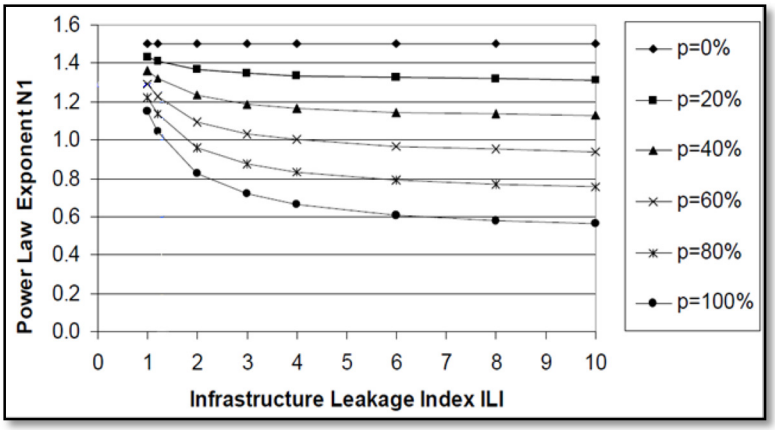

Figure 2-21: N1 relation to ILI number for pipe materials with varying rigidity (Thornton & Lambert, 2005)

The findings in the above studies indicate a clear and reversible pressure dependant relationship for all tested materials operating within their elastic ranges.

It must however be mentioned here, that with a recent summary of head-area sloped found in studies thus far, van Zyl and Malde (2017) conclude that the head-area slopes of all leak types in steel pipes are very small and may be assumed to be zero, except for leaks caused by corrosion failures.

2.8.5.2 Leak Type, Size and Shape

Greyvenstein & van Zyl (2007) performed experimental studies on failed pipes taken from the Johannesburg water distribution system in South Africa, as well as on pipes with artificially induced

leaks in a laboratory environment. By conducting pressure tests on these pipe sections, leakage numbers were obtained for various leak types, sizes and shapes.

The results of Greyvenstein & van Zyl support the findings by Hiki (1981), which indicate that leakage exponent values (or N1 values) for round holes remain close to 0.5, irrespective of hole diameter or pipe material, pointing to negligible change in area as pressure increases. In a summary of head-area slopes observed in recent studies, van Zyl and Malde (2017) also conclude that the head-area slopes or round holes may be assumed to be zero. Van Zyl and Malde then confirm this behaviour through an experimental study of round leaks in various pipe materials.

In the study by Greyvenstein and van Zyl, corrosion holes in steel pipes, however, were found to exhibit considerably higher exponent values (equivalent to N1 values) of between 0.67 and 2.3. The high exponents were observed in pipes with significant corrosion damage to the pipe wall and surrounding material. It is suggested that the weakened support and loss of supporting material around the hole contributes to higher stresses and strains around the hole, in turn leading to higher exponent values.

By testing longitudinal cracks in uPVC and Asbestos Cement pipes, Greyvenstein and van Zyl also show that longitudinal cracks can lead to considerably higher exponent values, with values up to 1.85 observed on uPVC test pieces. Circumferential cracks exhibited lower values between 0.41 and 0.53 in uPVC pipes. Narrow cracks were also shown to have higher leakage exponents than wider cracks of equal length. It is argued that this phenomenon occurs due to the circumferential stresses being higher than longitudinal stresses in pipes, resulting in the widening of longitudinal cracks as pressure increases.

Overall, Greyvenstein and van Zyl conclude that the leakage type is a larger contributor to the leakage exponent in comparison to the pipe material. This contradicts the common perception that plastic pipes will automatically result in higher leakage exponents than steel pipes, due to their lower modulus of elasticity only. The results of Greyvenstein & van Zyl are summarised in Table 2-6.

Table 2-6: Leakage exponents (or N1 values) for different materials and different leak types (Greyvenstein & Van Zyl, 2007)

Failure Type	uPVC	Asbestos Cement	Mild Steel
Round hole	**0.524**	**-**	**0.518**
Longitudinal crack	**1.38-1.85**	**0.79-1.04**	**-**
Circumferential crack	**0.41-0.53**	**-**	**-**
Corrosion cluster	**-**	**-**	**0.67-2.3**

The finite element study by Cassa and Van Zyl (2010), already referred to in paragraph 2.8.5.1, indicates increasing exponent numbers with increasing hole diameters. Cassa & Van Zyl show that for circular holes the crack area increases slightly while the shape changes to an ellipse under pressure, with this

effect emphasised as the elasticity of the material increases. If the FAVAD equation is considered, the pressure-area slope (m) was shown to increase exponentially with leak size. The results in terms of the N1 exponent are plotted in Figure 2-22.

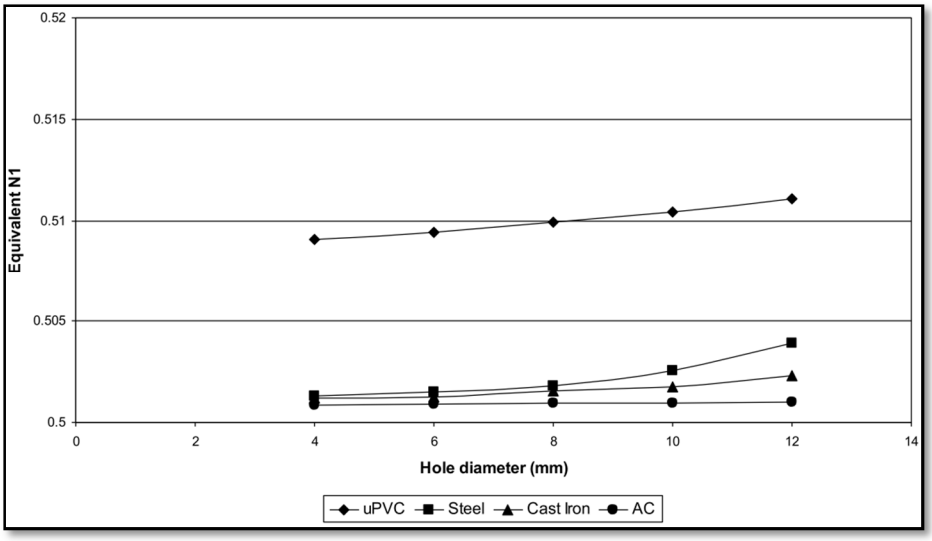

Figure 2-22: Variation of N1 with increasing hole diameter for various pipe materials (Cassa et al., 2010)

Again, the reader is reminded here, that the study by Cassa and Van Zyl is a theoretical finite element study. In contrast to this study, Bennis et al (2011) showed through experimental studies on steel and PVC pipe sections, that the N1 exponent for round holes decreases slightly as the hole diameter increases, indicating a slight decrease in pressure dependant flow as the hole diameter increases, as shown in Figure 2-23. For both studies, however, the N1 variation appears to be small.

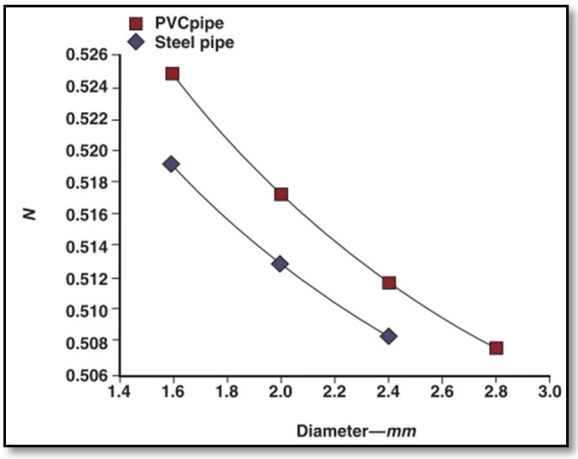

Figure 2-23: Variation of N1 exponent with leak diameter for round leaks (Bennis et al., 2011)

For longitudinal cracks, Cassa & Van Zyl (Cassa et al., 2010) show through the finite element study that pipe stresses are significantly affected by the leak opening, and that the material yield strength is easily exceeded in the vicinity of the opening. Longitudinal cracks, for instance, showed a clear increase

in leak area under increasing pressure, with considerable deformation and high stress concentrations at the crack tips, ultimately leading to local plastic deformation. An exponential pressure-area slope increase with leak size was observed for longitudinal leaks. Cassa and Van Zyl also show that an increase in length of a longitudinal or centrifugal crack is expected to have an exponential effect on the N1 value or the pressure-area gradient, again, with this effect emphasised by the elasticity of the pipe material.

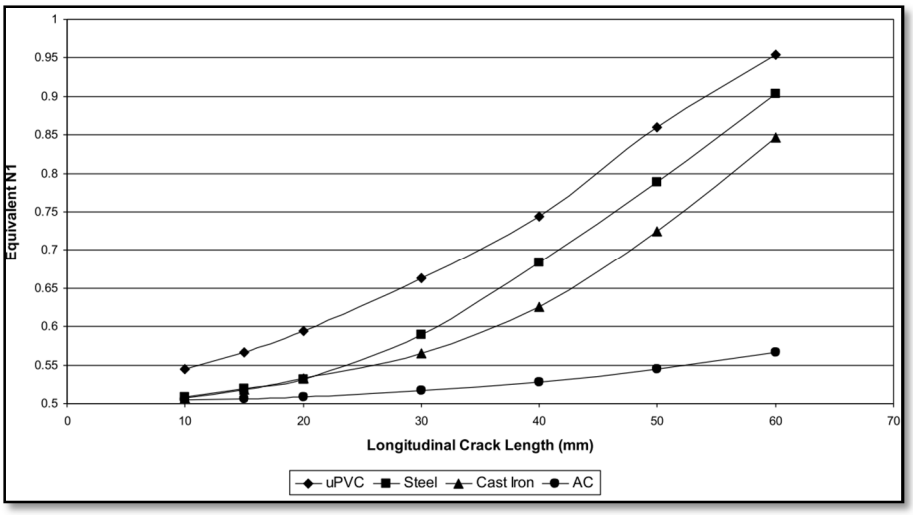

Figure 2-24: Variation of N1 with length of longitudinal crack for various pipe materials (Cassa et al., 2010)

Finally, in a recent experimental study by van Zyl and Malde (2017), the head-area slopes of various leak types in a range of different pipe materials were observed under controlled conditions. The behaviour observed in previous studies was confirmed, with longitudinal cracks showing the most expansion under increasing pressure, while round holes showed the least expansion, and circumferential holes showed negative expansion.

2.8.5.3 Soil Hydraulics

Already in 1981, Hiki (1981) investigated the influence of the medium surrounding the leak on the leakage exponent, which is equivalent to the N1 number. Exponents were measured for leaks discharging into air, water and sand, but no direct influence could be detected.

Walski et al. (2006) modelled leakage in a controlled environment using test apparatus that simulated typical soil conditions. By analysing test data and by assuming the Darcy's law for the leak flow through the soil, Walski et al. developed the Orifice/Soil number. This number indicates whether the leak is more soil or orifice dependant. The number represents the ratio between the head loss resulting from the orifice to the head loss resulting from the soil. The orifice/soil number is directly related to the flow rate, with higher flow rates resulting in more orifice dependent leakage.

For large leaks, with high flow rates, the water will create its own path upwards to the surface, essentially removing the effect of the soil and creating a static head immediately outside the leak. When soil permeability is low and leaks are small, however, additional friction head builds up on the water path between the leak and the soil, resulting in situations where the soil head loss can exceed the orifice head loss.

Walski et al. also found through a number of field tests that for most real-world situations, leaks are dominated by orifice dependence, rather than soil dependence. The nature and size of the orifice was therefore found to have a much greater effect on the leakage characteristics, compared to the effect of the porous media flow through the soil, unless the flow rates from the leaks are high.

Van Zyl and Clayton (2007) point out the complexity of characterising the leak-soil flow behaviour. They highlight the effects of fluidisation and scouring of the soil adjacent to the leak, which leads to the modification of the boundary of the leak/soil interface; the inconsistency of the soil permeability surrounding the pipe; the effect of the permeability of the ground on the flow condition; and the effect of the stress conditions in the ground. They argue that flow rates in the soil-leak interface will unlikely follow a linear function of pressure, as assumed by Walski et al. for their calculation of the leakage Orifice/Soil number referred to above, and is considerably more complex than often assumed.

A number of studies have since been conducted on the effect of the surrounding soil on the leakage characteristics. In a literature review by van Zyl (2014) on the latest theoretical developments on the pressure-leakage relationship, however, van Zyl concludes that the high pressures commonly found in distribution systems are unlikely to be contained by any soils, and that the impact of the soil on the pressure-leakage behaviour, and therefore the N1 and FAVAD parameters, is most likely to be small. Further investigation into the effect of the soil will therefore fall outside the scope of this study.

2.8.5.4 Initial Pressure and Pressure Reduction Range

Cassa & van Zyl (2014) show through analytical exploration of the N1 equation, that different N1 values can be obtained for the same leak when the pressures are varied. In this study it is shown that N1 values tend to 0.5 as the system pressure approaches zero, and tend to 1.5 as the pressure approaches infinity.

Experiments performed by Bennis et al (2011) on steel and PVC pipes support the dependence of the N1 value on the system pressure. A higher initial pressure resulted in higher N1 values, meaning that, the reduction of flow rate for a given pressure reduction, will be greater for higher initial pressures.

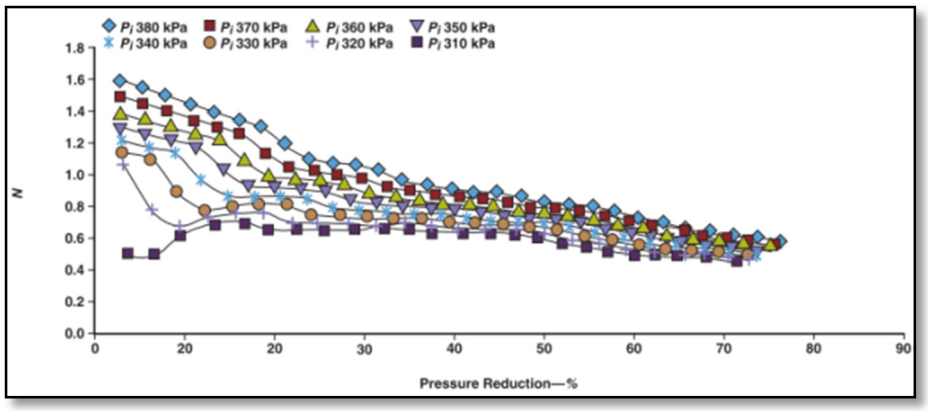

Figure 2-25: Variation of N1 in response to pressure reduction rates for various initial pressures on steel pipes (Bennis et al., 2011)

According to Cassa and van Zyl (2014), however, the above pressure dependence of the N1 value may point to a critical flaw of the N1 equation, which is not contained within the FAVAD equation. The variables of the FAVAD equation are not influenced by the initial system pressure or the pressure reduction range.

2.8.5.5 Leak Flow Type:

The type of flow can vary from turbulent flow to laminar flow. Fully turbulent flow is a requirement for the theoretical leakage exponent of 0.5 for an orifice, and in some cases, leakage exponents of 1 can be explained by laminar flow, as flow rate and pressure become linearly related with laminar flow (Van Zyl, 2014).

The Reynolds number is dependent on the leak perimeter and the kinematic viscosity of the fluid. The kinematic viscosity, in turn, is temperature dependent. Therefore, only the leak perimeter, leakage flow rate and temperature affect the state of the fluid. The Reynolds number for a leak or orifice can be written as Equation 2-27:

$$Re = \frac{4V \times r_h}{\mathcal{V}} = \frac{4Q}{\mathcal{V} P_w} \qquad \textbf{2-27}$$

Where V equals velocity, $\mathcal{V}$ kinematic viscosity, r_h the hydraulic radius of the orifice and P_w, the wetted perimeter.

Van Zyl & Clayton (2007) assumed constant kinematic viscosity, and investigated the effect of the wetted perimeters. They found larger wetted perimeters of longitudinal and circumferential cracks in

comparison to round holes, resulting in a higher possibility of laminar or transitional flow rates, which in turn result in higher N1 exponent values. This effect is supported by experimental results quoted by Thornton and Lambert (2005) from John May that clearly show that N1 values increase to above 0.5 as the Reynolds number decreases to below 4000, representing transitional or laminar flow.

Clayton & van Zyl, however, also show that for flow in leaks to be laminar, the leak must be less than 3 litres per day for a leak with an aspect ratio of 10 000, which means that the leaks in the laminar zone are unlikely to contribute substantially to pipeline leakage. The leakage from pipes with mainly background losses and without significant leaks or bursts, as defined in paragraph 2.2.2, are more likely to show transitional flow, which can result in N1 values higher than 0.5.

2.8.6 FAVAD and N1 for Systems with Multiple Leaks

2.8.6.1 The N1 Equation for Systems with Multiple Leaks

Applying the N1 equation to systems with multiple leaks is not new. Already in 1979 Ogura (cited in (Allan Lambert, 2000)) performed field tests on small sections of distribution systems in Japan, most of which consisted of metal pipes. N1 exponent values were obtained by isolating sections of the distribution systems and recording the inflow needed to maintain leakage rates at different pressures, with the pressures varying between 5 and 40 metres head. N1 exponents ranging between 0.65 and 2.12 were calculated, resulting in a weighted average of 1.15. Based on this result, the Japanese standard value for the N1 exponent remained 1.15 for the next 20 years.

Lambert (2000), in a brief literature overview of pressure-leakage relationships, also refers to studies by Goodwin performed in 1980 on UK distributions systems with the 'customer night use' approach. In this case, the detectable leaks were repaired before the tests, with the remaining leaks expected to be small background leaks. N1 values of between 0.7 and 1.68 where obtained, averaging at 1.13, with the lower numbers possibly resulting from the water used by customers during the test.

According to Lambert's research, similar and more recent tests with minimal customer night use in Australia and New Zealand have resulted in N1 values closer to 1.5 for background leakage.

Lambert (2000) concludes that, if all tests are considered, before and after leak detection, an average N1 value of 1 must be expected for complete systems if the details of the pipe materials are not known, and an N1 value of 1.5 should be estimated for small background leakage in general.

The N1 values observed in field tests, however, often tend to deviate considerably from the values proposed by Ogura and Lambert. In a more recent study, for instance, Deyi et al. (2014) performed field

tests on pressure management zones within the distribution systems of KwaDabeka, a low to middle income earning township in KwaZulu-Natal, South Africa, where they attempted to characterise the leakage with the FAVAD and the N1 equation. This township represents distribution systems common to South Africa, being comprised of various pipe materials, but mostly plastic and asbestos cement.

In this investigation, an unrealistically large range of N1 values between 0.18 and 3.33 was obtained. They also concluded that all N1 values higher than 1.5 signified a system leakage area smaller than zero, which is not physically possible. Reasons for this anomaly are suggested to be measurement errors, an underestimated role played by plastic deformation, or the leaking of valves on the system boundary. This study therefore highlights the complexity and high error potential of implementing this method to large pressure management zones. The results are tabulated in Table 2-5, together with results from other similar studies.

2.8.6.2 The Applicability of the N1 Equation for Systems with Multiple Leaks

Investigations were conducted by Ferrante et al. (2014) to determine whether the mean values of the parameters of the power law, or N1 equation, for individual leaks can be used to characterise systems with multiples leaks. In a statistical study, the functional dependence of the parameters is investigated by applying spatial variation to the parameters at a local scale, and translating the effect to the global scale. Flat, horizontal systems with negligible friction were assumed for this study.

First, it was shown that the power law has the same functional dependence in a local scale compared to a global scale. This was shown by first writing the N1 equation in mean terms for each leak, with the bar representing mean values. Assuming that the pipe and leak properties remain fairly constant throughout the system, the mean values for C and $N1$ can be estimated for each leak as $\overline{C_{N1}}$ and $\overline{N1}$ and the pressure for the whole system can be represented and measured by a constant head value of $\bar{H}$.

$$\bar{Q} = \overline{C_{N1}}\,\bar{H}^{\overline{N1}}$$

2-28

The leakage for the system can then simply be characterised by the sum of the leakages of all individual leaks:

$$Q_{System} = \sum_{i=1}^{n} Q_i = n\bar{Q} = (n\overline{C_{N1}})\bar{H}^{\overline{N1}} = C_{System}\bar{H}^{\overline{N1}}$$

2-29

The above equation therefore shows the same functional dependence on the N1 exponent for individual leaks and leaks in systems.

Similarly Ferrante et al. show, through another example of spatial variation, that even if the variation of parameter C_{N1} between individual leaks is high, the variation on the global scale, of random systems consisting of leaks with the same local variation, is low. This confirms that the N1 equation can be applied to a system of leaks, if the N1 exponent is the same for all the local leaks.

If, however, the N1 exponents vary over a mean N1 value, the combined N1 value will not necessarily equal the mean value of all the individual leaks. Ferrante et al. show that systems with random leaks of the same variation are not necessarily characterised by the mean exponent if the exponent varies from leak to leak. Differences do therefore exist when applying local leak laws to the global scale.

2.8.6.3 The Applicability of the FAVAD Equation for System with Multiple Leaks

In another analytical investigation by Ferrante et al. (2014), similar to the one discussed in paragraph 2.8.6.2, it is shown, by varying unrelated and random parameters of the power law and FAVAD equation, that the FAVAD equation outperforms the power law or N1 equation when the functional dependence is compared between the local and the global scale.

In this investigation, parameters of the N1 equation and the FAVAD equation were spatially varied according to distributions that suit their character best. The random variation of the parameters was applied to 100 single leaks, and then to 100 systems with 100 single leaks each. By comparing the resulting sample means, the local variation was compared to the global variation. The global mean N1 exponent was shown to generally be higher than the local N1 exponent, while the parameters of the FAVAD equation were shown to result in a similar head versus leakage relationship, whether in the global or local scale.

The effectiveness of the FAVAD equation was confirmed by Schwaller & van Zyl (2015) in another statistical investigation into the feasibility of the FAVAD equation for characterising pressure management areas (PMAs).

A Spreadsheet model for a distribution system was developed with a number of random distributions of leak quantities, areas, discharge coefficients and head area slopes typically found in real distribution systems. A pressure management area consisting of 40 km of pipes and 2500 service connections was used as a basis.

A sensitivity analysis was then conducted on a number of networks. These networks consist of distribution systems with 100, 1000 and 10 000 leaks. For each of these cases, 100 randomised networks were generated, amounting to 300 artificial network models with randomly distributed leaks.

In order to perform realistic statistical analyses, Schwaller and Van Zyl fitted the most suitable distributions and ranges to the various leak parameters. The discharge coefficient C_d and the initial leak area A_0 were modelled with normal distributions, the head-area slope m was modelled as a power function of the leak area, and the pressure head H was modelled with a uniform distribution. The distribution system was assumed to exist on a constant elevation.

For each network, the sum of all the initial leak areas was plotted against the leak area measured for the network according to the FAVAD equation. The initial leakage area (A_0) was found to be approximately equal to the sum of all the individual initial leakage areas, as shown in Figure 2-26. Similarly, the head-area slope (m) for each network was found to approximately equal the sum of all the individual head-area slopes of the network, as shown in Figure 2-27.

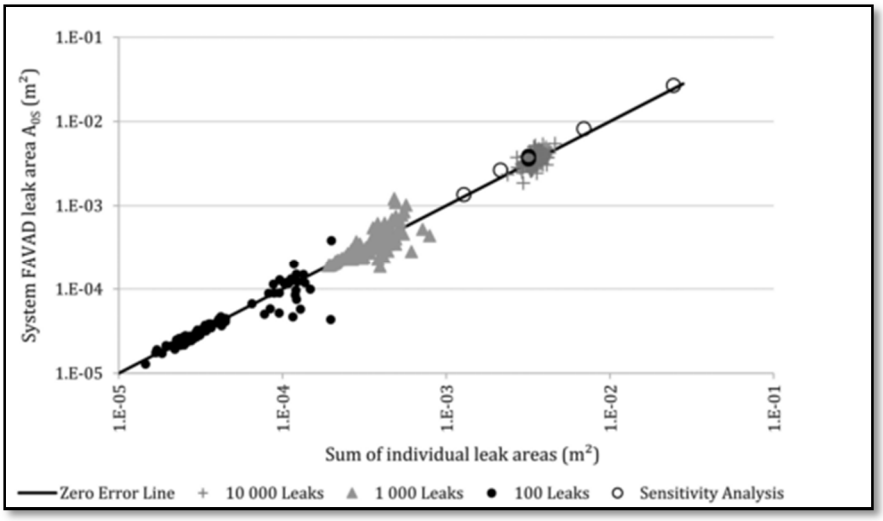

Figure 2-26: Initial system leakage area compared to sum of individual leakage areas (Schwaller et al., 2015)

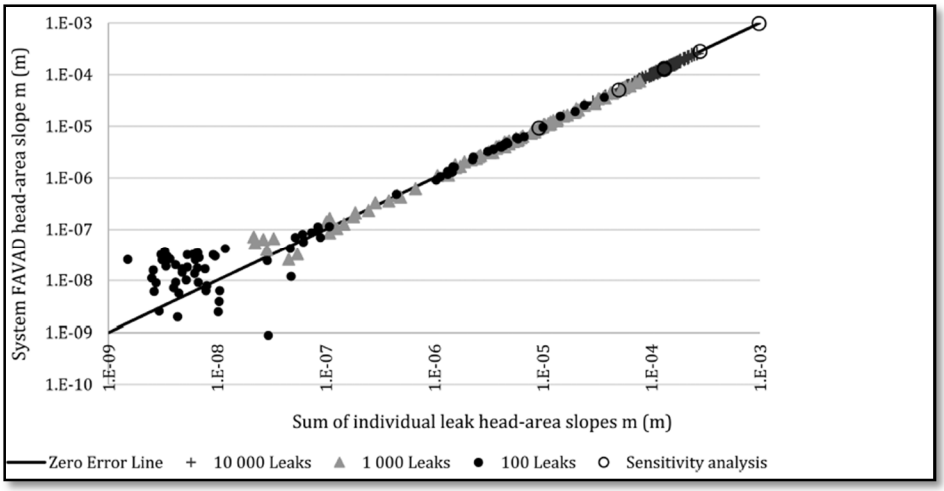

Figure 2-27: System head-area slope compared to sum of individual head-area slopes(Schwaller et al., 2015)

Schwaller and van Zyl found that the initial leakage area and head-area slope of any system can be estimated using the FAVAD equation with the leakage rate and average zone pressure head before and after pressure reduction. These initial leakage areas, as well as the head-area slopes, were found to provide good estimates of the sums of the individual leakage areas and head-area slopes of all the leaks in the system.

$$\boldsymbol{Q_D = \sum_{i=1}^{n} \overline{Q} = n\overline{Q} = n\overline{C}\sqrt{2g}\left(\overline{A_0}h^{0.5} + \overline{m}h^{1.5}\right)}$$

2-30

Schwaller & van Zyl concluded that the application of the FAVAD equation for characterising leakage in systems is feasible, because leaks deform linearly under changing pressure. The system initial area and the system head-area slope are meaningful properties, independent of pressure, characterising the state of the system. Estimates of the total initial leakage area as well as the sum of all head-area slopes can therefore be obtained by applying the FAVAD equation together with pressure reduction.

The high errors resulting when varying elevations are taken into consideration remain a concern. By performing a sensitivity analysis, Schwaller & van Zyl showed that the FAVAD parameters are sensitive to the slope of the system and that the equation works most accurately on horizontal systems. They did, however, also find that the errors remain small, if the head-area slope is high in relation to the slope of the pipe. Although, in this study, systems with big head-area slopes ($m > 10^{-5}$) resulted in small errors, even though the systems had significant static head variation, the study was focused specifically on distribution systems, which, in general, present significantly smaller slopes than transmission lines.

In another study, Schwaller and van Zyl (2014) make use of the same hypothetical Spreadsheet model to investigate whether the variations in N1 exponents observed in the field can be attributed to the elastic expansion of the areas of individual leaks.

Simulations were carried out to reproduce conditions typically observed in real distribution systems, such as the condition involving two pressures, as experienced during night tests. Random leaks were created by varying the FAVAD equation parameters according to suitable distributions and within realistic ranges, assuming a linear head-area relationship. The N1 leakage exponent was then calculated for each leak and the mean and range of the N1 exponents for all the leaks in the system was then calculated. Repeatability analysis applied for distribution systems with 100, 1000 and 10 000 leaks. The resulting N1 leakage exponents were estimated as displayed in Table 2-7 below:

Table 2-7: Leakage exponents for 100 random networks with 100, 1 000 and 10 000 leaks respectively (Schwaller & Van Zyl, 2014)

Number of System Leaks	Mean N1	Range of N1
100	**0.66**	**0.46 - 1.67**
1000	**0.92**	**0.46 - 1.59**
10 000	**1.08**	**0.81 – 1.26**

As seen above, the N1 values largely ranged between 0.5 and 1.5, as expected from field studies. This investigation therefore shows that the combined effect of individual elastically deforming leaks, characterised by the FAVAD equation, can produce a range of leakage exponents that is typical to the range observed in field studies.

Finally, in a study by Kanaasha, Piller and van Zyl (2018), the FAVAD equation was incorporated into the hydraulic formulation of a network modelling software, which, in its conventional form, uses the power equation to measure pressure-dependent outflows. The effect of replacing the power equation with the FAVAD equation was tested on 600 instances of stochastic leakage distributions in three differently sized pipe networks.

All example networks were supplied from a single point by gravity, and both a high and low input pressure was simulated in order to represent the implementation of pressure management. When comparing the power equation results to the FAVAD results, significant errors were observed for the power equation, if the FAVAD simulations were assumed to be accurate. These errors were especially apparent for individual nodes at elevations which differed extensively from the average zonal pressures, and when simulating system pressures that significantly differed from the nominal range.

It can be concluded that the FAVAD equation is not only excellent for characterising individual elastically deforming leaks, but is also suited for investigating horizontal systems with multiple leaks. The FAVAD equation therefore outperforms the N1 equation when leaks of systems are analysed collectively.

2.8.7 The Leakage Number

It is clear from the preceding paragraph 2.8.5, that the FAVAD equation outperforms the N1 or power law equation for systems with multiple leaks. In addition, Cassa & van Zyl (2014) conducted a comparison study to evaluate the performance of the FAVAD and N1 parameters for individual leaks. The leak characterisation capabilities of the FAVAD and N1 equation were compared with results from a finite element analysis study by predicting the leakage through a 60 mm long split in a PVC pipe.

Again, the FAVAD equation was shown to outperform the N1 equation. This is supported by van Zyl, Lambert and Collins (2018), who also cite various studies which point to the FAVAD equation being superior over the power equation, and which also confirm the linear variation in leak area with pressure, on which the FAVAD leakage model is based. They also mathematically show that the N1 equation will likely lead to significant errors when the equation is used at pressures different from the ones at which it was calibrated.

A considerable amount of literature, however, presents results, data and guidelines in terms of N1 exponent values. It has therefore become desirable to relate the N1 exponent value to the variables of the FAVAD equation, which take the changing area under pressure into account. The leakage number was derived and defined by van Zyl & Cassa (2014) as a more consistent way to characterise pressure leakage response. Van Zyl, Lambert and Collins (2018) provide mathematical proof that the leakage number can be used to link the FAVAD equation to the power equation.

For the derivation, Equation 2-14 and 2-22 were equated, and after manipulation, the following expression was found:

$$N1 = \frac{\ln(N_L+1)-\ln C}{\ln h} + \frac{1}{2}$$

2-31

With the leakage number defined as:

$$N_L = \frac{mh}{A_0}$$

2-32

The leakage number can therefore be defined as the ratio between the flow through the expanded leak and the initial area of the leak. Thus, with the above relation, the leakage exponent can be easily determined for any leak if the head-area slope and initial area are known.

A plot of the leakage exponent versus the leakage number was generated, as shown in Figure 2-28, and it was shown that the relationship remains the same, irrespective of the values of A_0, m and h.

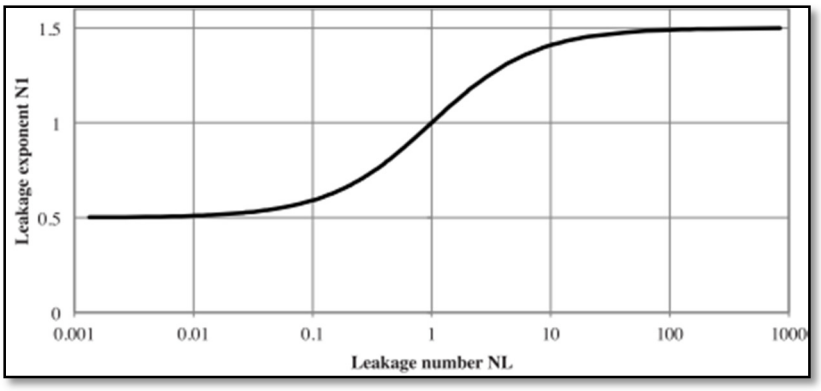

Figure 2-28: Leakage Number N_L corresponding to Leakage Exponent N (Cassa & Van Zyl, 2014)

The formula describing this relationship was manipulated to the following form:

$$N_L = \frac{N1-0.5}{1.5-N1} \quad or \quad N1 = \frac{1.5N_L+0.5}{N_L+1} \qquad \textbf{2-33}$$

The leakage number will equal one if the leakage amount through the expanded portion of the leak equals the leakage through the initial leakage area. A leakage number smaller than one, indicates that the leakage through the initial area contributes more than the leakage through the expanded area (Schwaller et al., 2015). A leakage number of -1 will occur if the leak area is equal to zero at any non-zero pressure differential (van Zyl, Lambert & Collins, 2018).

In a field study by Deyi & van Zyl (2014), the N1 exponents, as well as the FAVAD variables were obtained for existing distribution systems. Even though the resulting N1 values reflected an unrealistic range of between 0.18 and 3.33, an interesting observation was made when plotting the N1 exponents in relation to the leak number. As shown in the figure below, the N1 exponents higher than 1.5 appeared to fit a seemingly different relationship, compared to the N1 values below 1.5, which followed the expected relationship.

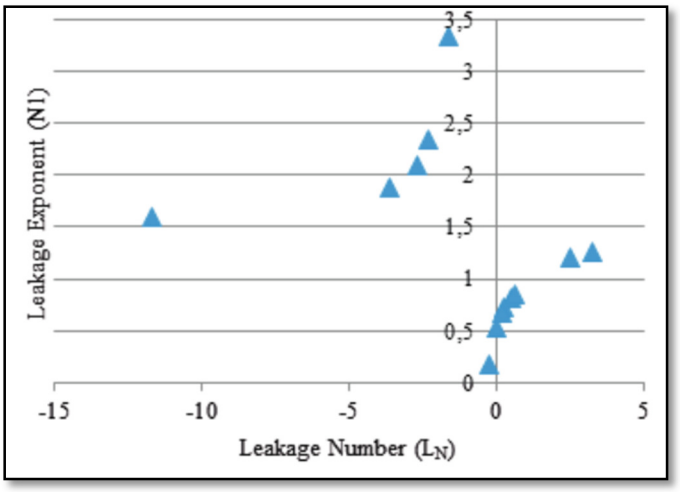

Figure 2-29: Relationship between N1 and Leakage Number (N_L), here indicated as L_N (Deyi et al., 2014)

This phenomenon is confirmed in the statistical investigation into the effectiveness of the FAVAD equation for systems, by Schwaller & van Zyl (2015), which was already referred to in paragraph 2.8.6.3. In this study, Schwaller & van Zyl briefly investigate the application of the leakage number to systems with multiple leaks. By using the total system leakage area and the system head-area slope, the study concludes that the leakage number can be used for future field applications for converting between the FAVAD variables and the N1 exponent value.

The above behaviour of the N1 exponent is confirmed through a mathematical analysis of the leakage number by Van Zyl, Lambert and Collins (2018). This study shows that this behaviour is a shortcoming of the power equation, and can be expected if the pressures exceed a certain range. The study also shows that, by first converting the leakage exponent to a leakage number using Equation 2-33, and then by proportionally adjusting the leakage number for the new pressure calculated with Equation 2-32, and then converting the adjusted number back to a leakage exponent, a more realistic N1 number can be obtained.

Chapter 3

3 Methodology

3.1 Introduction to Methodology

From the Literature Review, the need for a simple, low cost pipe condition assessment technique, which can survey large sections of pipe infrastructure in short periods of time with minimal disturbance to the operation of the infrastructure, is highlighted.

Equipment satisfying the above need was initially developed and successfully implemented by the University of Cape Town for distribution networks. This equipment generates and records leakage flow rates for various pressures, providing pressure-flow relationships for the tested pipes, which can subsequently be interpreted to provide information on the pipe condition and the extent of pipe leakage.

After the successful implementation of this technique on distribution networks, equipment limitations for testing larger bulk transfer pipelines became apparent, leading to the development of new equipment for this purpose. René Nsanzubuhoro, under the supervision of Professor Kobus van Zyl (2016), designed and developed such equipment for bulk transfer pipelines.

This methodology chapter explains how this newly developed Pipe Condition Assessment Equipment (PCAE) is tested on available bulk pipelines in the field.

The chapter starts off with a detailed description of the testing equipment, as well as a description of the parts acquired for connecting onto the various possible connection points encountered in the field. The process for acquiring and identifying pipes in the field for testing purposes, is then discussed.

This section is followed by a detailed explanation of the test procedure, in which all the activities for testing the pipelines with the PCAE, and for recording the test data, are explained. The methodology for processing the recorded data into useful pipe information is then discussed. In this section, an Excel tool that was developed for interpreting the data, is also described in detail.

Finally, the section concludes with observations made during the application of the methodology.

3.2 Testing Equipment

3.2.1 Detailed description of the testing equipment

Figure 3-1 provides an annotated image of the PCAE setup, and Figure 3-2 shows a schematic of the equipment. These two figures are referred to in the description of the equipment, which follows in the next paragraph. The technical detail and the detailed function of each component is discussed in Table 3-1.

The PCAE is installed onto a tanker trailer. A 1000 litre tank serves as the source and storage of water for the equipment. A 50mm rigid PVC pipe extends from the base of the tank, and branches into two supply pipes, each fitted with a camlock hose connection point.

A pump unit is installed on the front A-frame of the trailer. This unit consists of the pump, measuring and data recording equipment, as well as a pump control device; all neatly fitted into a galvanised steel frame. A flexible and detachable hose connects the supply from the tank with the pump unit through camlock couplings.

In the pump unit, the flow first enters the pump, where pressure is added. An air relief valve is situated on a high point immediately after the pump, in order to collect and remove all the air that has potentially accumulated in the equipment.

The flow then passes through a magnetic flow meter that continuously measures and transmits the flow rate to a data recorder. In order to ensure that the magnetic flow meter performs optimally, the whole pump can be levelled with a levelling mechanism that consists of a scissor jack on one side of the frame, and a pivot connection on the other. This system ensures that the flow meter operates in a horizontal position at all times, as specified by the flow meter manufacturer.

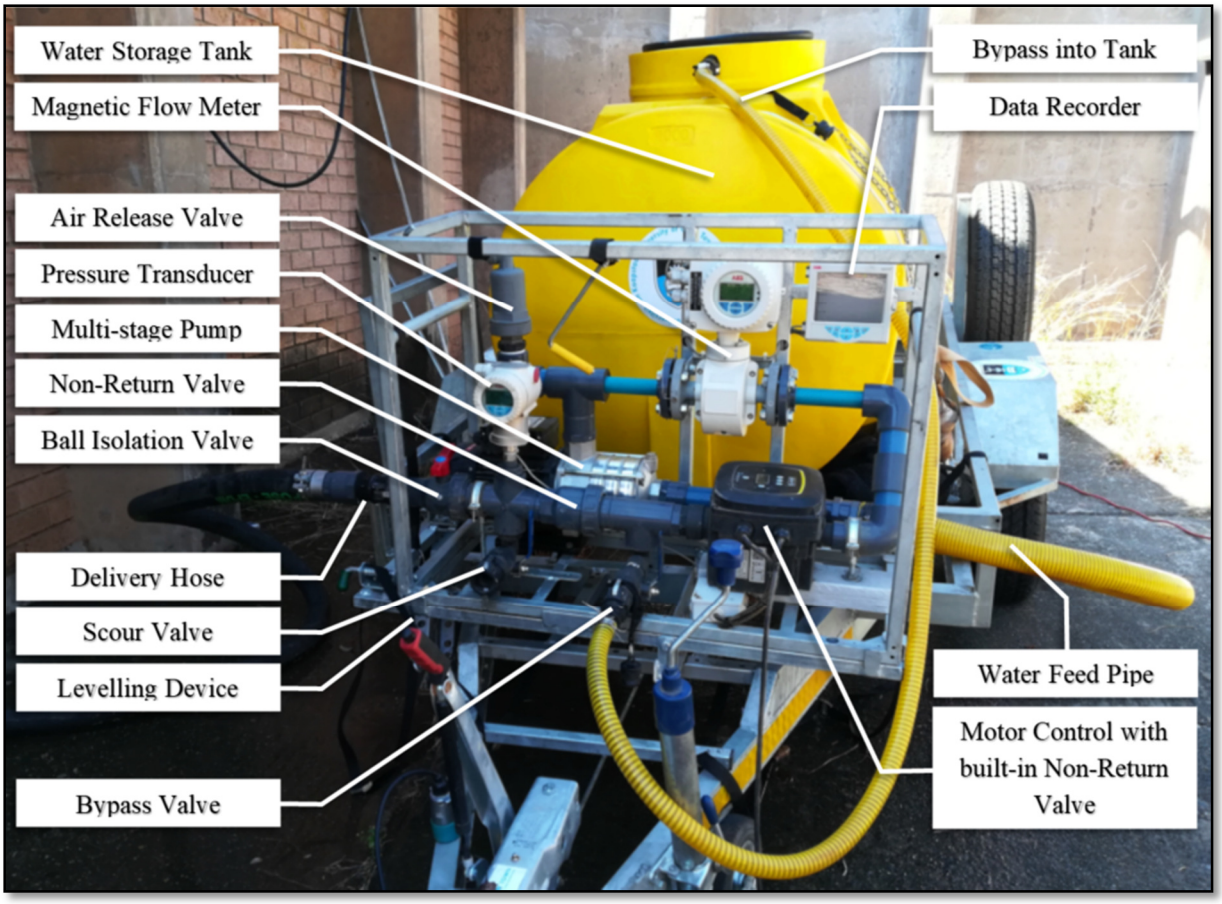

Figure 3-1: Annotated illustration of the testing equipment

Following the flow meter, the flow enters the motor control unit. This unit consists of a variable speed drive for the pump motor, a pressure transducer and a non-return valve. The desired pressure can be easily set on the unit, which then constantly records the system pressure, while regulating the speed of the pump motor to achieve and maintain the desired system pressure.

After the pump control unit, a branch pipe is installed, which is fitted with an isolating ball valve and a camlock hose coupling. A flexible pipe, leading back to the tank, then connects to the coupling, allowing the pump to circulate the flow, in order to maintain pressure in the system without flow entering the test pipe.

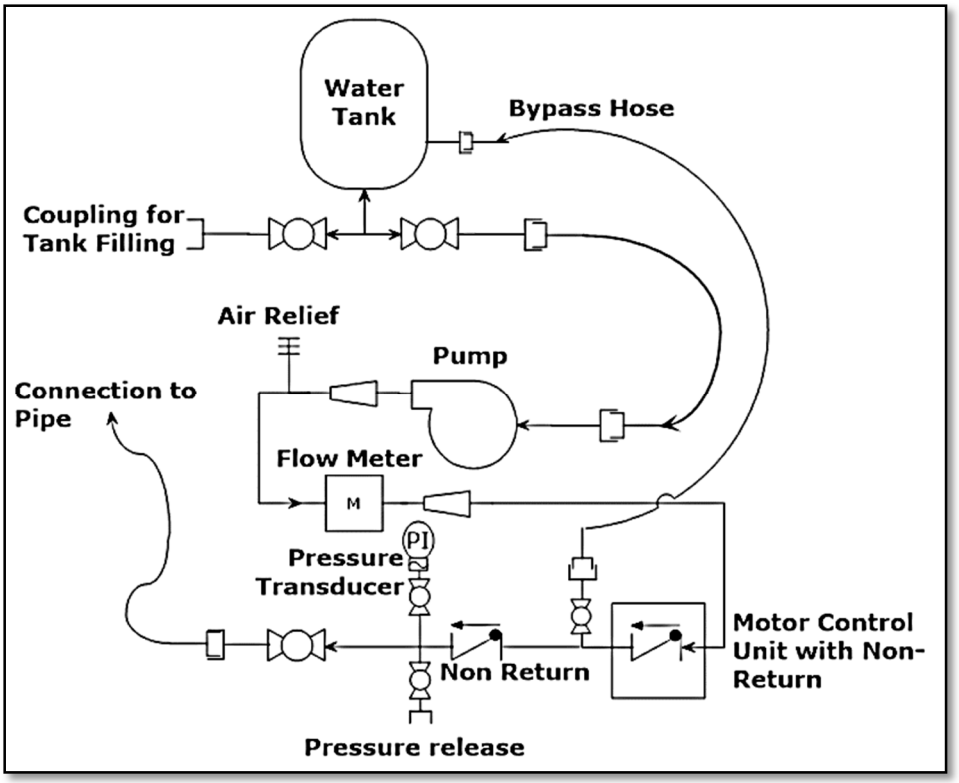

Figure 3-2: Test Equipment Schematic

This branch is followed by a non-return valve and a cross-connection. One of the connections opens up to atmosphere with an isolating ball valve, allowing for the de-pressurisation of the delivery hose and test pipe. On the other connection, a pressure transducer is installed that continuously measures and transmits the system pressure to a data recorder.

Following the cross connection, the flow is directed through an isolating ball valve and a camlock coupling into the ten metre long delivery house. This hose then connects to the test pipe with a suitable coupling, depending on the type of connection point.

A data recorder with a display unit continuously plots and updates the pressure and flow data, providing the operator with a visual graph of the test data being recorded. This device stores the data directly onto a memory card, with which the data can then be transferred to a personal computer for further interpretation.

Table 3-1: Detailed Test Equipment Components Description

Component	Specification	Description and Function
Water Tank	1000 Litres capacity. Original purpose of trailer is for diesel transportation and storage.	The water tank is rigid and manufactured from plastic/PVC. It is fixed onto the trailer and it can be closed with a lid to keep the interior clean, so that the water in the test pipe does not contaminate. Its purpose is to store water and to provide a water source to the PCAE.
Multi-Stage Pump	Model: Euroflow HS18-40N-1 Maximum head: 42 m Maximum Q at 17m: 16 m^3/h Maximum Q at 41m: 4 m^3/h	The centrifugal pump is a four stage pump, allowing it to add a large range of pressures to the test pipe.
Air-Relief Valve	25 mm	The air-relief valve is situated on a high point on the equipment and ensures that no air is trapped in any of the components.
Magnetic Flow Meter	Model: ABB FEX500 (25mm) Flow Range: 4-200 l/min Measuring accuracy: 0.2%	An electromagnetic flow meter accurately measures flow within the flow range, and continuously transmits the reading to the data recorder.
Motor Control Unit / Inverter unit	Model: DAB Active Driver Plus M/M 1.1 Pressure range: 1-9 bar Pressure rating: 13 bar Maximum Flow: 300 l/m	The motor control unit consists of a variable speed drive that regulates the pump speed, in order to maintain a selected pressure. It includes a non-return valve and a pressure transducer. From this unit, the pump is started and stopped. By simply changing the pressure setting, new data points along the pressure-flow curve are obtained.
Bypass to Tank	25 mm ball valve with flexible hose.	This bypass circulates the pumped flow back into the water tank. This allows the operator to start the pump in advance, pressurising the system without introducing flow into the pipe. Flow can then be introduced gradually, without the pipe pressure dropping, ensuring that no air enters the pipe.
Non-Return Valve	50mm Non-Return Valve	The non-return valve ensures that a pressurised test cannot reverse the flow direction. Only once the pumping pressure exceeds the test pipe pressure, flow will start. The non-return valve also protects the PCAE from excessive pressures in the test pipe.
Pressure Transducer	Model: ABB 2600T Pressure Range: 0-10 bar Calibrated: 01/10/2017	The pressure transducer continually records, displays and transmits pressure data to the data recorder.
Data Recorder	Model: ABB SM500F Frequency: 10 Hz	The data recorder displays the pressure and flow data on a continuously updated plot. The data is also recorded onto an SD-Card, enabling data transfer to a PC for interpretation.
Water Feed Pipe	Material: Rubber Class: 10 OD: 50 mm, ID: 45.2 mm Length: 10 m	This feed pipe is very flexible to ensure that it can easily be routed to the ideal connection point. It transfers pressurised water from PCAE to test pipe.
Generator	Model: Ryobi RG-2700 Capacity: 2.7 kW	A portable petrol generator forms part of the PCAE. The generator provides a power source when a power point is out of reach at the testing location.

3.2.2 Test Pipe Connection

The PCAE must connect to the test pipe on an existing connection point. Pipes in the field, however, do not have uniform and consistent connection points, and often do not have any connection point at a desired location at all. For this reason, the PCAE must be equipped with an adaptable connection mechanism, so that it can connect to any type of connection point available. If no connection point is available, pipe equipment, such as an air valve, can be removed to create an entry point to the pipe where the PCAE must be able to connect.

The PCAE has a geka-type quick coupling at the end of the feed pipe, with which it must connect to the test pipe. Before this study, the PCAE was already equipped with a number of interchangeable threaded connections and fire-hose connections, which are assembled with geka-type connection points, onto which the feed pipe can connect. During the study, more connections were acquired as needed, including flanged connections for connecting to air valve and scour valve connections in the field. The flanged connections were also adapted to suit various flange specifications and pressure rating classes by slotting the holes. Even though this weakened the flanges, it is no reason for concern, as the pressures are unlikely to exceed 500kPa.

The equipment can now connect to almost any connection point commonly encountered in the field, from 15 mm threaded pipes up to 100 mm flanged connections. Figure 3-3 shows examples of some of the different fittings that from part of the PCAE.

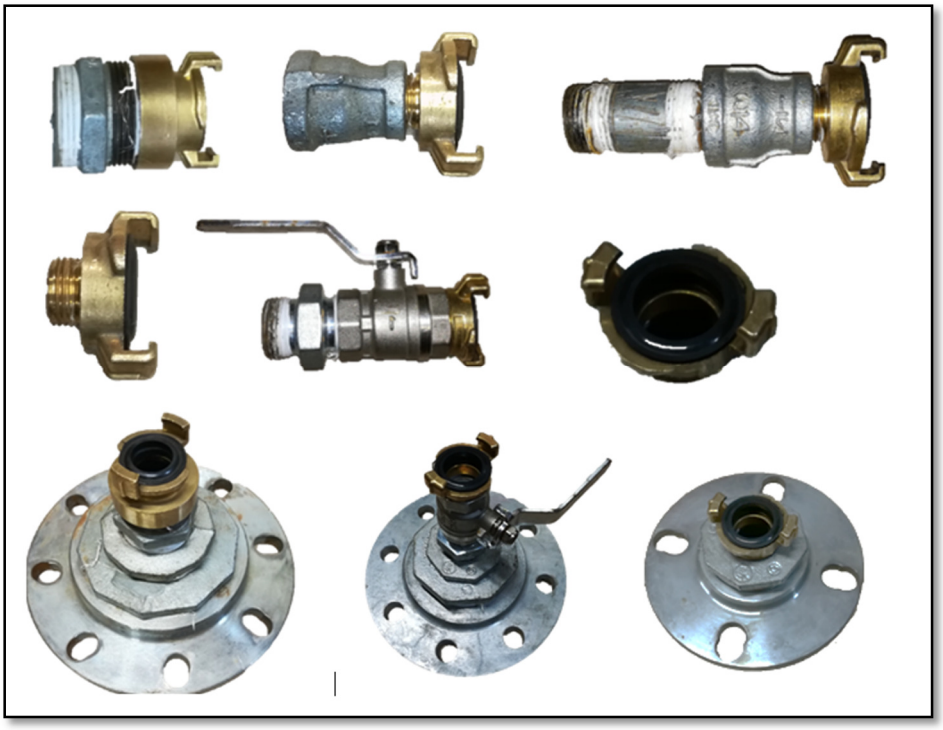

Figure 3-3: Examples of connection fittings for the PCAE feed pipe to connect to existing connection points.

3.2.3 Modifications and Additions to the PCAE

The design and assembly of the PCAE did not from part of the scope of this study. Experiences in the field, however, prompted the implementation of minor modifications to the equipment. These modifications are listed below:

a) A ball valve open to the atmosphere, downstream of the non-return valve on the PCAE, was installed to allow the operator to relieve the pressure in the equipment, facilitating the disconnection of the hose from the PCAE. Often, the test pipe takes very long to depressurise naturally from leakages, especially if the pipe is in a good condition. Opening this valve allows for controlled depressurisation for disconnecting the feed hose on completion of the test, or for refilling the tank.

b) Feed pipe extension: A 10m extension to the 50mm pipe was borrowed during the testing period, doubling the reach of the equipment in chambers and areas of rough terrain, where the trailer was restricted from reaching the test point.

c) Additional access point adaptor fittings: All the flanged connection fittings, from 50 mm up to 100 mm, were acquired during the test period for connecting onto air valves and scour valves on bulk pipelines. The flanges were also adapted to fit pipes of various pressure classes.

3.3 Identification of Pipelines

3.3.1 Pipeline Requirements

To identify pipes for testing, clear selection criteria first had to be defined. For pipes to be deemed suitable for testing with the PCAE, the pipeline must have the following properties:

a) The pipeline must be isolatable. The pipeline must therefore be fitted with an isolation valve on either end of the section to be tested, and both isolation valves must ideally seal effectively.

b) An access point, where the PCAE can be connected to the pipeline, must exist. On a pipeline with a considerable elevation difference, the connection point must ideally be situated as high as possible, so that the PCAE can induce a wider range of pressures. The maximum pressure, that the PCAE can induce, is approximately 40 metres. If the connection point is at a low point on the pipeline, the PCAE can only add the difference in pressure between the high point and its maximum capacity. Also, if the pressure exceeds approximately 40 metres, or 4 bar, at the connection point, no pressure can be added at all, and the test cannot be conducted.

The connection point can be any point onto which a threaded or flanged fitting can be connected to. It can also be created by removing currently installed equipment, such as air valves.

c) The area around the test point must be accessible by the PCAE trailer, and the trailer must ideally be able to reach within 10 metres of the testing point. An extension of the PCAE feed pipe allows for the trailer to be parked a maximum of 20 metres from the testing point.

d) The pipeline sizes and lengths were not strictly considered as eliminating factors for selecting pipelines, but consideration was given to the limitation of the equipment capacity. For instance, long and large pipes could be tested if it is known that the leakage is small. To be considered as a bulk transfer line, a minimum diameter of 200mm was set, and the pipe function was confined to pipes transferring water between two points.

e) It must be possible to take the pipeline out of operation for the duration of the test. Although the test duration is short, the pipeline flow must be stopped and supply will be interrupted.

From the above list, it is clear that the pipe properties required for a successful test are realistic, and a large number of pipes in the field should be suitable for this type of testing. With the pipeline requirements set, the next step was to identify and approach pipe owners.

3.3.2 Identifying Suitable Pipelines for Testing

An unpopulated spreadsheet was compiled to specify every potential pipeline. The spreadsheet would list the basic pipeline properties, the pipeline location, its owner and the contact details of the person with whom access could be arranged. The next step was to approach various pipeline owners and identify pipes to populate the spreadsheet with.

3.3.2.1 Department of Water and Sanitation Pipelines

The DWS implements bulk transfer projects on a regular basis, and it was initially anticipated, that a number of pipelines meeting the criteria listed in paragraph 3.3.1 would be on offer at DWS. The student, in his position as an employee at the Department of Water and Sanitation (DWS), first approached officials in the department on a national and regional level.

After contacting a number of officials in the various clusters, it was realised that, even though the DWS implements a number of bulk pipeline installations, it is not responsible for operating and maintaining most of these bulk-pipeline schemes.

Irrespectively, the operations personnel in the various clusters across the country were enquired about pipes meeting the criteria, and a number of short pipe sections were identified. These pipes mainly consists of short pipes from dam outlets up to connections points, where bulk transfer systems, which are operated by water boards, carry the flow further.

The pipes that were proposed were scattered across the country, with large distances between the potential pipes sections. It was decided not to investigate these pipes, due to the extensive travel requirements in comparison to the number of pipes that could be tested.

Other than the relatively short pipes on dam outlet works, the only bulk transfer systems that remain under operation and maintenance by DWS, are the Usutu-River, Usutu-Vaal and Komati Government Water Schemes, as well as the Vaal River Eastern Sub-System Augmentation Scheme, all of which are located in the Mpumalanga Province. These are large bulk schemes with pipelines ranging between a minimum of 900 mm up to 1.9 m in diameter, with long lengths exceeding 10 kilometres between isolation valves, and high pressures exceeding 30 bar.

Even though it was possible to arrange for short down-time periods and testing of these pipelines, it was decided that they would not be tested for the purpose of this study. The reasons were the location of the pipes from Pretoria, which is more than 200 km away; the fact that a 150 mm flanged connection piece would need to be purchased to replace existing air valves with a connection point; as well as the capacity constraint of the equipment.

Due to the limited pipes available at the DWS, water boards and municipalities where approached for alternative pipe sections.

3.3.2.2 Water Boards

Even though the bulk water transfer infrastructure remains the property of the DWS, most of the operation and maintenance services of bulk transfer systems, including bulk storage dams, have been delegated to water boards. There are 15 water boards across South Africa, and their mandate it to provide water services to water service institutions (DWS, n.d.), such as municipalities and other bulk water users.

A number of water boards were approached, and varied levels of cooperation was received. Responses to emails were seldom, prompting the student to telephonically identify responsible persons to enable discussions. If discussions were favourable, further arrangements were made via email.

Little support was received from the water boards. Further attempts to gain access to water boards in the vicinity of Gauteng were made, due to the favourable location and abundance of pipes suiting the

testing requirements. A meeting was arranged with the responsible persons at Rand Water, but unfortunately they were not keen to take pipes out of operation for the duration of the test.

3.3.2.3 Municipalities

In the large metropolitan areas, bulk water is supplied to municipalities by the water boards, who then distribute this water to the end-users. Both Tshwane Water and Johannesburg Water were initially approached.

The City of Tshwane reacted favourably and offered a number of pipelines suiting the requirements. A meeting was held with the operational staff, and an artisan was assigned the responsibility of assisting with the organisation of the tests.

In addition to approaching municipalities directly, consultants, who were contracted to municipalities were also approached. One of the consultants, namely Ceenex Consulting, reacted favourably to the enquiry and made arrangements with the Thembisile-Hani Local Municipality in the KwaMhlanga region in Mpumalanga for their pipelines to be made available for testing. The consultant and the municipality were enthusiastic to assist, and a meeting was arranged to discuss the proposed pipes. The proposed pipes met the testing requirements, and further arrangements were made for conducting the pipe tests.

3.4 Testing Procedure

When arriving on site to test a particular pipeline, the following procedure is proposed for setting up the equipment. It is recommended that the schematic of the equipment (Figure 3-2) is viewed alongside the explanation of the testing procedure.

a) **Identify the ideal connection point:**

   Any type of pipe access between 15 mm and up to 100 mm in diameter, can be utilised as a connection point, because a wide range of adaptable fittings are available. If no dedicated connection points are available on a pipeline, installed components, such an air valve, can be replaced with a connection point.

   The best connection point is, however, at the highest elevation on the pipeline. The pressure range added by the PCAE must be as high as possible, so that a curve can be accurately fitted to the plotted data. It must therefore start at a low pressure, and add as much pressure as possible, within the limitations of the pipe strength and the equipment capacity. At the highest

point, the static head in the pipe is at its lowest, meaning that the PCAE can utilise its full capacity to add the most pressure.

Connection points that are already fitted with isolation valves are ideal, as they can be connected to, without any water leaving or air entering the pipe.

b) Fill the water tank:

Once the PCAE has been transported to the identified connection point, the PCAE hose is connected using the most suitable fitting. The other end of the hose is then connected to the water tank of the PCAE, allowing the tank to be filled from the pipeline.

If the pipeline connection point is fitted with an isolation valve, the connection of the pipe and the tank filling can be achieved while the pipe is in operation. However, if no isolation valve is fitted at the connection point, the pipeline must be stopped and depressurised first.

c) Setup the PCAE:

While the tank is being filled, the PCAE can be setup. This includes the levelling of the pump unit using the built-in scissor jack levelling mechanism, as well as the connecting of the equipment to a power source, which can be the portable petrol generator, should an alternative power source not be available. Once the PCAE is powered, the data recorder can be activated and set to start recording the pressure and flow data.

Once the tank is full, the hose is removed from the coupling leading to the tank, and connected to the delivery coupling of the pump unit. The pressure in the pipeline can now be observed.

d) Close isolation valves and start pump:

The downstream isolation valve on the test pipe must be closed first, to ensure that the pipeline remains under pressure and no air is able to enter the pipe.

Then, while the upstream valve is being closed, the pump can already be started. No flow from the PCAE will enter the pipe until the pressure in the pipe drops to a level lower than the capacity of the pump (approximately 40 metres). The valve for circulating the flow back into

the supply tank must, however, be open, in order to prevent a no-flow condition, under which the pump would automatically switch off.

The pressure in the pipeline must then be observed. If the pressure remains constant, it means that the pipe has no leakage, or the upstream valve does not seal. To test whether the pressure is maintained through a leaking upstream valve, flow must be released from the pipe until the pressure drops. If the pressure recovers after the flow has been released, it is clear that the upstream valve is not sealing. If the reduced pressure is maintained, it is clear that the pipe is not leaking.

If, however, the pressure immediately drops when the upstream valve is closed, the pipe is suspected of leaking. As the pressure drops and the pipe pressure approaches the maximum pump pressure (approximately 4 bar), the valve for circulating the flow back into the supply tank must be closed. The pump and VSD will then maintain the pressure in the test pipe by adapting the pump speed to generate a constant flow rate equal to the leakage rate.

The maximum pressure that can be maintained by the PCAE is determined by the leakage flow rate. Approximately 4 bar can be maintained if the pipeline leakage is low. If the leakage is high, it can be expected that the equipment will not be able to achieve the desired maximum pressure, due to capacity constraints. In such cases, a reduced maximum pressure will be acceptable as a starting point.

If no significant pressure can be added at all, it means that there is a large leak that requires urgent attention, or one of the isolation valves are not sealing. If this situation is encountered, it is advised that the isolation valves are jerked slightly, while the pressure is observed. If any change in pressure is witnessed, the likelihood is high that the valve is not sealing.

e) Vary the pressure in the pipeline:

If the pipe is leaking and the PCAE pump is maintaining a set maximum pressure at a stable flow rate, the pressure setting on the pump control unit can be reduced by suitably sized increments to achieve a range of pressure-flow points which characterise the leak. In most cases, 0.5 bar increments are appropriate. For each incremental pressure drop, the pump will slow down to match the reduced leakage flow rate required at the lower pipe pressure. It is important that the flow and pressure is allowed to stabilise for each point.

Once the pressure has stabilised at the lowest setting, the pressure setting is increased by equal increments. This process can be repeated until the water in the tank is depleted. It is

recommended that the test be run through at least two cycles of dropping and increasing the pressure. Should the tank empty before this has been achieved, the tank filling procedure must be repeated, which requires the upstream isolation valve of the pipeline to be opened again.

Once the above steps have been completed, the equipment can be disconnected and disassembled. The pressure and flow data is continuously logged and stored for the whole testing period, and can now be transferred to a PC for processing.

3.5 Data Processing

3.5.1 Overview of the Approach Followed

One of the goals of this study, is to test the effectiveness of pressure testing as a technique to assess leakage in pipelines in the field. For this technique to be effective, the processing of data should be simple, quick and require little input from the equipment user. It was therefore decided to develop a user friendly Excel workbook template with automated functions, which simplifies data processing and reduces processing time.

The development of this workbook, therefore, not only has the purpose of processing the data obtained in this study, but it also aims to demonstrate, that the characteristics of a pipeline can be determined in minimal time and with minimum effort, following a successful test in the field.

The Excel workbook template also serves as the test report. Once the template has been populated, it can be printed in the form of a document that contains all the relevant test information. The test report consists of ten sheets, and is structured as follows:

- Following the cover page, table of contents and list of constants, a spreadsheet with all the equipment detail and specifications is presented. These sheets remain the same for all the tests.

- The next three sheets provide a short description of the pipe and testing procedure, as well as a detailed list of the pipe information and specifications. The elevation profile of the pipe is also included.

- The next set of sheets present the collected data. The first sheet of these sheets imports and plots the pressure and flow data against time. It then assists the user to identify the converged flow values which were required to maintain the various set pressures. These pressure and flow data points are then recorded and transferred to the next sheet.

- The pressure values of the various nodes are then calculated by correcting the recorded pressure values at the test point with the estimated elevation differences, minor losses and friction losses up to the respective nodes.

- Finally, the corrected pressure and flow data is used to estimate the N1 and FAVAD equation parameters. A short analysis of the obtained results concludes the test report.

The methods used for processing the data, as well as more detail on the functioning of the active Excel workbook, are discussed in the next paragraphs.

3.5.2 Converting and Importing the Raw Data

The data from the ABB data logger must first be converted to a format that can be imported into an Excel workbook. *DataManager Pro* is software that has been developed by ABB for viewing, analysing and converting data from its data recorders.

For each test, the data is transferred from the data recorder to a PC with a SD-card. It is then opened with the *DataManager Pro* software, with which the whole data range can then be viewed. The desired data range must then be selected and converted into Excel format. Due to the large amount of data often recorded during tests in the field, it is recommended that only the relevant data is carefully selected for each test cycle, in order to minimise the resulting Excel spreadsheet size.

The data is then imported into the Excel workbook for further processing. As shown in the Figure 3-4, the macro-enabled Excel worksheet has an import function, which allows the user to easily import and format the selected test data in minimal time and with minimal effort.

By selecting the *"Import Data"* button, a File Explorer window opens and prompts the user to select a file containing the desired test data. An Excel sheet, that was creating using *DataManager Pro*, must be then be selected. The data will then be transferred into the spreadsheet, as time (in milliseconds), flow (in litres / minute) and pressure (in bar).

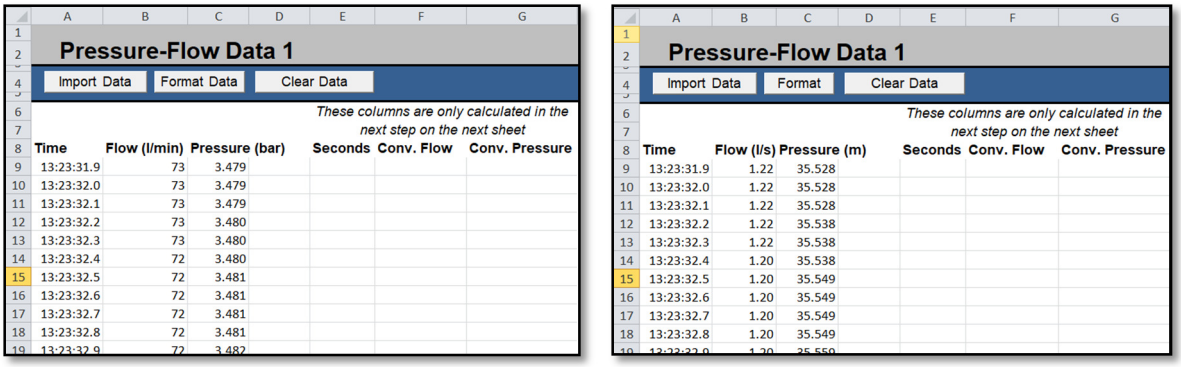

Pressure-Flow Data 1

Import Data | Format Data | Clear Data

These columns are only calculated in the next step on the next sheet

Time	Flow (l/min)	Pressure (bar)	Seconds	Conv. Flow	Conv. Pressure
13:23:31.9	73	3.479			
13:23:32.0	73	3.479			
13:23:32.1	73	3.479			
13:23:32.2	73	3.480			
13:23:32.3	73	3.480			
13:23:32.4	72	3.480			
13:23:32.5	72	3.481			
13:23:32.6	72	3.481			
13:23:32.7	72	3.481			
13:23:32.8	72	3.481			
13:23:32.9	72	3.482			

Pressure-Flow Data 1

Import Data | Format | Clear Data

These columns are only calculated in the next step on the next sheet

Time	Flow (l/s)	Pressure (m)	Seconds	Conv. Flow	Conv. Pressure
13:23:31.9	1.22	35.528			
13:23:32.0	1.22	35.528			
13:23:32.1	1.22	35.528			
13:23:32.2	1.22	35.538			
13:23:32.3	1.22	35.538			
13:23:32.4	1.20	35.538			
13:23:32.5	1.20	35.549			
13:23:32.6	1.20	35.549			
13:23:32.7	1.20	35.549			
13:23:32.8	1.20	35.549			
13:23:32.9	1.20	35.559			

Figure 3-4: Workbook Screenshot of Data Import Function

The "*Format"* button is linked to a VBA programme that converts the flow and pressure from litres per minute and bars, to litres per second and metres head, respectively.

3.5.3 Calculating Pressure-Flow Data Points

The pressure and flow data over time is plotted in the Excel workbook by selecting the *"Plot Graph"* button on the spreadsheet depicted in Figure 3-5. The programme automatically aligns the pressure access on the right, to the flow axis on the left to clearly illustrate the relationship between pressure and flow with time.

The time is plotted in seconds, starting at 0 seconds for the first data point on the imported data set. When *"Plot Graph"* is selected, the whole data set of the imported data is initially plotted. By selecting *"Set Data Range"*, the programme prompts the user for the start and end time of the desired data range. Figure 3-5 illustrates an example, where the data has been plotted and the range selected, resulting in a clear plot, with only the relevant test data on display.

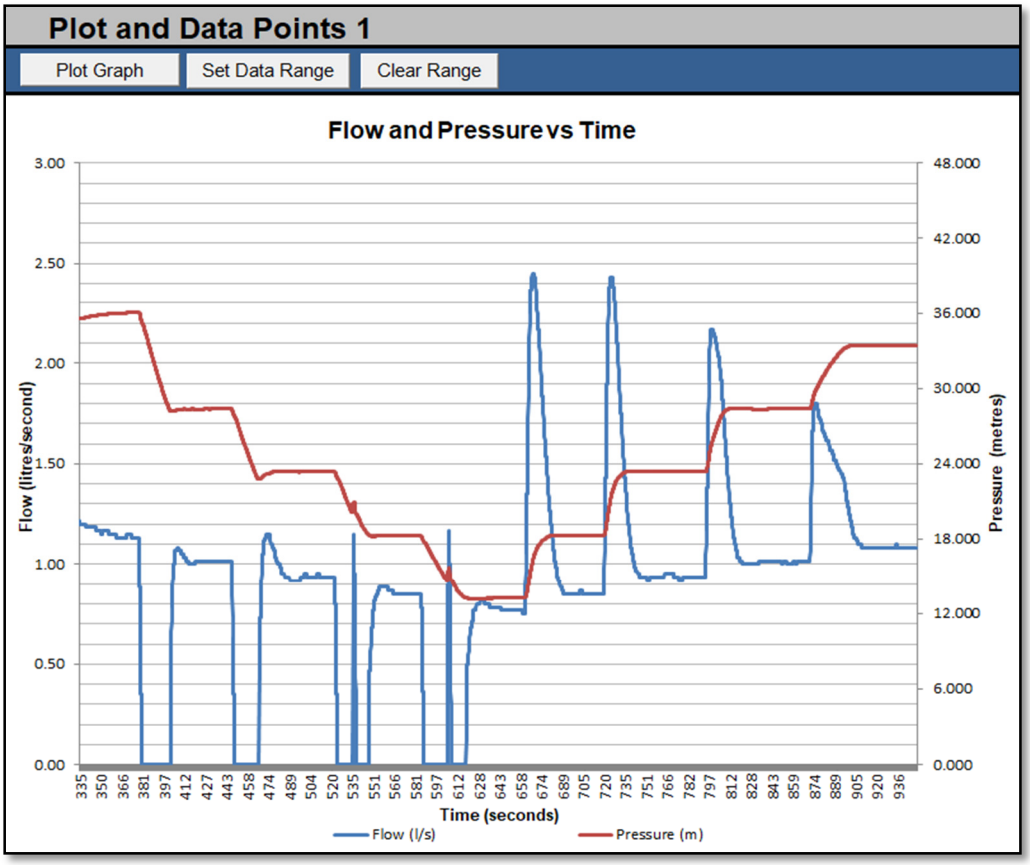

Figure 3-5: Pressure vs flow plot in Excel workbook, before calculation of average data points

The plot provides the user with a good overview of the test, as well as the different pressures at which the flow was measured. Now, a single flow versus pressure value must be derived for every pressure setting. To determine the pressure and its corresponding flow value, the average pressure and average flow must be calculated for every pressure setting, but only after the readings have stabilised.

Due to irregular fluctuations in the flow, as well as varying times required for convergence, user judgement is required to determine the most appropriate range over which the averages must be calculated. A tool has therefore been programmed and incorporated into the Excel workbook to assist the user with identifying these points.

Figure 3-6 is a screenshot of the tool in the workbook. The start and end time of the data range, which was recorded for a single pressure setting, is requested. The approximate times can be read off the graph in Figure 3-5.

The programme then plots the specific range on separate plots for both pressure and flow. The user must then apply his/her judgement to decide which part of the range best reflects steady and converged readings. By selecting the *"Calculate & Plot"* button, the programme calculates the average flow and pressure over this range and plots the result on the two graphs.

If the user is satisfied that the average value accurately follows the trend of the recorded readings, the *"Record Point"* button can be selected. The average flow and pressure will then be recorded as a data point, and the values will be plotted on the main pressure and flow plot of Figure 3-5. Figure 3-7 depicts an example of the resulting plot, once all the data points have been calculated and plotted.

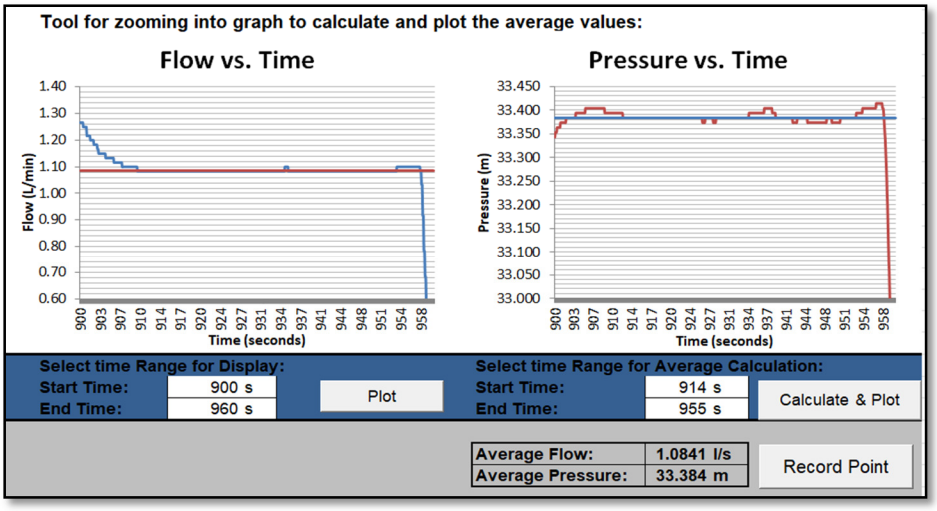

Figure 3-6: A built-in tool in the Excel workbook to determine the converged pressure vs flow data points

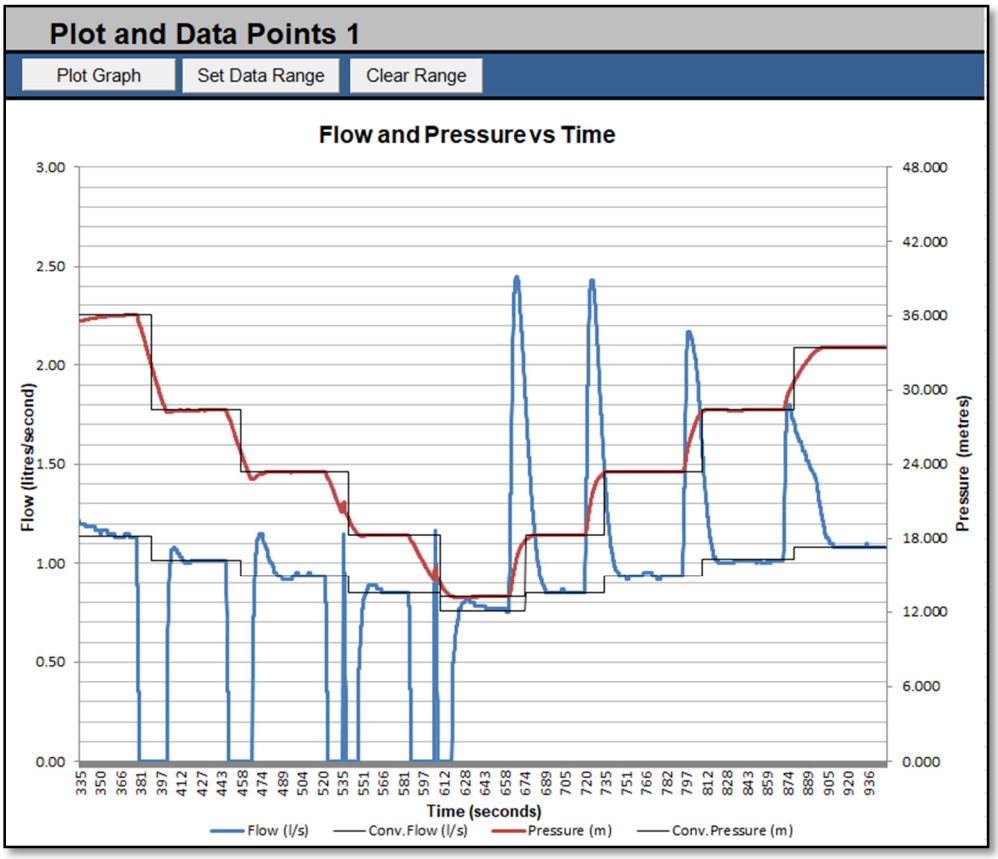

Figure 3-7: The Pressure and flow plot in the Excel Workbook, after calculation of average pressure vs flow data points

3.5.4 Correcting the Pressure at each Node

The recorded pressures on the PCAE do not accurately reflect the pressures at the leak locations, because they do not take the elevation difference, as well as the minor and friction losses, into consideration. For the leak to be accurately characterised, however, the flow versus pressure relationship must be known at the leak location.

The Excel programme has been developed to incorporate all these losses, in order to estimate the actual flow versus pressure relationship at selected node points. Figure 3-8 is a screenshot from the Excel programme, and indicates the node points along the pipeline elevation profile.

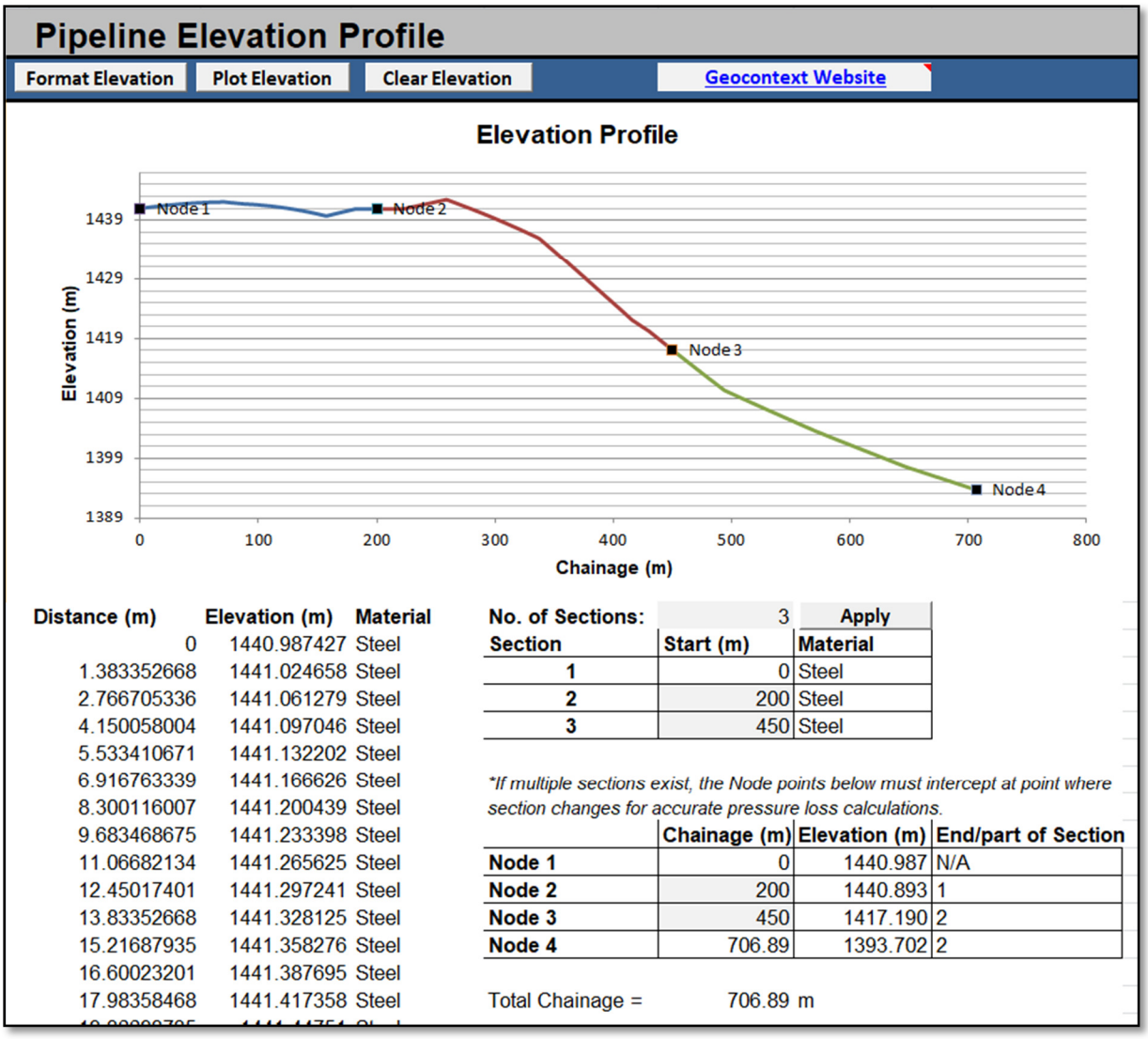

Figure 3-8: Excel workbook elevation profile and node selection example

Note that, in Figure 3-8, the pipeline can be divided into sections and nodes can applied along the length of the pipeline. Setting the pipeline sections, specifying the nodes and importing the pipeline elevation profile will be is discussed in more detail in the next paragraphs.

3.5.4.1 Separating the Pipeline into Sections

The friction and minor losses depend on the pipeline properties, which may change along the pipeline length. The Excel programme, therefore, makes provision for separating the pipe into a maximum of three different sections, which can vary in terms of pipe material, pipe diameter, minor losses and pipe roughness.

The details of these sections are inserted into a spreadsheet with general pipeline information, as depicted in Figure 3-9.

General Test Information

Pipeline:	Lynnwood Road to Koedoesnek Reservoir
Area:	Pretoria East, Lynnwood/Faerie Glen
Pipe Owner:	Tshwane Municipality
Date:	06 Jun 18
Time:	08:00 - 15:00

Pipeline Section:	Section 1	Section 2	Section 3	
Pipe length (m):	200	250	256.89	
Pipe Diameter (mm):	500	300	400	
Pipe Material:	Steel	Steel	Steel	
Absolute Roughness e (mm)	0.5	0.5	0.5	
Minor Losses/km	1	1	1	
Upstream Isolation:	Butterfly Valve			
Upstream Source:	Pressured Pipe			
Upstream Pressure (Bar) approx:	>10			
Upstream Isolation Elevation (m):	1390			
Downstream Isolation:	Pressure Reg. Valve			
Downstream Delivery:	Reservoir			
Downstream Pressure (Bar) approx:	<1			
Downstream Isolation Elevation (m):	1440			

Figure 3-9: Populated Excel spreadsheet with pipeline information, as an example.

3.5.4.2 Identifying Node Points

Nodes along the pipeline, at which the actual pressure will be estimated, must then be chosen by the user. The Excel programme requires four nodes to be specified. If the pipeline consists of more than one section, the first two or three nodes will be selected automatically to coincide with the points where the pipeline sections meet.

Nodes must either be selected at locations where leakage is expected, or, if the leak location is not known, at high and low peaks along the elevation profile. This will provide a wide spectrum of leakage characteristics, which can then assist the user with identifying possible leak locations.

3.5.4.3 Importing the Pipeline Elevation Profile

To determine the elevation of the nodes along the pipeline, a pipeline elevation profile must be obtained. If one is available, the data can be inserted directly into the Excel workbook

If, however, no elevation data is available, the spreadsheet provides a link to a free online tool called *"Geocontext"* that allows the user to obtain estimated chainages and elevation data. Figure 3-10 displays a screenshot of the online tool.

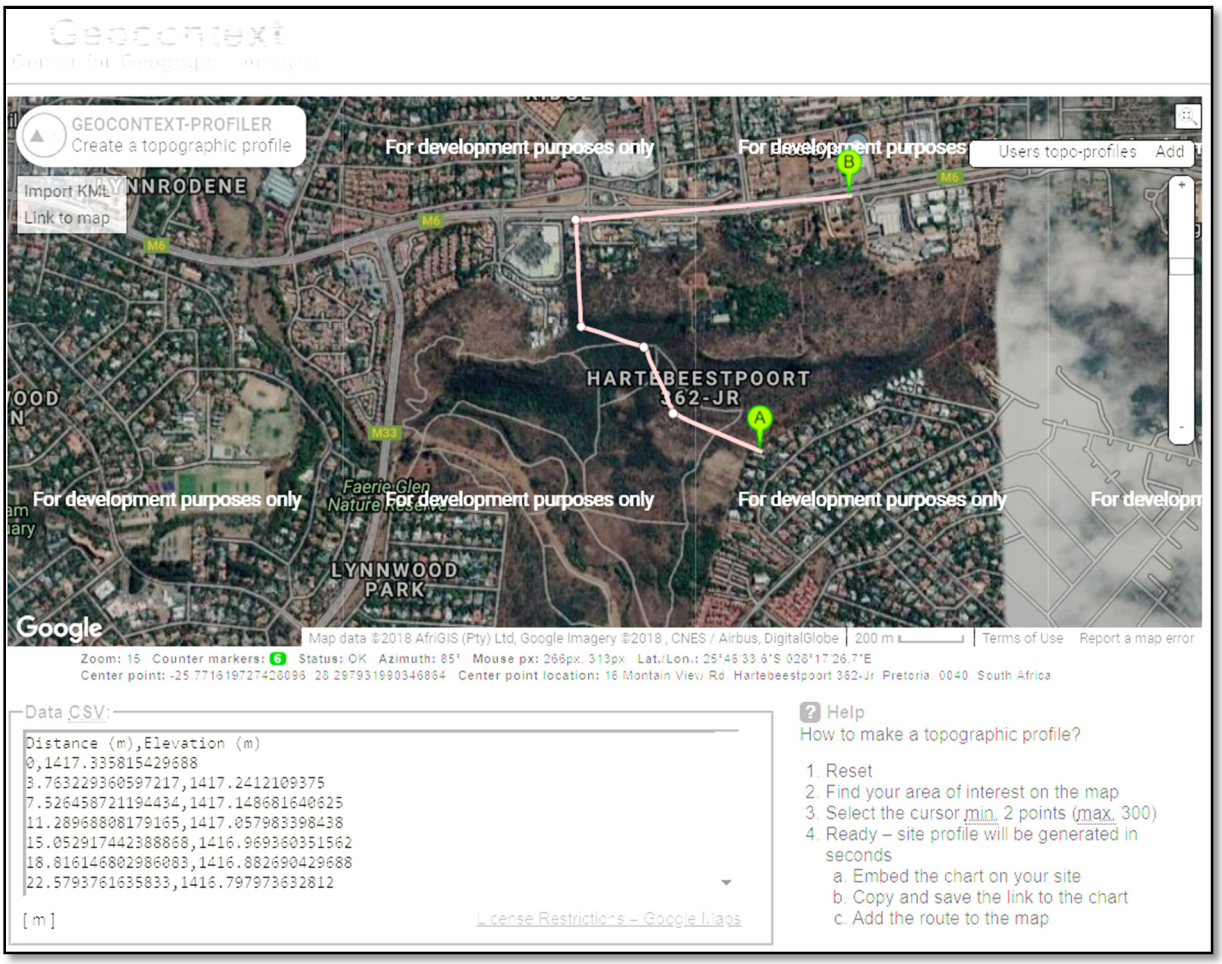

Figure 3-10: Screenshot of *Geocontext* online elevation profile tool

Once the *Geocontext* website has been opened, the user identifies the pipeline area on the satellite image, and then plots the pipeline along its route. The online tool then generates the approximate pipeline profile and displays it either as a graphic, or as a table in CSV data format. The CSV data can be copied directly from the *Geocontext* website to the Excel spreadsheet, depicted in Figure 3-8.

The CSV data separates the elevations and chainages by commas. By selecting the *"Format Elevation"* button, after pasting the data, the elevations and chainages are automatically separated into two columns. The elevation is then plotted along the pipeline chainage.

3.5.4.4 Friction and Minor Head Losses

In addition to the elevation difference, the pressure at the leak location is also influenced by friction and minor losses, which result from the flow induced into the pipe by the PCAE.

Various fittings exists downstream of the pressure transducer on the PCAE, which contribute to the head losses. The fittings on the PCAE and the fittings on the connection pipework, leading up to the main test pipe, can create significant head losses, due to the high velocities that occur in these small diameter pipes.

The Excel worksheet contains a spreadsheet that calculates all the friction and minor losses from the pressure transducer on the PCAE, all the way to the last node on the pipeline.

The Colebrook-White method (Equation 3-1) is used to calculate the friction factor, and the Darcy-Weisbach equation (Equation3-2) is then applied to calculate the head loss resulting from the friction factor. The minor losses are calculated with the Minor Loss formula (Equation 3-3).

$$\frac{1}{\sqrt{f}} = -2\log_{10}\left(\frac{\varepsilon}{3.7\,D} + \frac{2.51}{R_e\sqrt{f}}\right) \quad \textbf{3-1}$$

$$h_f = f\frac{L}{D}\frac{V^2}{2g} \quad \textbf{3-2}$$

$$h_l = K_L\frac{V^2}{2g} \quad \textbf{3-3}$$

With every pressure-flow point obtained in Paragraph 3.5.3, the implicit Colebrook-White friction factor is solved with the Excel programme, and the head losses are calculated.

Figure 3-11 shows the pressure head correction tool for calculating the corrected pressure at the PCAE connection point to the pipeline. The same table and method is repeated to calculate the friction and minor losses through the connecting pipework and through the sections of pipe between the nodes, using the properties of the respective pipe sections.

Pressure Head Correction

Calculate Friction

Calculate the Pressure as expected at the Connection Point (Node 0)

Length: 10 m
Diameter: 0.0452 m

Area: 0.0016046 m^2
Δh(static) 1.85 m

Point	Flow (l/s)	Measured Head (m)	Velocity(m/s)	Reynolds No	CW LHS	CW RHS	CW diff.	f	hf	hm	h
1	1.14	36.02	0.7096	28158.32	6.26	6.26	-8.92E-04	0.02549	0.144721161	0.50717	37.22
2	1.02	28.36	0.6336	25143.55	6.20	6.20	-3.06E-04	0.02605	0.117920793	0.40438	29.69
3	0.93	23.37	0.5817	23082.60	6.14	6.14	-1.32E-04	0.02649	0.101076477	0.34081	24.77
4	0.85	18.27	0.5297	21021.65	6.09	6.09	-5.13E-05	0.027	0.085437639	0.28266	19.75
5	0.76	13.25	0.4718	18721.37	6.01	6.01	-1.51E-05	0.02766	0.069418407	0.22419	14.81
6	0.85	18.27	0.5297	21021.65	6.09	6.09	-5.13E-05	0.027	0.085437639	0.28266	19.75
7	0.93	23.36	0.5817	23082.60	6.14	6.14	-1.32E-04	0.02649	0.101076477	0.34081	24.77
8	1.02	28.36	0.6362	25248.05	6.20	6.20	-3.18E-04	0.02603	0.118806855	0.40775	29.69
9	1.08	33.39	0.6757	26812.74	6.23	6.23	-5.64E-04	0.02573	0.132442635	0.45985	34.64
10			0.0000	0.00	5.12	#DIV/0!	#DIV/0!	0.03808	0	0	0.00
11			0.0000	0.00	#NUM!	#NUM!	#NUM!	-0.0997	0	0	0.00
12			0.0000	0.00	#NUM!	#NUM!	#NUM!	-0.1308	0	0	0.00
13			0.0000	0.00	#NUM!	#NUM!	#NUM!	-0.1618	0	0	0.00
14			0.0000	0.00	#NUM!	#NUM!	#NUM!	-0.1929	0	0	0.00
15			0.0000	0.00	#NUM!	#NUM!	#NUM!	-0.224	0	0	0.00

Figure 3-11: Screenshot of Pressure Head Correction tool in the Excel Programme

The generic Excel programme has been programmed with sufficient capacity to calculate the friction and minor losses for the following pipe sections:

- The PCAE hose, connecting the PCAE equipment to the pipeline.
- Two different connecting pipes between the PCAE connection point and the main pipeline to be tested. One or both of these pipes must be specified to define the connection point to the main pipeline. An example of such a pipe would be the branch to an air valve or scour valve.
- The main pipeline can be divided into three different pipe sections if the properties along the length of the tested section change.

Figure 3-12 shows a screenshot of the Excel tool, where the various connecting pipe and coupling details must be specified. Note that, apart from the hose coupling, the friction losses through two connection pipes, and the minor losses through four different pipe fitting types can be specified.

To simplify the operation of the Excel programme, the minor loss factors for all the adaptable hose connections in the PCAE toolbox, as well as for various standard pipe fittings, have been calculated and included in the spreadsheet. The programme user can simply select the desired coupling or fitting from a drop-down list, as displayed in Figure 3-13.

Connection of Testing Equipment

Connection Type:	Connection on PRV	
Connection Fitting size (mm):	50	
Comment on Fitting:	50mm female connection: Male threaded 50mm to 1 inch reducer. 1 inch female to male, 1 inch Geka coupling	
Minor loss coefficient of fitting	50 mm Flanged or 50 Threaded	19.66
Static height difference (A) in (m):	1.85	

Connection pipes*:

	Pipe 1	Pipe 2
Length of connection pipe* (mm):	300	
Diameter of connection pipes (mm)	50	
Absolute Roughness e (mm)	0.2	
Static height difference (B) in (mm):	800	

Minor losses of fittings on connection pipes*:

	Fitting 1	Fitting 2	Fitting 3	Fitting 4
Fitting type:	Butterfly valve	Instant diffuser	None	None
Pipe 1 or Pipe 2	1	1	1	1
Fitting diameter in (mm):	50	50	0.05	0.05
Fitting diameter out (mm):	50	400	0.05	0.05
Absolute Roughness e (mm)	0.5	0.5	0.5	0.5
No. of fittings:	1	1	1	1
Fitting Minor Loss Coefficient:	1.3266	0.9690	0.0000	0.0000
			SUM:	2.29562

** Pipes and Fittings between the connection point and the main pipeline*

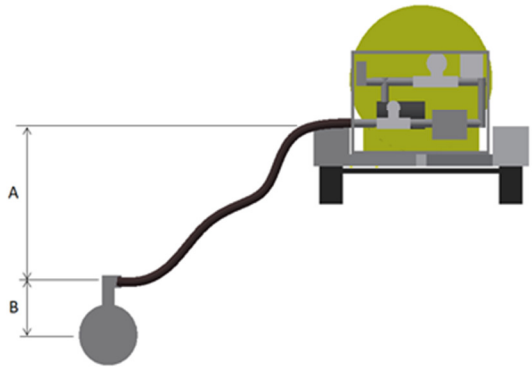

Figure 3-12: A screenshot of the Excel spreadsheet where the connecting pipework is specified

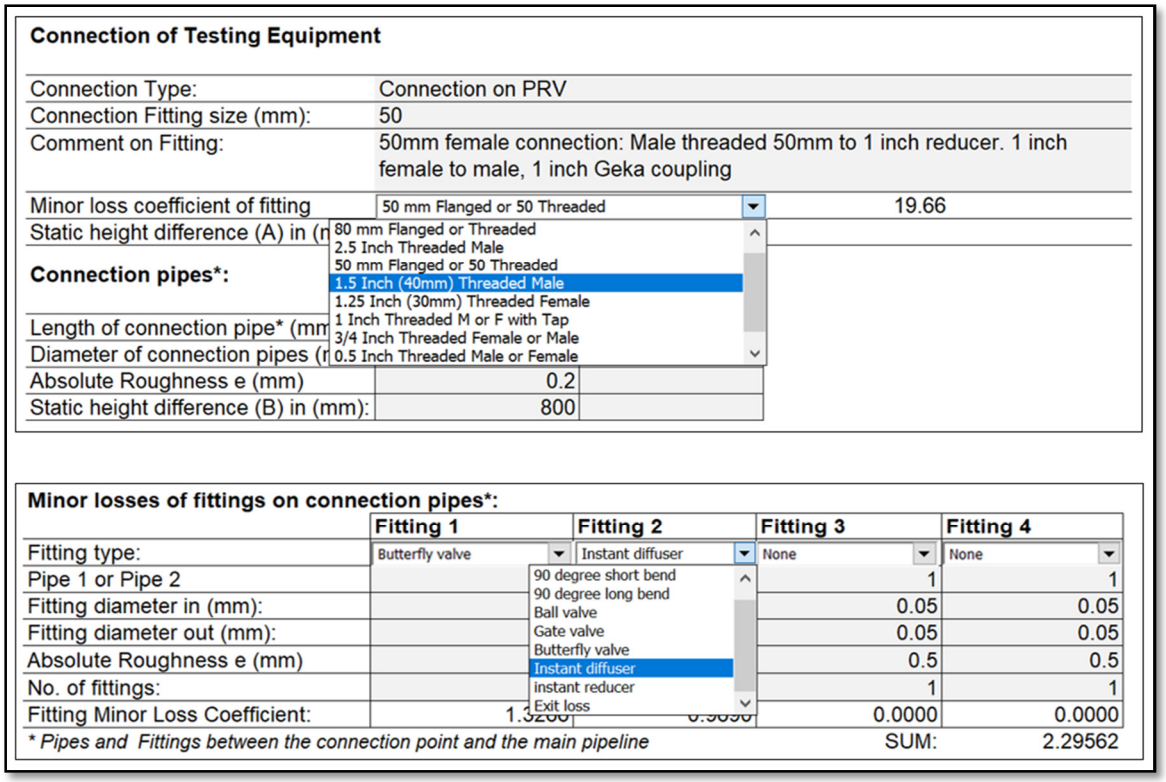

Figure 3-13: The selection of the connection coupling and pipe fittings in the Excel programme

3.5.4.5 Calculating Minor Loss Coefficients

The minor loss coefficients for various fittings commonly encountered in the field, as well as for all the pipe connection point adaptors, are calculated in the Excel programme. For general pipe fittings, the CRANE Nuclear "*General Engineering Information*" (2013) guideline for minor loss coefficients provided the loss coefficients as listed in Table 3-2.

Table 3-2: Minor Loss Coefficients from CRANE Nuclear *General Engineering Information* (CRANE Nuclear, 2013)

90 degree short bend	$K_l = 20f_T$
90 degree long bend	$K_l = 12f_T$
Ball valve	$K_l = 3f_T$
Gate valve	$K_l = 8f_T$
Butterfly valve	$K_l = 35f_T$
Exit loss	$K_l = 1$
Where $f_T = \frac{0.25}{\left[log\left(\frac{\varepsilon/D}{3.7}\right)\right]^2}$	

From the *Fluid Mechanics* text book by F. White (2008), the following equations were applied for sudden expansions and contractions. Note that, with both equations, for calculating the resulting pressure loss, the velocity in Equation 3-3 refers to the velocity in the smaller pipe.

- For sudden expansions:

$$K_{se} = \left(1 - \frac{{D_1}^2}{{D_2}^2}\right)^2 \qquad \textbf{3-4}$$

- For sudden contractions

$$K_{sc} = 0.42\left(1 - \frac{{D_2}^2}{{D_1}^2}\right) \qquad \textbf{3-5}$$

For the various connection point adaptors, the minor loss coefficients of all the reducers and diffusers that make up the adaptor were combined into one coefficient for the complete adaptor. Figure 3-14 illustrated how the adaptor can be componentised into sections, with each change in diameter regarded as an expansion or contraction. Equations 38 to 39 were then applied to calculate the cumulative K factor.

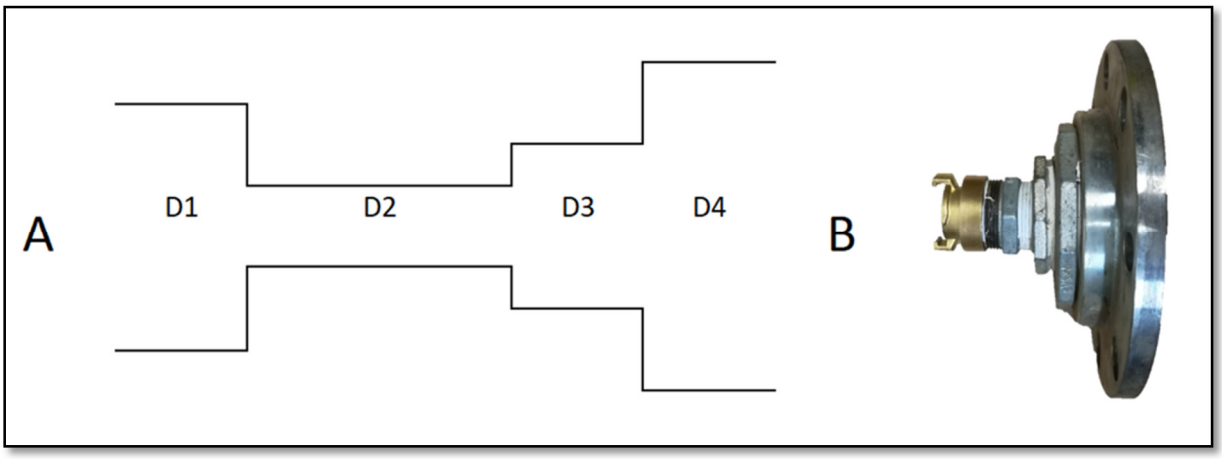

Figure 3-14: Diagram showing how a connection coupling was dissected into components for calculating minor losses between point A and B.

In the illustration of Figure 3-14, D1 represents the flexible 50mm hose, D2 represents the quick coupling and D3 up to D4 represent the expansion or contractions between the coupling and the connection point. If D3 is very short, it was often neglected and the assumption was made that D2 expands directly to D4.

The K-factors for every section, however, relate to different diameters. In order to calculate K-factors that can be added together, all factors must relate to the same pipeline diameter. Therefore, to combine the K-factors of Figure 3-14, the following derivation was applied:

- First, Equation 3-3 is expanded to include the Equations 3-4 and 3-5.

$$h_l = K_{Combined}\frac{v^2}{2g}$$

$$h_l = \frac{{V_1}^2}{2g}\left(\frac{f_1 L_1}{D_1}\right) + \frac{{V_2}^2}{2g}\left(\frac{f_2 L_2}{D_2} + K_{sc} + K_{se}\right) + \frac{{V_3}^2}{2g}\left(\frac{f_3 L_3}{D_3} + K_{se}\right) + \ \ldots$$

$$\therefore h_l = \frac{{V_1}^2}{2g}\left(\frac{f_1 L_1}{D_1}\right) + \frac{{V_2}^2}{2g}\left(\frac{f_2 L_2}{D_2} + 0.42\left(1 - \frac{{D_2}^2}{{D_1}^2}\right) \ + \left(1 - \frac{{D_2}^2}{{D_3}^2}\right)^2\right) + \frac{{V_3}^2}{2g}\left(\frac{f_3 L_3}{D_3} + \left(1 - \frac{{D_3}^2}{{D_4}^2}\right)^2\right)$$

- Then, the velocity is written as a function of the pipe diameters:

$$V_2 = \frac{V_1 A_1}{A_2} = \frac{V_1 D_1^2}{D_2^2}, \ \ V_3 = \frac{V_1 A_1}{A_3} = \frac{V_1 D_1^2}{D_3^2}$$

$$\therefore h_l = \frac{{V_1}^2}{2g}\left(\frac{f_1 L_1}{D_1}\right) + \frac{{V_2}^2}{2g}\left(\frac{f_2 L_2}{D_2} + 0.42\left(1 - \frac{{D_2}^2}{{D_1}^2}\right) \ + \left(1 - \frac{{D_2}^2}{{D_3}^2}\right)^2\right) + \frac{{V_3}^2}{2g}\left(\frac{f_3 L_3}{D_3} + \left(1 - \frac{{D_3}^2}{{D_4}^2}\right)^2\right)$$

$$\therefore h_l = \frac{{V_1}^2}{2g}\left(\left(\frac{f_1 L_1}{D_1}\right) + \left(\frac{D_1}{D_2}\right)^4\left(\frac{f_2 L_2}{D_2} + 0.42\left(1 - \frac{{D_2}^2}{{D_1}^2}\right) \ + \left(1 - \frac{{D_2}^2}{{D_3}^2}\right)^2\right) + \left(\frac{D_1}{D_3}\right)^4\left(\frac{f_3 L_3}{D_3} + \left(1 - \frac{{D_3}^2}{{D_4}^2}\right)^2\right)\right)$$

$$\therefore K_{Combined} = \left(\frac{f_1 L_1}{D_1}\right) + \left(\frac{D_1}{D_2}\right)^4\left(\frac{f_2 L_2}{D_2} + 0.42\left(1 - \frac{{D_2}^2}{{D_1}^2}\right) \ + \left(1 - \frac{{D_2}^2}{{D_3}^2}\right)^2\right) + \left(\frac{D_1}{D_3}\right)^4\left(\frac{f_3 L_3}{D_3} + \left(1 - \frac{{D_3}^2}{{D_4}^2}\right)^2\right)$$

3-6

The 50mm hose coupling (D1), with an internal diameter of 45.2mm is, therefore, a common reference to all the pipe couplings. Note that the friction factor, which is included in the combined K-factor formula (3-6), changes with velocity. The Excel programme takes this into account, and the K-factors therefore vary depending on the test.

3.5.5 Analysis of the Data using the N1 and FAVAD approach

Once the pressure data has been corrected for each node, the leak at the node can be analysed. Two methods are applied in this study. The N1 equation is used to characterise the pipeline empirically, and the FAVAD equation is used as a fundamental approach. For each test, the leakage will be briefly investigated with the empirical N1 method, after which a more in-depth investigation will follow, using the fundamental FAVAD approach.

3.5.5.1 Applying the N1 Concept

As discussed under Paragraph 2.8.4.1 in the Literature Review, the N1 equation provides an empirical relationship between leakage and pressure. The N1 equation (Equation 2-22) is in the form of a power function, with two unknowns, namely the N1 leakage coefficient (C_{N1}) and the N1 exponent.

For the N1 approach, the flow rate is simply plotted against the corrected pressure head, and a trend-line for a power function is applied to the plotted data. The R-squared value is then calculated to determine how accurately the trend-line represents the recorded data. By eliminating points that are clearly outliers, the fitment of the trend-line can be significantly improved. The resulting exponent is then recorded as the N1 value of a potential leak occurring at the respective node.

The N1 exponent for the potential leak at every node is then compared to N1 values that have been recorded under similar conditions, and for similar pipe materials, in previous studies. Certain leak types, and their corresponding N1 values, can then be anticipated. By comparing the N1 values obtained at every node with the anticipated N1 value, the likelihood of the potential leak existing at the respective node can be determined.

3.5.5.2 Applying the FAVAD Equation Concept

The FAVAD equation (Equation 2-14), which is discussed in detail in Paragraph 2.8.3, characterises the leak in terms of its initial leak area (A_0), its head-area slope (m) and its FAVAD leakage coefficient (C_d). The equation is repeated below:

$$Q = C_d\sqrt{2g}(A_0H^{0.5} + mH^{1.5})$$

The pressure-flow data points are first converted to effective leak area versus pressure head points. To convert the flow measurements to effective areas, Equation 2-9 in Paragraph 2.8.2 can be re-written as Equation 3-7 below:

$$C_dA = Q/\sqrt{2gH} \qquad \textbf{3-7}$$

The effective area is calculated for every flow-pressure point, and is then plotted against the pressure head. According to the FAVAD theory, for elastic conditions, it is expected that a linear relationship exists between the effective leak area and the pressure head. A trend-line for a linear function is therefore applied to the plot.

Similarly to the N1 concept approach, outliers are identified and removed in order to ensure a high r-squared value for the trend-line. The intercept on the effective area axis at zero pressure head is then recorded as the initial effective leak area, and the gradient of the trend-line is recorded as the effective head-area slope.

The FAVAD parameters are then compared to previous studies in the field, and the node with the most probable parameters – taking into consideration the pipe type and material – is then identified as the node closest to which a leak potentially exists.

Figure 3-15 displays a screenshot from the Excel workbook. In the screenshot, the N1 and FAVAD plots are included for Node 1 only. The combined FAVAD plots for all four nodes are displayed in Figure 3-16. From this plot, the node with the most probable FAVAD parameters can be identified.

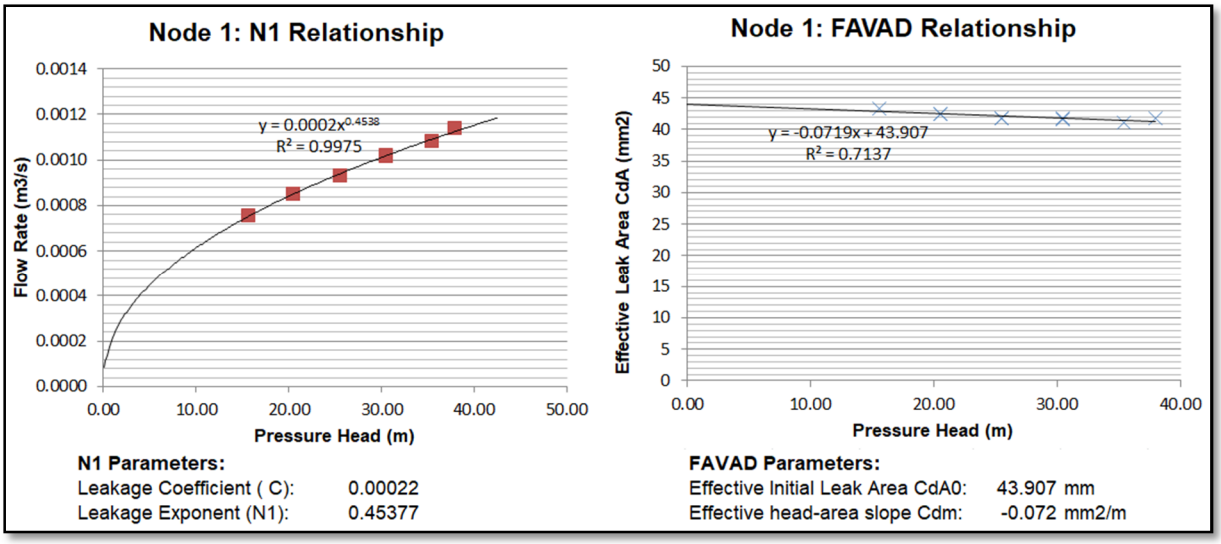

Figure 3-15: Example from Excel workbook, indicating the N1 and FAVAD Equation plots for Node 1

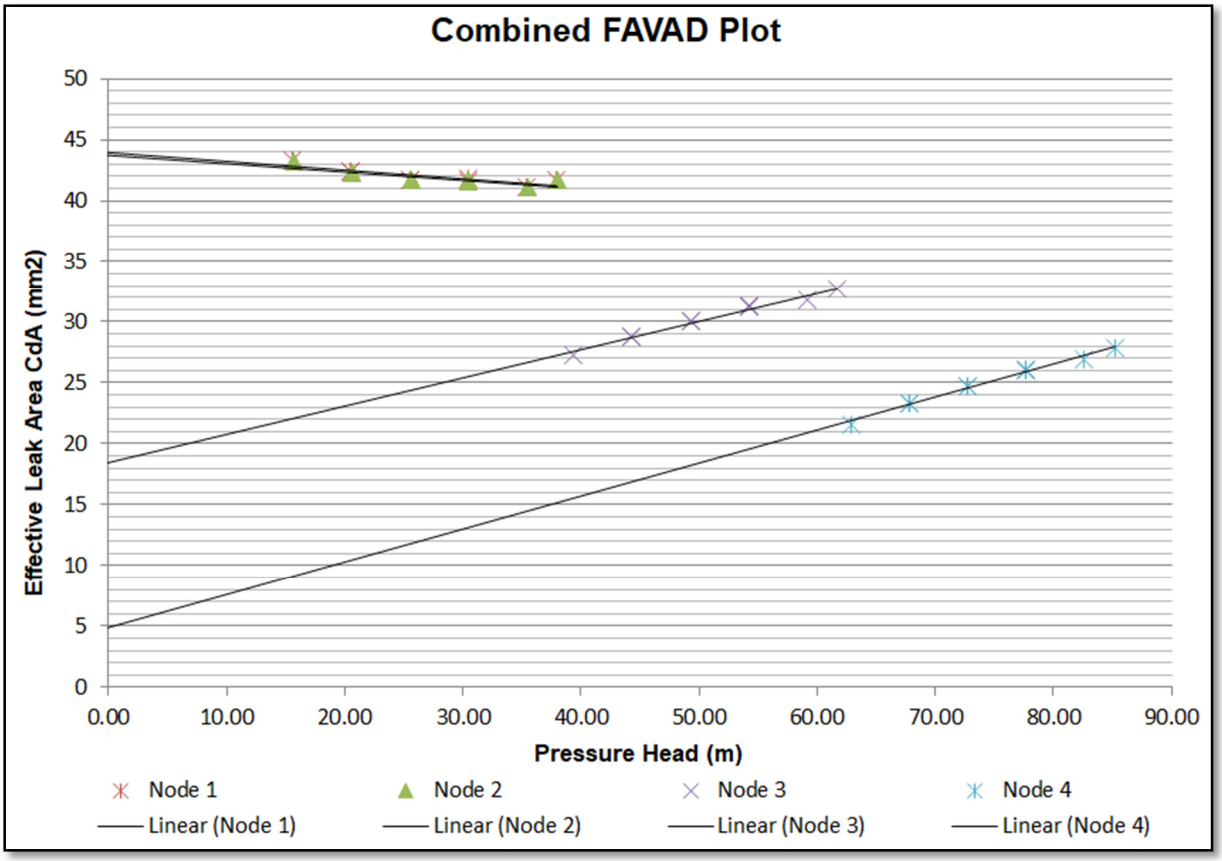

Figure 3-16: A Screenshot from the Excel workbook, displaying the combined FAVAD plots for all four nodes.

3.5.6 Pressure Drop Analysis

The flow that is required to maintain pressure in the pipe is often lower than the minimum flow that the flow meter can measure. In these cases, a pressure drop test is performed, and the drop in pressure is recorded with time. Any leak, no matter how small, will lead to the pressure in an isolated pipe dropping over time, and by measuring both the time and the drop in pressure, the leak can be characterised.

In a study by R. Nsanzubuhoro (2018), a formula is derived that can be applied to interpret the pressure drop with time data. This comprehensive formula takes the variation of the pipe diameter into account, which subsequently results in changes in the pipe volume. This occurs due to the varying pipe wall strains that result from the pressure changes.

Equation 3-8 is derived from the conservation of mass principle, and the leakage is characterised by the modified orifice equation.

$$h(t) = \frac{A_0'}{m}\tan^2\left[\frac{\sqrt{m'}\sqrt{A_0'}}{2}\left(-\left(\frac{C_d\sqrt{2g}}{\rho g V_0\left[\frac{d_0}{bE}\left(\frac{5}{4}-v\right)\right]+\frac{1}{K}}\right)t + C(m', A_0')\right)\right] \quad \textbf{3-8}$$

R. Nsanzubuhoro uses a numerical approach, based on the conservation of mass formula, to verify the derived equation. R. Nsanzubuhoro explains the numerical approach as follows.

Firstly, the conservation of mass formula can be simplified by removing the term for mass entering the pipe, as mass will only exit the pipe at the leak.

$$\dot{M}_{in} - \dot{M}_{out} = \frac{\delta M}{\delta t} \quad \rightarrow \quad -\dot{M}_{out} = \frac{\delta M}{\delta t} \quad \textbf{3-9}$$

Now, the mass flow rate can be written in terms of the volumetric flow rate:

$$-Q_{out}\rho = \frac{\delta M}{\delta t} \quad \textbf{3-10}$$

The volumetric flow rate equals the leakage exiting the pipe, and can therefore be written in the form of the modified orifice equation: $Q = C_d\sqrt{2g}(A_0H^{0.5} + mH^{1.5})$).

The following formula was derived by R. Nsanzubuhoro to calculate the pipe volume as a function of pressure, by taking the expansion and contraction of the pipe into account:

$$V = \frac{\pi d^2}{4} l\left[2\varepsilon_{circ} + \varepsilon_{long} + 1\right]$$

3-11

In the above formula, l is the length of pipe, and d is the internal diameter. By applying Hooke's law, the strain can be written in terms of the internal pipe pressure and the Modulus of Elasticity (E). Also, by simply dividing the volume with density, the mass can be obtained:

$$M = \frac{\pi d^2}{4} l\left[\left(\frac{5\rho g d}{4bE} - \upsilon\frac{\rho g d}{2bE}\right)h + 1\right]\rho$$

3-12

The mass, however, is a function of time. By applying the conservation of mass formula (Equation 3-10), the mass can be written as Equation 3-13 below:

$$M_j = M_0 - \sum_{j=0}^{n} (Q_{out}\rho)_j \ \delta t$$

3-13

In this equation, M_0 represents the initial mass at time zero, and is calculated with Equation 3-12, by setting h to h_0. Then, by rearranging Equation 3-12, so that h becomes the subject of the equation, R. Nsanzubuhoro derived the following equation for the pressure head in terms of the mass in the pipe.

$$h(M_j) = h_j \ = \frac{4bE}{\rho g d_0\,(5 - 2\upsilon)}\left[\left(\frac{M_j}{\rho V_0}\right) - 1\right]$$

3-14

In order to apply the above theory, the FAVAD equation parameters are first assumed, and then used to calculated the flow rate corresponding to the recorded pressure for every time step. After solving Equation 3-12 for the initial mass, Equation 3-13 is then calculated for every time step, in order to obtain the remaining mass in the pipe. The corresponding pressure head is then calculated with Equation 3-14, and plotted alongside the recorded pressure head.

By adjusting the initially assumed FAVAD parameters, the parameters can be optimised until the resulting pressure head behaviour best resembles the recorded pressure head behaviour. The resulting flow rate can then be plotted against the recorded pressure, from which relation the N1 value can be obtained.

3.6 Experimental Observations

3.6.1 Factors Eliminating Pipelines from the Leak Characterisation Test

Even though major municipalities, water boards and the national Department of Water and Sanitation responded favourably when asked to make pipes available for testing, surprisingly few pipelines were deemed feasible for the application of the leak characterisation test. Most of the reasons observed, however, did not eliminate this testing method as an appropriate means to assess these pipes, but rather eliminated the pipes from being made available for research purposes.

The following reasons were given for pipes being eliminated from the study:

a) **No isolation valves exist, or isolation valves could not be identified:** Some pipes were eliminated, due to isolation valves not being existent either upstream or downstream of the connection point. Unless the pipe is a rising main that is open to the atmosphere, this scenario is not desirable for any pipe, and should be addressed, irrespective of the requirements of this testing method.

b) **Isolation valves that leak excessively or are inoperable:** For a number of pipes, the pipe owner was already aware of excessively leaking isolation valves, and therefore the pipes were not investigated further. Also, a number of isolation valves were known to be inoperable, as they have not been operated for years and have seized up. Both these scenarios are, again, not desirable, and should be addressed, irrespective of this test.

c) **No connection point / access point:** The complete non-existence of an access point has also been encountered, especially on shorter pipes. Although installing an access point would not be a major operation, this was not feasible for testing purposes.

d) **No downtime available:** Non-availability of downtime was the most common reason for pipes not being available for testing. Most of the pipes that were made available, were pipes that deliver bulk water to reservoirs. Shutting these pipes off for the short duration of the test was feasible, as the reservoir would store sufficient capacity to overcome the down period. The bulk of the pipes are, however, downstream of the reservoir and can therefore not store water for down periods.

e) **Access point out of reach:** In some cases, potential pipe tests were eliminated, due to pipe access points that could not be reached with the PCAE. These access points were found to be out of reach of the closest position that the PCAE trailer could be brought.

Rough terrain conditions were encountered, especially in reaching high lying air valves. With enough preparation and with suitable vehicles, these points could mostly be reached, but for the purpose of this study, these pipes were eliminated.

Also, cases were observed where the ideal access points were deep inside buildings, or fenced-into yards with only pedestrian entrances. For this testing method to be implemented, modifications to improve site access, or alternative access points, must first be implemented.

f) **Extensive Leakage:** Pipe owners were aware of pipes with leakage rates that were significantly higher than the maximum capacity of the PCAE. The fact that the pipe owners were aware of the high leakages, but did not have the resources or incentives to address the high leakage, is a major concern, as the cost of the leak is most probably considerable higher than the cost of intervention.
It is, however, not recommended to increase the capacity of the PCAE in order to accommodate these types of pipes, because this type of leakage is sufficient to motivate urgent intervention, and the leak location may be detectable by visual inspection.

g) **Flooded chambers:** On more than one occasion, isolation valve chambers were flooded due to leaking flanges. If de-watering equipment was available, these chambers were first emptied before the pipe was isolated, however, this equipment was not always available, leading to the elimination of these pipes for this study.

h) **Pipes not full:** One of the potential pipelines is in a remote area, where water rationing is being implemented. The pipe was visited three times, and found to be either empty or only half-full, even though the necessary arrangements were made in advance. After the third visit, the test of this pipeline was abandoned.

Chapter 4

4 Results and Discussion

In this chapter, the results of all the pipe tests are presented and discussed. The first test is discussed and analysed in detail, in order to demonstrate the application of the methodology presented in Chapter 3. As further tests are presented and discussed, the level of detail decreases as the reader becomes familiar with the repetitive elements of the tests. The level of detail is then limited to what is required to understand the new and interesting observations made, which contribute to the lessons learned and the aims of this study.

Finally, this chapter concludes with a summary and discussion of the combined results and observations of all tests. For more detail on each individual test, the spreadsheets for all the pressure tests are attached in Appendix A. Table 4-1 below contains a list of all the tests as an overview.

Table 4-1: List of all tests

No	Name	Length (m)	Diameter (mm)	Type
1	Lynnwood Road to Koedoesnek Reservoir	707	500	Steel rising main
2	Garsfontein to Parkmore High Level Reservoir	2 640	500	Steel rising main
3	Queenswood Reservoir Supply Line	2 853	500 (1 133 m), 600 (1 720 m)	Steel rising main
4	Muckleneuk Reservoir Supply Line	247 (AC) 1 017 (Steel)	300 (AC) 496 (Steel)	AC & Steel mains
5	Florauna High Level Reservoir Supply Line	1 260	300	Steel rising main
6	Fort Klapperkop to Carina Street Reservoir	3245	406	Steel rising main
7	Simon Vermooten to Murrayfield Reservoir	1650	500	Steel rising main
8	Brickfields to Constantia Reservoir	+/- 650	450	Steel rising main
9	KwaMhlanga: Vlaklaagte to Verena Line	8 740 & 3 800 & 9 400	400	Steel gravity main (divided into 3 sections)
10	KwaMhlanga: Moloto Pipeline	+/-3 750	300	Steel gravity main

Even though the tests listed in Table 4-1 were not specifically selected to present a diverse set of results, but rather comprise of all the pipelines that where available for testing in the Gauteng area, the observations, lessons learned and findings varied significantly.

4.1 Lynnwood Road to Koedoesnek Reservoir

4.1.1 Test Description

The pipeline from Lynnwood Road to Koedoesnek Reservoir is a 500 mm diameter, 707 metre long pipe steel pipeline. It is a rising main that branches off a pressurised main supply pipe, and supplies a reservoir approximately 47 metres higher. Immediately after the branch, an isolating butterfly valve is located in a valve chamber next to the road (V1 in Figure 4-1). The downstream isolation valve (V2) is a PRV, which is located inside a valve chamber just upstream of the Koedoesnek reservoir.

The pressure upstream of the pipeline is above 10 bar, and provides the driving force for the flow from Lynnwood road to the Koedoesnek reservoir. The pressure downstream of the pipeline is low and mainly results from the slightly elevated reservoir and the reservoir level.

The most suitable connection location was identified to be the valve chamber at V2, as this is the highest point on the pipeline section. Upon inspection, the most suitable connection point was identified to be a 50 mm connection on a PRV, already fitted with an isolating ball valve. A second and a third PRV exist downstream and adjacent to this PRV, which were then used for isolating the pipe.

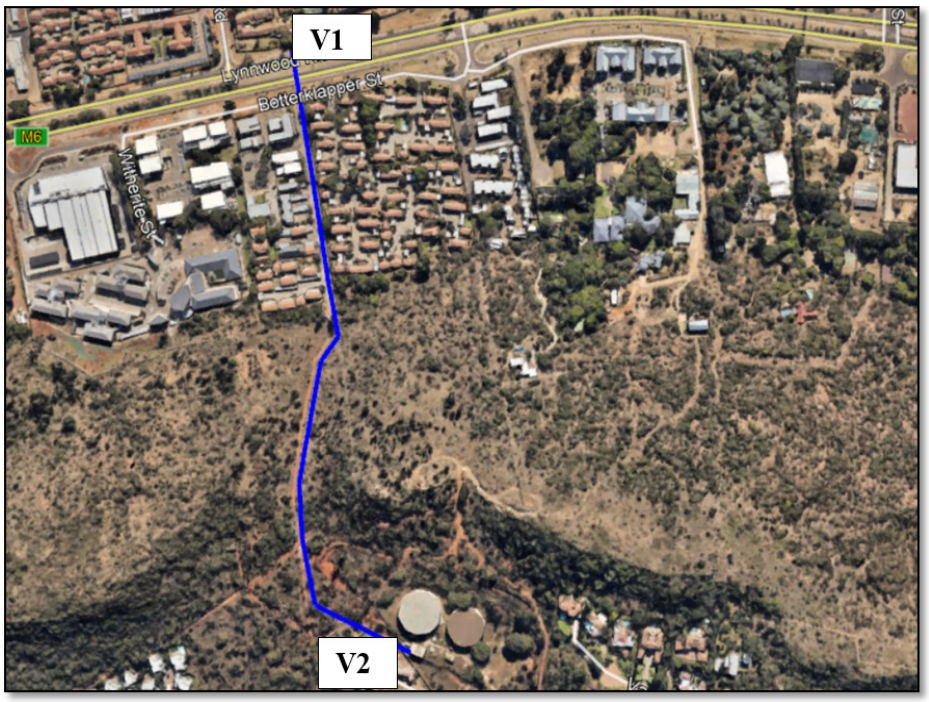

Figure 4-1: Lynnwood Road to Koedoesnek pipeline route starting at V1 and ending at V2. The equipment was connected inside the valve chamber at V2.

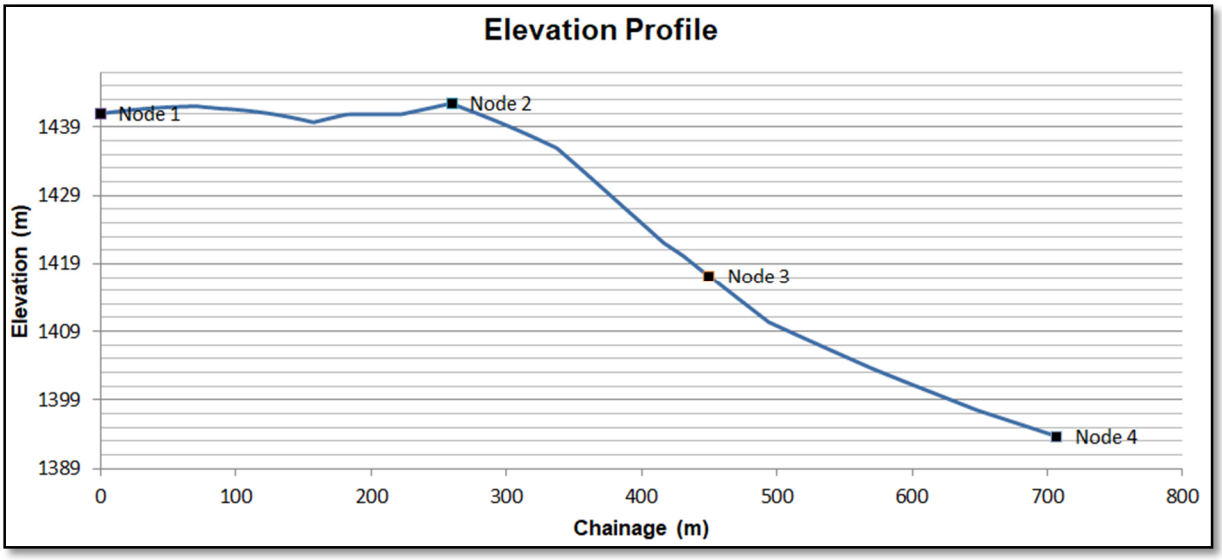

Figure 4-2: Elevation Profile for Koedoesnek Reservoir, with node points indicating where the potential leak will be characterised.

The isolating ball valve on the connection point allowed for the PCAE to be connected to the PRV, while the pipe was still in operation. The hose was then connected to the PCAE water tank, and the isolation valve was slightly opened to fill the tank. Once the tank was full, the next step was to close the ball valve and isolate the pipeline.

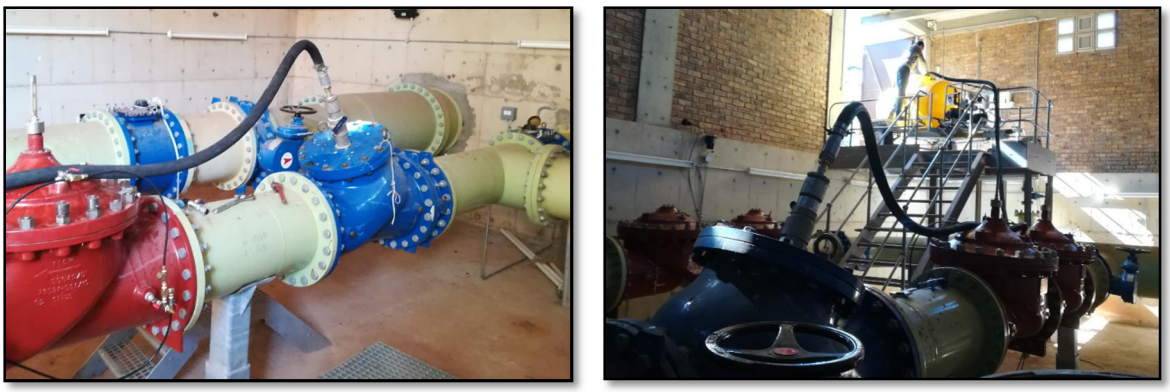

Figure 4-3: PCAE setup and connection point at Koedoesnek reservoir valve chamber.

In this case, it was believed that the isolation valve closing sequence did not have an influence, as the pipe was pressurised from both ends. For convenience, it was decided to deviate from the proposed methodology and first close the upstream valve.

The valve chamber of the upstream valve (V1) was, however, completely flooded upon arrival. This was due to leaking adaptable flanges on the high pressure pipe upstream of the isolation valve. The operations team, therefore, first had to get hold of dewatering equipment, after which the chamber could be drained. The isolation valve (V1) was then closed until no sound of passing liquid could be heard, and the hand wheel reached its maximum closed position.

After returning to the valve chamber (V2), the hose was connected to the delivery of the PCAE, and the PCAE was prepared for starting the test. When the ball valve at the connection point was opened, however, a sense of air flowing into the pipe was noticed. This indicated that the pipe was already draining, and that, contrary to the assumption that the pipe is pressurised from both ends, the downstream PRV (V2) acted as a check valve, preventing return flow.

The PRV (V2) was immediately closed and the pump on the PCAE was started at its maximum pressure setting. Flow from the PCAE filled the pipe and the pressure stabilised at the maximum pressure within 60 seconds. The fact that the equipment was installed at a high point, and that the pressure stabilised quickly, provided sufficient reasons to assume that the pipe was fully filled and that all the air was expelled.

Figure 4-4 shows a plot of all the flow and pressure measurements over time. The highest stable pressure that could be achieved was 36.02 metres head. At this pressure, the leakage was measured to be 1.14 litres per second (4.104 m^3/h). Once stable, the pressure was dropped to obtain a second data point. This process was repeated for four downward adjustments of the pressure, down to a lowest pressure of 13.25 metres, before the pressure was incrementally increased on an upward adjustment cycle. After the fourth upward pressure adjustment, the water in the tank reached its minimum draw down level and the test was stopped.

The quick and stable conversions, as well as the consistency between the downward and the upward pressure adjustment cycles, support the assumption that no air had been entrapped in the system. The test was therefore concluded, as sufficient data points were obtained. ‘

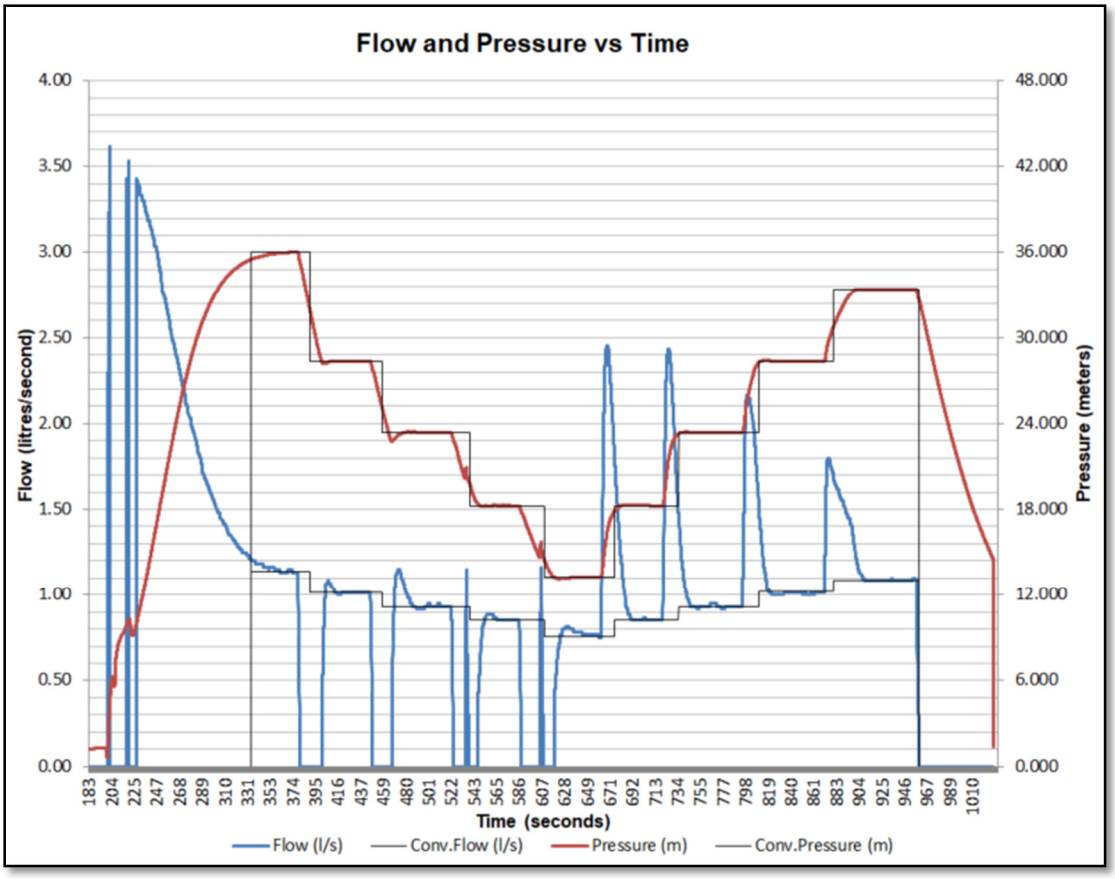

Figure 4-4: Pressure and flow versus time for Koedoesnek Pipeline, including the estimated converged values.

4.1.2 Test Results

The Excel tool, which was developed for this study, and which is described in detail under Paragraph 3.5, was used to record and interpret the test results. First, the pressure and flow over time data was plotted with this tool, generating the plot depicted in Figure 4-4 in the previous paragraph. The tool was then used to estimate the average stabilised pressure and flow values by fitting a straight horizontal lines through the pressure and flow readings on the plot, which are also displayed in Figure 4-4.

Once the set of pressure vs flow points have been obtained, the pressures had to be corrected for the nodes at which the leakage was being analysed. To correct the pressures, the Excel tool takes into consideration all the minor losses, friction losses and elevation differences.

The nodes were carefully selected to reflect the widest range of scenarios. The elevation profile in Figure 4-2 shows the final node locations. By inserting the pipe details and by selecting the coupling types, the Excel tool then automatically presents the pressure versus flow data for each node.

By fitting a trendline of an exponential equation, the N1 leakage exponent was estimated. In Figure 4-5, the flow versus pressure data points are plotted for each of the four nodes, as well as their respective trendlines.

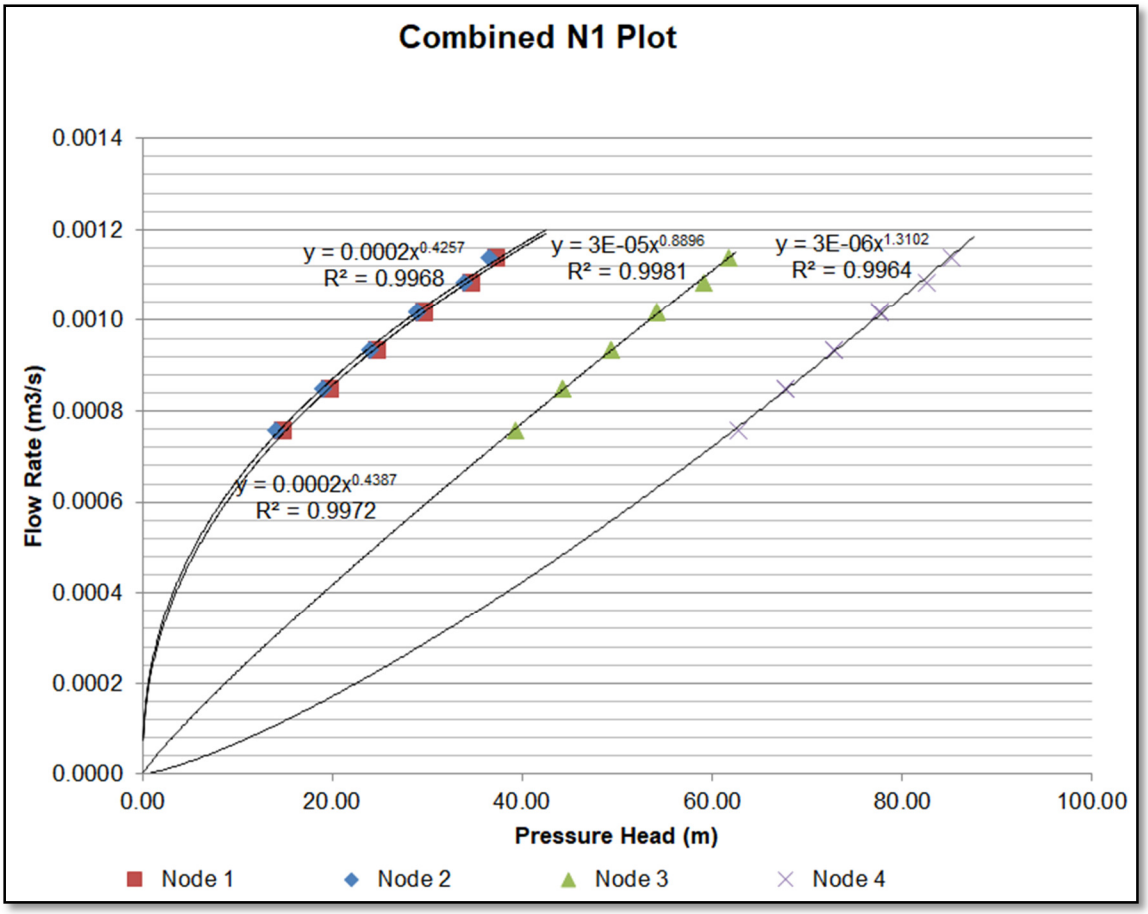

Figure 4-5: N1 plot for four nodes along the pipeline to Koedoesnek reservoir

From the plot in Figure 4-5, it is clear that the N1 equation approximations fit the data points very well. No far outliers exist, and the R-squared value (R^2) exceeds 0.996 at all four nodes. The resulting N1 leakage exponent values are listed in Table 4-2.

Table 4-2: N1 and FAVAD parameters for pipeline to Koedoesnek reservoir

Node	N1 Exp.	Effective Initial Leak Area (mm^2)	Effective Pressure-Area Slope (mm^2/m)	Initial Leak Area, C_d=0.65 (mm^2)	Pressure-Area Slope C_d=0.65 (mm^2/m)
1	0.4387	43.907	-0.0719	67.5	-0.111
2	0.4257	46.554	-0.1288	71.6	-0.198
3	0.8896	18.449	0.2322	28.4	0.357
4	1.3102	4.904	0.2703	7.5	0.416

Similarly, the effective leak area (C_dA) was calculated, as explained in Paragraph 3.5.5.2, and plotted against the pressure. A trendline of a linear equation was then generated for each node, as shown in Figure 4-6.

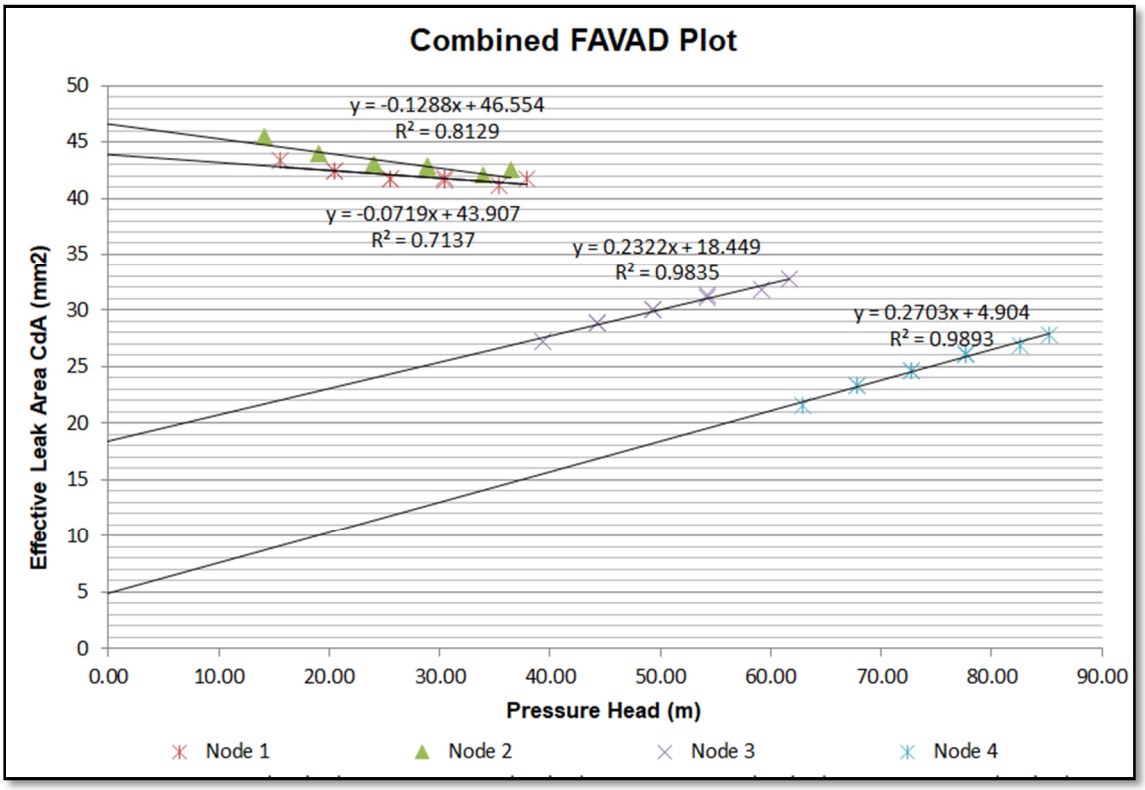

Figure 4-6: FAVAD plot for four nodes along the pipeline to Koedoesnek reservoir

A linear relationship fits the data points well, and no clear outliers were recorded. Especially for the third and fourth node, the R^2 value exceeds 0.98. The resulting FAVAD parameters are also listed in Table 4-2, together with the actual initial leakage areas, if a discharge coefficient (C_d) value of 0.65 is assumed.

4.1.3 Interpretation of Results

From the results, it appears that the leakage emanates from a pipeline leak, rather than from a leaking valve. This is suggested for the following reasons:

- At Node 1, where the downstream valve is located, a negative pressure-area slope is observed, which is not characteristic of a leaking valve.
- The pressure upstream of the upstream isolation valve, at Node 4, exceeds the pressure in the tested pipe section, preventing outflow through the valve.

As discussed in the Literature Review under Section 2.8.5, the characteristics of a leak are related to a number of factors, including the pipe material, leak hydraulics, as well as the soil conditions

surrounding the leak. By comparing the leak characteristics of potential leaks at every node to the characteristics of similar pipes and leaks in literature, the most probable leak type and leak location can estimated. The expected

The pipe feeding Koedoesnek reservoir consists of steel and a significant elastic deformation of the leak area is therefore expected. In the literature review reference is made to a study by Van Zyl and Clayton, (2007), which concludes that the pipe material type has a strong influence on the leakage characteristics of leaks existing on the pipe.

Reference is also made in Paragraph 2.8.5.1, to a numerical investigation into the effects of pressure on holes and cracks by Cassa and Van Zyl (2010). In this investigation, small pressure-area slopes for round holes in steel pipes were estimated, with values of approximately 0.00001 for 12 mm holes, and lower for smaller holes. For longitudinal cracks in steel pipes, the predicted pressure-area slopes are significantly higher, with approximate values of 0.0001 for 30 mm long cracks and 0.0004 for 50 mm long cracks. Negative pressure-area slopes were found to only result from circumferential cracks, which are uncommon in steel pipes.

However, in an experimental setup by Greyvenstein and Van Zyl (2007), a wide range of N1 leakage exponents where observed for corrosion clusters on steel pipes, ranging from 0.67 to 2.3. Greyvenstein and Van Zyl suggest that this variation could result from the weakening of the thinning material surrounding the hole. Clayton and Van Zyl (2007) support these findings in a field investigation, and also make an observation, that the highest leakage exponents are often found in corroded pipes.

By comparing the Koedoesnek pipeline with the leak characteristics found in literature, the following scenarios are likely:

- All the dominant leaks are downstream of Node 2
- Longitudinal cracks of approximately 40 mm in length exist along the pipeline from Node 3 up to Node 4. This scenario is uncommon for steel pipes, and is therefore unlikely.
- Longitudinal cracks exist on gaskets or flexible couplings between nodes 3 and 4. The existence of such leaks can easily be verified by a quick visual inspection of all the air valve and scour valve chambers.
- Round holes exist somewhere between Nodes 2 and 3, where the pressure-area slope is expected to be closer to 0.
- Corrosion holes exist between Nodes 2 and 4. This is a likely scenario, but due to the range of exponent values or pressure-area slopes that can result from corrosion holes, the location cannot be pinpointed any further, other than that they most likely exist between Nodes 2 and 4.

A leakage of 1.14 litres per second (4.1m3/hour) at 36 metres pressure head was recorded. Considering the scarcity of water, as well as the high cost of this purified water, which has been transported a considerable distance from its original source, this leakage rate is significant. It is therefore recommended that further inspections are carried out on the pipeline in order to identify and address the source of the leak.

4.1.4 Test Observations

The following observations were made during this test:

- Air entered the pipeline at the connection point, because the valve closing sequence was incorrect, and the isolation valve at the higher end of the pipeline acted as a non-return valve. From the results, however, it appears that no air was trapped in the pipeline. In order to prevent air entering the pipeline during future tests, it is important that the isolation valves are closed in the correct sequence in order to maintain the pressure until the PCAE equipment is ready to add pressure to the pipe.

- The presence of an isolation valve on the connection point was greatly beneficial in reducing downtime, as the PCAE could be installed and removed while the pipe remained in operation.

- The test itself was quick and required less than 20 minutes to complete after the equipment setup. The downtime was, however, much longer, due to the unforeseen circumstances on site. If, however, proper preparations were made in advance to ensure that both isolation valves were accessible, the total downtime could have been reduced significantly.

- Apart from preparing the site, also preparing the Excel spreadsheet tool in advance, by filling in the basic pipe information and elevation profile data, would allow for test results to be made available within minutes after the completion of the test.

4.2 Garsfontein to Parkmore High Level Reservoir

4.2.1 Test Description

The Garsfontein to Parkmore reservoir pipeline is a 406 mm diameter, steel rising main that is supplied by a high pressure main. The elevation difference between the start and end of the pipeline is similar, but the pipeline passes through a deep valley. The pressure upstream of the first isolation valve is above 5 bar, which is sufficient to drive the flow through the pipeline up to the Parkmore reservoir.

The pipeline section starts with a PRV at V1, as indicated in the satellite image in Figure 4-7, and ends at a valve chamber at V2, shortly before the Parkmore High Level Reservoir. Although the image shows reservoirs at the starting point, the system is not supplied by these reservoirs.

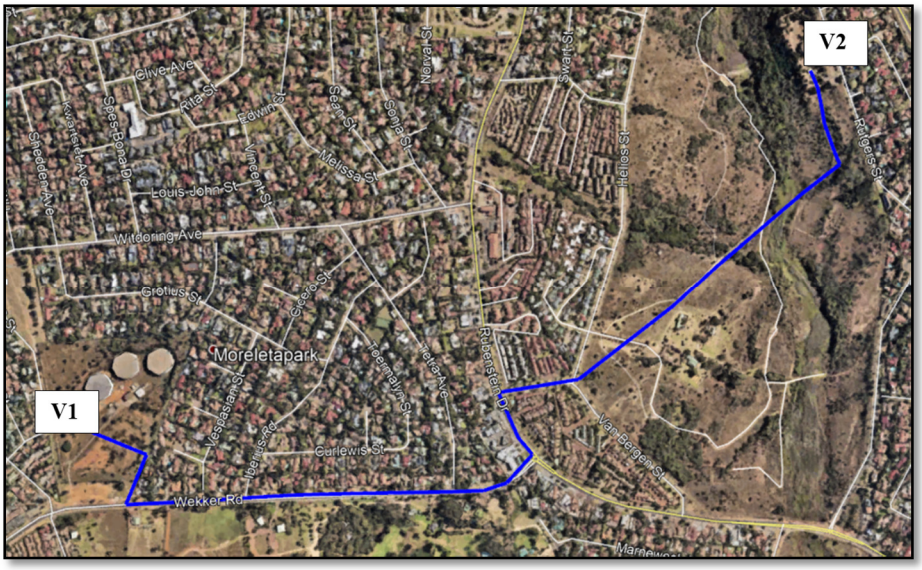

Figure 4-7: Satellite image of the pipeline from Garsfontein to Parkmore High Level Reservoirs.

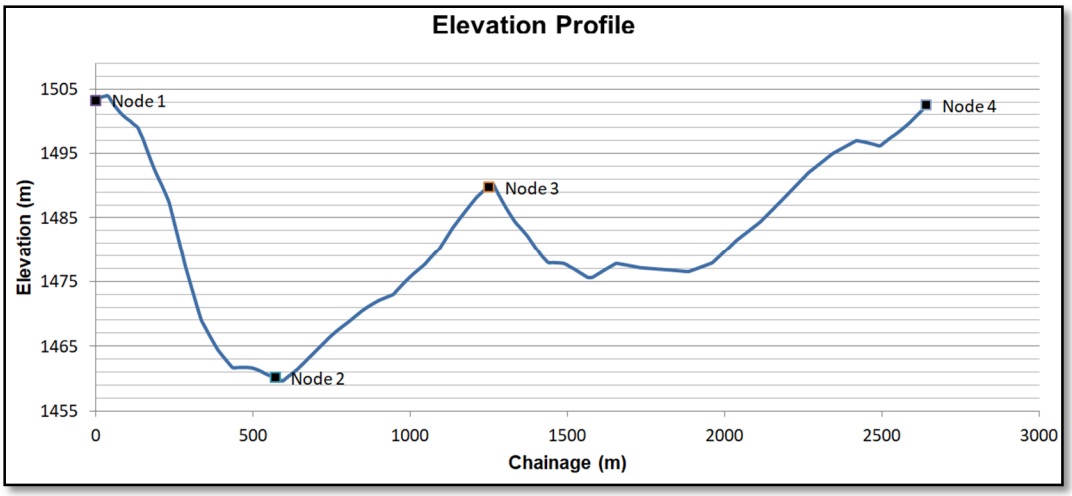

Figure 4-8: Elevation Profile of the Parkmore reservoir supply pipeline.

The valve chamber at V2 is slightly lower than Parkmore reservoir, and pressure gauges in the valve chamber indicated that the downstream pressure resulting from the reservoir elevation difference was approximately 5 metres.

The valve chamber at V2, as pictured in Figure 4-9, provided various options for connecting the PCAE and for isolating the pipeline. The first connection point (CP1) is larger and is already fitted with an isolating valve, while the second connection point (CP2) is significantly more difficult to connect to, as it is not fitted with a valve. The drawback of CP1, however, is that it depends on the isolating capabilities of three valves. Two of these valves are located on branches, which bypass the reservoir and supply the outgoing supply line directly. These valves are in a permanently closed position, and the pressure downstream of these valves is governed by the reservoir level.

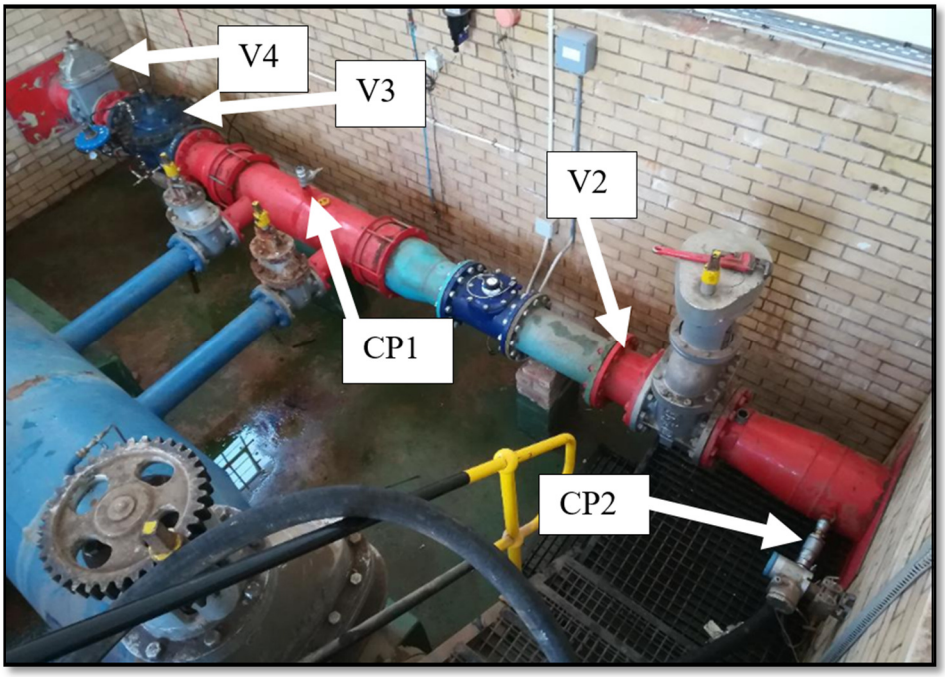

Figure 4-9: Valve chamber at V2, indicating valves 2 to 4, and potential connection points CP1 and CP2.

In total, five test runs were carried out on this pipe section on two separate dates. For the first two test runs, the PCAE was connected to CP1, and both the PRV (V3) and the gate valve (V4) were closed. For the third test, the connection point was moved to CP2, and only the gate valve (V2) was closed. On a second visit, two additional tests were performed by connecting to CP2 and isolating with the gate valve at V2.

4.2.2 Test Results

The results of all five tests varied, and little consistency was observed. Figure 4-10 and Figure 4-11 are plots of the FAVAD equation parameters for the highest and lowest node on the pipeline. The nodes locations are indicated on the elevation profile in Figure 4-8.

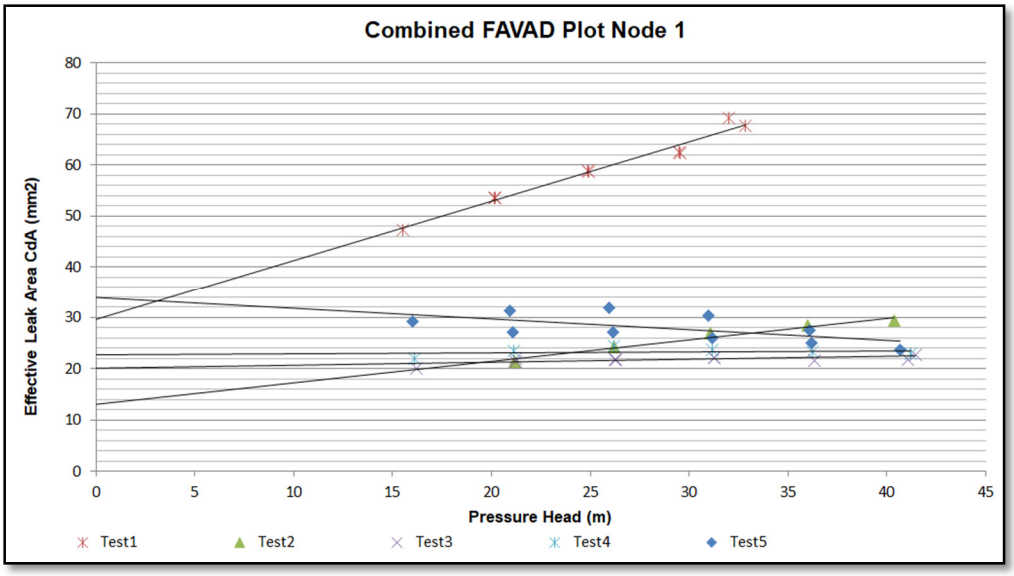

Figure 4-10: Effective Leak are versus Pressure at Node 1 for 5 test runs on the Parkmore reservoir pipeline

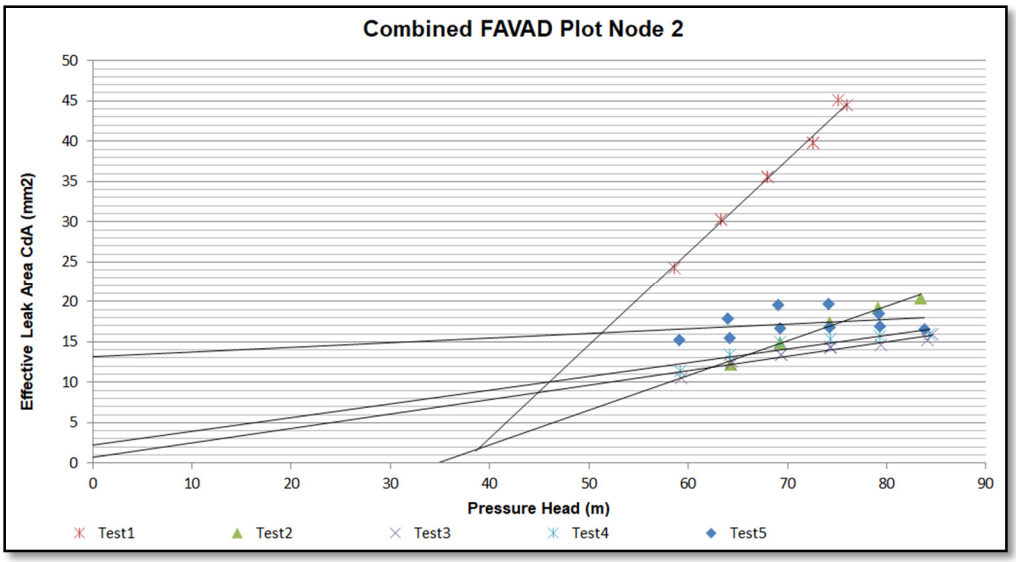

Figure 4-11: Effective Leak are versus Pressure at Node 2 for 5 test runs on the Parkmore reservoir pipeline

4.2.3 Interpretation of Results

For the first test, the results in Figure 4-10 and in Figure 4-11 indicate a large, pressure sensitive leak, which stands out from the other tests. The test was repeated after opening and closing valves V1, V3 and V4 for filling the tank. The results of the second test indicate a significantly smaller leak, with an area that remains sensitive to pressure.

This significant change in results after opening and closing the valves, strongly hints at the possibility of the valves not sealing effectively during the first test. If the upstream valve, V1, did not seal, however,

the pipe would not have depressurised, due to the high upstream pressure. It is, therefore, likely that both valves V3 and V4, or one of the bypass valves, did not seal effectively.

When the first test was performed, it was noticed that, once all the valves were closed, the pressure in the test pipe dropped to a lower level than the downstream pressure of the isolation valves. This indicates that a leak exists on the pipeline, causing the pipeline to lose pressure. If the valves on the bypasses were leaking, this behaviour would not have been witnessed, as the leakage through the valves would maintain the pressure in the tested pipe, eliminating this possibility.

If the gate valve V4, however, leaked, and the PRV (V3) did not fully close, the behaviour described above would have been witnessed. The PRV would act as a non-return valve, allowing the pipe to depressurise once all valves were closed; then, when pressurising the pipe with the PCAE, the PRV would allow flow to pass through the leaking gate valve, indicating an excessively large leak.

The leakage of valves in the vicinity of the connection point can also be interpreted from the FAVAD parameters of the test data. At Node 1, which is approximately 3 metres from the suspected leaking valves, the test results in Figure 4-10 indicate a leak with a steep pressure-area slope and an initial leak area of 30 mm^2. Any point at a lower elevation will lead to an even steeper pressure-area slope. Figure 4-11 shows how, at the lowest extreme, the FAVAD parameters indicate unrealistic pressure-area slopes and negative initial leak areas, which are not possible. The most likely leak position is, therefore, at the highest node, which is at Node 1.

From the interpretation of the FAVAD parameters, it appears likely that the leakage through Valves V3 and V4 persisted in the second test. Figure 4-11 indicates that, in comparison to later tests, the characteristics of this leak still point to a leak location at a high elevation, such as the location of valves V3 and V4.

For the remaining tests, it was decided to move the connection point to CP2, and to utilise V2 as an isolation valve, as this would reduce the number of isolation valves that could potentially leak. As seen in Figure 4-10 and Figure 4-11, the results for both tests 3 and 4 were significantly more consistent, although they were performed approximately 3 weeks apart. It is therefore assumed that these results most accurately represent the characteristics of the real leak.

Table 4-3: N1 and FAVAD parameters for pipeline to Parkmore High Level reservoir, for Tests 3 & 4.

Node	N1 Exponent (Test 3/4)	Initial Leak Area (mm^2) (Test 3/4) C_d=0.65	Pressure-Area Slope (mm^2/m) (Test 3/4) C_d=0.65
1	0.581 / 0.5363	30.8 / 34.9	0.088 / 0.028
2	1.486 / 1.39	1.1 / 3.5	0.275 / 0.263
3	0.871 / 0.811	17.6 / 20.7	0.230 / 0.201
4	0.59725 / 0.552	29.9 / 33.9	0.102 / 0.047

The results of tests 3 and 4 are summarised in

Table 4-3. A discharge coefficient of 0.65 was assumed. By comparing the test results to the expected results for steel pipelines from literature, as was done for the Lynnwood to Koedoespoort pipeline in Paragraph 4.1.3. The following conclusions can be made:

- Round holes, with leak areas insensitive to pressure, possibly occur at the high lying nodes. Such round and rigid holes, however, are uncommon in steel pipes, and this scenario is deemed unlikely.
- Either longitudinal cracks or corrosion holes exist at the lower elevations. Both of these types of leaks exhibit a large range of N1 values and steep pressure-area slopes. Corrosion holes would be likely in steel pipes.
- If the leak is at a low point, the initial leak area will be smaller than at higher elevations.

The pipe passes through a valley and underneath a small river. The corrosive conditions resulting from the moist soil at the river are likely to lead to corrosion of the pipe. If the valve chambers are inspected and no leaks exist from the air valves or gaskets, the next most likely scenario would be the existence of small corrosion holes at the low points of the pipeline.

The leakage is between 0.35 and 0.65 litres per second, depending on the applied pressure. This is a significant leak and it is recommended that the leak is investigated further.

Finally, the fifth test provided completely different results and leak characteristics that do not follow a consistent trend. Figure 4-12 shows the recorded test data for the fifth and final test, from which it can be observed that the leakage flow rates were higher while the pressure was incrementally increased, in comparison to the following phase of the test, during which the pressure was incrementally decreased.

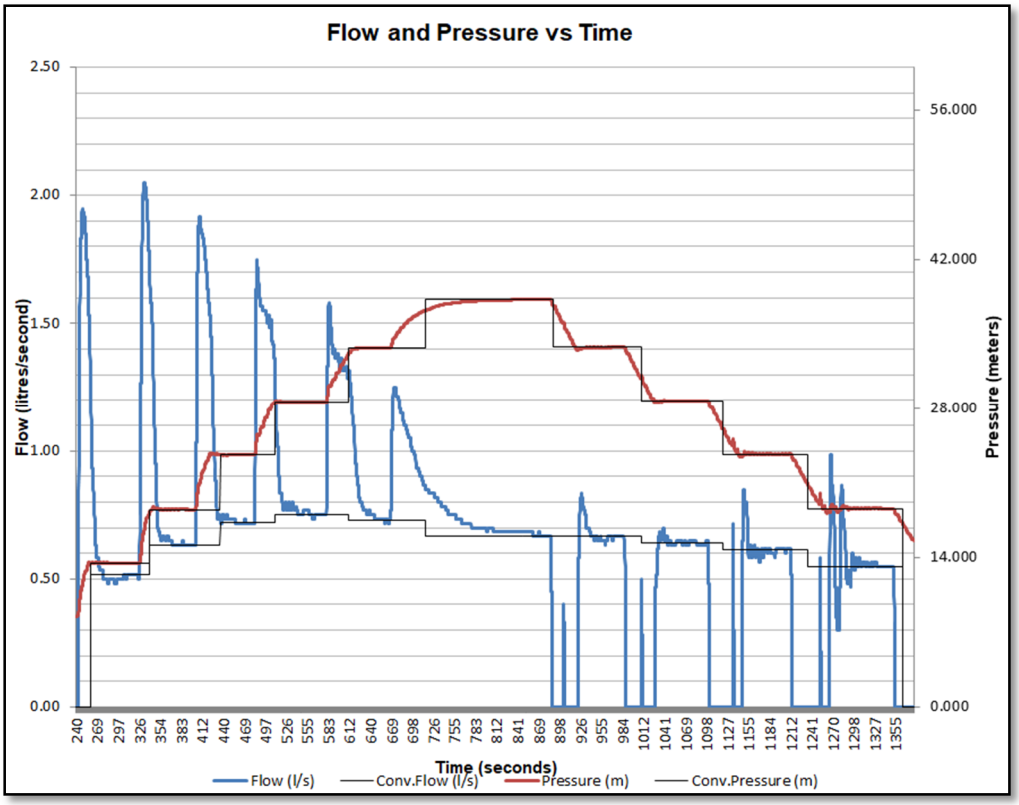

Figure 4-12: Flow and pressure over time for fifth test on the Parkmore High Level reservoir pipeline.

Figure 4-13 compares the pressure and flow points of the fifth test to the third and fourth test at the fourth node. In the first plot, the FAVAD relationship was plotted for the entire data set, assuming no changes in the leak characteristics during the test. For the second and third plot, the data points where split into two sets, with the one set representing the characteristics before a change in behaviour, and the second set representing the characteristics after the change.

The second plot shows only the first three readings, which appear to be consistent in Figure 4-12 and precede the sudden change in characteristics. The third plot in Figure 4-13 shows the last 5 points, which follow after the change in leak behaviour.

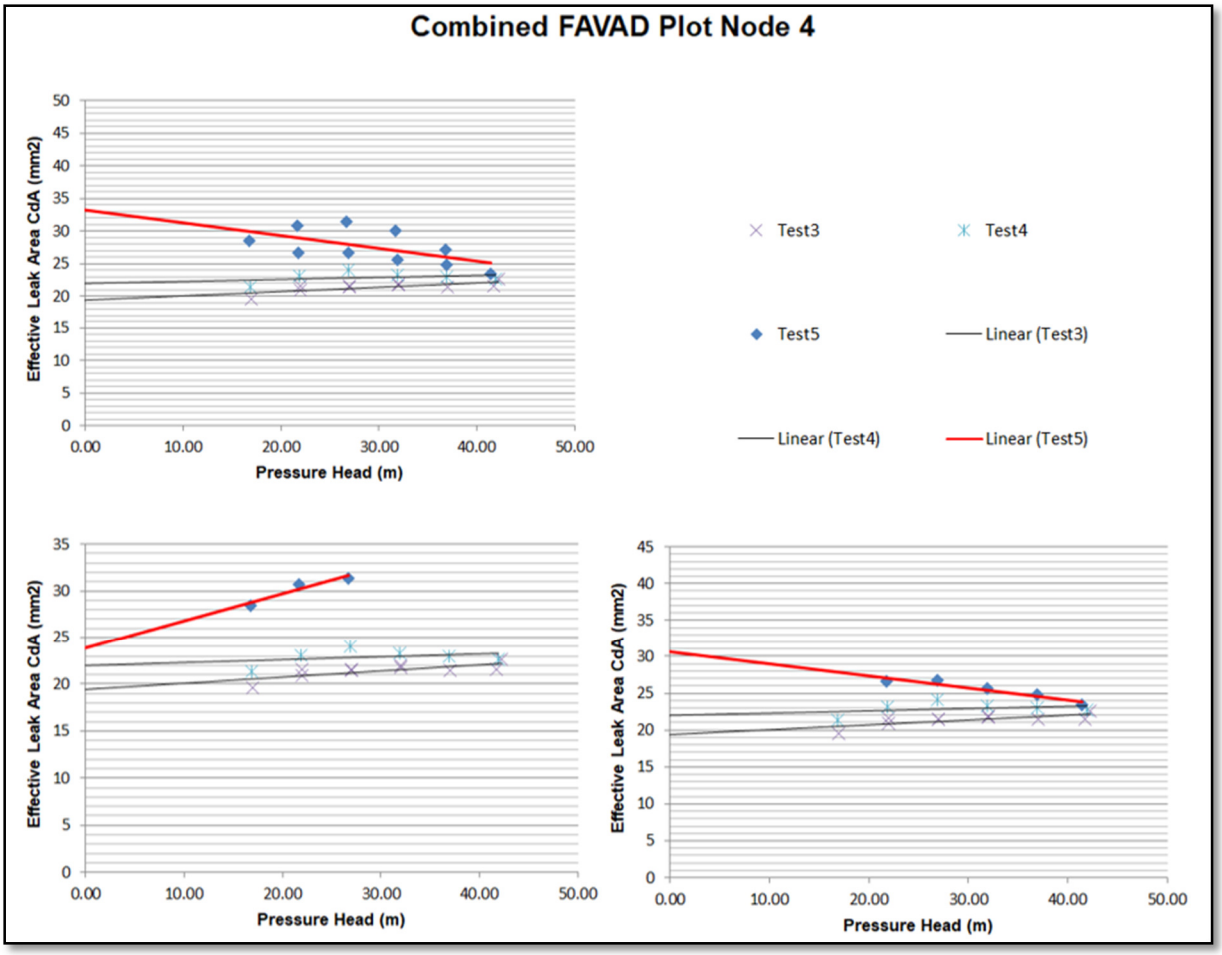

Figure 4-13: Combined FAVAD plot for tests 3, 4 and 5 at node 4 at Parkmore HL, showing the different possible trends from the fifth test.

By interpreting the plots in Figure 4-13, an initial leak through the upstream isolation valve, at Node 4, is suspected to be the cause of the deviation in results, for the following reasons:

- The leak characteristics appear to have changed during the test. This dynamic behaviour is not expected for fixed leaks in the pipeline, but rather points to a valve opening or closing during the test.
- At Node 1 (refer to Figure 4-10) the head-area slope is flatter for the fifth test, in comparison to the slopes obtained in the other tests. It is, therefore, expected that the characteristics of the event must have a very flat or negative slope at Node 1 in order to pull the slope of the existing leak down to such an extent. A leaking valve at Node 1 would not create such a negative pressure-area slope, and the leak is expected to be lower than Node 1.
- At the nodes which are lower than Node 4, the initial leak areas are negative before the change in the leak behaviour, indicating that the event most likely occurred at an elevation not lower than Node 4.

- The third plot in Figure 4-13 shows a negative slope at Node 4, indicating that, for the second part of the test, the leak most probably shifted to a lower elevation. The data in this plot, therefore, most likely describes the characteristics of the leak that was observed in the preceding tests.

It is clear that these tests provided characteristics of different leaks that cannot exist at the same location. The only explanation is, that the upstream isolation valve at the start of the pipeline, which is a PRV, was not yet fully closed after it was opened for filling the PCAE tank for the fifth test. It then closed further during the test, resulting in the sudden change in characteristics.

4.2.4 Observations

A number of observations were made during these five tests, which can provide useful information for recognising events in future tests.

a) Leakage through isolation valves

In this test, two cases of leaking isolation valves were witnessed and interpreted.

In the first case, the isolation gate valve on a high elevation, close to the PCAE connection point, failed to isolate the pipe. A steep positive pressure-area slope at the node closest to the valve suggested the possible failure.

In the second case, a PRV isolation valve at the furthest end of the pipeline failed to isolate the pipeline during the initial stages of the test, as it was still in the process of closing. Even though the observed data can possibly be of benefit in identifying leaking isolation valves in future test, the characteristics of a leaking valve at the far end of the pipeline is harder to distinguish from a leak that results from the failure of the pipeline.

The one characteristic of a leaking isolation valve, that clearly distinguishes it from a pipeline leak, is the changing behaviour of the leak with repetition. For future tests, if a leaking valve is suspected, it is recommended that the suspect valve is opened and closed before repeating the test. If the results of the two tests differ, a leaking valve is a likely contributor to the leak.

b) Air in the pipeline

During the third and fourth test, it was impossible to prevent air from entering the pipe through the connection point, as the connection point (CP2) was positioned on the side of the main pipeline, and was not fitted with an isolation valve. To connect the PCAE hose, the existing fitting had to be removed and replaced, during which a significant amount of water drained from the pipe.

Ideally, after such a connection, both upstream and downstream isolation valves should first be opened for a period of time in order for the air to be transported out of the pipeline. This was not done in this case, as it was initially not realised that the PRV valve acted as a non-return valve.

It is not believed that the air significantly affected the results, as the flow stabilised well at every pressure increment. However, it is worth noting that the occurrence of air in the pipeline clearly shows in the test data. An extract from the flow and pressure over time data recordings for the fourth test are shown in Figure 4-14, which clearly shows the dampening effect of the air on the pressure change in the pipeline, as well as the increased fluctuations in flow, before both the flowrate and pressure stabilised.

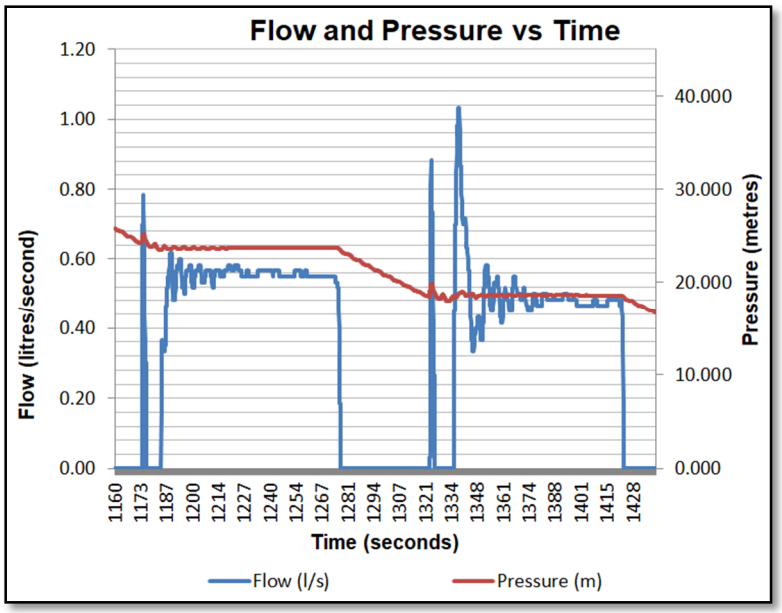

Figure 4-14: Example of flow and pressure vs. time plot from fourth test on Parkmore pipeline.

c) Benefits of on-site data processing

Finally, this test demonstrates the benefits of being able to process and analyse the testing data on site. Although the data was not analysed on site for these tests, the test demonstrated that unwanted events that require re-testing often only emerge once the data is processed.

The Excel tool (described in Paragraph 3.5), which was developed to simplify and accelerate the data processing, allows for data to be processed on site within a reasonable time period, making on-site processing with a laptop computer possible.

4.3 Queenswood Reservoir Supply Line

4.3.1 Test Description

The supply pipeline to the Queenswood reservoir consists of two steel pipe sections. One section is 1133 metre long with a diameter of 500 mm, and the other section is 1720 metre long with a diameter of 600 mm. The two sections where tested together and could not be isolated from each other. A butterfly valve on the upstream end and a PRV on the downstream end were used to isolate the combined pipe section for the test. The pressure upstream of V2 is significantly higher than the downstream pressure, preventing leakage out of the pipe section.

Figure 4-15 and Figure 4-16 show the pipeline route and elevation profile for the combined section. The connection point for the PCAE is located next to the PRV in the same valve chamber at high point on the pipeline. The PCAE was connected with a flanged coupling to a 50 mm unused off-take, which was already fitted with an isolation valve. It is important to note that the pipeline crosses a railway line and a freeway at Node 3 in Figure 4-16.

During the first pressure test, the tank emptied before sufficient satisfactory results were obtained. The tank was then refilled, during which valve V2 was opened and closed, and the test was repeated.

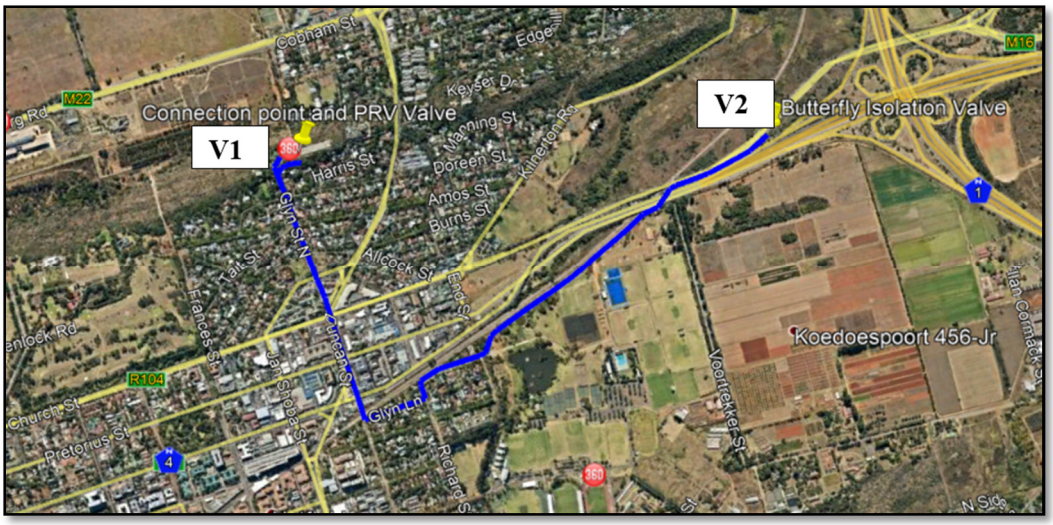

Figure 4-15: Satellite image of the supply pipeline to the Queenswood Reservoirs.

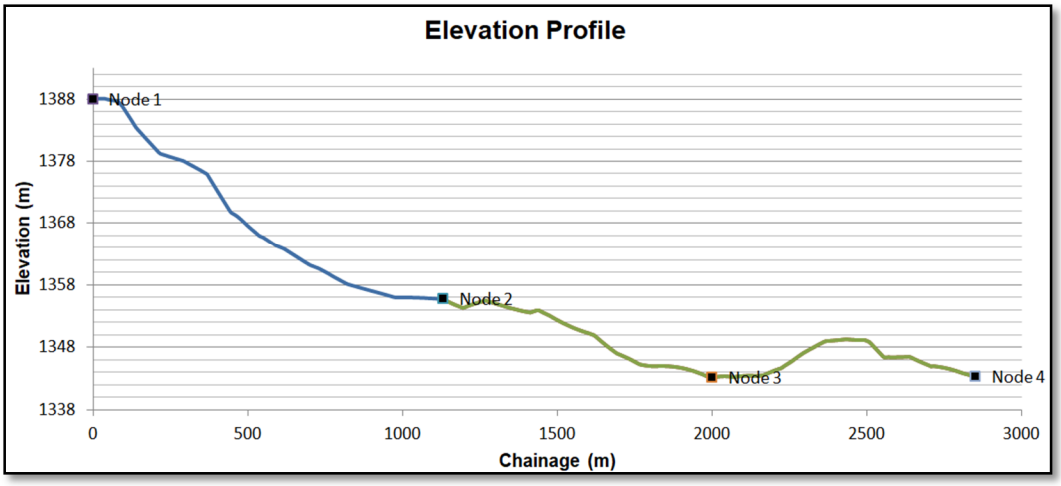

Figure 4-16: Elevation profile of the supply line to the Queenswood Reservoirs

4.3.2 Test Results and Interpretation

For both tests, the pressure was first increased to the maximum, after which it was incrementally dropped. In each case, the tank emptied during the pressure hiking cycle. Figure 4-17 shows the recorded data for the first test.

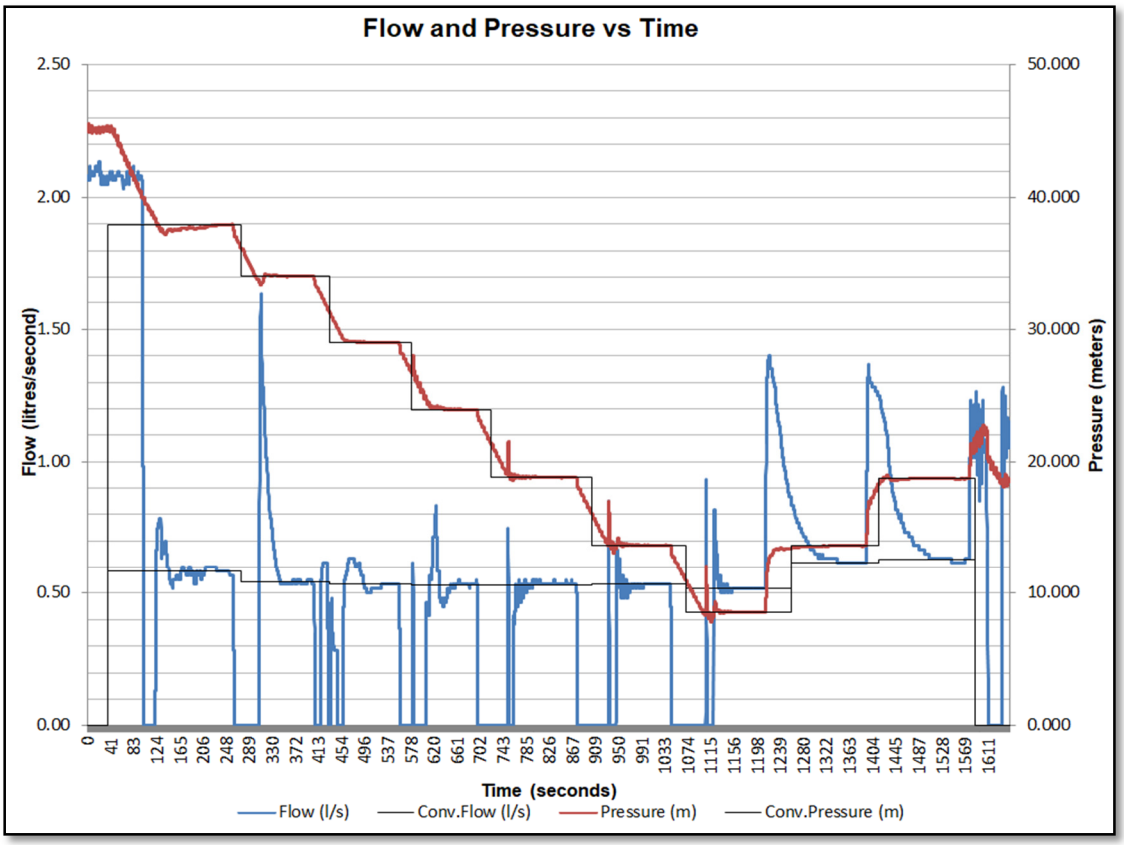

Figure 4-17: Pressure and flow over time for Test 1 on Queenswood supply pipeline

As seen in Figure 4-17, the leakage flow rate remained fairly independent of pressure as the pressure was incrementally reduced. However, a clear increase in flow rate was observed immediately after the cycle was reversed and pressure was being added. Interestingly, both tests showed the same trend.

Figure 4-18 shows a plot of the FAVAD parameters for both tests at Node 3, the lowest of the four nodes. A leak at the lowest node is the most likely leak location, because a leak at any higher node would result in even more negative head-area slopes, which are not expected in steel pipes. As the trendlines show, even though all the gradients are negative, they are very close to zero. This means that, even at the lowest node, the leak area shows very little dependence on pressure.

Due to the significant difference between the results from the pressure adding and pressure relieving cycles, the results were split to reflect the properties of the cycles individually. Note from Figure 4-18 that the results from both tests are similar for the pressure relieving cycle.

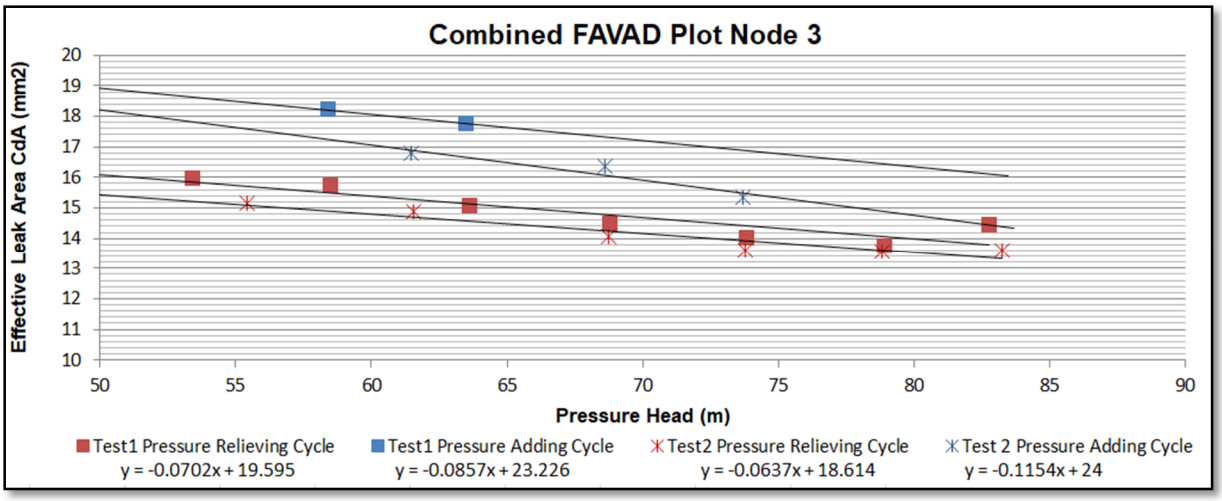

Figure 4-18: Combined FAVAD plot for both tests at lowest node on the Queenswood supply line

The following conclusions can be made from the above results:

- The lowest pipeline elevation has the highest probability of a leak or leaks, as the leak characteristics become more realistic for steel pipelines as the elevation drops. The low pressure dependence also supports this assumption.
- Even at the lowest elevation, the head-area slope remains negative. However, it becomes very small, indicating that the leak area is insensitive to pressure. The negative slope could also result from an underestimation of the frictional head losses, which were calculated to correct the pressure at the node.

- At the lowest elevation, the pipeline crosses a railway line close to a wetland area. This is a very corrosive environment, where corrosion holes would be likely causes of leaks. Round pinhole, which closely resemble small orifices, are therefore likely causes of the leaks.
- The cause of the clear and significant increase in initial leak area witnessed during the pressure hiking cycle remains unclear and requires further analysis.
- The leak consistently remained above 0.5 litres per second. This is a high leakage rate and the identification and elimination of the leak source should be prioritised.
- A pressure in the upstream isolation pipe exceeds the pressure in the tested pipe. It is therefore not possible for this valve to contribute to the observed leakage.

4.3.3 Test Observations

The following observations are worth noting and contribute to the lessons learned:

- Due to the high leakage flow rate, the water tank of the PCAE emptied quickly. A full test, which includes a complete pressure relieving and pressure hiking cycle, could therefore not be achieved. Also, in these tests, where the pressure dependence of the leak area is low, it would have been beneficial to increase the duration of flow for each pressure increment, in order to allow more time for convergence and stabilisation of the flow. This would have resulted in more accurate measurements, but would require a larger tank capacity.
- Alternatively, more tests should have been conducted on this pipe line, especially for the pressure hiking cycle. For future tests, this test shows the importance of running the test through both a pressure hiking and a pressure relieving cycle.
- Even though the results show unexpected and unexplained behaviour for leaks in steel pipes, the results still provide clear and useful information on the leakage rate and the most likely leak area, with minimal effort, time and interruption to the system.
- These tests again demonstrate the ease and simplicity of applying pressure tests to assess pipe conditions and to identify potential pipe leakage areas. If the Excel tool (described in Paragraph 3.5) was available and populated with all the pipeline information in preparation for the test, the results could have been interpreted on site within minimal time.

4.4 Muckleneuk Reservoir Supply Line

4.4.1 Test Description

The Muckleneuk Reservoir is supplied by a 230 metre long, 300 mm Asbestos Cement (AC) pipe. The AC pipe is supplied by 500 mm steel pipeline, which was isolated 1010 metres from the AC connection point. The two pipes could be isolated from each other, but no connection point existed on the steel pipeline. After the PCAE was connected to the AC pipe, in a valve chamber close to the reservoir, the AC pipe section was tested, followed by a combined test of the AC and steel pipe.

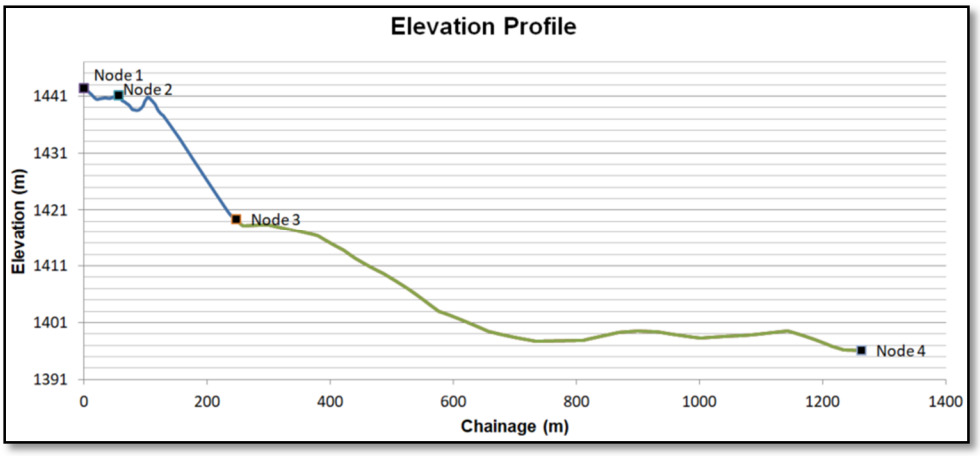

Figure 4-19: Elevation Profile for Muckleneuk Reservoir Supply Line

An unused offtake at Node 2 in Figure 4-19, approximately 60 metres from the PCAE connection point, exists on the pipeline. With an existing 5mm ball valve, the offtake could be opened to atmosphere. This provided an ideal opportunity to simulate a leak on this pipe, with controlled leak characteristics.

4.4.2 Test Results and Interpretation

For tests on the AC pipe sections, the leakage flow was lower than the minimum flow that could be recorded by the flow meter. The pipe was therefore pressurised to the highest possible pressure, after which the pump was switched off and the pressure was recorded as it dropped with time.

The methodology for analysing a pressure drop test, as explained in detail in Paragraph 3.5.6, was followed. By estimating the leakage parameters of the FAVAD equation, the flow rate was calculated for the pressure at every reading. From the estimated flow rate, the resulting pressure head was calculated and plotted against the recorded head. The effective head-area slope and the effective initial leak area were then optimised so that the calculated pressure curve matched the recorded curve best.

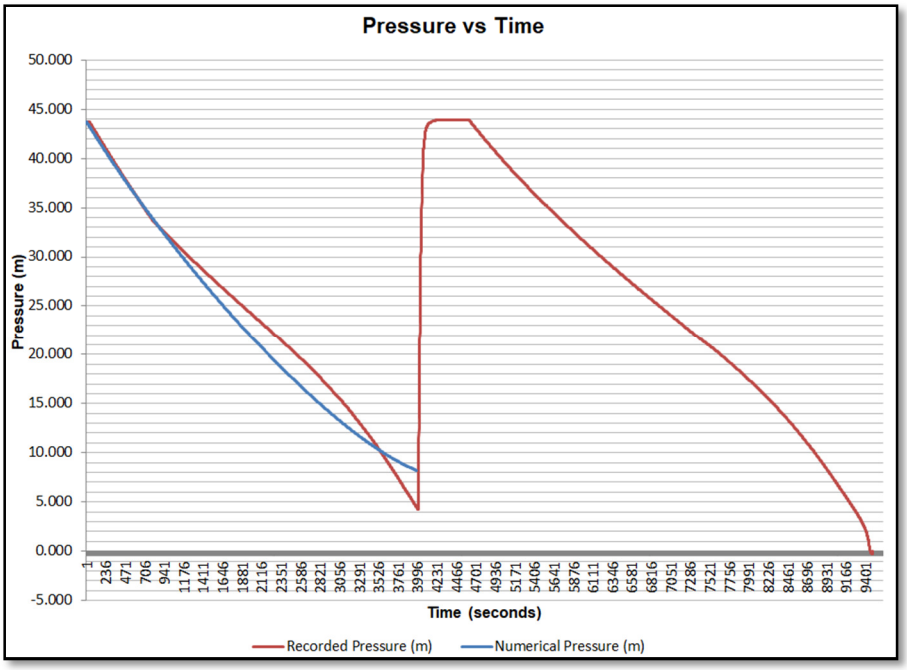

Figure 4-20: Pressure drop test on Muckleneuk 300mm AC pipe

As seen in Figure 4-20, two pressure drop tests were performed on the AC pipe in close succession. The measured pressure drop, however, did not follow the expected trajectory. For AC pipes, the expected leaks would result from cracks in the pipe which, due to the crack opening under pressure, would leak more at a high pressure, after which the leakage rate would steadily decrease as the pressure drops. In this case, it appears that the pressure initially drops at a high rate, after which the rate starts to steadily decrease, as expected, until the rate suddenly starts to unexpectedly increase again. The second test confirms this behaviour.

The witnessed behaviour could not be matched by estimating the FAVAD leakage flow rate and calculating the resulting pressure head. As seen in Figure 4-20, the closest calculated head follows a different trajectory. Further analysis of this leak behaviour, however, falls beyond the scope of this study.

The steel and AC pipe where then tested as one section. Again, the leakage could not be detected with the PCAE, but a pressure drop over time was observed. The pressure drop was analysed by assuming the steel pipe properties for the entire length of pipe. In this case, the calculated pressure head, using the optimised FAVAD parameters, perfectly matched the recorded pressure behaviour over time.

For both tests, the resulting N1 and FAVAD parameters are presented in Table 4-4 below. The calculated flow rate at the maximum pressure that can be delivered by the PCAE equipment is very low, confirming why no flow reading was recorded.

Table 4-4: Estimated N1 and FAVAD parameters for Muckleneuk supply pipes (C_d = 0.65)

Pipe Section	N1	A_0 (mm^2)	m (mm^2/m)	Q at h=40m (l/s)
Section 1 (AC Pipe)	0.755	0.325	0.015	0.024
Section 1&2 (AC & Steel Pipe)	1.498	0.00065	0.015	0.011

The estimated flow rates, however, indicate a lower flow rate for the combined pipes, which should not be possible. This could be attributed to the following:

- The FAVAD and N1 parameters have not been adapted for the leak elevation and friction losses.
- For the combined pipe tests, the properties of the steel pipe were assumed for the entire length. This leaves room for error, which could reflect in such a discrepancy.

The fact that the estimated flow rate has not increased when the steel pipe section was added, however, suggests that it is improbable that the steel pipe contributed to the leakage.

4.4.3 Test Observations

For the purpose of this study, the fact that the leakage is below the measurable rate is already sufficient to suggest that the pipelines are in good condition and do not currently require intervention. The observation of the pressure drop over time, however, provided an opportunity for further exploring the application of the FAVAD and N1 concepts.

From the above tests it appears possible to characterise leakage to some extent, even if the flow rate cannot be recorded. This could be beneficial in scenarios where small leaks are investigated, or where access to the pipe for connecting the PCAE is not available, and the pipe can be pressurised by alternative means.

The interesting pressure drop behaviour that was observed also suggests that further analysis and investigation of this behaviour could contribute to our understanding of leak behaviour in AC pipes.

4.4.4 Leak Simulation

The existence of a 5 mm ball valve on an unused offtake, 60 metres from the connection point, provided an ideal opportunity to validate the methodology on a simulated leak with known characteristics. The low flow rate observed in the pipeline test is also beneficial, as it can be assumed that the leakage from the pipeline is negligible.

Figure 4-21 below shows the pressure and flow values that were measured with the ball valve in a fully open position. The resulting N1 and FAVAD parameters at the leak location follow in Figure 4-22. The

pressure head for the N1 and FAVAD plots have been adjusted to include the friction and minor losses, as well as the leak elevation.

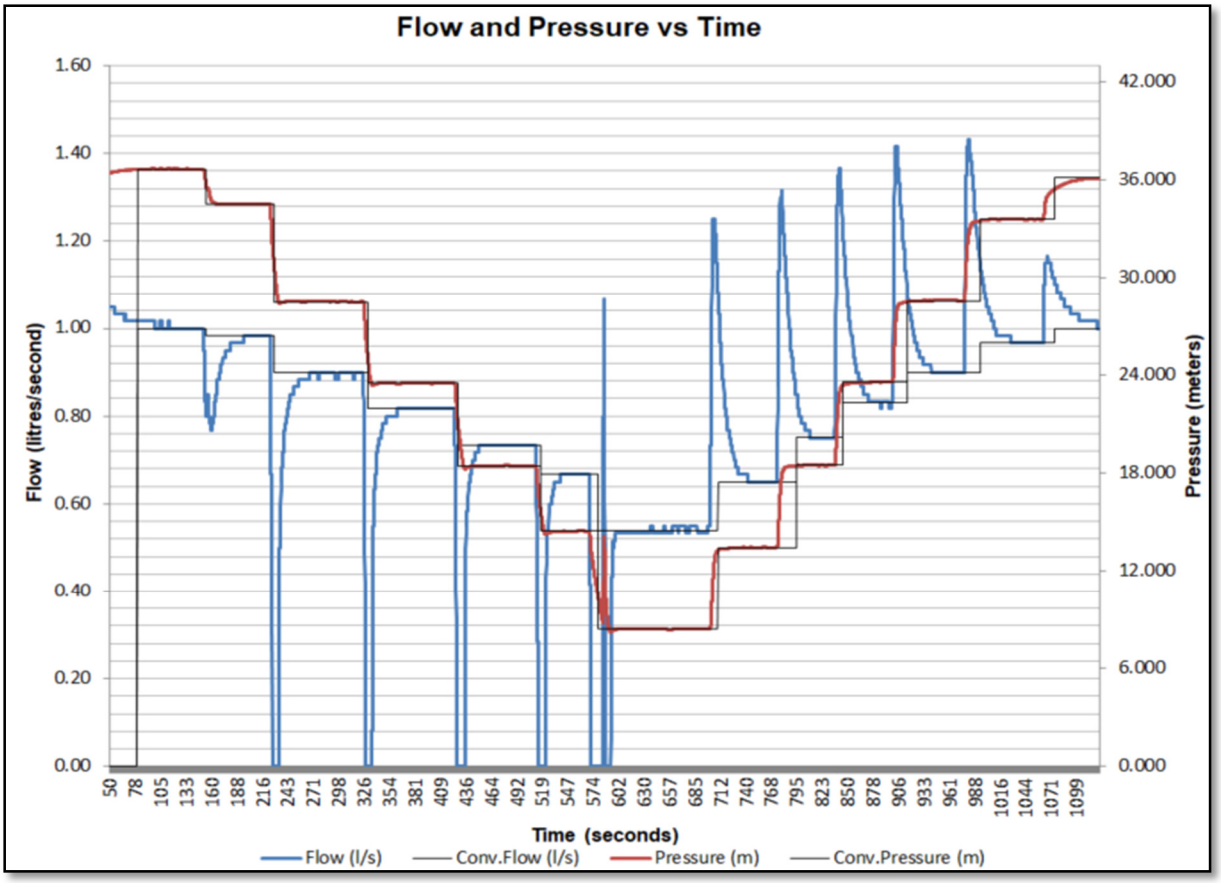

Figure 4-21: Pressure and flow over time for simulated leak on the Muckleneuk supply line

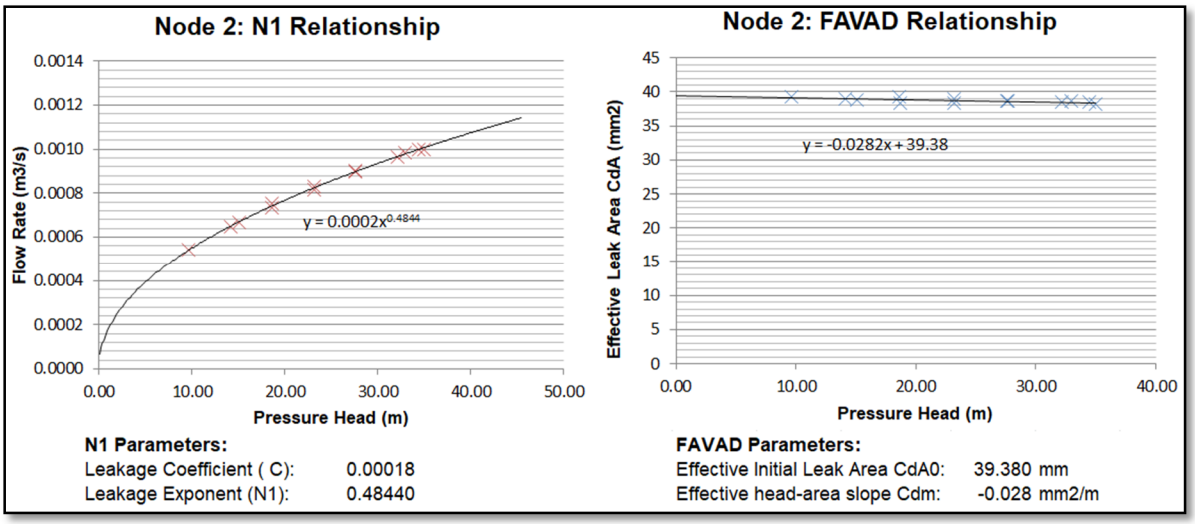

Figure 4-22: FAVAD and N1 Parameters at simulated leak location

From Figure 4-22, it can be observed that the data accurately follows a trajectory that suits the expected N1 and FAVAD behaviour for a round and rigid leak. The N1 exponent is very close to 0.5 and the effective head-area slope is very close to 0, indicating a leak area with an area that is pressure independent and meets the characteristics of an orifice.

The round and rigid opening created by a steel ball valve is expected to simulate such behaviour. In addition, the effective initial leak area is 39.380 mm^2, which is close to the 32 mm^2 area of the open ball valve. This test, therefore, validates the methodology.

4.5 Florauna Reservoir Supply Line

4.5.1 Test Description

The Florauna Reservoir is supplied by a pump station through a 1260 metre long, 300 mm diameter rising main. For the test, the pipeline was isolated by a PRV valve downstream of the connection point, before the reservoir, and a butterfly valve upstream of the connection point, close to the pump station.

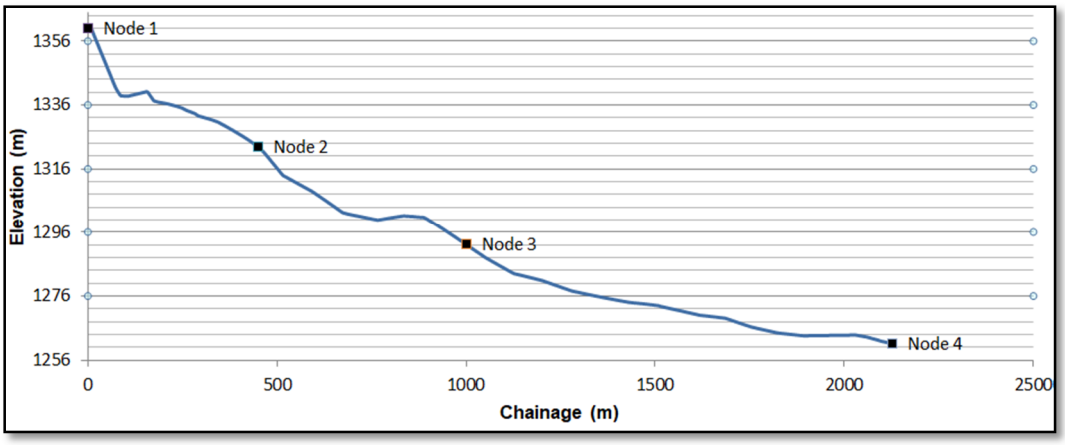

Figure 4-23: Elevation profile for Florauna Reservoir supply pipeline

The PCAE was connected at a high point on the pipeline, in the same chamber as the downstream isolation valve. The test initially indicated a significant leak, however, after tweaking the isolating gate valve during the test, the leak disappeared. The results of this test can therefore provide a good indication of the leak behaviour that can be expected for a leaking isolation valve.

4.5.2 Test Results and Discussion

The recorded data is displayed in Figure 4-24. As can be seen in the figure, a leak was initially detected and the test was commenced. After the pressure was incrementally dropped for a second time, it was realised that the upstream isolation valve leaked. The valve was closed further, after which the leakage

stopped. Small pressure fluctuations can be seen in the figure, which presumably result from the sudden reduction in leakage flow through the valve.

The flow rate then dropped to a level which was lower than the minimum flow rate which the flow meter could record. The bypass to the PCAE tank was then opened and closed repeatedly, resulting in a flow reading every time the bypass was opened. After it was realised that the flow was below the minimum recordable level, a pressure drop test was performed, which was then repeated.

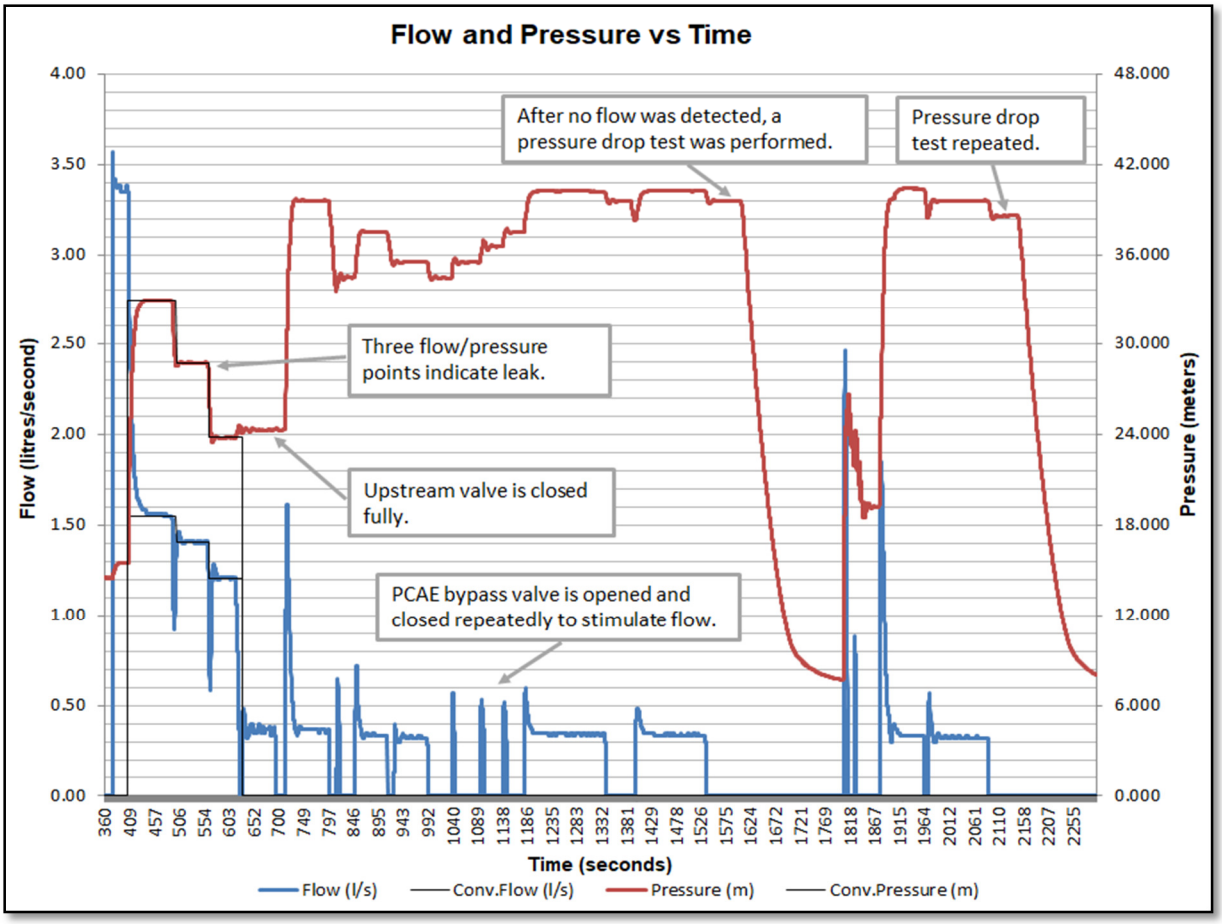

Figure 4-24: Florauna Reservoir supply line flow and pressure plot over time

The first three points were analysed by using the methodology for leaks with recordable flow rates. The FAVAD parameters were then calculated for all the nodes, with Node 1 representing the highest point at the PCAE connection point, and Node 4 representing the upstream isolation valve, which is at the lowest point. It can be clearly seen in Figure 4-25 below, that the detected leak was most likely at Node 1, as this would be the only node at which the leak characteristics would result in a positive initial leak area.

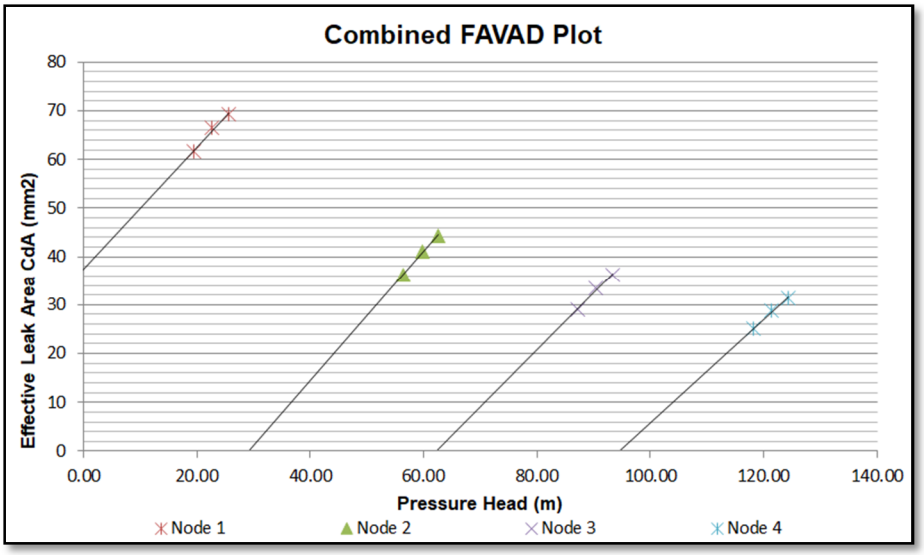

Figure 4-25: Combined FAVAD plot for Florauna reservoir supply line with leaking isolation valve

In this case, the leaking valve, therefore, results in an effective head-area slope of **C_dm = 1.258 mm²/m** and an N1 exponent of **N1 = 0.93**. The analysis of the above test confirms that the leaking valve would have been identified as the cause of the leak, even if it was not realised on site during the test.

Finally, the pressure drop test was analysed using the same methodology as applied in Paragraph 0, in order to interpret the remaining leakage in the pipe. The FAVAD parameters where estimated and optimised until the calculated pressure trajectory best matched the recorded trajectory.

As shown in Figure 4-26, the trajectory could be matched to a satisfactory accuracy, until the measured pressure head starts to level out at a pressure of approximately 7.7 metres. Considering that the connection point was at the highest elevation level of the isolated pipeline section, the fact that the pressure did not drop to zero suggests that the remaining leakage is most likely through the downstream isolation valve, from the filled pipeline leading up to the reservoir.

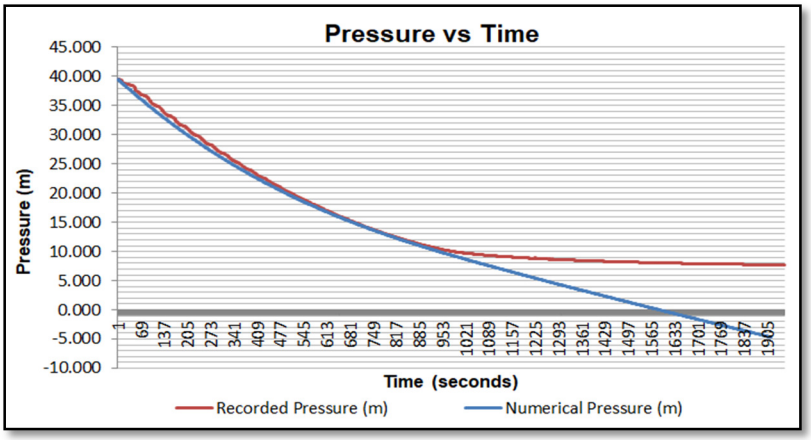

Figure 4-26: Florauna pipeline pressure drop over time, showing the recorded and calculated trajectory.

4.5.3 Test Observations

Similarly to the Parkmore High Level test, discussed under Paragraph 4.2, the leak characteristics of a leaking isolation valve were observed during this test. It was also shown that a leaking isolation valve can be identified by interpreting the test results. Understanding the behaviour of a leaking valve, and being able to identify such a leak, is important so that valve failures can be differentiated from pipeline failures.

Furthermore, this test again demonstrated how a pressure test can provide useful information on the pipe in a very short period and with minimal interference and effort. This test was carried out only by the writer and with the assistance of an artisan who is familiar with the pipe infrastructure. Within 18 minutes from arrival on site, the PCAE was set up, the hose was connected and the tank was filled. The test was then started and completed within 40 minutes, after which the equipment was disassembled. The entire duration spent on site was less than 75 minutes.

4.6 Further Tests

The remaining tests will only be briefly discussed in this section in order to avoid repetition, as most observations and lessons learned have already been raised in the five tests discussed in the preceding paragraphs. For more information, Appendix A contains detailed spreadsheets on all the pressure tests, and Appendix B contains a photo report on the remaining tests, where no pressure tests were carried out.

4.6.1 Fort Klapperkop to Carina Reservoir Pipeline

A 3245 metre long, 406 mm internal diameter steel pipeline supplies the Carina reservoir with water from a pressurised pipeline at the Fort Klapperkop Reservoirs in Pretoria. The pipeline was isolated from the supply, which has a pressure exceeding 500 kPa, by a PRV located at Node 4 in Figure 4-27. Prior to the valve chamber at Node 1, the pipeline splits into a number of branches, which all enter the valve chamber. In the chamber, four PRV's and three gate valves had to be closed in order to isolate the pipeline. A corroded strainer, located in close vicinity to the connection point, was observed to be leaking significantly, with water spraying from a crack in the strainer body.

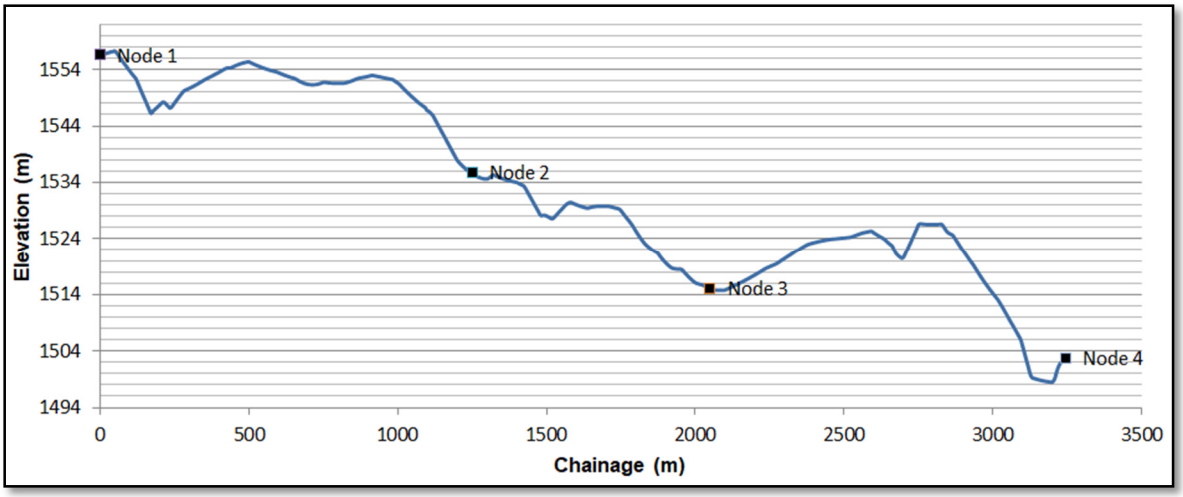

Figure 4-27: Fort Klapperkop to Carina Reservoir pipeline elevation profile

As shown Figure 4-28, the high leakage rate limited the PCAE's capacity to add pressure, and the maximum pressure that could be attained was less than 16 metres head. Nonetheless, four data points where obtained and corrected for each node, as displayed in Figure 4-29.

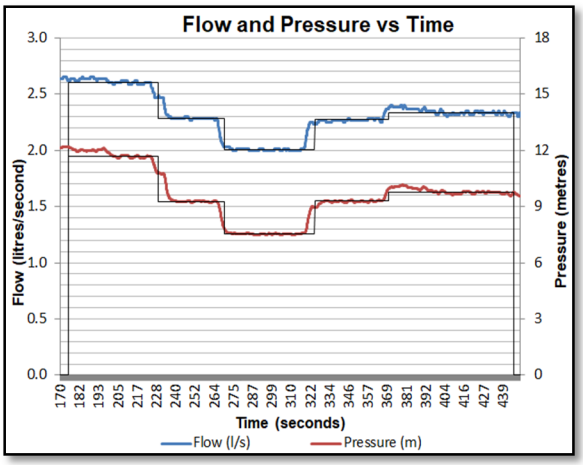

Figure 4-28: Flow and pressure plot over time for Carina supply line

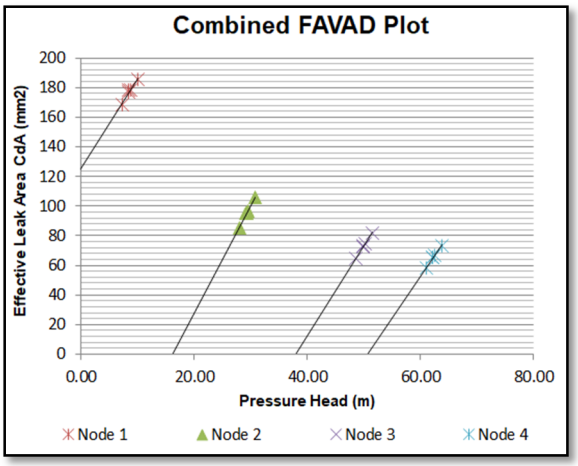

Figure 4-29: FAVAD plot for each node on the Carinal Reservoir supply line

From the FAVAD plots in Figure 4-29, it is clear that the main contributor to the leakage is within close proximity to Node 1. Similarly to the leaking valves at the Parkmore High Level and Florauna Reservoirs, discussed under Paragraph 4.2 and 0, only Node 1 yields realistic leakage characteristics.

The test was repeated, and the resulting estimated FAVAD relations for both tests are plotted in Figure 4-30. For both tests, the leak characteristics point to an initial leak area of approximately 78mm, assuming a discharge coefficient (C_d) of 0.65. The effective head-area slope, which is above 6 mm^2/m, is, however, almost six times higher than the one observed for the leaking gate valve of the Florauna supply pipe.

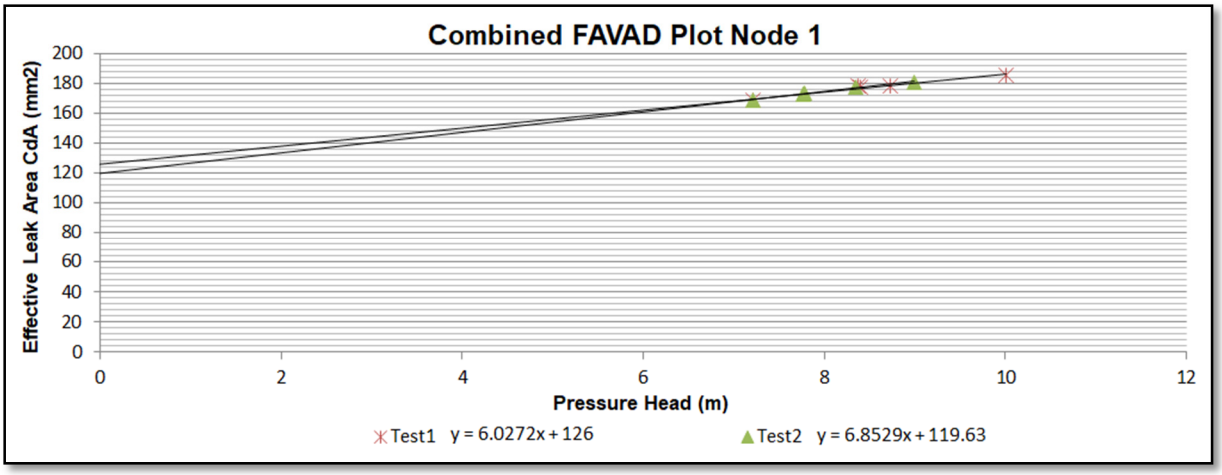

Figure 4-30: FAVAD plot at Node 1 for both tests on the Carina Reservoir supply line

The high head-area slope, therefore, suggests that the main contributor to the leak is the crack in the strainer, which expands under pressure to significantly increase the leak area as the pressure is increased.

Even though the leaking strainer prevented a proper pipeline leakage assessment, due to its high leakage rate potentially disguised further leaks along the pipeline, the test showed the extent of this leakage, which well exceeds 2.5 l/s at only 15 metres pressure head.

Finally, the test again demonstrated the effectiveness of this pipe testing technique, with the data collection for two test runs being achieved within 70 minutes from arrival on site.

4.6.2 Simon Vermooten to Murrayfield Reservoir

The supply pipeline to the Murrayfield Reservoir in Pretoria consists of an approximately 1650 metre long, 500 mm diameter, pressurised pipeline, with an elevation difference between its start and end node of approximately 90 meters.

Two butterfly valve are installed on the pipeline, with the first one located at the start of the pipeline, and the second one approximately halfway to the reservoir. A gate valve exists close to the reservoir at the end of the pipeline. The pipeline is supplied by a high pressure main, with the pressure upstream of the isolating butterfly valve exceeding 1700 kPa.

After connecting the PCAE at the high point, within close vicinity to the gate valve at the Murrayfield Reservoir, the butterfly valve at the pipeline supply was closed. The pressure, however, did not drop, prompting the removal of the hose from the PCAE in order to observe the flow behaviour. A consistent flow was witnesses exiting the pipeline, indicating that the butterfly valve did not seal.

Similar behaviour was witnessed when closing the second butterfly valve, as depicted in Figure 4-31.

Figure 4-31: Consistent flow from the Murrayfield Reservoir supply pipeline after isolation of the first valve (left) and the second valve (right).

Even though a pressure test could not be performed, the leaking valves were identified and the pipe owner was informed.

4.6.3 Brickfields to Constantia Reservoir

The Brickfields to Constantia Reservoir pipeline is approximately 600 metre long, 450 mm diameter pipeline. The pipeline is supplied by a high pressure main supply pipe, from which it can be isolated by a butterfly valve.

Similarly to the Murrayfield pipeline discussed in the previous paragraph, the isolating butterfly valve did not seal, even after repeated efforts from the pipe owner's operations team to close the valve. In this case, the flow leaking through the closed valve could be heard and sensed, prompting the termination of the test with the conclusion that the pipeline could not be isolated.

4.6.4 KwaMhlanga: Vlaklaagte to Verena Pipeline

The Vlaklaagte to Verenea pipeline is an approximately 21 km long steel gravity pipeline with a diameter of 400 mm. It is owned and operated by the Thembisile-Hani Municipality in the KwaMhlanaga region, which is approximately 80 km north-west of Pretoria.

The pipeline can be isolated into three sections by closing butterfly valves between the Vlaklaagte and Verena reservoirs. Air-valves exist along the pipeline, which can be removed in order to gain access to the pipe for the PCAE equipment.

Figure 4-32 shows the pipeline route on a satellite image. From the image it can be seen that the pipeline is situated in a very rural area and crosses the countryside. Access to the pipeline is difficult as it does not follow a road.

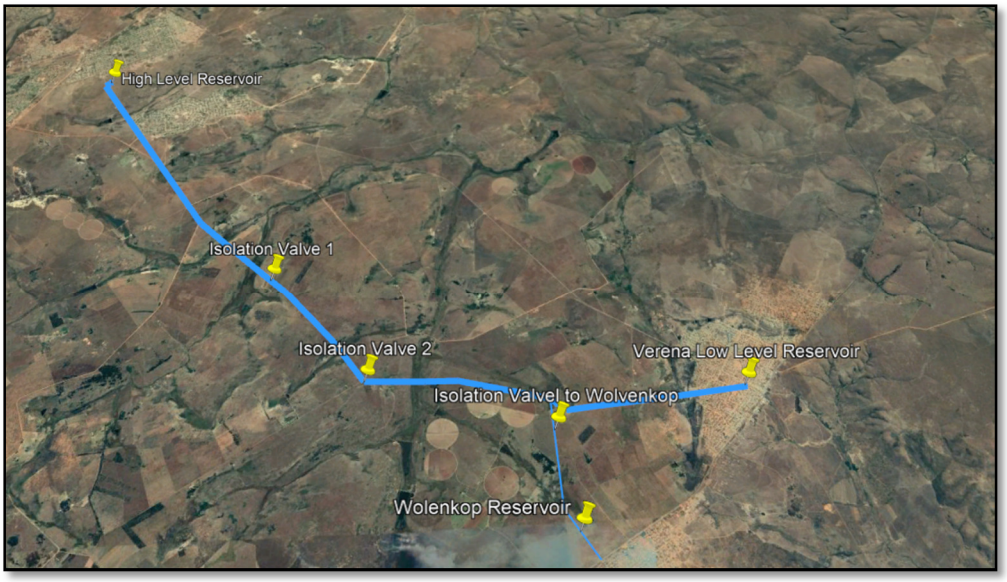

Figure 4-32: Satellite image showing the pipeline route from Vlaklaagte to Verena

Tests on all three pipeline section were attempted, starting with the last section, which ends at the Verena reservoir.

a) Isolation Valve 2 to Verena Reservoir:

The pipe section from Isolation Valve 2 is approximately 9.4 km long and traverses a hill. Attempts were made to reach the air valve on top of the hill, but the terrain proved to be inaccessible with the available vehicles and the PCAE. The PCAE was then connected to an alternative air valve located at a lower elevation, but the pipeline pressure exceeded the maximum PCAE capacity by a considerable margin. The test on this pipeline section was therefore aborted.

b) Isolation Valve 1 to Isolation Valve 2:

The second section of pipe, from Isolation Valve 1 to Isolation Valve 2, is approximately 3.8 km long, with an elevation range of approximately 43 metres. After both the isolation valves were closed, the pressure in the pipe was observed with the PCAE. As displayed in Figure 4-33, the pipeline continued to maintain the pressure that was observed before the upstream isolation valve was closed, which exceeded 80 metres.

Immediately after opening the relief valve on the PCAE, the pressure in the pipeline dropped until the relief valve was closed again, resulting in a small pressure wave, which can be recognised by

the dampening oscillating pressure behaviour in Figure 4-33. The pipeline was then pressurised by the PCAE to its maximum capacity. The pipe again maintained its pressure, with only a slight loss observed over time.

The test, therefore, concludes that this pipe section is in an excellent condition with no noteworthy leakage, and that both isolation valves sealed tightly.

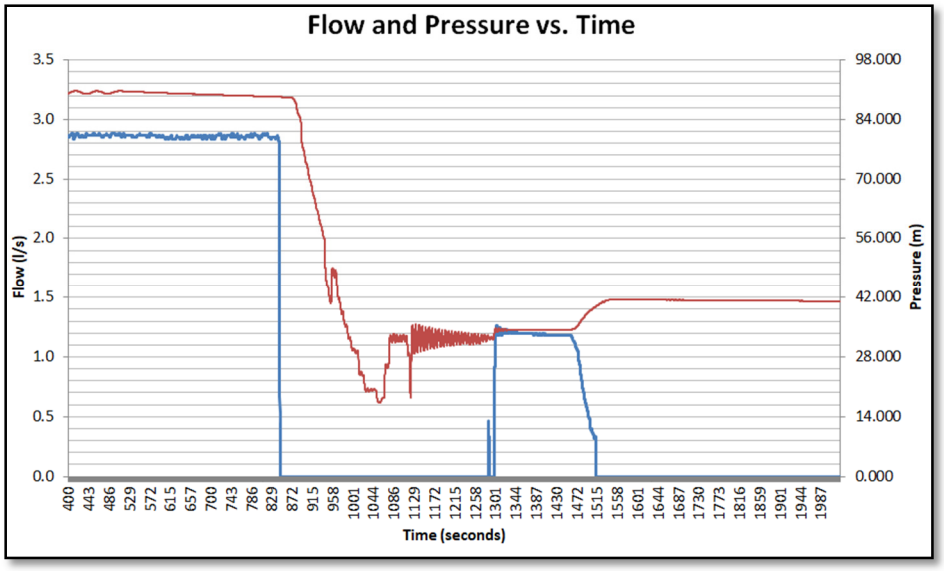

Figure 4-33: Pressure and Flow over time for Section 2 of the Verena Reservoir pipeline

c) Vlaklaagte Reservoir to Isolation Valve 1:

The first section of pipe is approximately 9 km long, and drops by an elevation difference of approximately 123 metres. The PCAE was connected by removing an air valve at a high point along the pipeline. After closing Isolation Valve 1 and filling the tank, the municipality's operations team isolated the reservoir from the pipeline.

After 3 minutes of pumping, the pressure did not increase at all. The pump was then switched off and the pressure was observed over a further 10 minutes, over which it remained constant. Realising that the pipe could not be pressurised, the test was terminated.

The most likely reason for this behaviour is that the pipeline was not full. This is likely, as water rationing was regularly taking place in the area. The pressure witnessed at the connection point was approximately 20 metres, which is similar to the estimated elevation difference between the connection point and the ground level of the reservoir, indicating that the pipeline was close to full. The fact that the pressure stayed constant, however, indicates that no significant leakage is likely.

4.6.5 KwaMhlanga: Moloto Reservoir Supply Line

The Moloto Reservoir is supplied by 300 mm diameter, 3.75 km long steel pipeline. A gate valve is installed at both the upstream and downstream end of the pipeline, allowing for isolation of the pipeline. Water rationing regularly takes place in this area, resulting in irregular use of this pipeline. This pipeline was visited with the PCAE on three occasions:

a) **Visit 1:** Arrangements were made with the municipality to test the pipe while water rationing was not taking place. When arriving on site at time on the suggested date, it was noticed, while fitting the PCAE, that the pipeline was running half empty. After a significant delay, the municipality was able to gain access to the downstream isolation valve, which they then closed. Unfortunately, however, the flow in the pipeline stopped completely before it was filled. The test was therefore postponed.

b) **Visit 2:** After arrival on site, the municipal staff member, with whom arrangements for the test were made, could not be reached. It was later discovered that the staff member was on sick leave. No other assistance was available during the limited time period while flow was expected in the pipe. The test was therefore postponed again.

c) **Visit 3:** Upon arrival on site at the suggested time and date, the pipe was completely dry. While waiting for water in the pipeline, the tests on the Vlaklaagte to Verena pipelines were carried out, which are discussed in Paragraph 4.6.4. The Moloto pipeline remained dry for the remainder of the day. It was decided to cancel further visits to this pipeline, in order not to risk more time and further travel costs.

By comparing the experiences of this test to those of some of the previous tests, the importance of having knowledgeable technical support from the entity that is responsible for the pipeline is highlighted. Even though previous tests have shown that similar pipeline tests can be performed in minimal time, this test shows that they can take considerably longer, especially if the pipeline use is unpredictable.

4.7 Summary of the Test Results and Discussion

As mentioned in the introductory paragraph of this chapter, even though the tested pipelines shared a lot of similarities, the observations made and the results obtained varied significantly. To summarise the results, the pie chart in Figure 4-34 provides an overview of all the pipeline sections tested. The white numbers refer to the number of pipe sections falling into the labelled field.

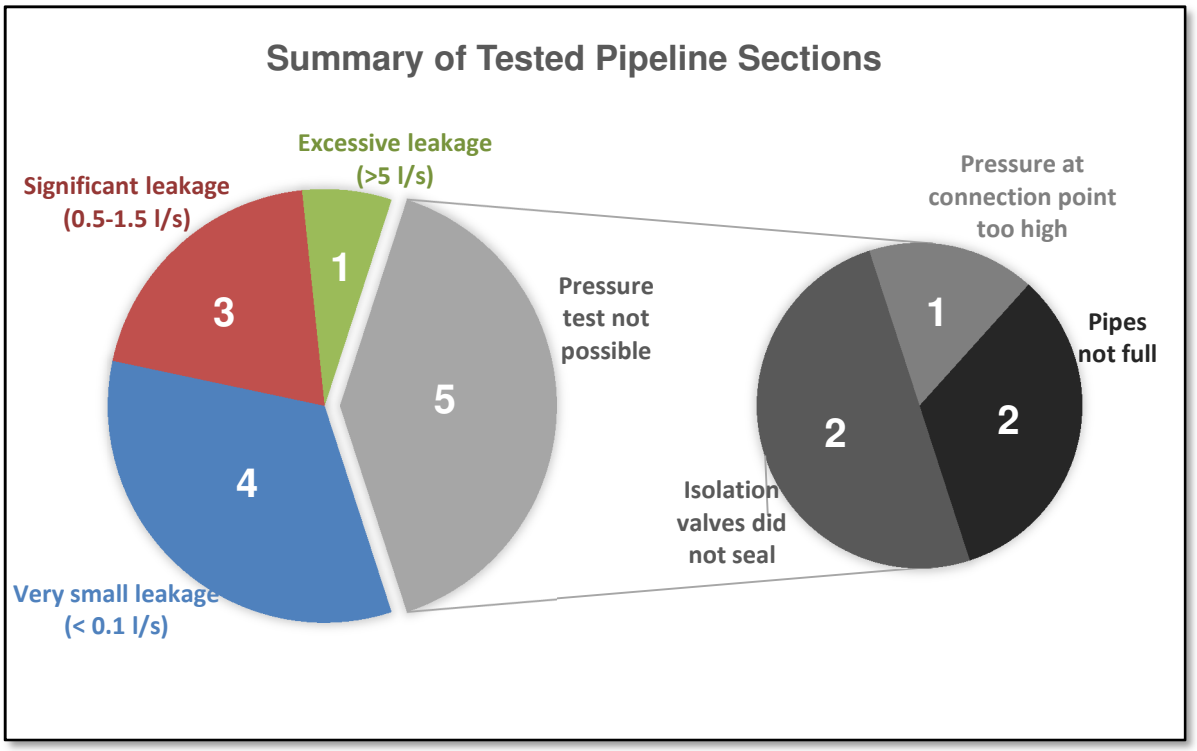

Figure 4-34: Pie chart of all pipeline sections tested

The following paragraphs group the results into outcomes of this study. The first paragraph discusses the pipeline leakage as an indicator of the pipe conditions. This is followed by a summary of the leak characteristics found in the field and discussion on the capability of the isolation valves to isolate the pipe sections.

4.7.1 Pipe Leakage

One outcome of the tests was to test the application of the PCAE for assessing the condition of pipes in the field. Although pipeline leakage is only one of numerous factors that describe the condition of a pipe, it provides a good indication of which pipelines are in more urgent need of attention.

In Table 4-5 below, the leakage rate is compared for all the pipes tested. The leakage flow rate, which is presented for each pipe test, has been standardised at an applied pressure head of 30 metres at the connection point. The ranking indicates how intervention to repair the pipelines should be prioritised.

Table 4-5: Summary of pipe leakage and general condition of all pipes tested

Pipeline Name	Leakage Rate Q (l/s) *	Rank	Comment
Lynnwood Road to Koedoesnek Reservoir	1.02	3	High leakage detected. Intervention to rectify leak strongly recommended.
Garsfontein to Parkmore High Level Reservoir	0.53	4	Significant leakage detected. Intervention to rectify leak recommended.
Queenswood Reservoir Supply Line	0.52	5	Significant leakage detected. Intervention to rectify leak recommended.
Muckleneuk Reservoir Supply Line	0.0073	✓	Leak is insignificant. No need for intervention in both AC and steel pipe.
Florauna High Level Reservoir Supply Line	0.078	✓	Leak is small. No need for intervention.
Fort Klapperkop Reservoirs to Carina Street Reservoir	6.0**	1	Extreme leakage. Urgent intervention required on Strainer.
Simon Vermooten to Murrayfield Reservoir	Unknown	6	Pipe appeared to be in good condition. Isolation valve must first be attended to before pipe leakage can be assessed further on both sections.
Brickfields to Constantia Reservoir	Unknown	2	Pipe did not appear to be in a good condition. Valve did not isolate at all and must be fixed urgently before pipeline can be assessed further.
KwaMhlanga: Vlaklaagte to Verena Line	Insignificant	7	No significant leakage in 2 of 3 sections. Pipe appears to be in a very good condition, except for a visual leak on an air-valve on the untested section.
KwaMhlanga: Moloto Pipeline	Unknown	8	Pipe not tested, but from visual inspection appears to be in a good condition.

* Leakage rate at connection point (at high point on pipeline), with 30 metres of pressure head applied.

** Maximum recorded flow was 2.6l/s at 12m head. 6 l/s is estimated if the trend is extended.

To put the observed leakages into perspective, Table 4-6 below shows the total water lost per annum, as well as the estimated annual direct loss in revenue resulting from these leakages. A production cost of 5 Rand/m^3 is assumed for this calculation, considering that the water source is a long distance away from the leak location for all the tested pipelines in Table 4-6.

All of the mains listed in Table 4-6, remain pressurised permanently, irrespective of the reservoir level. The leakage is therefore assumed to be at a constant rate over 24 hours per day for 365 days of the year.

Table 4-6: Annual water and revenue loss from detected leakage

Pipeline Name	Leakage Rate Q (l/s) *	Annual Leakage Volume (m^3/annum)	Annual Lost Revenue (Rands/annum)
Lynnwood Road to Koedoesnek Reservoir	1.02	37 843	189 216
Garsfontein to Parkmore High Level Reservoir	0.53	16 714	83 570
Queenswood Reservoir Supply Line	0.52	16 398	81 993
Fort Klapperkop Reservoirs to Carina Street Reservoir	6.0	189 216	946 080
Totals:		**260 172.00**	**1 300 860.00**

Table 4-6 presents the direct financial implications of leaving leaks unattended. The high revenue loss resulting from the leaking strainer at the Carina Street Reservoir, is of particular concern, as such a visible leak can be prevented or repaired at a minimal cost and with little effort.

However, even if the excessive leakage from the strainer is attended to, the loss from the remaining pipes is significant. The size of the leakages observed in these pipelines are often perceived to be negligible by pipe operators, because the leakage flow rates are small compared to the volumes transferred in bulk pipelines. In this case, however, the leakage from these pipes can amount to over 350 000 Rand per annum, which should be sufficient reason to motivate for the identification and repair of such leaks.

It must also be noted that the measured leakages, apart from the visible strainer leakage, would not be detected without condition assessments, and the pipe owner was, in fact, not aware of the leakages. Considering that only a small sample of the whole bulk infrastructure was tested, it is highly likely that a large number of leaks exist without the knowledge of the pipe owner.

Performing condition assessments on pipes, and subsequently identifying and repairing leaks, therefore, has the potential to greatly reduce revenue losses. This is over and above the fact that water should be treated as a limited and scarce resource, which must be responsibly managed to ensure sustainability.

4.7.2 Leak Characteristics

Another outcome of this study is to characterise the leaks that where identified. Table 4-7 below provides approximate possible locations for the leaks, as well as the respective characteristics of the leaks, if the leaks indeed exist in the suggested locations.

It must be noted here, however, that the high elevation differences in bulk pipelines, as well as the potential errors in estimating frictional losses, significantly affect the resulting leak characteristics. The N1 exponent, the initial leak area and the head-area slope can therefore vary significantly, as the exact leak locations are not known. Nonetheless, these values still provide valuable information for assessing the source of the leak.

Table 4-7: Leak characteristics of all the pipelines tested (C_d =0.65)

Pipeline	Estimated Leak Area:	Leak Characteristics:	Comment
Lynnwood Road to Koedoesnek Reservoir	Low section, from Node 3 to Node 4.	N1: 0.89-1.31 A_0: 7.5-50.0 mm^2 m: 0 – 0.42 mm^2/m	N1 and A_0 vary significantly depending on the leak location. m remains fairly constant.
Garsfontein to Parkmore High Level Reservoir	Low section, closer to Node 2. Higher Nodes also possible.	N1: 0.84-1.45 A_0: 1.1 – 3.5 mm^2 m: 0.26-0.28 mm^2/m	N1 and A_0 vary significantly, as the leak can be within a large elevation range. m remains fairly constant.
Queenswood Reservoir Supply Line	Lowest section, at Node 3	N1: 0.18 - 0.19 A_0: 31.7 – 35.2 mm^2 m: -0.08 -0.04 mm^2/m	An N1<0.5 and a negative m value is not expected. Possibly the frictional loss was underestimated. Large leak area expected.
Muckleneuk Reservoir Supply Line	At low point, but negligible.	N1*: 1.5 A_0*: 0.770 mm^2 m*: 0.015 mm^2/m	Pressure drop test was performed. Leakage is minor.
Florauna High Level Reservoir Supply Line	Possibly through valve, but negligible,	N1*: 0.83 A_0*: 1.8 mm^2 m*: 0.042 mm^2/m	Pressure drop test was performed. Leakage is minor.
Fort Klapperkop Reservoirs to Carina Street Reservoir	At strainer at Node 1.	N1: 0.79 A_0: 184-193 mm^2 m: 9.3-10.5 mm^2/m	High flow rate through strainer possibly hides smaller leaks on pipeline. Very large leak area detected.
Simon Vermooten to Murrayfield Reservoir	Unknown	Unknown	Isolation valves did not seal.
Brickfields to Constantia Reservoir	Unknown	Unknown	Isolation valves did not seal.
KwaMhlanga: Vlaklaagte to Verena Line	No leaks suspected	N/A	Unknown
KwaMhlanga: Moloto Pipeline	Unknown	Unknown	Unknown

* Characteristics at connection point and not at most likely leak location.

4.7.3 Isolation Valve Conditions

The condition of the isolation valves was found to play a critical role in the success of the tests. It was therefore decided to summarise the findings, specifically of the isolation valves, in order to provide the reader with an overview of the amount of valves that were effective. The valve types encountered, as well as the number of valves that failed to isolate for each valve type, are displayed in the pie chart in Figure 4-35.

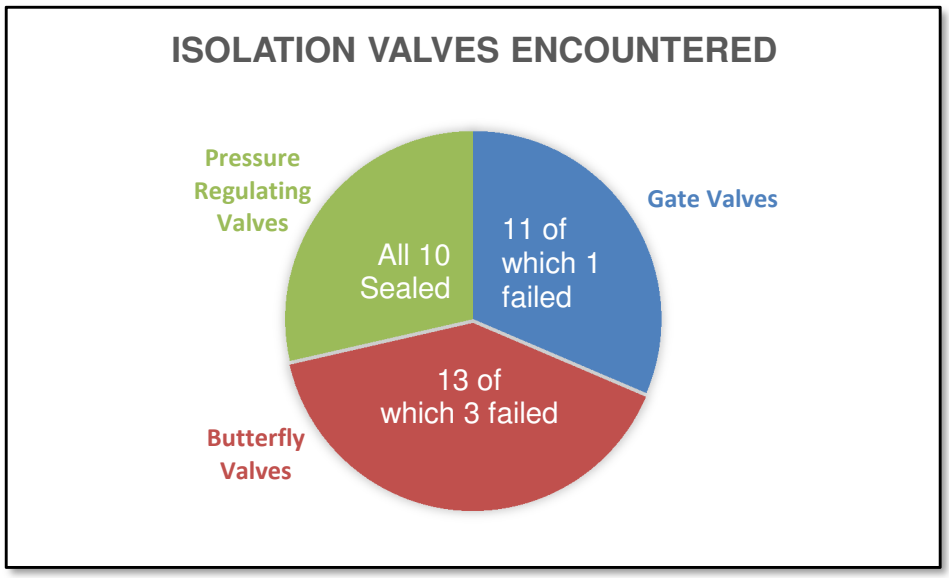

Figure 4-35: Summary of all isolation valves encountered

From Figure 4-35, it is clear that, of the 34 valves encountered, only 4 were found to be leaking significantly. None of the PRVs failed, and most failures were observed on butterfly valves.

Table 4-8 lists all the valves encountered, as well as their ability to isolate the pipeline.

Table 4-8: Summary of isolation valves for all pipelines tested

Pipeline	Upper Isolation Valve	Seal/not Seal	Lower Isolation Valve	Seal/not Seal
Lynnwood Road to Koedoesnek Reservoir	PRV	- sealed	Butterfly	- sealed
Garsfontein to Parkmore High Level Reservoir	2x Gate	- one did not seal - one sealed	PRV	- sealed
Queenswood Reservoir Supply Line	PRV	- sealed	Butterfly	- sealed
Muckleneuk Reservoir Supply Line	PRV	- sealed	2x Gate Valves	- both sealed
Florauna High Level Reservoir Supply Line	Gate	- sealed, negligible leakage. - initially did not seal (N1=0.93, C_dm=1.26mm^2/m, C_dA_0=37mm)	PRV	- sealed
Fort Klapperkop to Carina Street Reservoir	3x Gate 4x PRV	- appeared to seal - High leakage in strainer could have disguised valve leak.	PRV	- sealed
Simon Vermooten to Murrayfield Reservoir	Gate	- appeared to seal	2x Butterfly	- both did not seal
Brickfields to Constantia Reservoir	2x Gate	- not tested	Butterfly	- did not seal
KwaMhlanga: Vlaklaagte to Verena Line	4x Butterfly	- 2 sealed - 2 unknown	3x Butterfly	- all three sealed
KwaMhlanga: Moloto Pipeline	Butterfly	- appeared to seal	Butterfly	- unknown

Chapter 5

5 Conclusion and Recommendations

5.1 Summary of Study

In this study, the application of a pipe condition assessment technique, which uses pressure tests to characterise leakage in pipelines, was tested for its application on bulk transfer pipelines in the field. This investigation included the implementation and testing of equipment, which was developed by the University of Cape Town for this purpose. It also included the processing, analysis and interpretation of the results, using the FAVAD and N1 concepts.

Through a great deal of correspondence with various pipe owners, a number potential pipelines were identified for testing. After filtering the proposed pipes with the requirements needed for applying the testing technique, ten pipelines remained. One of the pipelines could be divided into three separate sections, and another pipeline could be divided into two sections, increasing the total number of pipe sections to thirteen.

Pressure tests were attempted on all of these pipes using the pressure testing equipment provided. For the tests which provided pressure versus leakage flow rate data, the results were processed according to the FAVAD and N1 leakage concepts. In cases where the flow rate was too small to be recorded, a pressure drop test was performed, from which flow rates were estimated based on FAVAD behaviour.

The study also includes the development of an Excel spreadsheet tool, which was developed to simplify the processing of the test data. Although the tool greatly assisted by minimising the repetitive work during the analysis of all the tests, the main aim for developing this tool to such detail, was to demonstrate the ease and effectiveness with which valuable results could be obtained from the test data.

After analysis of the tested pipelines, the results were summarised according to the recorded pipeline leakage, the likely leak characteristics and the ability of the isolation valves to effectively isolate the pipe. The severity of the pipeline conditions were assessed according to these factors, and a ranking was allocated to indicate which pipelines were in most urgent need of intervention.

Of the pipelines tested, the leakage was determined for eight of the pipe sections. Of the remaining pipe sections, two could not be isolated, due to the isolation valves leaking significantly; one could not

provide test results at all, as it was either empty or short from full on all three test attempts; and one failed to provide a suitable, accessible connection point, at which the static pipe pressure did not exceed the maximum capacity of the equipment.

A wide range of leakage flow rates were recorded. Four pipe sections provided clear pressure-leakage data points that were further processed and analysed to determine the most likely leakage characteristics. In another four pipe sections, the leakage was below the minimum flow rate that the equipment could detect. In two of these cases, a pressure drop test was performed, and the characteristics, matching the observed pressure drop best, were estimated.

For comparison reasons, the leakages were all estimated at an applied pressure of 30 metres at the connection point. Of the four pipelines that showed measurable leakage, two leaked significantly, with leakage flow rates above 0.5 l/s. One leaked at double the rate, at approximately 1.0 l/s, and one leaked excessively at above 6 l/s.

For all the leaking pipes, the leakage was analysed to obtain the N1 leakage number and characterised according to the FAVAD leakage model. By comparing the characteristics of well-defined leaks in literature to the observed behaviour in the field, valuable clues relating to the possible leak location and type were obtained. This was achieved by adapting the recorded data by incorporating the pressure losses or gains according to the elevation profile, friction losses and minor losses at theoretical leak locations, strategically placed along the pipeline length.

Apart from characterising actual leakage from the pipeline, other interesting events were observed. The pressure-leakage behaviour of these events were reported and analysed to demonstrate the capability of the technique to identify the cause of such behaviour:

- Leaking valves: Leaking valves were detected a number of times during the pressure tests. After processing the data using the FAVAD model, a clear indication was obtained on the likelihood of an isolation valve not sealing. The results were also able to indicate at which end of the pipeline the isolation valve was likely failing. By adjusting or jerking the suspected leaking valve in a subsequent test, changes in the results were able to confirm if the suspected valve was indeed the source of the leakage.

- Air in the pipeline: An air bubble in the pipeline dampens the effect of sudden pressure changes. In one test, air was unintentionally introduced into the pipeline. The presence of the air could be clearly recognised by the oscillating pressures, which took longer to stabilise.

- An open ball valve along the pipeline: The analysis of an open ball valve not only validated the methodology, but it also demonstrated the behaviour that would result from an off-take along the pipeline, which is open to the atmosphere, such as an open tap.

- A leak from a cracked strainer: The analysis of the leakage behaviour in one of the tests pointed to a leak close to the connection point, with an area that was highly pressure dependent. This finding was validated, as a cracked and corroded strainer was leaking excessively in the vicinity of the connection point.

One test, however, provided different pressure-leakage characteristics for the pressure hiking cycle, in comparison to the pressure dropping cycle. The cause of this behaviour could not be identified and further investigation, beyond the scope of this study, is required.

Finally, it is important to note that the number of pipe sections that could be tested was limited in comparison to the number of bulk pipelines that exist in Pretoria and the surrounding region. The reasons for a large number of pipes not being suitable for testing should, however, not reflect negatively on the applicability of this test to assess pipes in the field, as most of these reasons could be resolved should this testing technique be adopted in practice.

The main reason for a number of pipes not being accessible, was the lack of cooperation or the unwillingness of major pipe owners or pipe operators to make pipes available for testing purposes, presumably due to the perceived risk involved. The tests did show, however, that it is possible to apply this test without exceeding the pipe operating pressure, thereby not posing any risk to the integrity of the pipe.

The second most common reason was due to downtime not being available for testing purposes. Should the technique be implemented in practice in a planned and systematic fashion, however, downtime could be arranged. The tests in this study also show that, if sufficient preparation is made, downtime can be limited to periods shorter than 1 hour.

Certain pipes did not have a connection points at suitable locations. Should this method of testing be adopted as a condition assessment technique by the pipe owner, this restriction could be resolved by the installation of connection points, which could then be used for recurring tests.

Other reasons indicate that the pipe requires intervention, irrespective of the test being applied. These include pipes where the operators were aware of excessive leakage, which exceeded the capacity of the test equipment and pipes that were not isolatable due to inoperable, flooded or excessively leaking isolation valves.

Only pipelines with no installed isolation valves, or isolation valves leaking at rates that were deemed acceptable by the pipe owner, posed a limitation to this testing technique.

5.2 Main Findings and Lessons Learned

- The application of the pressure testing equipment and the testing technique was found to be effective for assessing the condition of most bulk pipelines encountered in the field in terms of their leakage characteristics.

- By interpreting the leakage characteristics, clues could be obtained on the most likely leak source, even though the technique is not suitable for pinpointing the exact leak location.

- The leakage flow rates, together with the likely leak sources, can be used to rank the tested pipes according to the severity of their condition and their need for intervention. Pipe owners or operators can therefore use this technique as an initial screening tool, to determine the order in which pipes must be repaired to optimally allocate resources and funding.

- The effectiveness of the equipment is limited to the sealing capability of the isolation valves. Of the 35 isolation valves encountered during the tests, however, only four leaking valves were identified, which continued to leak significantly after repeated efforts to close the valve.

- The elevation profiles of bulk pipelines were found to vary significantly along the length. Due to the leak characteristic's sensitivity to pressure, the varying elevations were observed to have a dominating effect on the resulting leak characteristics. On the one hand, this allows for the identification of the most likely leak elevation, and subsequently the most likely leak location. On the other hand, the high dependence of the leak characteristics on the leak location made accurate characterisation of the leak, in terms of the leak size, type and shape, unpredictable.

- Similar to the effect of the elevation variation, the frictional and minor losses increasingly influence the leak characteristics as the leak location moves further away from the connection point. Due to the long lengths of bulk pipelines, the accuracy of the loss calculations, which are based on assumed pipe properties, can affect the resulting leak characteristics, especially if the leak is large and the pipe diameter is small.

- The downtime required to perform the test can be minimised by proper preparation. If the details of the connection point are known in advance, and the isolation valves are tested in advance, the test can be completed with less than 1 hour of downtime. After the downtime, the pipe can immediately be operated, as it remains filled with water.

- The downtime and ease of implementing the test is greatly influenced by the existence of valves on the connection points. This allows for connection and removal of the equipment, as well as tank filling, while the pipe remains in operation.

- The results can be processed and interpreted with minimal effort and in little time by using basic software programmes to assist with this task. If the pipe information is obtained in advance, the information can be loaded into the data processing programme prior to the test, making on-site evaluation of the results even more achievable.

5.3 Recommendations

5.3.1 Recommendations for future tests

For future tests, the following recommendations derive from the lessons learned in this study:

- The pipeline operating pressure and operating flow rate should be obtained while the pipe is in normal operation. The leakage characteristics can then be used to estimate the actual leakage during operation, rather than the leakage at a theoretical benchmark value, as was done in this study. This would also allow for the calculation of the Infrastructure Leakage Index (ILI) and the Unavoidable Annual Real Losses (UARL), so that the extent of leakage can be related to the characteristics of the pipe.

- In addition to the operating flow rate and pressure, effort should be made to obtain more pipeline information in general, such as the exact pipe diameters, wall thicknesses and surface roughness valves. This would assist with the friction calculations required for adapting the recorded data to the different node locations.

- Where possible, it would be of great benefit if the tests could be followed by an extensive investigation of the tested pipeline, in order to verify the findings of the test.

- Ideally, the pipeline should be inspected before the test is attempted and the equipment is transported to site. Such an inspection should include the identification of a suitable connection point and a check on the operability of the isolation valves.

5.3.2 Proposed enhancements to the technique and equipment

The equipment performed well and no major changes are required. Should the technique and equipment be commercialised, however, the following improvements are proposed:

- A pump with an increased capacity to add pressure at higher heads would be beneficial in cases where the highest point on the pipeline cannot be accessed or exists in an inconvenient location. Even though the current equipment can add up to 40 metres in head, any connection point at a lower level decreases the pressure range that can be applied for obtaining data points.

- A higher water tank capacity would be desirable. During more than one test, the tank emptied before the test was completed. The tank also had to be refilled on numerous occasions if the test had to be repeated. Filling the tank requires the opening and closing of the isolation valves on the pipeline, which can significantly increase the downtime required.

- Rough or inaccessible terrain surrounding the ideal connection point was encountered. A more rugged vehicle or a considerably longer hose from the testing equipment to the connection point would assists in such cases.

- A device to verify isolation valve leakage would complement the equipment well. A basic acoustic device is suggested, with which a closed isolation valve can be assessed.

- Separate pressure transducers with fittings are recommended as part of the testing equipment. These can then be used to measure the normal operating pressure in the pipe, before or after the pipeline is isolated.

References

(SAICE), S. A. I. of C. E. (2011). *Infrastructure Report Card for South Africa*.

Bennis, S., Fares, R., Guemouria, N., & Dubois, M. (2011). Theoretical modeling and experimental validation of leakage in drinking water networks. *Journal American Water Works Association*, *103*(12), 61–+.

Boulos, P. F., & Aboujaoude, A. S. (2011). Managing leaks using flow step-testing, network modeling, and field measurement. *Journal / American Water Works Association*, *103*(2), 90–97.

Cassa, A. M., & Van Zyl, J. E. (2014). Predicting the leakage exponents of elastically deforming cracks in pipes. *Procedia Engineering*, *70*, 302–310. http://doi.org/10.1016/j.proeng.2014.02.034

Cassa, A. M., van Zyl, J. E., & Laubscher, R. F. (2010). A numerical investigation into the effect of pressure on holes and cracks in water supply pipes. *Urban Water Journal*, *7*(2), 109–120. http://doi.org/10.1080/15730620903447613

Cataldo, a., Persico, R., Leucci, G., De Benedetto, E., Cannazza, G., Matera, L., & De Giorgi, L. (2014). Time domain reflectometry, ground penetrating radar and electrical resistivity tomography: A comparative analysis of alternative approaches for leak detection in underground pipes. *NDT & E International*, *62*, 14–28. http://doi.org/10.1016/j.ndteint.2013.10.007

Cataldo, A., Cannazza, G., Benedetto, E. De, & Giaquinto, N. (2012). Underground Water Pipelines, *12*(6), 1660–1667.

Cataldo, A., De Benedetto, E., Cannazza, G., Piuzzi, E., & Giaquinto, N. (2015). Embedded TDR wire-like sensing elements for monitoring applications. *Measurement: Journal of the International Measurement Confederation*, *68*, 236–245. http://doi.org/10.1016/j.measurement.2015.02.050

Charalambous, B. (2005). Experiences in DMA redesign at the Water Board of Lemesos, Cyprus. *Leakage 2005*, 1–11.

Clayton, C. R. I., & van Zyl, J. E. (2007). The effect of pressure on leakage in water distribution systems. *Water Management*, *160*(June), 109–114. http://doi.org/10.1680/wama.2007.160.2.109

Colombo, A. F., & Karney, B. W. (2002). Energy and Costs of Leaky Pipes: Toward Comprehensive Picture. *Journal of Water Resources Planning and Management*, *128*(6), 441–450. http://doi.org/10.1061/(ASCE)0733-9496(2002)128:6(441)

Colombo, A. F., Lee, P., & Karney, B. W. (2009). A selective literature review of transient-based leak detection methods. *Journal of Hydro-Environment Research*, *2*(4), 212–227. http://doi.org/10.1016/j.jher.2009.02.003

Costello, S. B., Chapman, D. N., Rogers, C. D. F., & Metje, N. (2007). Underground asset location and condition assessment technologies. *Tunnelling and Underground Space Technology*, *22*(5–6), 524–542. http://doi.org/10.1016/j.tust.2007.06.001

CRANE Nuclear. (2013). *General Engineering Data*.

de Miranda, S., Molari, L., Scalet, G., & Ubertini, F. (2014). A physically-based analytical relationship for practical prediction of leakage in longitudinally cracked pressurized pipes. *Engineering Structures*, *79*, 142–148. http://doi.org/10.1016/j.engstruct.2014.08.011

de Wit, M., & Stankiewicz, J. (2006). Changes in Surface Water Supply Across Africa with Predicted Climate Change. *Science*, *311*(5769), 1917–1921. http://doi.org/10.1126/science.1119929

Deyi, M., Van Zyl, J., & Shepherd, M. (2014). Applying the FAVAD concept and leakage number to real networks: A case study in Kwadabeka, South Africa. *Procedia Engineering*, *89*, 1537–1544. http://doi.org/10.1016/j.proeng.2014.11.450

Dobbs, R., Pohl, H., Lin, D.-Y., Mischke, J., Garemo, N., Hexter, J., … Nanavatty, R. (2013). Infrastructure productivity: how to save $1 trillion a year. *McKinsey Global Institute*, (January), 100.

DWS. (n.d.). Water Service Institutions. Retrieved November 20, 2018, from http://www.dwa.gov.za/IO/wsi.aspx

DWS, & Sussens, H. (2015). *Metropolitan Municipality Water Balance Assessment*.

Environmental Protection Authority. (2007). *Leakage Management Technologies*. *American Water Works Association*.

Essop, R. (2016, June 10). Eight Provinces Declared Disaster Areas due to Drought. *Eyewitness News*. Cape Town. Retrieved from http://ewn.co.za/2016/06/10/Eight-provinces-declared-drought-disaster-areas

Farley, M. (2003). NON REVENUE WATER Paper presented to 12 th Annual CWWA Water , Wastewater & Solid Waste. *Paper Presented To 12Th Annual Cwwa Water, Wastewater and Soil Waste Conference 28 Sept-3 Oct 2003- Atlantis, Paradise Island Bahamas*, (Ili).

Ferrante, M. (2011). Experimental investigation of the effects of pipe material on the leak law : leak in a steel pipe. *Journal of Hydraulic Engineering*, *under revi*(August), 736–743. http://doi.org/10.1061/(ASCE)HY.1943-7900.0000578.

Ferrante, M., Brunone, B., Meniconi, S., Capponi, C., & Massari, C. (2014). The leak law: From local to global scale. *Procedia Engineering*, *70*, 651–659. http://doi.org/10.1016/j.proeng.2014.02.071

Ferrante, M., Massari, C., Brunone, B., & Meniconi, S. (2011). Experimental Evidence of Hysteresis in the Head-Discharge Relationship for a Leak in a Polyethylene Pipe. *Journal of Hydraulic Engineering*, *137*(7), 775–780. http://doi.org/10.1061/(ASCE)HY.1943-7900.0000360

Ferrante, M., Meniconi, S., & Brunone, B. (2014). Local and global leak laws: The relationship between pressure and leakage for a single leak and for a district with leaks. *Water Resources Management*, *28*(11), 3761–3782. http://doi.org/10.1007/s11269-014-0708-x

Frauendorfer, R., & Liemberger, R. (2010). *The Issues and Challenges of Reducing Non-Revenue Water*.

Gao, Y., Brennan, M. J., Joseph, P. F., Muggleton, J. M., & Hunaidi, O. (2005). On the selection of acoustic / vibration sensors for leak detection in plastic water pipes. *Journal of Sound and Vibration*, *283*, 927–941. http://doi.org/10.1016/j.jsv.2004.05.004

Greyvenstein, B., & Van Zyl, J. E. (2007). An experimental investigation into the pressure - Leakage relationship of some failed water pipes. *Journal of Water Supply: Research and Technology - AQUA*, *56*(2), 117–124. http://doi.org/10.2166/aqua.2007.065

Hamilton, S., & Charalambous, B. (2013). *Leak Detection Technology and Implementation*. *CAS Vacuum Technology*. IWA Publishing.

Hamilton, S., McKenzie, R., & Seago, C. (2006). A review of performance indicators for real losses from water supply systems. *UK House of Commons Report*, (July), 1–9. Retrieved from http://www.iwaponline.com/jws/048/jws0480227.htm

Hannaford, M. A., & Melia, W. J. (2010). An Advanced Method of Condition Assessment for Large-Diameter Mortar-Lined Steel Pipelines. *Hetch Hetchy Water and Power Project San Francisco Public Utilities Commission*, (Figure 1), 1–11.

Hao, T., Rogers, C. D. F., Metje, N., Chapman, D. N., Muggleton, J. M., Foo, K. Y., … Saul, A. J. (2012). Condition assessment of the buried utility service infrastructure. *Tunnelling and Underground Space Technology Incorporating Trenchless Technology Research*, *28*, 331–344.

Hedden, S., & Cilliers, J. (2014). Parched prospects: The emerging water crisis in South Africa. *Water Wheel*, *13*(6), 42–47.

Hedden, S., ISS, & WRC. (2016). Parched prospects II A revised long-term water supply and demand forecast for South Africa. *African Futures*, *16*(March), 1–18.

Herbst, P., & Raletjena, M. (2015). No Drop in the Context of Water Security. In *5th Regional Annual Water Leakage Summit* (pp. 1–52).

Hiki, S. (1981). Relationship between Leakage Quantity and Pressure. *Journal of Japan Waterworks Association*, *51*(5), 50–54.

Hunaidi, O., & Giamou, P. (1998). Ground-penetrating radar for detection of leaks in buried plastic water distribution pipes. *Proceedings of the 7th International Conference on Ground Penetrating Radar*, (May), 783–786.

Hunaidi, O., Wang, A., & Bracken, M. (2004). Acoustic methods for locating leaks in municipal water pipe networks. *Conference on Water*, 1–14.

Idelchik, I. E. (1966). *Handbook of Hydraulic Resistance*. (D. Grunaer, Ed.). Springfield.

Innospection. (n.d.). Remote Field Eddy Current Technique. Retrieved April 1, 2016, from http://www.innospection.com/pdfs/Remote Field Eddy Current.pdf

Kabaasha, A.M., Piller, O., and Van Zyl, J.E. (2018). "Incorporating the modified orifice equation into pipe network solvers for more realistic leakage modeling." Journal of Hydraulic Engineering, 144(2) 1-8

Karney, B., Khani, D., & Halfawy, M. R. (2009). A Simulation Study on Using Inverse Transient Analysis for Leak Detection in Water Distribution Networks, *6062*. http://doi.org/10.14796/JWMM.R235-23.

Kingdom, B., Liemberger, R., & Marin, P. (2006). The Challenge of Reducing Non-Revenue Water (NRW) in Developing Countries: How the Private Sector Can Help. *WATER SUPPLY AND SANITATION SECTOR BOARD DISCUSSION*, (No. 8).

Lai, W. W. L., Chang, R. K. W., Sham, J. F. C., & Pang, K. (2016). Perturbation mapping of water leak in buried water pipes via laboratory validation experiments with high-frequency ground penetrating radar (GPR). *Tunnelling and Underground Space Technology*, *52*, 157–167.

Lambert, A. (2000). What do we know about pressure leakage relationships in distribution systems? *IWA Conference System Approach to Leakage Control and Water Distribution System Management*, (May), 1–9.

Lambert, A., & Hirner, W. (2000). Losses from Water Supply Systems: Standard Terminology and Recommended Performance Measeures. *IWA: The Blue Pages*, (3).

Laven, K. (2012). Original Copy of Article for Water 21 , February 2012 Towards Improved Management of Transmission Mains Leakage Frequency of Unreported Bursts on Transmission Mains, (February), 0–5.

Laven, K., & Lambert, A. O. (2012). What Do We Know About Real Losses On Transmission Mains ? Component Analysis Concepts applied to Unreported Leak Data.

Ledochowski, W. (1956). An analytic method of locating leaks in pressure pipelines. *The South African Institution of Civil Engineers*, *December*, 341–344.

Leinov, E., Cawley, P., & Lowe, M. J. (2015). Guided wave attenuation in pipes buried in sand, *227*, 227–236. http://doi.org/10.1063/1.4914614

Liemberger, R., Brothers, K., Lambert, A., McKenzie, R., Rizzo, A., & Waldron, T. (2017). Water Loss Performance Indicators, (September). Retrieved from https://www.researchgate.net/publication/265063780

Liu, Z., & Kleiner, Y. (2013). State of the art review of inspection technologies for condition assessment of water pipes. *Measurement: Journal of the International Measurement Confederation*, *46*(1), 1–15.

Liu, Z., Kleiner, Y., Rajani, B., Condit, W., & Wang, L. (2012). *EPA: Condition Assessment Technologies for Water Transmission and Distribution Systems*.

Macdonald, G., & Yates, C. D. (2005). DMA Design and Implementation , a North American Context. *Leakage 2005*, 1–8.

Mckenzie, R., Siqalaba, Z., & Wegelin, W. (2012). *The State of Non-Revenue Water in South Africa (2012)*.

Mergelas, B., & Henrich, G. (2005). Leak locating method for precommissioned transmission pipelines: North American case studies. *Leakage 2005*, (50 mm), 1–7.

Mpesha, W., Gassman, S., & Chaudhry, H. (2001). Leak Detection in Pipes by Frequency Response Method. *Journal of Hydraulic Engineering*, *127*(February), 134–147.

Muller, M. (2016). Urban water security in Africa: The face of climate and development challenges. *Development Southern Africa*, *33*(1), 67–80. http://doi.org/10.1080/0376835X.2015.1113121

Muller, M., Schreiner, B., Smith, L., Koppen, B. Van, Sally, H., Aliber, M., … Pietersen, K. (2009). Water security in South Africa. *Development Planning Division Working Paper Series*, *12*(12), 40.

Nsanzubuhoro, R., & van Zyl, J. E. (2016). LEAKAGE CHARACTERIZATION OF BULK WATER PIPELINES Deliverable 3 : Pipe condition assessment device design report, (December).

Nsanzubuhoro, R., & van Zyl, J. E. (2018). Dynamic Pressure Analysis. University of Cape Town.

Oliveira, F., Ross, T., & Trovato, A. (2011). Smartball : a New Pipeline Leak Detection System , and Its Survey of Two Petrobras / Transpetro Pipelines Field Tests . *Rio Pipeline Confernce 2011*, 1–10.

Orazem, M. E. (2014). *Underground Pipeline Corrosion - Detection, analysis and prevention. Woodhead Publishing Series in Metals and Surface Engineering*. Woodhead Elsevier. http://doi.org/10.1007/s13398-014-0173-7.2

Orazem, M. E., & Tribollet, B. (2008). List of symbols. *Electrochemical Impedance Spectroscopy*, *7*(1), 481–493. http://doi.org/10.1093/jicru/ndm007

Ostapkowicz, P. (2016). Leak detection in liquid transmission pipelines using simplified pressure analysis techniques employing a minimum of standard and non-standard measuring devices. *Engineering Structures*, *113*, 194–205. http://doi.org/10.1016/j.engstruct.2016.01.040

PICA. (n.d.). RFT Technology Described. Retrieved April 1, 2016, from http://www.picacorp.com/technology/entryid/144/rft-technology-described.aspx

Price, M., & Reed, D. W. (1989). The influence of mains leakage and urban drainage on ground water levels beneath conurbations in the UK. *Proceedings of the Institution of Civil Engineers*, *86*(1), 31–39.

Prinsloo, K., Wrigglesworth, M., & Webb, M. (2011). Advancement of condition assessment techniques for large diameter pipelines. *SAICE Civil Engineering Magazine*, (October), 20–26. Retrieved from http://reference.sabinet.co.za/sa_epublication_article/civeng_v19_n9_a7

Rezaei, H., Ryan, B., & Stoianov, I. (2015). Pipe failure analysis and impact of dynamic hydraulic conditions in water supply networks. *Procedia Engineering*, *119*(1), 253–262. http://doi.org/10.1016/j.proeng.2015.08.883

Rogers, D. (2014). Leaking water networks: An economic and environmental disaster. *Procedia Engineering*, *70*, 1421–1429. http://doi.org/10.1016/j.proeng.2014.02.157

Schwaller, J., & Van Zyl, J. E. (2014). Implications of the known pressure-response of individual leaks for whole distribution systems. *Procedia Engineering*, *70*, 1513–1517. http://doi.org/10.1016/j.proeng.2014.02.166

Schwaller, J., van Zyl, J. E., & Kabaasha, A. M. (2015). Characterising the pressure-leakage response of pipe networks using the FAVAD equation. *Water Science and Technology: Water Supply*, *15*(6), 1373–1382. http://doi.org/10.2166/ws.2015.101

Shakmak, B., & Al-Habaibeh, A. (2015). Detection of water leakage in buried pipes using infrared technology; A comparative study of using high and low resolution infrared cameras for evaluating distant remote detection. *2015 IEEE Jordan Conference on Applied Electrical Engineering and Computing Technologies (AEECT)*, 1–7. http://doi.org/10.1109/AEECT.2015.7360563

Ssozi, E. N., Malekpour, A., B.W.Karney, & J.Nault. (2015). Physical Understanding of Sudden Pressurization of Pipe Systems with Entrapped Air: Energy Auditing Approach. *ASCE Journal of Hydraulic Engineering*, *138*(July), 642–652. http://doi.org/10.1061/(ASCE)HY.1943-7900

Stampolidis, A., Soupios, P., Vallianatos, F., & Tsokas, G. N. (2003). Detection of leaks in buried plastic water distribution pipes in urban places - A case study. *Proceedings of the 2nd International Workshop on Advanced Ground Penetrating Radar*, 120–124.

Thornton, J., & Lambert, a. (2005). Progress in practical prediction of pressure: leakage, pressure: burst frequency and pressure: consumption relationships. … *of IWA Special Conference'Leakage*, 1–10. Retrieved from http://www.leakssuite.com/Research Papers/2005_ThorntonLambert IWA Halifax.pdf

Tse, P. W., & Wang, X. (2009). Semi-quantitative analysis of defect in pipelines through the use of technique of ultrasonic guided waves. *Key Engineering Materials*, *413–414*, 109–116. http://doi.org/10.4028/www.scientific.net/KEM.413-414.109

Turkowski, M., & Bratek, A. (2007). METHODS AND SYSTEMS OF LEAK DETECTION IN LONG RANGE PIPELINES. *Journal of Automation, Mobile Robotics & Intelligent Systems*, *1*(3 September), 39–46.

United Nations. (2012). *The United Nations Worls Water Development Report 4: Managing Water under Uncertainty and Risk* (Vol. 1–3). UNESCO.

United Nations. (2015). *The United Nations World Water Development Report 2015: Water for a sustainable world*.

van den Berg, C. (2015). Drivers of non-revenue water: A cross-national analysis. *Utilities Policy*, *36*, 71–78. http://doi.org/10.1016/j.jup.2015.07.005

Van Vuuren, S. J. (2014). Theoretical Overview of Surge Analysis - University of Pretoria Lecture Material. University of Pretoria.

Van Zyl, J. E. (2014). Theoretical modeling of pressure and leakage in water distribution systems. *Procedia Engineering*, *89*, 273–277. http://doi.org/10.1016/j.proeng.2014.11.187

Van Zyl, J. E., & Malde, R. (2017). Evaluating the pressure-leakage behaviour of leaks in water pipes. *Journal of Water Supply: Research and Technology - AQUA*, *66*(5), 287–299. http://doi.org/10.2166/aqua.2017.136

Van Zyl, J.E., Lambert, A., and Collins, R. (2017). "Realistic modeling of leakage and intrusion flows through leak openings in pipes." Journal of Hydraulic Engineering, 143(9) 1-7.

Walski, T., Bezts, W., Posluzny, E., Weir, M., & Whitman, B. (2006). Modelling Leakage Reduction Through Pressure Control. *Journal of the American Water Work Association*, *98*(4), 147–152.

Walski, T., Whitman, B., Baron, M., & Gerloff, F. (2009). Pressure vs . Flow Relationship for Pipe Leaks. *World Environmental and Water Resources Congress*, (1), 93–102. http://doi.org/10.1061/41036(342)10

Webb, M. C., Mergelas, B., & Laven, K. (2009). Transmission Main Leak Detection in Sub-Saharan Africa. In *International No-Dig (NASTT & ISTT)* (pp. 1–10).

Wegelin, W. A., Mckenzie, R. S., Herbst, P., & Wensley, A. (2010). Benchmarking and tracking of water losses in all municipalities of South Africa. *Institute of Municipal Engineering of Southern Africa*, (1).

Wegelin, W., Barnard, S., & Mckenzie, R. (2016). *Status Report on Water Losses within Eight Large Water Supply Systems*.

White, F. M. (2008). *Fluid Mechanics* (6th ed.). Rhode Island: McGraw-Hill.

World Bank. (2016). *High and Dry: Climate Change, Water and the Economy*. *World Bank Group*.

APPENDICES

Appendix A: Spreadsheets for Pressure Tests

Appendix B: Photo Report of Further Tests

Appendix C: Visual Basic Code for Spreadsheet Tool

Appendix A:

Spreadsheets for Pressure Tests

Test Report and Analysis

Pipe:

Lynnwood Road to Koedoesnek Reservoir

Testing Date:

06 June 2018

Contents:

Constants

Constant:	Symbol	Value	Unit
Water Density (@20degC):	q	998.19	kg/m3
Gravitational Acceleration:	g	9.81	m/s2
Fluid Kinematic Viscosity:	v	1.14E-06	kg/m.s

Test Equipment Information

Pump	
Make	Euroflow
Model	HS18-40N-1
Maximum h (m)	42
Maximum Flow rate at 17m pressure (m3/h	16
Minimum flow rate at 41m pressure (m3/hr)	4
Flow meter	
Make	ABB
Model	FEX500
Signal type	4-20mA
Signal parameters	Flow rate
Flow Range(l/min)	0-200
Flow direction	Forward flow
Measuring accuracy of rate	0.20%
Type	Electromagnetic
Min. flow range (l/min)	4
Max. flow range (l/min)	200
Pressure Transducer	
Make	ABB
Model	2600T
Pressure Range (bar)	0-10
Signal type	4-20mA
Signal parameters	Pressure
Last callibrated date	01/10/2017
Recorder	
Make	ABB
Model	SM500F
Time step (seconds)	0.1
Channel Tags	Pressure and Flow
Password	N/A
Inverter	
Make	Active Driver Plus
Model	M/M 1.1
Pressure regulating Range (bar)	1-9
Maximum Pressure (bar)	13
Q max (l/min)	300
Non Return Valve flow direction	Forward
Generator	
Make	RYOBI
Model	RG-2700
Power output (kW)	2.7
Fuel type	Unleaded Petrol
Fuel Tank capacity (l)	12
Water Source	
Type	Water Tank on trailer
Size (l)	1000

Delivery line from equipment to test pipe connection		*Ref*
Material	Rubber	
Class	10	
Nominal diameter (mm)	50	
ID (mm)	45.2	
Length (m)	10	
Roughness coefficient (estimated mm)	0.03	

Components on delivery line	**Minor Loss Coefficient**	
1 x 50mm Ball Valve	0.029	*[2]*
1 x 50mm Straight Connector	0.077	*[2]*
Total minor loss coefficient	0.1061	

Minor losses of test equipment fittings:		*[2]&[1]*
100mm Flanged or Threaded	16.26	
80 mm Flanged or Threaded	23.30	
2.5 Inch Threaded Male	21.33	
50 mm Flanged or 50 Threaded	19.66	
1.5 Inch (40mm) Threaded Male	14.97	
1.25 Inch (30mm) Threaded Female	15.13	
1 Inch Threaded M or F with Tap	8.05	
3/4 Inch Threaded Female or Male	35.35	
0.5 Inch Threaded Male or Female	29.76	

Ball Valve Friciton Loss — Reference: [2]

$$K_{ball} = 3\frac{0.25}{\left[log\left(\frac{\varepsilon/D}{3.7}\right)\right]^2}$$

Straight Connector (similar to open fully open gate valve) [2]

$$K_{con} = 8\frac{0.25}{\left[log\left(\frac{\varepsilon/D}{3.7}\right)\right]^2}$$

Sudden Contraction / Reduction [1]

$$K_{sc} = 0.42\left(1 - \frac{{D_2}^2}{{D_1}^2}\right)$$

Sudden Expansion [1]

$$K_{se} = \left(1 - \frac{{D_1}^2}{{D_2}^2}\right)^2$$

References:

[1] White, F. M. (2008). Fluid Mechanics (6th ed.). Rhode Island: McGraw-Hill

[2] CRANE Nuclear. (2013). General Engineering Data.

Test Equipment Information (continued)

Test Equipment Fittings:

The K-factors represent the loss from the point where the 50mm pipe reduces to a "Geka" coupling, up to the point where the connection is fitted to the pipe.

100 mm Flanged or 100mm Threaded (4 Inch)	Components
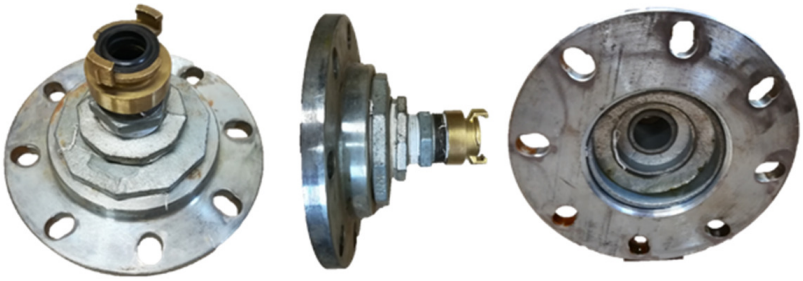	100mm Flange 4 inch x 2.5 inch 2.5 inch x 1.5 inch 1.5 inch male to female 1.5 inch female coupling Minor Loss: 16.2636
80 mm Flanged or 80mm Threaded (3 Inch)	**Components**
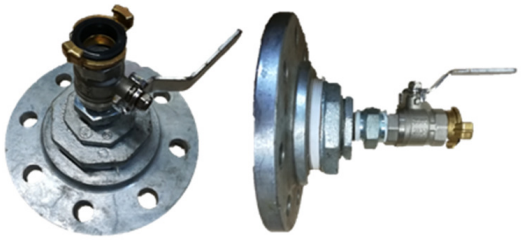	80mm Flange 3 inch x 2 inch 2 inch x1 inch 1 inch male to female 1 inch ball valve 1 inch male coupling Minor Loss: 23.2958
2.5 Inch Threaded Male	**Components**
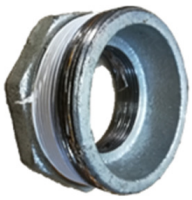	2.5 inch x 1.5 inch 1.5 inch male to female 1.5 inch male coupling Minor Loss: 21.3306
50 mm Flanged or Threaded (2 Inch) with Tap	**Components**
	50mm Flange 2 inch x 1 inch 1 inch male coupling Optional: 1 inch male to female 1 inch ball valve Minor Loss: 19.6575
1.5 Inch (40mm) Threaded Male	**Components**
	1.5 male to female 1.5 inch female coupling Minor Loss: 14.9665
1.25 Inch (30mm) Threaded Female	**Components**
	1.25 inch (30mm) x 1 inch 1 inch male to female 1 inch ball valve 1 Inch male coupling Minor Loss: 15.1312

Test Equipment Information (continued)

1 Inch Threaded Male or Female with Tap	Components
	1 inch male to female 1 inch ball valve 1 inch male coupling
	Minor Loss: 8.04883
3/4 Inch Threaded Female or Male	Components
	3/4 inch x 0.5 inch 0.5 inch male coupling (3/4 inch male to female)
	Minor Loss: 35.3457
0.5 Inch Threaded Male or Female	Components
	0.5 Inch Male Coupling
	Minor Loss: 29.7644

General Test Description

Description:

The pipeline from Lynnwood Road to Koedoesnek Reservoir is a 500 mm diameter, 707 metre long pipe steel pipeline. It is a rising main that branches off a pressurised main supply pipe, and supplies a reservoir approximately 47 metres higher. Immediately after the branch, an isolating butterfly valve is located in a valve chamber next to the road (V1 in Figure 1). The downstream isolation valve (V2) is a PRV, which is located inside a valve chamber just upstream of the Koedoesnek reservoir.

The pressure upstream of the pipeline is above 10 bar, and provides the driving force for the flow from Lynnwood road to the Koedoesnek reservoir. The pressure downstream of the pipeline is low and mainly results from the slightly elevated reservoir and the reservoir level.

The most suitable connection location was identified to be the valve chamber at V2, as this is the highest point on the pipeline section.

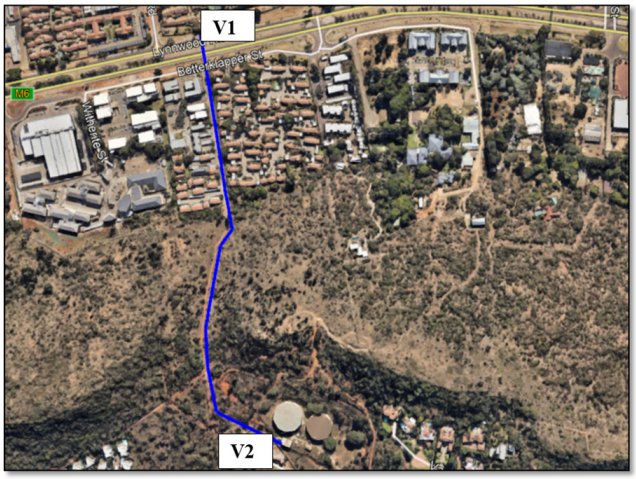

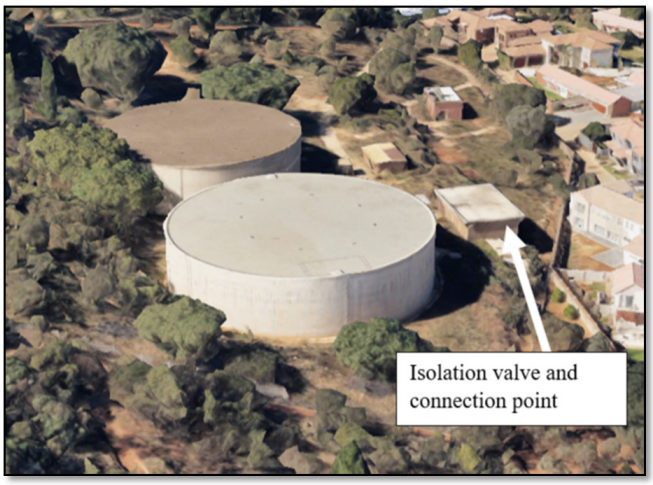

Figure 1 & 2: Map showing pipeline route starting at V1 and ending at V2

The isolating ball valve on the connection point allowed for the equipment to be connected to the PRV, while the pipe was still in operation. The hose was then connected to the equipment water tank, and the isolation valve was slightly opened to fill the tank. Once the tank was full, the next step was to close the ball valve and isolate the pipeline.

Figure 3 & 4: Equipment setup and connection point at Koedoesnek reservoir valve chamber.

General Test Description (Continued)

Upon arrival at the solation valve at location V2, as indicated on the map in Figure 1, it was noticed that the chamber was full of water. A team fwas then arranged to pump the water out of the chamber. The chamber was emptied at close to 13:00. Valve V2 was then closed and a leak on a coupling was identified to be responsible for the flooded chamber. The leak was, however, on the supply side of the isolation valve and not on the pipe that we tested. The isolation valve appeared to seal effectively.

We then returned to the testing equipment at the connection point. The pipeline was already depressurised upon arrival. Slight suction of air into the rubber hose, which was still connected to the pipeline, was observed. The pipe was then connected to the pump and the pump was started and allowed to run at maximum flow and pressure. The pressure stabilised at approximately 3.6 bar and the flow was measured to be 68 litres per minute.
The pressure was then dropped at increments of 0.5 bar up to 1.5 bar, and the flow was allowed to stabilise for each case. Thereafter the pressure was increased at increments of 0.5 bar up to 3.5 bar..

General Test Information

Pipeline:	Lynnwood Road to Koedoesnek Reservoir
Area:	Pretoria East, Lynnwood/Faerie Glen
Pipe Owner:	Tshwane Municipality
Date:	06 Jun 18
Time:	08:00 - 15:00

Pipeline Section:	**Section 1**	**Section 2**	**Section 3**	
Pipe length (m):	707			
Pipe Diameter (mm):	500			
Pipe Material:	Steel			
Absolute Roughness e (mm)	0.5			
Minor Losses/km	1			
Upstream Isolation:	Butterfly Valve			
Upstream Source:	Pressured Pipe			
Upstream Pressure (Bar) approx:	>10			
Upstream Isolation Elevation (m):	1390			
Downstream Isolation:	Pressure Reg. Valve			
Downstream Delivery:	Reservoir			
Downstream Pressure (Bar) approx:	<1			
Downstream Isolation Elevation (m):	1440			

Connection of Testing Equipment

Connection Type:	50 mm Flanged or 50 Threaded	
Connection Fitting size (mm):	50	
Comment on Fitting:	50mm female connection: Male threaded 50mm to 1 inch reducer. 1 inch female to male, 1 inch Geka coupling	
Minor loss coefficient of fitting	4	19.66
Static height difference (A) in (m):	1.85	

Connection pipes*:

	Pipe 1	**Pipe 2**
Length of connection pipe* (mm):	300	
Diameter of connection pipes (mm)	50	
Absolute Roughness e (mm)	0.2	
Static height difference (B) in (mm):	800	

Minor losses of fittings on connection pipes*:

	Fitting 1	**Fitting 2**	**Fitting 3**	**Fitting 4**
Fitting type:	Butterfly valve	Instant diffuser	None	None
Pipe 1 or Pipe 2	1	1	1	1
Fitting diameter in (mm):	50	50	0.05	0.05
Fitting diameter out (mm):	50	400	0.05	0.05
Absolute Roughness e (mm)	0.5	0.5	0.5	0.5
No. of fittings:	1	1	1	1
Fitting Minor Loss Coefficient:	1.3266	0.9690	0.0000	0.0000
			SUM:	2.29562

** Pipes and Fittings between the connection point and the main pipeline*

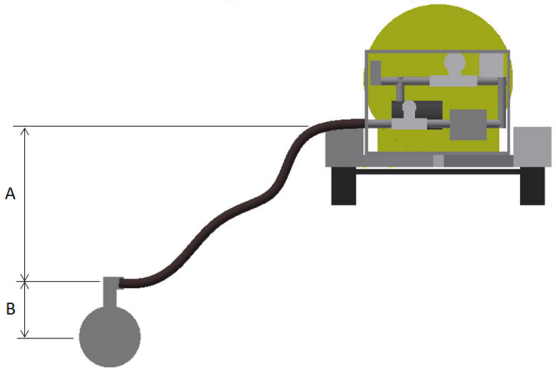

Pipeline Elevation Profile

Geocontext Website

Elevation Profile

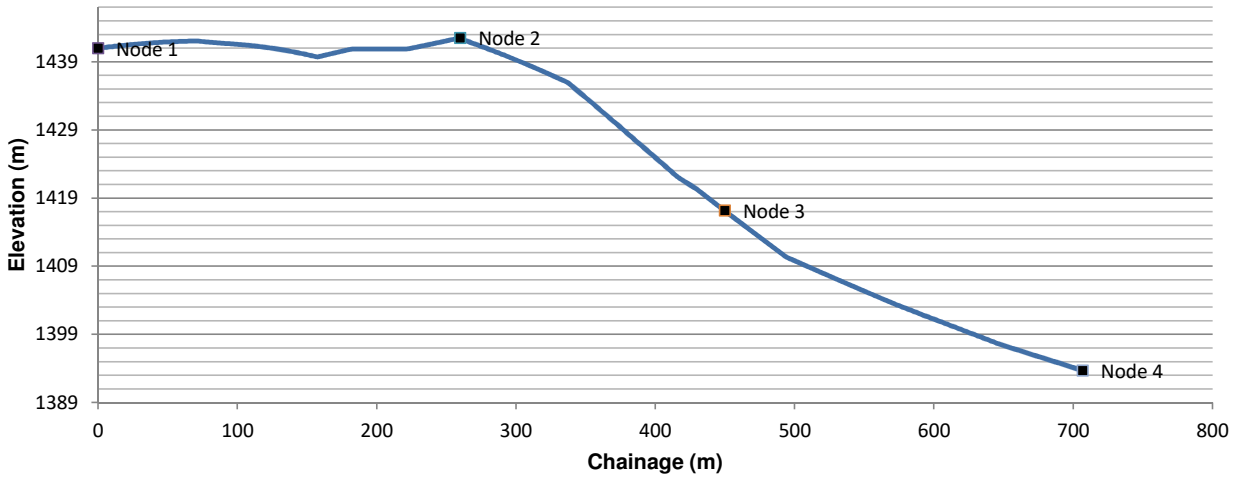

Distance (m)	Elevation (m)	Material
0	1440.987427	Steel
1.383352668	1441.024658	Steel
2.766705336	1441.061279	Steel
4.150058004	1441.097046	Steel
5.533410671	1441.132202	Steel
6.916763339	1441.166626	Steel
8.300116007	1441.200439	Steel
9.683468675	1441.233398	Steel
11.06682134	1441.265625	Steel
12.45017401	1441.297241	Steel
13.83352668	1441.328125	Steel
15.21687935	1441.358276	Steel
16.60023201	1441.387695	Steel
17.98358468	1441.417358	Steel
19.36693735	1441.44751	Steel
20.75029002	1441.476807	Steel
22.13364269	1441.505493	Steel
23.51699535	1441.533447	Steel
24.90034802	1441.560669	Steel
26.28370069	1441.587158	Steel
27.66705336	1441.613037	Steel
29.05040602	1441.638062	Steel
30.43375869	1441.662476	Steel
31.81711136	1441.686157	Steel
33.20046403	1441.709106	Steel
34.5838167	1441.731323	Steel
35.96716936	1441.75293	Steel
37.35052203	1441.773804	Steel
38.7338747	1441.793823	Steel
40.11722737	1441.813232	Steel
41.50058004	1441.832031	Steel
42.8839327	1441.849976	Steel
44.26728537	1441.867188	Steel
45.65063804	1441.883789	Steel
47.03399071	1441.899658	Steel
48.41734337	1441.914795	Steel
49.80069604	1441.929199	Steel
51.18404871	1441.942993	Steel
52.56740138	1441.955933	Steel
53.95075405	1441.968262	Steel

No. of Sections:	1	
Section	**Start (m)**	**Material**
1	0	Steel
2		0
3		0

**If multiple sections exist, the Node points below must intercept at point where section changes for accurate pressure loss calculations.*

	Chainage (m)	Elevation (m)	End/part of Section
Node 1	0	1440.987	N/A
Node 2	260	1442.463	1
Node 3	450	1417.190	1
Node 4	706.89	1393.702	1

Total Chainage = 706.89 m

Distance/Elevation Data Continues

Plot and Data Points

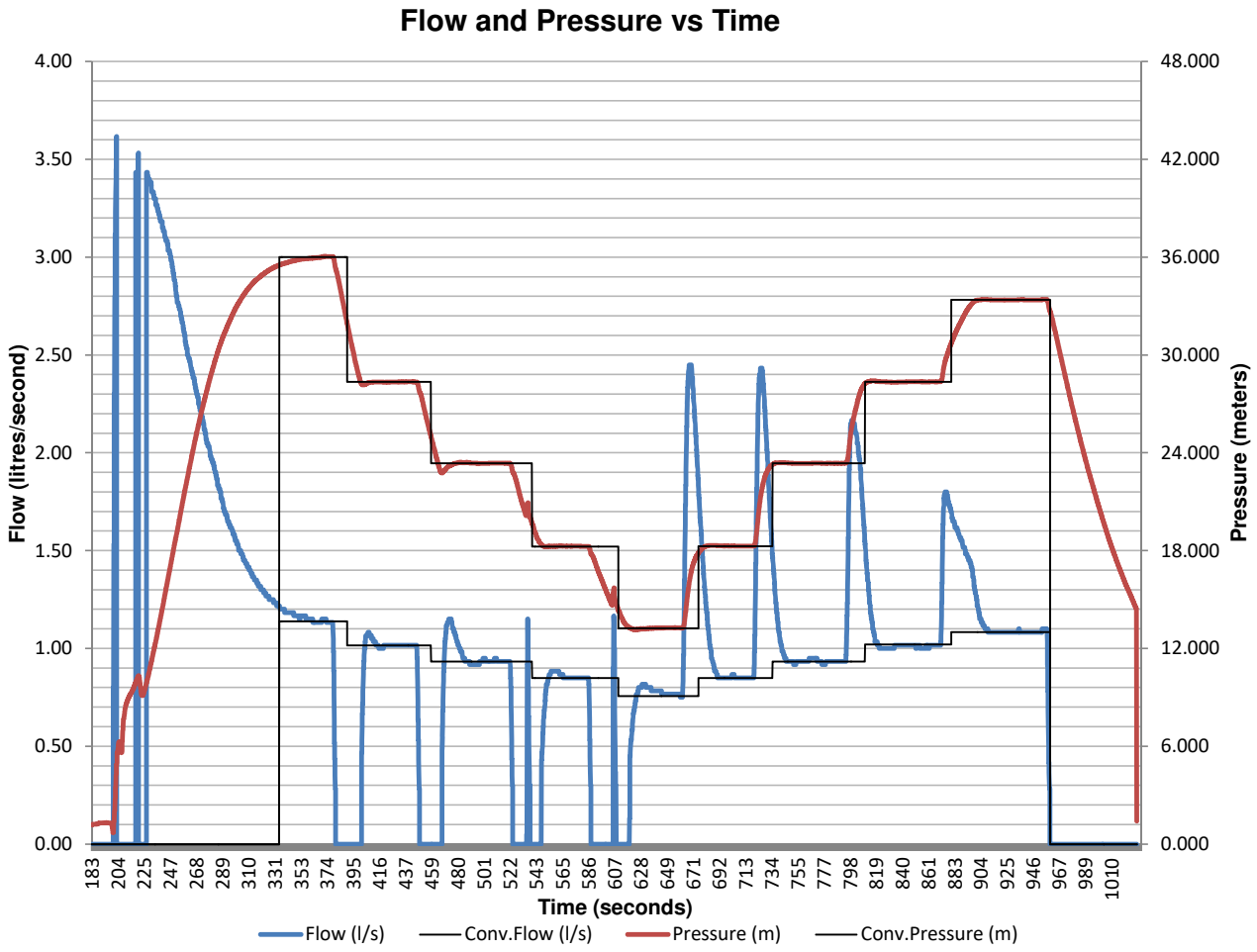

Tool for zooming into graph to calculate and plot the average values:

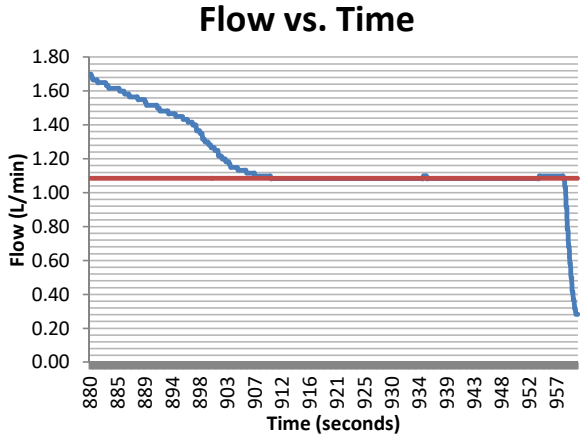

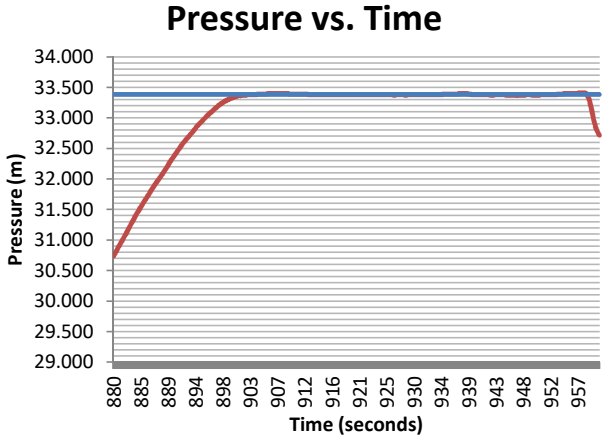

Select time Range for Display:		Select time Range for Average Calculation:	
Start Time:	880 s	Start Time:	925 s
End Time:	960 s	End Time:	937 s

Average Flow:	1.0842 l/s
Average Pressure:	33.385 m

Pressure Head Correction

Corrected pressure at every Node:

Reynold's Number

$$\mathrm{Re} = \frac{\rho \mathrm{VD}}{\mu} = \frac{\mathrm{VD}}{\nu} = \frac{\mathrm{QD}}{\nu A}$$

Colebrook-White

$$\frac{1}{\sqrt{f}} = -2\log_{10}\left(\frac{\varepsilon}{3.7D} + \frac{2.51}{R_e\sqrt{f}}\right)$$

Minor Loss Equation

$$h_L = K_L\frac{V^2}{2g}$$

Darcy-Weissbach

$$h_f = f\frac{L}{D}\frac{V^2}{2g}$$

			Corrected Head (m)				
Point	**Flow (l/s)**	**Measured Head (m)**	**Node 0**	**Node 1**	**Node 2**	**Node 3**	**Node 4**
1	1.14	36.02	37.22	37.940	36.464	61.736	85.224
2	1.02	28.36	29.69	30.421	28.945	54.217	77.705
3	0.93	23.37	24.77	25.520	24.044	49.316	72.804
4	0.85	18.27	19.75	20.503	19.027	44.299	67.787
5	0.76	13.25	14.81	15.573	14.097	39.369	62.857
6	0.85	18.27	19.75	20.507	19.031	44.303	67.791
7	0.93	23.36	24.77	25.513	24.037	49.309	72.797
8	1.02	28.36	29.69	30.421	28.945	54.218	77.705
9	1.08	33.39	34.64	35.370	33.894	59.166	82.654
10	0.00	0.00	0.00	0.000	0.000	0.000	0.000
11	0.00	0.00	0.00	0.000	0.000	0.000	0.000
12	0.00	0.00	0.00	0.000	0.000	0.000	0.000
13	0.00	0.00	0.00	0.000	0.000	0.000	0.000
14	0.00	0.00	0.00	0.000	0.000	0.000	0.000
15	0.00	0.00	0.00	0.000	0.000	0.000	0.000

N1 And FAVAD Parameters

N1 Equation:

$$Q = C_d A\sqrt{2gh}$$
$$Q = C_d\sqrt{2g}\,Ah^{0.5}$$
$$Q = C_{N1}Ah^{N1}$$

FAVAD Equation:

$$Q = C_d A\sqrt{2gh} \quad but \quad A = A_0 + mH$$
$$\therefore C_d A = Q/\sqrt{2gh} \qquad Q = C_d\sqrt{2gh}(A_0 + mh)$$
$$Q = C_d\sqrt{2g}\,(A_0 h^{0.5} + mh^{1.5})$$

Node 0: N1 Relationship

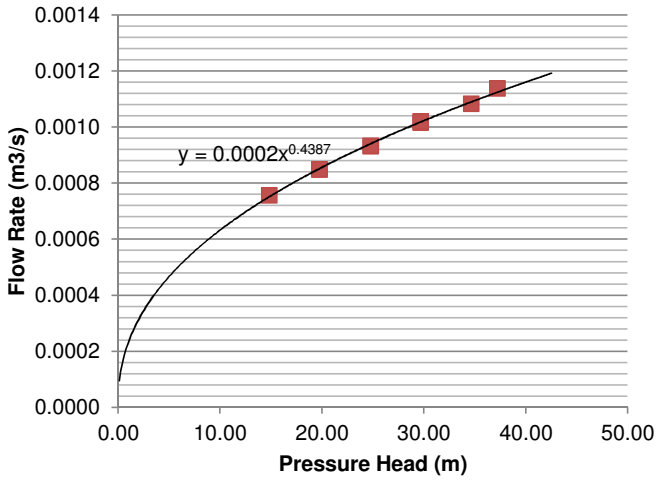

N1 Parameters:

Leakage Coefficient (CN1):	0.00023
Leakage Exponent (N1):	0.43869

Node 0: FAVAD Relationship

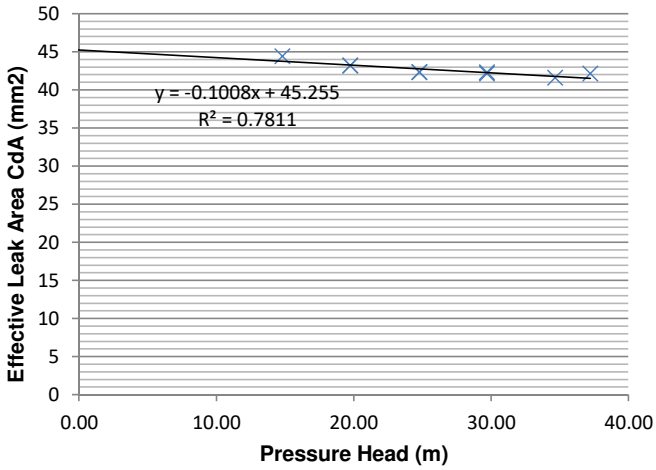

FAVAD Parameters:

Effective Initial Leak Area CdA0:	45.255 mm
Effective head-area slope Cdm:	-0.101 mm2/m

Node 1: N1 Relationship

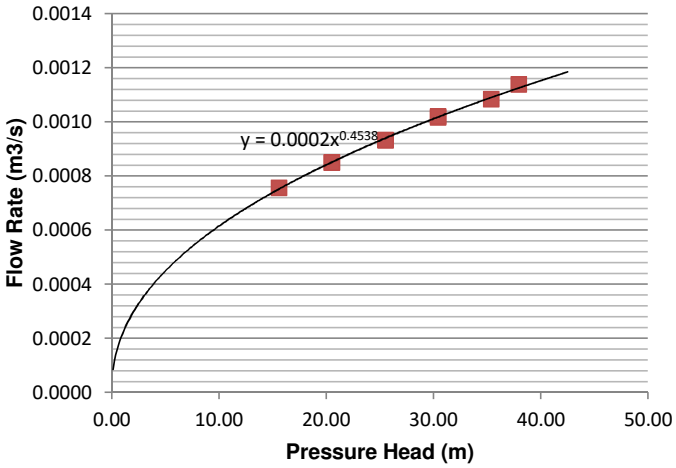

N1 Parameters:

Leakage Coefficient (C):	0.00022
Leakage Exponent (N1):	0.45377

Node 1: FAVAD Relationship

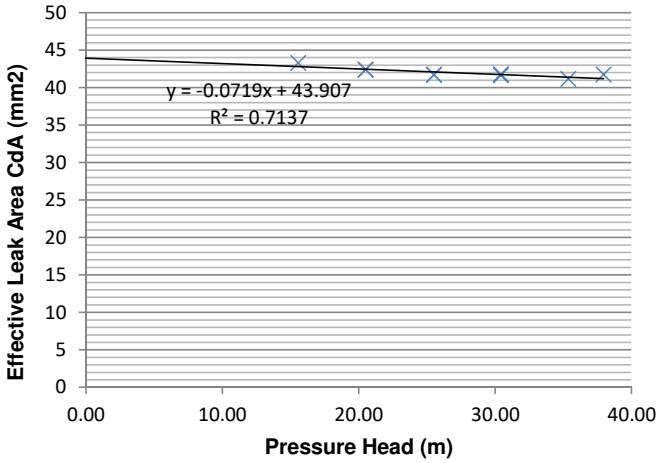

FAVAD Parameters:

Effective Initial Leak Area CdA0:	43.907 mm
Effective head-area slope Cdm:	-0.072 mm2/m

N1 And FAVAD Parameters

Node 2: N1 Relationship

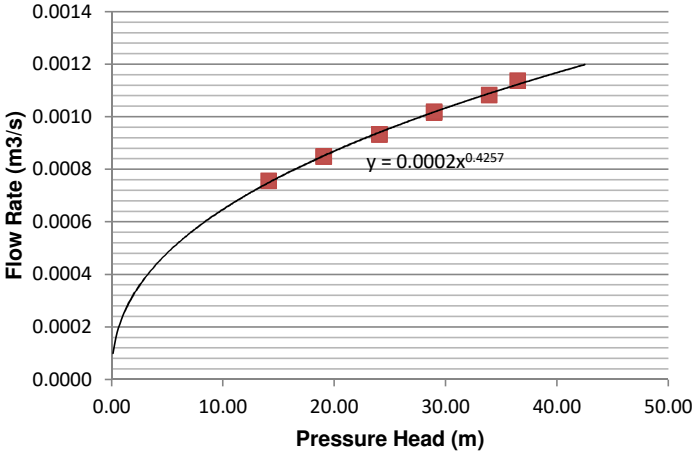

N1 Parameters:

Leakage Coefficient (C): #####

Leakage Exponent (N1): #####

Node 2: FAVAD Relationship

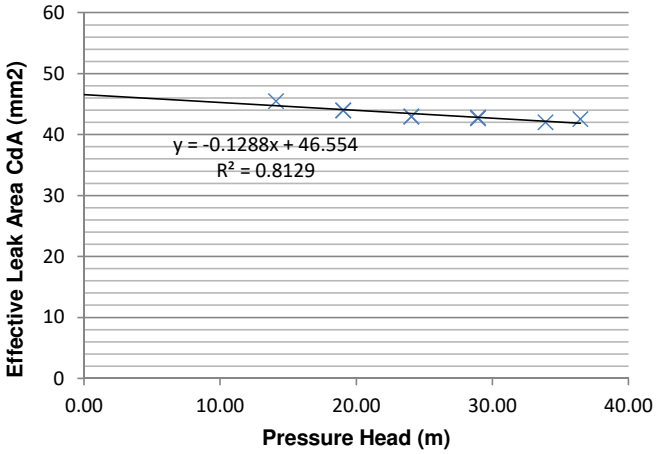

FAVAD Parameters:

Effective Initial Leak Area CdA0: 46.554 mm

Effective head-area slope Cdm: -0.129 mm2/m

Node 3: N1 Relationship

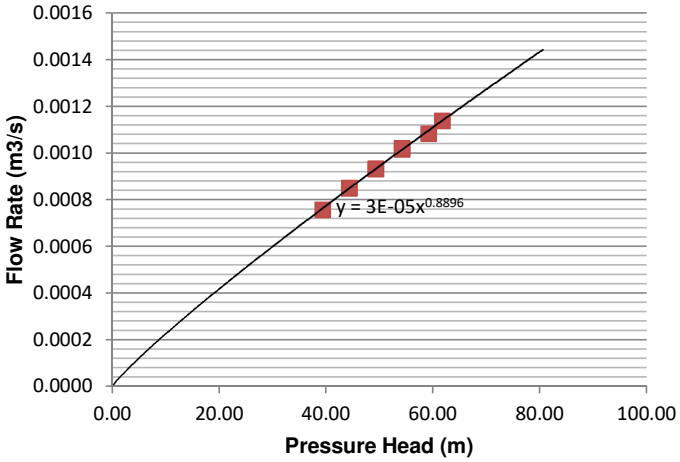

N1 Parameters:

Leakage Coefficient (C): 0.00003

Leakage Exponent (N1):

Node 3: FAVAD Relationship

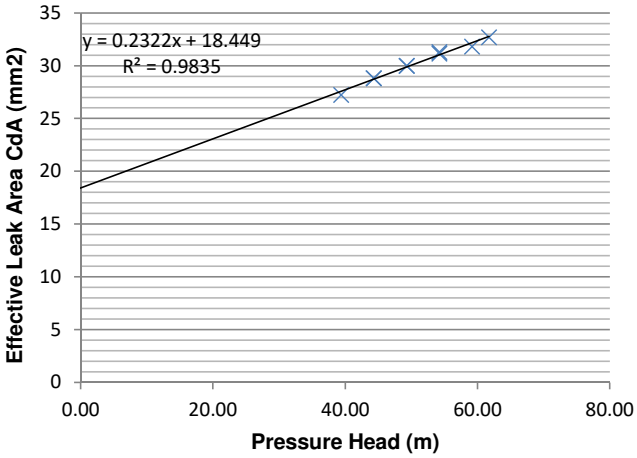

FAVAD Parameters:

Effective Initial Leak Area CdA0: 18.449 mm

Effective head-area slope Cdm: 0.232 mm2/m

Node 4: N1 Relationship

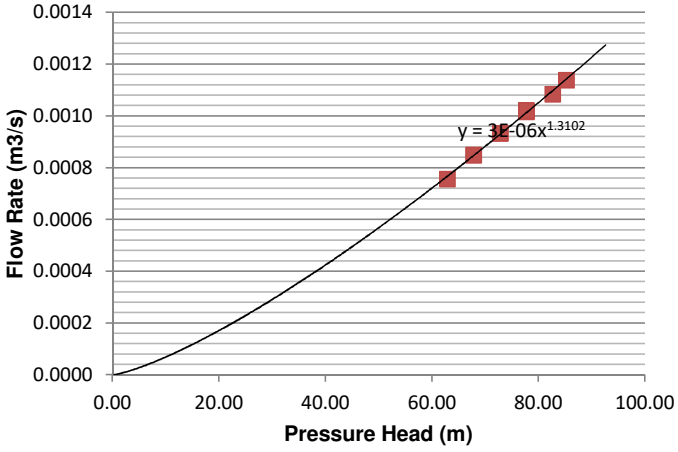

N1 Parameters:

Leakage Coefficient (C): 0.00000

Leakage Exponent (N1): 1.31022

Node 4: FAVAD Relationship

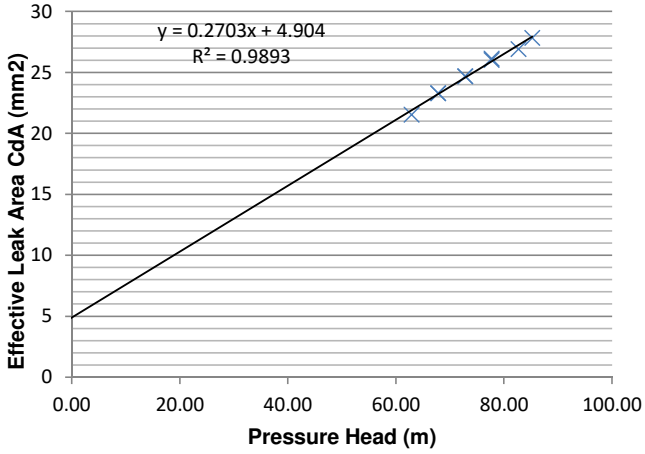

FAVAD Parameters:

Effective Initial Leak Area CdA0: 4.904 mm

Effective head-area slope Cdm: 0.270 mm2/m

Combined FAVAD Plot

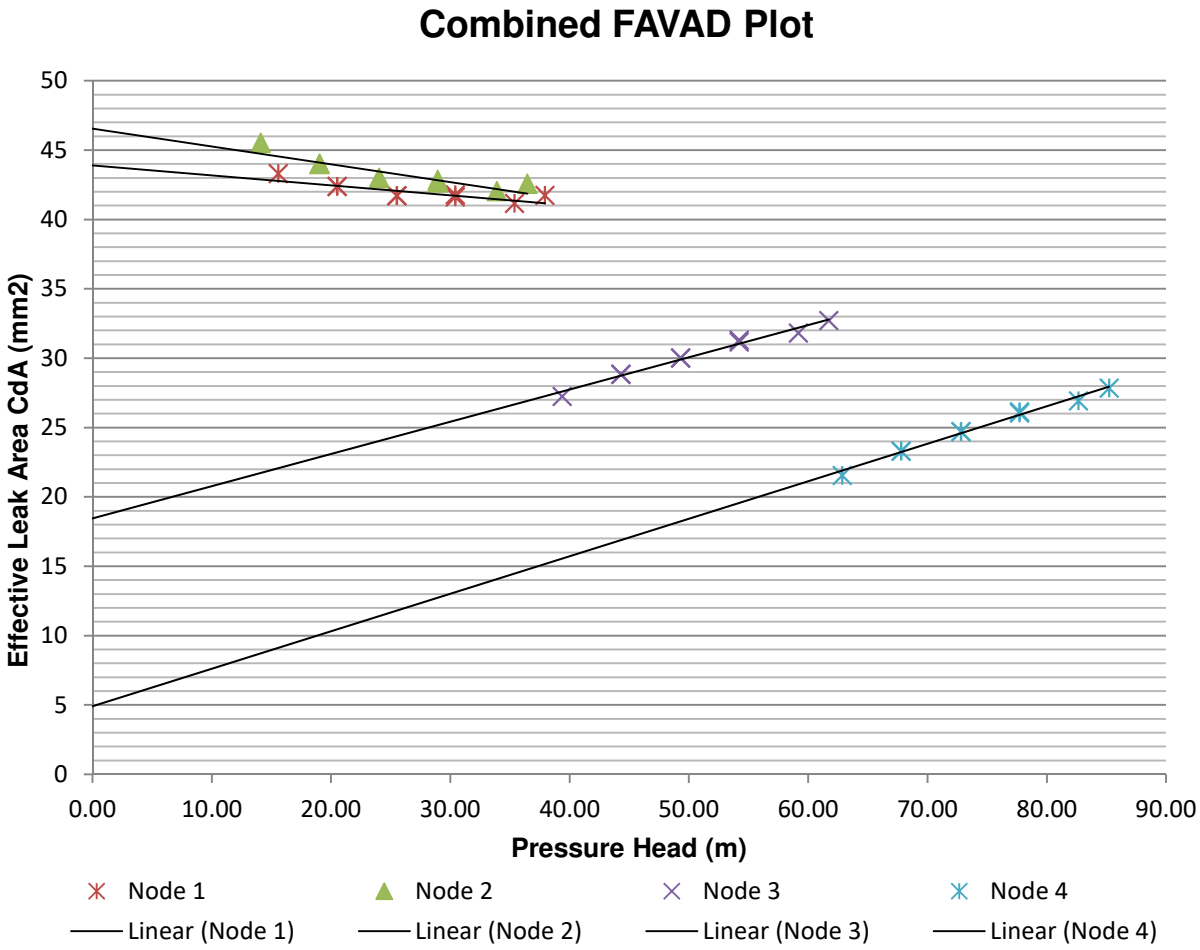

Conclusion:

By comparing the Koedoesnek pipeline with the leak characteristics found in literature, the following scenarios are likely:

- All the dominant leaks are downstream of Node 2
- Longitudinal cracks of approximately 40 mm in length exist along the pipeline from Node 3 up to Node 4. This scenario is uncommon for steel pipes, and is therefore unlikely.
- Longitudinal cracks exist on gaskets or flexible couplings between nodes 3 and 4. The existence of such leaks can easily be verified by a quick visual inspection of all the air valve and scour valve chambers.
- Round holes exist somewhere between nodes 2 and 3, where the pressure-area slope is expected to be closer to 0.
- Corrosion holes exist between nodes 2 and 4. This is a likely scenario, but due to the range of exponent values or pressure-area slopes that can result from corrosion holes, the location cannot be pinpointed, other than that they are most likley between nodes 2 and 4.

A leakage of 1.14 litres per second (4.1m3/hour) at 36 metres pressure head was recorded. Considering the scarcity of water, as well as the high cost of this purified water, which has been transported a considerable distance from its original source, this leakage rate is significant. It is therefore recommended that further inspections are carried out on the pipeline in order to identify and address the source of the leak.

K-Factor Calculator

Connection:

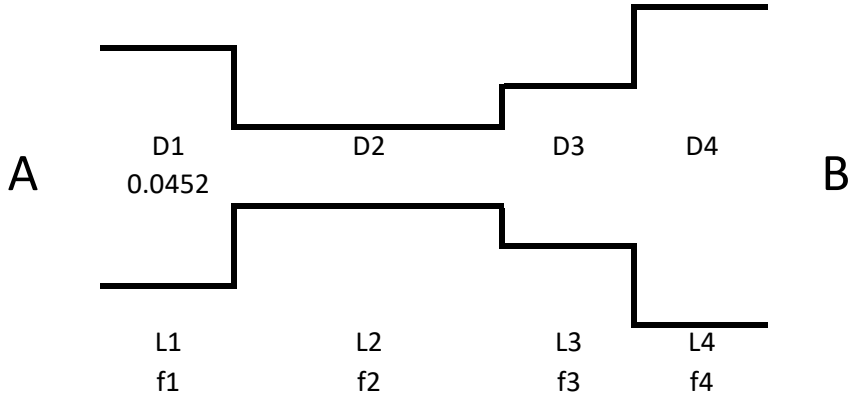

$$\Delta h_{a\to b} = h_{m1} + h_{m2} + h_{m3} \dots$$

$$\Delta h_{a\to b} = \frac{V_1^2}{2g}\left(\frac{f_1 L_1}{D_1}\right) + \frac{V_2^2}{2g}\left(\frac{f_2 L_2}{D_2} + K_{sc} + K_{se}\right) + \frac{V_3^2}{2g}\left(\frac{f_3 L_3}{D_3} + K_{se}\right) + \dots$$

but

$K_{sc} = 0.42\left(1 - \frac{D_2^2}{D_1^2}\right)$ *(sudden contraction, reference velocity 2)*

$K_{se} = \left(1 - \frac{D_1^2}{D_2^2}\right)^2$ *(sudden expansion, reference velocity 1)*

⋮

and $Q_1 = Q_2 = Q_3$, $V_1 A_1 = V_2 A_2 = V_3 A_3$, $V_2 = \frac{V_1 A_1}{A_2}$, $V_3 = \frac{V_1 A_1}{A_3}$

$$\therefore \Delta h_{a\to b} = \frac{V_1^2}{2g}\left(\frac{f_1 L_1}{D_1}\right) + \frac{V_2^2}{2g}\left(\frac{f_2 L_2}{D_2} + 0.42\left(1 - \frac{D_2^2}{D_1^2}\right) + \left(1 - \frac{D_2^2}{D_3^2}\right)^2\right) + \frac{V_3^2}{2g}\left(\frac{f_3 L_3}{D_3} + \left(1 - \frac{D_3^2}{D_4^2}\right)^2\right)$$

$$\therefore \Delta h_{a\to b} = \frac{V_1^2}{2g}\left(\frac{f_1 L_1}{D_1}\right) + \frac{1}{2g}\left(\frac{V_1 A_1}{A_2}\right)^2\left(\frac{f_2 L_2}{D_2} + 0.42\left(1 - \frac{D_2^2}{D_1^2}\right) + \left(1 - \frac{D_2^2}{D_3^2}\right)^2\right) + \frac{1}{2g}\left(\frac{V_1 A_1}{A_3}\right)^2\left(\frac{f_3 L_3}{D_3} + \left(1 - \frac{D_3^2}{D_4^2}\right)^2\right)$$

$$\therefore \Delta h_{a\to b} = \frac{V_1^2}{2g}\left(\left(\frac{f_1 L_1}{D_1}\right) + \left(\frac{A_1}{A_2}\right)^2\left(\frac{f_2 L_2}{D_2} + 0.42\left(1 - \frac{D_2^2}{D_1^2}\right) + \left(1 - \frac{D_2^2}{D_3^2}\right)^2\right) + \left(\frac{A_1}{A_3}\right)^2\left(\frac{f_3 L_3}{D_3} + \left(1 - \frac{D_3^2}{D_4^2}\right)^2\right)\right)$$

$$\therefore K_{combined} = \left(\frac{f_1 L_1}{D_1}\right) + \left(\frac{A_1}{A_2}\right)^2\left(\frac{f_2 L_2}{D_2} + 0.42\left(1 - \frac{D_2^2}{D_1^2}\right) + \left(1 - \frac{D_2^2}{D_3^2}\right)^2\right) + \left(\frac{A_1}{A_3}\right)^2\left(\frac{f_3 L_3}{D_3} + \left(1 - \frac{D_3^2}{D_4^2}\right)^2\right)$$

$$\therefore K_{combined} = \left(\frac{f_1 L_1}{D_1}\right) + \left(\frac{D_1}{D_2}\right)^4\left(\frac{f_2 L_2}{D_2} + 0.42\left(1 - \frac{D_2^2}{D_1^2}\right) + \left(1 - \frac{D_2^2}{D_3^2}\right)^2\right) + \left(\frac{D_1}{D_3}\right)^4\left(\frac{f_3 L_3}{D_3} + \left(1 - \frac{D_3^2}{D_4^2}\right)^2\right)$$

With $\frac{1}{f^{\frac{1}{2}}} \approx -1.8 \log\left[\frac{6.9}{Re_d} + \left(\frac{\epsilon/d}{3.7}\right)^{1.11}\right]$

K-Factor Calculator

100 mm Flanged or 100mm Threaded (4 Inch)	Kcomb	16.26		Assumptions:
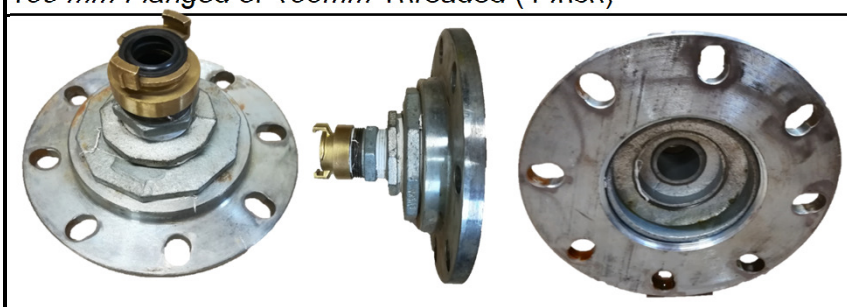	D2=	0.022	m	> Sudden expansion from D2 to D3 to D4
	L2=	0.04	m	
	e2	0.05	mm	
	f2=	*0.027*		> Friction due to L4 negligible, because D4 is large
	D3=	0.039	m	
	L3=	0.06	m	
	e3=	0.26	mm	>V1 stays constant*
	f3=	*0.036*		
	D4=	0.1	m	
80 mm Flanged or 80mm Threaded (3 Inch)	Kcomb	23.3		Assumptions:
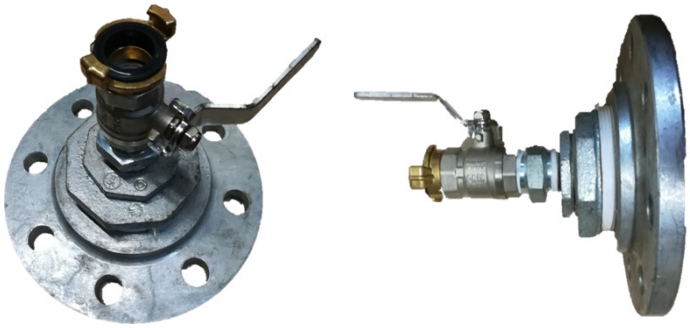	D2=	0.022	m	> Sudden expansion from D2 to D4
	L2=	0.108	m	
	e2=	0.05	mm	
	f2=	*0.027*		> Friction due to L3 & L4 negligible, because D4 is large
	D4=	0.08	m	>V1 stays constant*
2.5 Inch Threaded Male	Kcomb	21.33		Assumptions:
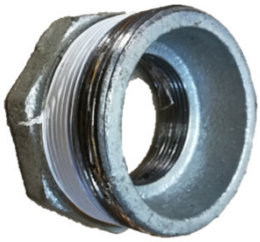	D2=	0.022	m	> Sudden expansion from D2 to D3
	L2=	0.04	m	
	e=	0.26	mm	
	f2=	*0.041*		negligible, because D4 is large and L3 short
	D3=	0.068	m	
				>V1 stays constant*
50 mm Flanged or Threaded (2 Inch) with tap	Kcomb	19.66		Assumptions:
	D2=	0.022	m	> Sudden expansion from D2 to D4
	L2=	0.108	m	
	e=	0.05	mm	
	f2=	*0.027*		> Friction due to L3 & L4 negligible, because D4 is large
	D4=	0.05	m	
				>V1 stays constant*

* V1 stays constant at approximately 0.59 m/s

K-Factor Calculator

1.5 Inch (40mm) Threaded Male	Kcomb.	14.967		Assumptions:
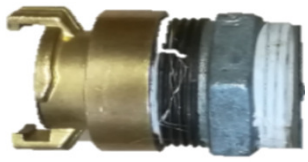	D2=	0.022	m	> Sudden expansion from D2 to D3
	L2=	0.04	m	
	e2=	0.05	mm	
	f2=	*0.027*		> Friction due to L4 negligible,
	D3=	0.039	m	because D4 is large, and L4 short.
	L3=	0.06	m	
	e3=	0.26	mm	>V1 stays constant*
	f3=	*0.036*		
1.25 Inch (30mm) Threaded Female	Kcomb.	15.131		Assumptions:
	D2=	0.022	m	> Sudden expansion from D2 to D3
	L2=	0.107	m	
	e2=	0.05	mm	
	f2=	*0.027*		> Friction due to L4 negligible,
	D3=	0.036	m	because D4 is large, and L4 short.
	L3=	0.035	m	
	e3=	0.26	mm	>V1 stays constant*
	f3=	*0.036*		
1 Inch Threaded Female or Male with Tap	Kcomb.	8.0488		Assumptions:
 	D2=	0.022	m	>V1 stays constant*
	L2=	0.107	m	
	e2=	0.05	mm	
	f2=	*0.027*		
3/4 Inch Threaded Female (or Male)	Kcomb.	35.346		Assumptions:
 	D2=	0.022	m	> Sudden reduction from D2 to D3
	L2=	0.03	m	and expansion for D3 to D4
	e2=	0.05	mm	
	2=	*0.027*		> Friction due to L4 negligible,
	D3=	0.016	m	because D4 is large and short.
	L3=	0.02	m	
	e3=	0.05	mm	>V1 stays constant*
	f3=	*0.028*		
	D4=	0.022	m	
0.5 Inch Threaded Male / Female	Kcomb.	29.764		Assumptions:
	D2=	0.022	m	> Sudden reduction from D2 to D3.
	L2=	0.03	m	
	e2=	0.05	mm	>V1 stays constant*
	f2=	*0.027*		> Friction due to L3 negligible,
	D3=	0.016	m	because D3 is large

Test Report and Analysis

Pipe:

Garsfontein to Parkmore High Level Reservoir 1

Testing Date:

07 & 28 June 2018

Contents:

Test Equipment Information

Pump	
Make	Euroflow
Model	HS18-40N-1
Maximum h (m)	42
Maximum Flow rate at 17m pressure (m3/h	16
Minimum flow rate at 41m pressure (m3/hr	4
Flow meter	
Make	ABB
Model	FEX500
Signal type	4-20mA
Signal parameters	Flow rate
Flow Range(l/min)	0-200
Flow direction	Forward flow
Measuring accuracy of rate	0.20%
Type	Electromagnetic
Min. flow range (l/min)	4
Max. flow range (l/min)	200
Pressure Transducer	
Make	ABB
Model	2600T
Pressure Range (bar)	0-10
Signal type	4-20mA
Signal parameters	Pressure
Last callibrated date	01/10/2017
Recorder	
Make	ABB
Model	SM500F
Time step (seconds)	0.1
Channel Tags	Pressure and Flow
Password	N/A
Inverter	
Make	Active Driver Plus
Model	M/M 1.1
Pressure regulating Range (bar)	1-9
Maximum Pressure (bar)	13
Q max (l/min)	300
Non Return Valve flow direction	Forward
Generator	
Make	RYOBI
Model	RG-2700
Power output (kW)	2.7
Fuel type	Unleaded Petrol
Fuel Tank capacity (l)	12
Water Source	
Type	Water Tank on trailer
Size (l)	1000

Delivery line from equipment to test pipe connection		*Ref*
Material	Rubber	
Class	10	
Nominal diameter (mm)	50	
ID (mm)	45.2	
Length (m)	10	
Roughness coefficient (estimated mr	0.03	

Components on delivery line	**Minor Loss Coefficient**	
1 x 50mm Ball Valve	0.029	*[2]*
1 x 50mm Straight Connector	0.077	*[2]*
Total minor loss coefficient	0.1061	

Minor losses of test equipment fittings:		*[2]&[1]*
100mm Flanged or Threaded	16.24	
80 mm Flanged or Threaded	23.23	
2.5 Inch Threaded Male	21.32	
50 mm Flanged or 50 Threaded	19.60	
1.5 Inch (40mm) Threaded Male	14.94	
1.25 Inch (30mm) Threaded Female	15.07	
1 Inch Threaded M or F with Tap	7.99	
3/4 Inch Threaded Female or Male	35.29	
0.5 Inch Threaded Male or Female	29.75	

Ball Valve Friciton Loss — Reference: [2]

$$K_{ball} = 3\frac{0.25}{\left[log\left(\frac{\varepsilon/D}{3.7}\right)\right]^2}$$

Straight Connector (similar to open fully open gate valve) [2]

$$K_{con} = 8\frac{0.25}{\left[log\left(\frac{\varepsilon/D}{3.7}\right)\right]^2}$$

Sudden Contraction / Reduction [1]

$$K_{sc} = 0.42\left(1 - \frac{{D_2}^2}{{D_1}^2}\right)$$

Sudden Expansion [1]

$$K_{se} = \left(1 - \frac{{D_1}^2}{{D_2}^2}\right)^2$$

References:

[1] White, F. M. (2008). Fluid Mechanics (6th ed.). Rhode Island: McGraw-Hill

[2] CRANE Nuclear. (2013). General Engineering Data.

General Test Description

Description:

The map in figure 1 shows the pipeline route, starting at an isolation valve at the Garsfontein reservoirs (V1), which is pressurised by a Rand Water line to a pressure of at least 6 bar. The pipe then dips down through a 60m deep valley and then rises to the Parkmore High Level reservoir. Approximately 40m upstream of the reservoir, the final isolation valves (V2, V3 and V4) are situated. V2 is a gate valve, V3 a PRV and V4 another gate valve. Two off-takes exist between V2 and V4 and supply a distribution network from the reservoir.

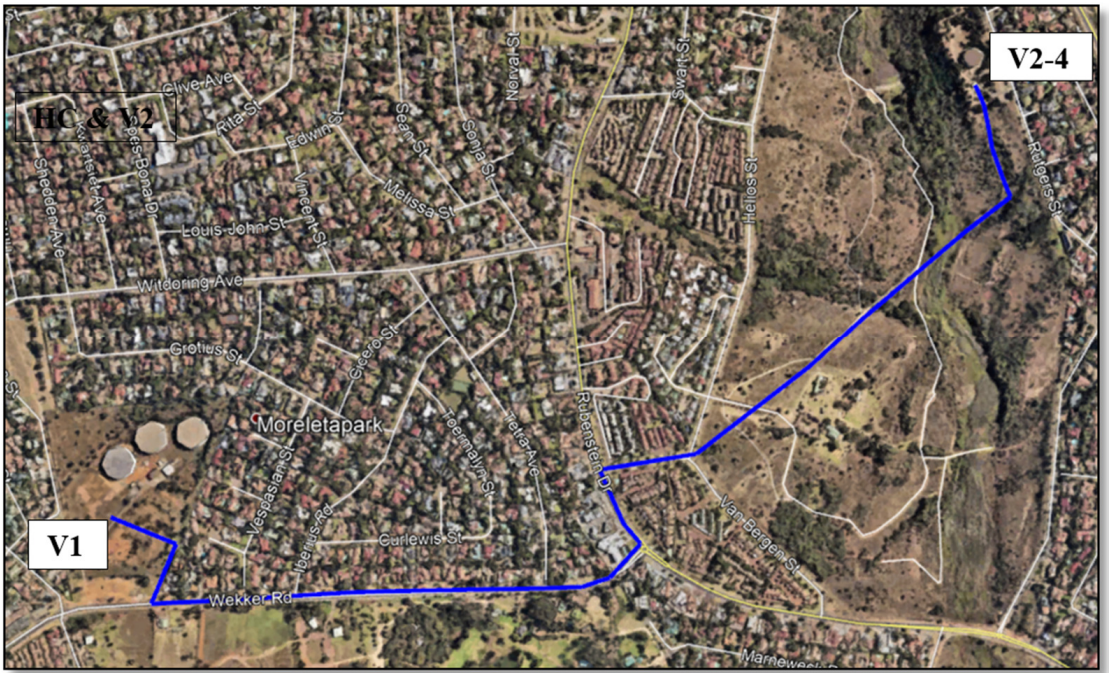

Figure 1: Map showing pipeline route starting at V1 and ending at V2-4

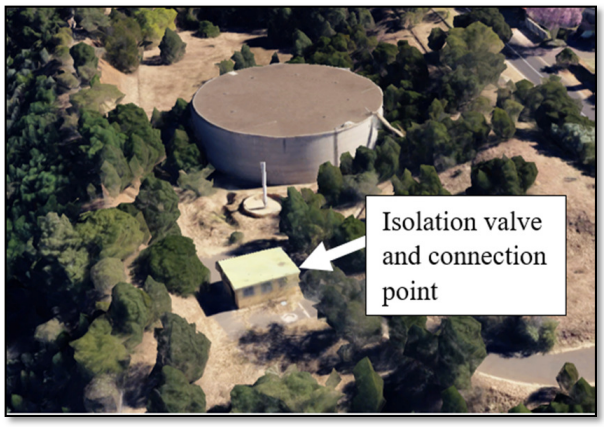

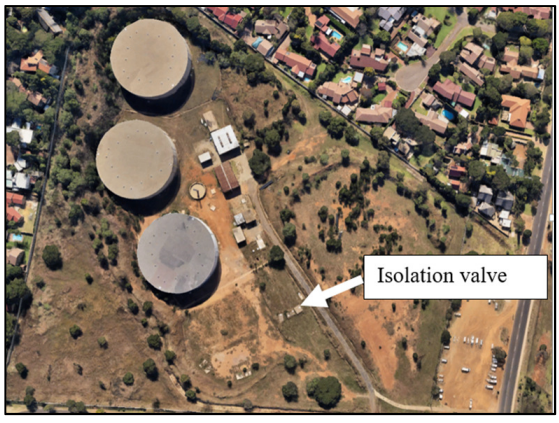

Figures 2&3: Arial images of the connection point at Parkmore High Level and the isolation valve at Garsfontein Reservoirs

General Test Description

In total, five test runs were carried out on this pipe section on two separate dates. For the first two test runs, the testing equipment was connected to CP1, and both the PRV (V3) and the gate valve (V4) were closed. For the third test, the connection point was moved to CP2, and only the gate valve (V2) was closed. On a second visit, two additional tests were performed by connecting to CP2 and isolating with the gate valve at V2.

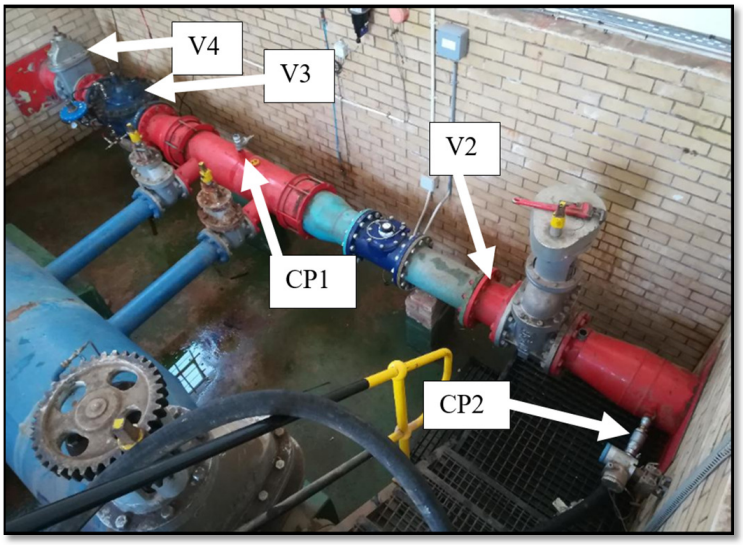

Figure 4: Valve chamber at V2, indicating valves 2 to 4, and potential connection points CP1 and CP2

General Test Information (Test 1)

Pipeline:	Garsfontein to Parkmore High Level Reservoir 1
Area:	Pretoria East, Garsfontein/Moreleta Park
Pipe Owner:	Tshwane Municipality
Date:	07 Jun 18
Time:	08:00 - 14:40

Pipeline Section:	**Section 1**	**Section 2**	**Section 3**	
Pipe length (m):	2640			
Pipe Diameter (mm):	500			
Pipe Material:	Steel			
Absolute Roughness e (mm)	0.05			
Minor Losses/km	0.5			
Upstream Isolation:	Pressure Reg. Valve			
Upstream Source:	Pressured Pipe			
Upstream Pressure (Bar) approx:	>5			
Upstream Isolation Elevation (m):	1503			
Downstream Isolation:	Gate Valve			
Downstream Delivery:	Reservoir			
Downstream Pressure (Bar) approx:	-5			
Downstream Isolation Elevation (m):	15002			

Connection of Testing Equipment

Connection Type:	Connection on PRV	
Connection Fitting size (mm):	30	
Comment on Fitting:	30mm female connection: Male threaded 1.25 to 1 inch reducer, 1 inch female to male, 1inch ball valve, 1 inch Geka coupling	
Minor loss coefficient of fitting	1.25 Inch (30mm) Threaded Female	15.07
Static height difference (A) in (m):	1.85	

Connection pipes*:

	Pipe 1	**Pipe 2**
Length of connection pipe* (mm):	30	
Diameter of connection pipes (mm)	30	
Absolute Roughness e (mm)	0.2	
Static height difference (B) in (mm):	800	

Minor losses of fittings on connection pipes*:

	Fitting 1	**Fitting 2**	**Fitting 3**	**Fitting 4**
Fitting type:	Instant diffuser	None	None	None
Pipe 1 or Pipe 2	1	1	1	1
Fitting diameter in (mm):	30	50	0.05	0.05
Fitting diameter out (mm):	500	400	0.05	0.05
Absolute Roughness e (mm)	0.05	0.2	0.5	0.5
No. of fittings:	0.2	0.2	0.2	0.2
Fitting Minor Loss Coefficient:	0.1986	0.0000	0.0000	0.0000
** Pipes and Fittings between the connection point and the main pipeline*			SUM:	0.19856

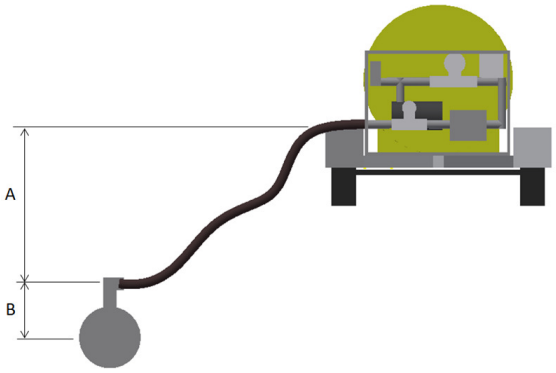

Pipeline Elevation Profile

Geocontext Website

Elevation Profile

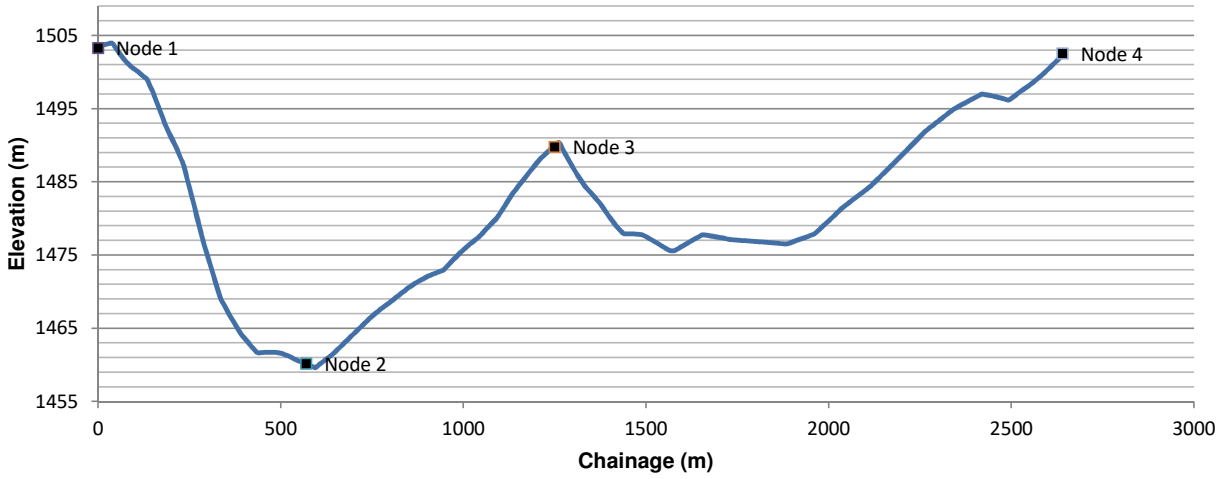

	Distance (m)	Elevation (m)	Material
1	0	1503.251099	Steel
1	5.16661139	1503.599121	Steel
1	10.33322278	1503.663452	Steel
1	15.49983417	1503.727905	Steel
1	20.66644556	1503.792358	Steel
1	25.83305695	1503.856689	Steel
1	30.99966834	1503.921143	Steel
1	36.16627973	1503.985474	Steel
1	41.33289112	1503.809448	Steel
1	46.49950251	1503.4021	Steel
1	51.6661139	1503.015015	Steel
1	56.83272529	1502.648193	Steel
1	61.99933668	1502.301514	Steel
1	67.16594807	1501.975098	Steel
1	72.33255946	1501.668823	Steel
1	77.49917085	1501.382935	Steel
1	82.66578224	1501.117065	Steel
1	87.83239363	1500.871582	Steel
1	92.99900502	1500.64624	Steel
1	98.16561641	1500.441162	Steel
1	103.3322278	1500.256348	Steel
1	108.4988392	1500.086304	Steel
1	113.6654506	1499.842407	Steel
1	118.832062	1499.618774	Steel
1	123.9986734	1499.415405	Steel
1	129.1652848	1499.2323	Steel
1	134.3318961	1498.974243	Steel
1	139.4985075	1498.399658	Steel
1	144.6651189	1497.837402	Steel
1	149.8317303	1497.287476	Steel
1	154.9983417	1496.588867	Steel
1	160.1649531	1495.890991	Steel
1	165.3315645	1495.205444	Steel
1	170.4981759	1494.532227	Steel
1	175.6647873	1493.871338	Steel
1	180.8313987	1493.225464	Steel
1	185.99801	1492.595947	Steel
1	191.1646214	1492.012085	Steel
1	196.3312328	1491.464355	Steel
1	201.4978442	1490.926392	Steel

No. of Sections:	1	
Section	**Start (m)**	**Material**
1	0	Steel
2		0
3		0

**If multiple sections exist, the Node points below must intercept at point where section changes for accurate pressure loss calculations.*

	Chainage (m)	Elevation (m)	End/part of Section
Node 1	0	1503.251	N/A
Node 2	570	1460.151	1
Node 3	1250	1489.735	1
Node 4	2640.14	1502.513	1

Total Chainage = 2640.14 m

Distance/Elevation Data Continues

Plot and Data Points (Test 1)

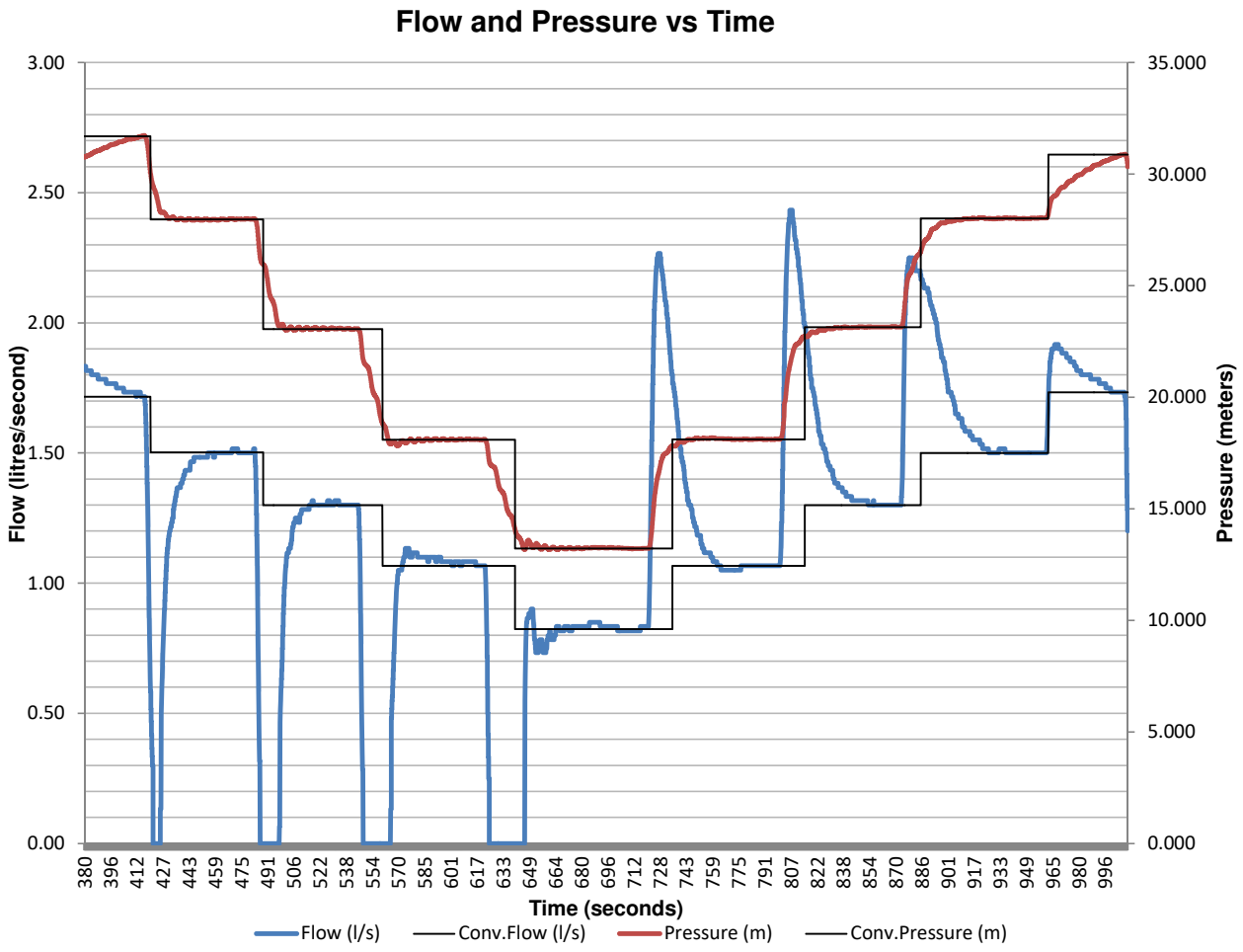

Pressure Head Correction (Test 1)

Corrected pressure at every Node:

Reynold's Number

$$\mathrm{Re} = \frac{\rho \mathrm{VD}}{\mu} = \frac{\mathrm{VD}}{\nu} = \frac{\mathrm{QD}}{\nu A}$$

Colebrook-White

$$\frac{1}{\sqrt{f}} = -2\log_{10}\left(\frac{\varepsilon}{3.7D} + \frac{2.51}{R_e\sqrt{f}}\right)$$

Minor Loss Equation

$$h_L = K_L\frac{V^2}{2g}$$

Darcy-Weissbach

$$h_f = f\frac{L}{D}\frac{V^2}{2g}$$

			Corrected Head (m)				
Point	**Flow (l/s)**	**Measured Head (m)**	**Node 0**	**Node 1**	**Node 2**	**Node 3**	**Node 4**
1	1.72	31.70	32.36	32.865	75.963	46.378	33.596
2	1.50	27.98	28.91	29.488	72.587	43.002	30.221
3	1.30	23.06	24.22	24.855	67.954	38.370	25.589
4	1.07	18.10	19.48	20.166	63.265	33.681	20.901
5	0.82	13.23	14.80	15.530	58.630	29.046	16.267
6	1.07	18.12	19.50	20.182	63.282	33.697	20.918
7	1.30	23.15	24.31	24.940	68.039	38.455	25.675
8	1.50	28.02	28.95	29.529	72.627	43.043	30.261
9	1.73	30.88	31.52	32.020	75.118	45.533	32.751
10	0.00	0.00	0.00	0.000	0.000	0.000	0.000
11	0.00	0.00	0.00	0.000	0.000	0.000	0.000
12	0.00	0.00	0.00	0.000	0.000	0.000	0.000
13	0.00	0.00	0.00	0.000	0.000	0.000	0.000
14	0.00	0.00	0.00	0.000	0.000	0.000	0.000
15	0.00	0.00	0.00	0.000	0.000	0.000	0.000

N1 And FAVAD Parameters (Test 1)

N1 Equation:

$$Q = C_d A\sqrt{2gh}$$
$$Q = C_d\sqrt{2g}Ah^{0.5}$$
$$Q = C_{N1}Ah^{N1}$$

FAVAD Equation:

$$Q = C_d A\sqrt{2gh} \quad but \quad A = A_0 + mH$$
$$\therefore C_d A = Q/\sqrt{2gh} \qquad Q = C_d\sqrt{2gh}(A_0 + mh)$$
$$Q = C_d\sqrt{2g}(A_0 h^{0.5} + mh^{1.5})$$

Node 0: N1 Relationship

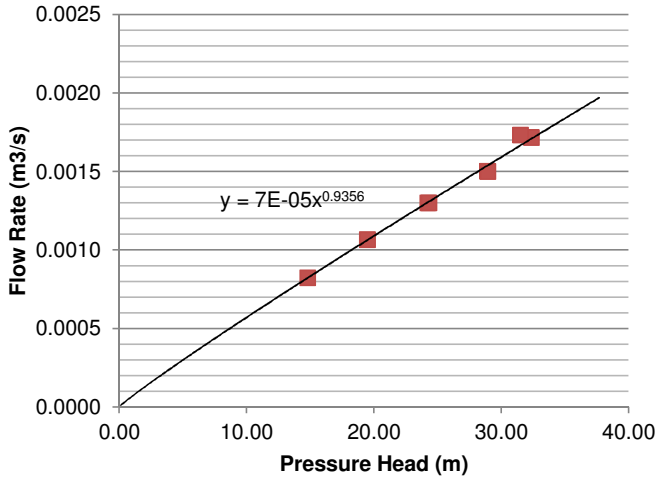

N1 Parameters:

Leakage Coefficient (CN1):	0.00007
Leakage Exponent (N1):	0.93559

Node 0: FAVAD Relationship

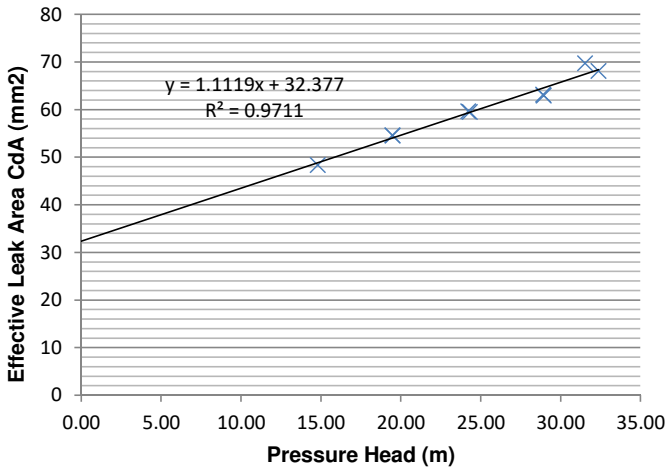

FAVAD Parameters:

Effective Initial Leak Area CdA0:	32.377	mm
Effective head-area slope Cdm:	1.112	mm2/m

Node 1: N1 Relationship

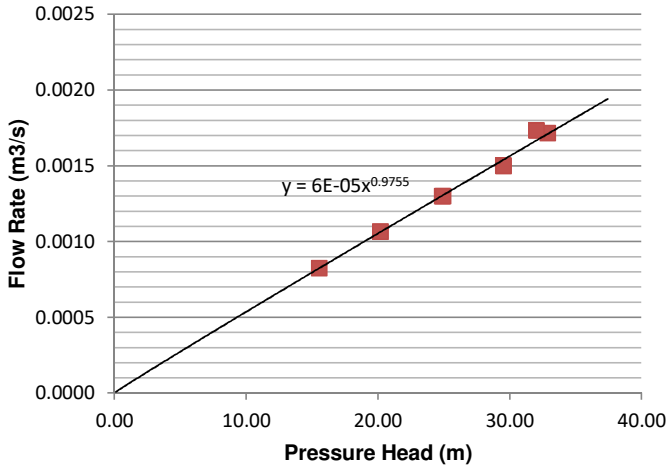

N1 Parameters:

Leakage Coefficient (C):	0.00006
Leakage Exponent (N1):	0.97553

Node 1: FAVAD Relationship

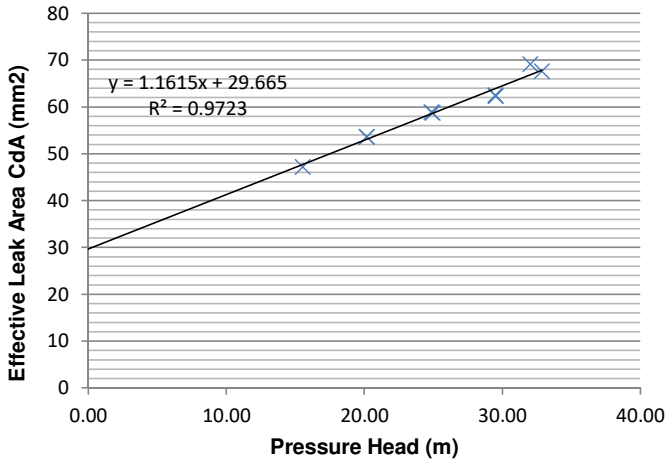

FAVAD Parameters:

Effective Initial Leak Area CdA0:	29.665	mm
Effective head-area slope Cdm:	1.162	mm2/m

N1 And FAVAD Parameters (Test 1)

Node 2: N1 Relationship

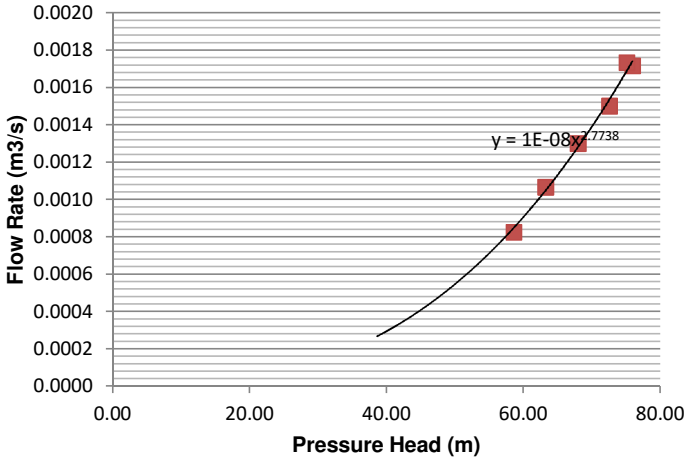

N1 Parameters:

Leakage Coefficient (C):	0.00000
Leakage Exponent (N1):	2.77379

Node 2: FAVAD Relationship

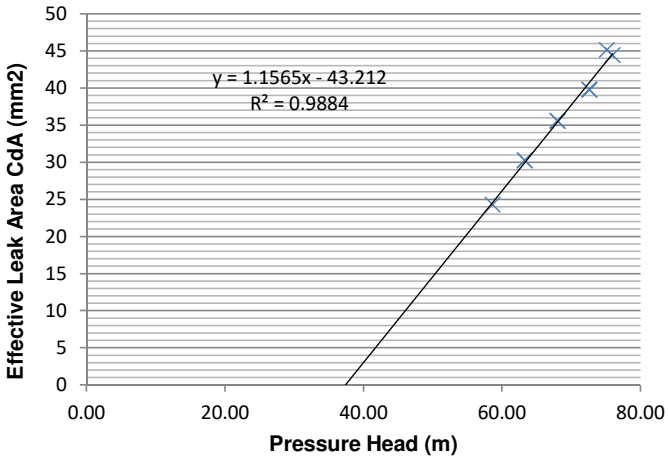

FAVAD Parameters:

Effective Initial Leak Area CdA0:	-43.212	mm
Effective head-area slope Cdm:	1.157	mm2/m

Node 3: N1 Relationship

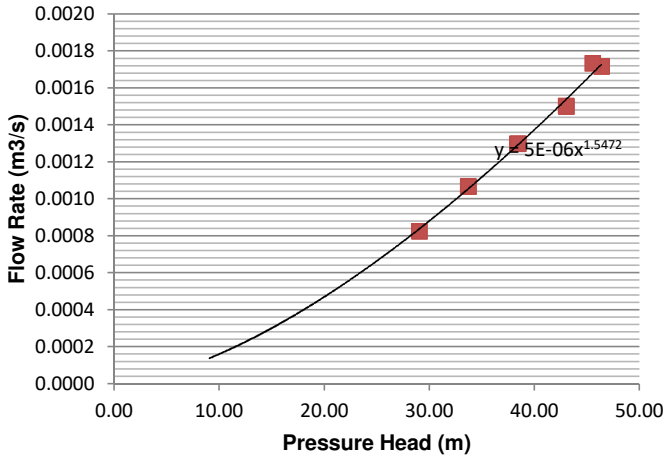

N1 Parameters:

Leakage Coefficient (C):	0.00000
Leakage Exponent (N1):	1.54719

Node 3: FAVAD Relationship

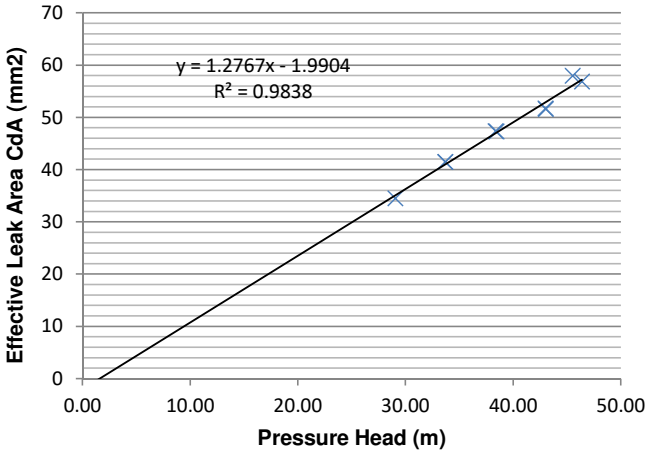

FAVAD Parameters:

Effective Initial Leak Area CdA0:	-1.990	mm
Effective head-area slope Cdm:	1.277	mm2/m

Node 4: N1 Relationship

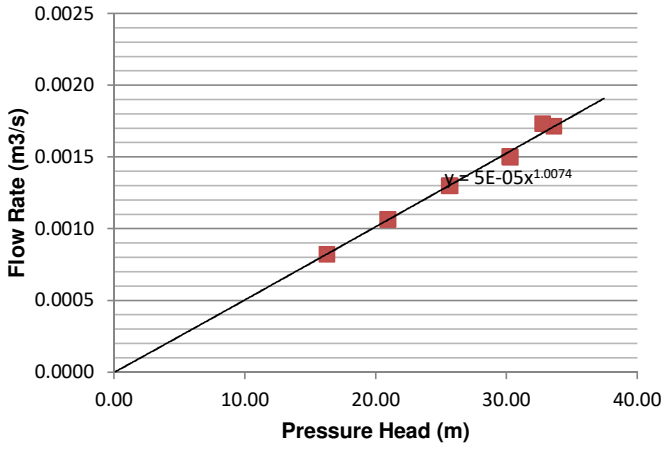

N1 Parameters:

Leakage Coefficient (C):	0.00005
Leakage Exponent (N1):	1.00742

Node 4: FAVAD Relationship

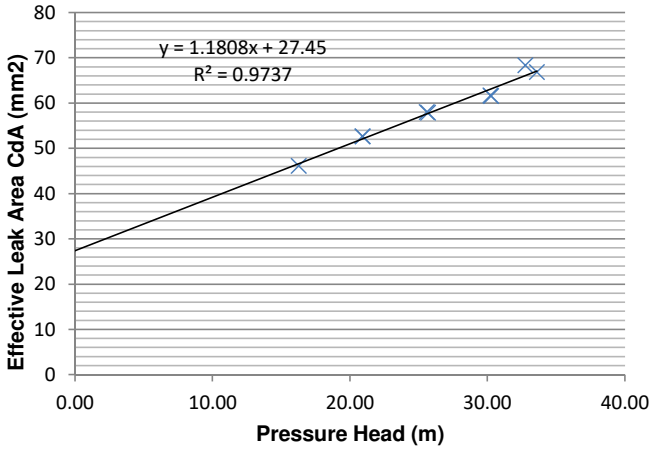

FAVAD Parameters:

Effective Initial Leak Area CdA0:	27.450	mm
Effective head-area slope Cdm:	1.181	mm2/m

Summary (Test 1)

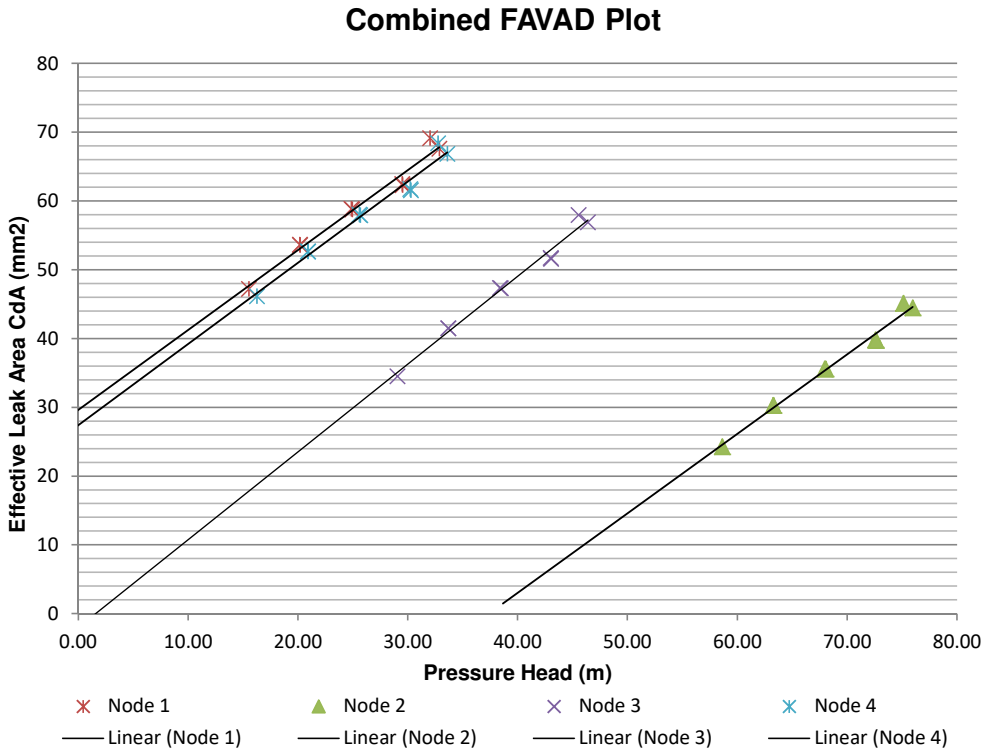

Discussion (Test 1):

A large leak with a pressure sensitive leak area was detected. The leak can only be above node 2 and node 3. Possibly a leaking isolation valve at node 1.

Plot and Data Points (Test 2)

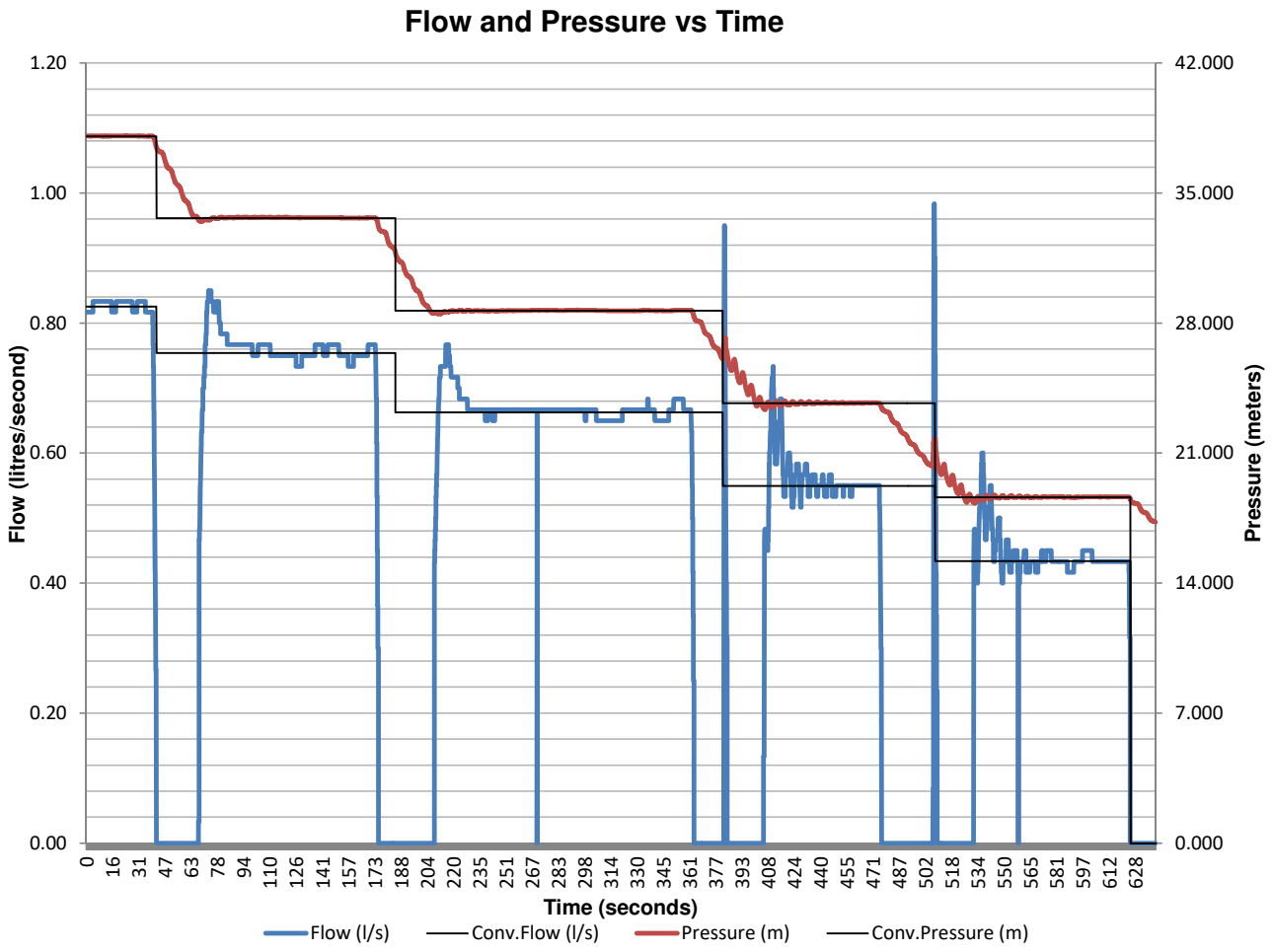

Pressure Head Correction (Test 2)

Corrected pressure at every Node:

Reynold's Number

$$\mathrm{Re} = \frac{\rho \mathrm{VD}}{\mu} = \frac{\mathrm{VD}}{\nu} = \frac{\mathrm{QD}}{\nu A}$$

Colebrook-White

$$\frac{1}{\sqrt{f}} = -2\log_{10}\left(\frac{\varepsilon}{3.7D} + \frac{2.51}{R_e\sqrt{f}}\right)$$

Minor Loss Equation

$$h_L = K_L\frac{V^2}{2g}$$

Darcy-Weissbach

$$h_f = f\frac{L}{D}\frac{V^2}{2g}$$

			Corrected Head (m)				
Point	**Flow (l/s)**	**Measured Head (m)**	**Node 0**	**Node 1**	**Node 2**	**Node 3**	**Node 4**
1	0.83	38.07	39.63	40.361	83.460	53.876	41.097
2	0.75	33.66	35.27	36.015	79.114	49.531	36.752
3	0.66	28.68	30.34	31.096	74.195	44.612	31.833
4	0.55	23.70	25.42	26.187	69.287	39.703	26.925
5	0.43	18.63	20.40	21.183	64.282	34.699	21.920
6	0.00	0.00	0.00	0.000	0.000	0.000	0.000
7	0.00	0.00	0.00	0.000	0.000	0.000	0.000
8	0.00	0.00	0.00	0.000	0.000	0.000	0.000
9	0.00	0.00	0.00	0.000	0.000	0.000	0.000
10	0.00	0.00	0.00	0.000	0.000	0.000	0.000
11	0.00	0.00	0.00	0.000	0.000	0.000	0.000
12	0.00	0.00	0.00	0.000	0.000	0.000	0.000
13	0.00	0.00	0.00	0.000	0.000	0.000	0.000
14	0.00	0.00	0.00	0.000	0.000	0.000	0.000
15	0.00	0.00	0.00	0.000	0.000	0.000	0.000

N1 And FAVAD Parameters (Test 2)

N1 Equation:

$$Q = C_d A\sqrt{2gh}$$
$$Q = C_d\sqrt{2g}\,Ah^{0.5}$$
$$Q = C_{N1}Ah^{N1}$$

FAVAD Equation:

$$Q = C_d A\sqrt{2gh} \quad but \quad A = A_0 + mH$$
$$\therefore C_d A = Q/\sqrt{2gh} \qquad Q = C_d\sqrt{2gh}(A_0 + mh)$$
$$Q = C_d\sqrt{2g}\,(A_0 h^{0.5} + mh^{1.5})$$

Node 0: N1 Relationship

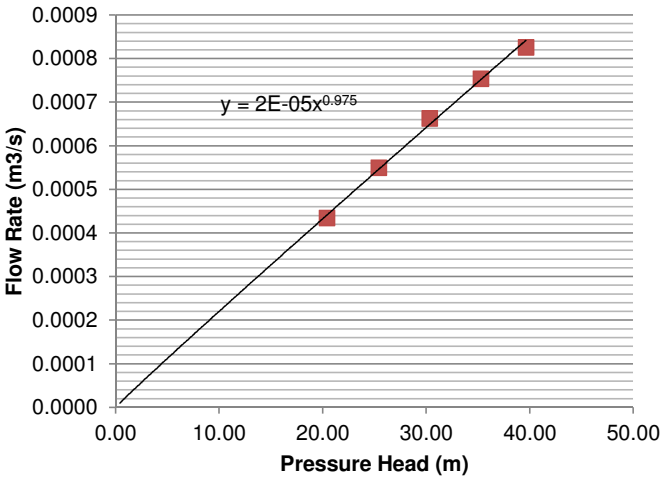

N1 Parameters:

Leakage Coefficient (CN1):	0.00002
Leakage Exponent (N1):	0.97499

Node 0: FAVAD Relationship

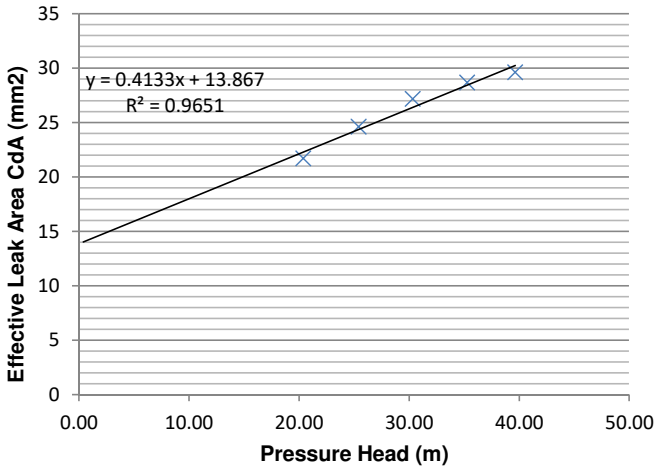

FAVAD Parameters:

Effective Initial Leak Area CdA0	13.867	mm
Effective head-area slope Cdm:	0.413	mm2/m

Node 1: N1 Relationship

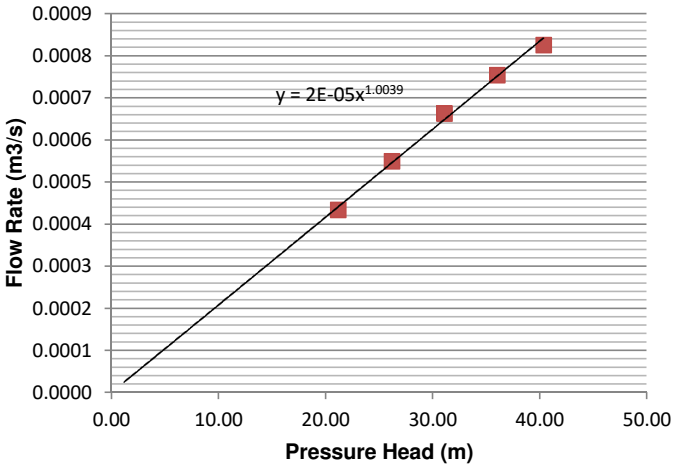

N1 Parameters:

Leakage Coefficient (C):	0.00002
Leakage Exponent (N1):	1.00395

Node 1: FAVAD Relationship

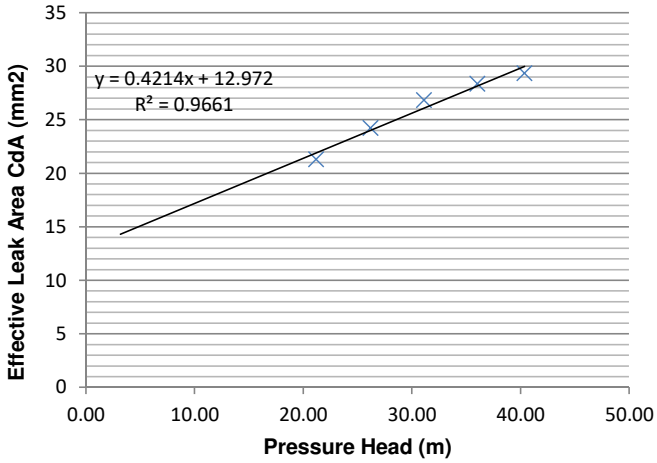

FAVAD Parameters:

Effective Initial Leak Area CdA0	12.972	mm
Effective head-area slope Cdm:	0.421	mm2/m

N1 And FAVAD Parameters (Test 2)

Node 2: N1 Relationship

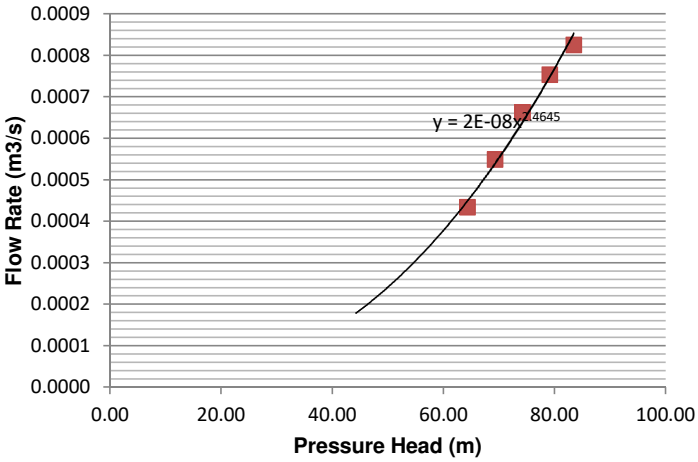

N1 Parameters:

Leakage Coefficient (C):	0.00000
Leakage Exponent (N1):	2.46453

Node 2: FAVAD Relationship

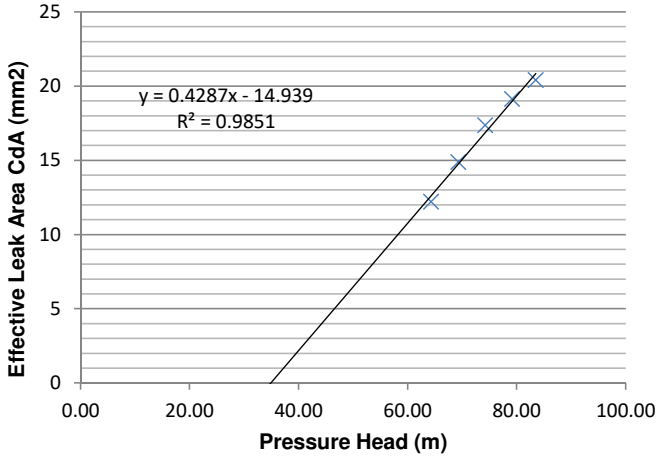

FAVAD Parameters:

Effective Initial Leak Area CdA0	-14.939	mm
Effective head-area slope Cdm:	0.429	mm2/m

Node 3: N1 Relationship

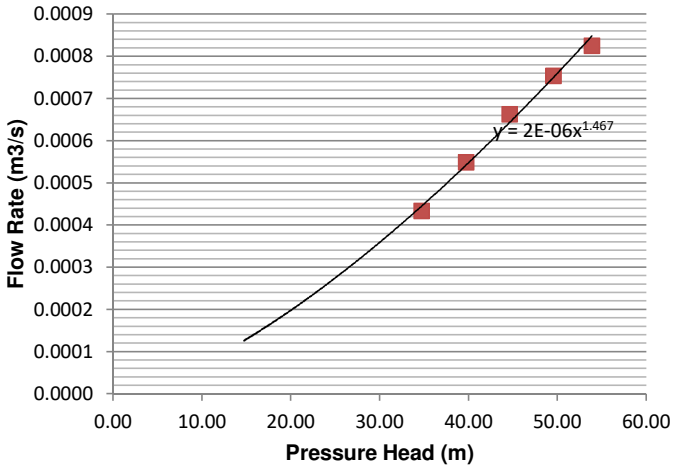

N1 Parameters:

Leakage Coefficient (C):	0.00000
Leakage Exponent (N1):	1.46697

Node 3: FAVAD Relationship

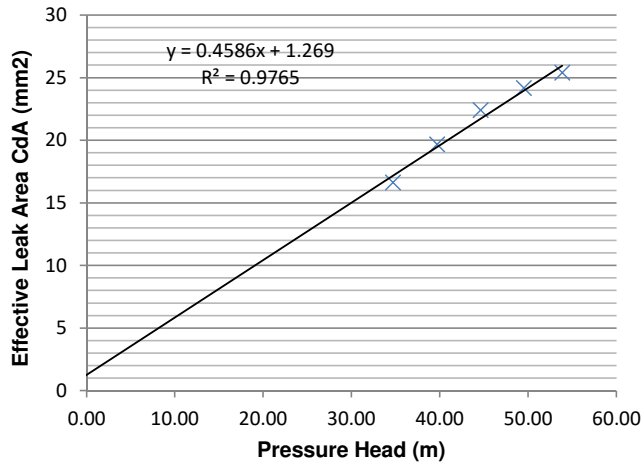

FAVAD Parameters:

Effective Initial Leak Area CdA0	1.269	mm
Effective head-area slope Cdm:	0.459	mm2/m

Node 4: N1 Relationship

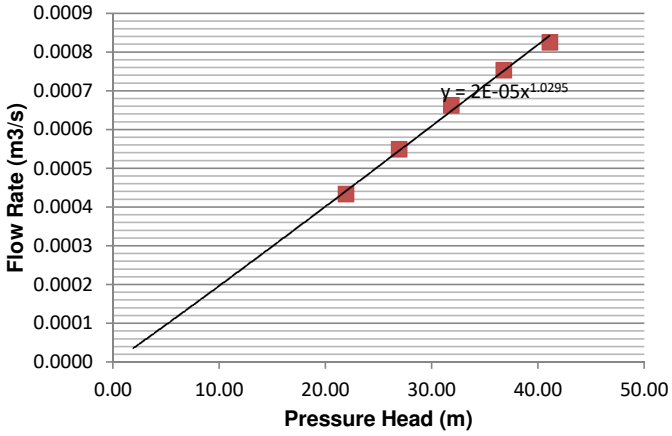

N1 Parameters:

Leakage Coefficient (C):	0.00002
Leakage Exponent (N1):	1.02955

Node 4: FAVAD Relationship

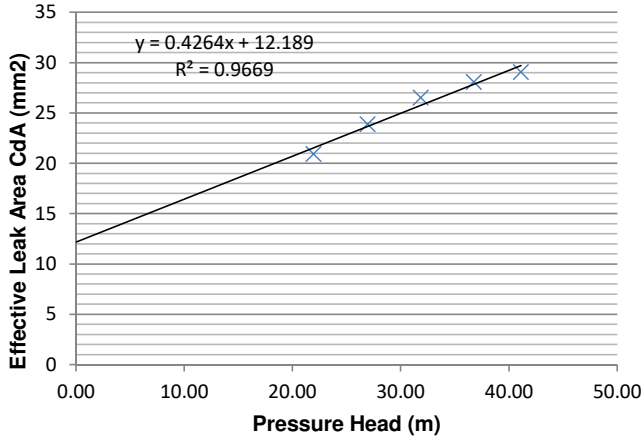

FAVAD Parameters:

Effective Initial Leak Area CdA0	12.189	mm
Effective head-area slope Cdm:	0.426	mm2/m

Summary (Test2)

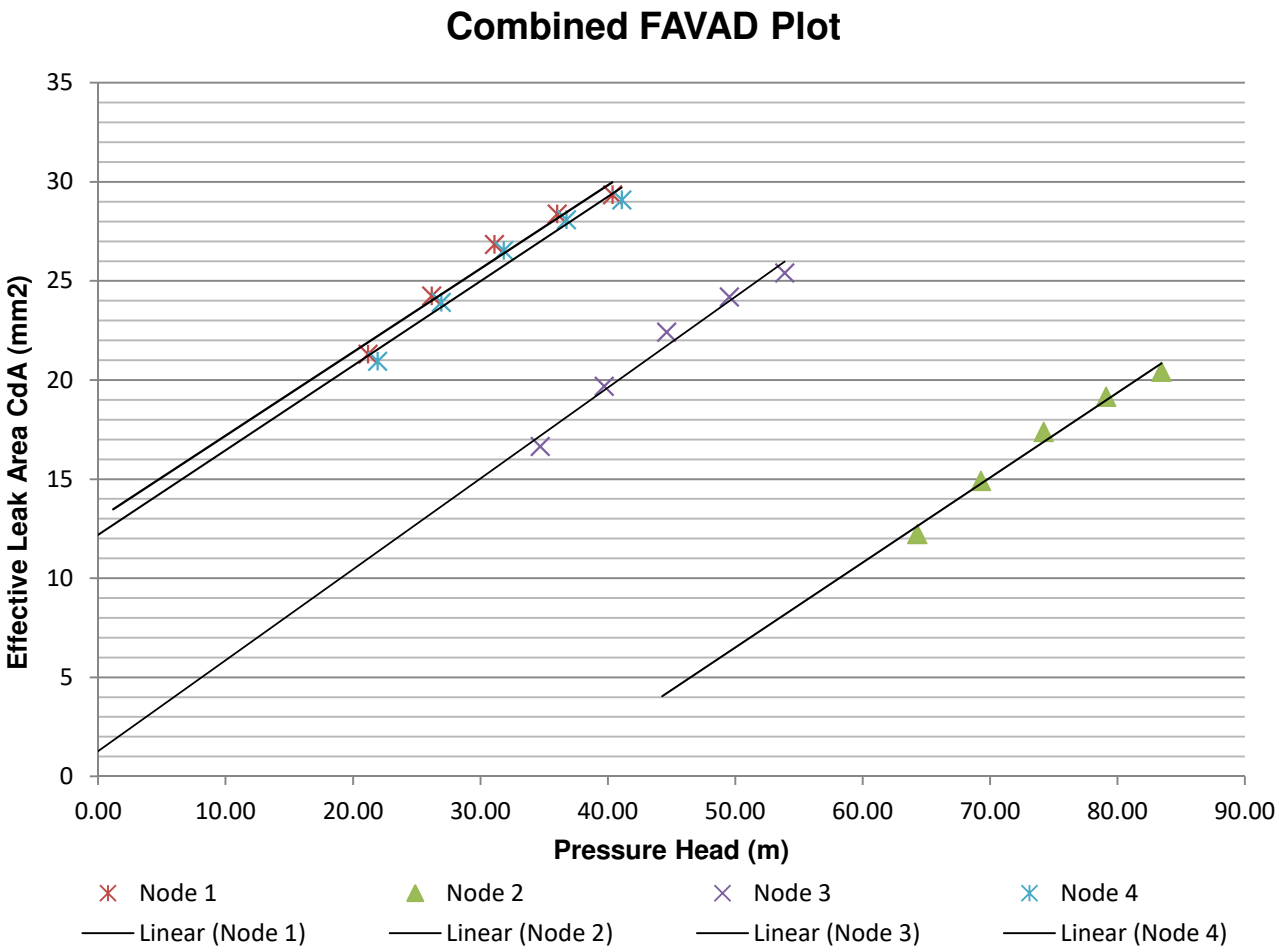

Discussion (Test 2):

Smaller leak than Test 1. Leak again most probably above nodes 2 & 3. The change from the previous leak links this leak to the valve's operation. Possibly tests 1 and 2 point to a leakaing isolatoin valve.

Plot and Data Points (Test 3)

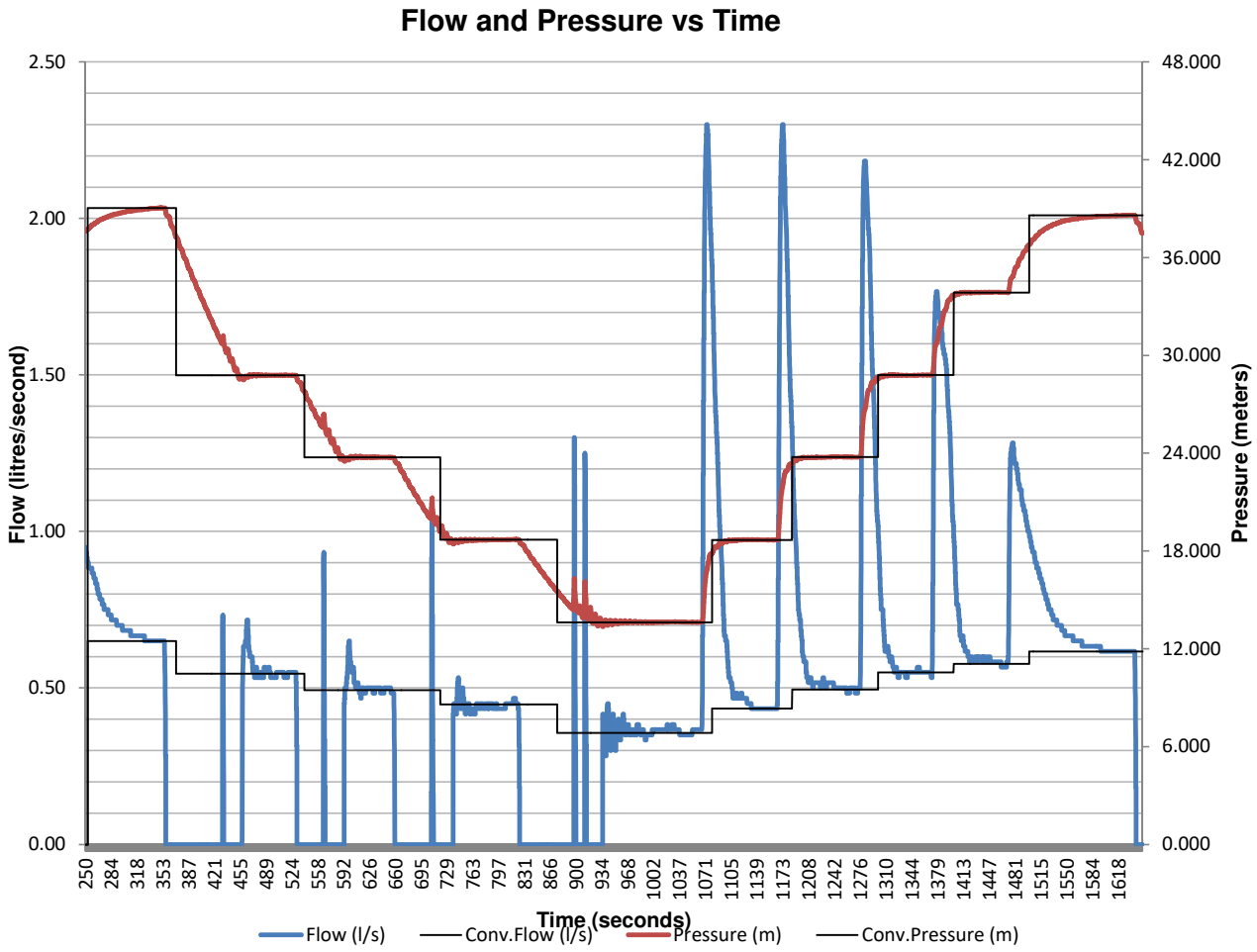

Pressure Head Correction (Test 3)

Corrected pressure at every Node:

Reynold's Number

$$\mathrm{Re} = \frac{\rho \mathrm{VD}}{\mu} = \frac{\mathrm{VD}}{\nu} = \frac{\mathrm{QD}}{\nu A}$$

Colebrook-White

$$\frac{1}{\sqrt{f}} = -2\log_{10}\left(\frac{\varepsilon}{3.7D} + \frac{2.51}{R_e\sqrt{f}}\right)$$

Minor Loss Equation

$$h_L = K_L\frac{V^2}{2g}$$

Darcy-Weissbach

$$h_f = f\frac{L}{D}\frac{V^2}{2g}$$

			Corrected Head (m)				
Point	**Flow (l/s)**	**Measured Head (m)**	**Node 0**	**Node 1**	**Node 2**	**Node 3**	**Node 4**
1	0.65	39.04	40.71	41.470	84.570	54.986	42.207
2	0.55	28.79	30.51	31.277	74.376	44.793	32.014
3	0.49	23.75	25.49	26.269	69.368	39.785	27.006
4	0.45	18.70	20.46	21.242	64.341	34.758	21.979
5	0.36	13.63	15.43	16.213	59.313	29.729	16.951
6	0.43	18.68	20.44	21.224	64.323	34.740	21.961
7	0.50	23.77	25.51	26.288	69.388	39.804	27.026
8	0.55	28.80	30.52	31.288	74.388	44.804	32.025
9	0.58	33.87	35.57	36.339	79.438	49.855	37.076
10	0.62	38.60	40.29	41.050	84.150	54.566	41.787
11	0.00	0.00	0.00	0.000	0.000	0.000	0.000
12	0.00	0.00	0.00	0.000	0.000	0.000	0.000
13	0.00	0.00	0.00	0.000	0.000	0.000	0.000
14	0.00	0.00	0.00	0.000	0.000	0.000	0.000
15	0.00	0.00	0.00	0.000	0.000	0.000	0.000

N1 And FAVAD Parameters (Test 3)

N1 Equation:

$$Q = C_d A\sqrt{2gh}$$
$$Q = C_d\sqrt{2g}\,Ah^{0.5}$$
$$Q = C_{N1}Ah^{N1}$$

FAVAD Equation:

$$Q = C_d A\sqrt{2gh} \quad but \quad A = A_0 + mH$$
$$\therefore C_d A = Q/\sqrt{2gh} \qquad Q = C_d\sqrt{2gh}(A_0 + mh)$$
$$Q = C_d\sqrt{2g}\,(A_0 h^{0.5} + mh^{1.5})$$

Node 0: N1 Relationship

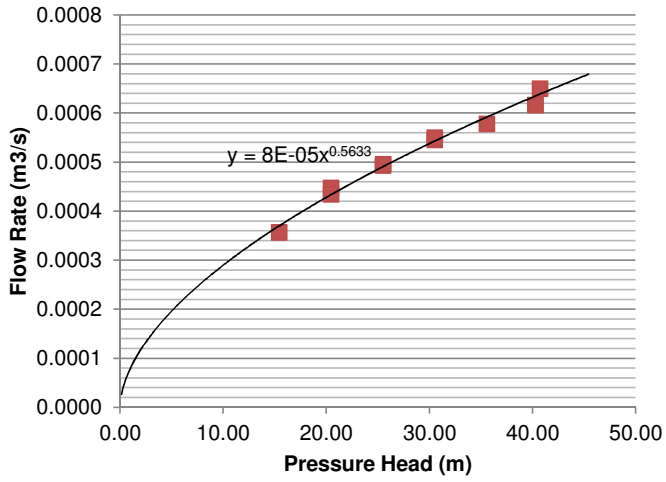

N1 Parameters:

Leakage Coefficient (CN1):	0.00008
Leakage Exponent (N1):	0.56334

Node 0: FAVAD Relationship

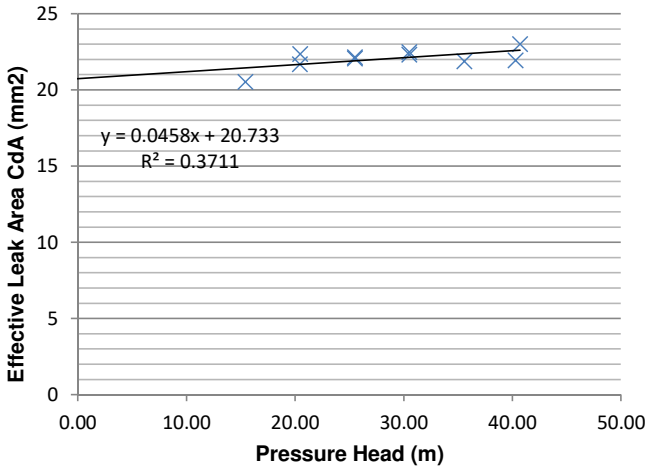

FAVAD Parameters:

Effective Initial Leak Area CdA0:	20.733	mm
Effective head-area slope Cdm:	0.046	mm2/m

Node 1: N1 Relationship

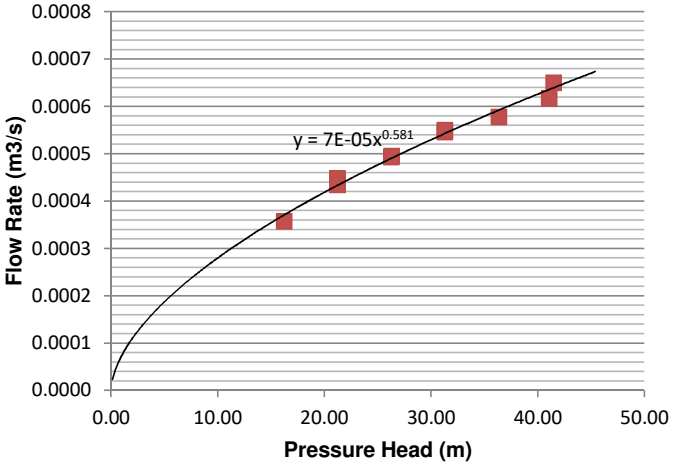

N1 Parameters:

Leakage Coefficient (C):	0.00007
Leakage Exponent (N1):	0.58104

Node 1: FAVAD Relationship

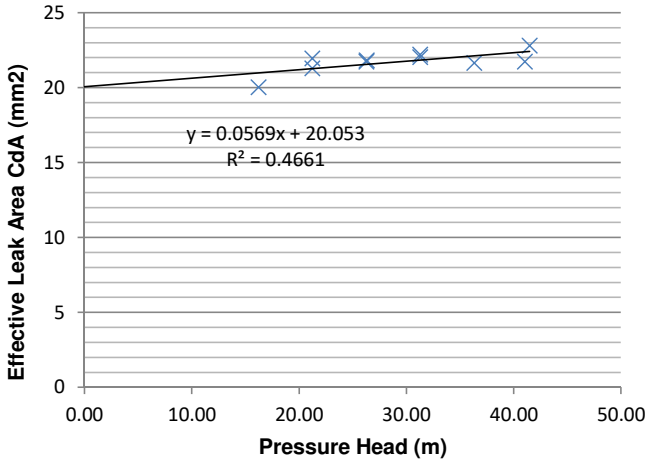

FAVAD Parameters:

Effective Initial Leak Area CdA0:	20.053	mm
Effective head-area slope Cdm:	0.057	mm2/m

N1 And FAVAD Parameters (Test 3)

Node 2: N1 Relationship

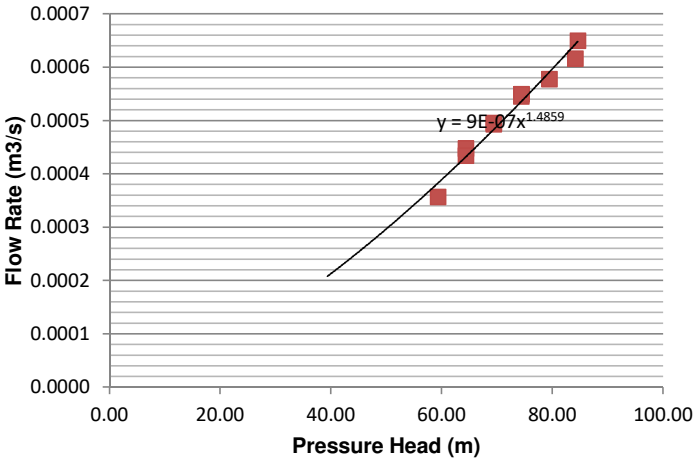

N1 Parameters:

Leakage Coefficient (C):	0.00000
Leakage Exponent (N1):	1.48586

Node 2: FAVAD Relationship

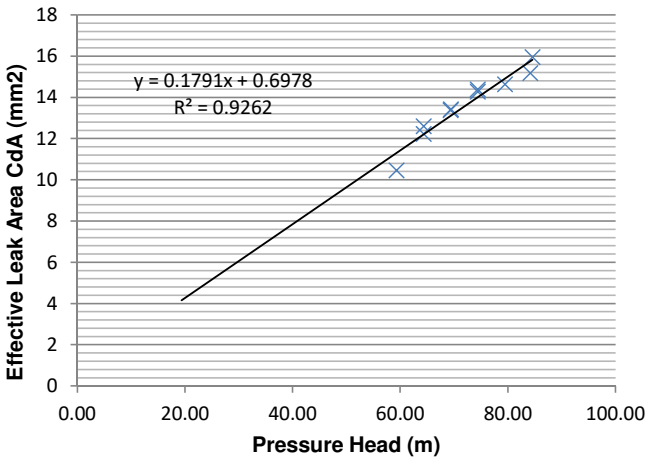

FAVAD Parameters:

Effective Initial Leak Area CdA0:	0.698	mm
Effective head-area slope Cdm:	0.179	mm2/m

Node 3: N1 Relationship

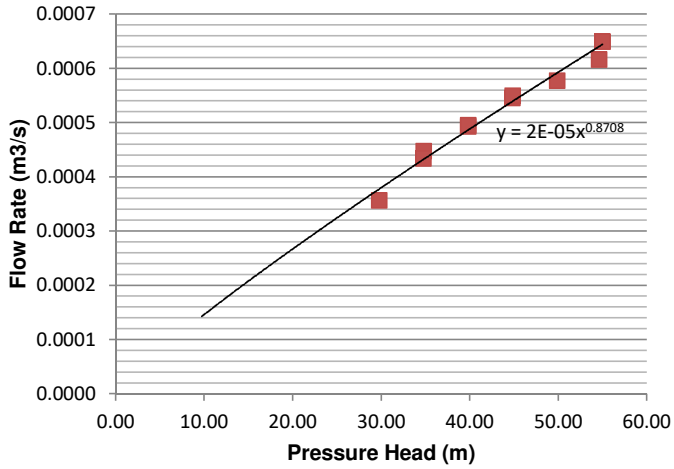

N1 Parameters:

Leakage Coefficient (C):	0.00002
Leakage Exponent (N1):	0.87078

Node 3: FAVAD Relationship

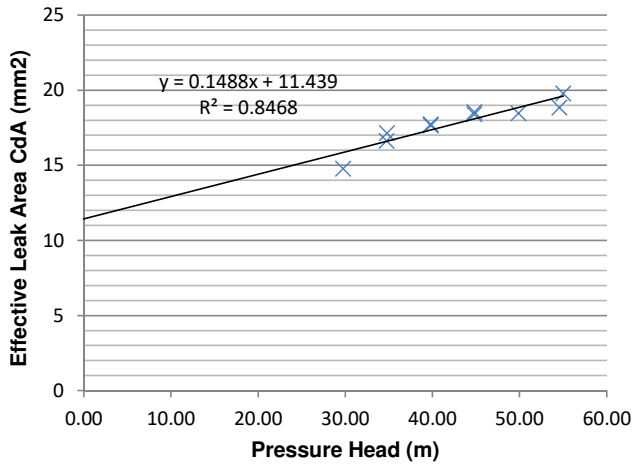

FAVAD Parameters:

Effective Initial Leak Area CdA0:	11.439	mm
Effective head-area slope Cdm:	0.149	mm2/m

Node 4: N1 Relationship

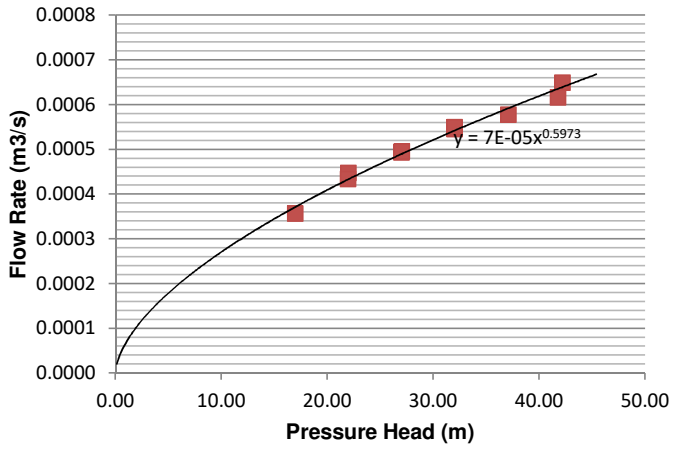

N1 Parameters:

Leakage Coefficient (C):	0.00007
Leakage Exponent (N1):	0.59725

Node 4: FAVAD Relationship

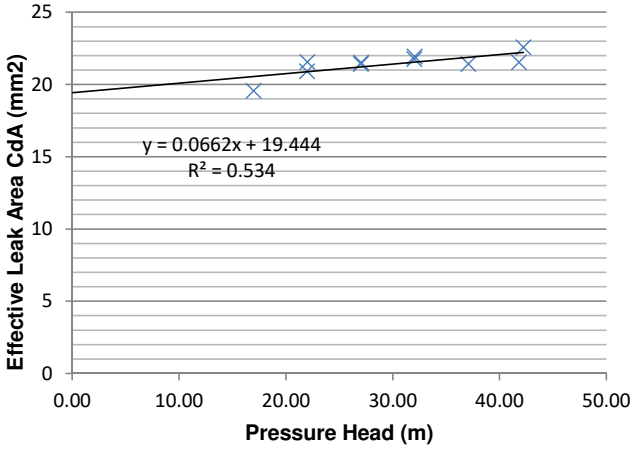

FAVAD Parameters:

Effective Initial Leak Area CdA0:	19.444	mm
Effective head-area slope Cdm:	0.066	mm2/m

Summary (Test 3)

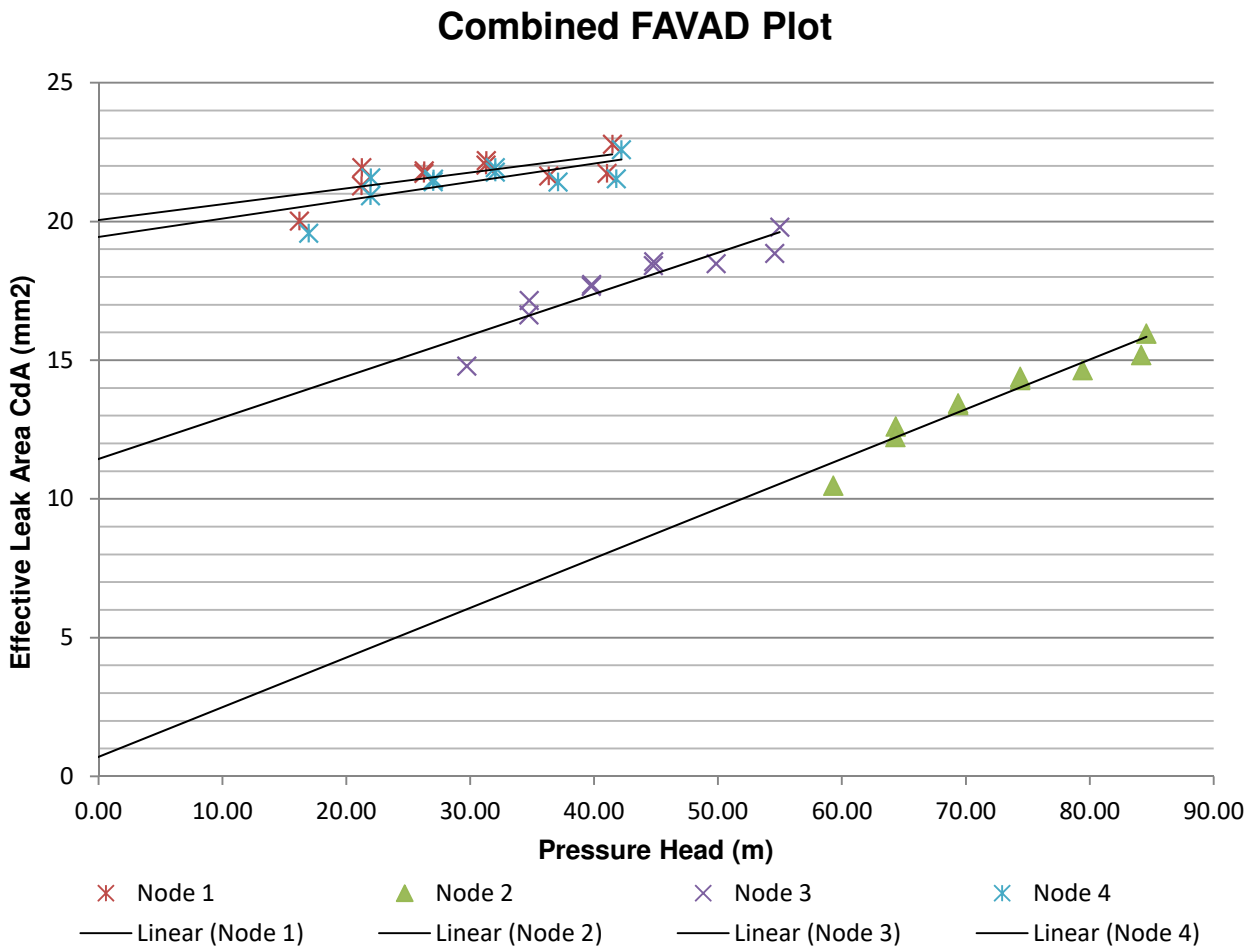

Discussion:

The following conclusions can be made:

- Round holes, with leak areas insensitive to pressure, possibly occur at the high lying nodes. Such round and rigid holes, however, are uncommon in steel pipes, and this scenario is deemed unlikely.
- Either longitudinal cracks or corrosion holes exist at the lower elevations. Both of these types of leaks exhibit a large range of N1 values and steep pressure-area slopes. Corrosion holes would be likely in steel pipes.
- If the leak is at a low point, the initial leak area will be smaller than at higher elevations.

The pipe passes through a valley and underneath a small river. The corrosive conditions resulting from the moist soil at the river are likely to lead to corrosion of the pipe. If the valve chambers are inspected and no leaks exist from the air valves or gaskets, the next most likely scenario would be the existence of small corrosion holes at the low points of the pipeline.

Summary (Test 4)

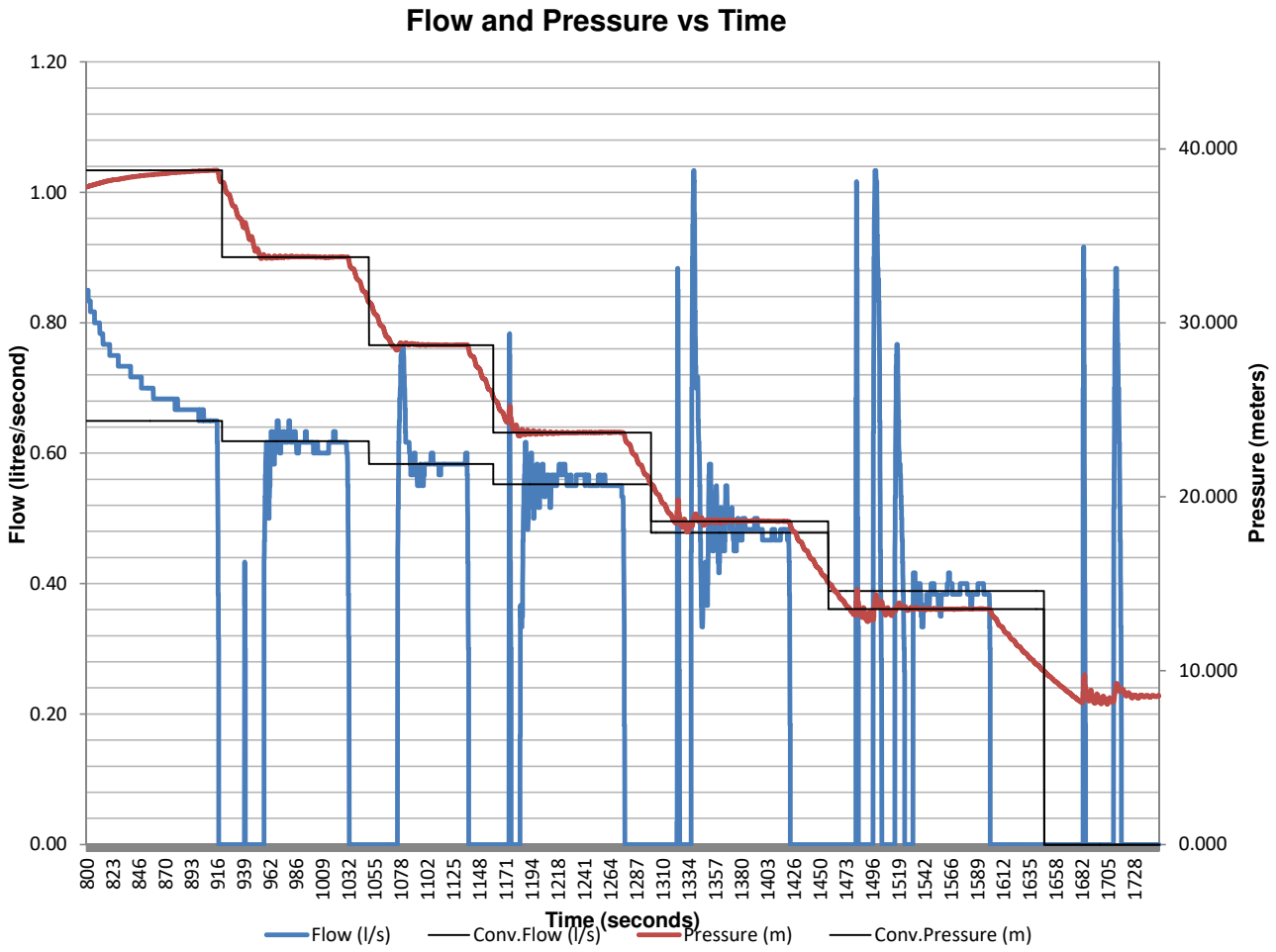

Pressure Head Correction (Test 4)

Corrected pressure at every Node:

Reynold's Number

$$\mathrm{Re} = \frac{\rho \mathrm{VD}}{\mu} = \frac{\mathrm{VD}}{\nu} = \frac{\mathrm{QD}}{\nu A}$$

Colebrook-White

$$\frac{1}{\sqrt{f}} = -2\log_{10}\left(\frac{\varepsilon}{3.7D} + \frac{2.51}{R_e\sqrt{f}}\right)$$

Minor Loss Equation

$$h_L = K_L\frac{V^2}{2g}$$

Darcy-Weissbach

$$h_f = f\frac{L}{D}\frac{V^2}{2g}$$

			Corrected Head (m)				
Point	**Flow (l/s)**	**Measured Head (m)**	**Node 0**	**Node 1**	**Node 2**	**Node 3**	**Node 4**
1	0.65	38.77	40.44	41.201	84.301	54.717	41.938
2	0.62	33.79	35.47	36.233	79.333	49.749	36.970
3	0.58	28.73	30.43	31.197	74.297	44.713	31.935
4	0.55	23.69	25.41	26.181	69.280	39.697	26.918
5	0.48	18.60	20.35	21.125	64.225	34.641	21.863
6	0.39	13.55	15.33	16.116	59.216	29.632	16.854
7	0.00	0.00	0.00	0.000	0.000	0.000	0.000
8	0.00	0.00	0.00	0.000	0.000	0.000	0.000
9	0.00	0.00	0.00	0.000	0.000	0.000	0.000
10	0.00	0.00	0.00	0.000	0.000	0.000	0.000
11	0.00	0.00	0.00	0.000	0.000	0.000	0.000
12	0.00	0.00	0.00	0.000	0.000	0.000	0.000
13	0.00	0.00	0.00	0.000	0.000	0.000	0.000
14	0.00	0.00	0.00	0.000	0.000	0.000	0.000
15	0.00	0.00	0.00	0.000	0.000	0.000	0.000

N1 And FAVAD Parameters (Test 4)

N1 Equation:

$$Q = C_d A\sqrt{2gh}$$
$$Q = C_d\sqrt{2g}\,Ah^{0.5}$$
$$Q = C_{N1}Ah^{N1}$$

FAVAD Equation:

$$Q = C_d A\sqrt{2gh} \quad but \quad A = A_0 + mH$$
$$\therefore C_d A = Q/\sqrt{2gh} \qquad Q = C_d\sqrt{2gh}(A_0 + mh)$$
$$Q = C_d\sqrt{2g}\,(A_0 h^{0.5} + mh^{1.5})$$

Node 0: N1 Relationship

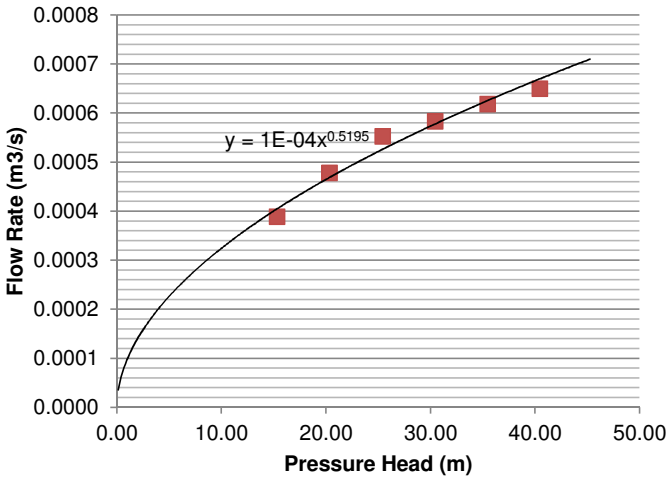

N1 Parameters:

Leakage Coefficient (CN1):	0.00010
Leakage Exponent (N1):	0.51952

Node 0: FAVAD Relationship

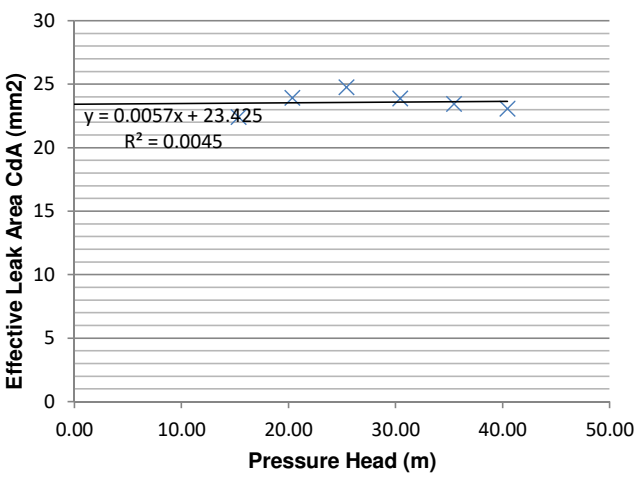

FAVAD Parameters:

Effective Initial Leak Area CdA0:	23.425	mm
Effective head-area slope Cdm:	0.006	mm2/m

Node 1: N1 Relationship

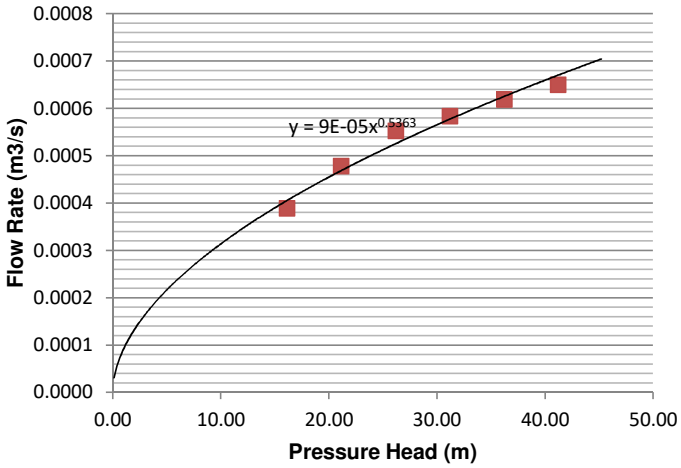

N1 Parameters:

Leakage Coefficient (C):	0.00009
Leakage Exponent (N1):	0.53629

Node 1: FAVAD Relationship

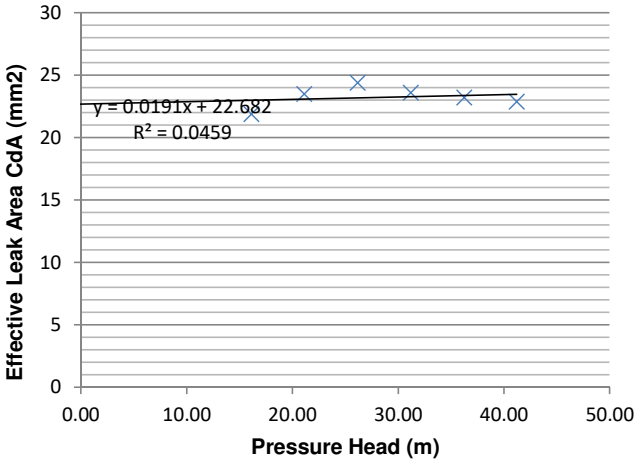

FAVAD Parameters:

Effective Initial Leak Area CdA0:	22.682	mm
Effective head-area slope Cdm:	0.019	mm2/m

N1 And FAVAD Parameters (Test 4)

Node 2: N1 Relationship

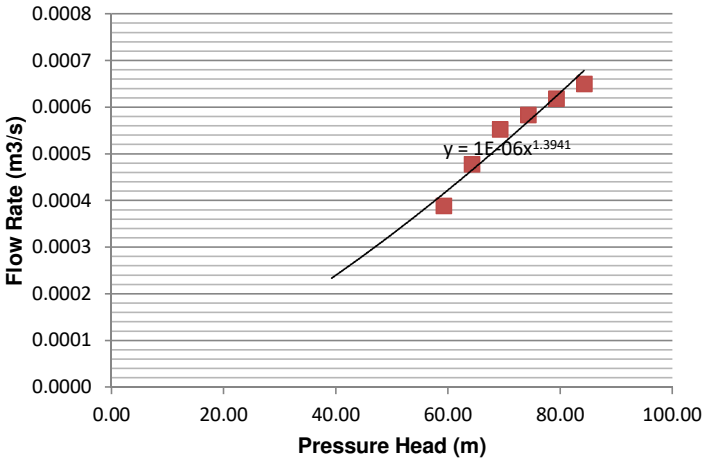

N1 Parameters:

Leakage Coefficient (C):	0.00000
Leakage Exponent (N1):	1.39408

Node 2: FAVAD Relationship

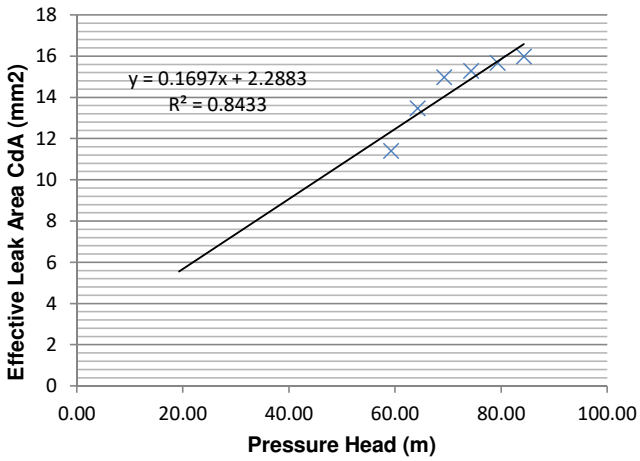

FAVAD Parameters:

Effective Initial Leak Area CdA0:	2.288	mm
Effective head-area slope Cdm:	0.170	mm2/m

Node 3: N1 Relationship

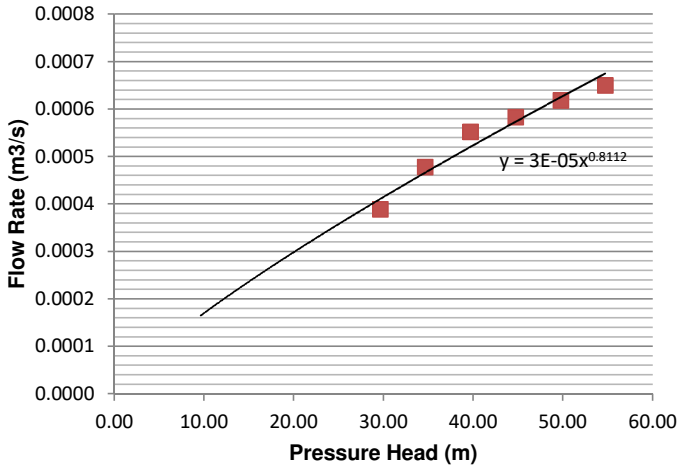

N1 Parameters:

Leakage Coefficient (C):	0.00003
Leakage Exponent (N1):	0.81120

Node 3: FAVAD Relationship

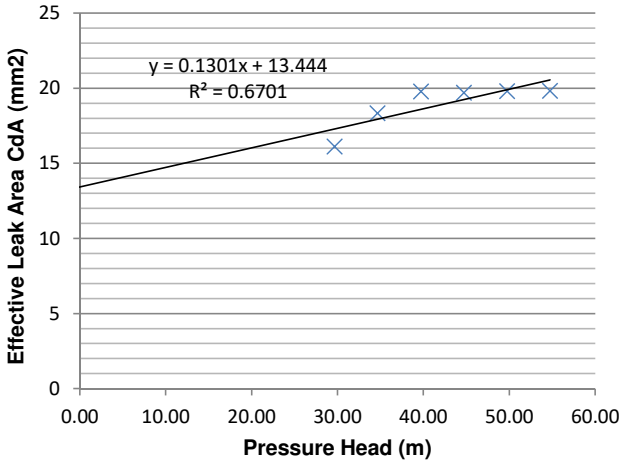

FAVAD Parameters:

Effective Initial Leak Area CdA0:	13.444	mm
Effective head-area slope Cdm:	0.130	mm2/m

Node 4: N1 Relationship

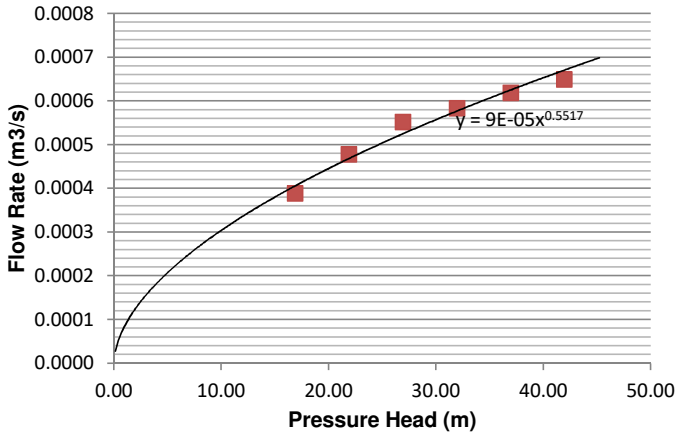

N1 Parameters:

Leakage Coefficient (C):	0.00009
Leakage Exponent (N1):	0.55169

Node 4: FAVAD Relationship

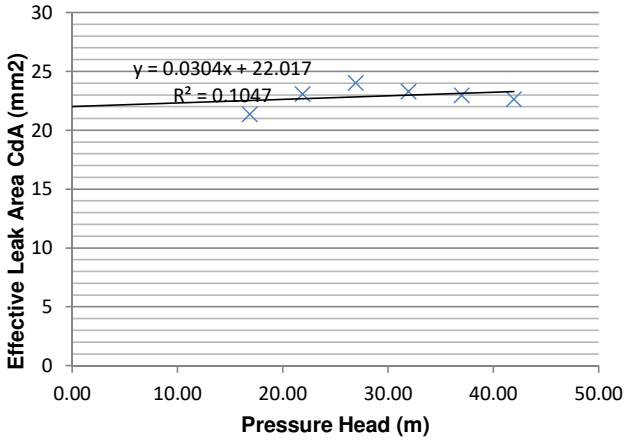

FAVAD Parameters:

Effective Initial Leak Area CdA0:	22.017	mm
Effective head-area slope Cdm:	0.030	mm2/m

Summary (Test 4)

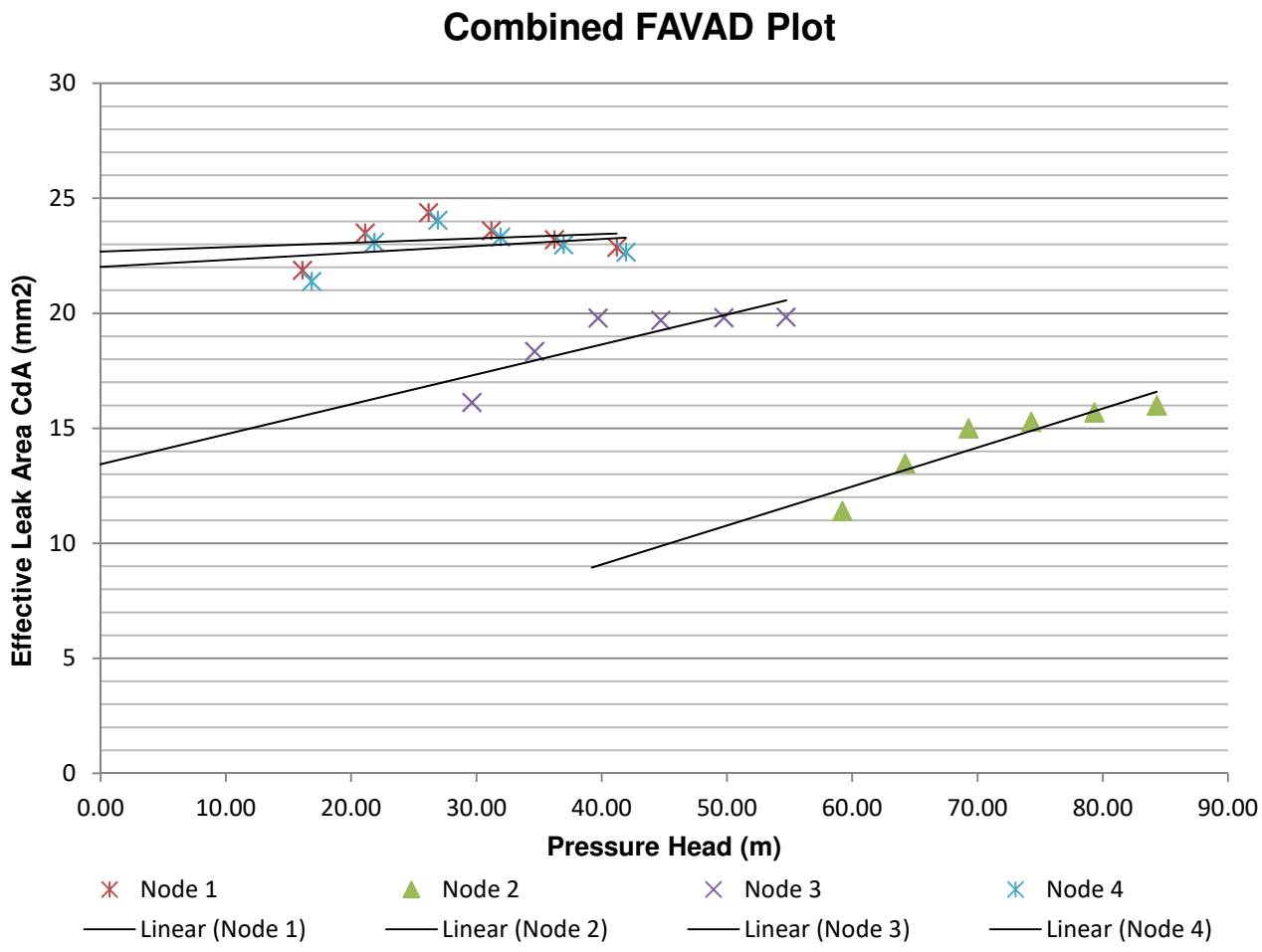

Discussion:

Very similar results to previous test.

Plot and Data Points (Test 5)

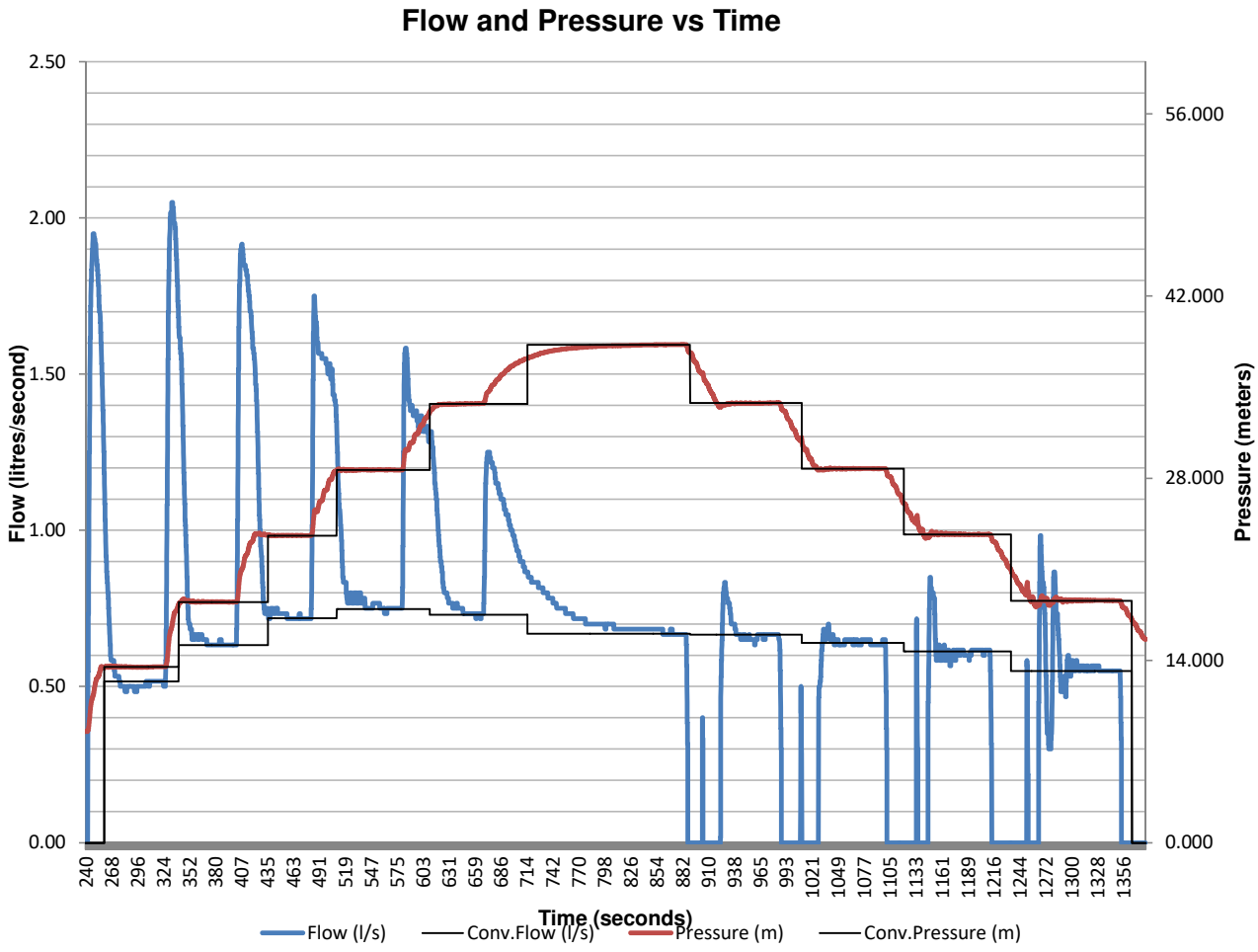

Pressure Head Correction (Test 5)

Corrected pressure at every Node:

Reynold's Number

$$\mathrm{Re} = \frac{\rho \mathrm{VD}}{\mu} = \frac{\mathrm{VD}}{\nu} = \frac{\mathrm{QD}}{\nu A}$$

Colebrook-White

$$\frac{1}{\sqrt{f}} = -2\log_{10}\left(\frac{\varepsilon}{3.7D} + \frac{2.51}{R_e\sqrt{f}}\right)$$

Minor Loss Equation

$$h_L = K_L\frac{V^2}{2g}$$

Darcy-Weissbach

$$h_f = f\frac{L}{D}\frac{V^2}{2g}$$

			Corrected Head (m)				
Point	**Flow (l/s)**	**Measured Head (m)**	**Node 0**	**Node 1**	**Node 2**	**Node 3**	**Node 4**
1	0.52	13.51	15.25	16.020	59.120	29.536	16.758
2	0.63	18.50	20.18	20.937	64.036	34.453	21.674
3	0.72	23.60	25.23	25.979	69.079	39.495	26.716
4	0.75	28.64	30.25	30.997	74.097	44.513	31.734
5	0.73	33.74	35.36	36.109	79.208	49.624	36.845
6	0.67	38.27	39.93	40.681	83.780	54.197	41.418
7	0.67	33.79	35.45	36.208	79.308	49.724	36.945
	0.64	28.74	30.42	31.176	74.275	44.691	31.913
9	0.61	23.69	25.38	26.142	69.241	39.658	26.879
10	0.55	18.60	20.32	21.086	64.185	34.602	21.823
11	0.00	0.00	0.00	0.000	0.000	0.000	0.000
12	0.00	0.00	0.00	0.000	0.000	0.000	0.000
13	0.00	0.00	0.00	0.000	0.000	0.000	0.000
14	0.00	0.00	0.00	0.000	0.000	0.000	0.000
15	0.00	0.00	0.00	0.000	0.000	0.000	0.000

N1 And FAVAD Parameters (Test 5)

N1 Equation:

$$Q = C_d A\sqrt{2gh}$$
$$Q = C_d\sqrt{2g}Ah^{0.5}$$
$$Q = C_{N1}Ah^{N1}$$

FAVAD Equation:

$$Q = C_d A\sqrt{2gh} \quad but \quad A = A_0 + mH$$
$$\therefore C_d A = Q/\sqrt{2gh} \qquad Q = C_d\sqrt{2gh}(A_0 + mh)$$
$$Q = C_d\sqrt{2g}\,(A_0 h^{0.5} + mh^{1.5})$$

Node 0: N1 Relationship

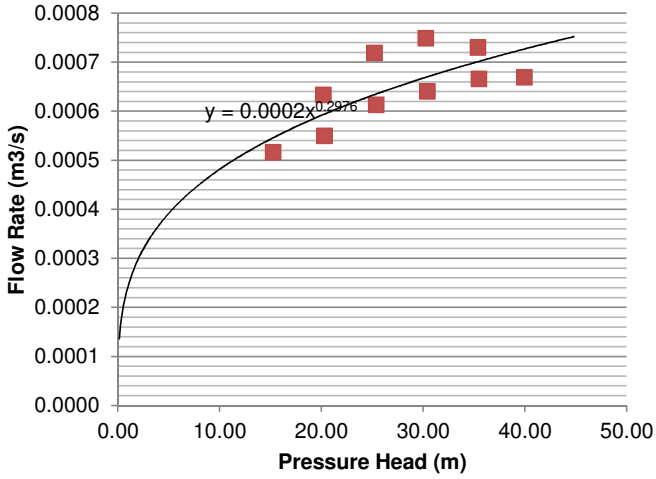

N1 Parameters:

Leakage Coefficient (CN1):	0.00024
Leakage Exponent (N1):	0.29763

Node 0: FAVAD Relationship

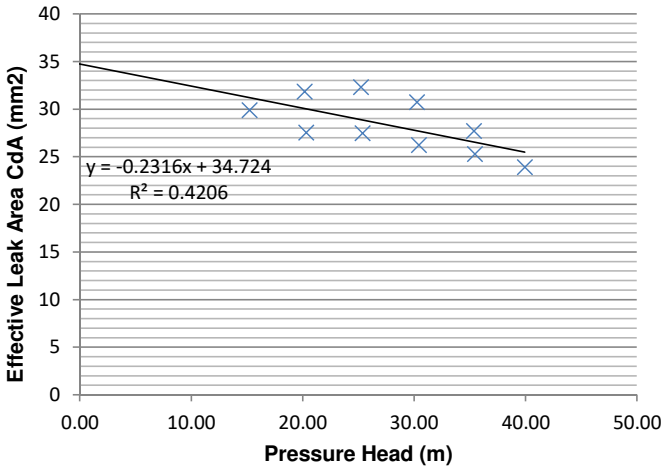

FAVAD Parameters:

Effective Initial Leak Area CdA0:	34.724	mm
Effective head-area slope Cdm:	-0.232	mm2/m

Node 1: N1 Relationship

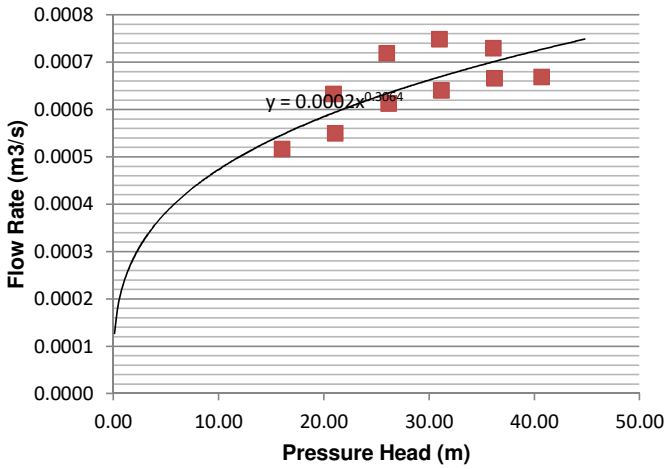

N1 Parameters:

Leakage Coefficient (C):	0.00023
Leakage Exponent (N1):	0.30639

Node 1: FAVAD Relationship

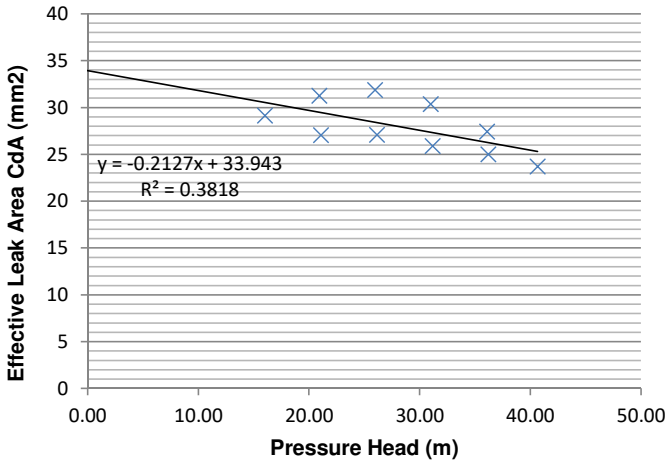

FAVAD Parameters:

Effective Initial Leak Area CdA0:	33.943	mm
Effective head-area slope Cdm:	-0.213	mm2/m

N1 And FAVAD Parameters (Test 5)

Node 2: N1 Relationship

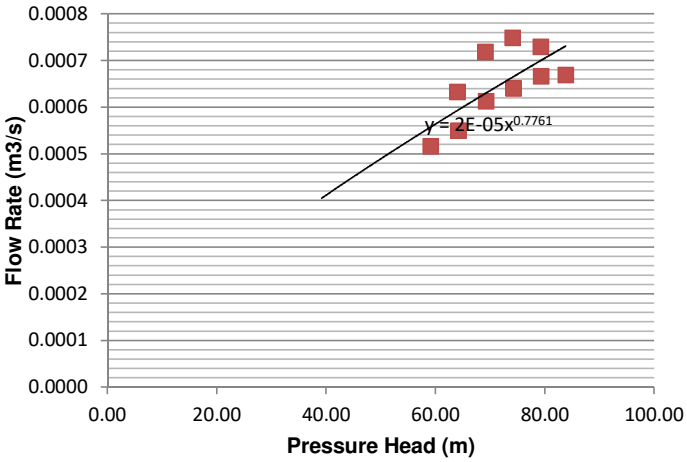

N1 Parameters:

Leakage Coefficient (C):	0.00002
Leakage Exponent (N1):	0.77615

Node 2: FAVAD Relationship

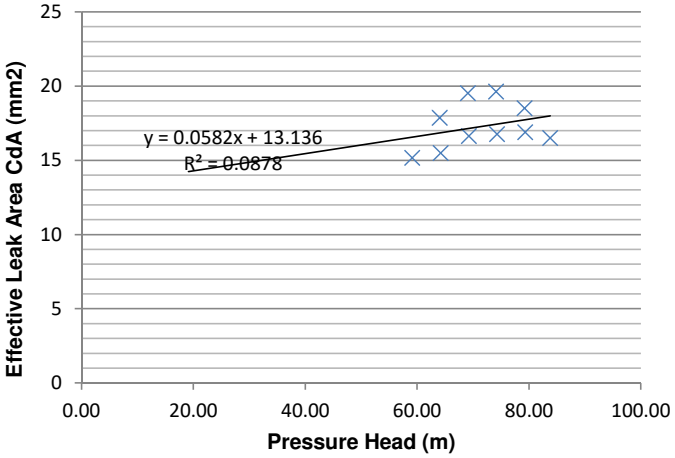

FAVAD Parameters:

Effective Initial Leak Area CdA0:	13.136 mm
Effective head-area slope Cdm:	0.058 mm2/m

Node 3: N1 Relationship

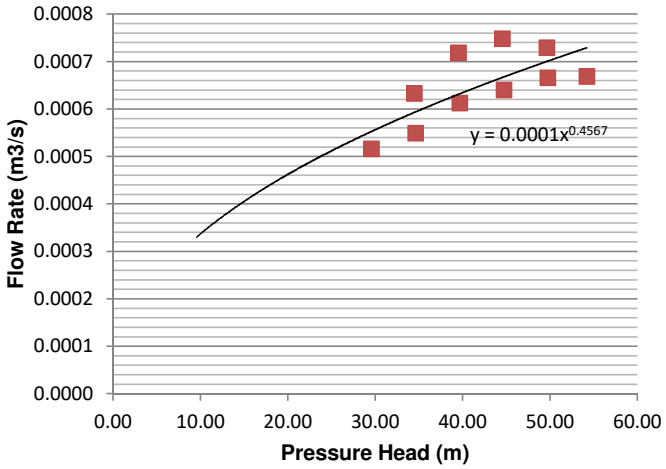

N1 Parameters:

Leakage Coefficient (C):	0.00012
Leakage Exponent (N1):	0.45672

Node 3: FAVAD Relationship

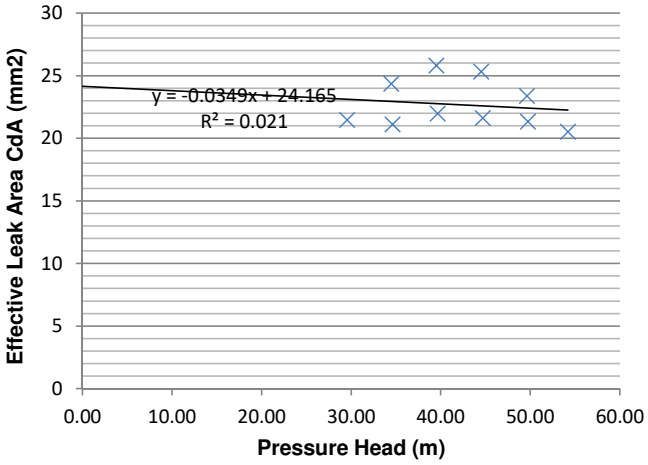

FAVAD Parameters:

Effective Initial Leak Area CdA0:	24.165 mm
Effective head-area slope Cdm:	-0.035 mm2/m

Node 4: N1 Relationship

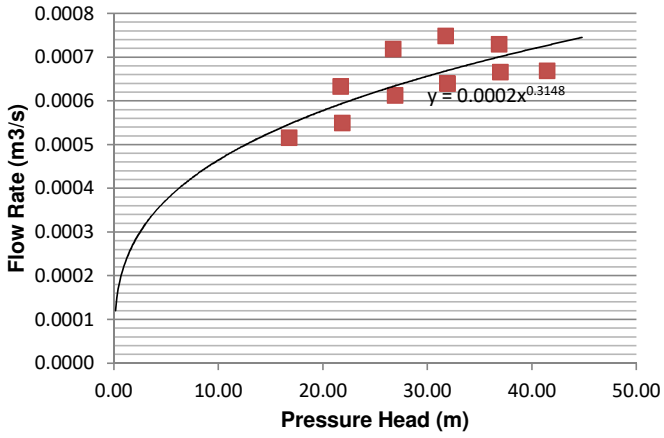

N1 Parameters:

Leakage Coefficient (C):	0.00023
Leakage Exponent (N1):	0.31479

Node 4: FAVAD Relationship

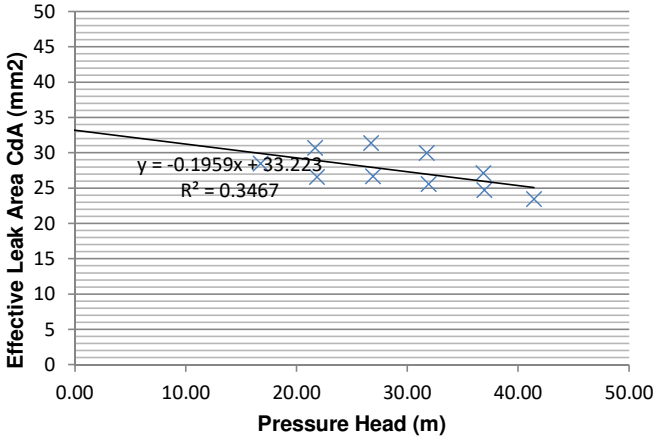

FAVAD Parameters:

Effective Initial Leak Area CdA0:	33.223 mm
Effective head-area slope Cdm:	-0.196 mm2/m

Summary (Test 5)

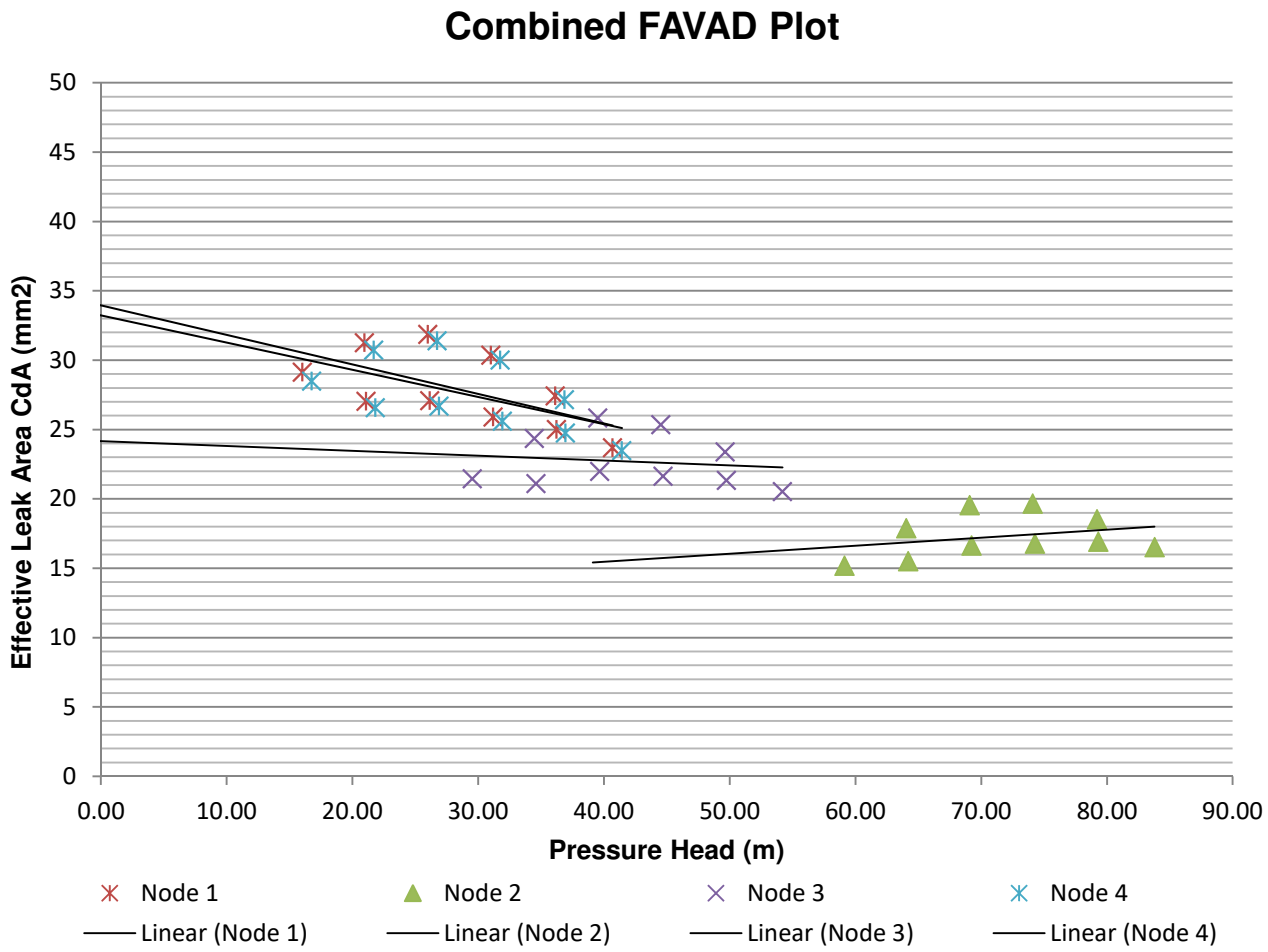

Discussion:

A change in behaviour occured during the test. It is proposed that the data points are split into two sets, with the one set representing the characteristics before a change in behaviour, and the second set representing the characteristics after the change.

N1 And FAVAD Combined

Node 1

Test 1 2018-06-07

Point	Flow (m3/s)	Corrected Head (m)	Effective Leak Area CdA (mm2)	Log(Q)	Log(H)
1	0.00172	32.865124	67.60344627	-2.7653	1.517
2	0.0015	29.488176	62.48578259	-2.823	1.47
3	0.0013	24.85504	58.86899454	-2.8861	1.395
4	0.00107	20.165854	53.62544541	-2.972	1.305
5	0.00082	15.530365	47.21461561	-3.084	1.191
6	0.00107	20.182363	53.60350798	-2.972	1.305
7	0.0013	24.940442	58.76811763	-2.8861	1.397
8	0.0015	29.528704	62.3188696	-2.8239	1.47
9	0.00173	32.019701	69.15505844	-2.7611	1.505
10	#N/A	#N/A	FALSE	FALSE	#####
11	#N/A	#N/A	FALSE	FALSE	#####
12	#N/A	#N/A	FALSE	FALSE	#####
13	#N/A	#N/A	FALSE	FALSE	#####
14	#N/A	#N/A	FALSE	FALSE	#####
15	#N/A	#N/A	FALSE	FALSE	#####

Test 2 2018-06-07

Flow (m3/s)	Corrected Head (m)	Effective Leak Area CdA (mm2)	Log(Q)	Log(H)
0.000826	40.36	29.346695	-3.0831	1.60596
0.000754	36.01	28.373662	-3.1225	1.55648
0.000663	31.10	26.839255	-3.1785	1.4927
0.000550	26.19	24.244751	-3.26	1.41809
0.000434	21.18	21.301408	-3.3623	1.32598
#N/A	#N/A	FALSE	FALSE	FALSE
#N/A	#N/A	FALSE	FALSE	FALSE
#N/A	#N/A	FALSE	FALSE	FALSE
#N/A	#N/A	FALSE	FALSE	FALSE
#N/A	#N/A	FALSE	FALSE	FALSE
#N/A	#N/A	FALSE	FALSE	FALSE
#N/A	#N/A	FALSE	FALSE	FALSE
#N/A	#N/A	FALSE	FALSE	FALSE
#N/A	#N/A	FALSE	FALSE	FALSE
#N/A	#N/A	FALSE	FALSE	FALSE

Test 3 2018-06-07

Point	Flow (m3/s)	Corrected Head (m)	Effective Leak Area CdA (mm2)	Log(Q)	Log(H)
1	0.000650	41.47	22.78742909	-3.1871	1.618
2	0.000546	31.28	22.02849076	-3.2631	1.495
3	0.000493	26.27	21.73743474	-3.3067	1.419
4	0.000448	21.24	21.93941649	-3.3488	1.327
5	0.000357	16.21	20.01882191	-3.4473	1.21
6	0.000434	21.22	21.28586886	-3.3621	1.327
7	0.000496	26.29	21.82283767	-3.3049	1.42
8	0.000550	31.29	22.19852845	-3.2596	1.495
9	0.000578	36.34	21.64314597	-3.2381	1.56
10	0.000617	41.05	21.72920327	-3.2099	1.613
11	#N/A	#N/A	FALSE	FALSE	#####
12	#N/A	#N/A	FALSE	FALSE	#####
13	#N/A	#N/A	FALSE	FALSE	#####
14	#N/A	#N/A	FALSE	FALSE	#####
15	#N/A	#N/A	FALSE	FALSE	#####

Test 4 2018-06-28

Flow (m3/s)	Corrected Head (m)	Effective Leak Area CdA (mm2)	Log(Q)	Log(H)
0.000650	41.20	22.861751	-3.1871	1.61491
0.000619	36.23	23.204841	-3.2085	1.55911
0.000584	31.20	23.586496	-3.2339	1.49412
0.000553	26.18	24.381364	-3.2576	1.41798
0.000478	21.13	23.484378	-3.3205	1.3248
0.000389	16.12	21.865653	-3.4103	1.20726
#N/A	#N/A	FALSE	FALSE	FALSE
#N/A	#N/A	FALSE	FALSE	FALSE
#N/A	#N/A	FALSE	FALSE	FALSE
#N/A	#N/A	FALSE	FALSE	FALSE
#N/A	#N/A	FALSE	FALSE	FALSE
#N/A	#N/A	FALSE	FALSE	FALSE
#N/A	#N/A	FALSE	FALSE	FALSE
#N/A	#N/A	FALSE	FALSE	FALSE
#N/A	#N/A	FALSE	FALSE	FALSE

Test 5 2018-06-28

Point	Flow (m3/s)	Corrected Head (m)	Effective Leak Area CdA (mm2)	Log(Q)	Log(H)
1	0.00052	16.020279	29.14243939	-3.2868	1.205
2	0.00063	20.936641	31.25434395	-3.1983	1.321
3	0.00072	25.979045	31.84757013	-3.1433	1.415
4	0.000749	31.00	30.36881932	-3.1256	1.491
5	0.000730	36.11	27.42739956	-3.1367	1.558
6	0.00067	40.680859	23.68944807	-3.1744	1.609
7	0.00067	36.208276	25.00796222	-3.1762	1.559
8	0.00064	31.175565	25.89681314	-3.1935	1.494
9	0.00061	26.141787	27.072595	-3.2125	1.417
10	0.00055	21.085801	27.04071276	-3.2596	1.324
11	#N/A	#N/A	FALSE	FALSE	#####
12	#N/A	#N/A	FALSE	FALSE	#####
13	#N/A	#N/A	FALSE	FALSE	#####
14	#N/A	#N/A	FALSE	FALSE	#####
15	#N/A	#N/A	FALSE	FALSE	#####

Node 2

Test 1 2018-06-07

Point	Flow (m3/s)	Corrected Head (m)	Effective Leak Area CdA (mm2)	Log(Q)	Log(H)
1	0.00172	75.963375	44.46664324	-2.7653	1.881
2	0.0015	72.58677	39.82689324	-2.823	1.861
3	0.0013	67.953919	35.6030003	-2.8861	1.832
4	0.00107	63.265009	30.27592599	-2.972	1.801
5	0.00082	58.62975	24.30011177	-3.084	1.768
6	0.00107	63.281518	30.27197645	-2.972	1.801
7	0.0013	68.03932	35.58064914	-2.8861	1.833
8	0.0015	72.627303	39.73670023	-2.8239	1.861
9	0.00173	75.117924	45.15031663	-2.7611	1.876
10	#N/A	#N/A	FALSE	FALSE	#####
11	#N/A	#N/A	FALSE	FALSE	#####
12	#N/A	#N/A	FALSE	FALSE	#####
13	#N/A	#N/A	FALSE	FALSE	#####
14	#N/A	#N/A	FALSE	FALSE	#####
15	#N/A	#N/A	FALSE	FALSE	#####

Test 2 2018-06-07

Flow (m3/s)	Corrected Head (m)	Effective Leak Area CdA (mm2)	Log(Q)	Log(H)
0.000826	83.46	20.407927	-3.0831	1.92148
0.000754	79.11	19.143831	-3.1225	1.89826
0.000663	74.20	17.375353	-3.1785	1.87038
0.000550	69.29	14.905221	-3.26	1.84065
0.000434	64.28	12.227899	-3.3623	1.80809
#N/A	#N/A	FALSE	FALSE	FALSE
#N/A	#N/A	FALSE	FALSE	FALSE
#N/A	#N/A	FALSE	FALSE	FALSE
#N/A	#N/A	FALSE	FALSE	FALSE
#N/A	#N/A	FALSE	FALSE	FALSE
#N/A	#N/A	FALSE	FALSE	FALSE
#N/A	#N/A	FALSE	FALSE	FALSE
#N/A	#N/A	FALSE	FALSE	FALSE
#N/A	#N/A	FALSE	FALSE	FALSE

Test 3 2018-06-07

Point	Flow (m3/s)	Corrected Head (m)	Effective Leak Area CdA (mm2)	Log(Q)	Log(H)
1	0.000650	84.57	15.95718197	-3.1871	1.927
2	0.000546	74.38	14.28492335	-3.2631	1.871
3	0.000493	69.37	13.37662834	-3.3067	1.841
4	0.000448	64.34	12.60593601	-3.3488	1.808
5	0.000357	59.31	10.46642973	-3.4473	1.773
6	0.000434	64.32	12.22690987	-3.3621	1.808
7	0.000496	69.39	13.43228498	-3.3049	1.841
8	0.000550	74.39	14.39669967	-3.2596	1.872
9	0.000578	79.44	14.63829895	-3.2381	1.9
10	0.000617	84.15	15.17661171	-3.2099	1.925
11	#N/A	#N/A	FALSE	FALSE	#####
12	#N/A	#N/A	FALSE	FALSE	#####
13	#N/A	#N/A	FALSE	FALSE	#####
14	#N/A	#N/A	FALSE	FALSE	#####
15	#N/A	#N/A	FALSE	FALSE	#####

Test 4 2018-06-28

Flow (m3/s)	Corrected Head (m)	Effective Leak Area CdA (mm2)	Log(Q)	Log(H)
0.000650	84.30	15.982639	-3.1871	1.92583
0.000619	79.33	15.68216	-3.2085	1.89945
0.000584	74.30	15.283988	-3.2339	1.87097
0.000553	69.28	14.987992	-3.2576	1.84061
0.000478	64.22	13.468753	-3.3205	1.8077
0.000389	59.22	11.407084	-3.4103	1.77244
#N/A	#N/A	FALSE	FALSE	FALSE
#N/A	#N/A	FALSE	FALSE	FALSE
#N/A	#N/A	FALSE	FALSE	FALSE
#N/A	#N/A	FALSE	FALSE	FALSE
#N/A	#N/A	FALSE	FALSE	FALSE
#N/A	#N/A	FALSE	FALSE	FALSE
#N/A	#N/A	FALSE	FALSE	FALSE
#N/A	#N/A	FALSE	FALSE	FALSE
#N/A	#N/A	FALSE	FALSE	FALSE

Test 5 2018-06-28

Point	Flow (m3/s)	Corrected Head (m)	Effective Leak Area CdA (mm2)	Log(Q)	Log(H)
1	0.00052	59.119872	15.17030101	-3.2868	1.772
2	0.00063	64.036166	17.87109776	-3.1983	1.806
3	0.00072	69.078512	19.53063704	-3.1433	1.839
4	0.00075	74.096838	19.64222388	-3.1256	1.87
5	0.00073	79.208024	18.51847242	-3.1367	1.899
6	0.00067	83.780361	16.50740808	-3.1744	1.923
7	0.00067	79.30778	16.89757311	-3.1762	1.899
8	0.00064	74.275085	16.77768005	-3.1935	1.871
9	0.00061	69.241325	16.63469476	-3.2125	1.84
10	0.00055	64.185376	15.49869538	-3.2596	1.807
11	#N/A	#N/A	FALSE	FALSE	#####
12	#N/A	#N/A	FALSE	FALSE	#####
13	#N/A	#N/A	FALSE	FALSE	#####
14	#N/A	#N/A	FALSE	FALSE	#####
15	#N/A	#N/A	FALSE	FALSE	#####

Node 3

Test 1		2018-06-07				Test 2		2018-06-07		
Point	Flow (m3/s)	Corrected Head (m)	Effective Leak Area CdA (mm2)	Log(Q)	Log(H)	Flow (m3/s)	Corrected Head (m)	Effective Leak Area CdA (mm2)	Log(Q)	Log(H)
1	0.00172	46.378236	56.90879132	-2.7653	1.666	0.000826	53.88	25.400342	-3.0831	1.7314
2	0.0015	43.00204	51.74407614	-2.823	1.633	0.000754	49.53	24.194664	-3.1225	1.69487
3	0.0013	38.369527	47.38060769	-2.8861	1.584	0.000663	44.61	22.407706	-3.1785	1.64945
4	0.00107	33.680947	41.49416918	-2.972	1.527	0.000550	39.70	19.690201	-3.26	1.59883
5	0.00082	29.045963	34.52426196	-3.084	1.463	0.000434	34.70	16.643349	-3.3623	1.54031
6	0.00107	33.697457	41.48400339	-2.972	1.528	#N/A	#N/A	FALSE	FALSE	FALSE
7	0.0013	38.454929	47.32796634	-2.8861	1.585	#N/A	#N/A	FALSE	FALSE	FALSE
8	0.0015	43.042578	51.61698362	-2.8239	1.634	#N/A	#N/A	FALSE	FALSE	FALSE
9	0.00173	45.53275	57.99234213	-2.7611	1.658	#N/A	#N/A	FALSE	FALSE	FALSE
10	#N/A	#N/A	FALSE	FALSE	#####	#N/A	#N/A	FALSE	FALSE	FALSE
11	#N/A	#N/A	FALSE	FALSE	#####	#N/A	#N/A	FALSE	FALSE	FALSE
12	#N/A	#N/A	FALSE	FALSE	#####	#N/A	#N/A	FALSE	FALSE	FALSE
13	#N/A	#N/A	FALSE	FALSE	#####	#N/A	#N/A	FALSE	FALSE	FALSE
14	#N/A	#N/A	FALSE	FALSE	#####	#N/A	#N/A	FALSE	FALSE	FALSE
15	#N/A	#N/A	FALSE	FALSE	#####	#N/A	#N/A	FALSE	FALSE	FALSE

Test 3		2018-06-07				Test 4		2018-06-28		
Point	Flow (m3/s)	Corrected Head (m)	Effective Leak Area CdA (mm2)	Log(Q)	Log(H)	Flow (m3/s)	Corrected Head (m)	Effective Leak Area CdA (mm2)	Log(Q)	Log(H)
1	0.000650	54.99	19.78960486	-3.1871	1.74	0.000650	54.72	19.838225	-3.1871	1.73812
2	0.000546	44.79	18.40735768	-3.2631	1.651	0.000619	49.75	19.803379	-3.2085	1.69679
3	0.000493	39.78	17.66317992	-3.3067	1.6	0.000584	44.71	19.7017	-3.2339	1.65044
4	0.000448	34.76	17.15116492	-3.3488	1.541	0.000553	39.70	19.800272	-3.2576	1.59875
5	0.000357	29.73	14.7835869	-3.4473	1.473	0.000478	34.64	18.339269	-3.3205	1.53959
6	0.000434	34.74	16.63747683	-3.3621	1.541	0.000389	29.63	16.125396	-3.4103	1.47177
7	0.000496	39.80	17.73481552	-3.3049	1.6	#N/A	#N/A	FALSE	FALSE	FALSE
8	0.000550	44.80	18.5504587	-3.2596	1.651	#N/A	#N/A	FALSE	FALSE	FALSE
9	0.000578	49.85	18.47788722	-3.2381	1.698	#N/A	#N/A	FALSE	FALSE	FALSE
10	0.000617	54.57	18.8468926	-3.2099	1.737	#N/A	#N/A	FALSE	FALSE	FALSE
11	#N/A	#N/A	FALSE	FALSE	#####	#N/A	#N/A	FALSE	FALSE	FALSE
12	#N/A	#N/A	FALSE	FALSE	#####	#N/A	#N/A	FALSE	FALSE	FALSE
13	#N/A	#N/A	FALSE	FALSE	#####	#N/A	#N/A	FALSE	FALSE	FALSE
14	#N/A	#N/A	FALSE	FALSE	#####	#N/A	#N/A	FALSE	FALSE	FALSE
15	#N/A	#N/A	FALSE	FALSE	#####	#N/A	#N/A	FALSE	FALSE	FALSE

Test 5		2018-06-28			
Point	Flow (m3/s)	Corrected Head (m)	Effective Leak Area CdA (mm2)	Log(Q)	Log(H)
1	0.00052	29.536333	21.46261584	-3.2868	1.47
2	0.00063	34.452546	24.36426031	-3.1983	1.537
3	0.00072	39.494822	25.82960797	-3.1433	1.597
4	0.00075	44.513122	25.3423257	-3.1256	1.648
5	0.00073	49.624324	23.39604483	-3.1367	1.696
6	0.00067	54.196712	20.52407197	-3.1744	1.734
7	0.00067	49.724134	21.3402065	-3.1762	1.697
8	0.00064	44.69146	21.62923791	-3.1935	1.65
9	0.00061	39.65772	21.98030175	-3.2125	1.598
10	0.00055	34.601816	21.10880966	-3.2596	1.539
11	#N/A	#N/A	FALSE	FALSE	#####
12	#N/A	#N/A	FALSE	FALSE	#####
13	#N/A	#N/A	FALSE	FALSE	#####
14	#N/A	#N/A	FALSE	FALSE	#####
15	#N/A	#N/A	FALSE	FALSE	#####
	#N/A	#N/A	#N/A	#N/A	#N/A
	#N/A	#N/A	#N/A	#N/A	#N/A

Node 4

Test 1		2018-06-07				Test 2		2018-06-07		
Point	Flow (m3/s)	Corrected Head (m)	Effective Leak Area CdA (mm2)	Log(Q)	Log(H)	Flow (m3/s)	Corrected Head (m)	Effective Leak Area CdA (mm2)	Log(Q)	Log(H)
1	0.00172	33.596306	66.86374711	-2.7653	1.526	0.000826	41.10	29.082572	-3.0831	1.61381
2	0.0015	30.220947	61.72358358	-2.823	1.48	0.000754	36.75	28.087846	-3.1225	1.56528
3	0.0013	25.589127	58.01844891	-2.8861	1.408	0.000663	31.83	26.526746	-3.1785	1.50288
4	0.00107	20.901221	52.67364747	-2.972	1.32	0.000550	26.92	23.910485	-3.26	1.43015
5	0.00082	16.266798	46.13348441	-3.084	1.211	0.000434	21.92	20.93996	-3.3623	1.34084
6	0.00107	20.91773	52.65285709	-2.972	1.321	#N/A	#N/A	FALSE	FALSE	FALSE
7	0.0013	25.674529	57.92187445	-2.8861	1.41	#N/A	#N/A	FALSE	FALSE	FALSE
8	0.0015	30.261496	61.55970983	-2.8239	1.481	#N/A	#N/A	FALSE	FALSE	FALSE
9	0.00173	32.75075	68.37887702	-2.7611	1.515	#N/A	#N/A	FALSE	FALSE	FALSE
10	#N/A	#N/A	FALSE	FALSE	#####	#N/A	#N/A	FALSE	FALSE	FALSE
11	#N/A	#N/A	FALSE	FALSE	#####	#N/A	#N/A	FALSE	FALSE	FALSE
12	#N/A	#N/A	FALSE	FALSE	#####	#N/A	#N/A	FALSE	FALSE	FALSE
13	#N/A	#N/A	FALSE	FALSE	#####	#N/A	#N/A	FALSE	FALSE	FALSE
14	#N/A	#N/A	FALSE	FALSE	#####	#N/A	#N/A	FALSE	FALSE	FALSE
15	#N/A	#N/A	FALSE	FALSE	#####	#N/A	#N/A	FALSE	FALSE	FALSE

Test 3		2018-06-07				Test 4		2018-06-28		
Point	Flow (m3/s)	Corrected Head (m)	Effective Leak Area CdA (mm2)	Log(Q)	Log(H)	Flow (m3/s)	Corrected Head (m)	Effective Leak Area CdA (mm2)	Log(Q)	Log(H)
1	0.000650	42.21	22.58759378	-3.1871	1.625	0.000650	41.94	22.659971	-3.1871	1.62261
2	0.000546	32.01	21.77334077	-3.2631	1.505	0.000619	36.97	22.972344	-3.2085	1.56785
3	0.000493	27.01	21.43858982	-3.3067	1.431	0.000584	31.93	23.312654	-3.2339	1.50426
4	0.000448	21.98	21.56816849	-3.3488	1.342	0.000553	26.92	24.045132	-3.2576	1.43004
5	0.000357	16.95	19.57835426	-3.4473	1.229	0.000478	21.86	23.084883	-3.3205	1.3397
6	0.000434	21.96	20.92536542	-3.3621	1.342	0.000389	16.85	21.381785	-3.4103	1.2267
7	0.000496	27.03	21.52303902	-3.3049	1.432	#N/A	#N/A	FALSE	FALSE	FALSE
8	0.000550	32.03	21.94150428	-3.2596	1.505	#N/A	#N/A	FALSE	FALSE	FALSE
9	0.000578	37.08	21.42688391	-3.2381	1.569	#N/A	#N/A	FALSE	FALSE	FALSE
10	0.000617	41.79	21.53669803	-3.2099	1.621	#N/A	#N/A	FALSE	FALSE	FALSE
11	#N/A	#N/A	FALSE	FALSE	#####	#N/A	#N/A	FALSE	FALSE	FALSE
12	#N/A	#N/A	FALSE	FALSE	#####	#N/A	#N/A	FALSE	FALSE	FALSE
13	#N/A	#N/A	FALSE	FALSE	#####	#N/A	#N/A	FALSE	FALSE	FALSE
14	#N/A	#N/A	FALSE	FALSE	#####	#N/A	#N/A	FALSE	FALSE	FALSE
15	#N/A	#N/A	FALSE	FALSE	#####	#N/A	#N/A	FALSE	FALSE	FALSE

Test 5		2018-06-28			
Point	Flow (m3/s)	Corrected Head (m)	Effective Leak Area CdA (mm2)	Log(Q)	Log(H)
1	0.00052	16.757676	28.49404152	-3.2868	1.224
2	0.00063	21.673723	30.71829711	-3.1983	1.336
3	0.00072	26.715856	31.40532896	-3.1433	1.427
4	0.00075	31.734102	30.01424264	-3.1256	1.502
5	0.00073	36.845339	27.15179033	-3.1367	1.566
6	0.00067	41.417831	23.47774181	-3.1744	1.617
7	0.00067	36.945257	24.75727743	-3.1762	1.568
8	0.00064	31.912625	25.59600709	-3.1935	1.504
9	0.00061	26.878927	26.69878832	-3.2125	1.429
10	0.00055	21.823114	26.57999084	-3.2596	1.339
11	#N/A	#N/A	FALSE	FALSE	#####
12	#N/A	#N/A	FALSE	FALSE	#####
13	#N/A	#N/A	FALSE	FALSE	#####
14	#N/A	#N/A	FALSE	FALSE	#####
15	#N/A	#N/A	FALSE	FALSE	#####
	#N/A	#N/A	#N/A	#N/A	#N/A
	#N/A	#N/A	#N/A	#N/A	#N/A

N1 And FAVAD Combined

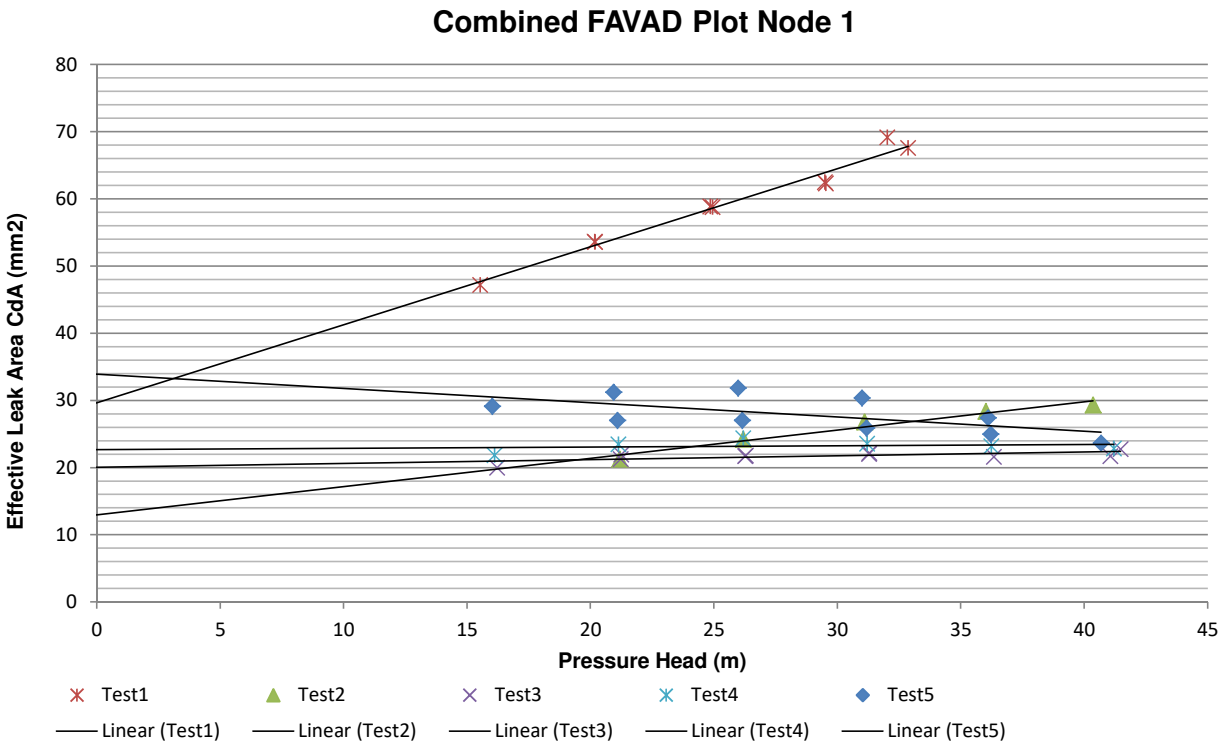

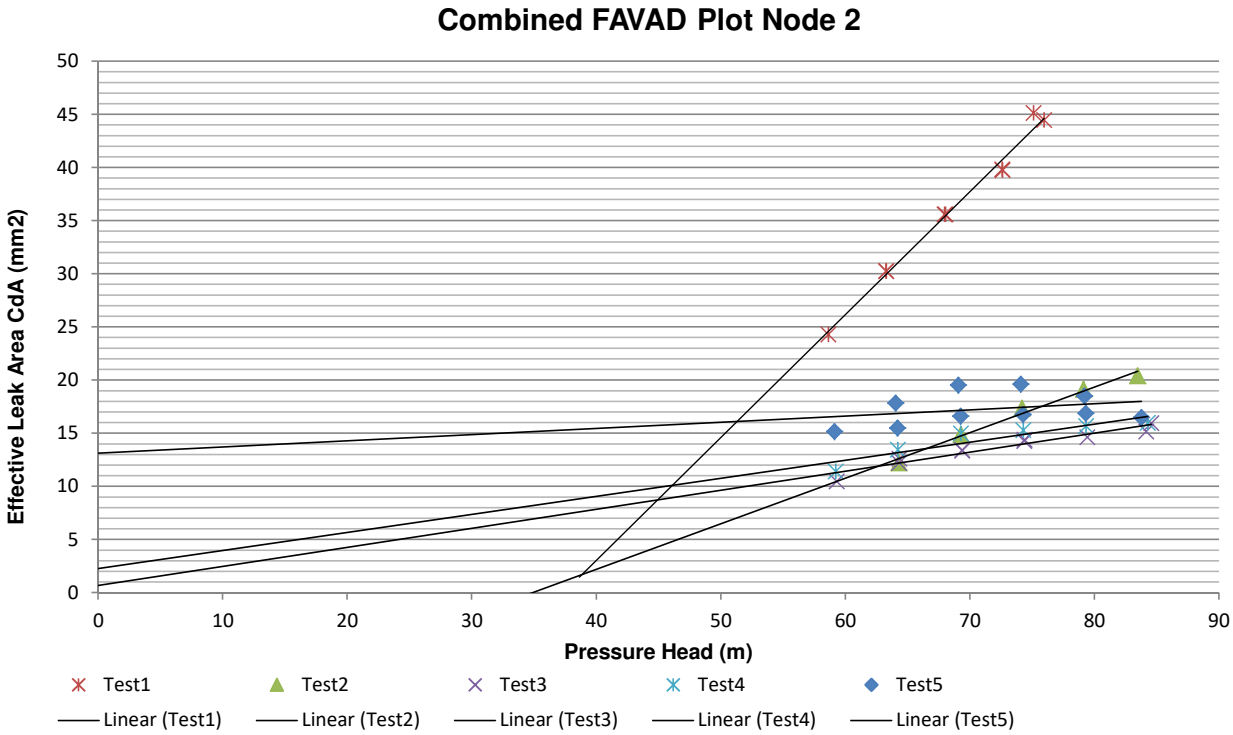

N1 And FAVAD Combined (Continued)

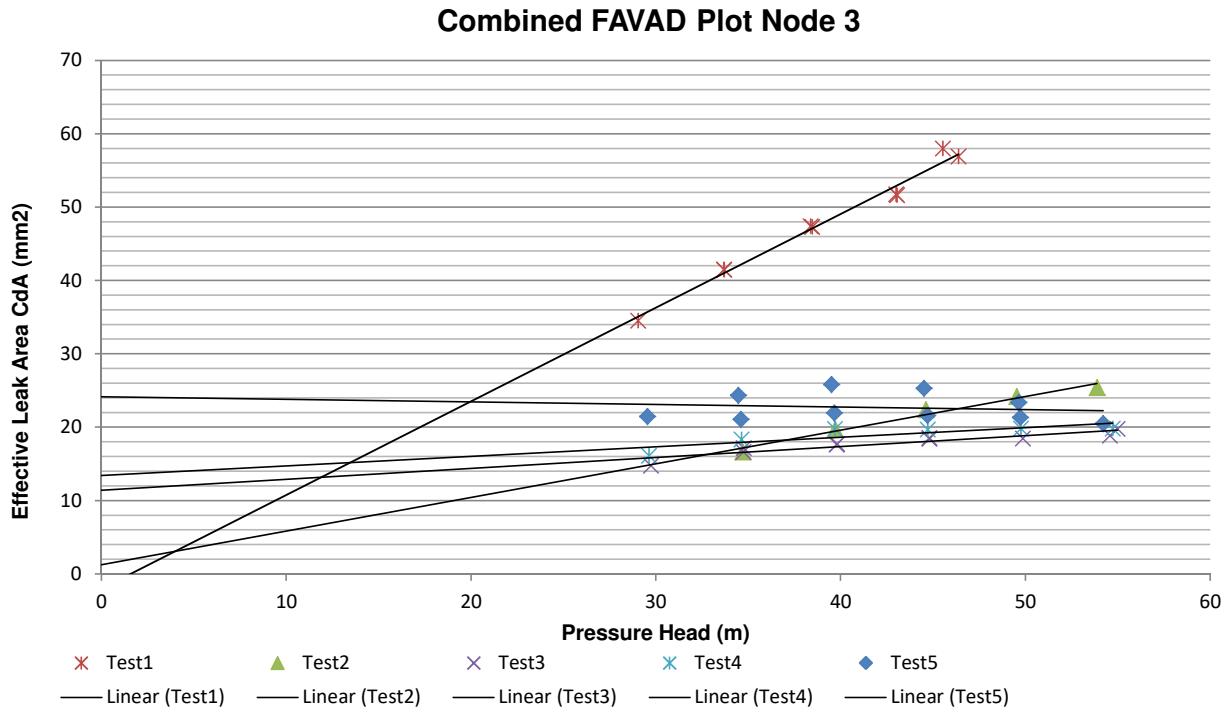

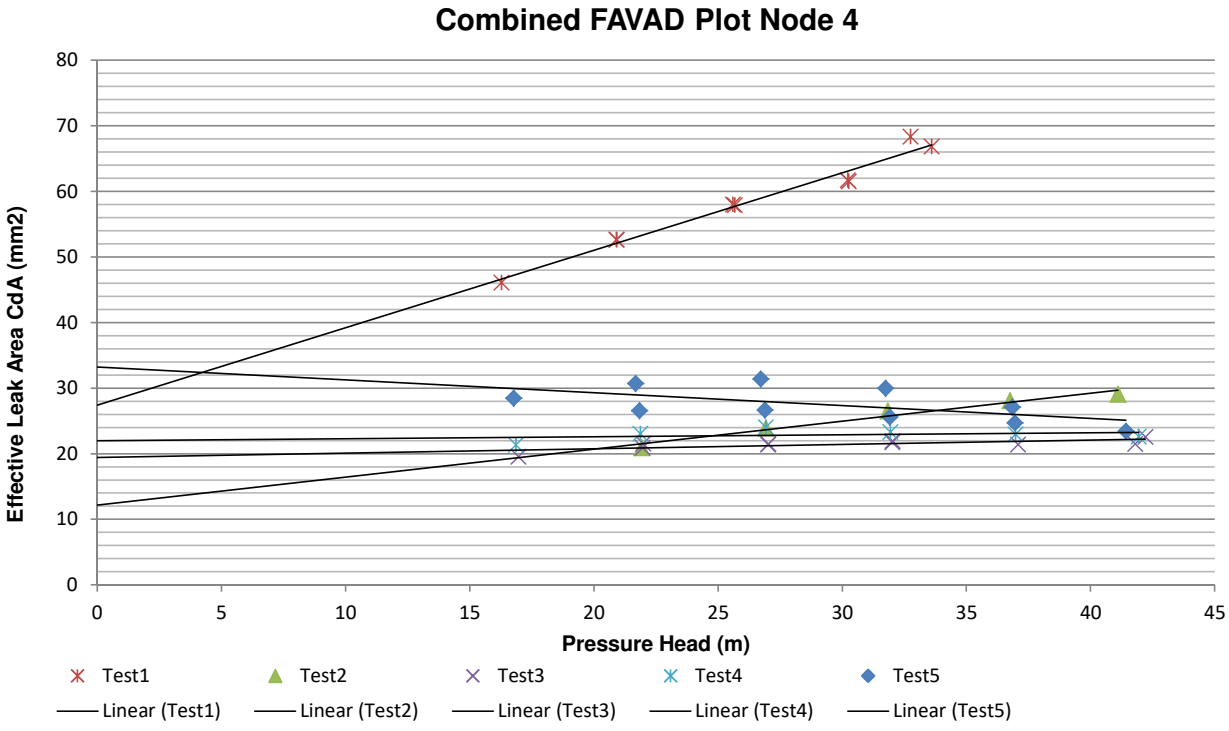

Test Report and Analysis

Pipe:

Supply Line to Queenswood Reservoir

Testing Date:

08 June 2018

Contents:

General Test Description

Description:

The map in figure 1 shows the pipeline route. The Queenswood Reservoir is fed by this pipeline, which is pressurised by gravity all the way from the Garsfontein Reservoirs. A butterfly isolation valve, as shown in Figure 1, is situated at a low point on the pipeline, and allows for the rising section of the pipeline (from this valve up to the reservoir) to be tested.

Just upstream of the reservoir, the line splits into three smaller lines which all enter a valve chamber. In the valve chamber, each line is fitted with two PRV's. A non-return valve ensures that the reservoir cannot drain into the supply pipe should the line pressure drop.

An 80mm off-take, with an isolation valve and a flanged end, upstream of the PRVs in the valve chamber is ideally suited as a connection point for the testing equipment.

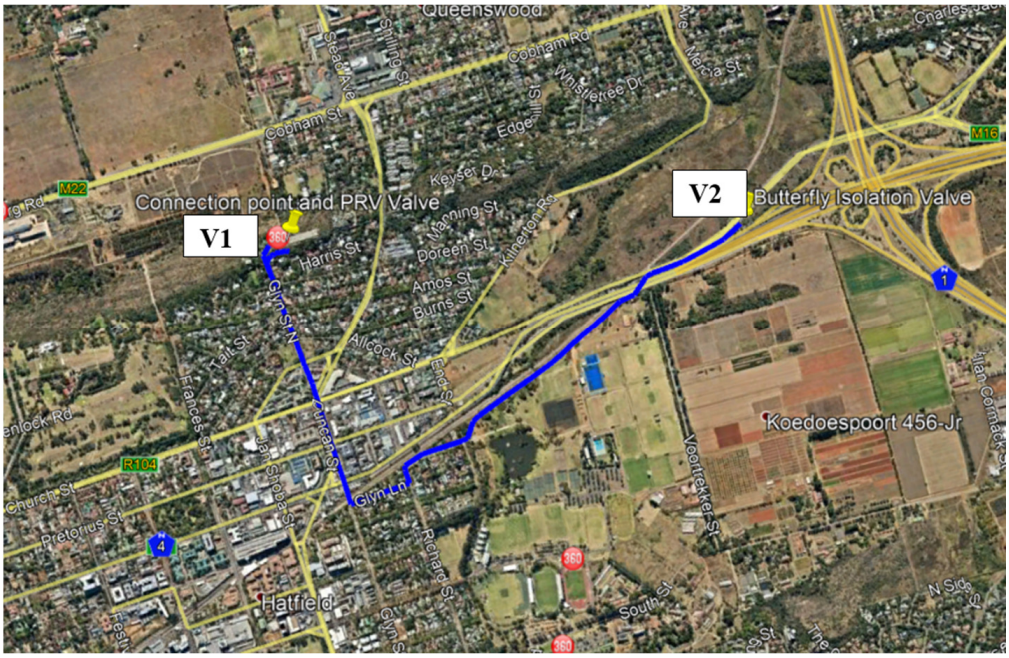

Figure 1: Map showing pipeline route starting at V1 and ending at V2

Figure 2: Test setup at reservoir

Figure 3&4: Connection Point at Queenswood Reservoir

Figure 5: Layout and isolation valves at Queenswood Reservoir.

General Test Information

Pipeline:	Supply Line to Queenswood Reservoir
Area:	Pretoria, Queeswood/Colbyn
Pipe Owner:	Tshwane Municipality
Date:	08 Jun 18
Time:	09:00 - 11:30

Pipeline Section:	**Section 1**	**Section 2**	**Section 3**	
Pipe length (m):	1133	1720		
Pipe Diameter (mm):	500	600		
Pipe Material:	Steel	Steel		
Absolute Roughness e (mm)	0.5	0.5		
Minor Losses/km	1	1		
Upstream Isolation:	Butterfly Valve			
Upstream Source:	Pressured Pipe			
Upstream Pressure (Bar) approx:	>14			
Upstream Isolation Elevation (m):	1390			
Downstream Isolation:	PRV			
Downstream Delivery:	Reservoir			
Downstream Pressure (Bar) approx:	<1			
Downstream Isolation Elevation (m):	1345			

Connection of Testing Equipment

Connection Type:	80mm Flanged Coupling	
Connection Fitting size (mm):	80	
Comment on Fitting:	80mm Flange, 3 inch x 2 inch,reducer, 2 inch x1 inch reducer, 1 inch male to female, 1 inch ball valve and 1 inch male Geka coupling	
Minor loss coefficient of fitting	80 mm Flanged or Threaded	23.43
Static height difference (A) in (m):	1.05	

Connection pipes*:

	Pipe 1	**Pipe 2**
Length of connection pipe* (mm):	3900	850
Diameter of connection pipes (mm)	80	200
Absolute Roughness e (mm)	0.2	0.2
Static height difference (B) in (mm):	-850	800

Minor losses of fittings on connection pipes*:

	Fitting 1	**Fitting 2**	**Fitting 3**	**Fitting 4**
Fitting type:		Gate valve		Exit loss
Pipe 1 or Pipe 2	1	1	1	2
Fitting diameter in (mm):	80	80	80	200
Fitting diameter out (mm):	80	80	200	400
Absolute Roughness e (mm)	0.5	0.5	0.5	0.5
No. of fittings:	3	1	1	1
Fitting Minor Loss Coefficient:	1.1710	0.2602	1.0000	0.0256
			SUM:	2.45682

** Pipes and Fittings between the connection point and the main pipeline*

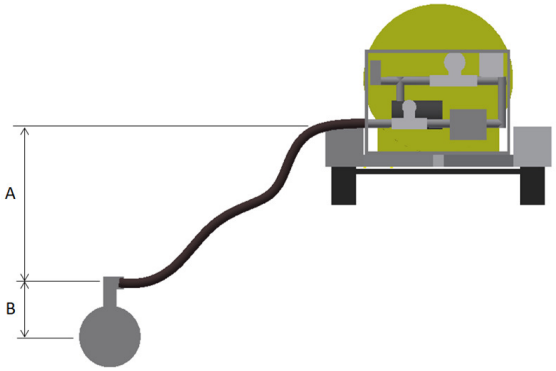

Pipeline Elevation Profile

Geocontext Website

Elevation Profile

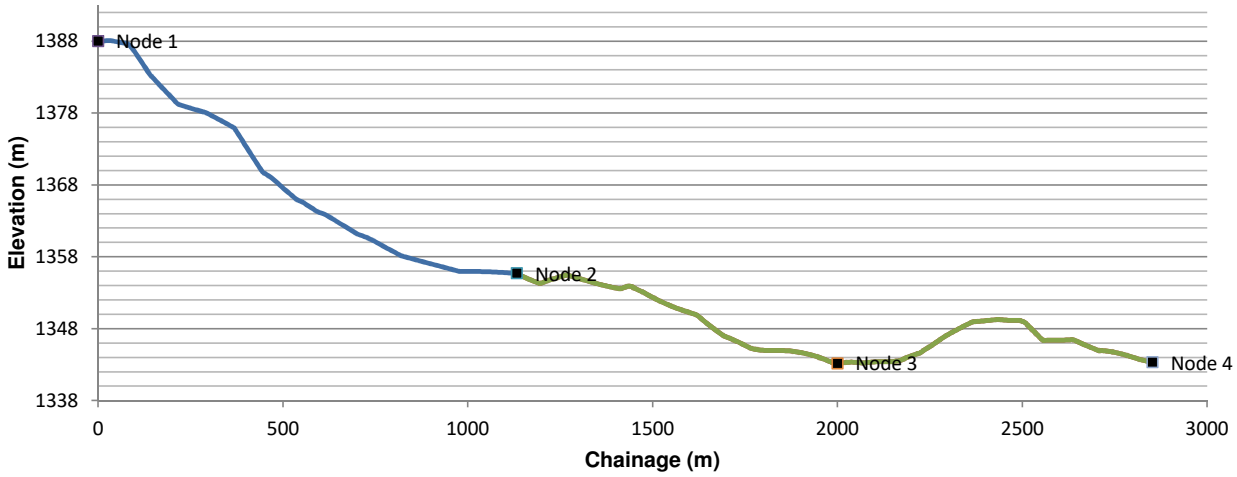

	Distance (m)	Elevation (m)	Material
1	0	1387.986084	Steel
1	5.582233384	1388.07251	Steel
1	11.16446677	1388.06897	Steel
1	16.74670015	1388.06897	Steel
1	22.32893354	1388.072632	Steel
1	27.91116692	1388.079956	Steel
1	33.4934003	1388.090698	Steel
1	39.07563369	1388.0625	Steel
1	44.65786707	1387.993286	Steel
1	50.24010045	1387.931519	Steel
1	55.82233384	1387.876953	Steel
1	61.40456722	1387.829712	Steel
1	66.98680061	1387.789795	Steel
1	72.56903399	1387.743774	Steel
1	78.15126737	1387.698242	Steel
1	83.73350076	1387.503296	Steel
1	89.31573414	1387.170288	Steel
1	94.89796752	1386.834229	Steel
1	100.4802009	1386.40918	Steel
1	106.0624343	1385.983643	Steel
1	111.6446677	1385.557617	Steel
1	117.2269011	1385.130981	Steel
1	122.8091344	1384.696167	Steel
1	128.3913678	1384.259155	Steel
1	133.9736012	1383.820679	Steel
1	139.5558346	1383.392212	Steel
1	145.138068	1383.081787	Steel
1	150.7203014	1382.771362	Steel
1	156.3025347	1382.460938	Steel
1	161.8847681	1382.154785	Steel
1	167.4670015	1381.852905	Steel
1	173.0492349	1381.551147	Steel
1	178.6314683	1381.249268	Steel
1	184.2137017	1380.947388	Steel
1	189.795935	1380.64563	Steel
1	195.3781684	1380.34375	Steel
1	200.9604018	1380.04187	Steel
1	206.5426352	1379.740112	Steel
1	212.1248686	1379.438232	Steel
1	217.707102	1379.217896	Steel

No. of Sections:	2	
Section	**Start (m)**	**Material**
1	0	Steel
2	1133	Steel
3		0

**If multiple sections exist, the Node points below must intercept at point where section changes for accurate pressure loss calculations.*

	Chainage (m)	Elevation (m)	End/part of Section
Node 1	0	1387.986	N/A
Node 2	1133	1355.721	1
Node 3	2000	1343.174	2
Node 4	2852.52	1343.346	2

Total Chainage = 2852.52 m

Distance/Elevation Data Continues

Plot and Data Points (Test 1)

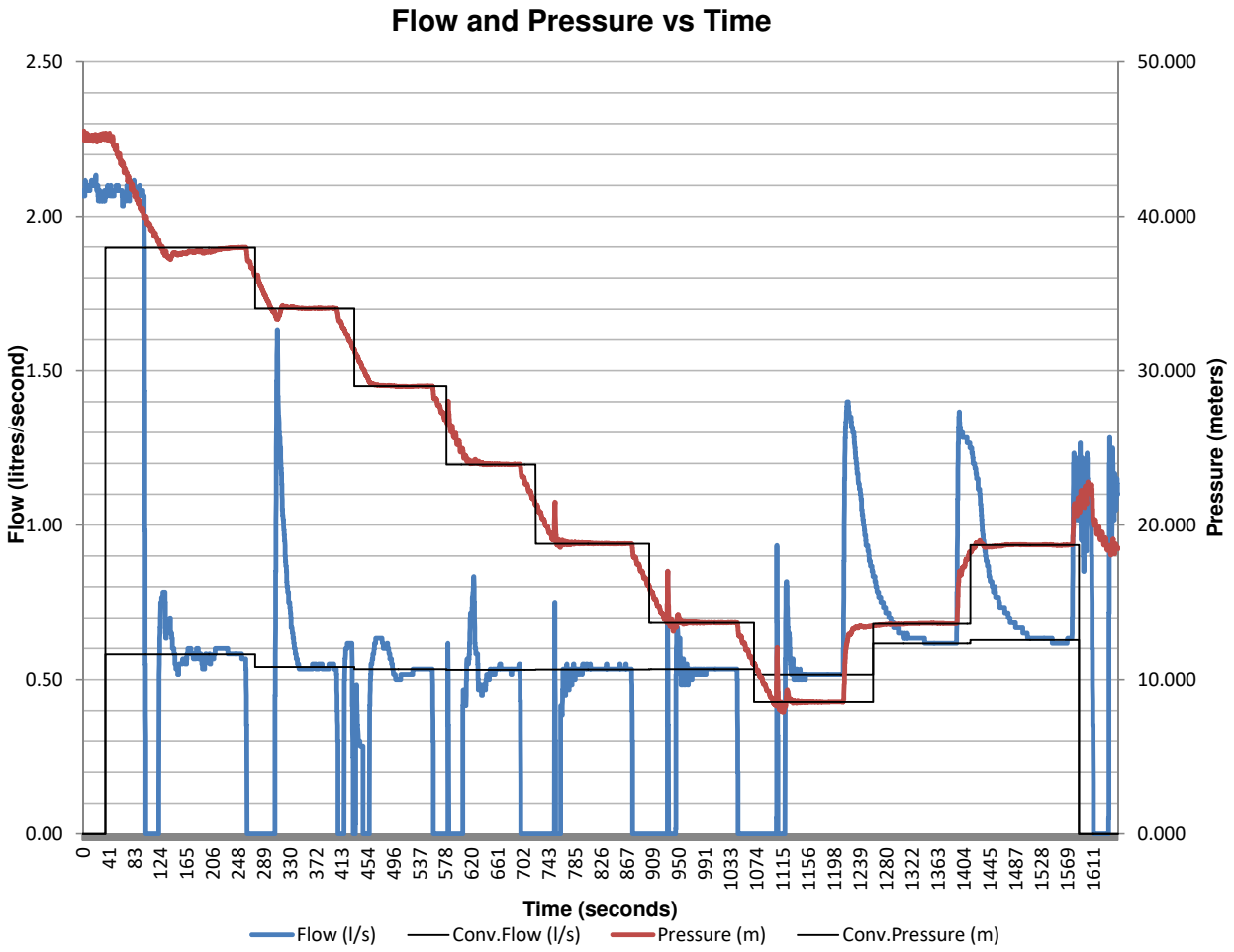

Tool for zooming into graph to calculate and plot the average values:

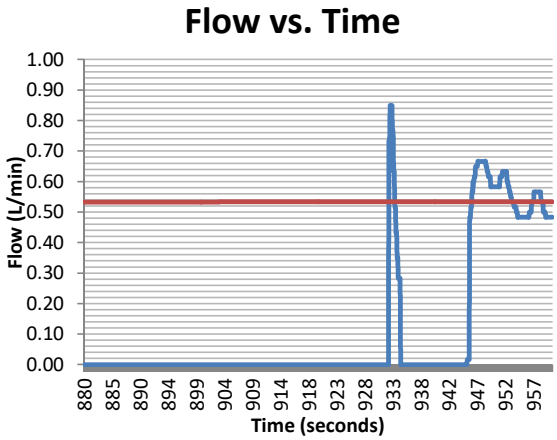

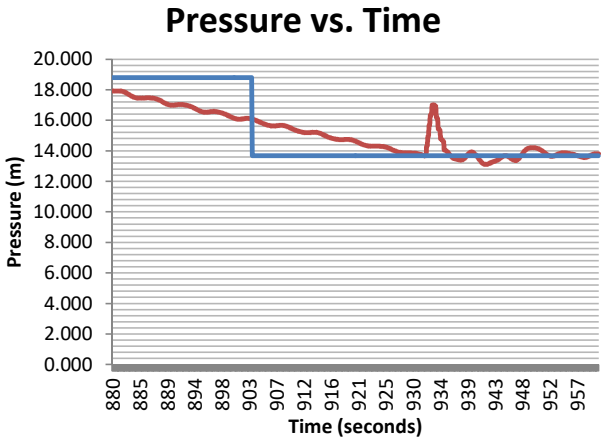

Select time Range for Display:		Select time Range for Average Calculation:	
Start Time:	## s	Start Time:	925 s
End Time:	## s	End Time:	937 s

Average Flow:	1.0842 l/s
Average Pressure:	33.385 m

Pressure Head Correction (Test 1)

Corrected pressure at every Node:

Reynold's Number

$$\mathrm{Re} = \frac{\rho \mathrm{VD}}{\mu} = \frac{\mathrm{VD}}{\nu} = \frac{\mathrm{QD}}{\nu A}$$

Colebrook-White

$$\frac{1}{\sqrt{f}} = -2\log_{10}\left(\frac{\varepsilon}{3.7D} + \frac{2.51}{R_e\sqrt{f}}\right)$$

Minor Loss Equation

$$h_L = K_L\frac{V^2}{2g}$$

Darcy-Weissbach

$$h_f = f\frac{L}{D}\frac{V^2}{2g}$$

			Corrected Head (m)				
Point	**Flow (l/s)**	**Measured Head (m)**	**Node 0**	**Node 1**	**Node 2**	**Node 3**	**Node 4**
1	0.58	37.96	38.81	38.753	70.218	82.764	82.592
2	0.54	34.07	34.95	34.891	66.356	78.903	78.730
3	0.53	29.01	29.89	29.832	61.297	73.843	73.671
4	0.53	23.93	24.81	24.755	56.220	68.767	68.594
5	0.53	18.79	19.67	19.613	51.078	63.625	63.452
6	0.53	13.67	14.55	14.496	45.961	58.508	58.336
7	0.52	8.58	9.47	9.411	40.876	53.423	53.251
8	0.62	13.62	14.44	14.378	45.843	58.390	58.217
9	0.63	18.71	19.52	19.462	50.927	63.473	63.301
10	0.00	0.00	0.00	0.000	0.000	0.000	0.000
11	0.00	0.00	0.00	0.000	0.000	0.000	0.000
12	0.00	0.00	0.00	0.000	0.000	0.000	0.000
13	0.00	0.00	0.00	0.000	0.000	0.000	0.000
14	0.00	0.00	0.00	0.000	0.000	0.000	0.000
15	0.00	0.00	0.00	0.000	0.000	0.000	0.000

N1 And FAVAD Parameters (Test 1)

N1 Equation:

$$Q = C_d A\sqrt{2gh}$$
$$Q = C_d\sqrt{2g}\,Ah^{0.5}$$
$$Q = C_{N1}Ah^{N1}$$

FAVAD Equation:

$$Q = C_d A\sqrt{2gh} \quad but \quad A = A_0 + mH$$
$$\therefore C_d A = Q/\sqrt{2gh} \qquad Q = C_d\sqrt{2gh}(A_0 + mh)$$
$$Q = C_d\sqrt{2g}\,(A_0 h^{0.5} + mh^{1.5})$$

Node 0: N1 Relationship

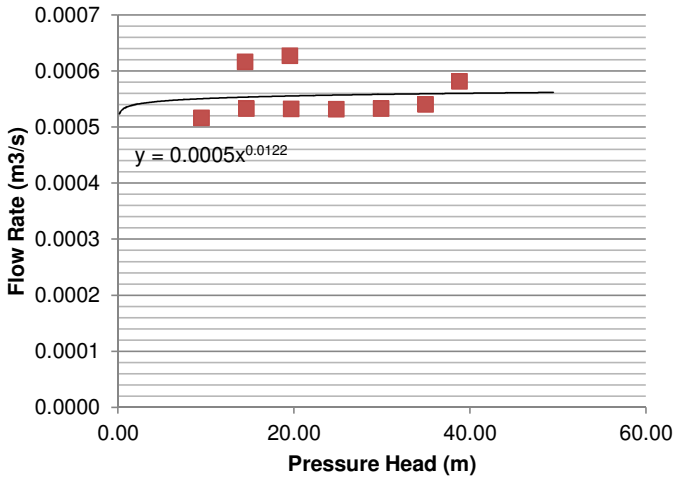

N1 Parameters:

Leakage Coefficient (CN1): 0.00054
Leakage Exponent (N1): 0.01219

Node 0: FAVAD Relationship

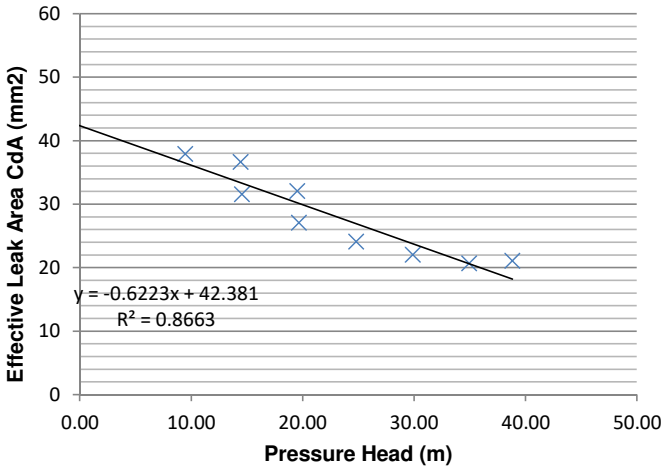

FAVAD Parameters:

Effective Initial Leak Area CdA0: 42.381 mm
Effective head-area slope Cdm: -0.622 mm2/m

Node 1: N1 Relationship

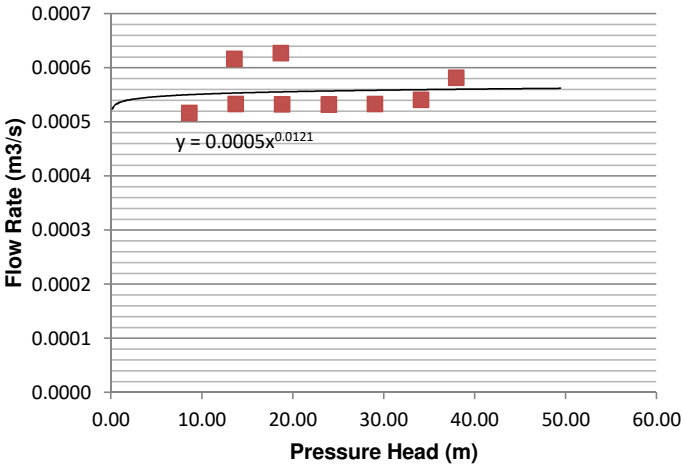

N1 Parameters:

Leakage Coefficient (C): 0.00054
Leakage Exponent (N1): 0.01213

Node 1: FAVAD Relationship

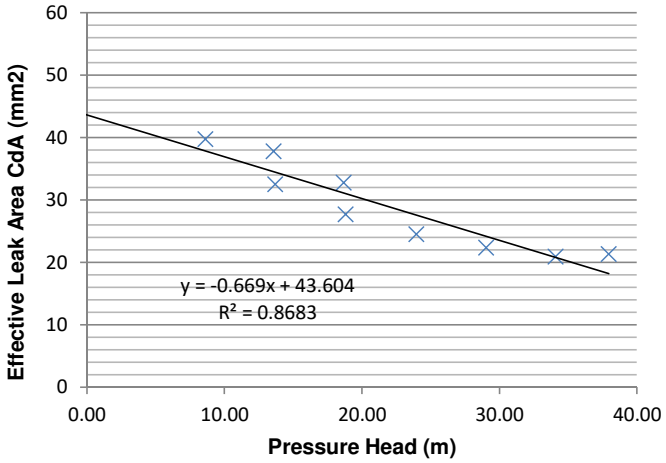

FAVAD Parameters:

Effective Initial Leak Area CdA0: 43.604 mm
Effective head-area slope Cdm: -0.669 mm2/m

N1 And FAVAD Parameters (Test 1)

Node 2: N1 Relationship

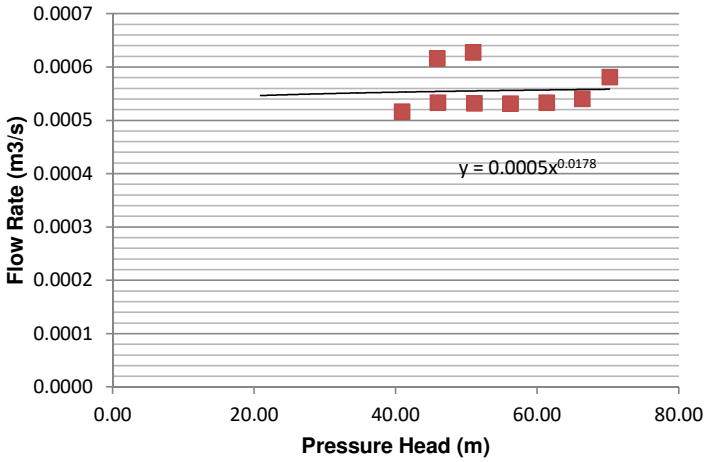

N1 Parameters:

Leakage Coefficient (C): 0.00052
Leakage Exponent (N1): 0.01779

Node 2: FAVAD Relationship

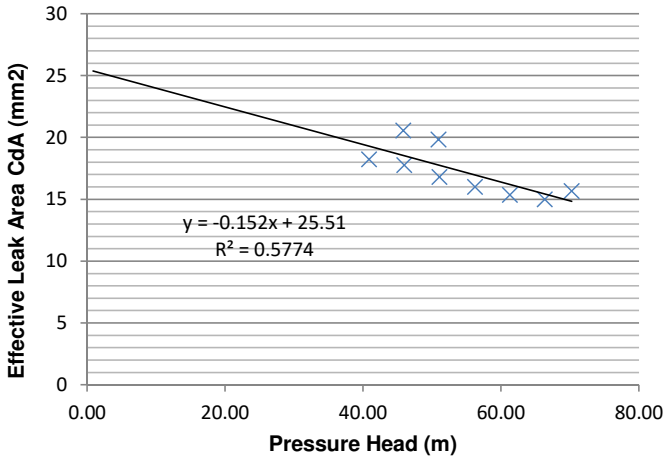

FAVAD Parameters:

Effective Initial Leak Area CdA0: 25.510 mm
Effective head-area slope Cdm: -0.152 mm2/m

Node 3: N1 Relationship

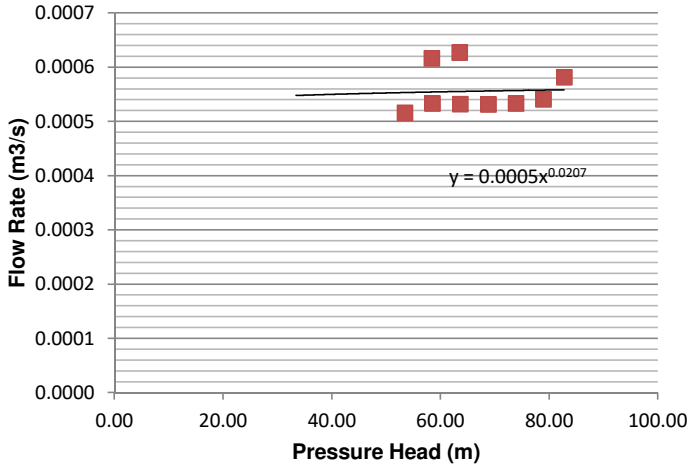

N1 Parameters:

Leakage Coefficient (C): 0.00051
Leakage Exponent (N1): 0.02072

Node 3: FAVAD Relationship

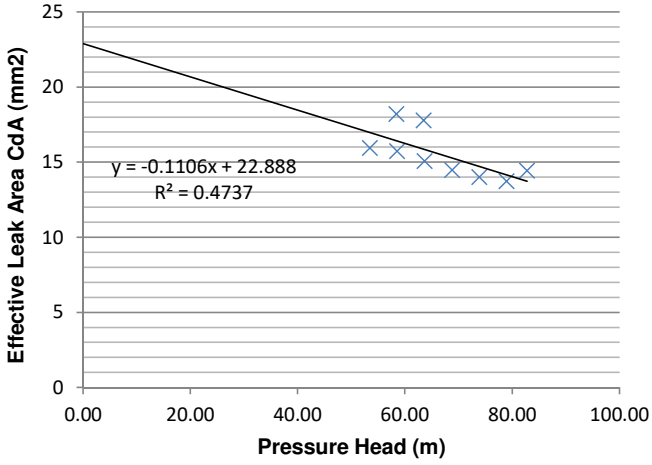

FAVAD Parameters:

Effective Initial Leak Area CdA0: 22.888 mm
Effective head-area slope Cdm: -0.111 mm2/m

Node 4: N1 Relationship

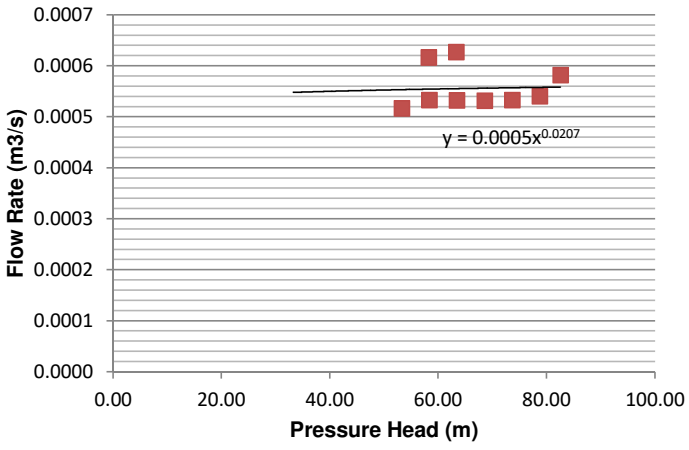

N1 Parameters:

Leakage Coefficient (C): 0.00051
Leakage Exponent (N1): 0.02068

Node 4: FAVAD Relationship

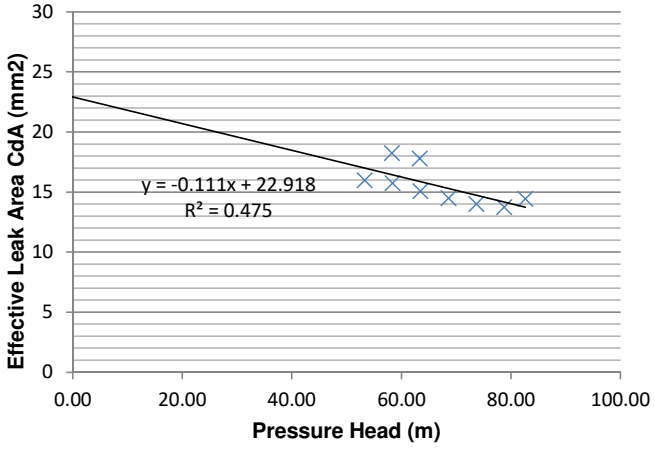

FAVAD Parameters:

Effective Initial Leak Area CdA0: 22.918 mm
Effective head-area slope Cdm: -0.111 mm2/m

Summary (Test 1)

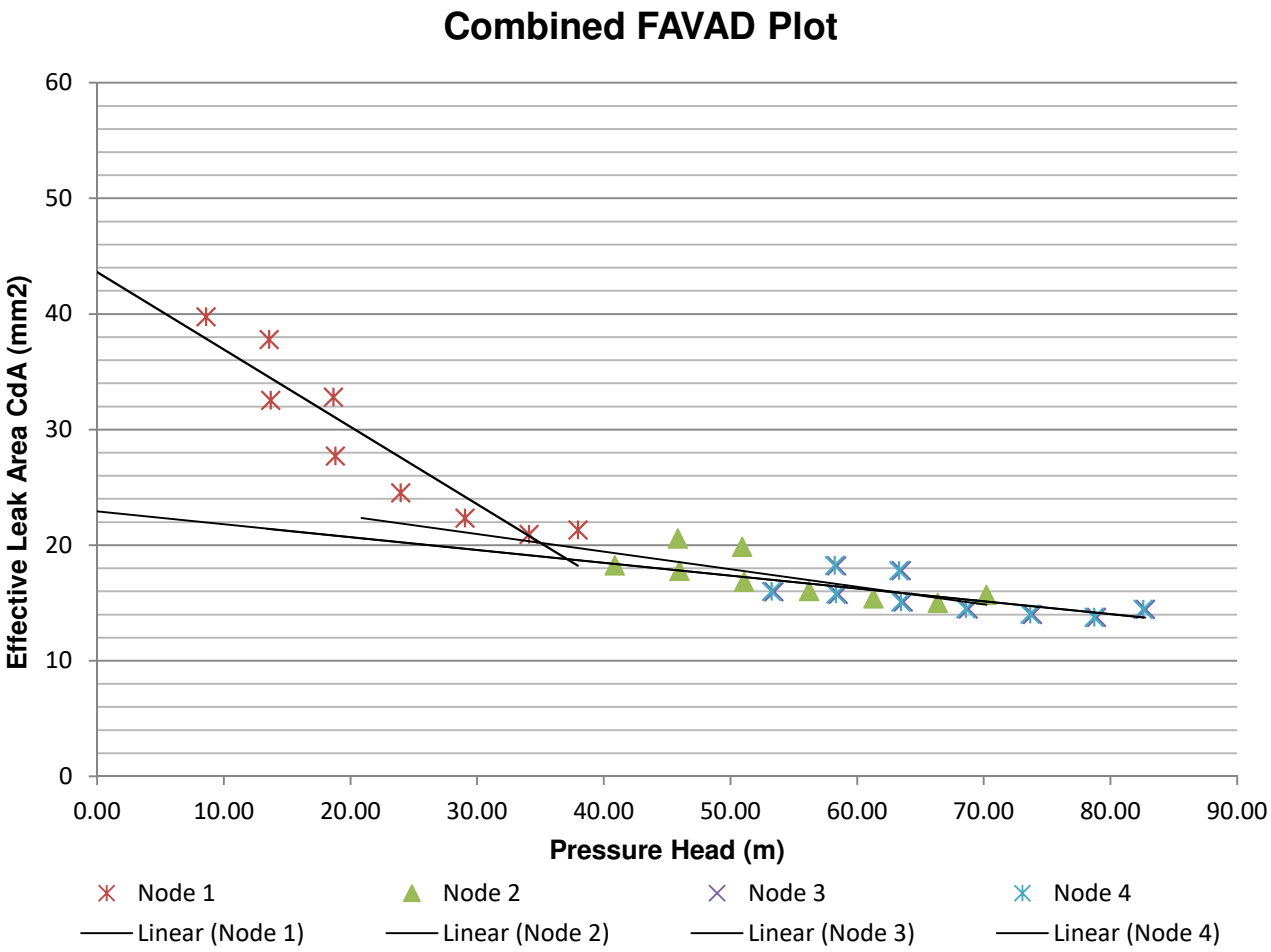

Discussion:

All leaks result in negative pressure-area slopes. This is not expected for steel pipes, therefore the node with the least negative slope most likely best represents the approximate leak location. Possibly errors from the assumptions made for calculating the adapted pressures, and the elavtion, is underestimated, leading to the negative readings.

The difference between the upward and downward pressure adjustment cycle cannot be explained and requires further investigation.

Plot and Data Points (Test 2)

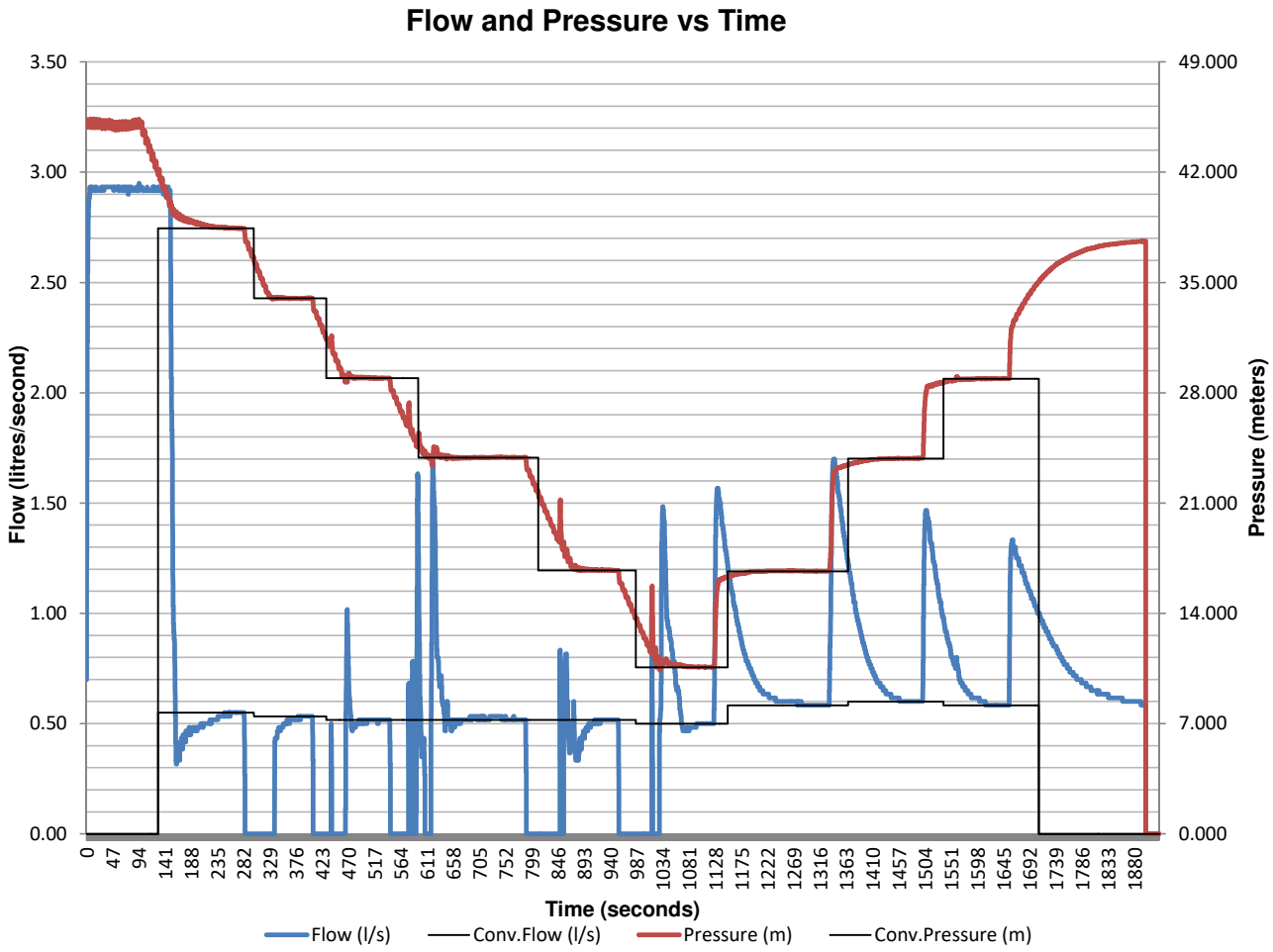

Tool for zooming into graph to calculate and plot the average values:

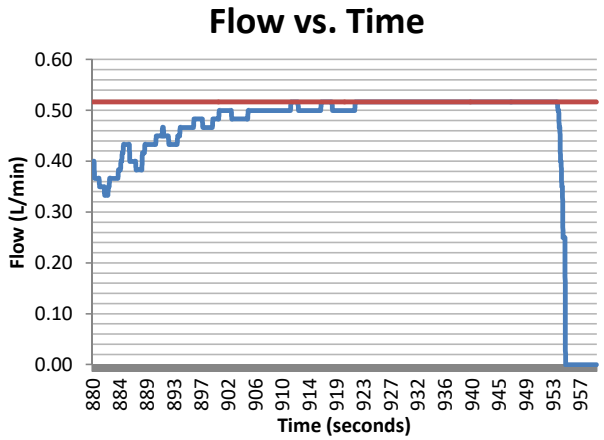

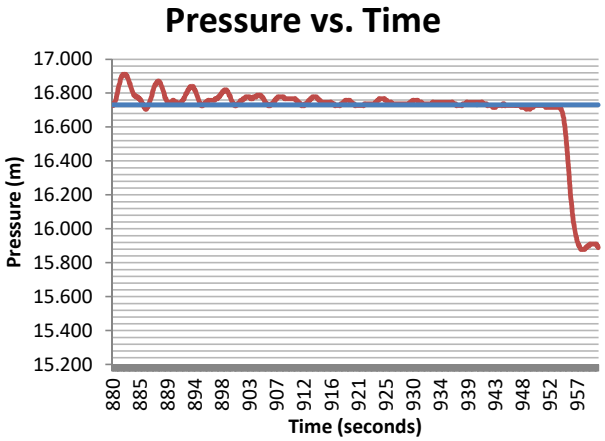

Select time Range for Display:		Select time Range for Average Calculation:	
Start Time:	880 s	Start Time:	925 s
End Time:	960 s	End Time:	937 s

Average Flow:	1.0842 l/s
Average Pressure:	33.385 m

Pressure Head Correction (Test 2)

Corrected pressure at every Node:

Reynold's Number

$$\mathrm{Re} = \frac{\rho \mathrm{VD}}{\mu} = \frac{\mathrm{VD}}{\nu} = \frac{\mathrm{QD}}{\nu A}$$

Colebrook-White

$$\frac{1}{\sqrt{f}} = -2\log_{10}\left(\frac{\varepsilon}{3.7D} + \frac{2.51}{R_e\sqrt{f}}\right)$$

Minor Loss Equation

$$h_L = K_L\frac{V^2}{2g}$$

Darcy-Weissbach

$$h_f = f\frac{L}{D}\frac{V^2}{2g}$$

			Corrected Head (m)				
Point	**Flow (l/s)**	**Measured Head (m)**	**Node 0**	**Node 1**	**Node 2**	**Node 3**	**Node 4**
1	0.55	38.44	39.31	39.252	70.717	83.264	83.091
2	0.53	34.01	34.89	34.830	66.295	78.841	78.669
3	0.52	28.93	29.82	29.766	61.231	73.778	73.606
4	0.52	23.89	24.78	24.727	56.192	68.738	68.566
5	0.52	16.73	17.62	17.563	49.028	61.574	61.402
6	0.50	10.59	11.49	11.428	42.894	55.440	55.268
7	0.58	16.67	17.52	17.462	48.927	61.474	61.302
8	0.60	23.84	24.68	24.617	56.082	68.629	68.456
9	0.58	28.90	29.74	29.685	61.150	73.696	73.524
10	0.00	0.00	0.00	0.000	0.000	0.000	0.000
11	0.00	0.00	0.00	0.000	0.000	0.000	0.000
12	0.00	0.00	0.00	0.000	0.000	0.000	0.000
13	0.00	0.00	0.00	0.000	0.000	0.000	0.000
14	0.00	0.00	0.00	0.000	0.000	0.000	0.000
15	0.00	0.00	0.00	0.000	0.000	0.000	0.000

N1 And FAVAD Parameters (Test 2)

N1 Equation:

$$Q = C_d A\sqrt{2gh}$$
$$Q = C_d\sqrt{2g}\,Ah^{0.5}$$
$$Q = C_{N1}Ah^{N1}$$

FAVAD Equation:

$$Q = C_d A\sqrt{2gh} \quad but \quad A = A_0 + mH$$
$$\therefore C_d A = Q/\sqrt{2gh} \qquad Q = C_d\sqrt{2gh}(A_0 + mh)$$
$$Q = C_d\sqrt{2g}\,(A_0 h^{0.5} + mh^{1.5})$$

Node 0: N1 Relationship

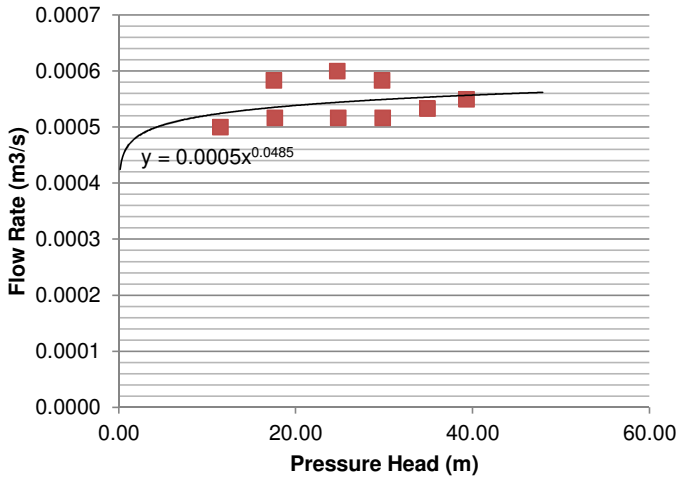

N1 Parameters:

Leakage Coefficient (CN1):	0.00047
Leakage Exponent (N1):	0.04850

Node 0: FAVAD Relationship

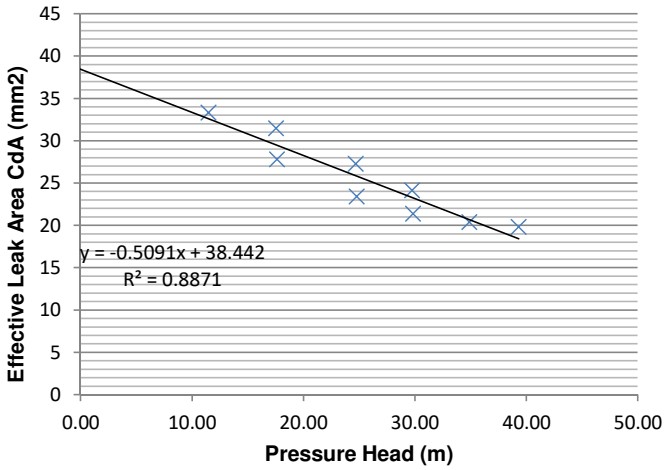

FAVAD Parameters:

Effective Initial Leak Area CdA(	38.442	mm
Effective head-area slope Cdm	-0.509	mm2/m

Node 1: N1 Relationship

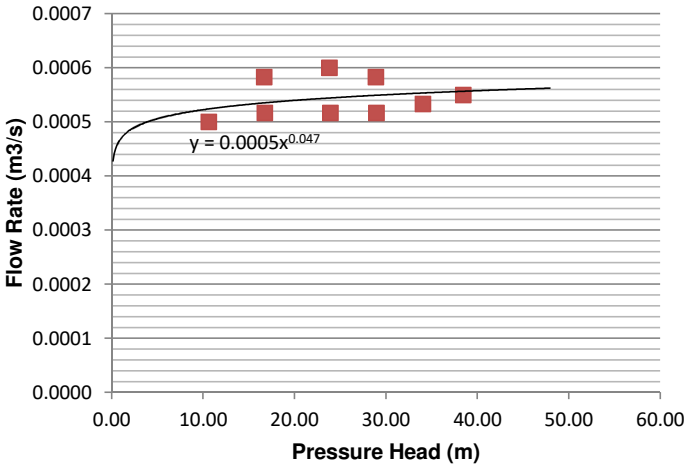

N1 Parameters:

Leakage Coefficient (C):	0.00047
Leakage Exponent (N1):	0.04695

Node 1: FAVAD Relationship

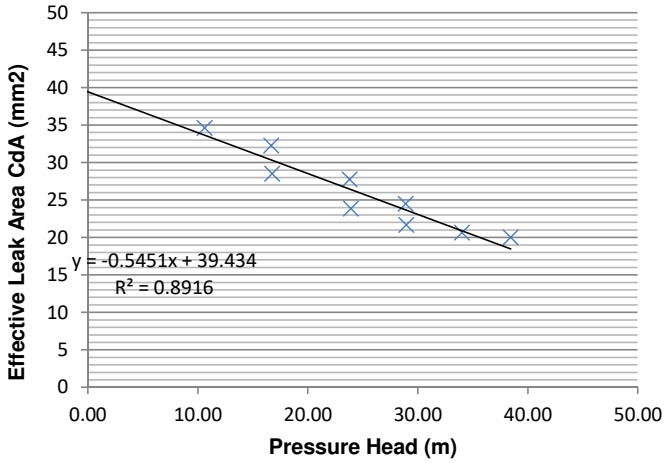

FAVAD Parameters:

Effective Initial Leak Area CdA(	39.434	mm
Effective head-area slope Cdm	-0.545	mm2/m

N1 And FAVAD Parameters (Test 2)

Node 2: N1 Relationship

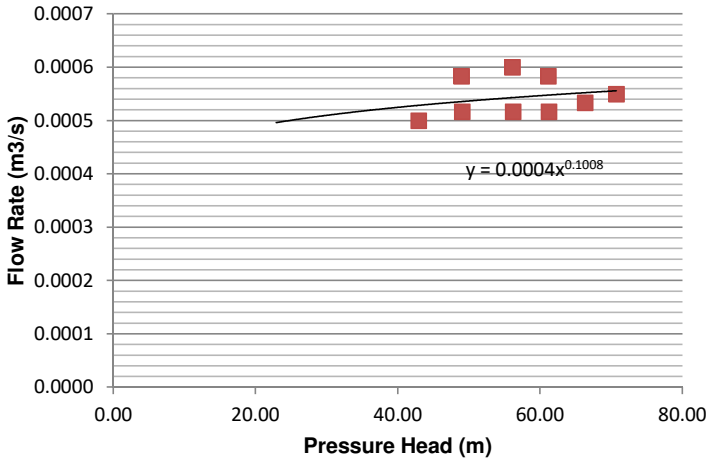

N1 Parameters:

Leakage Coefficient (C):	0.00036
Leakage Exponent (N1):	0.10077

Node 2: FAVAD Relationship

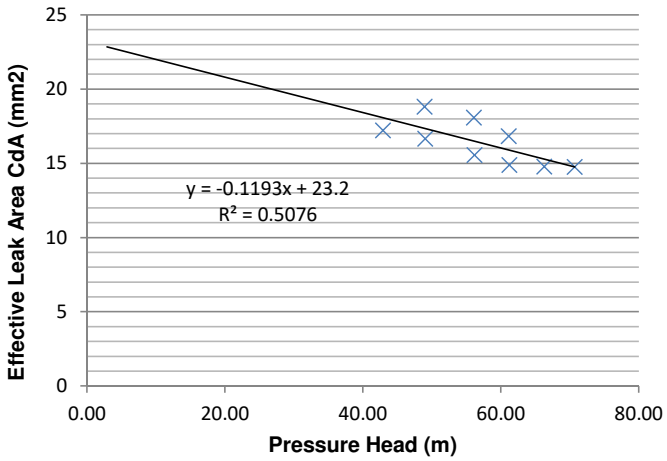

FAVAD Parameters:

Effective Initial Leak Area CdA(	23.200	mm
Effective head-area slope Cdm	-0.119	mm2/m

Node 3: N1 Relationship

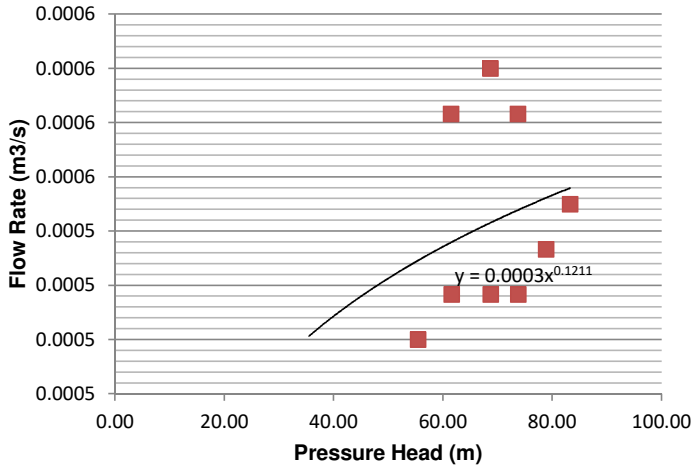

N1 Parameters:

Leakage Coefficient (C):	0.00033
Leakage Exponent (N1):	0.12114

Node 3: FAVAD Relationship

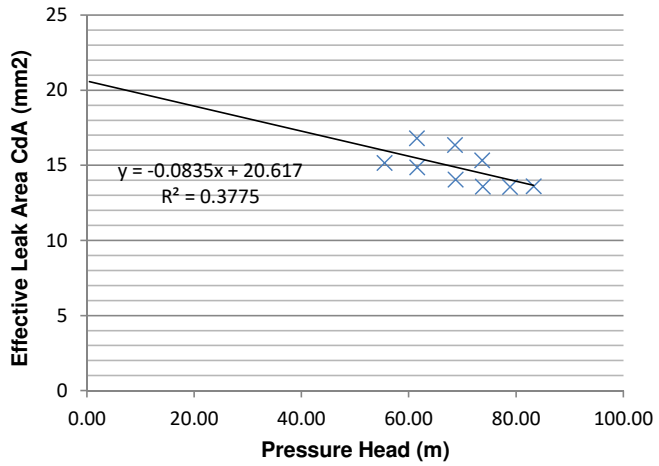

FAVAD Parameters:

Effective Initial Leak Area CdA(	20.617	mm
Effective head-area slope Cdm	-0.083	mm2/m

Node 4: N1 Relationship

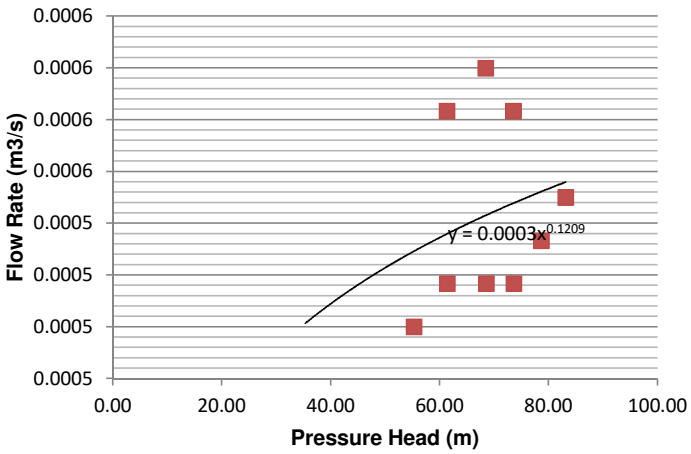

N1 Parameters:

Leakage Coefficient (C):	0.00033
Leakage Exponent (N1):	0.12086

Node 4: FAVAD Relationship

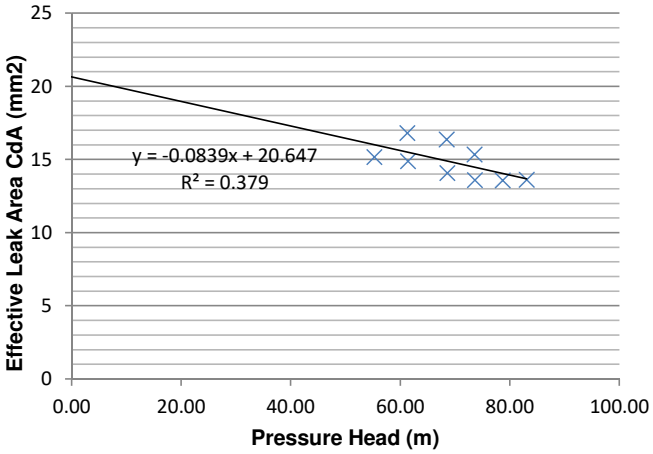

FAVAD Parameters:

Effective Initial Leak Area CdA(	20.647	mm
Effective head-area slope Cdm	-0.084	mm2/m

Summary (Test 2)

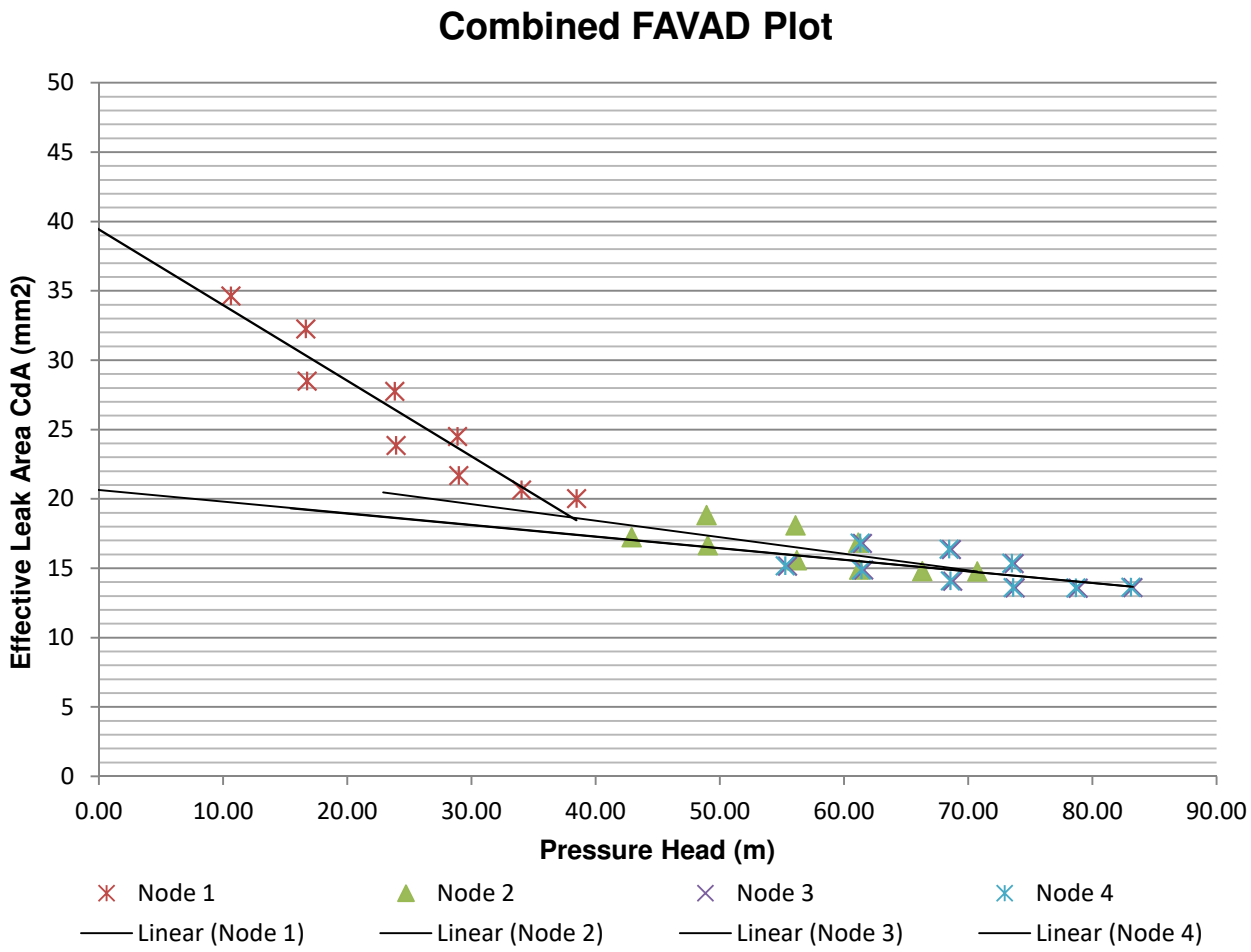

Discussion:

Very similar to test 1.

N1 And FAVAD Combined

Node 1

Test 1 2018-06-08

Point	Flow (m3/s)	Corrected Head (m)	Effective Leak Area CdA (mm2)	Log(Q)	Log(H)
1	0.00058	37.95266	21.32499116	-3.235	1.579
2	0.00054	34.091181	20.91541532	-3.267	1.533
3	0.00053	29.03178	22.3466485	-3.273	1.463
4	0.00053	23.955131	24.53790006	-3.274	1.379
5	0.00053	18.813171	27.71668101	-3.274	1.274
6	0.00053	13.696329	32.53472446	-3.273	1.137
7	0.00052	8.6111855	39.74929868	-3.287	0.935
8	0.00062	13.578386	37.78129989	-3.21	1.133
9	0.00063	18.66221	32.79670918	-3.202	1.271
10	#N/A	#N/A	FALSE	FALSE	#####
11	#N/A	#N/A	FALSE	FALSE	#####
12	#N/A	#N/A	FALSE	FALSE	#####
13	#N/A	#N/A	FALSE	FALSE	#####
14	#N/A	#N/A	FALSE	FALSE	#####
15	#N/A	#N/A	FALSE	FALSE	#####

Test 2 2018-06-08

Flow (m3/s)	Corrected Head (m)	Effective Leak Area CdA (mm2)	Log(Q)	Log(H)
0.000550	38.45	20.02409635	-3.26	1.58492
0.000533	34.03	20.64048134	-3.273	1.53186
0.000517	28.97	21.67272253	-3.287	1.46189
0.000517	23.93	23.84616174	-3.287	1.37888
0.000517	16.76	28.48956013	-3.287	1.22435
0.000500	10.63	34.62458637	-3.301	1.02647
0.000583	16.66	32.26253271	-3.234	1.22174
0.000600	23.82	27.75593476	-3.222	1.37689
0.000583	28.88	24.5037968	-3.234	1.46067
#N/A	#N/A	FALSE	FALSE	FALSE
#N/A	#N/A	FALSE	FALSE	FALSE
#N/A	#N/A	FALSE	FALSE	FALSE
#N/A	#N/A	FALSE	FALSE	FALSE
#N/A	#N/A	FALSE	FALSE	FALSE
#N/A	#N/A	FALSE	FALSE	FALSE

Test 3 2018-06-07

Point	Flow (m3/s)	Corrected Head (m)	Effective Leak Area CdA (mm2)	Log(Q)	Log(H)
1					
2					
3					
4					
5					
6					
7					
8					
9					
10					
11					
12					
13					
14					
15					

Test 4 2018-06-28

Flow (m3/s)	Corrected Head (m)	Effective Leak Area CdA (mm2)	Log(Q)	Log(H)

Test 5 2018-06-28

Point	Flow (m3/s)	Corrected Head (m)	Effective Leak Area CdA (mm2)	Log(Q)	Log(H)
1					
2					
3					
4					
5					
6					
7					
8					
9					
10					
11					
12					
13					
14					
15					

Node 2

Test 1 2018-06-08

Point	Flow (m3/s)	Corrected Head (m)	Effective Leak Area CdA (mm2)	Log(Q)	Log(H)
1	0.00058	70.217562	15.67787136	-3.235	1.846
2	0.00054	66.356164	14.99156185	-3.267	1.822
3	0.00053	61.296777	15.37908181	-3.273	1.787
4	0.00053	56.220131	16.01735285	-3.274	1.75
5	0.00053	51.07817	16.8211066	-3.274	1.708
6	0.00053	45.961326	17.76040844	-3.273	1.662
7	0.00052	40.876214	18.2442331	-3.287	1.611
8	0.00062	45.843215	20.56190924	-3.21	1.661
9	0.00063	50.927015	19.85352792	-3.202	1.707
10	#N/A	#N/A	FALSE	FALSE	#####
11	#N/A	#N/A	FALSE	FALSE	#####
12	#N/A	#N/A	FALSE	FALSE	#####
13	#N/A	#N/A	FALSE	FALSE	#####
14	#N/A	#N/A	FALSE	FALSE	#####
15	#N/A	#N/A	FALSE	FALSE	#####

Test 2 2018-06-08

Flow (m3/s)	Corrected Head (m)	Effective Leak Area CdA (mm2)	Log(Q)	Log(H)
0.000550	70.72	14.76559483	-3.26	1.84952
0.000533	66.29	14.7880072	-3.273	1.82148
0.000517	61.23	14.90643013	-3.287	1.78697
0.000517	56.19	15.56052691	-3.287	1.74967
0.000517	49.03	16.65861762	-3.287	1.69044
0.000500	42.89	17.23552383	-3.301	1.63239
0.000583	48.93	18.82745644	-3.234	1.68955
0.000600	56.08	18.08795726	-3.222	1.74882
0.000583	61.15	16.84110155	-3.234	1.78639
#N/A	#N/A	FALSE	FALSE	FALSE
#N/A	#N/A	FALSE	FALSE	FALSE
#N/A	#N/A	FALSE	FALSE	FALSE
#N/A	#N/A	FALSE	FALSE	FALSE
#N/A	#N/A	FALSE	FALSE	FALSE
#N/A	#N/A	FALSE	FALSE	FALSE

Test 3 2018-06-07

Point	Flow (m3/s)	Corrected Head (m)	Effective Leak Area CdA (mm2)	Log(Q)	Log(H)
1					
2					
3					
4					
5					
6					
7					
8					
9					
10					
11					
12					
13					
14					
15					

Test 4 2018-06-28

Flow (m3/s)	Corrected Head (m)	Effective Leak Area CdA (mm2)	Log(Q)	Log(H)

Test 5 2018-06-28

Point	Flow (m3/s)	Corrected Head (m)	Effective Leak Area CdA (mm2)	Log(Q)	Log(H)
1					
2					
3					
4					
5					
6					
7					
8					
9					
10					
11					
12					
13					
14					
15					

Node 3

Test 1		2018-06-08				Test 2		2018-06-08		
Point	Flow (m3/s)	Corrected Head (m)	Effective Leak Area CdA (mm2)	Log(Q)	Log(H)	Flow (m3/s)	Corrected Head (m)	Effective Leak Area CdA (mm2)	Log(Q)	Log(H)
1	0.00058	82.763978	14.4407348	-3.235	1.918	0.000550	83.26	13.60773176	-3.26	1.92045
2	0.00054	78.902609	13.7480732	-3.267	1.897	0.000533	78.84	13.56040343	-3.273	1.89675
3	0.00053	73.843227	14.01179884	-3.273	1.868	0.000517	73.78	13.57993677	-3.287	1.86793
4	0.00053	68.766582	14.48264718	-3.274	1.837	0.000517	68.74	14.06894501	-3.287	1.8372
5	0.00053	63.62462	15.07160923	-3.274	1.804	0.000517	61.57	14.86485639	-3.287	1.7894
6	0.00053	58.507776	15.74136649	-3.273	1.767	0.000500	55.44	15.1603348	-3.301	1.74382
7	0.00052	53.422674	15.95872273	-3.287	1.728	0.000583	61.47	16.79664529	-3.234	1.78869
8	0.00062	58.389605	18.21936365	-3.21	1.766	0.000600	68.63	16.3511918	-3.222	1.8365
9	0.00063	63.473396	17.78344654	-3.202	1.803	0.000583	73.70	15.34070438	-3.234	1.86744
10	#N/A	#N/A	FALSE	FALSE	#####	#N/A	#N/A	FALSE	FALSE	FALSE
11	#N/A	#N/A	FALSE	FALSE	#####	#N/A	#N/A	FALSE	FALSE	FALSE
12	#N/A	#N/A	FALSE	FALSE	#####	#N/A	#N/A	FALSE	FALSE	FALSE
13	#N/A	#N/A	FALSE	FALSE	#####	#N/A	#N/A	FALSE	FALSE	FALSE
14	#N/A	#N/A	FALSE	FALSE	#####	#N/A	#N/A	FALSE	FALSE	FALSE
15	#N/A	#N/A	FALSE	FALSE	#####	#N/A	#N/A	FALSE	FALSE	FALSE

Test 3		2018-06-07				Test 4		2018-06-28		
Point	Flow (m3/s)	Corrected Head (m)	Effective Leak Area CdA (mm2)	Log(Q)	Log(H)	Flow (m3/s)	Corrected Head (m)	Effective Leak Area CdA (mm2)	Log(Q)	Log(H)
1										
2										
3										
4										
5										
6										
7										
8										
9										
10										
11										
12										
13										
14										
15										

Test 5		2018-06-28			
Point	Flow (m3/s)	Corrected Head (m)	Effective Leak Area CdA (mm2)	Log(Q)	Log(H)
1					
2					
3					
4					
5					
6					
7					
8					
9					
10					
11					
12					
13					
14					
15					

Node 4

Test 1 2018-06-08

Point	Flow (m3/s)	Corrected Head (m)	Effective Leak Area CdA (mm2)	Log(Q)	Log(H)
1	0.00058	82.59177	14.45578184	-3.235	1.917
2	0.00054	78.730429	13.76309821	-3.267	1.896
3	0.00053	73.671052	14.02816263	-3.273	1.867
4	0.00053	68.594407	14.50081175	-3.274	1.836
5	0.00053	63.452446	15.09204335	-3.274	1.802
6	0.00053	58.335601	15.76457936	-3.273	1.766
7	0.00052	53.25051	15.98449999	-3.287	1.726
8	0.00062	58.217371	18.24629445	-3.21	1.765
9	0.00063	63.301154	17.80762451	-3.202	1.801
10	#N/A	#N/A	FALSE	FALSE	#####
11	#N/A	#N/A	FALSE	FALSE	#####
12	#N/A	#N/A	FALSE	FALSE	#####
13	#N/A	#N/A	FALSE	FALSE	#####
14	#N/A	#N/A	FALSE	FALSE	#####
15	#N/A	#N/A	FALSE	FALSE	#####

Test 2 2018-06-08

Flow (m3/s)	Corrected Head (m)	Effective Leak Area CdA (mm2)	Log(Q)	Log(H)
0.000550	83.09	13.62182379	-3.26	1.91956
0.000533	78.67	13.57523447	-3.273	1.8958
0.000517	73.61	13.59580926	-3.287	1.86691
0.000517	68.57	14.08659695	-3.287	1.83611
0.000517	61.40	14.88568139	-3.287	1.78818
0.000500	55.27	15.18392788	-3.301	1.74247
0.000583	61.30	16.8202215	-3.234	1.78747
0.000600	68.46	16.37174696	-3.222	1.83541
0.000583	73.52	15.35865959	-3.234	1.86643
#N/A	#N/A	FALSE	FALSE	FALSE
#N/A	#N/A	FALSE	FALSE	FALSE
#N/A	#N/A	FALSE	FALSE	FALSE
#N/A	#N/A	FALSE	FALSE	FALSE
#N/A	#N/A	FALSE	FALSE	FALSE
#N/A	#N/A	FALSE	FALSE	FALSE

Test 3 2018-06-07

Point	Flow (m3/s)	Corrected Head (m)	Effective Leak Area CdA (mm2)	Log(Q)	Log(H)
1					
2					
3					
4					
5					
6					
7					
8					
9					
10					
11					
12					
13					
14					
15					

Test 4 2018-06-28

Flow (m3/s)	Corrected Head (m)	Effective Leak Area CdA (mm2)	Log(Q)	Log(H)

Test 5 2018-06-28

Point	Flow (m3/s)	Corrected Head (m)	Effective Leak Area CdA (mm2)	Log(Q)	Log(H)
1					
2					
3					
4					
5					
6					
7					
8					
9					
10					
11					
12					
13					
14					
15					

N1 And FAVAD Combined

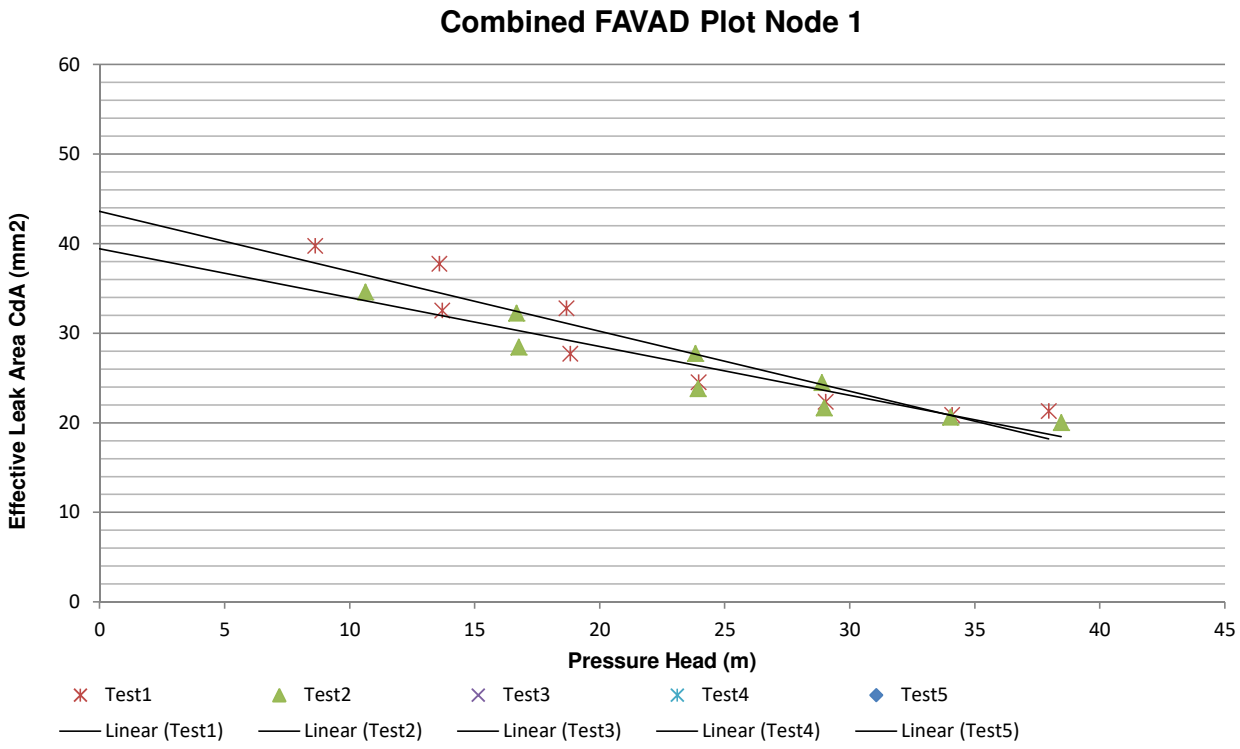

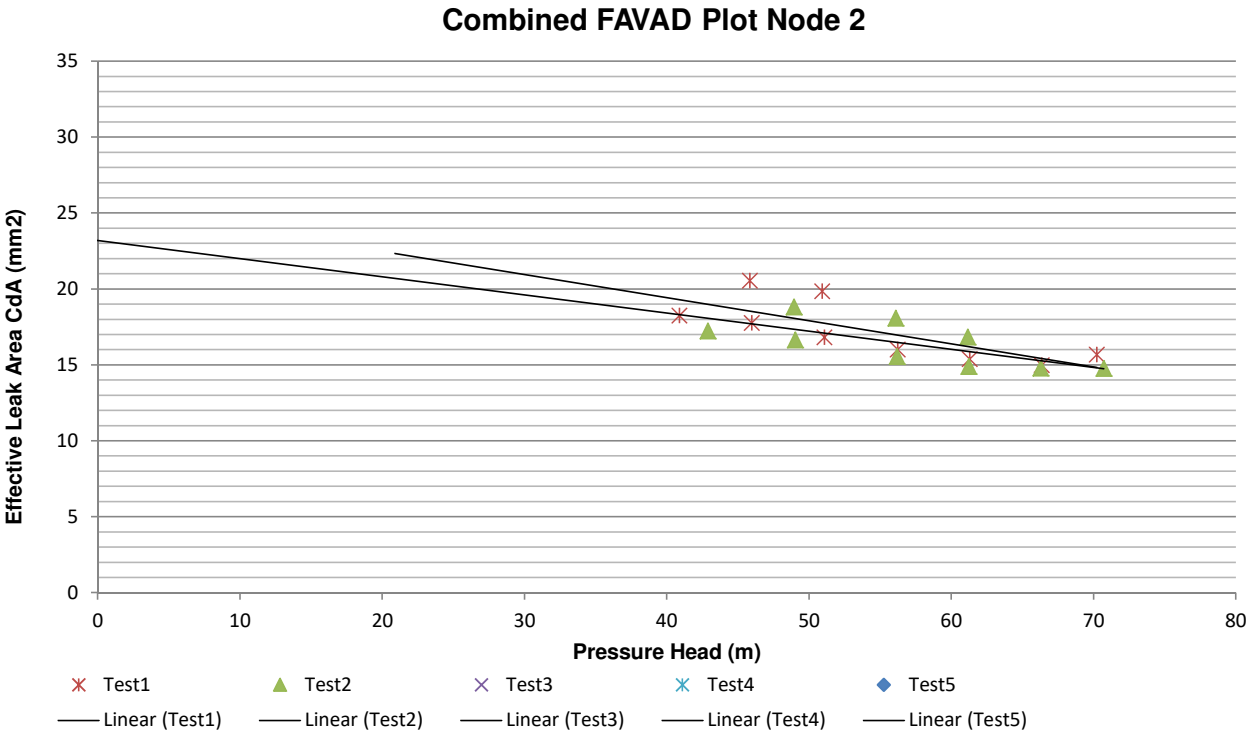

N1 And FAVAD Combined (Continued)

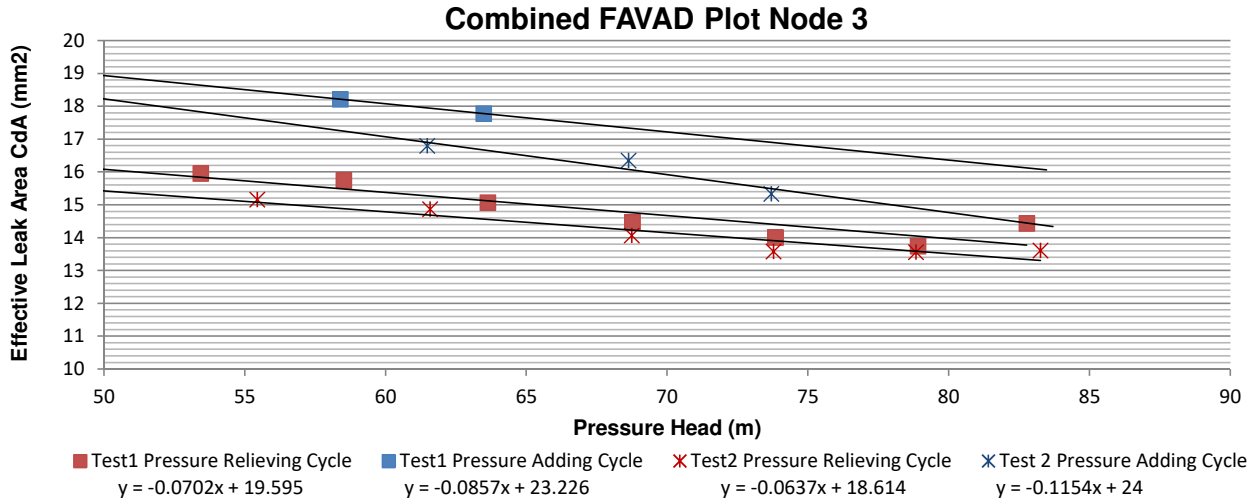

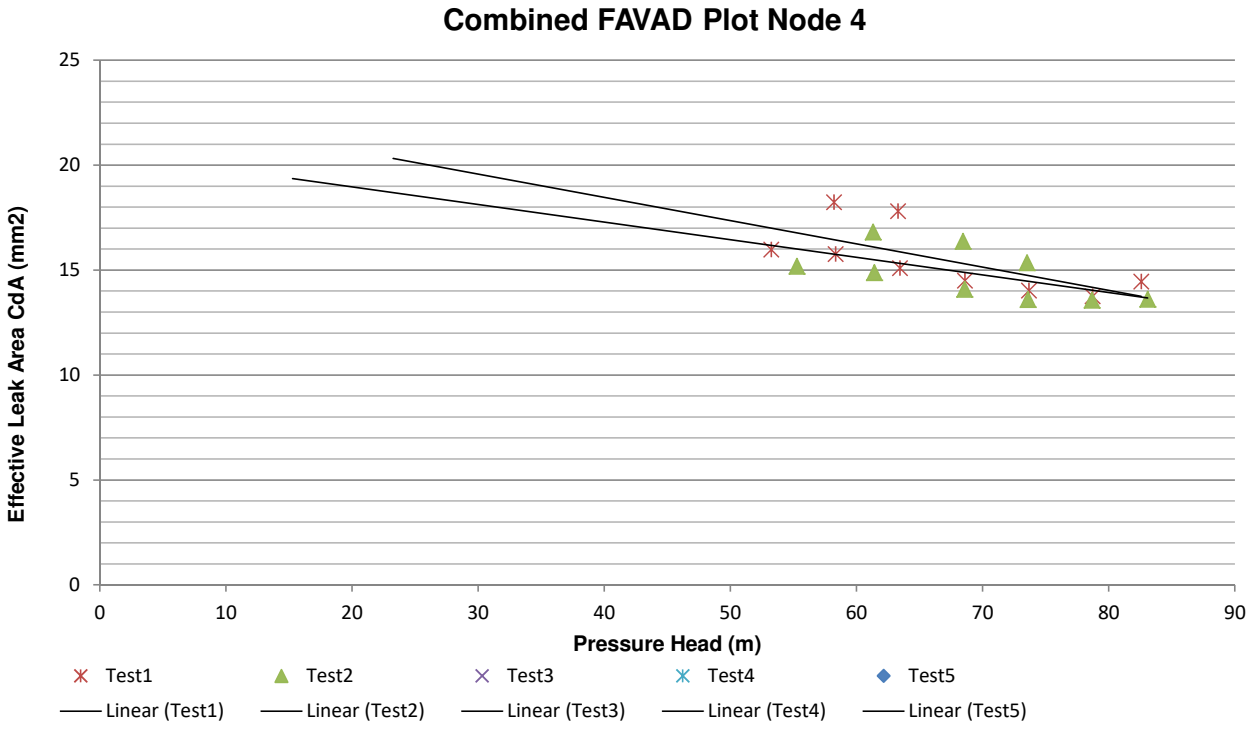

Test Report and Analysis

Pipe:

Supply Line to Muckleneuk Reservoir

Testing Date:

02 August 2018

Contents:

General Test Description

Description:

The map in figure 1 shows the pipeline route. The blue line shows the smaller AC pipe which can be isolated with a butterfly valve from a larger 1m diameter supply line. This pipe enters a valve chamber next to the reservoir. Inside the chamber, it splits into three pipes, two of which are fitted with two PRVs in series, and one is isolated with a gate valve that is in a permanently closed position. Before the split, an 80mm pipe branches off the main pipe and is fitted with a one inch pipe connection onto which the testing equipment could be connected to.

The green line shows the larger 1m diameter steel pipe that feeds the AC pipe. This pipe can be isolated upstream and downstream with a butterfly valve, but due to there not being a connection point, the pipe must be tested together with the AC pipe from the same connection point.

Figure 1: Map showing pipeline route starting at V1 and ending at V3

The first test discussed in this test report, is a simulated leak 60 metres from the connection point. A leak was simulated by opening a 6.35 mm ball valve on an offtake to the pipe. For this test, valve V3 was closed and V2 was open.

For the second test in this report, V3 was closed and V2 open. Both the steel and AC pipe were tested as one pipe.

For the third test, valve V2 was closed and only the AC pipe is tested.

General Test Description (Continued)

Figure 2: Test Equipment Setup

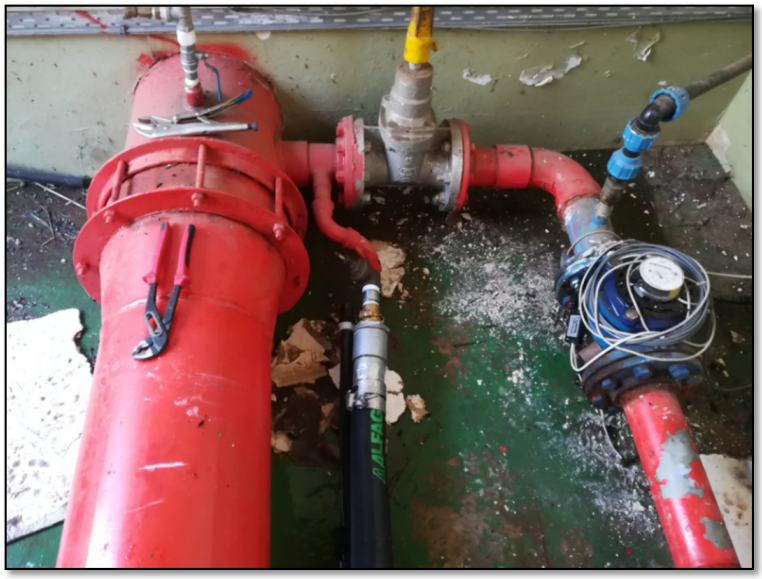

Figure 3 & 4: Connection point and Simulated leak from ball valve, respectively.

General Test Information

Pipeline:	Supply Line to Muckleneuk Reservoir
Area:	Pretoria, Muckleneuk
Pipe Owner:	Tshwane Municipality
Date:	02 Aug 18
Time:	09:00 - 11:30

Pipeline Section:	**Section 1**	**Section 2**	**Section 3**	
Pipe length (m):	247	1017		
Pipe Diameter (mm):	300	496		
Pipe Material:	Asbestos Cement	Steel		
Absolute Roughness e (mm)	0.5	0.5		
Minor Losses/km	1	1		
Pipe Wall Thickness (mm)	8	4		
Upstream Isolation:	Butterfly Valve	Butterfly Valve		
Upstream Source:	Pressured Pipe	Pressured Pipe		
Upstream Pressure (Bar) approx:	>8	>10		
Upstream Isolation Elevation (m):				
Downstream Isolation:	PRV			
Downstream Delivery:	Reservoir			
Downstream Pressure (Bar) approx:	<1			
Downstream Isolation Elevation (m):				

Connection of Testing Equipment

Connection Type:	1 Inch Threaded Connection	
Connection Fitting size (mm):	25	
Comment on Fitting:	1 inch isolation valve, 1 inch connection piece, 1 inch Geka coupling, 1 inch pipework into 80mm branch pipe, into 300mm main pipe.	
Minor loss coefficient of fitting	1 Inch Threaded M or F with Tap	8.08
Static height difference (A) in (m):	1.15	

Connection pipes*:

	Pipe 1	**Pipe 2**
Length of connection pipe* (mm):	400	100
Diameter of connection pipes (mm)	25	80
Absolute Roughness e (mm)	0.2	0.1
Static height difference (B) in (mm):	-80	0

Minor losses of fittings on connection pipes*:

	Fitting 1	**Fitting 2**	**Fitting 3**	**Fitting 4**
Fitting type:		Exit loss		Exit loss
Pipe 1 or Pipe 2	1	1	2	2
Fitting diameter in (mm):	25	25	80	200
Fitting diameter out (mm):	25	25	80	400
Absolute Roughness e (mm)	0.1	0.1	0.1	0.2
No. of fittings:	2	1	1	1
Fitting Minor Loss Coefficient:	0.6820	1.0000	0.0095	0.0002
** Pipes and Fittings between the connection point and the main pipeline*			SUM:	1.69175

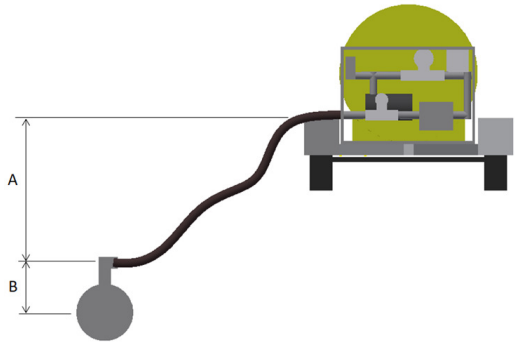

Pipeline Elevation Profile

Geocontext Website

Elevation Profile

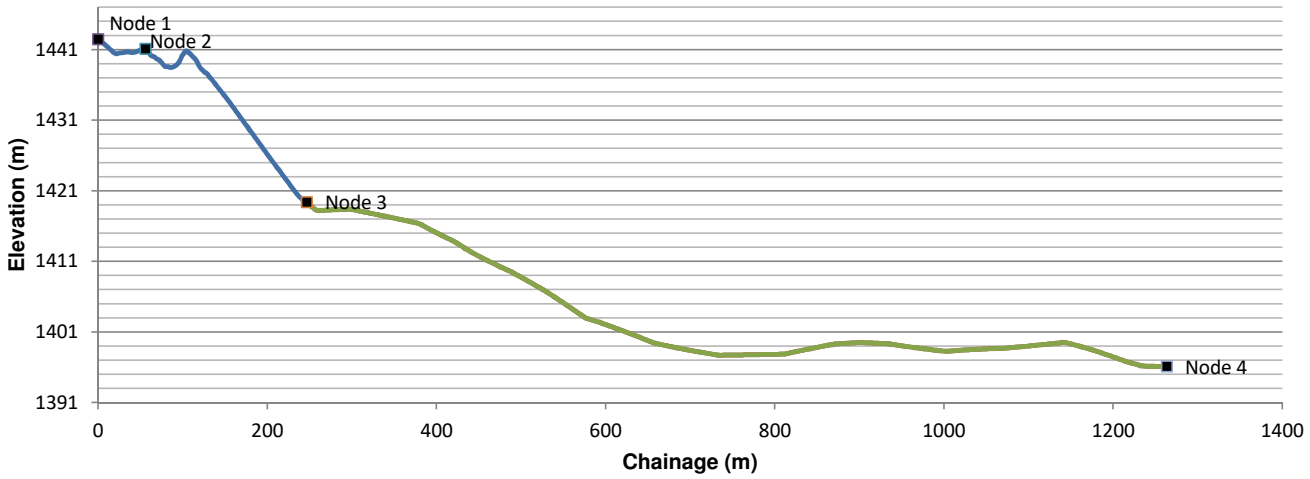

	Distance (m)	Elevation (m)	Material
1	0	1442.459106	Asbestos Cement
1	2.472397034	1442.272827	Asbestos Cement
1	4.944794069	1442.042847	Asbestos Cement
1	7.417191103	1441.765869	Asbestos Cement
1	9.889588138	1441.500977	Asbestos Cement
1	12.36198517	1441.287842	Asbestos Cement
1	14.83438221	1440.970337	Asbestos Cement
1	17.30677924	1440.706543	Asbestos Cement
1	19.77917628	1440.484863	Asbestos Cement
1	22.25157331	1440.425171	Asbestos Cement
1	24.72397034	1440.520386	Asbestos Cement
1	27.19636738	1440.561035	Asbestos Cement
1	29.66876441	1440.607788	Asbestos Cement
1	32.14116145	1440.652344	Asbestos Cement
1	34.61355848	1440.697754	Asbestos Cement
1	37.08595552	1440.641357	Asbestos Cement
1	39.55835255	1440.619141	Asbestos Cement
1	42.03074959	1440.611084	Asbestos Cement
1	44.50314662	1440.670898	Asbestos Cement
1	46.97554365	1440.811157	Asbestos Cement
1	49.44794069	1440.940552	Asbestos Cement
1	51.92033772	1441.064575	Asbestos Cement
1	54.39273476	1441.076904	Asbestos Cement
1	56.86513179	1440.917847	Asbestos Cement
1	59.33752883	1440.649292	Asbestos Cement
1	61.80992586	1440.241455	Asbestos Cement
1	64.28232289	1440.083984	Asbestos Cement
1	66.75471993	1439.953857	Asbestos Cement
1	69.22711696	1439.698853	Asbestos Cement
1	71.699514	1439.566528	Asbestos Cement
1	74.17191103	1439.296997	Asbestos Cement
1	76.64430807	1438.93042	Asbestos Cement
1	79.1167051	1438.61377	Asbestos Cement
1	81.58910214	1438.617676	Asbestos Cement
1	84.06149917	1438.51416	Asbestos Cement
1	86.5338962	1438.488281	Asbestos Cement
1	89.00629324	1438.563843	Asbestos Cement
1	91.47869027	1438.743408	Asbestos Cement
1	93.95108731	1439.005005	Asbestos Cement
1	96.42348434	1439.384277	Asbestos Cement

No. of Sections:	2	
Section	**Start (m)**	**Material**
1	0	Asbestos Cement
2	247	Steel
3		0

**If multiple sections exist, the Node points below must intercept at point where section changes for accurate pressure loss calculations.*

	Chainage (m)	Elevation (m)	End/part of Section
Node 1	0	1442.459	N/A
Node 2	56	1441.077	1
Node 3	247	1419.398	1
Node 4	1263.39	1396.132	1

Total Chainage = 1263.39 m

Distance/Elevation Data Continues

Plot and Data Points (Leak Simulation)

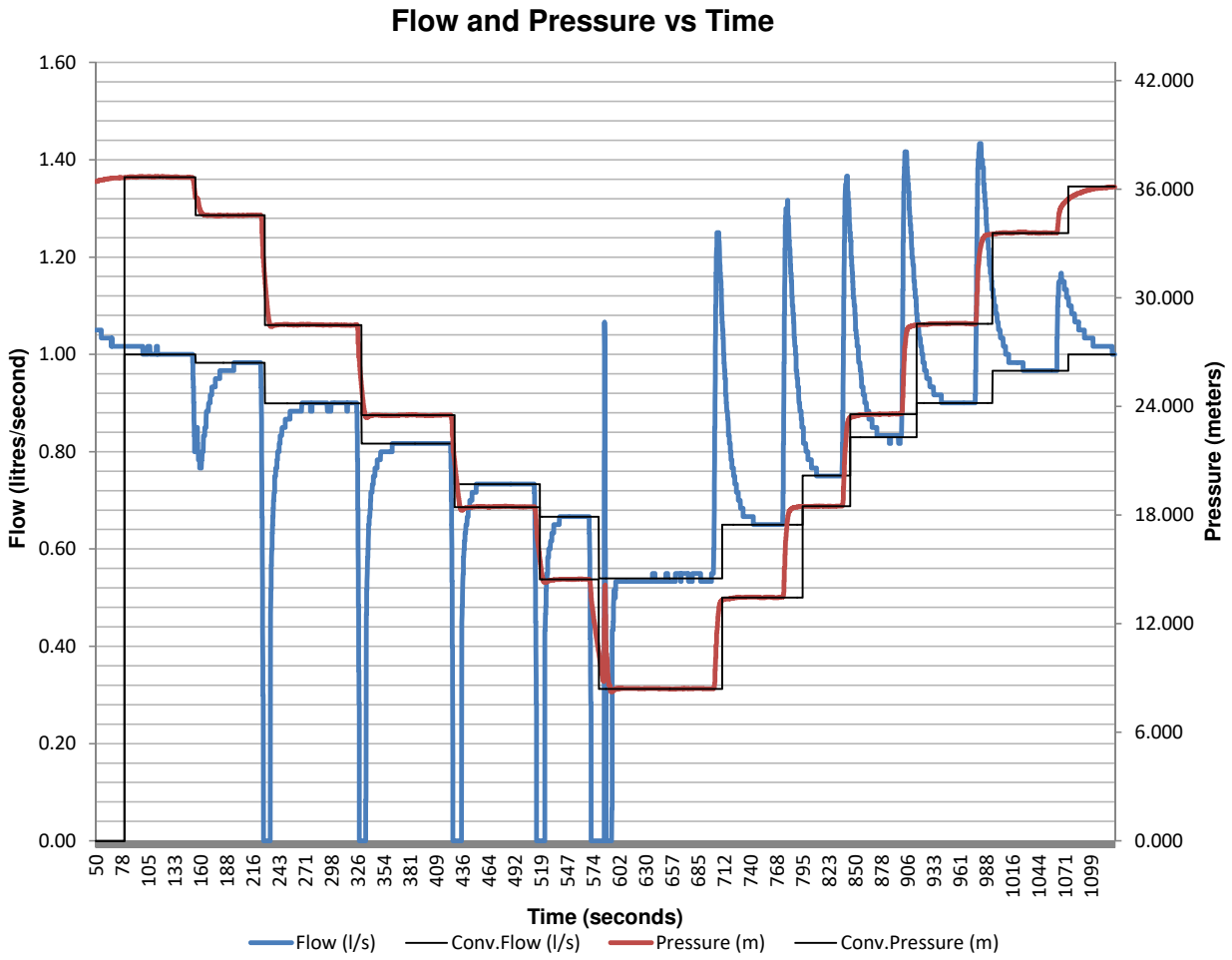

Pressure Head Correction (Leak Simulation)

Corrected pressure at every Node:

Reynold's Number

$$\mathrm{Re} = \frac{\rho \mathrm{VD}}{\mu} = \frac{\mathrm{VD}}{\nu} = \frac{\mathrm{QD}}{\nu A}$$

Colebrook-White

$$\frac{1}{\sqrt{f}} = -2\log_{10}\left(\frac{\varepsilon}{3.7D} + \frac{2.51}{R_e\sqrt{f}}\right)$$

Minor Loss Equation

$$h_L = K_L\frac{V^2}{2g}$$

Darcy-Weissbach

$$h_f = f\frac{L}{D}\frac{V^2}{2g}$$

			Corrected Head (m)				
Point	**Flow (l/s)**	**Measured Head (m)**	**Node 0**	**Node 1**	**Node 2**	**Node 3**	**Node 4**
1	1.00	36.66	37.54	33.560	34.942	56.618	79.870
2	0.98	34.57	35.45	31.601	32.982	54.658	77.911
3	0.90	28.49	29.42	26.186	27.568	49.244	72.500
4	0.82	23.52	24.48	21.801	23.182	44.859	68.117
5	0.73	18.45	19.45	17.273	18.654	40.331	63.591
6	0.67	14.46	15.48	13.670	15.052	36.729	59.990
7	0.54	8.41	9.47	8.258	9.640	31.318	54.580
8	0.65	13.45	14.48	12.755	14.137	35.815	59.075
9	0.75	18.49	19.48	17.202	18.584	40.261	63.519
10	0.83	23.58	24.54	21.773	23.155	44.831	68.089
11	0.90	28.57	29.49	26.256	27.638	49.314	72.570
12	0.97	33.59	34.48	30.759	32.140	53.816	77.070
13	1.00	36.16	37.03	33.057	34.439	56.114	79.367
14	0.00	0.00	0.00	0.000	0.000	0.000	0.000
15	0.00	0.00	0.00	0.000	0.000	0.000	0.000

N1 And FAVAD Parameters (Leak Simulation)

N1 Equation:

$$Q = C_d A\sqrt{2gh}$$
$$Q = C_d\sqrt{2g}\,Ah^{0.5}$$
$$Q = C_{N1}Ah^{N1}$$

FAVAD Equation:

$$Q = C_d A\sqrt{2gh} \quad but \quad A = A_0 + mH$$
$$\therefore C_d A = Q/\sqrt{2gh} \qquad Q = C_d\sqrt{2gh}(A_0 + mh)$$
$$Q = C_d\sqrt{2g}\,(A_0 h^{0.5} + mh^{1.5})$$

Node 0: N1 Relationship

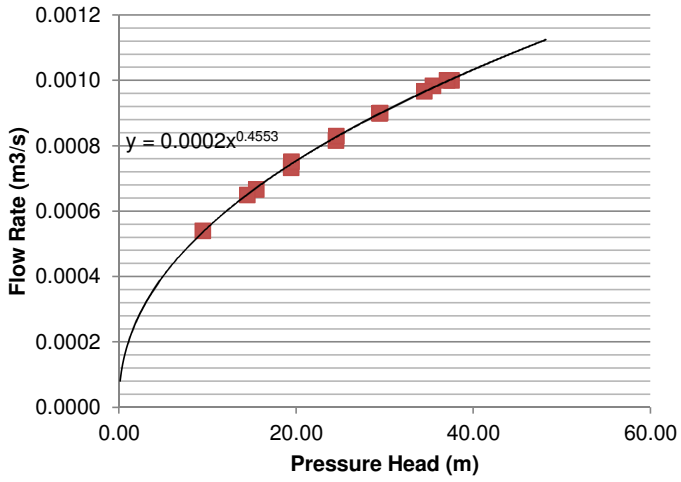

N1 Parameters:

Leakage Coefficient (CN1):	0.00019
Leakage Exponent (N1):	0.45530

Node 0: FAVAD Relationship

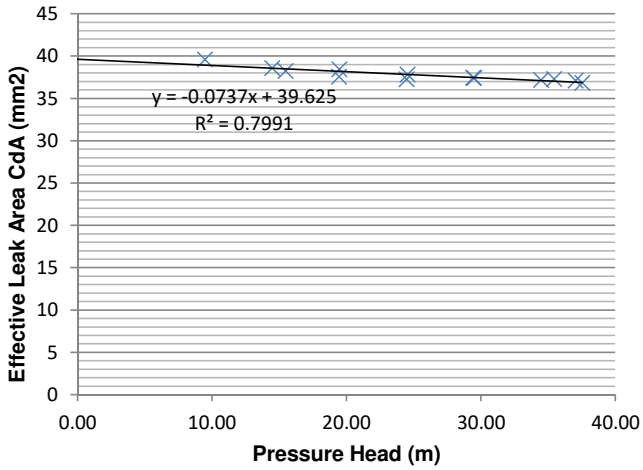

FAVAD Parameters:

Effective Initial Leak Area CdA0	39.625	mm
Effective head-area slope Cdm:	-0.074	mm2/m

Node 1: N1 Relationship

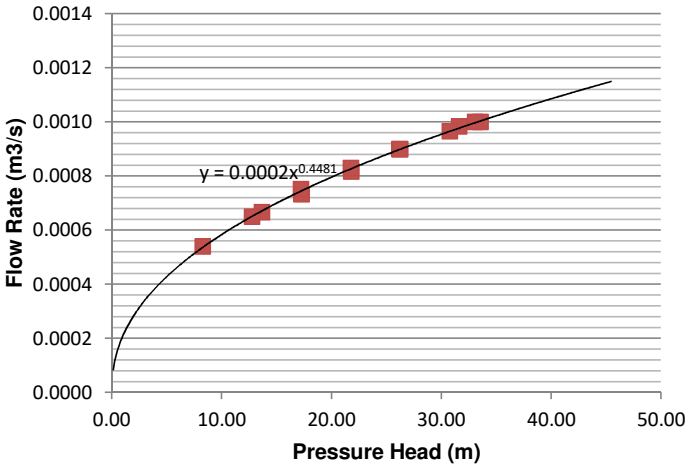

N1 Parameters:

Leakage Coefficient (C):	0.00021
Leakage Exponent (N1):	0.44805

Node 1: FAVAD Relationship

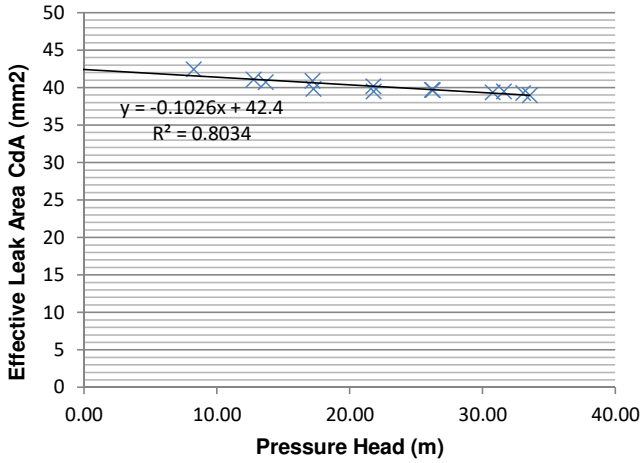

FAVAD Parameters:

Effective Initial Leak Area CdA0	42.400	mm
Effective head-area slope Cdm:	-0.103	mm2/m

N1 And FAVAD Parameters (Leak Simulation)

Node 2: N1 Relationship

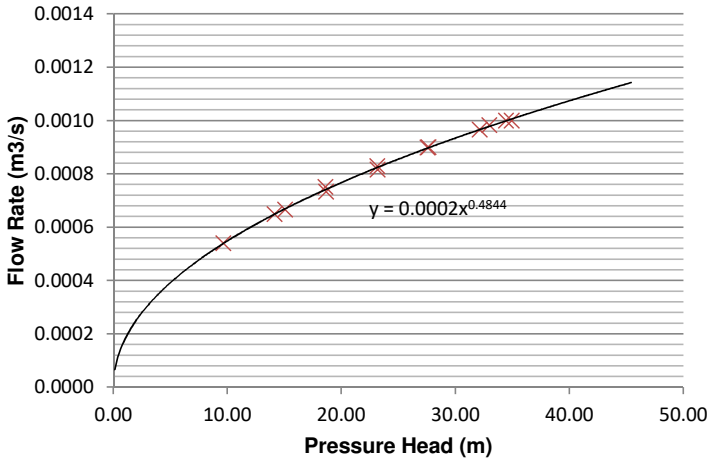

N1 Parameters:

Leakage Coefficient (C):	0.00018
Leakage Exponent (N1):	0.48440

Node 2: FAVAD Relationship

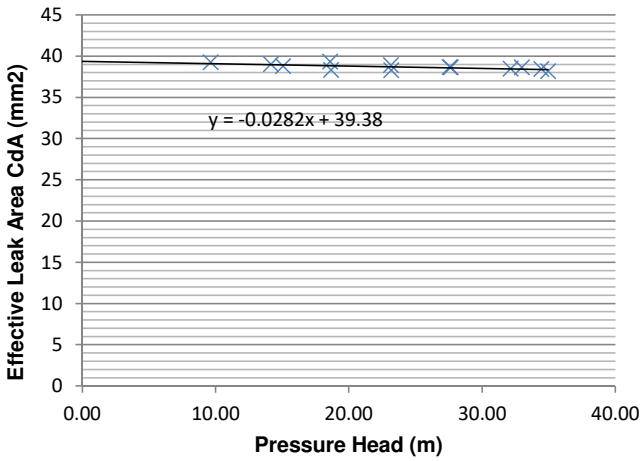

FAVAD Parameters:

Effective Initial Leak Area CdA0	39.380	mm
Effective head-area slope Cdm:	-0.028	mm2/m

Node 3: N1 Relationship

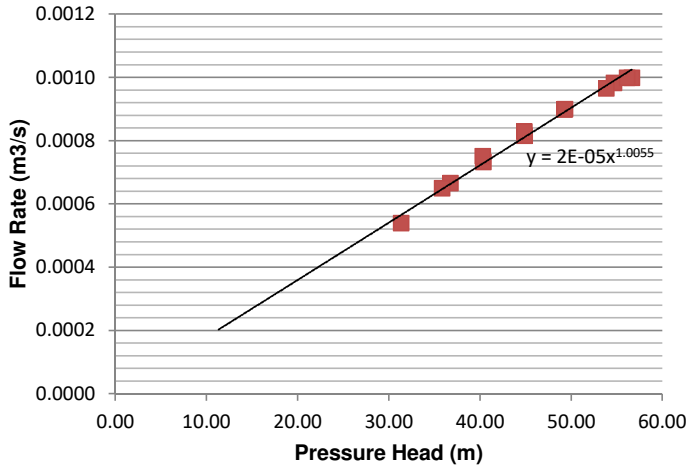

N1 Parameters:

Leakage Coefficient (C):	0.00002
Leakage Exponent (N1):	1.00551

Node 3: FAVAD Relationship

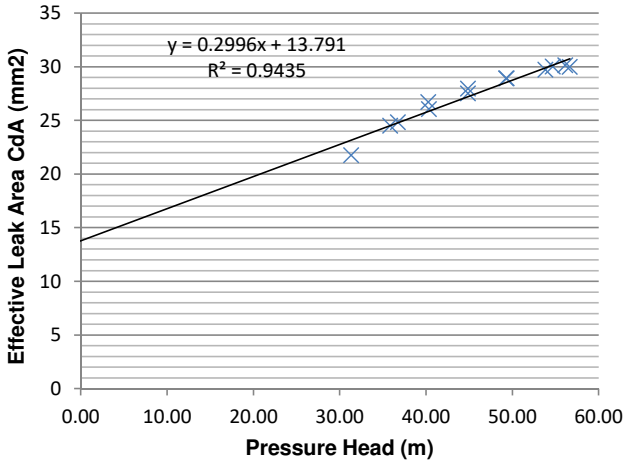

FAVAD Parameters:

Effective Initial Leak Area CdA0	13.791	mm
Effective head-area slope Cdm:	0.300	mm2/m

Node 4: N1 Relationship

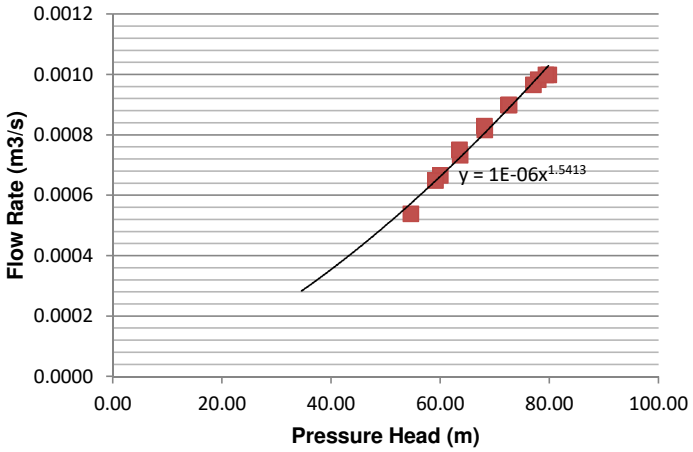

N1 Parameters:

Leakage Coefficient (C):	0.00000
Leakage Exponent (N1):	1.54133

Node 4: FAVAD Relationship

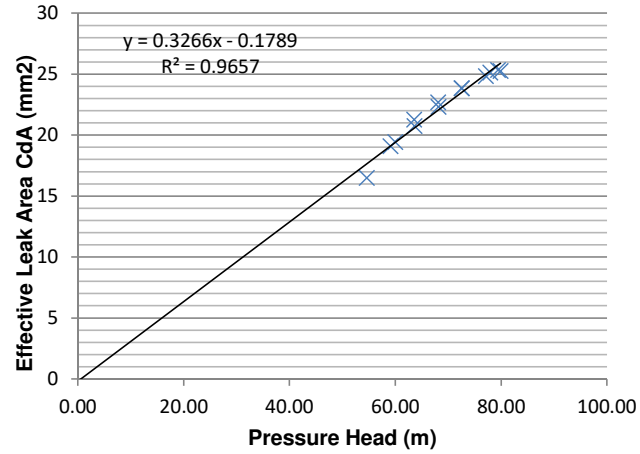

FAVAD Parameters:

Effective Initial Leak Area CdA0	-0.179	mm
Effective head-area slope Cdm:	0.327	mm2/m

Summary (Leak Simulation)

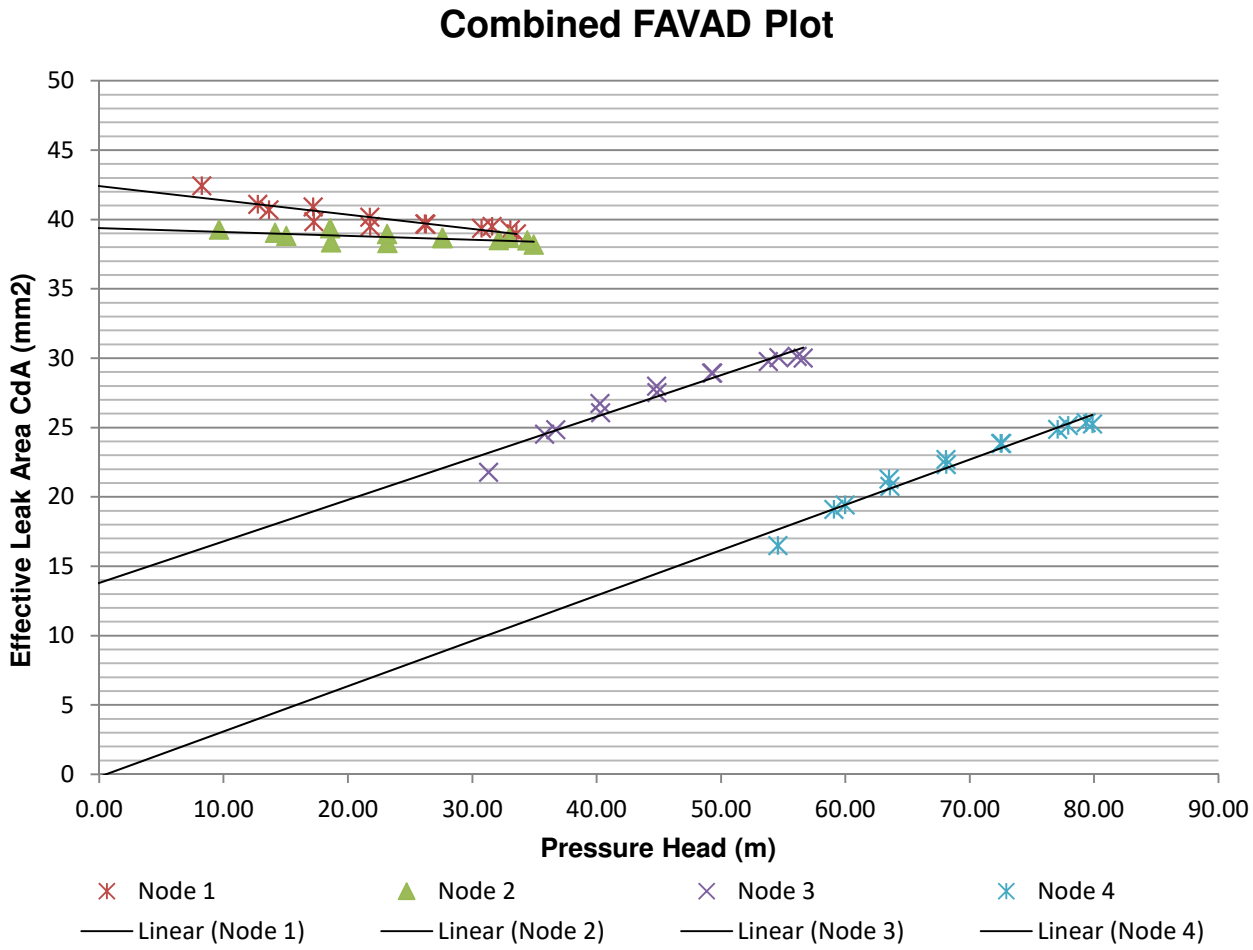

Conclusion:

At Node 2, where the leak was simualted, the head-area slope is very flat. This would be expected for a ball valve, as its area is rigid and resistant to changes resulting from pressure.

Pressure Drop Test (Section 1&2, AC and Steel pipe)

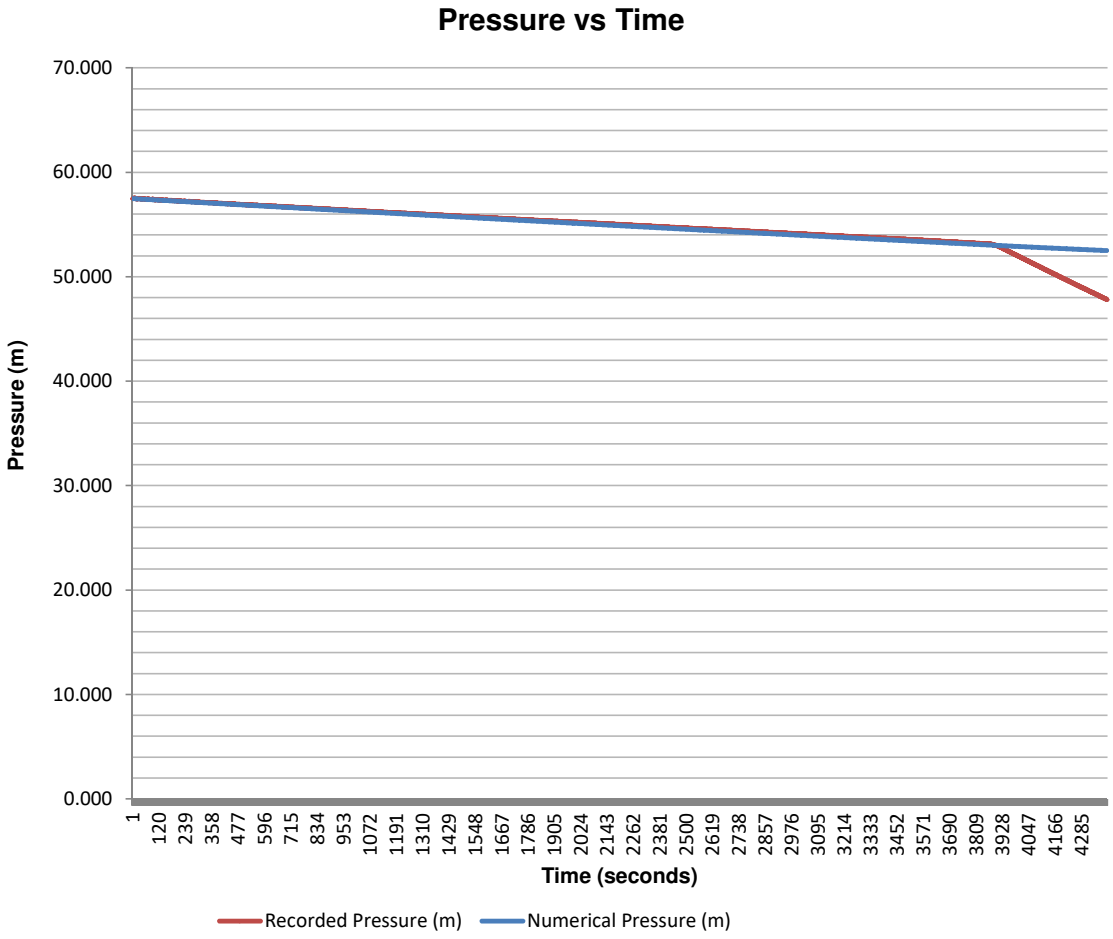

Mass Calculation:	Mo	2.44E+05	kg	
	CA0		**Cm**	
Optimised Effective Leak Area and Effective Pressure-Area Slope:	1.00E-09	m^2	1.00E-08	m^2/m
	1.00E-03	mm^2	1.00E-02	mm^2/m

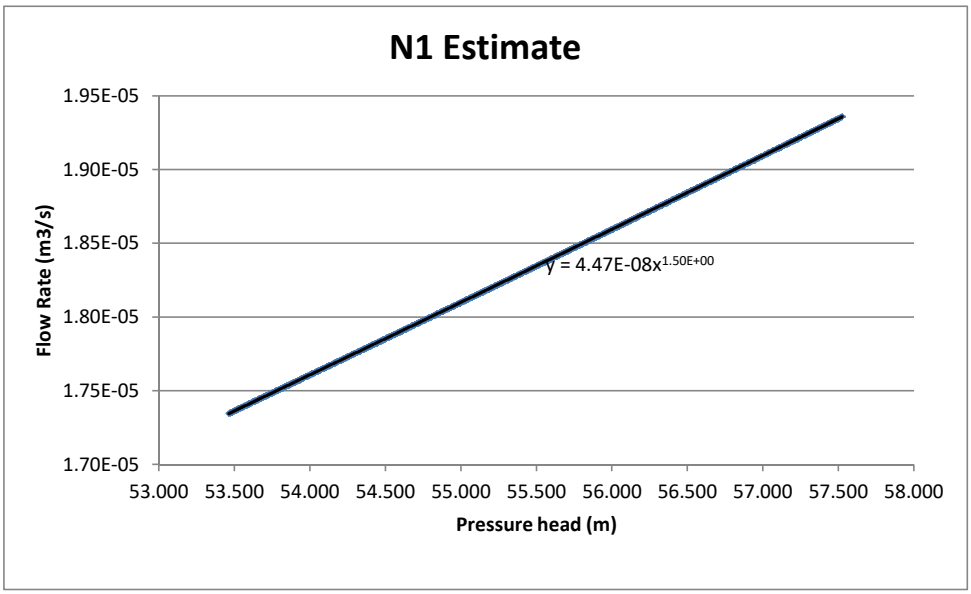

Pressure Drop Test (Section 1, AC Pipe)

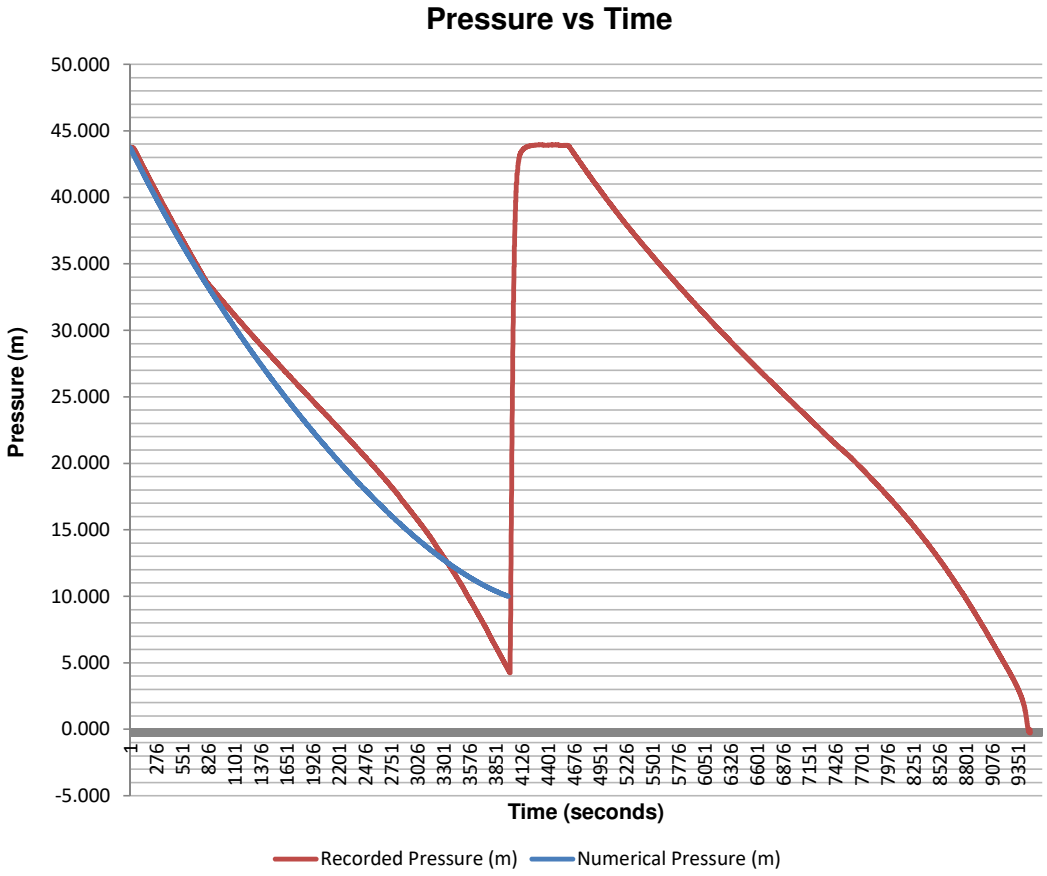

Mass Calculation: Mo		2.94E+04	kg	
	CA0		**Cm**	
Optimised Effective Leak Area	5.00E-07	m^2	1.00E-08	m^2/m
and Effective Pressure-Area Slope:	5.00E-01	mm^2	0.01	mm^2/m

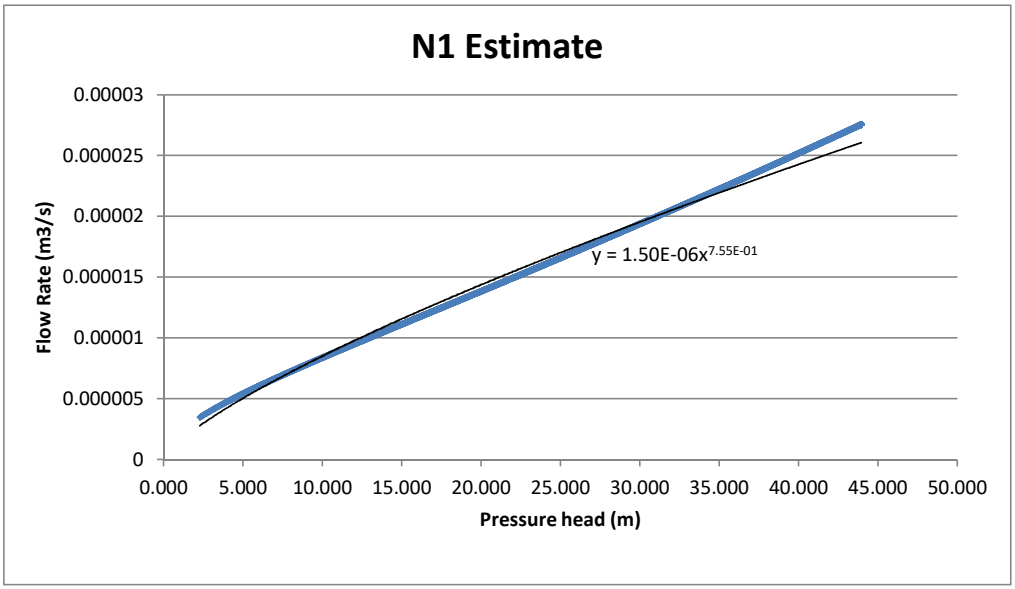

Test Report and Analysis

Pipe:

Florauna Reservoir Supply Line

Testing Date:

22 August 2018

Contents:

General Test Description

Description:

The map in figure 1 shows the pipeline route. The tested pipeline starts with a pressure regulating valve (PRV) (V1) just upstream of the duty and stand-by pumps. The pipeline then rises up to the valve chamber shortly before the Florauna Reservoir. The pipe then branches into a bypass and into a reservoir input. Both branches were isolated by gate valves. A 1 inch connection point directly to the main pipe in the valve chamber served as an ideal connection point for the equipment.
Due to the long length from the connection point to the trailer, the supply pipe was lengthened to 20 metres for this test.

Figure 1: Map showing pipeline route starting at V1 and ending at V2

Figure 2: Testing Equipment setup at Florauna reservoir

Figure 3&4: Connection point

General Test Information

Pipeline:	Florauna Reservoir Supply Line
Area:	Pretoria North, Florauna
Pipe Owner:	Tshwane Municipality
Date:	22 Aug 18
Time:	13:00 - 14:15

Pipeline Section:	**Section 1**	**Section 2**	**Section 3**	
Pipe length (m):	1260			
Pipe Diameter (mm):	300			
Pipe Material:	Steel			
Absolute Roughness e (mm)	0.5			
Minor Losses/km	1			
Upstream Isolation:	PRV			
Upstream Source:	Pump Station			
Upstream Pressure (Bar) approx:	low			
Upstream Isolation Elevation (m):				
Downstream Isolation:	Gate Valve			
Downstream Delivery:	Reservoir			
Downstream Pressure (Bar) approx:	<1			
Downstream Isolation Elevation (m):				

Connection of Testing Equipment

Connection Type:	1 Inch Threaded Connection **Length of Equipment Supply Pipe Double (20m)**	
Connection Fitting size (mm):	25	
Comment on Fitting:	1 inch isolation valve, 1 inch connection piece, 1 inch Geka coupling, 1 inch 300mm long pipework into main pipe.	
Minor loss coefficient of fitting	1 Inch Threaded M or F with Tap	7.98
Static height difference (A) in (m):	-0.1	

Connection pipes*:

	Pipe 1	**Pipe 2**
Length of connection pipe* (mm):	300	0
Diameter of connection pipes (mm)	25	25
Absolute Roughness e (mm)	0.2	0
Static height difference (B) in (mm):	300	0

Minor losses of fittings on connection pipes*:

	Fitting 1	**Fitting 2**	**Fitting 3**	**Fitting 4**
Fitting type:	Exit loss	None	None	None
Pipe 1 or Pipe 2	1	1	1	1
Fitting diameter in (mm):	25	25	80	200
Fitting diameter out (mm):	25	25	80	400
Absolute Roughness e (mm)	0.1	0.1	0.1	0.2
No. of fittings:	1	1	1	1
Fitting Minor Loss Coefficient:	1.0000	0.0000	0.0000	0.0000
** Pipes and Fittings between the connection point and the main pipeline*			SUM:	1.00000

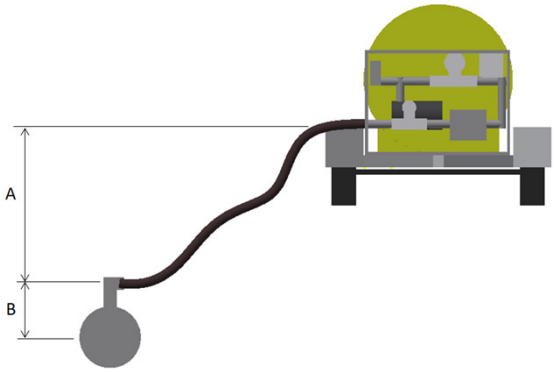

Pipeline Elevation Profile

Geocontext Website

Elevation Profile

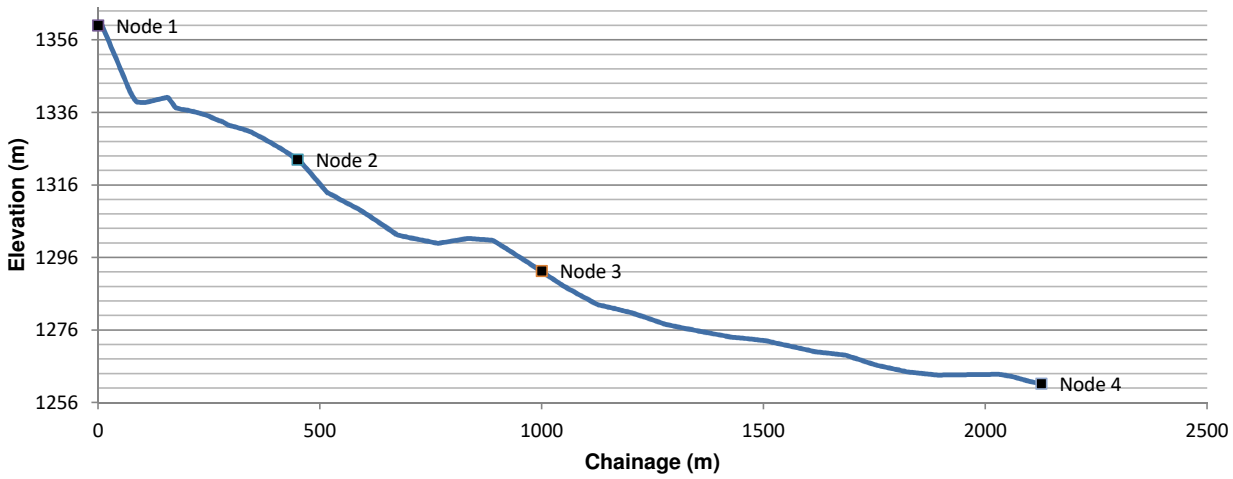

	Distance (m)	Elevation (m)	Material
1	0	1359.991821	Steel
1	4.160977879	1360.096802	Steel
1	8.321955758	1360.126343	Steel
1	12.48293364	1358.924683	Steel
1	16.64391152	1357.723022	Steel
1	20.8048894	1356.521362	Steel
1	24.96586727	1355.31958	Steel
1	29.12684515	1354.11792	Steel
1	33.28782303	1352.91626	Steel
1	37.44880091	1351.7146	Steel
1	41.60977879	1350.512939	Steel
1	45.77075667	1349.311279	Steel
1	49.93173455	1348.109619	Steel
1	54.09271243	1346.907959	Steel
1	58.25369031	1345.706299	Steel
1	62.41466819	1344.50415	Steel
1	66.57564606	1343.302124	Steel
1	70.73662394	1342.100098	Steel
1	74.89760182	1341.027466	Steel
1	79.0585797	1340.231445	Steel
1	83.21955758	1339.435791	Steel
1	87.38053546	1338.893677	Steel
1	91.54151334	1338.852783	Steel
1	95.70249122	1338.812012	Steel
1	99.8634691	1338.771118	Steel
1	104.024447	1338.730225	Steel
1	108.1854249	1338.817749	Steel
1	112.3464027	1338.938843	Steel
1	116.5073806	1339.059937	Steel
1	120.6683585	1339.181152	Steel
1	124.8293364	1339.302246	Steel
1	128.9903142	1339.42334	Steel
1	133.1512921	1339.544434	Steel
1	137.31227	1339.665649	Steel
1	141.4732479	1339.786743	Steel
1	145.6342258	1339.907837	Steel
1	149.7952036	1340.028931	Steel
1	153.9561815	1340.150146	Steel
1	158.1171594	1340.057129	Steel
1	162.2781373	1339.360229	Steel

No. of Sections:	1	
Section	**Start (m)**	**Material**
1	0	Steel
2	0	0
3		0

**If multiple sections exist, the Node points below must intercept at point where section changes for accurate pressure loss calculations.*

	Chainage (m)	Elevation (m)	End/part of Section
Node 1	0	1359.992	N/A
Node 2	450	1322.986	1
Node 3	1000	1292.236	1
Node 4	2126.26	1261.185	1

Total Chainage = 2126.26 m

Distance/Elevation Data Continues

Plot and Data Points 1

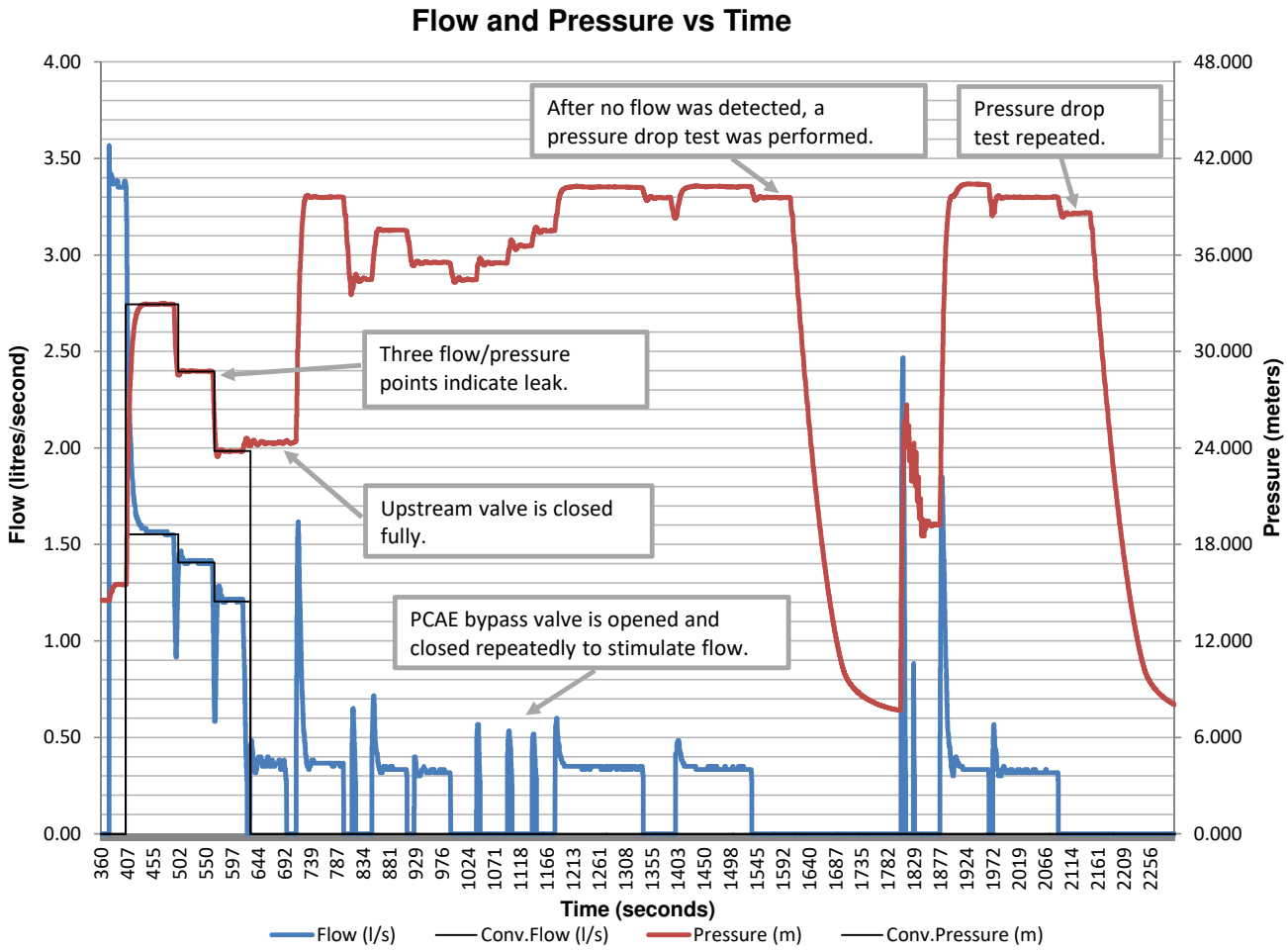

Pressure Head Correction

Corrected pressure at every Node:

Reynold's Number

$$\mathrm{Re} = \frac{\rho \mathrm{VD}}{\mu} = \frac{\mathrm{VD}}{\nu} = \frac{\mathrm{QD}}{\nu A}$$

Colebrook-White

$$\frac{1}{\sqrt{f}} = -2\log_{10}\left(\frac{\varepsilon}{3.7D} + \frac{2.51}{R_e\sqrt{f}}\right)$$

Minor Loss Equation

$$h_L = K_L\frac{V^2}{2g}$$

Darcy-Weissbach

$$h_f = f\frac{L}{D}\frac{V^2}{2g}$$

			Corrected Head (m)				
Point	**Flow (l/s)**	**Measured Head (m)**	**Node 0**	**Node 1**	**Node 2**	**Node 3**	**Node 4**
1	1.55	32.94	31.95	25.334	62.325	93.056	124.071
2	1.41	28.77	27.93	22.552	59.546	90.280	121.301
3	1.20	23.81	23.16	19.298	56.295	87.034	118.063
4	0.00	0.00	0.00	0.000	0.000	0.000	0.000
5	0.00	0.00	0.00	0.000	0.000	0.000	0.000
6	0.00	0.00	0.00	0.000	0.000	0.000	0.000
7	0.00	0.00	0.00	0.000	0.000	0.000	0.000
8	0.00	0.00	0.00	0.000	0.000	0.000	0.000
9	0.00	0.00	0.00	0.000	0.000	0.000	0.000
10	0.00	0.00	0.00	0.000	0.000	0.000	0.000
11	0.00	0.00	0.00	0.000	0.000	0.000	0.000
12	0.00	0.00	0.00	0.000	0.000	0.000	0.000
13	0.00	0.00	0.00	0.000	0.000	0.000	0.000
14	0.00	0.00	0.00	0.000	0.000	0.000	0.000
15	0.00	0.00	0.00	0.000	0.000	0.000	0.000

N1 And FAVAD Parameters

N1 Equation:

$$Q = C_d A\sqrt{2gh}$$
$$Q = C_d\sqrt{2g}Ah^{0.5}$$
$$Q = C_{N1}Ah^{N1}$$

FAVAD Equation:

$$Q = C_d A\sqrt{2gh} \quad but \quad A = A_0 + mH$$
$$\therefore C_d A = Q/\sqrt{2gh} \qquad Q = C_d\sqrt{2gh}(A_0 + mh)$$
$$Q = C_d\sqrt{2g}\,(A_0 h^{0.5} + mh^{1.5})$$

Node 0: N1 Relationship

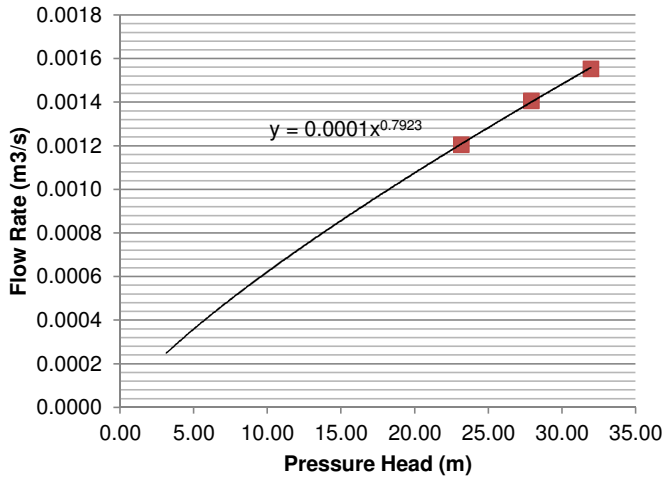

N1 Parameters:

Leakage Coefficient (CN1):	0.00010
Leakage Exponent (N1):	0.79234

Node 0: FAVAD Relationship

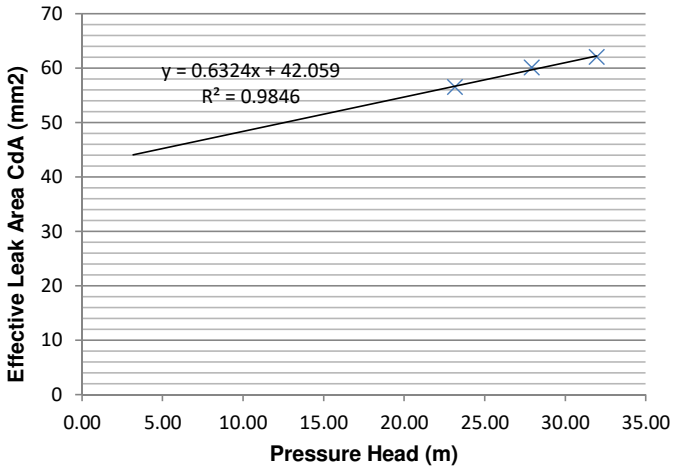

FAVAD Parameters:

Effective Initial Leak Area CdA0:	42.059	mm
Effective head-area slope Cdm:	0.632	mm2/m

Node 1: N1 Relationship

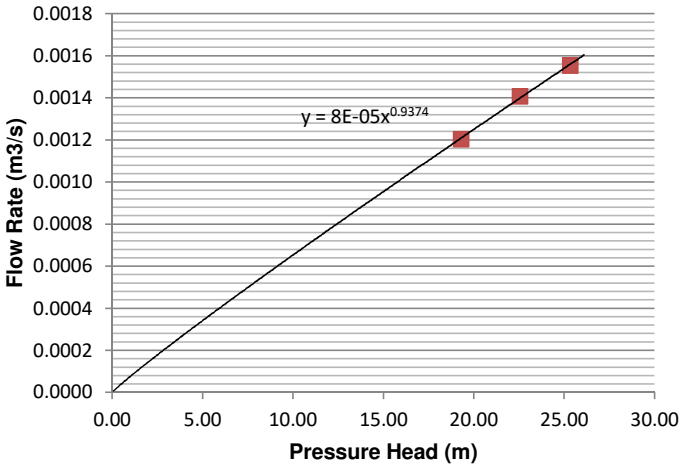

N1 Parameters:

Leakage Coefficient (C):	0.00008
Leakage Exponent (N1):	0.93743

Node 1: FAVAD Relationship

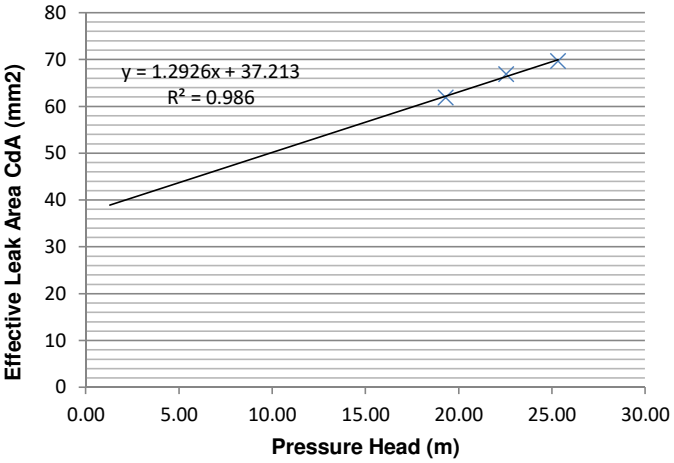

FAVAD Parameters:

Effective Initial Leak Area CdA0:	37.213	mm
Effective head-area slope Cdm:	1.293	mm2/m

N1 And FAVAD Parameters

Node 2: N1 Relationship

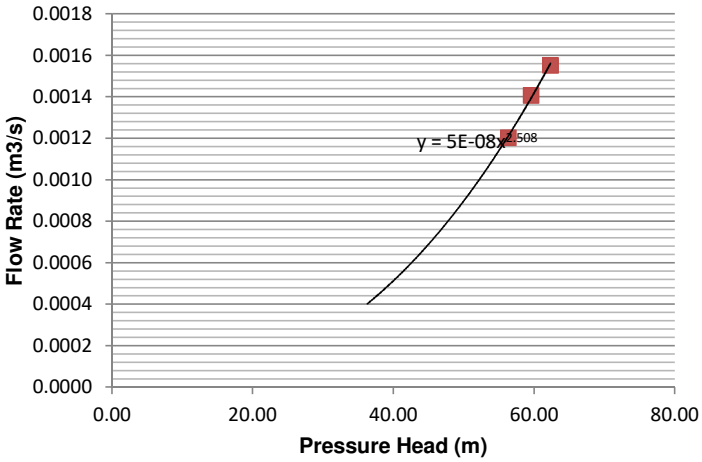

N1 Parameters:

Leakage Coefficient (C):	0.00000
Leakage Exponent (N1):	2.50798

Node 2: FAVAD Relationship

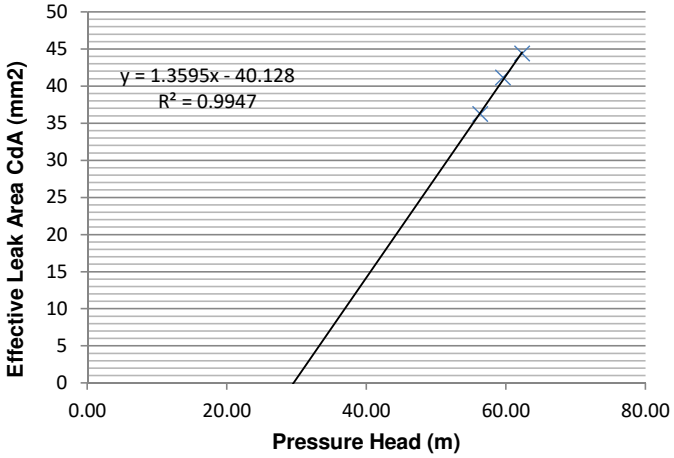

FAVAD Parameters:

Effective Initial Leak Area CdA0:	-40.128	mm
Effective head-area slope Cdm:	1.360	mm2/m

Node 3: N1 Relationship

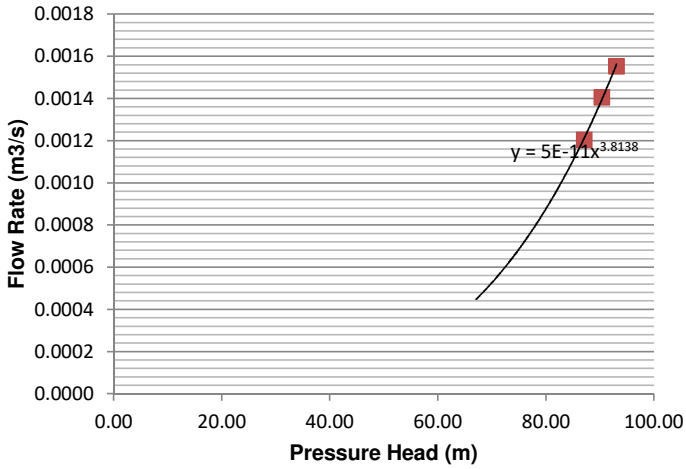

N1 Parameters:

Leakage Coefficient (C):	0.00000
Leakage Exponent (N1):	3.81380

Node 3: FAVAD Relationship

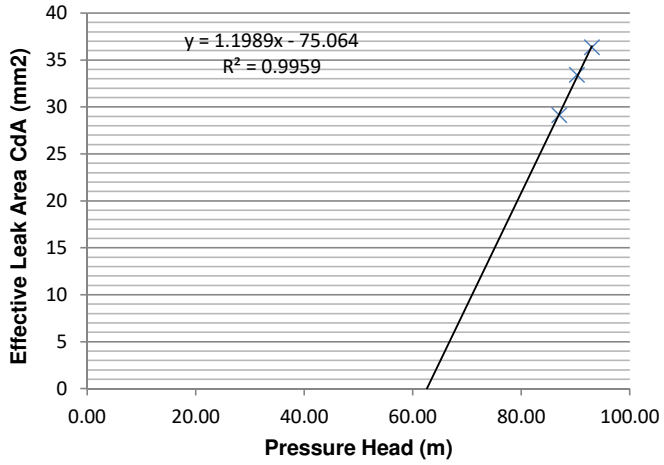

FAVAD Parameters:

Effective Initial Leak Area CdA0:	-75.064	mm
Effective head-area slope Cdm:	1.199	mm2/m

Node 4: N1 Relationship

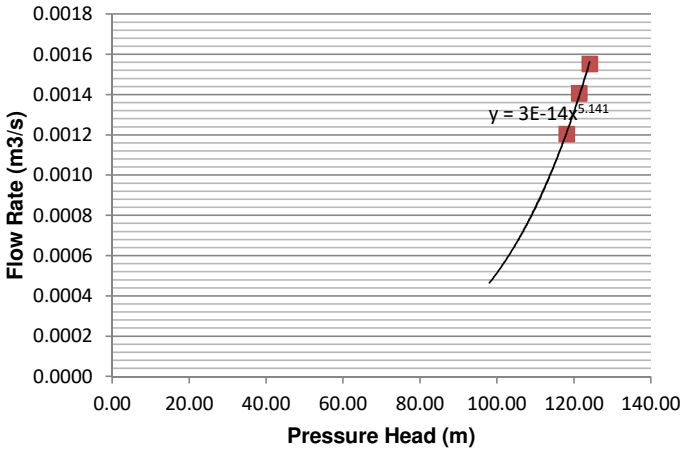

N1 Parameters:

Leakage Coefficient (C):	0.00000
Leakage Exponent (N1):	5.14096

Node 4: FAVAD Relationship

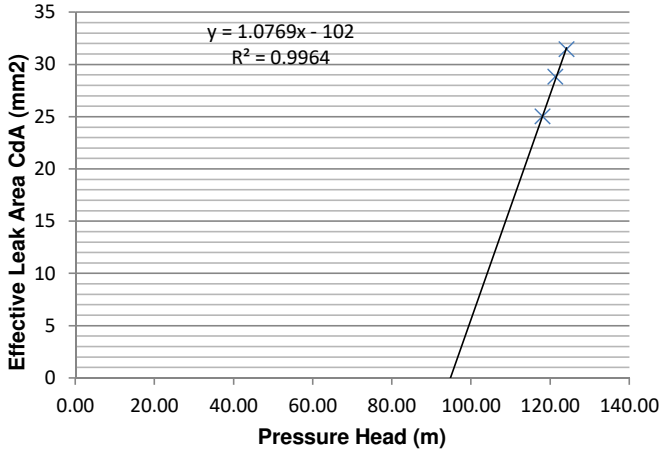

FAVAD Parameters:

Effective Initial Leak Area CdA0:	-102.004	mm
Effective head-area slope Cdm:	1.077	mm2/m

Summary

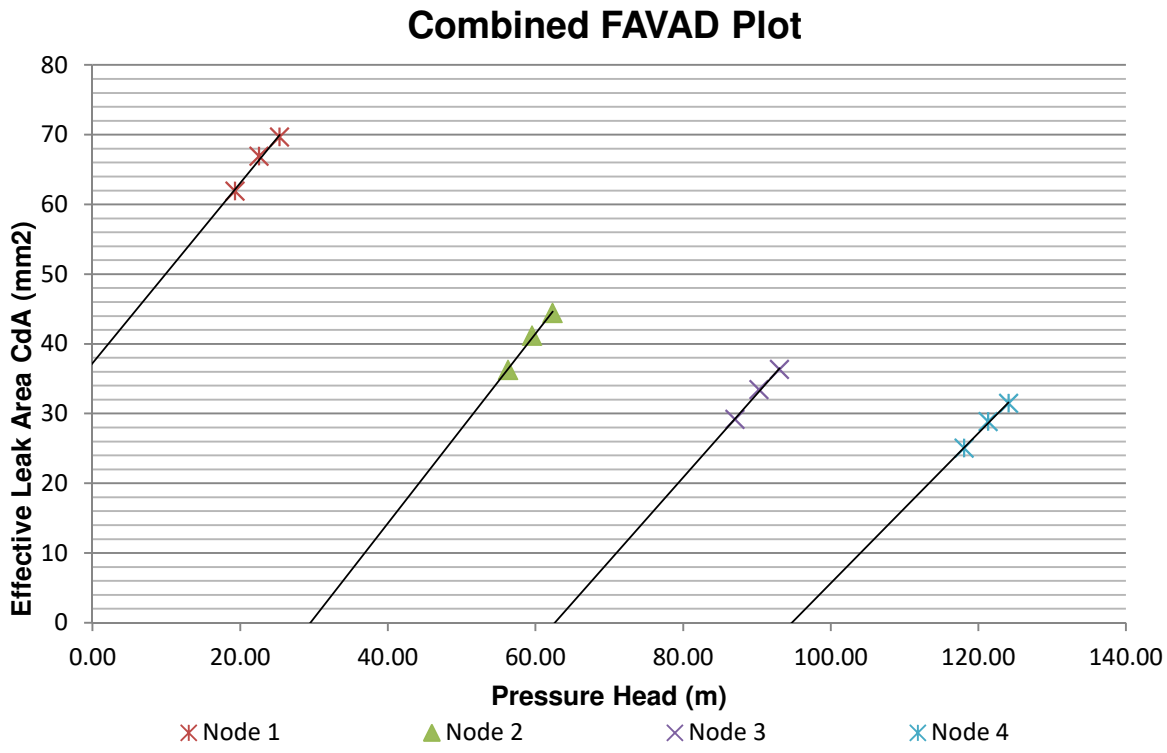

Conclusion:

Initially, the isolation valve at the reservoir-end of the pipeline did not seal. After closing this valve during the test, the leakage stopped.

The above results clearly show that the leak most likely at, or close to, Node 1, indicating a leakaing valve.

A pressure drop test was performed and a small leak was detected. The drop test data is included in the next sheet.

Pressure Drop Test

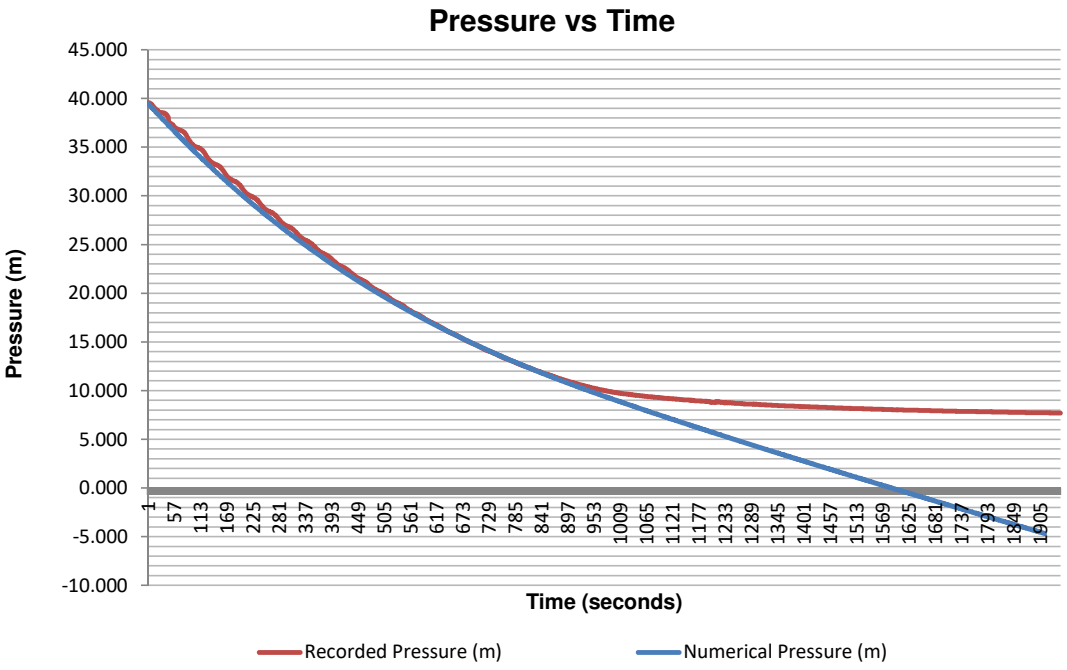

Mass Calculation: Mo		2.84E+04	kg	
	CA0		**Cm**	
Optimised Effective Leak Area and	1.80E-06	m^2	4.20E-08	m^2/m
Effective Pressure-Area Slope:	1.8	mm^2	0.042	mm^2/m

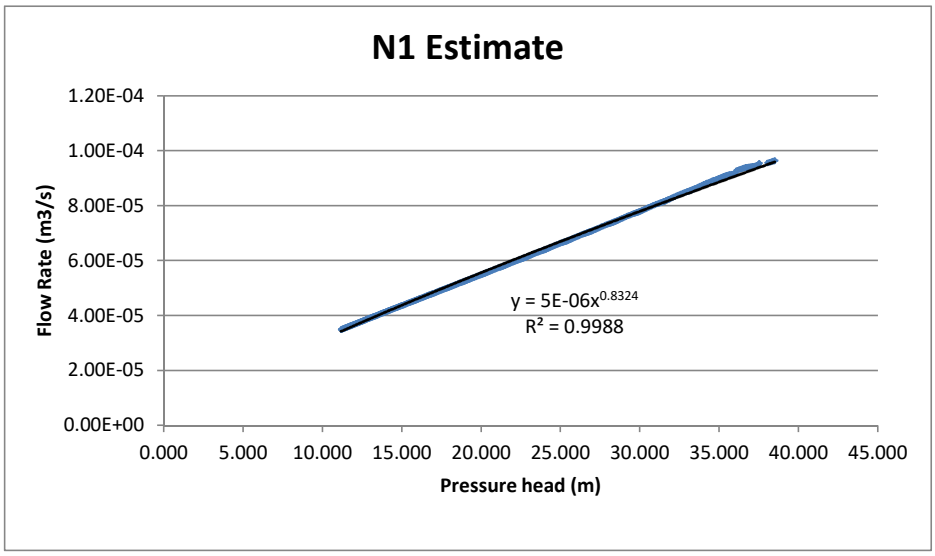

Test Report and Analysis

Pipe:

Fort Klapperkop to Carina Reservoir

Testing Date:

08 June 2018

Contents:

General Test Description

Description:

The map in figure 1 shows the pipeline route, starting at an isolation valve at the Fort Klapperkop reservoirs (V1), which is pressurised by a Rand Water line to a pressure of at least 5 bar. The pipe then rises to a maximum height after dropping down to the final isolation valves (V2) at Carina Street. At the isolating valve chamber, a number of PRVs on branches were observed, all of which had to be closed in order to isolate the pipeline.

It was also noted that a strainer on the tested pipe had a significant leak, resulting in a significant spray of water in the valve room. The spray appeared to be pressure dependant, as it significantly reduced immediately after the pipe was isolated. The size of this leak was unfortunately unknown.

Figure 1: Map showing pipeline route starting at V1 and ending at V2

Figure 2: Equipment Setup at Carina Reservoir

Figure 3: Valve Chamber Layout

Figure 4: Connection point on PRV.

General Test Information

Pipeline:	Fort Klapperkop to Carina Reservoir
Area:	Pretoria Old East, Groenkloof
Pipe Owner:	Tshwane Municipality
Date:	08 Jun 18
Time:	09:00 - 11:30

Pipeline Section:	**Section 1**	**Section 2**	**Section 3**	
Pipe length (m):	3245			
Pipe Diameter (mm):	406			
Pipe Material:	Steel			
Absolute Roughness e (mm)	0.5			
Minor Losses/km	1			
Upstream Isolation:	Pressure Reg. Valve			
Upstream Source:	Pressured Pipe			
Upstream Pressure (Bar) approx:	>5			
Upstream Isolation Elevation (m):				
Downstream Isolation:	Gate Valve			
Downstream Delivery:	Reservoir			
Downstream Pressure (Bar) approx:	>0.3			
Downstream Isolation Elevation (m):				

Connection of Testing Equipment

Connection Type:	Connection on PRV	
Connection Fitting size (mm):	30	
Comment on Fitting:	30mm female connection: Male threaded 1.25 to 1 inch reducer, 1 inch female to male, 1inch ball valve, 1 inch Geka coupling	
Minor loss coefficient of fitting	1.25 Inch (30mm) Threaded Female	15.00
Static height difference (A) in (m):	1.7	

Connection pipes*:

	Pipe 1	**Pipe 2**
Length of connection pipe* (mm):	0	1200
Diameter of connection pipes (mm)	30	150
Absolute Roughness e (mm)	0.2	0.2
Static height difference (B) in (mm):	0	0

Minor losses of fittings on connection pipes*:

	Fitting 1	**Fitting 2**	**Fitting 3**	**Fitting 4**
Fitting type:		Gate valve	None	None
Pipe 1 or Pipe 2	1	2	2	0
Fitting diameter in (mm):	30	150	150	0.05
Absolute Roughness e (mm)	0.5	0.5	0.5	0.5
No. of fittings:	1	1	1	1
Fitting Minor Loss Coefficient:	1.0000	0.0003	0.0000	0.0000
			SUM:	1.00035

** Pipes and Fittings between the connection point and the main pipeline*

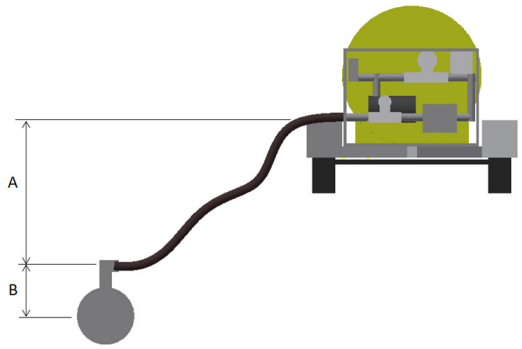

Pipeline Elevation Profile

Geocontext Website

Elevation Profile

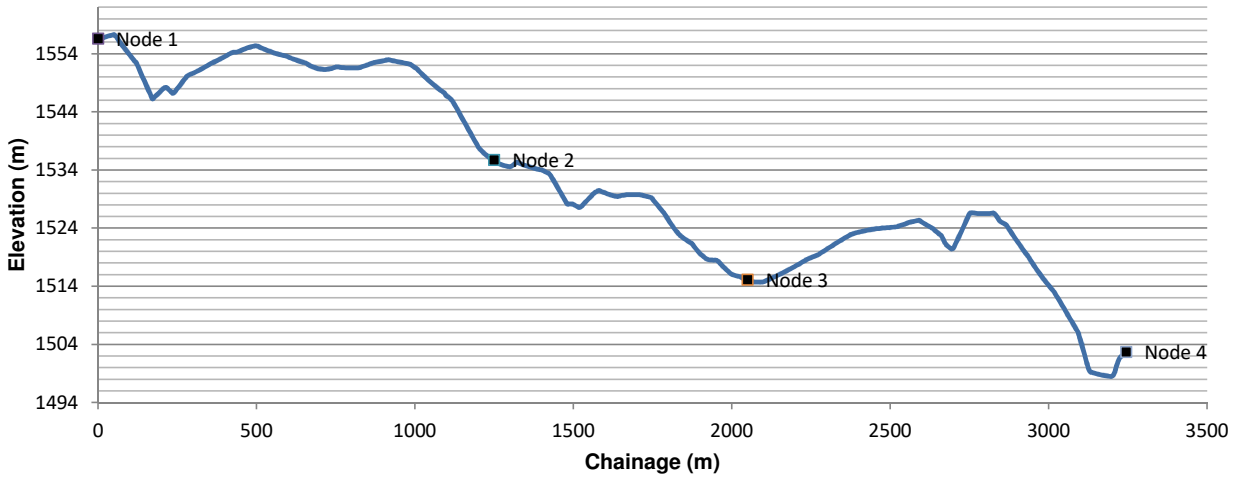

	Distance (m)	Elevation (m)	Material
1	0	1556.580811	Steel
1	6.350889428	1556.608154	Steel
1	12.70177886	1556.711914	Steel
1	19.05266828	1556.840332	Steel
1	25.40355771	1556.966309	Steel
1	31.75444714	1557.061157	Steel
1	38.10533657	1557.147339	Steel
1	44.45622599	1557.224854	Steel
1	50.80711542	1557.293701	Steel
1	57.15800485	1556.90271	Steel
1	63.50889428	1556.41394	Steel
1	69.85978371	1555.933716	Steel
1	76.21067313	1555.46228	Steel
1	82.56156256	1554.999512	Steel
1	88.91245199	1554.545288	Steel
1	95.26334142	1554.099854	Steel
1	101.6142308	1553.663086	Steel
1	107.9651203	1553.234985	Steel
1	114.3160097	1552.815552	Steel
1	120.6668991	1552.404785	Steel
1	127.0177886	1551.645752	Steel
1	133.368678	1550.849976	Steel
1	139.7195674	1550.060791	Steel
1	146.0704568	1549.277954	Steel
1	152.4213463	1548.501709	Steel
1	158.7722357	1547.731934	Steel
1	165.1231251	1546.968628	Steel
1	171.4740145	1546.258911	Steel
1	177.824904	1546.591309	Steel
1	184.1757934	1546.919556	Steel
1	190.5266828	1547.24353	Steel
1	196.8775723	1547.563354	Steel
1	203.2284617	1547.878906	Steel
1	209.5793511	1548.190308	Steel
1	215.9302405	1548.208008	Steel
1	222.28113	1547.876709	Steel
1	228.6320194	1547.542603	Steel
1	234.9829088	1547.205688	Steel
1	241.3337983	1547.421997	Steel

No. of Sections:	1	
Section	**Start (m)**	**Material**
1	0	Steel
2		0
3		0

**If multiple sections exist, the Node points below must intercept at point where section changes for accurate pressure loss calculations.*

	Chainage (m)	Elevation (m)	End/part of Section
Node 1	0	1556.581	N/A
Node 2	1250	1535.728	1
Node 3	2050	1515.119	1
Node 4	3245.30	1502.712	1

Total Chainage = 3245.30 m

Plot and Data Points (First Test)

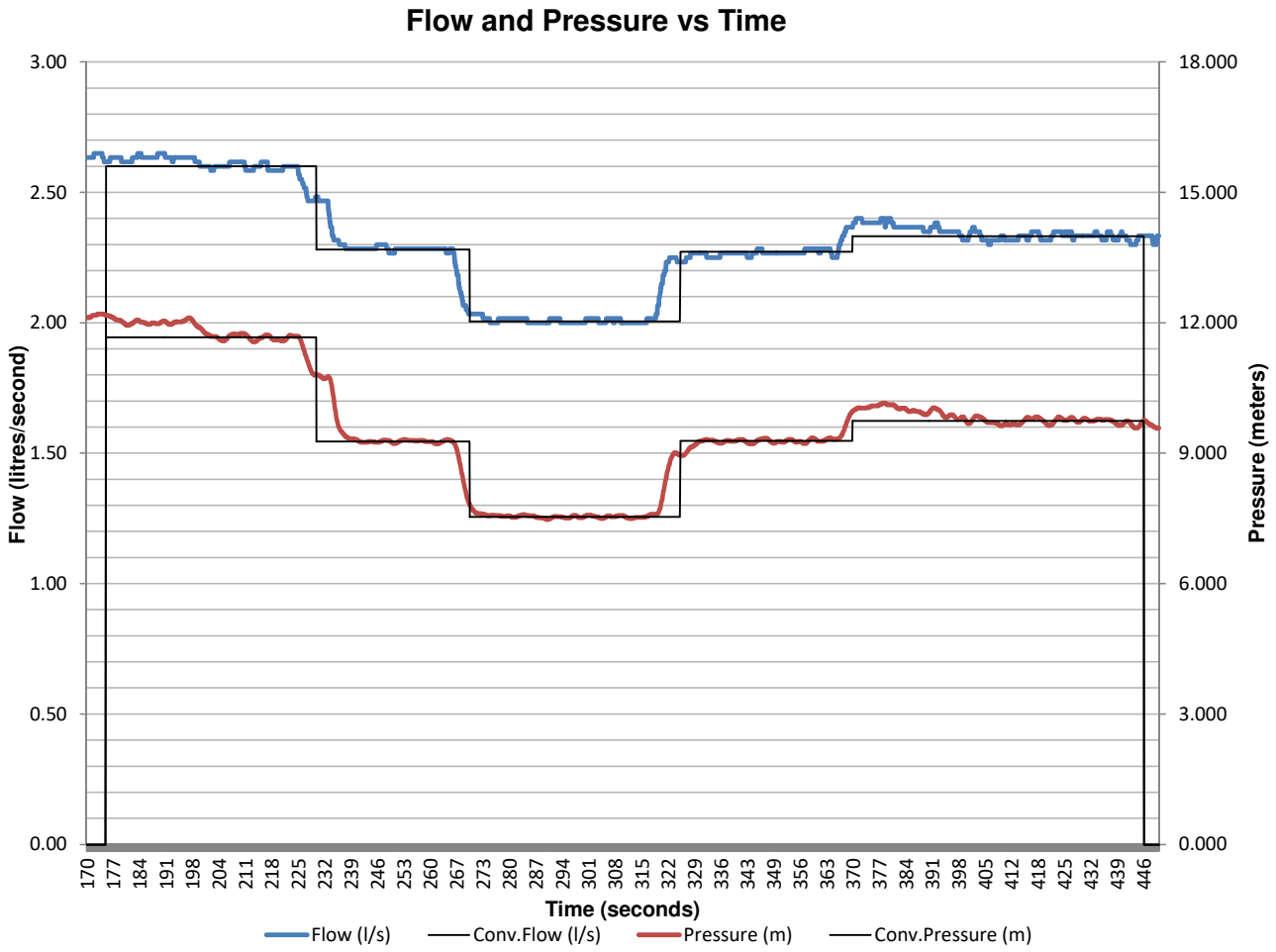

Pressure Head Correction (First Test)

Corrected pressure at every Node:

Reynold's Number

$$\mathrm{Re} = \frac{\rho \mathrm{VD}}{\mu} = \frac{\mathrm{VD}}{\nu} = \frac{\mathrm{QD}}{\nu A}$$

Colebrook-White

$$\frac{1}{\sqrt{f}} = -2\log_{10}\left(\frac{\varepsilon}{3.7D} + \frac{2.51}{R_e\sqrt{f}}\right)$$

Minor Loss Equation

$$h_L = K_L\frac{V^2}{2g}$$

Darcy-Weissbach

$$h_f = f\frac{L}{D}\frac{V^2}{2g}$$

			Corrected Head (m)				
Point	**Flow (l/s)**	**Measured Head (m)**	**Node 0**	**Node 1**	**Node 2**	**Node 3**	**Node 4**
1	2.60	11.67	10.69	10.001	30.823	51.411	63.789
2	2.28	9.27	8.90	8.371	29.200	49.793	62.177
3	2.01	7.54	7.63	7.217	28.051	48.648	61.037
4	2.27	9.29	8.93	8.405	29.234	49.827	62.211
5	2.33	9.75	9.28	8.727	29.555	50.147	62.531
6	0.00	0.00	0.00	0.000	0.000	0.000	0.000
7	0.00	0.00	0.00	0.000	0.000	0.000	0.000
8	0.00	0.00	0.00	0.000	0.000	0.000	0.000
9	0.00	0.00	0.00	0.000	0.000	0.000	0.000
10	0.00	0.00	0.00	0.000	0.000	0.000	0.000
11	0.00	0.00	0.00	0.000	0.000	0.000	0.000
12	0.00	0.00	0.00	0.000	0.000	0.000	0.000
13	0.00	0.00	0.00	0.000	0.000	0.000	0.000
14	0.00	0.00	0.00	0.000	0.000	0.000	0.000
15	0.00	0.00	0.00	0.000	0.000	0.000	0.000

N1 And FAVAD Parameters (First Test)

N1 Equation:

$$Q = C_d A\sqrt{2gh}$$
$$Q = C_d\sqrt{2g}Ah^{0.5}$$
$$Q = C_{N1}Ah^{N1}$$

FAVAD Equation:

$$Q = C_d A\sqrt{2gh} \quad but \quad A = A_0 + mH$$
$$\therefore C_d A = Q/\sqrt{2gh} \qquad Q = C_d\sqrt{2gh}(A_0 + mh)$$
$$Q = C_d\sqrt{2g}\,(A_0 h^{0.5} + mh^{1.5})$$

Node 0: N1 Relationship

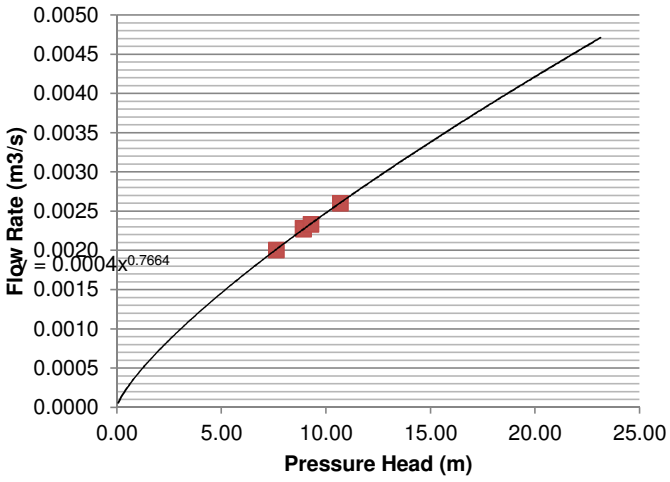

N1 Parameters:

Leakage Coefficient (CN1):	0.00042
Leakage Exponent (N1):	0.76640

Node 0: FAVAD Relationship

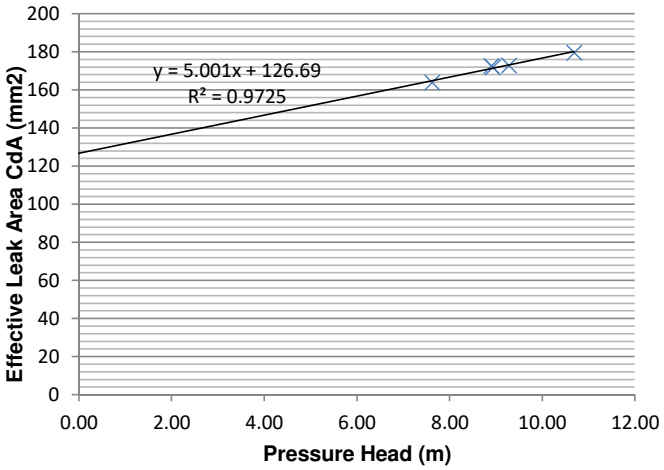

FAVAD Parameters:

Effective Initial Leak Area CdA0:	126.691	mm
Effective head-area slope Cdm:	5.001	mm2/m

Node 1: N1 Relationship

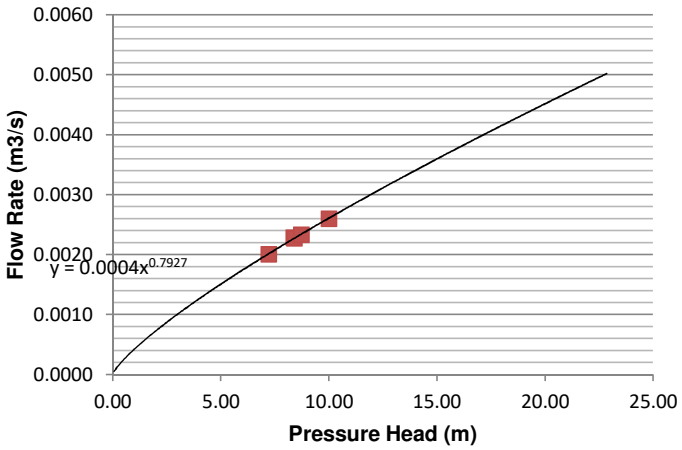

N1 Parameters:

Leakage Coefficient (C):	0.00042
Leakage Exponent (N1):	0.79274

Node 1: FAVAD Relationship

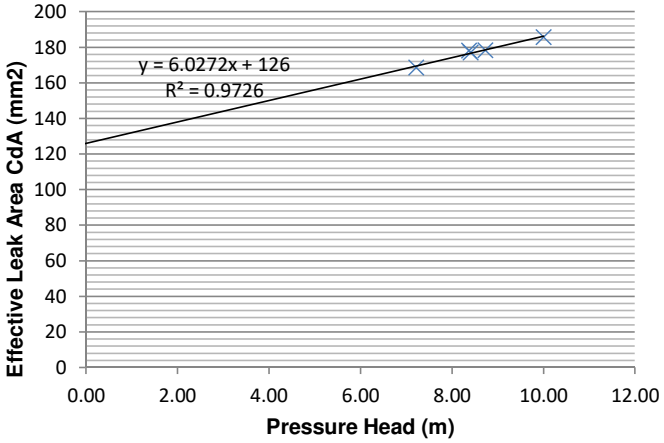

FAVAD Parameters:

Effective Initial Leak Area CdA0:	125.998	mm
Effective head-area slope Cdm:	6.027	mm2/m

N1 And FAVAD Parameters (First Test)

Node 2: N1 Relationship

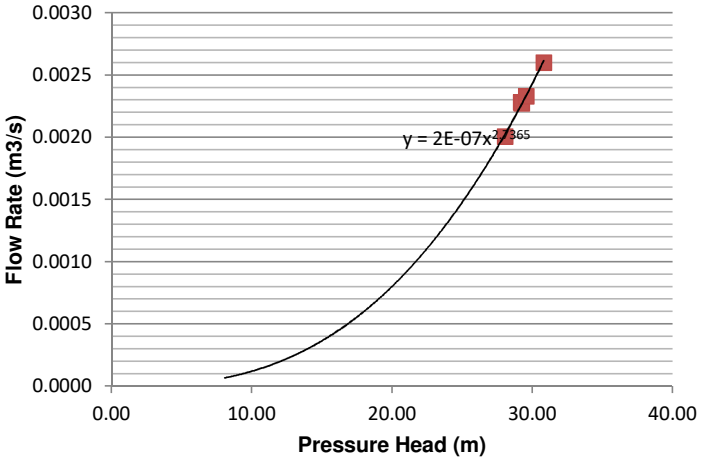

N1 Parameters:

Leakage Coefficient (C): 0.00000
Leakage Exponent (N1): 2.73650

Node 2: FAVAD Relationship

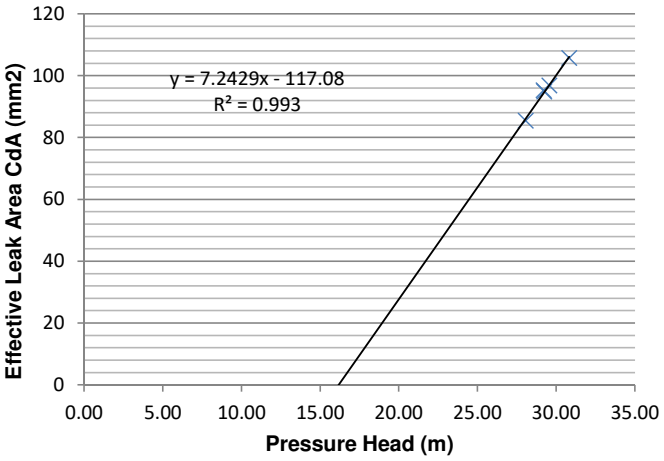

FAVAD Parameters:

Effective Initial Leak Area CdA0: -117.077 mm
Effective head-area slope Cdm: 7.243 mm2/m

Node 3: N1 Relationship

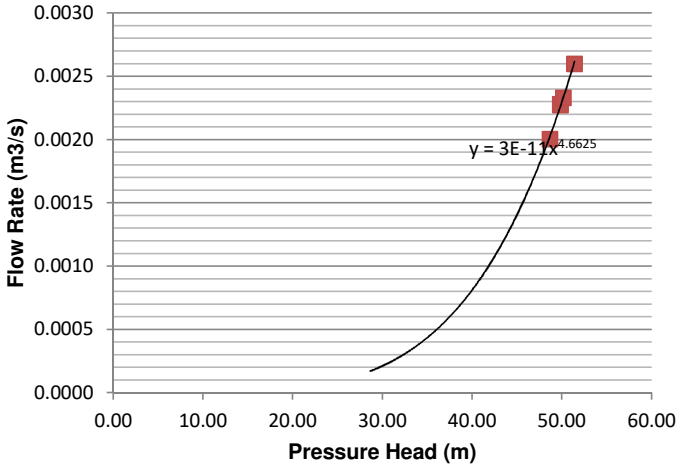

N1 Parameters:

Leakage Coefficient (C): 0.00000
Leakage Exponent (N1): 4.66252

Node 3: FAVAD Relationship

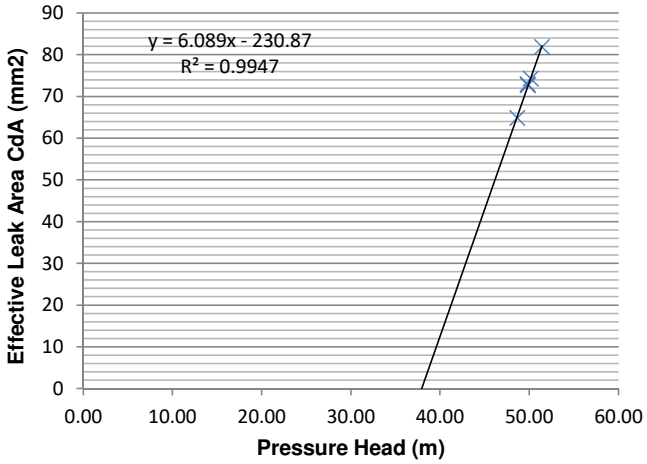

FAVAD Parameters:

Effective Initial Leak Area CdA0: -230.870 mm
Effective head-area slope Cdm: 6.089 mm2/m

Node 4: N1 Relationship

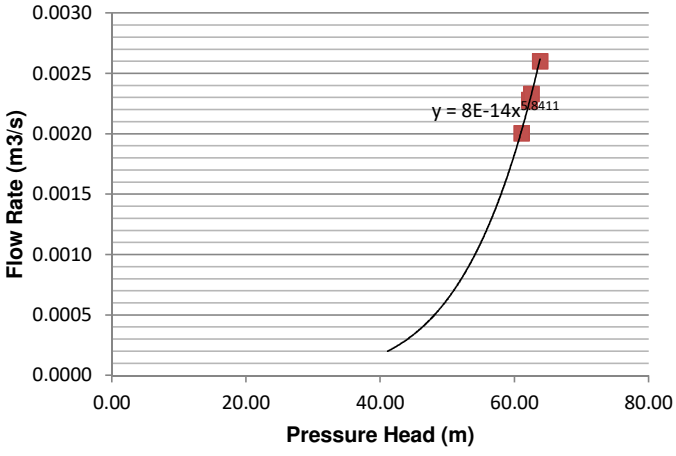

N1 Parameters:

Leakage Coefficient (C): 0.00000
Leakage Exponent (N1): 5.84107

Node 4: FAVAD Relationship

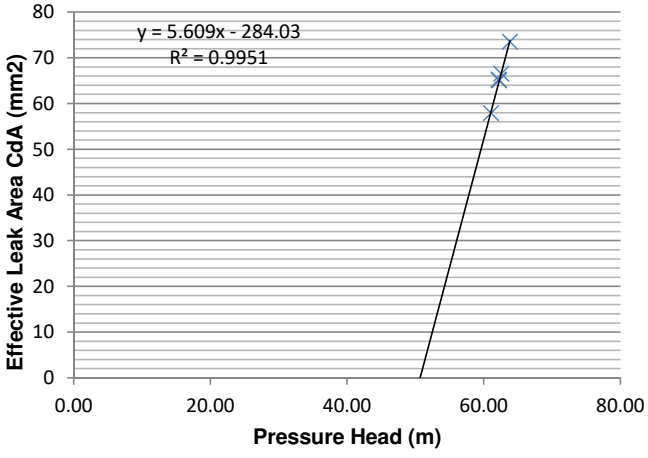

FAVAD Parameters:

Effective Initial Leak Area CdA0: -284.026 mm
Effective head-area slope Cdm: 5.609 mm2/m

Summary (First Test)

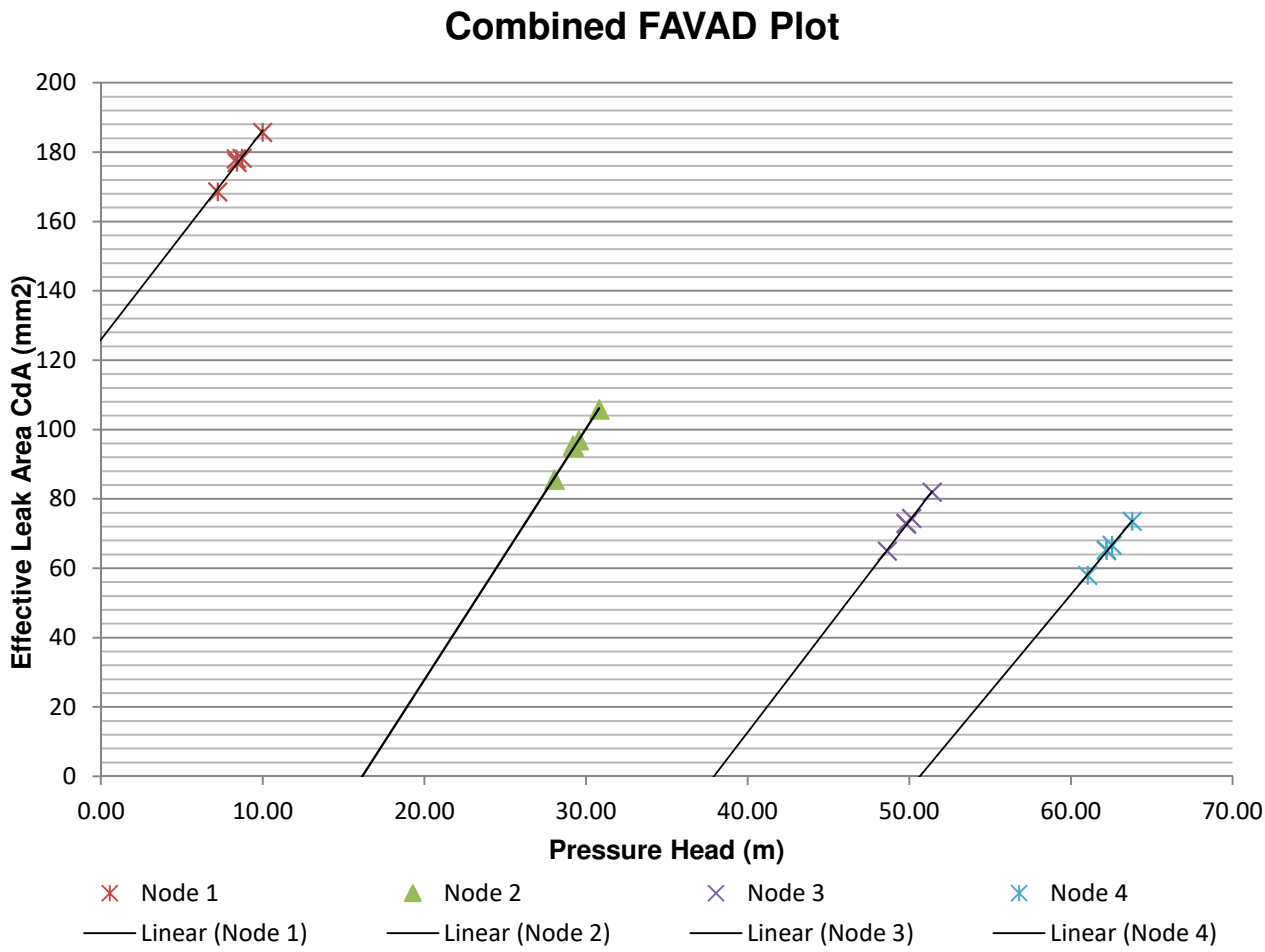

Discussion:

The existance of a very large leak close to Node 1 is clear from the results. The leaking strainer is most likely the main contributor to this leak, but due to its large size, smaller leaks along the pipeline, which are still sginificant, may be hidden.

Pressure-Flow Data (Second Test)

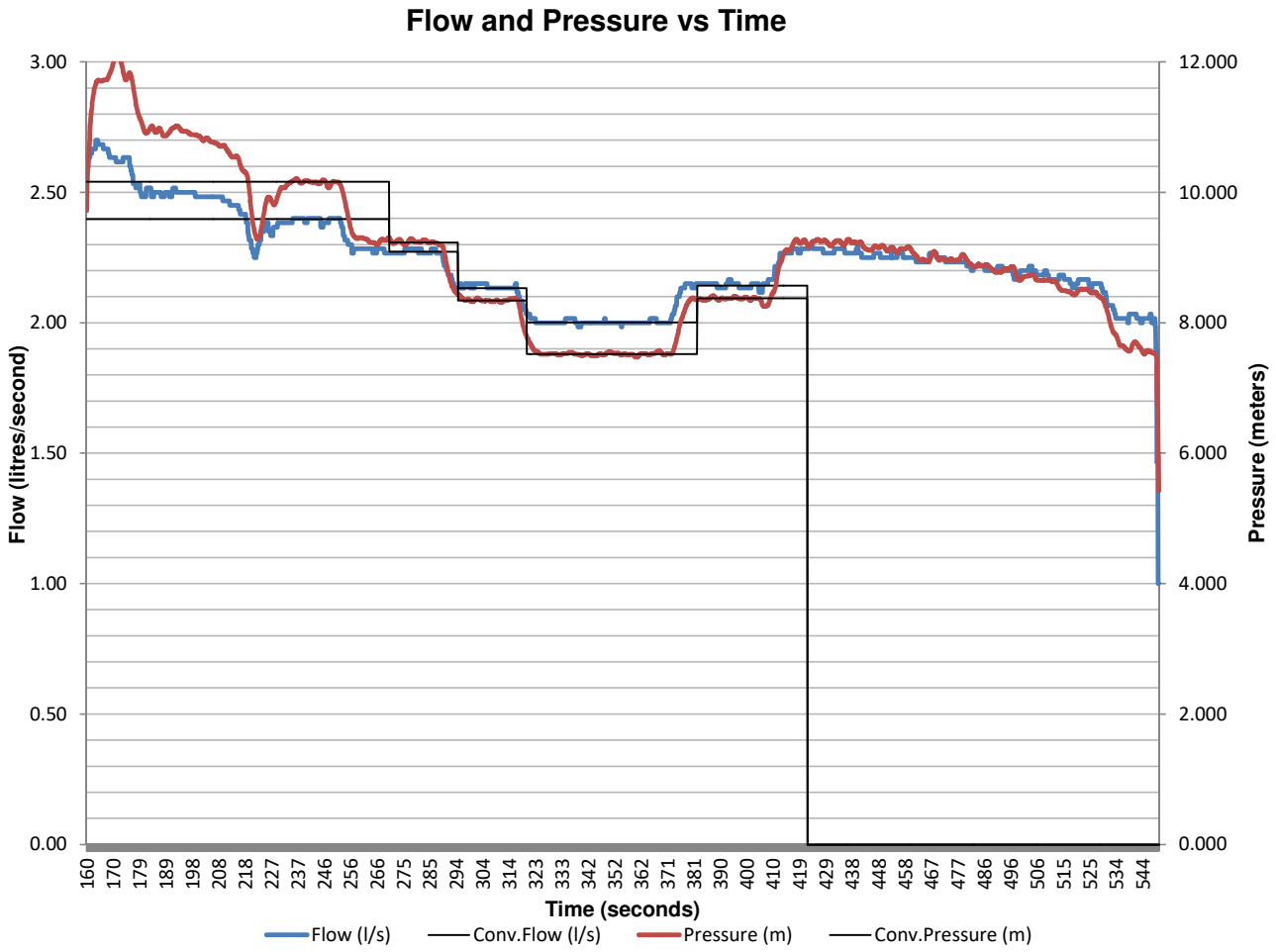

Pressure Head Correction (Second Test)

Corrected pressure at every Node:

Reynold's Number

$$\mathrm{Re} = \frac{\rho \mathrm{VD}}{\mu} = \frac{\mathrm{VD}}{\nu} = \frac{\mathrm{QD}}{\nu A}$$

Colebrook-White

$$\frac{1}{\sqrt{f}} = -2\log_{10}\left(\frac{\varepsilon}{3.7D} + \frac{2.51}{R_e\sqrt{f}}\right)$$

Minor Loss Equation

$$h_L = K_L\frac{V^2}{2g}$$

Darcy-Weissbach

$$h_f = f\frac{L}{D}\frac{V^2}{2g}$$

			Corrected Head (m)				
Point	**Flow (l/s)**	**Measured Head (m)**	**Node 0**	**Node 1**	**Node 2**	**Node 3**	**Node 4**
1	2.40	10.17	9.58	8.993	29.819	50.410	62.792
2	2.27	9.23	8.88	8.350	29.179	49.772	62.156
3	2.13	8.35	8.23	7.764	28.596	49.191	61.578
4	2.00	7.52	7.62	7.208	28.043	48.640	61.029
5	2.14	8.38	8.24	7.775	28.607	49.201	61.588
6	0.00	0.00	0.00	0.000	0.000	0.000	0.000
7	0.00	0.00	0.00	0.000	0.000	0.000	0.000
8	0.00	0.00	0.00	0.000	0.000	0.000	0.000
9	0.00	0.00	0.00	0.000	0.000	0.000	0.000
10	0.00	0.00	0.00	0.000	0.000	0.000	0.000
11	0.00	0.00	0.00	0.000	0.000	0.000	0.000
12	0.00	0.00	0.00	0.000	0.000	0.000	0.000
13	0.00	0.00	0.00	0.000	0.000	0.000	0.000
14	0.00	0.00	0.00	0.000	0.000	0.000	0.000
15	0.00	0.00	0.00	0.000	0.000	0.000	0.000

N1 And FAVAD Parameters (Second Test)

N1 Equation:

$$Q = C_d A\sqrt{2gh}$$
$$Q = C_d\sqrt{2g}Ah^{0.5}$$
$$Q = C_{N1}Ah^{N1}$$

FAVAD Equation:

$$Q = C_d A\sqrt{2gh} \quad but \quad A = A_0 + mH$$
$$\therefore C_d A = Q/\sqrt{2gh} \qquad Q = C_d\sqrt{2gh}(A_0 + mh)$$
$$Q = C_d\sqrt{2g}\,(A_0 h^{0.5} + mh^{1.5})$$

Node 0: N1 Relationship

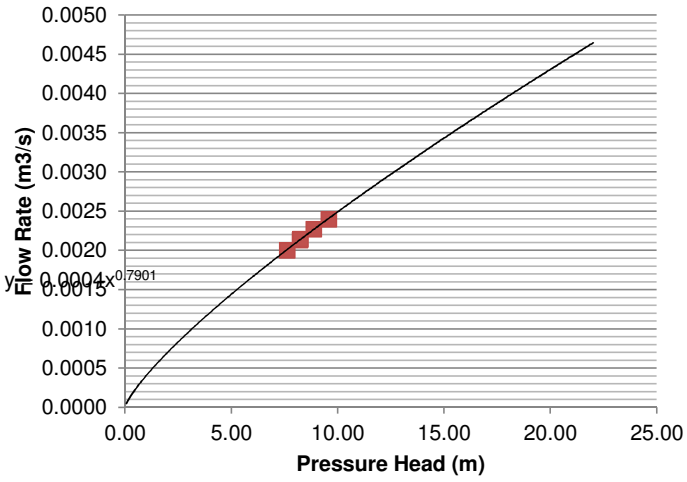

N1 Parameters:

Leakage Coefficient (CN1):	0.00040
Leakage Exponent (N1):	0.79007

Node 0: FAVAD Relationship

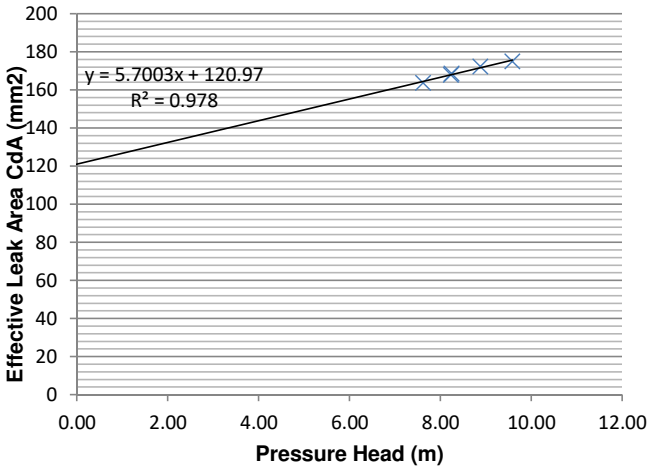

FAVAD Parameters:

Effective Initial Leak Area CdA0:	120.965	mm
Effective head-area slope Cdm:	5.700	mm2/m

Node 1: N1 Relationship

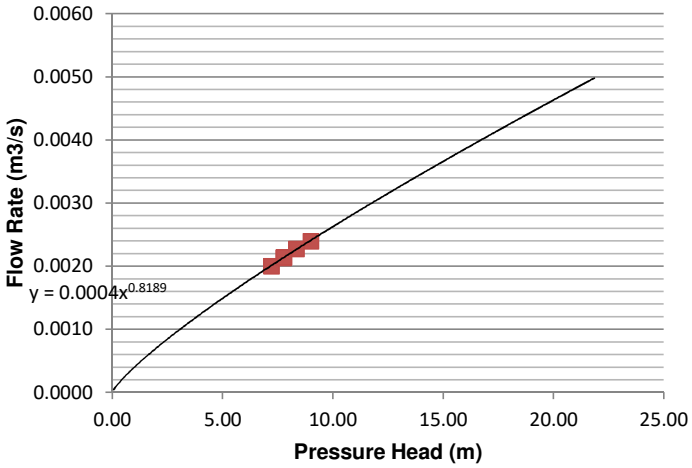

N1 Parameters:

Leakage Coefficient (C):	0.00040
Leakage Exponent (N1):	0.81894

Node 1: FAVAD Relationship

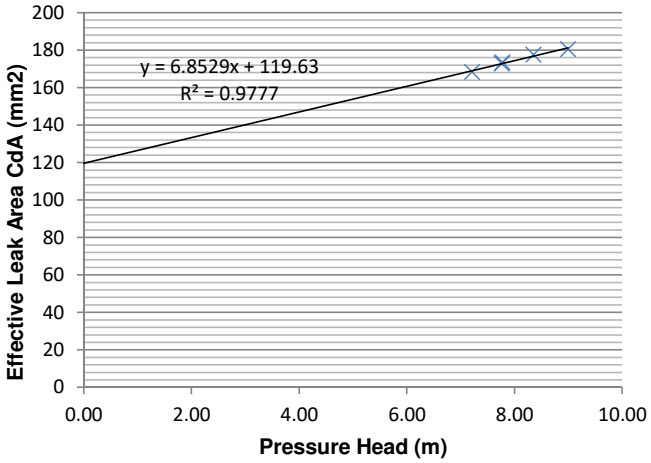

FAVAD Parameters:

Effective Initial Leak Area CdA0:	119.625	mm
Effective head-area slope Cdm:	6.853	mm2/m

N1 And FAVAD Parameters (Second Test)

Node 2: N1 Relationship

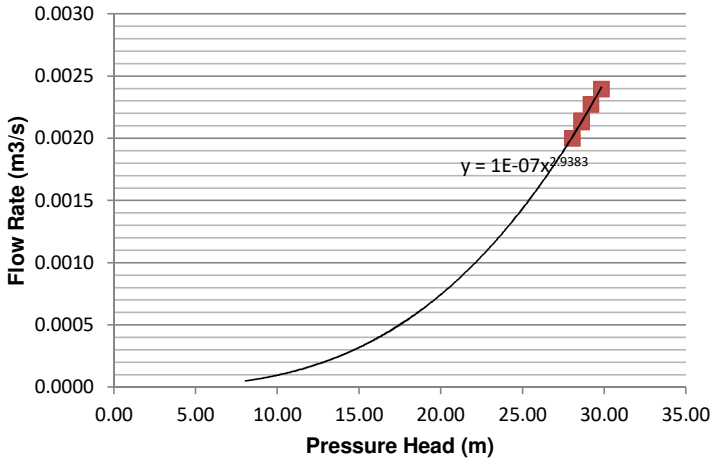

N1 Parameters:

Leakage Coefficient (C):	0.00000
Leakage Exponent (N1):	2.93826

Node 2: FAVAD Relationship

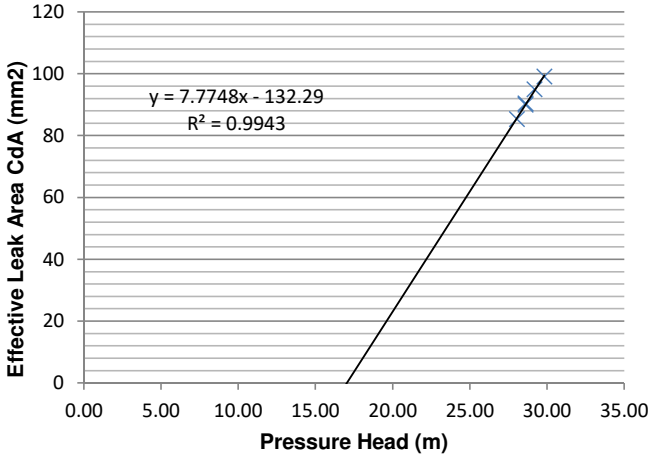

FAVAD Parameters:

Effective Initial Leak Area CdA0:	-132.289	mm
Effective head-area slope Cdm:	7.775	mm2/m

Node 3: N1 Relationship

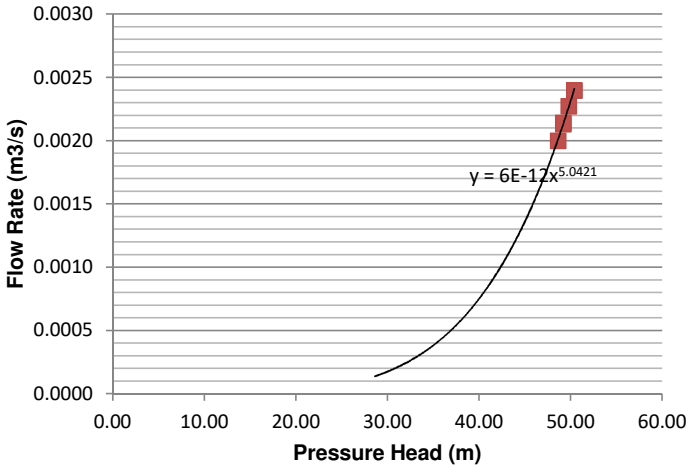

N1 Parameters:

Leakage Coefficient (C):	0.00000
Leakage Exponent (N1):	5.04213

Node 3: FAVAD Relationship

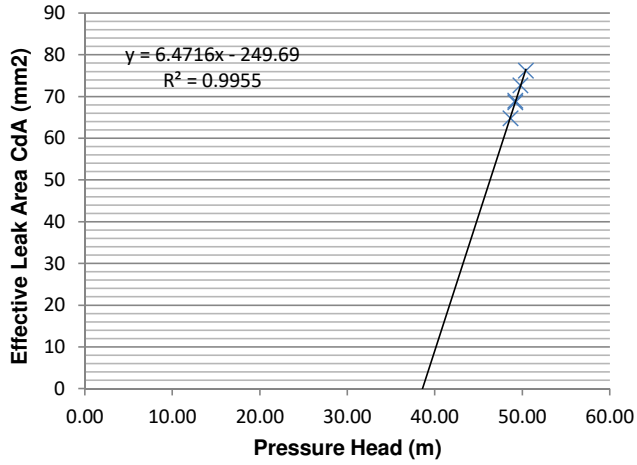

FAVAD Parameters:

Effective Initial Leak Area CdA0:	-249.685	mm
Effective head-area slope Cdm:	6.472	mm2/m

Node 4: N1 Relationship

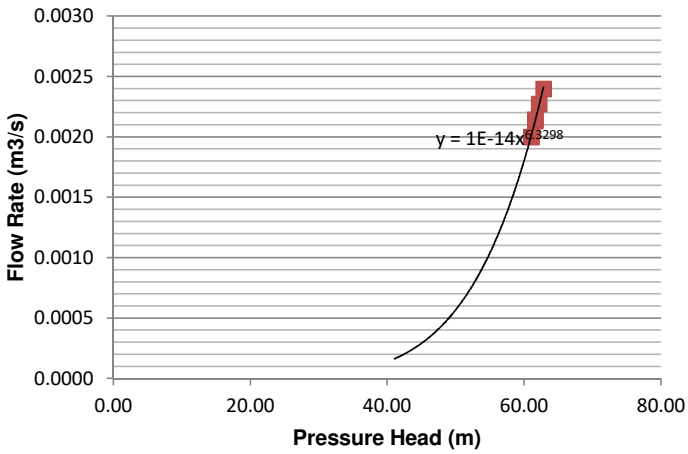

N1 Parameters:

Leakage Coefficient (C):	0.00000
Leakage Exponent (N1):	6.32977

Node 4: FAVAD Relationship

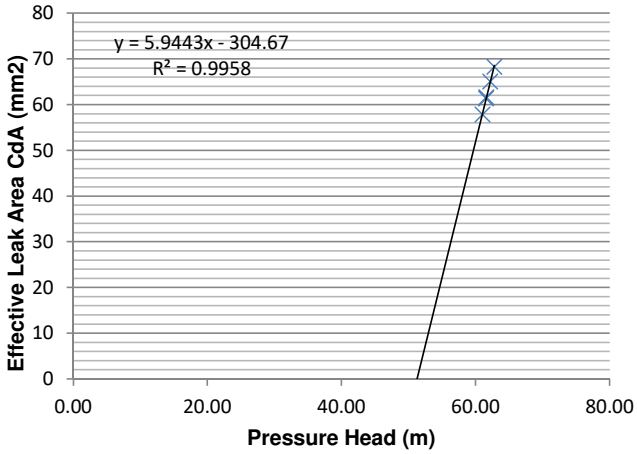

FAVAD Parameters:

Effective Initial Leak Area CdA0:	-304.669	mm
Effective head-area slope Cdm:	5.944	mm2/m

Summary (Second Test)

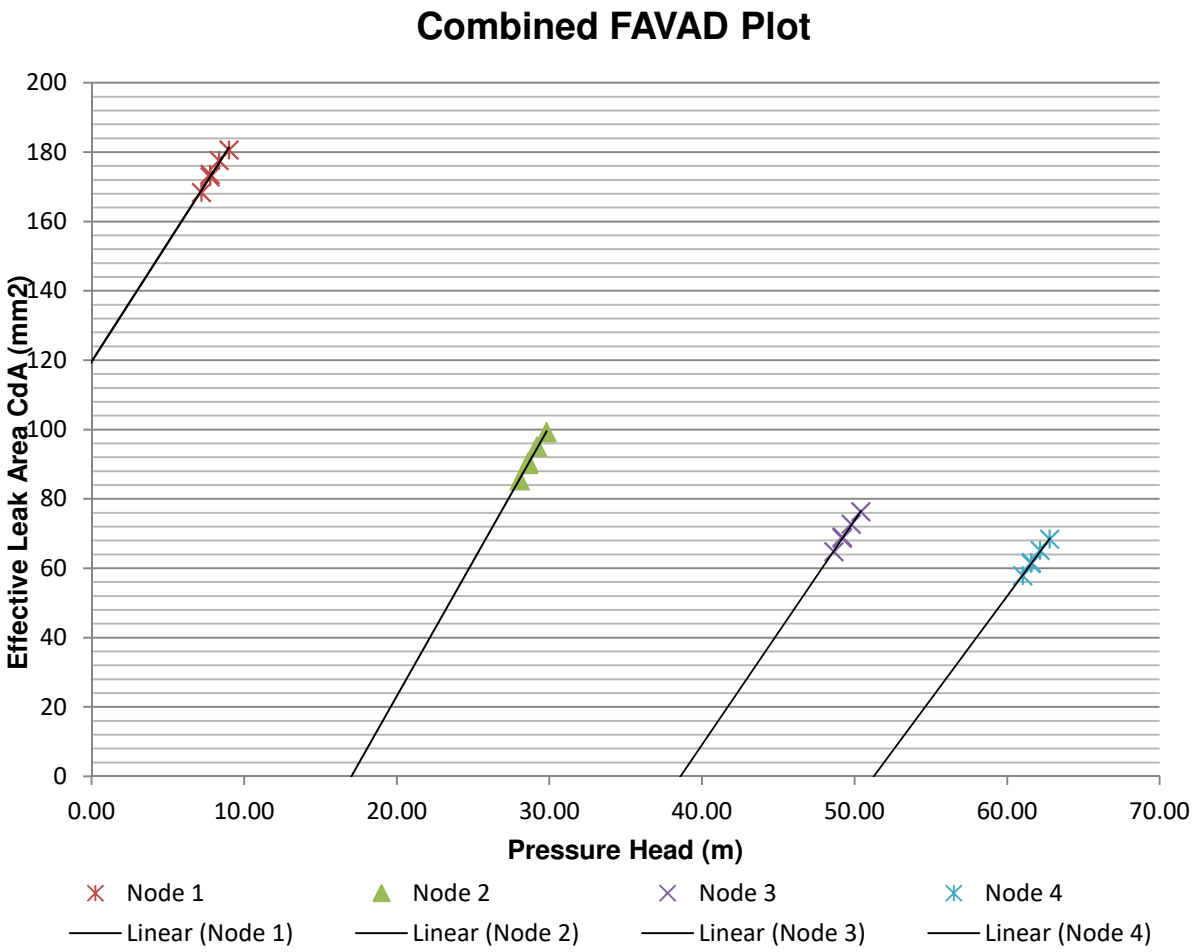

Discussion:

This test shows similar results to the first test, as expected.

N1 And FAVAD Combined (1&2) for Node 1 & 2

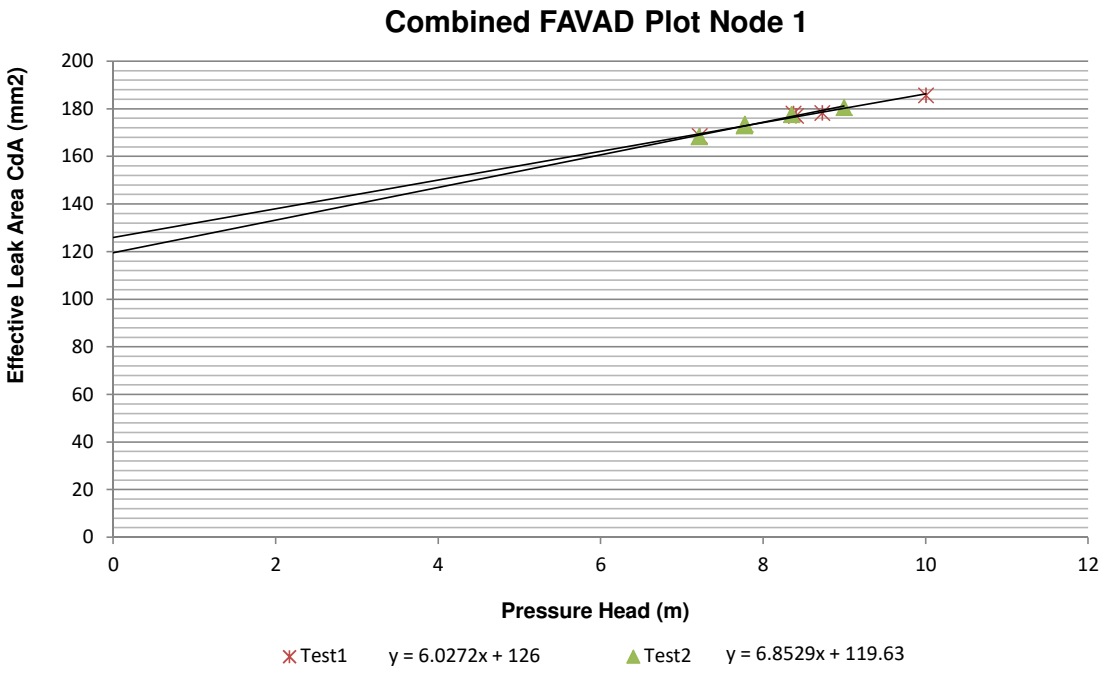

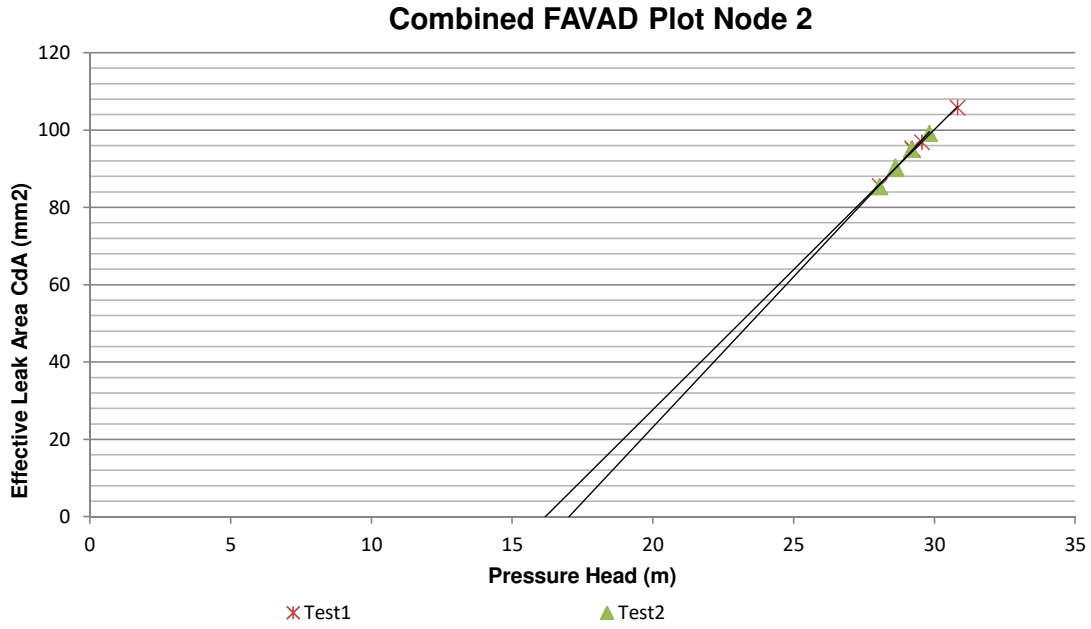

Appendix B:

Photo Report of Further Tests

Picture Report of Tests not Covered by Spreadsheets

Simon Vermooten to Murrayfield Reservoir:

The equipment was connected to the Murrayfield reservoir supply line, but both upstream isolation valves did not seal. Figure 3 below shows the flow exiting the pipe after one of the isolation valves was closed, and Figure 4 shows the flow after both valves were closed.

Figure 1 & 2: Equipment setup and connection point at the Murrayfield Reservoir

Figure 3 & 4: Flow exiting the pipe, after both isolation valves were closed.

KwaMhlanga: Vlaklaagte to Verena Pipeline:

This pipeline was divided into three sections by closing isolation valves along the pipeline. Figures 5 to 7 show the test of the middle section. Figure 8 and 10 show the tests of the last and first section respectively. For all three tests, the equipment was connected to 100 mm air valve connections as depicted in Figure 7.

The middle section was tested first, and the pipe maintained its pressure, indicating a very good pipe condition. A test on the last section was then attempted, but the pressure in the pipeline was too high at the connection point. On this same section, a leaking air valve was identified, as shown in Figure 9.

The first section was tested last. Unfortunately, this pipeline section could not be pressurised, possibly due to the pipeline supply having stopped as part of a water rationing programme.

Figures 5,6 & 7: Equipment setup on middle section; isolation butterfly valve; connection point by replacing 100 mm air valve.

Figure 8: Equipment setup on last section.

Figure 9: Leaking air valve on last section.

Figure 10: Equipment setup on first section.

KwaMhlanga: Moloto Reservoir Supply Line:

On three occasions a test was attempted on this pipeline. The test equipment was connected, but the pipe was always either empty or half-empty, due to water rationing taking place in the area.

Figure 11: Equipment setup at an air valve on the Moloto pipeline

Figure 12 & 13: Connection point to the pipeline by removal and replacement of 50 mm air valve

Appendix C:

Visual Basic Code for Spreadsheet Tool

Visual Basic Code for Excel Data Processing Tool

The code for the Excel Spreadsheet tool was developed specifically for this study, with the aim of demonstrating the ease with which the test data can be processed.

The comments describing the code are coloured green:

```
Sub FormatElevationProfile()
'
' Macro to format the elevation profile data to the desired and compatible format
'
Dim StringVal() As String
NumRows = Range("B8", Range("B8").End(xlDown)).Rows.Count
For x = 1 To NumRows
On Error Resume Next
StringVal = Split((Range("B8").Offset(x - 1, 0)), ",")
Range("B8").Offset(x - 1, 0) = StringVal(0)
Range("C8").Offset(x - 1, 0) = StringVal(1)
On Error GoTo 0
Next x

End Sub
```

```
Sub ClearElevationData()
'
' Macro to clear and reset elevation data
'
Application.ScreenUpdating = False
Range("B8", Range("B8").End(xlDown)).ClearContents
Range("C8", Range("C8").End(xlDown)).ClearContents
Range("B8") = "Paste here"

End Sub
```

```
Sub PlotElevationProfile()
'
'Macro to plot the elevation profile
'
Dim ElevationValues As Range
Dim ElevationChainage As Range
Set ElevationValues = Range("C8", Range("C8").End(xlDown))
Set ElevationChainage = Range("B8", Range("B8").End(xlDown))

ActiveSheet.ChartObjects("ElevationProfile").Activate
    With ActiveChart
    .SeriesCollection(1).Values = ElevationValues
    .SeriesCollection(1).XValues = ElevationChainage
    .Axes(xlValue).MinimumScale = Round(Application.WorksheetFunction.Min(Range("C8", Range("C8").End(xlDown)))) - 5
    .Axes(xlValue).MaximumScale = Round(Application.WorksheetFunction.Max(Range("C8", Range("C8").End(xlDown)))) + 5
    End With
End Sub
```

```
Sub ApplySections()
'
'Macro that seperates the elevation data of the whole pipeline into sections and indicates
'sections in different colours on the plot
'
Dim NumRows As Integer
NumRows = Range("B8", Range("B8").End(xlDown)).Rows.Count

If Not Range("G9") = 0 Then
 For x = 0 To NumRows - 1
    If Range("F7") = 1 Then
    Range("D8").Offset(x, 0) = Range("G9")
    ElseIf Range("B8").Offset(x, 0) < Range("F10") Then
    Range("D8").Offset(x, 0) = Range("G9")
    End If
 Next x
End If

If Not Range("G10") = 0 Then
 For x = 0 To NumRows - 1
    If Range("B8").Offset(x, 0) > Range("F10") Then
    Range("D8").Offset(x, 0) = Range("G10")
    End If
 Next x
End If

If Not Range("G11") = 0 Then
 For x = 0 To NumRows - 1
    If Range("B8").Offset(x, 0) > Range("F11") Then
    Range("D8").Offset(x, 0) = Range("G11")
    End If
 Next x
End If

For x = 0 To NumRows - 1
    If Not Range("D8").Offset(x, 0) = Range("D8").Offset(x + 1, 0) Then
    Range("D8").Offset(x, 0) = "End"
    End If
Next x

Dim ElevationValues1 As Range
Dim ElevationChainage1 As Range
Dim ElevationValues2 As Range
Dim ElevationChainage2 As Range
Dim ElevationValues3 As Range
Dim ElevationChainage3 As Range
Dim findrow As Long
Dim findrow2 As Long
Dim findrow3 As Long

    findrow = Range("D:D").Find("end", Range("D8")).Row
    findrow2 = Range("D:D").Find("end", Range("D" & findrow)).Row
    findrow3 = Range("D:D").Find("end", Range("D" & findrow2)).Row

Set ElevationValues1 = Range("C8" & ":C" & findrow)
Set ElevationChainage1 = Range("B8" & ":B" & findrow)
Set ElevationValues2 = Range("C" & findrow + 1 & ":C" & findrow2)
Set ElevationChainage2 = Range("B" & findrow + 1 & ":B" & findrow2)
Set ElevationValues3 = Range("C" & findrow2 + 1 & ":C" & findrow3)
Set ElevationChainage3 = Range("B" & findrow2 + 1 & ":B" & findrow3)

ActiveSheet.ChartObjects("ElevationProfile").Activate
    With ActiveChart
    .SeriesCollection(1).Values = ElevationValues1
    .SeriesCollection(1).XValues = ElevationChainage1
    .SeriesCollection(2).Values = ElevationValues2
    .SeriesCollection(2).XValues = ElevationChainage2
    .SeriesCollection(3).Values = ElevationValues3
    .SeriesCollection(3).XValues = ElevationChainage3
    .Axes(xlValue).MinimumScale = Round(Application.WorksheetFunction.Min(Range("C8", Range("C8").End(xlDown)))) - 5
    .Axes(xlValue).MaximumScale = Round(Application.WorksheetFunction.Max(Range("C8", Range("C8").End(xlDown)))) + 5
    End With
End Sub
```

```
Sub ImportData()
'
'   Import data from test file. Extracts the recorded data from a file selected by the user
'
Application.ScreenUpdating = False
    Dim wkbCrntWorkBook As Workbook
    Dim wkbSourceBook As Workbook
    Dim rngSourceRange1 As Range
    Dim rngSourceRange2 As Range
    Dim rngSourceRange3 As Range
    Dim rngDestination1 As Range
    Dim rngDestination2 As Range
    Dim rngDestination3 As Range
    Dim NumRows1 As Double
    Set wkbCrntWorkBook = ActiveWorkbook
    With Application.FileDialog(msoFileDialogOpen)
        .Filters.Clear
        .AllowMultiSelect = False
        .Show
        If .SelectedItems.Count > 0 Then
            Workbooks.Open .SelectedItems(1)
            Set wkbSourceBook = ActiveWorkbook
            Set rngSourceRange1 = Range("A9", Range("A9").End(xlDown))
            Set rngSourceRange2 = Range("B9", Range("B9").End(xlDown))
            Set rngSourceRange3 = Range("C9", Range("C9").End(xlDown))
            NumRows1 = Range("A9", Range("A9").End(xlDown)).Rows.Count
            wkbCrntWorkBook.Activate
            Set rngDestination1 = Range("A9", Range("A9").Offset(NumRows1, 0))
            rngSourceRange1.Copy rngDestination1
            Set rngDestination2 = Range("B9", Range("B9").Offset(NumRows1, 0))
            rngSourceRange2.Copy rngDestination2
            Set rngDestination3 = Range("C9", Range("C9").Offset(NumRows1, 0))
            rngSourceRange3.Copy rngDestination3
            wkbSourceBook.Close False
        End If
    End With
    Range("B8") = "Flow (l/min)"
    Range("C8") = "Pressure (bar)"
End Sub
```

```
Sub FormatData()

' Macro to change the fromat of the test data to a compatible format that can be processed further

    Application.ScreenUpdating = False
    Dim NumRows As Long
    Dim density1 As Double
    Dim gravity1 As Double

    Sheets("1Constants").Activate
    density1 = Range("D6").Value
    gravity1 = Range("D7").Value

    Sheets("6TestData").Activate
' Change Date Format to remove the date from the time
    Range("A:A").NumberFormat = "hh:mm:ss.0"
    NumRows = Range("A9", Range("A9").End(xlDown)).Rows.Count

' Convert Date to seconds and milliseconds, pressure to metres head and flow to l/s
    Range("B8") = "Flow (l/s)"
    Range("B:B").NumberFormat = "0.00"
    Range("C8") = "Pressure (m)"
    For x = 1 To NumRows - 1
    Range("E9") = 0
    Range("E9").Offset(x, 0) = Range("E9").Offset(x - 1, 0) + 0.1
    Range("B9").Offset(x - 1, 0) = Range("B9").Offset(x - 1, 0).Value / 60
    Range("C9").Offset(x - 1, 0) = Range("C9").Offset(x - 1, 0).Value * (100000 / (density1 * gravity1))
    Next x

'Turn Milliseconds into whole seconds
    For x = 1 To NumRows - 1
    Range("E9").Offset(x, 0) = Round(Range("E9").Offset(x, 0), 0)
    Next x

' Clean Data to remove all negative pressure data, such as the Error Values which are recorded as -999
    For x = 1 To NumRows
    If Range("B9").Offset(x, 0) < 0 Then
    Range("B9").Offset(x, 0) = 0
    End If
    Next x

' Add a row for the Averages before processing
    For x = 0 To NumRows
    Range("F9").Offset(x, 0) = 0
    Range("G9").Offset(x, 0) = 0
    Next x

End Sub
```

```
Sub ClearData()
'
' Clear the imported test data Macro
'
Application.ScreenUpdating = False
Range("A9", Range("G9").End(xlDown)).ClearContents

End Sub
```

```
Sub PlotGraph()
'
' Plot Graph Macro
'
    Application.ScreenUpdating = False

    Dim FTestData As Range
    Dim xTestData As Range
    Dim PTestData As Range
    Dim FTestAvg As Range
    Dim PTestAvg As Range
    Dim chart1 As Shape

    Set FTestData = Range("B9", Range("B9").End(xlDown))
    Set xTestData = Sheets("6TestData").Range("E9", Range("E9").End(xlDown))
    Set PTestData = Sheets("6TestData").Range("C9", Range("C9").End(xlDown))
    Set FTestAvg = Sheets("6TestData").Range("F9", Range("F9").End(xlDown))
    Set PTestAvg = Sheets("6TestData").Range("G9", Range("G9").End(xlDown))

    ActiveSheet.ChartObjects("FlowPressureVsTime1").Activate
    With ActiveChart
    .SeriesCollection(1).Values = FTestData
    .SeriesCollection(1).XValues = xTestData
    .SeriesCollection(2).Values = PTestData
    .SeriesCollection(2).AxisGroup = 2
    .SeriesCollection(3).AxisGroup = 1
    .SeriesCollection(3).Values = FTestAvg
    .SeriesCollection(3).XValues = xTestData
    .SeriesCollection(4).AxisGroup = 2
    .SeriesCollection(4).Values = PTestAvg
    .SeriesCollection(4).XValues = xTestData
    End With

' Align left and right axis
' Adjust the scale of the secondary Y axis to match the gridlines of both axes
'
    Dim Ymin    As Double
    Dim Ymax    As Double
    Dim Yscale  As Double
    Dim Ylines  As Integer
    Dim sYmin   As Double
    Dim sYmax   As Double
    Dim sYscale As Double

    With ActiveChart
        .Axes(xlValue).MinimumScaleIsAuto = True
        .Axes(xlValue).MaximumScaleIsAuto = True
        .Axes(xlValue).MajorUnitIsAuto = True
        .Axes(xlValue, xlSecondary).MinimumScaleIsAuto = True
        .Axes(xlValue, xlSecondary).MaximumScaleIsAuto = True
        .Axes(xlValue, xlSecondary).MajorUnitIsAuto = True
    End With
```

```
    Ymin = ActiveChart.Axes(xlValue).MinimumScale
    Ymax = ActiveChart.Axes(xlValue).MaximumScale
    Yscale = ActiveChart.Axes(xlValue).MajorUnit
    Ylines = Round((Ymax - Ymin) / Yscale)
    sYmin = ActiveChart.Axes(xlValue, xlSecondary).MinimumScale
    sYmax = ActiveChart.Axes(xlValue, xlSecondary).MaximumScale
    'Calculate the new major unit and maximum bound of the secondary Y axis.
    sYscale = Round((sYmax - sYmin) / Ylines)
    sYmax = sYmin + Ylines * sYscale

    With ActiveChart.Axes(xlValue, xlSecondary)
        .MinimumScale = 0
'        .MinimumScale = sYmin
        .MaximumScale = sYmax
        .MajorUnit = sYscale
    End With

End Sub
```

```
Sub SelectDataRange1()
'
' Macro that selects the data range to be shown on main plot, using the range requested from the user:
'
    Dim StartAt As Long
    Dim StopAt As Long
    StartAt = Application.InputBox("Enter Start Time")
    StopAt = Application.InputBox("Enter Stop Time")

    Dim FTestData As Range
    Dim xTestData As Range
    Dim PTestData As Range
    Dim FTestAvg As Range
    Dim PTestAvg As Range

    Set FTestData = Range(Range("B9").Offset(RowOffset:=(StartAt * 10)), Range("B9").Offset(RowOffset:=(StopAt * 10)))
    Set xTestData = Range(Range("E9").Offset(RowOffset:=(StartAt * 10)), Range("E9").Offset(RowOffset:=(StopAt * 10)))
    Set PTestData = Range(Range("C9").Offset(RowOffset:=(StartAt * 10)), Range("C9").Offset(RowOffset:=(StopAt * 10)))
    Set FTestAvg = Range(Range("F9").Offset(RowOffset:=(StartAt * 10)), Range("F9").Offset(RowOffset:=(StopAt * 10)))
    Set PTestAvg = Range(Range("G9").Offset(RowOffset:=(StartAt * 10)), Range("G9").Offset(RowOffset:=(StopAt * 10)))

    ActiveSheet.ChartObjects("FlowPressureVsTime1").Activate
    With ActiveChart
    .SeriesCollection(1).Values = FTestData
    .SeriesCollection(2).Values = PTestData
    .SeriesCollection(1).XValues = xTestData
    .SeriesCollection(3).Values = FTestAvg
    .SeriesCollection(4).Values = PTestAvg
    End With

End Sub
```

```
Sub ClearDataRange()
'
' Macro to clear data and reset
'
    NumRows = Range("A9", Range("A9").End(xlDown)).Rows.Count

    Set FTestData = Range(Range("B9").Offset(RowOffset:=(0)), Range("B9").Offset(RowOffset:=(NumRows)))
    Set xTestData = Range(Range("C9").Offset(RowOffset:=(0)), Range("C9").Offset(RowOffset:=(NumRows)))
    Set PTestData = Range(Range("E9").Offset(RowOffset:=(0)), Range("E9").Offset(RowOffset:=(NumRows)))

    ActiveSheet.ChartObjects("FlowPressureVsTime1").Activate
    With ActiveChart
    .SeriesCollection(1).Values = FTestData
    .SeriesCollection(2).Values = xTestData
    .SeriesCollection(1).XValues = PTestData
    End With

End Sub
```

```
Sub PlotRange()
'
'Macro to plot the desired zoomed-in range
'
 Application.ScreenUpdating = False

    Dim StartTime As Integer
    Dim StopTime As Integer

    StartTime = Range("L56")
    StopTime = Range("L57")

    Dim FTestData1 As Range
    Dim xTestData1 As Range
    Dim PTestData1 As Range

    Set FTestData1 = Range(Range("B9").Offset(RowOffset:=(StartTime * 10)), Range("B9").Offset(RowOffset:=(StopTime * 10)))
    Set PTestData1 = Range(Range("C9").Offset(RowOffset:=(StartTime * 10)), Range("C9").Offset(RowOffset:=(StopTime * 10)))
    Set xTestData1 = Range(Range("E9").Offset(RowOffset:=(StartTime * 10)), Range("E9").Offset(RowOffset:=(StopTime * 10)))

    ActiveSheet.ChartObjects("FlowVsTime").Activate
    With ActiveChart
    .SeriesCollection(1).Values = FTestData1
    .SeriesCollection(1).XValues = xTestData1
    End With
    ActiveSheet.ChartObjects("PressureVsTime").Activate
    With ActiveChart
    .SeriesCollection(1).Values = PTestData1
    .SeriesCollection(1).XValues = xTestData1
    End With

End Sub
```

```
Sub AverageCalc()
'
'Macro to calculate the average of the plotted value between the specified range
'
    Dim StartAvg As Integer
    Dim StopAvg As Integer
    Dim FAvg As Double
    Dim PAvg As Double

    StartAvg = Range("S56")
    StopAvg = Range("S57")

    Set FAverage = Range(Range("B9").Offset(RowOffset:=(StartAvg * 10)), Range("B9").Offset(RowOffset:=(StopAvg * 10)))
    Set PAverage = Range(Range("C9").Offset(RowOffset:=(StartAvg * 10)), Range("C9").Offset(RowOffset:=(StopAvg * 10)))

    FAvg = Application.Average(FAverage)
    PAvg = Application.Average(PAverage)
    Range("S59") = FAvg
    Range("S60") = PAvg

'   Plot the average values
    Dim StartDisp As Integer
    Dim StopDisp As Integer
    Dim RowCount As Integer
    Dim TempFlow As Range
    Dim TempPres As Range

    FAvg = Range("S59")
    PAvg = Range("S60")
    StartDisp = Range("L56") * 10
    StopDisp = Range("L57") * 10
    RowCount = StopDisp - StartDisp

    For x = StartDisp To StopDisp
    Range("F9").Offset(x, 0).Value = FAvg
    Range("G9").Offset(x, 0).Value = PAvg
    Next x

    Set TempFlow = Range(Range("F9").Offset(RowOffset:=(StartDisp)), Range("F9").Offset(RowOffset:=(StopDisp)))
    Set TempPres = Range(Range("G9").Offset(RowOffset:=(StartDisp)), Range("G9").Offset(RowOffset:=(StopDisp)))

    ActiveSheet.ChartObjects("FlowVsTime").Activate
    With ActiveChart
    .SeriesCollection(2).Values = TempFlow
    End With

    ActiveSheet.ChartObjects("PressureVsTime").Activate
    With ActiveChart
    .SeriesCollection(2).Values = TempPres
    End With

End Sub
```

```
Sub RecordPoint()
'
'Macro to record the average pressure vs flow point of the selected range
'
    Application.ScreenUpdating = False

    Dim PointNo As Integer
    PointNo = Application.InputBox("Please insert point no.")
    Range("S59").Select
    Selection.Copy
    Sheets("7PressureCorrection").Activate
    Range("B28").Offset(RowOffset:=(PointNo - 1)) = PointNo
    Range("C28").Offset(RowOffset:=(PointNo - 1)).PasteSpecial xlPasteValues
    Sheets("6TestData").Select
    Range("S60").Select
    Selection.Copy
    Sheets("7PressureCorrection").Activate
    Range("D28").Offset(RowOffset:=(PointNo - 1)).PasteSpecial xlPasteValues
    Sheets("6TestData").Activate
    Application.CutCopyMode = False
    Range("X59") = PointNo
End Sub
```

```
Sub GoalSeekFriction()
'
'This makro solves the friction coefficient in the Colebrook-White equation by solving equations simultaneously
'
Application.ScreenUpdating = False

    NumRows = Range("C28", Range("C28").End(xlDown)).Rows.Count
    For x = 0 To NumRows - 1
        Range("I28").Offset(x, 1) = 0.5
        Range("I28").Offset(x, 0).GoalSeek Goal:=0, ChangingCell:=Range("I28").Offset(x, 1)
    Next x
    For x = 0 To NumRows - 1
        Range("I50").Offset(x, 1) = 0.5
        Range("I50").Offset(x, 0).GoalSeek Goal:=0, ChangingCell:=Range("I50").Offset(x, 1)
    Next x
    If Range("P45") > 0 Or Range("P46") > 0 Then
    For x = 0 To NumRows - 1
        Range("V50").Offset(x, 1) = 0.5
        Range("V50").Offset(x, 0).GoalSeek Goal:=0, ChangingCell:=Range("V50").Offset(x, 1)
    Next x
    End If
    For x = 0 To NumRows - 1
        Range("I72").Offset(x, 1) = 0.5
        Range("I72").Offset(x, 0).GoalSeek Goal:=0, ChangingCell:=Range("I72").Offset(x, 1)
    Next x
    For x = 0 To NumRows - 1
        Range("I94").Offset(x, 1) = 0.5
        Range("I94").Offset(x, 0).GoalSeek Goal:=0, ChangingCell:=Range("I94").Offset(x, 1)
    Next x
    For x = 0 To NumRows - 1
        Range("I116").Offset(x, 1) = 0.5
        Range("I116").Offset(x, 0).GoalSeek Goal:=0, ChangingCell:=Range("I116").Offset(x, 1)
    Next x
End Sub
```